



NTIA Report 08-450

**POTENTIAL INTERFERENCE FROM  
BROADBAND OVER POWER LINE (BPL)  
SYSTEMS TO FEDERAL GOVERNMENT  
RADIOCOMMUNICATION SYSTEMS  
AT 1.7 - 80 MHz**

**Phase 2 Study**

**VOLUME I**  
*technical report*



NTIA Report 08-450

**POTENTIAL INTERFERENCE FROM BROADBAND OVER  
POWER LINE (BPL) SYSTEMS TO FEDERAL  
GOVERNMENT RADIOCOMMUNICATION SYSTEMS AT  
1.7 - 80 MHz**

**Phase 2 Study**

**VOLUME I**

**James C. Richards  
Jonathan V. Williams**



**U.S. Department of Commerce  
Carlos M. Gutierrez, Secretary**

John M. R. Kneuer, Assistant Secretary  
for Communications and Information

**October 2007**

## **ACKNOWLEDGEMENTS**

The authors would like to thank the many organizations and persons who contributed to the completion of this report. In particular, we wish to thank the federal agency representatives on the Interdepartment Radio Advisory Committee for providing vital comments, information, and review of this report.

We also wish to thank the following NTIA personnel who contributed substantially to this report and to the underlying studies: Alakananda Paul Cou-Way Wang, and Edward Drocella.

## **PREFACE**

This report contains two volumes. Volume I presents the main text and Volume II contains appendixes that provide additional technical supporting information that is summarized in Volume I.

## EXECUTIVE SUMMARY

On October 14, 2004, the Federal Communications Commission (Commission or FCC) adopted a Report and Order that defined new Part 15 rules for Access Broadband over Power Line (BPL) systems. The National Telecommunications and Information Administration (NTIA) contributed to the Commission's work by providing analysis to support recommendations for refinements in the rules and measurement guidelines in comments and staff correspondence filed in response to the Commission's earlier BPL Notice of Proposed Rulemaking (NPRM). The NTIA Phase 2 study of Access BPL systems expands on its earlier Phase 1 study by providing additional modeling results and analyses to evaluate the effectiveness of the FCC's rules and measurement guidelines in minimizing the potential for harmful interference to federal radiocommunication systems under worst-case conditions.

NTIA's simulations of overhead Medium Voltage (MV) power lines show that aspects of the measurement guidelines addressed in the BPL Report and Order, such as measurement distance, locations, height and height correction factor, and antenna type, effectively estimate the peak electric field strength that might be experienced in the vicinity of the Access BPL energized power line. These simulations employ the Numerical Electromagnetic Code (NEC) software package to model a variety of power line configurations. NTIA investigated the Commission's new methodology for extrapolating field strength limits when measurements must be made at distances other than those specified in the rules. NTIA's simulations confirm that the extrapolation methodology provides a reasonable approximation of the predicted rate of field strength roll-off with distance in close proximity to the BPL device and its associated power lines.

The FCC's rules include special mechanisms for minimizing the likelihood of harmful interference to critical federal radiocommunication systems in addition to the baseline protection afforded by field strength limits, prohibition of harmful interference from Access BPL systems, and compliance measurement provisions. These special protection provisions have the following forms: geographic consultation areas, wherein BPL deployments at any frequency in those areas must be preceded by consultations between BPL operators and nearby radio operators; excluded bands, in which certain frequencies are not to be used by BPL in any geographic area; and small geographic exclusion zones, wherein BPL emissions are forbidden at specified frequencies. NTIA's analysis shows that, at the distances corresponding to these protection areas, BPL emissions are expected to result in only small increases in the noise floor of protected communications receivers, or power flux density levels that fall below the interference protection requirement for sensitive radioastronomy or over-the-horizon radar receivers.

This Phase 2 report illustrates the application of the rules and measurement guidelines in a case study. Using the NEC software package, NTIA created an elaborate power line model that approximates an existing overhead Access BPL power line structure. After applying the emissions limits and methodology from the BPL measurement guidelines, NTIA analyzed the noise floor increase expected in nearby receivers as a result of BPL operations. In addition, NTIA used this power line model to

analyze the BPL emission levels that might be seen at more distant receivers. The results of the case study are consistent with NTIA's earlier analyses using simple power line models.

NTIA's Comments in response to the BPL NPRM included a preliminary analysis of the aggregation of overhead Access BPL emissions via ionospheric propagation in the 1.7 to 30 MHz frequency range. That analysis has been further refined in this report to include NEC simulations of both an elaborate overhead power line model and an underground power line model, and the adopted BPL measurement guidelines were employed to ensure compliance with Part 15 rules. As in the earlier analysis, the Voice of America Coverage Analysis Program (VOACAP) High Frequency (HF) propagation software package was used for predicting the propagation of radiated BPL emissions. Ionospheric propagation was analyzed using these overhead and underground models over a wide range of conditions. The results of this analysis show that a widespread deployment of Access BPL systems throughout the United States is not expected to pose a problem for federal radiocommunication systems operating in the 1.7 to 30 MHz band.

In summary, the Phase 2 study analyses expanded on the scope of NTIA's earlier analyses and applied the Commission's adopted rules and measurement guidelines for Access BPL systems. The results of these analyses confirm that these Access BPL rules, measurement guidelines, and special protection provisions will limit the interference risks for federal radiocommunication systems.

# VOLUME I

## TABLE OF CONTENTS

	ACKNOWLEDGEMENTS .....	iii
	PREFACE .....	iv
	EXECUTIVE SUMMARY .....	v
	.....	
	TABLE OF CONTENTS .....	vii
	GLOSSARY .....	x
	.....	
SECTION 1	INTRODUCTION	
1.1	Background .....	1-1
1.2	Objectives .....	1-2
1.3	Approach .....	1-2
SECTION 2	PART 15 MEASUREMENT GUIDELINES	
2.1	Introduction .....	2-1
2.2	Power Line Models Used in the Analysis .....	2-1
2.3	Measurement Antenna Height .....	2-5
2.3.1	Height Corresponding to Peak Field Strength .....	2-5
2.3.2	Peak Electric Field Strength at the Compliance Measurement Heights.....	2-8
2.3.3	Antenna Measurement Height Correction Factor above 30 MHz	2-13
2.4	Measurement Distance Along the Power Line .....	2-17
2.5	Measurement Distance Extrapolation .....	2-22
2.5.1	New Approach for Distance Extrapolation .....	2-22
2.5.2	Calculated Electric Field Strength Decay for Distance Extrapolation .....	2-26
2.6	Use of Loop Antenna Below 30 MHz .....	2-29
2.7	Measurement Antenna Polarization .....	2-30
2.8	Guidelines for Choosing Representative Systems .....	2-31
2.9	Summary .....	2-34
SECTION 3	SPECIAL PROVISIONS FOR PREVENTION OF INTERFERENCE FROM BPL SYSTEMS	
3.1	Introduction .....	3-1
3.1.1	Background .....	3-2
3.2	Potential Victim Receivers .....	3-3
3.2.1	Communications Receivers .....	3-3
3.2.2	Radar Receivers .....	3-5



3.2.3	Radioastronomy Receivers .....	3-6
3.3	Potential Sources of Interference .....	3-6
3.3.1	Overhead Power Line Model .....	3-6
3.3.2	Underground Power Line Model .....	3-7
3.3.3	Part 15 Scaling of Power Line Models .....	3-8
3.4	Analytical Approach .....	3-9
3.4.1	Communications Receivers .....	3-9
3.4.2	Radar Receivers .....	3-11
3.4.3	Radioastronomy Receivers .....	3-13
3.5	Simulation Results .....	3-14
3.5.1	Communications Receivers .....	3-16
3.5.2	Radar Receivers .....	3-23
3.5.3	Radioastronomy Receivers .....	3-23
3.6	Summary .....	3-25
SECTION 4	CASE STUDY OF POTENTIAL INTERFERENCE USING ADOPTED BPL RULES	
4.1	Introduction .....	4-1
4.2	Methodology .....	4-1
4.2.1	Structure Injection Points .....	4-2
4.2.2	Simulation Frequencies .....	4-3
4.2.3	Part 15 Scaling .....	4-5
4.2.4	Simulation of Potential Interference .....	4-7
4.3	Results .....	4-12
4.3.1	Receiver Noise Floor Increase Along the Power Line .....	4-14
4.3.2	Power Flux Density Away from the Power Line .....	4-16
4.4	Summary .....	4-19
SECTION 5	IONOSPHERIC PROPAGATION AND AGGREGATION OF BPL EMISSIONS	
5.1	Introduction .....	5-1
5.2	Analytical Modeling of Sky Wave Propagation .....	5-1
5.2.1	Background .....	5-1
5.2.2	Approach .....	5-2
5.3	Simulation Characteristics .....	5-6
5.4	Simulation Results .....	5-9
5.4.1	Comparison of Overhead and Underground Analysis Results.....	5-9
5.4.2	Maps of Ionospheric Aggregation .....	5-11
5.5	Summary .....	5-18
SECTION 6	SUMMARY OF RESULTS	
6.1	Introduction .....	6-1
6.2	Phase 2 Analyses .....	6-1
6.2.1	Part 15 Rules and Measurement Guidelines .....	6-1
6.2.2	Special Protection Provisions .....	6-3
6.2.3	Case Study Applying the Access BPL Measurement Guidelines	6-3

6.2.4	Aggregation of Emissions via Ionospheric Propagation .....	6-4
6.3	Conclusion .....	6-4

**TECHNICAL APPENDICES**

(See VOLUME II)

## GLOSSARY

AWG	American Wire Gauge
BPL	Broadband over Power Line(s)
BW	Bandwidth
CISPR	International Special Committee on Radio Interference
CONUS	Continental United States
COTHEN	Customs Over The Horizon Enforcement Network
dB	Decibel
dBi	Decibel referenced to an isotropic radiator
dBm	Decibel referenced to 1 milliwatt
dB $\mu$ V	Decibel referenced to 1 microvolt
dBW	Decibels referenced to 1 Watt
E	Electric Field Strength
EMC	Electromagnetic Compatibility
EUT	Equipment Under Test
FCC	Federal Communications Commission
G	Gain
GHz	Gigahertz
H	Magnetic Field Strength
HF	High Frequency
Hz	Hertz
I	Interference Power
ICAO	International Civil Aviation Organization
IRAC	Interdepartment Radio Advisory Committee
ITM	Irregular Terrain Model
ITS	Institute for Telecommunication Sciences
ITU	International Telecommunication Union
ITU-R	International Telecommunication Union Radiocommunication Sector
kHz	Kilohertz
km	Kilometer
LV	Low Voltage
m	Meter
MHz	Megahertz
mm	millimeter
mS	Siemens/meter
ms	Millisecond
MV	Medium Voltage
N	Noise Power
NEC	Numerical Electromagnetic Code
NOI	Notice of Inquiry
NPRM	Notice of Proposed Rulemaking
NTIA	National Telecommunications and Information Administration
OR	Off-Route

OTH	Over the Horizon
PFD	Power Flux Density
PLC	Power Line Communications
PLT	Power Line Telecommunications
R	Route
RF	Radio Frequency
RMS	Root Mean Square
RSMS	Radio Spectrum Measurement System
S	Signal Power
SNR	Signal-to-Noise Ratio
SSB	Single Sideband
SSN	Smoothed Sunspot Number
URD	Underground Residential Distribution
US&P	United States and Possessions
UTC	Universal Coordinated Time
VHF	Very High Frequency
VLA	Very Large Array
VOA	Voice of America
VOACAP	Voice of America Coverage Analysis Program
W	Watt
$\mu\text{A}$	Microampere
$\mu\text{V}$	Microvolt



# **SECTION 1 INTRODUCTION**

## **1.1 BACKGROUND**

The National Telecommunications and Information Administration (NTIA) Phase 1 Study of Access Broadband over Power Line (BPL) systems summarized federal use of the 1.7 – 80 MHz frequency range, presented measurement and modeling results for BPL emissions, defined interference risks to radio reception in the immediate vicinity of overhead power lines used by Access BPL systems, suggested refinements to Part 15 measurement guidelines applicable to BPL systems, and identified means for mitigating local interference should it occur.<sup>[1]</sup> Propagation and aggregation of emissions from BPL systems and the associated BPL deployment models were suggested as issues requiring further study.

In comments and staff correspondence filed in response to the Federal Communications Commission (Commission or FCC) BPL Notice of Proposed Rulemaking (BPL NPRM), NTIA provided a preliminary analysis to support recommendations for refinements in the rules and measurement guidelines.<sup>[2]</sup> In its comments, NTIA proposed a number of refinements to the measurement guidelines for BPL systems, such as the measurement locations along the power line, away from the power line, and at various measurement antenna heights. NTIA's preliminary analysis of these proposals confirmed that the measurement guidelines defined in the BPL NPRM strike a reasonable balance between measurement simplicity, accuracy and repeatability. NTIA also presented a worst-case analysis of ionospheric propagation and aggregation of emissions from wide scale deployment of Access BPL systems. This preliminary analysis showed that aggregation of BPL emissions via ionospheric propagation was not a near term problem; however, NTIA indicated that it would continue to study this issue. Finally, NTIA continued to evolve its analysis of interference risks to nearby radio receivers and proposed a framework for protection of critical federal radiocommunications.

## **1.2 OBJECTIVES**

The NTIA Phase 2 Study is intended to provide additional technical background for the rules and measurement guidelines for Access BPL systems. This report combines the preliminary Phase 2 analyses presented in other NTIA contributions in the FCC's BPL proceeding with additional analyses that extend both the depth and scope of the earlier work. It also offers a case study of calculated emission levels from a model of an actual BPL network for the purpose of demonstrating the effectiveness of the BPL rules and measurement guidelines adopted by the FCC in its BPL Report and Order.<sup>[3]</sup> This case study includes an analysis of the risk of interference that a representative BPL network might present to nearby radiocommunications.

### **1.3 APPROACH**

NTIA simulated a variety of power line structures using the Numerical Electromagnetic Code (NEC) software package and determined the expected field strength over a range of distances from the power line, along the length of the power line, and at various heights above the ground.<sup>[4]</sup>

The NEC simulations were used to evaluate the effectiveness of the FCC's recently adopted measurement guidelines at achieving a reasonable level of measurement accuracy with a practical number of measurements as discussed in Section 2.

In Section 3, the interference risk to fixed and mobile base station receivers from nearby BPL devices was analyzed to formulate suitable radii recommendations for exclusion zones and consultation areas.

Using an NEC model of an elaborate power line structure, NTIA applied the measurement guidelines adopted in the BPL Report and Order to evaluate their effectiveness as a means to limit the interference risk associated with these emissions to nearby radiocommunications as discussed in Section 4.

Based on the rules and measurement guidelines for Access BPL systems, NTIA updated and expanded upon its evaluation of the aggregation of their emissions via ionospheric propagation using the Voice of America Coverage Analysis Program (VOACAP) High Frequency (HF) propagation software package as discussed in Section 5.<sup>[5]</sup>

Finally, a summary of the results from these analyses is provided Section 6.

Supplemental data from these analyses are provided in Appendices A through D contained in Volume II of this report.





## SECTION 2 PART 15 MEASUREMENT GUIDELINES

### 2.1 INTRODUCTION

In the Phase 1 Study, NTIA stated that adopting effective BPL measurement guidelines is critical to reducing the risk of harmful interference to federal radiocommunications.<sup>[6]</sup> The NTIA Phase 1 Study comments on the FCC's BPL NPRM, and subsequent correspondence with the Commission described NTIA's measurements and analyses of BPL emissions.<sup>[7]</sup> Emissions from Access BPL systems operating on overhead Medium Voltage (MV) power lines are atypical of most Part 15 devices in that the peak field strength often occurs at heights significantly greater than 1 meter and may occur at various distances along the power line.

NTIA's measurements and analyses showed that the strength of radiated emissions diminished more slowly with distance from the BPL source than would be expected of a typical point source radiator. Measurements of BPL field strength are typically performed in the near field where the relationship between the electric and magnetic fields is not easily quantified. In its earlier filings in the FCC's BPL proceeding, NTIA presented measurements and computer modeling of emissions from Access BPL sources and connected power lines in order to characterize the nature of these emissions. In the Phase 2 Study, NTIA further analyzes these characteristics of BPL emissions using the Commission's recently adopted measurement guidelines to demonstrate that these guidelines effectively balance measurement accuracy with a reasonably limited number of measurements.

### 2.2 POWER LINE MODELS USED IN THE ANALYSIS

NTIA used the NEC software program to create a number of power line models to gain a greater understanding of the effects various physical topologies might have on the electric fields radiated by BPL signals on power lines. Below 30 MHz, the magnetic field that would be measured by rotating a vertically positioned loop antenna 180 degrees about its vertical axis was determined by simulation over a range of heights and all along the length of the power line model. Where results below 30 MHz are shown in terms of electric field strength, the magnetic field strength was converted to vertical electric field strength using Equation 2-1, assuming a Cartesian coordinate system as shown in Figure 2-1 below:

$$E_z = \eta \cdot \sqrt{H_x^2 + H_y^2}, \quad (\text{Equation 2-1})$$

where  $\eta$  is the impedance of free space, nominally 377 ohms ( $\Omega$ );

$H_x$  is the x-component of the horizontal magnetic field, in A/m;  
 $H_y$  is the y-component of the horizontal magnetic field, in A/m; and  
 $E_z$  is the vertical electric field strength in V/m.

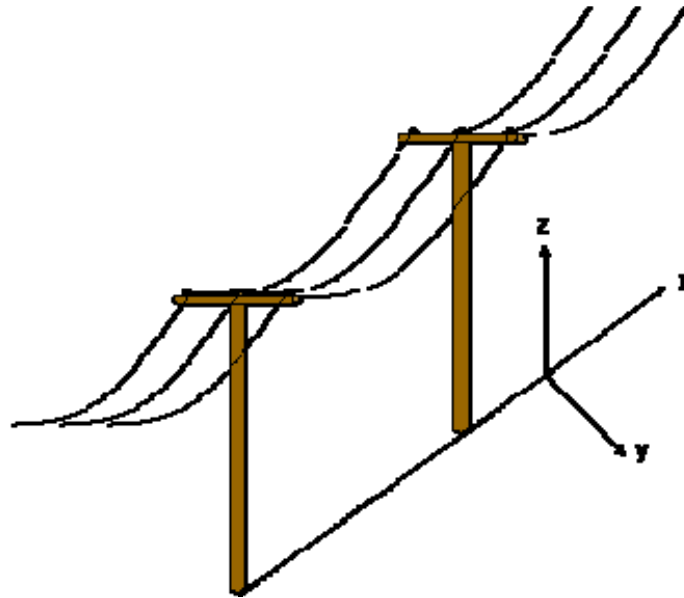


**Figure 2-1: Power line and coordinate system**

Above 30 MHz, the electric field strength in either the horizontal or vertical polarization was determined over a range of heights and at any position along the length of the NEC power line models.

NTIA evaluated a wide variety of power line topologies to calculate three-axis electric field values in a vertical grid located at a 10 meter horizontal distance from the power line (the measurement distance adopted in the BPL Report and Order), at heights ranging from 1 to 20 meters in one meter increments. These calculations were made horizontally along the length of the modeled power lines in one meter increments, and at frequencies ranging from 2 to 50 MHz in 2 MHz increments. Eighteen relatively simple power line topologies are listed in Table 2-1. Figure 2-2 depicts the orientation of power line conductors for each of these topologies.

**Table 2-1: Power line topologies used to model antenna measurement height**

Model Name	Number of Wires	Wire Configuration	Multi-grounded neutral with 3 transformers	Wire Spacing
------------	-----------------	--------------------	--	--------------

Model Name	Number of Wires	Wire Configuration	Multi-grounded neutral with 3 transformers	Wire Spacing
tri26	2	triangular-horizontal	not included	0.6 meters
tri210	2	triangular-horizontal	not included	1.0 meters
tri36	3	triangular-horizontal	not included	0.6 meters
tri310	3	triangular-horizontal	not included	1.0 meters
tri26n	2	triangular-horizontal	included	0.6 meters
tri210n	2	triangular-horizontal	included	1.0 meters
tri36n	3	triangular-horizontal	included	0.6 meters
tri310n	3	triangular-horizontal	included	1.0 meters
ver1	1	vertical	not included	n/a
ver26	2	vertical	not included	0.6 meters
ver210	2	vertical	not included	1.0 meters
ver36	3	vertical	not included	0.6 meters
ver310	3	vertical	not included	1.0 meters
ver1n	1	vertical	included	n/a
ver26n	2	vertical	included	0.6 meters
ver210n	2	vertical	included	1.0 meters
ver36n	3	vertical	included	0.6 meters
ver310n	3	vertical	included	1.0 meters

The power line models listed in Table 2-1 were 340 meters in length, 12 meters above ground, and consisted of eight segments of catenary (hanging) wires (with catenary lengths of 43 meters each) as would be suspended between nine utility poles. The signal injection point for these models was on the segment next to the model's mid-point, on one of the outside wires. All wires were assumed to be copper, and all models with neutral wires included three simulated distribution transformers wired between one of the phases and neutral, with  $7.7 \Omega$  of real impedance.<sup>[8]</sup> On the models with a neutral wire, the neutral was connected to ground at each transformer point (in the center of the model and at each end).

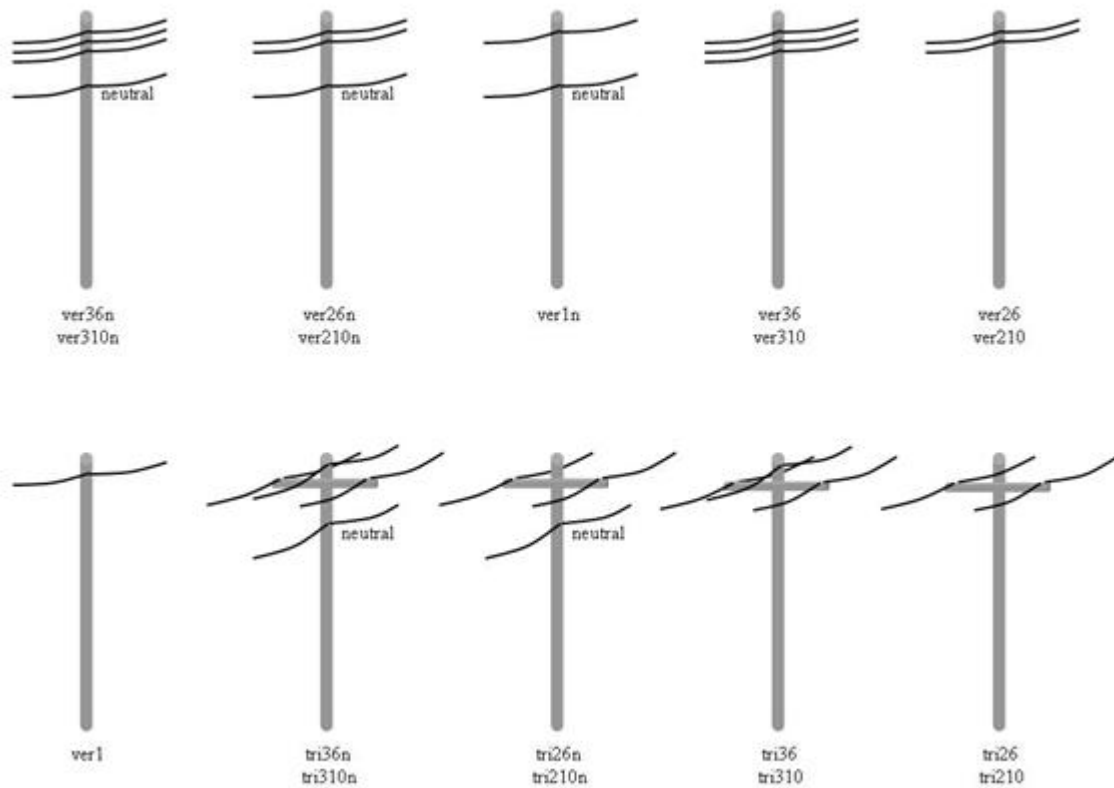


**Figure 2-2: Power line topologies**

Vertical-alignment models were designed such that all wires (including the neutral, if any) were arranged in a vertical line. Triangular-horizontal models with three wires were designed with the middle wire 0.25 meter higher than the outer two. The neutral wire (if one was included) was centered under the phase wires.

NTIA also constructed an elaborate NEC model based on the physical layout of an actual MV distribution branch in one of the BPL deployment areas where NTIA conducted field measurements. This model was designed using power line maps as well as actual observation (Figure 2-3). The model consisted of three-phase and multi-grounded neutral wiring. Included in the model are risers (connections of all three phases of overhead wiring to underground wiring having a characteristic impedance of 30  $\Omega$ ), wire intersections, transformers and neutral grounds. Along most of the power line, the wiring topology is vertical, but at one pole (at a riser) it shifts to a horizontal-triangular configuration and then back to vertical. The model covered an area of some 240,000 square meters (600m  $\times$  400m), and was segmented and tested at 4.303 MHz, 8.192 MHz, 22.957 MHz and 28.298 MHz (frequencies which corresponded with measurement frequencies in the field).

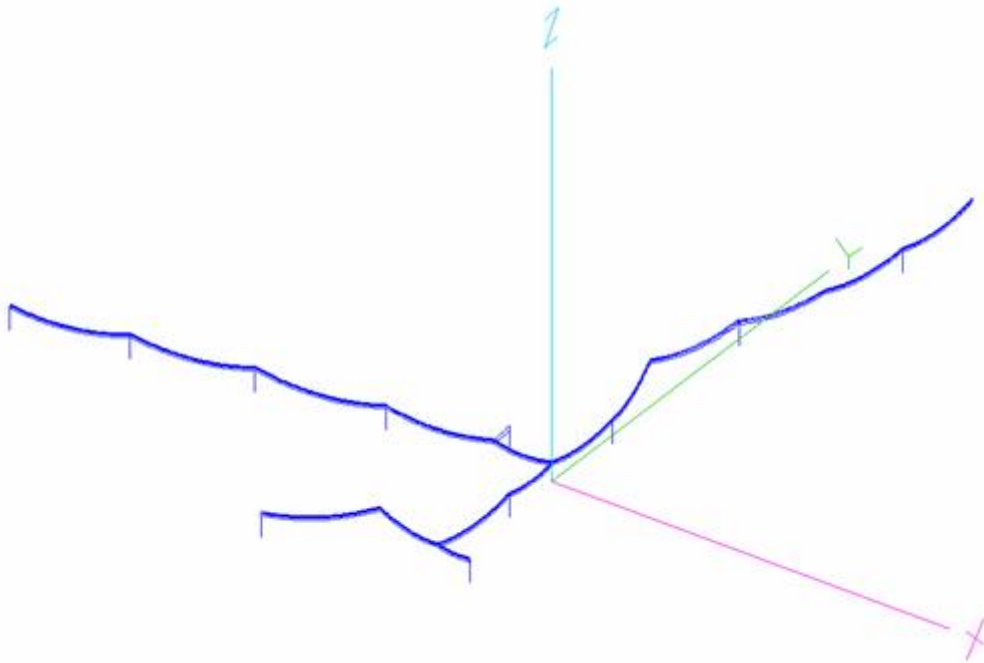


**Figure 2-3: NEC model of actual power line carrying BPL signals**

## **2.3 MEASUREMENT ANTENNA HEIGHT**

NTIA analyzed the electric field strength calculated from a variety of power line models to determine the strength of radiated emissions as a function of height. In addition, NTIA analyzed the difference in peak field strength over the range of simulated heights, and the peak field strength at 1 meter off the ground (below 30 MHz) and at 1 to 4 meters off the ground (30 MHz and above). These results were used to assess the effectiveness of the measurement antenna heights specified in the measurement guidelines for estimating the field strength radiated from Access BPL systems. In lieu of measurements performed at various antenna heights, NTIA proposed the application of a height correction factor. The Commission's rules for Access BPL systems adopted a 5 dB height correction factor with a 1 meter measurement height, as an alternative to measuring field strength from 1 to 4 meters at or above 30 MHz.<sup>[9]</sup>

### **2.3.1 Height Corresponding To Peak Field Strength**

Figures 2-4 through 2-7 show the heights where the peak electric field strength occurred over the frequency range of 2 to 50 MHz for two of the power line topologies described in Section 2.2. These results were obtained at a horizontal distance of 10 meters from the modeled power lines, and considered points all along the power line. The results for other power line configurations are provided in Appendix A.

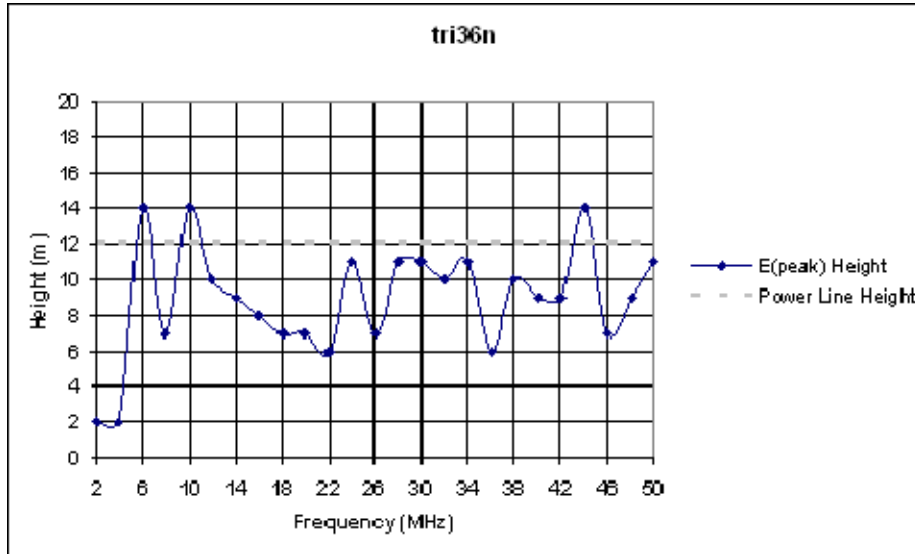
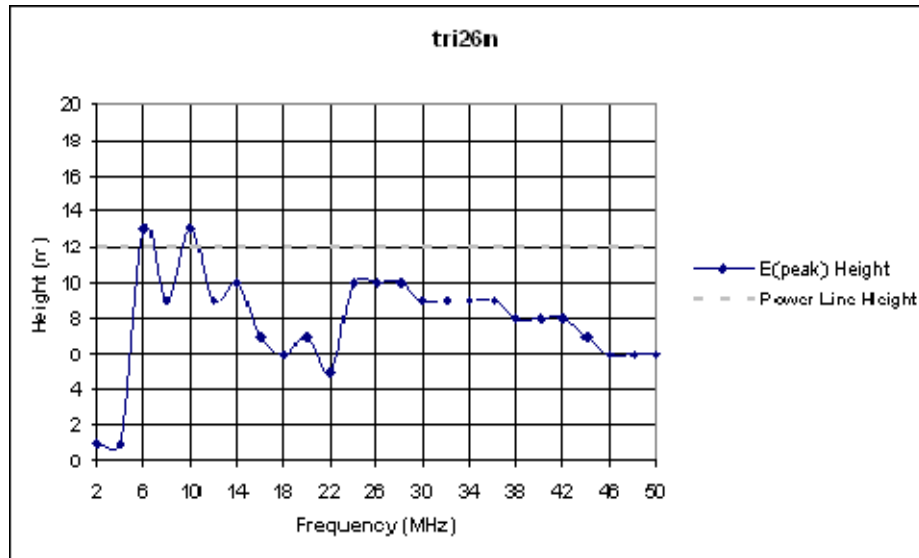


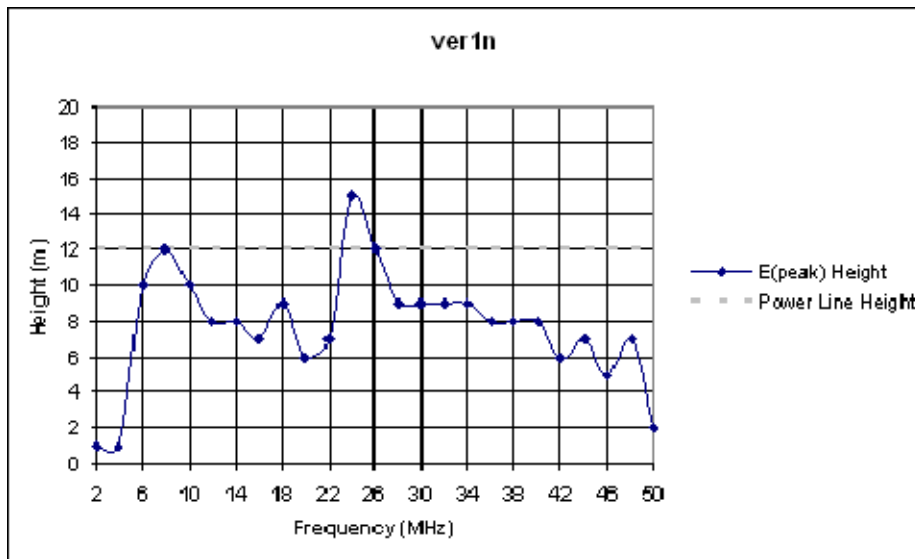
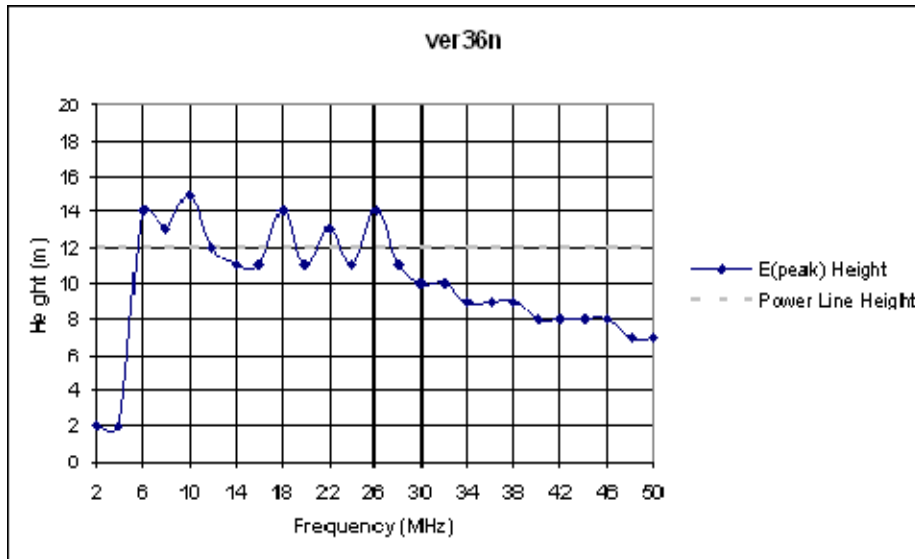
Figure 2-4: Height corresponding to peak electric field strength as a function of frequency

Figure 2-5: Height corresponding to peak electric field strength as a function of



frequency

**Figure 2-6: Height corresponding to peak electric field strength as a function of frequency**



**Figure 2-7: Height corresponding to peak electric field strength as a function of frequency**

Figures 2-4 through 2-7 illustrate the variability of heights at which the peak electric field strength occurs. This variability can be seen over both frequency and power line topology. In those cases where the operating frequency is above 6 MHz, the peak field strength typically occurred at heights greater than 1 meter. Below 6 MHz, where the wavelengths are greater than four times the modeled power line height (12 meters), the increased in-phase coupling between the power line and ground will generally lead to the highest values of electric field at or near ground level.

### 2.3.2 Peak Electric Field Strength at the Compliance Measurement Heights

Although the peak field strength may occur at any height, the rules for Access BPL systems specify measurement heights of 1 meter below 30 MHz, and 1 to 4 meters at or above 30 MHz.<sup>[10]</sup> Figures 2-8 through 2-17 show the 80<sup>th</sup> percentile of peak electric field strength values along the power lines and over the range of simulated heights, relative to the peak field strength seen at the Part 15 compliance measurement height.<sup>[11]</sup> As previously stated in Section 2.2, the power line simulations computed electric field strength values at heights of 1 to 20 meters in one meter increments. The 80<sup>th</sup> percentile values eliminate the localized peaks that are unlikely to be encountered by a radio receiver randomly located in close proximity to an Access BPL power line.<sup>[12]</sup>

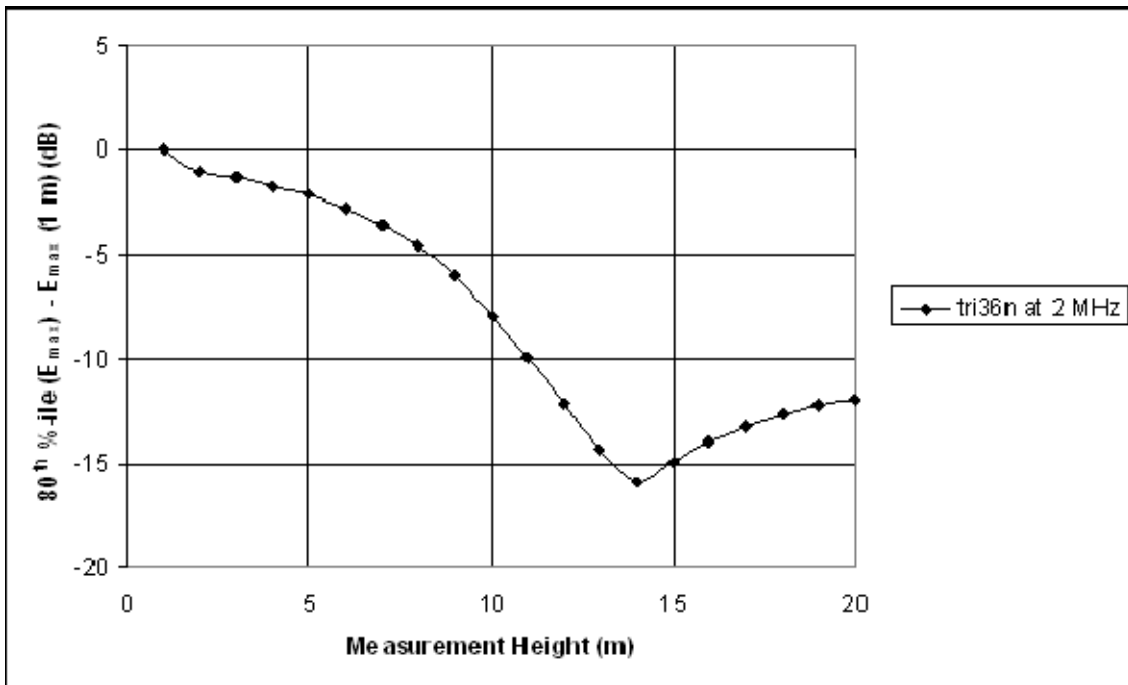


Figure 2-8: 80<sup>th</sup> percentile of peak electric field strength along the power line relative to the peak electric field strength at a 1 meter measurement height



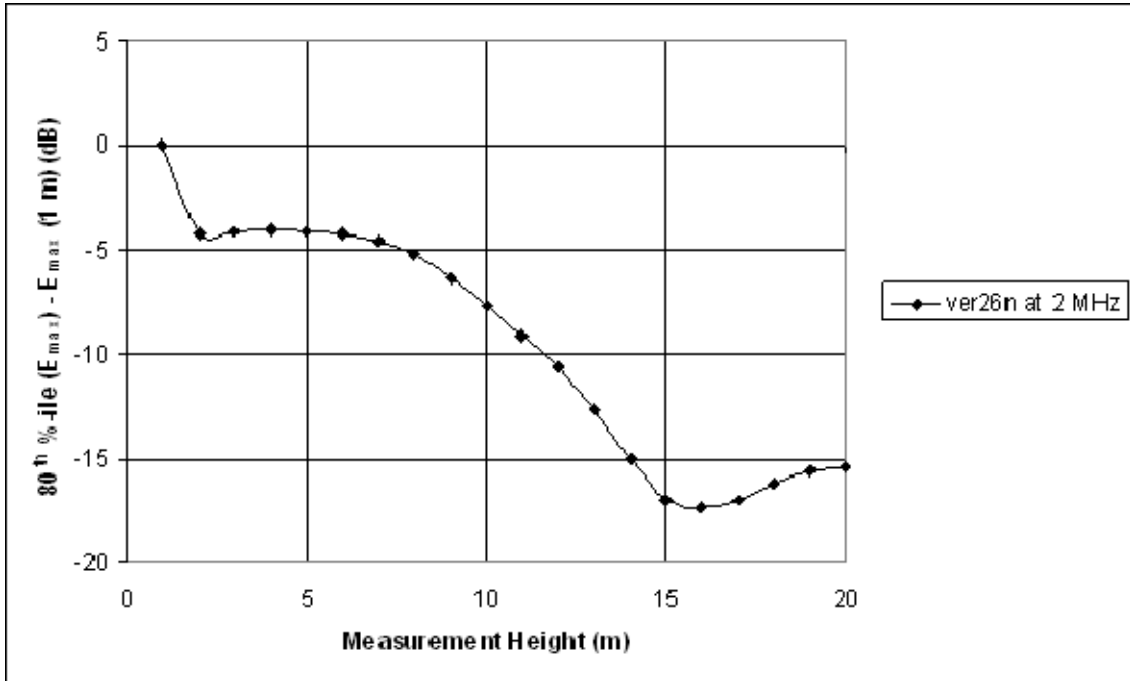


Figure 2-9: 80<sup>th</sup> percentile of peak electric field strength along the power line relative to the peak electric field strength at a 1 meter measurement height

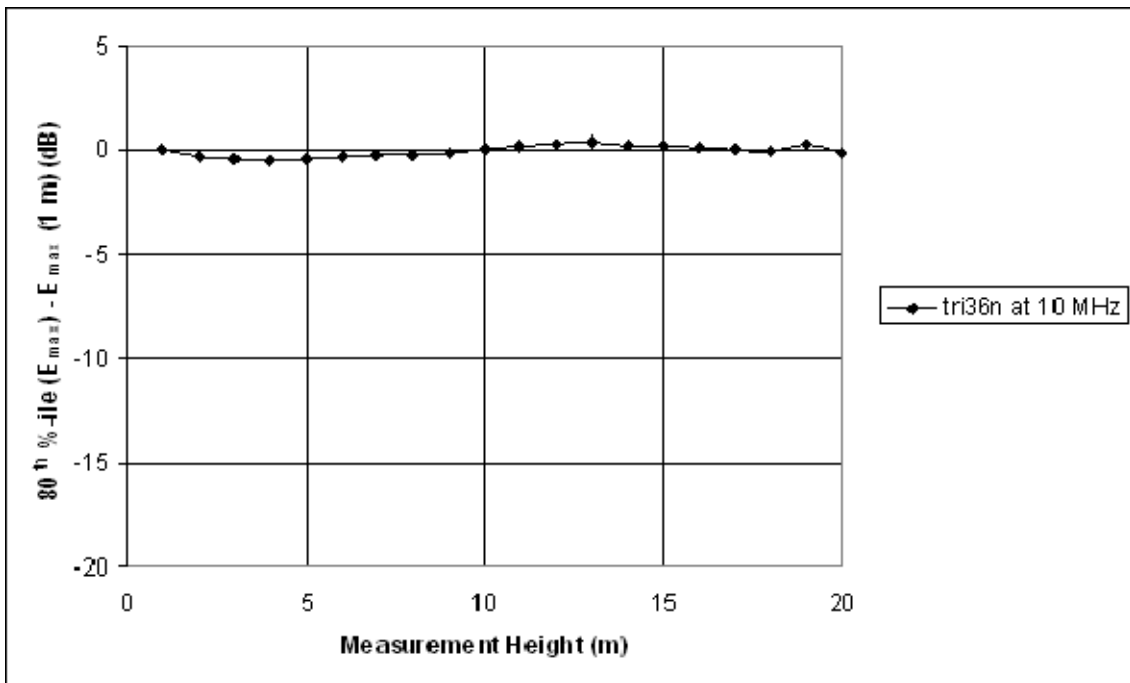


Figure 2-10: 80<sup>th</sup> percentile of peak electric field strength along the power line relative to the peak electric field strength at a 1 meter measurement height

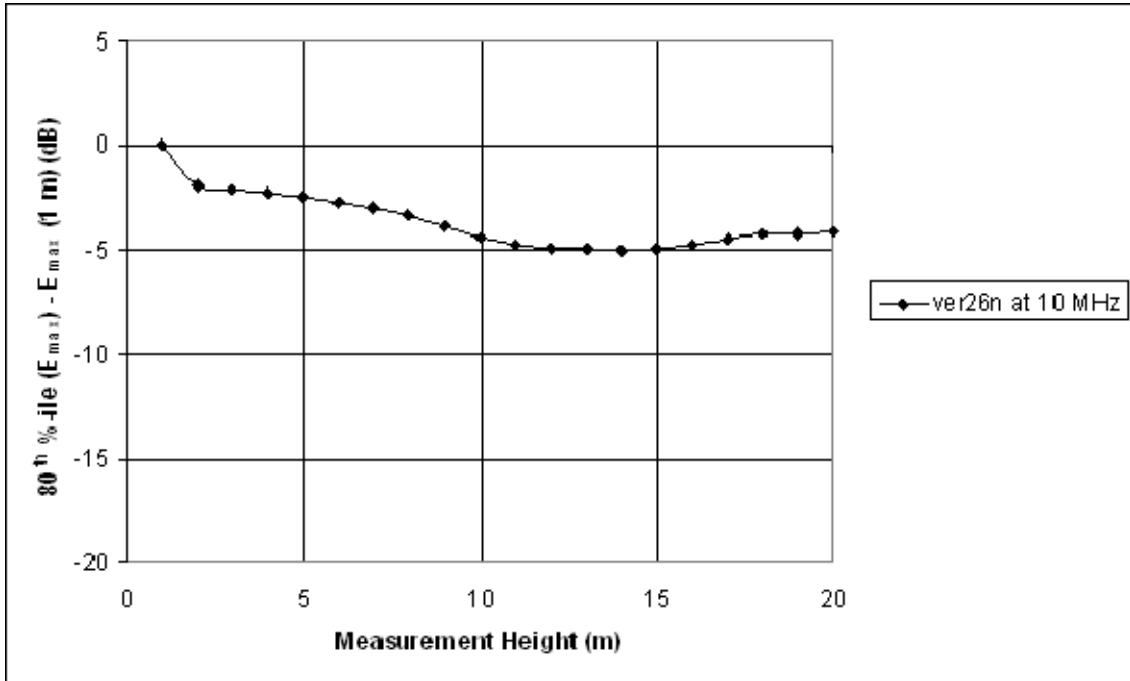


Figure 2-11: 80<sup>th</sup> percentile of peak electric field strength along the power line relative to the peak electric field strength at a 1 meter measurement height

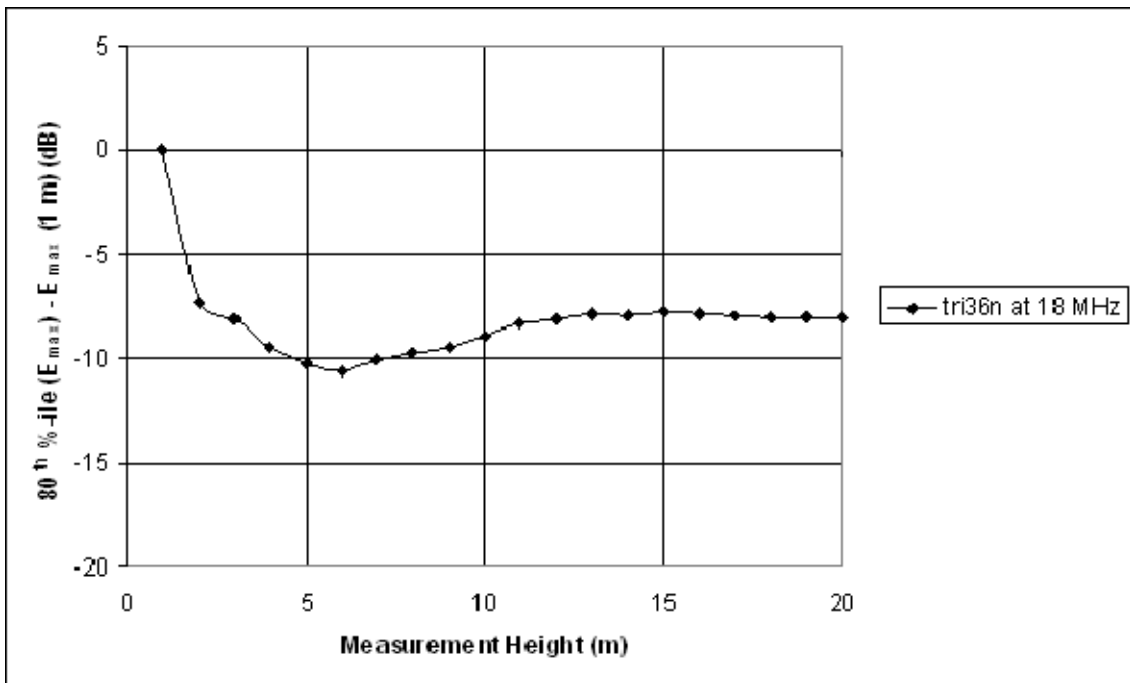


Figure 2-12: 80<sup>th</sup> percentile of peak electric field strength along the power line relative to the peak electric field strength at a 1 meter measurement height

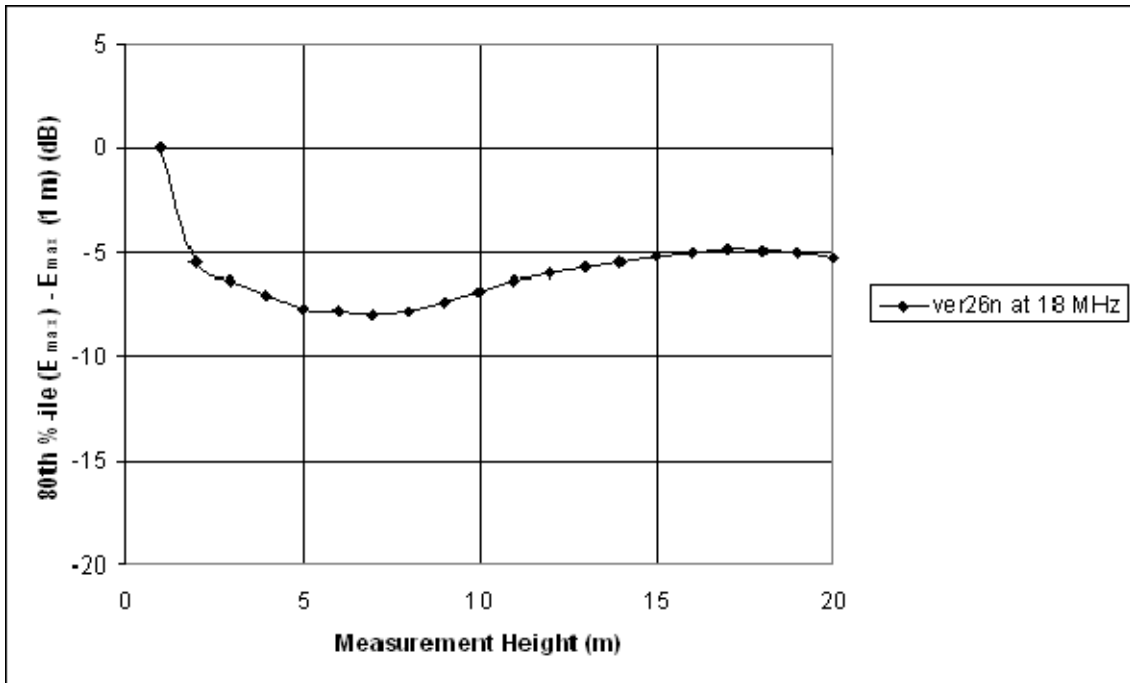


Figure 2-13: 80<sup>th</sup> percentile of peak electric field strength along the power line relative to the peak electric field strength at a 1 meter measurement height

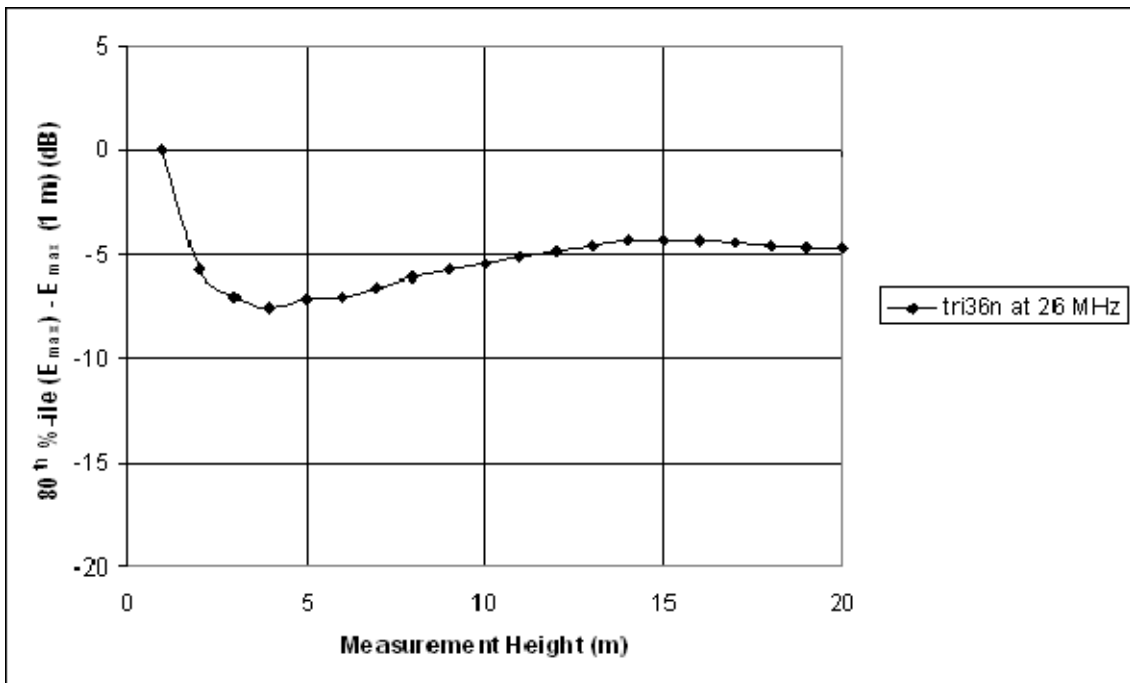


Figure 2-14: 80<sup>th</sup> percentile of peak electric field strength along the power line relative to the peak electric field strength at a 1 meter measurement height

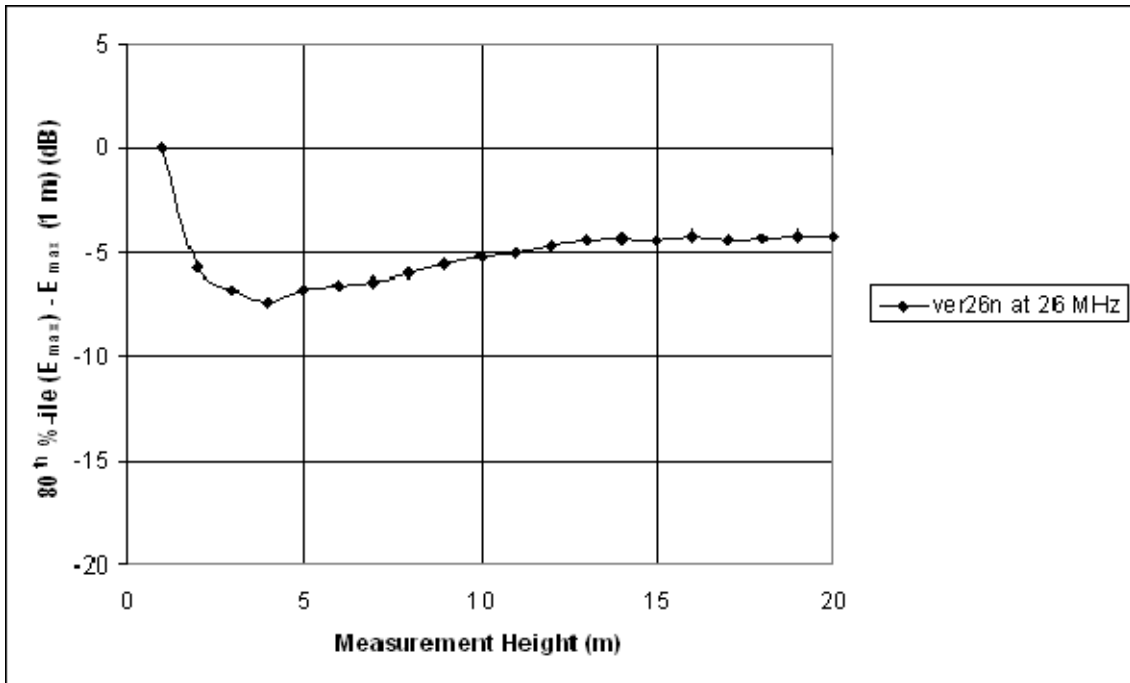


Figure 2-15: 80<sup>th</sup> percentile of peak electric field strength along the power line relative to the peak electric field strength at a 1 meter measurement height

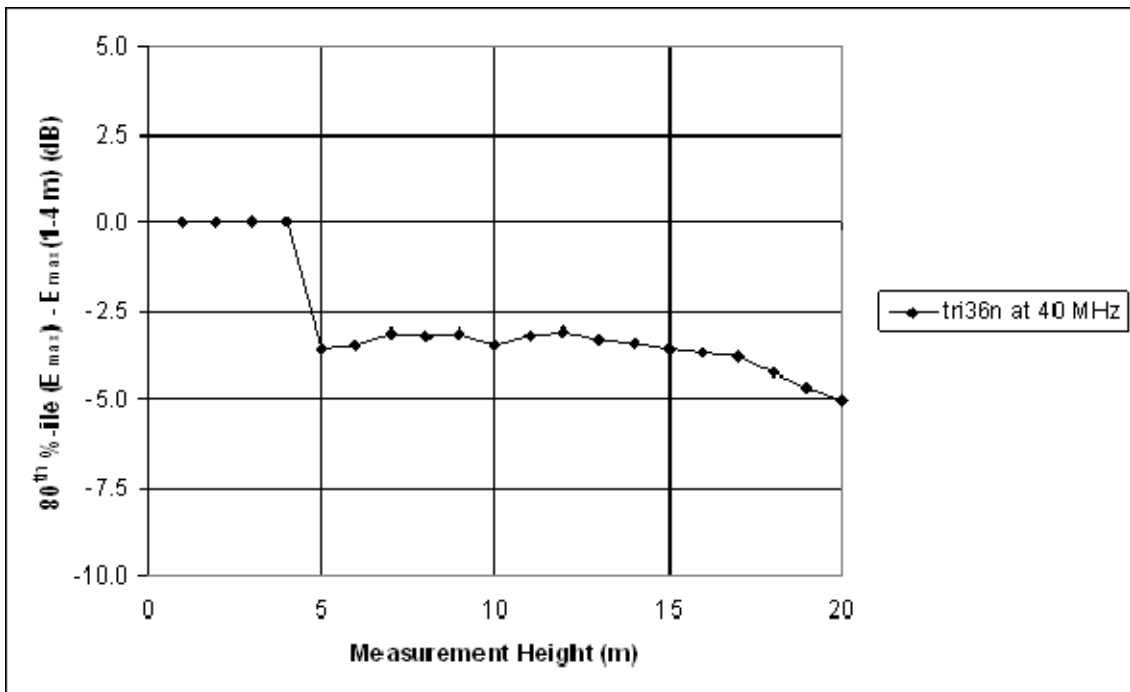
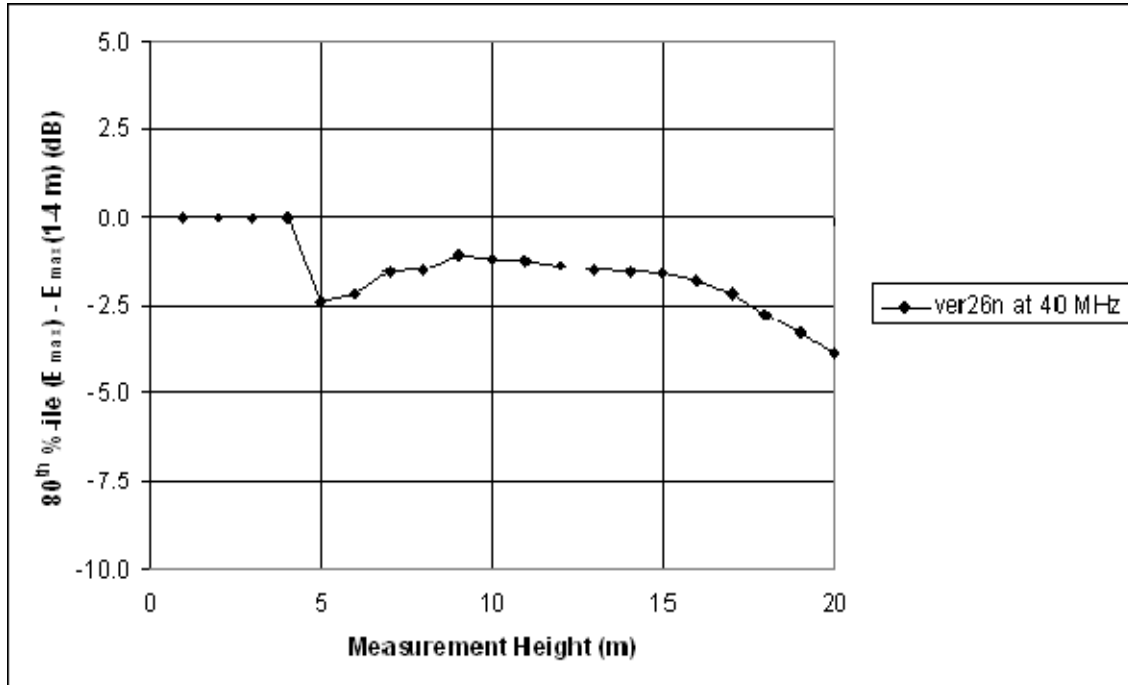


Figure 2-16: 80<sup>th</sup> percentile of peak electric field strength along the power line relative to the peak electric field strength at the 1 to 4 meter measurement height



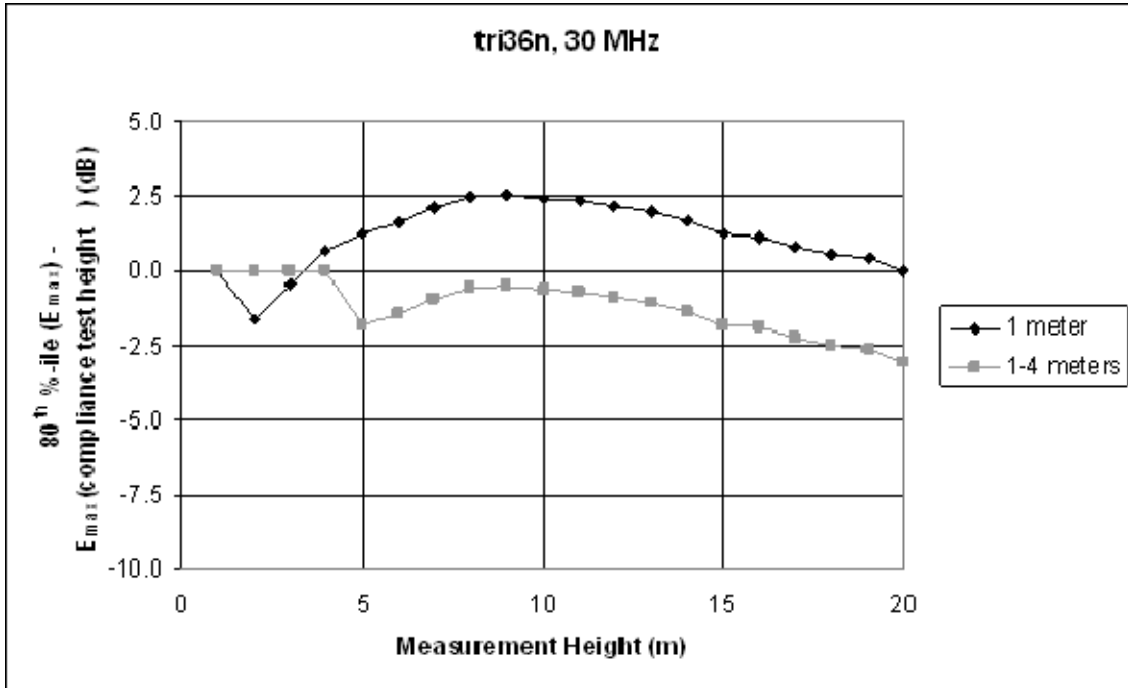
**Figure 2-17: 80<sup>th</sup> percentile of peak electric field strength along the power line relative to the peak electric field strength at the 1 to 4 meter measurement height**

As can be seen in Figures 2-8 through 2-17, and in Appendix A, the Part 15 measurement heights underestimated the 80<sup>th</sup> percentile of peak electric field strength for the various power line models by no more than 1 dB. The use of these measurement heights is expected to result in reasonable estimates of peak field strength at the most locations surrounding overhead Access BPL power lines.

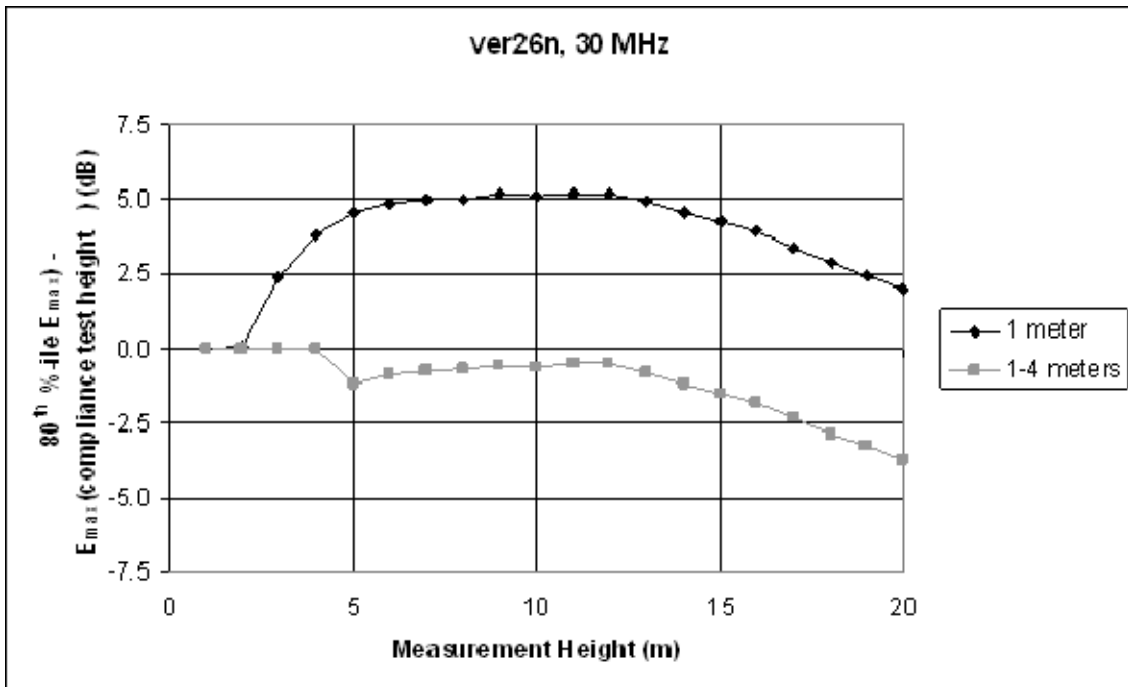
### 2.3.3 Antenna Measurement Height Correction Factor above 30 MHz

Above 30 MHz, the option to perform compliance measurements at a 1 meter measurement height coupled with a 5 dB height correction factor provides a much simpler measurement approach than to perform measurements over the specified 1 to 4 meter range of measurement heights. Figures 2-18 through 2-23 illustrate the difference between the overall peak field strength (80<sup>th</sup> percentile values), which could occur at any height, relative to the peak field strength at the specified measurement height(s) for two of the simulated power line configurations. These figures show two cases: use of the specified 1 to 4 meter measurement height, and use of the optional 1 meter measurement height. The NEC simulation data were scaled to the peak levels seen in either the horizontal or vertical polarizations at the FCC-specified compliance measurement locations for the 1 meter and 1 to 4 meter height cases. <sup>[13]</sup>

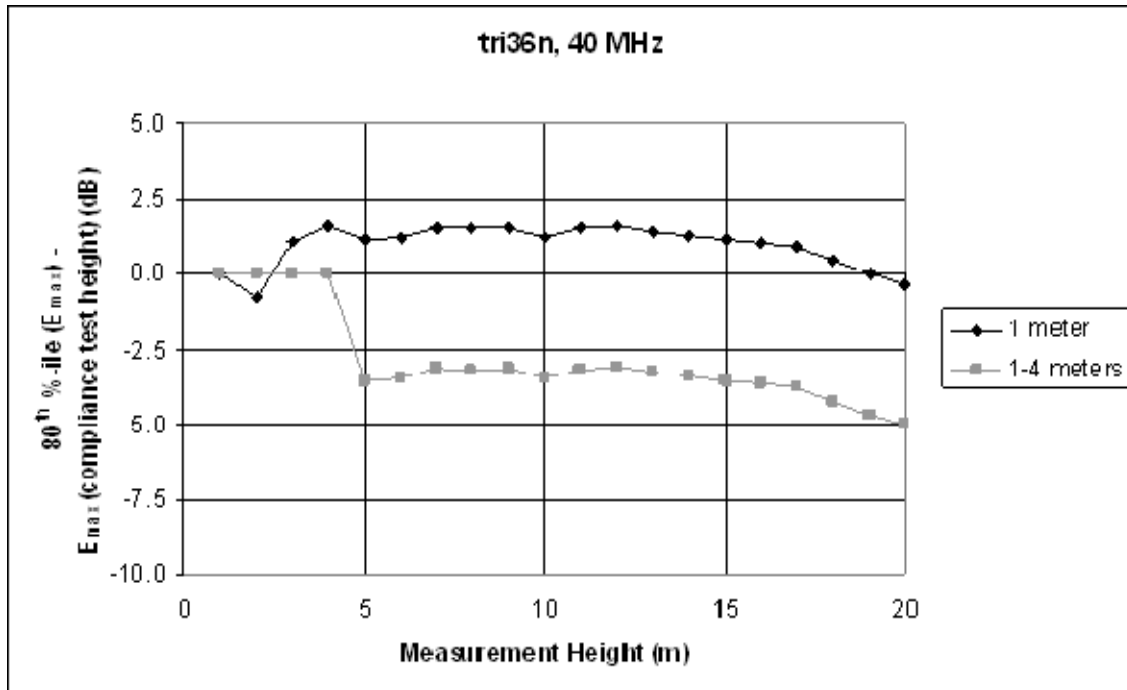
The results for other power line configurations modeled by NTIA are provided in Appendix A.



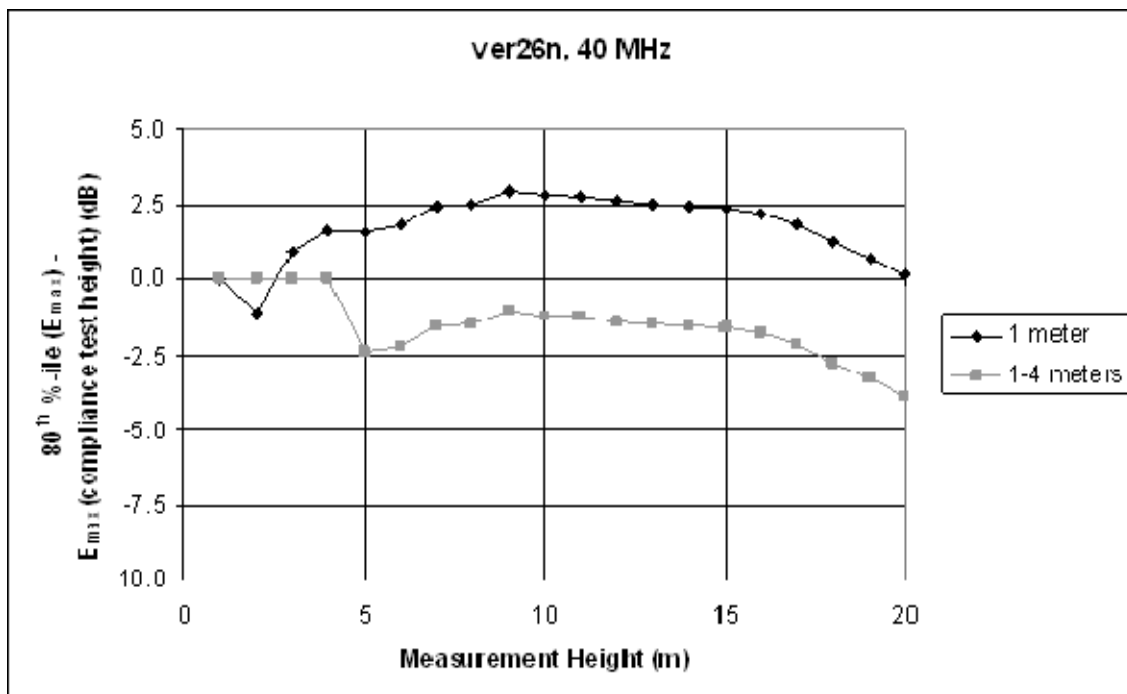
2-18: Comparison of electric field strength as a function of measurement height, if compliance measurements were performed at heights of 1 meter, or at 1 to 4 meters



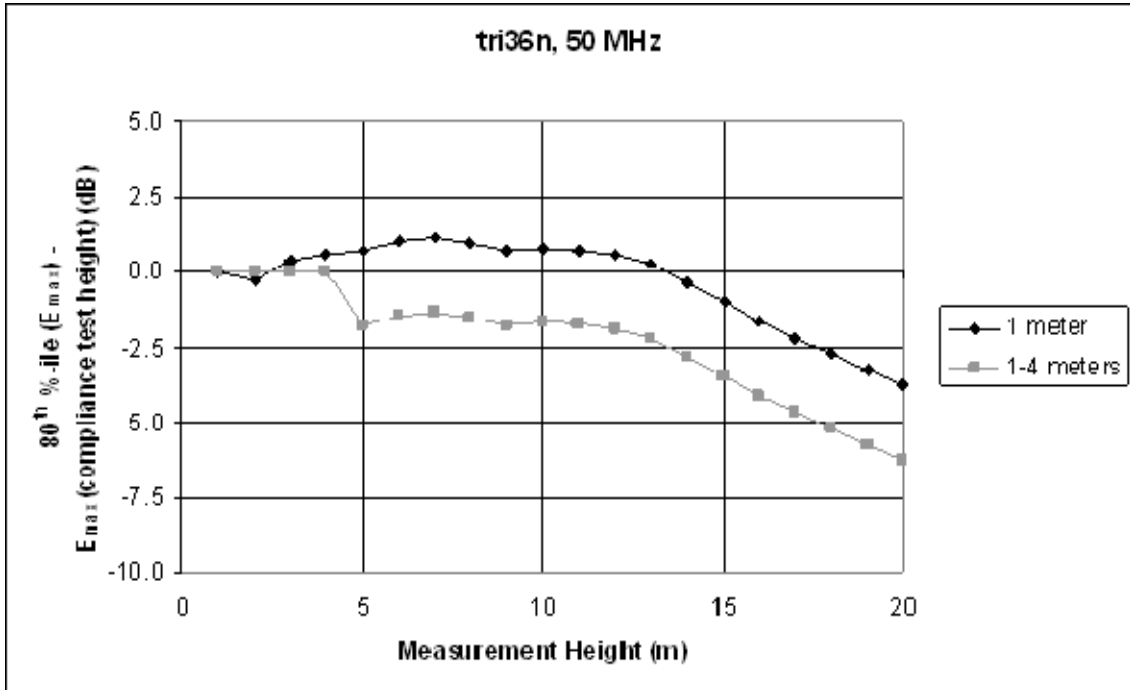
2-19: Comparison of electric field strength as a function of measurement height, if compliance measurements were performed at heights of 1 meter, or at 1 to 4 meters



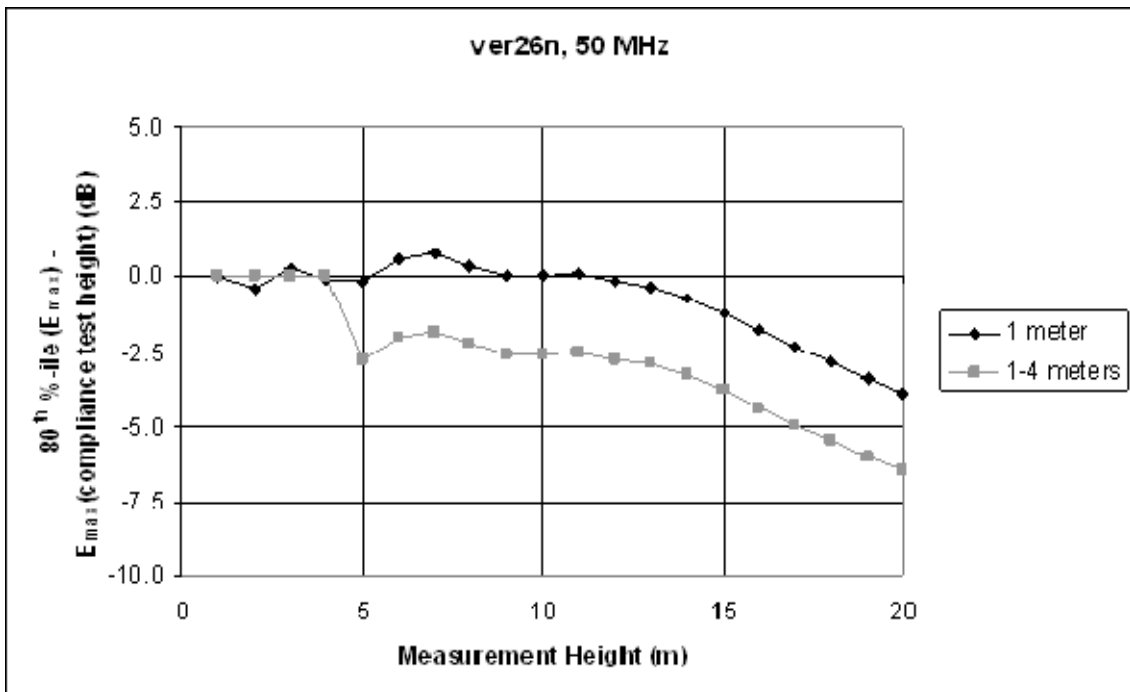
2-20: Comparison of electric field strength as a function of measurement height, if compliance measurements were performed at heights of 1 meter, or at 1 to 4 meters



2-21: Comparison of electric field strength as a function of measurement height, if compliance measurements were performed at heights of 1 meter, or at 1 to 4 meters



2-22: Comparison of electric field strength as a function of measurement height, if compliance measurements were performed at heights of 1 meter, or at 1 to 4 meters



2-23: Comparison of electric field strength as a function of measurement height, if compliance measurements were performed at heights of 1 meter, or at 1 to 4 meters



NTIA's simulation results shown here and in Appendix A indicate that scaling the field strength data to meet the Part 15 limits using a 1 meter antenna height tends to underestimate the peak field strength at any height by anywhere from 2.5 to 7.5 dB. The optional use of a 1 meter measurement height, with the corresponding 5 dB height correction factor, would result in limiting peak field strength to levels that would likely be seen if the measurements were performed at the specified 1 to 4 meter height above 30 MHz.

## **2.4 MEASUREMENT DISTANCE ALONG THE POWER LINE**

As noted in NTIA's Phase 1 Study, compliance measurement testing commissioned by BPL equipment vendors and service providers has generally focused on radiated emissions measured on radials from the BPL device under test. However, FCC rules state that Part 15 devices and all attached wiring should be considered when measuring radiated emissions.<sup>[14]</sup> In the Commission's BPL Report and Order, the measurement guidelines specify the measurement locations along the power line away from a BPL device.<sup>[15]</sup> In this section, NTIA provides its simulation results from evaluating the field strength along the length of the power line and comparing this to the field strength levels at the prescribed measurement locations.

NTIA evaluated the field strength along the length of the power line in 1 meter increments for six simulated power line configurations described in Section 2.2. These calculations were performed over the frequency range of 2 to 28 MHz. Figures 2-24 through 2-31 show the electric field strength levels along the power line for a subset of the cases considered. Each figure includes an electric field strength level that corresponds to the Part 15 radiated emissions limit, when extrapolated from a horizontal distance of 30 meters to the horizontal measurement distance of 10 meters, and assuming a power line height of 12 meters.<sup>[16]</sup> In addition, these figures show the Part 15 compliance measurement points specified in the measurement guidelines for overhead Access BPL systems. The peak value of electric field strength at these measurement points was used to scale the simulated signal source level so that the power line model satisfies the Part 15 limit based on the compliance measurement procedure. The emissions limit is extrapolated to the 10 meter measurement distance using the slant range distance between the simulated power line and the simulated measurement antenna at a height of 1 meter. Electric field strength values were determined from NEC magnetic field strength simulations of the power line models using the methodology described in Section 2.2. Results for other power line configurations are provided in Appendix B.

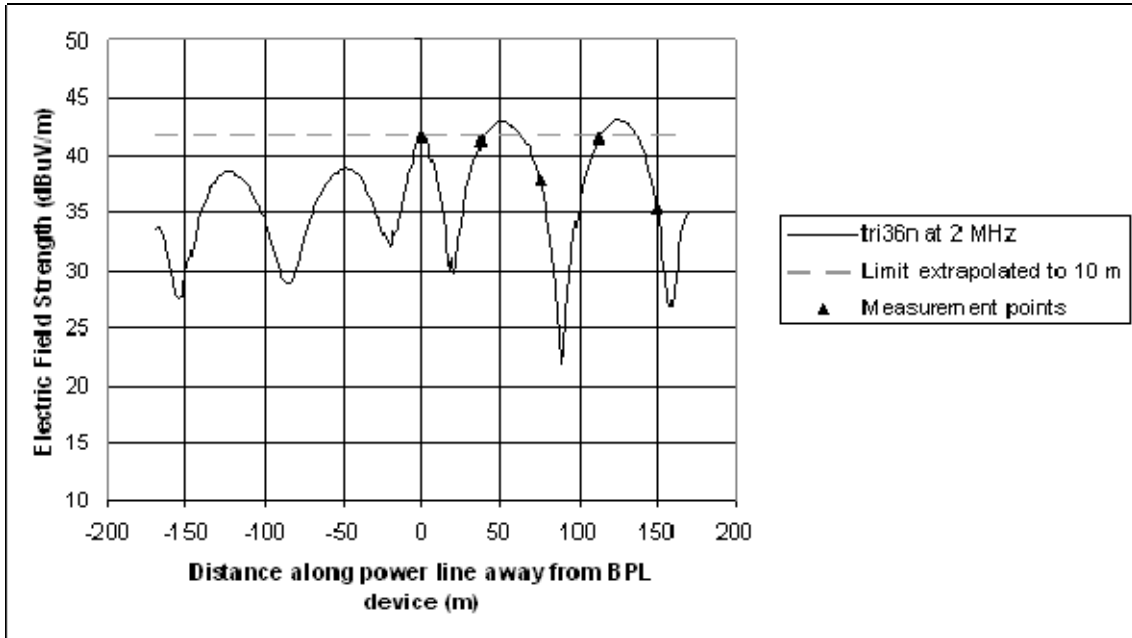


Figure 2-24: Vertical electric field strength along tri36n power line model at 2 MHz

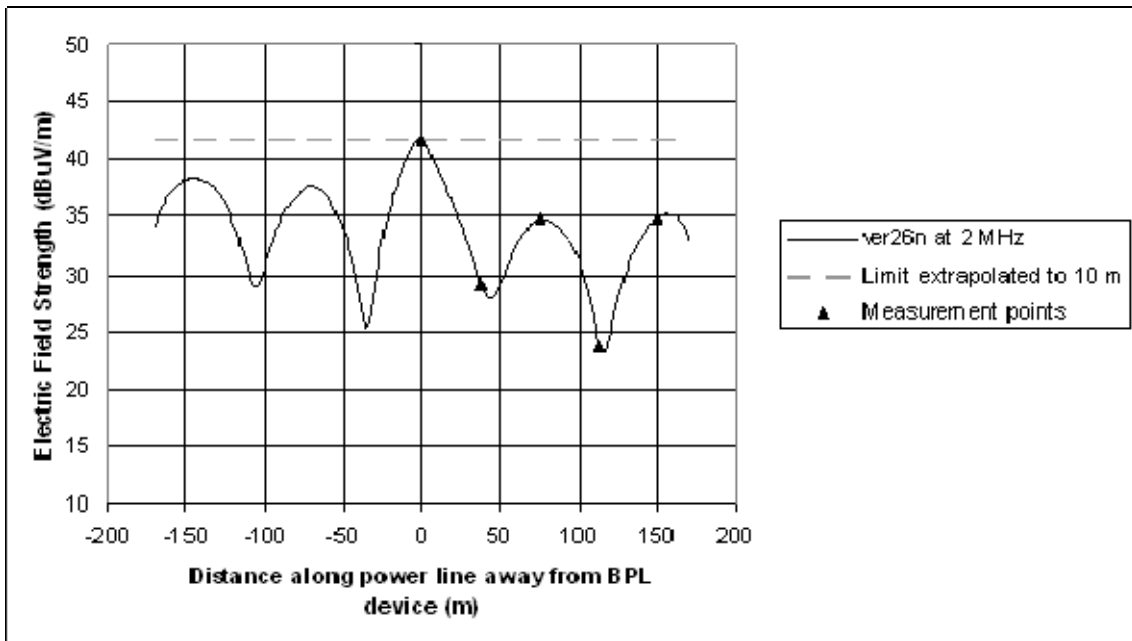


Figure 2-25: Vertical electric field strength along ver26n power line model at 2 MHz

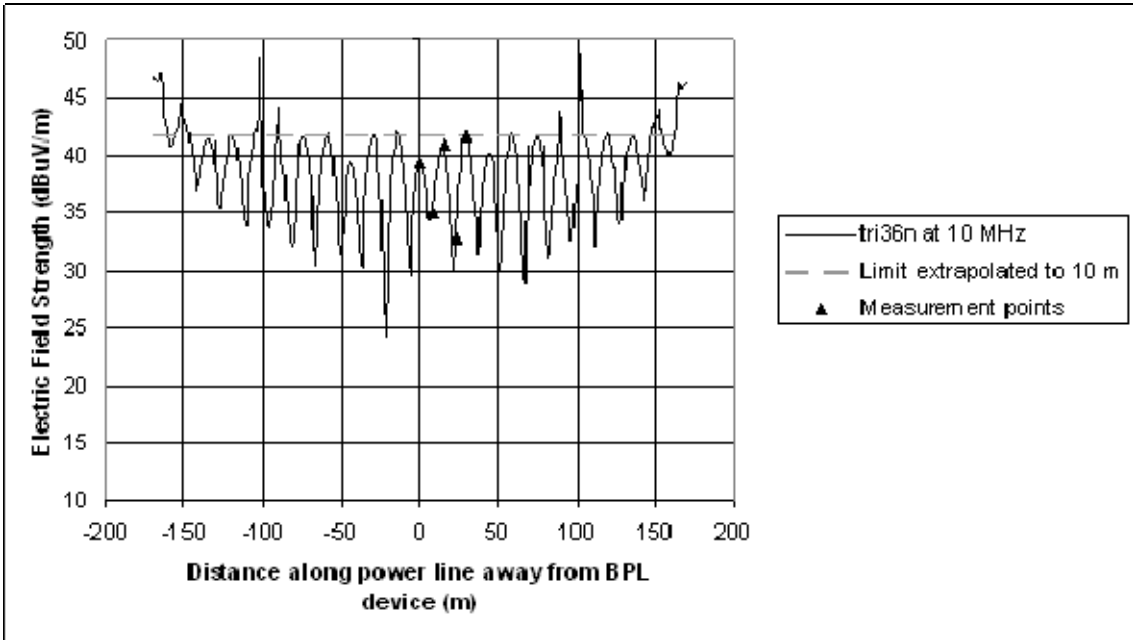


Figure 2-26: Vertical electric field strength along tri36n power line model at 10 MHz

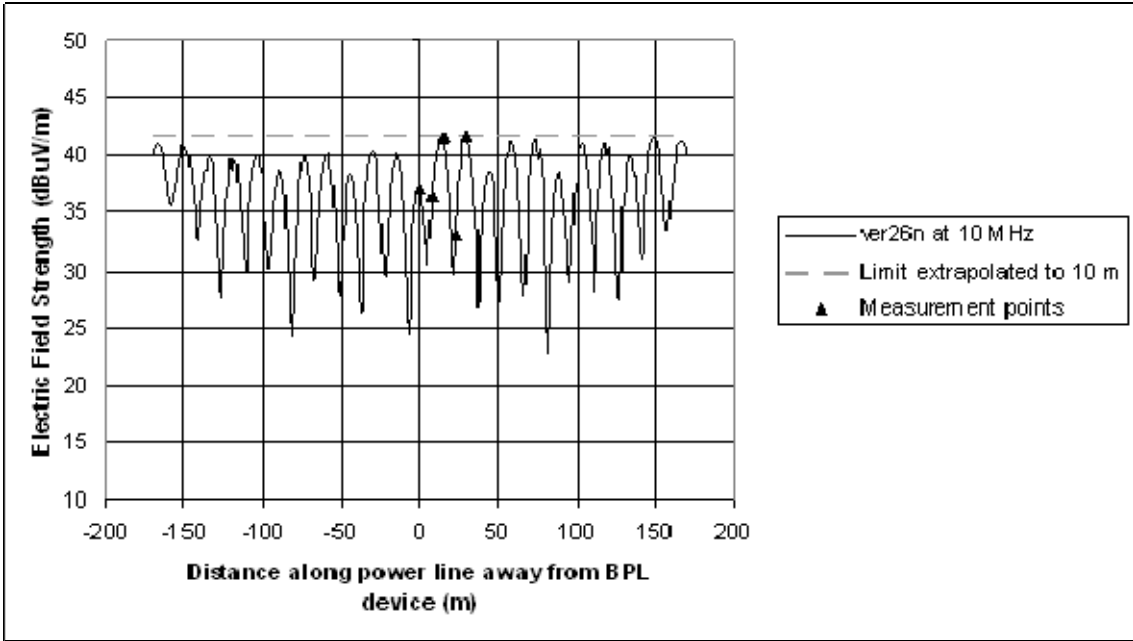


Figure 2-27: Vertical electric field strength along ver26n power line model at 10 MHz

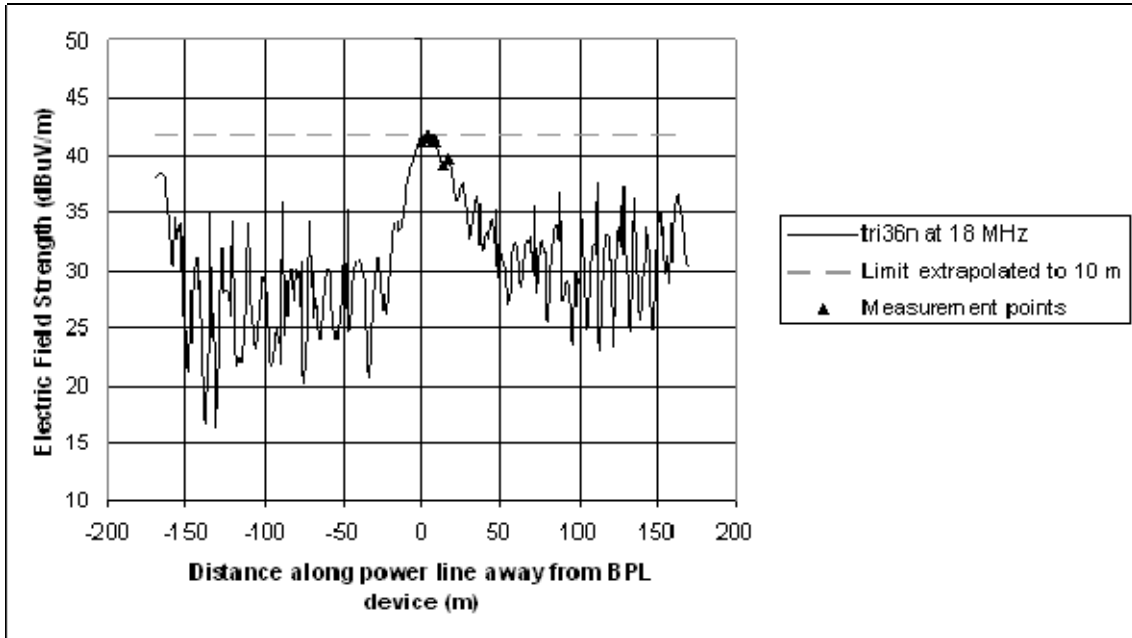


Figure 2-28: Vertical electric field strength along tri36n power line model at 18 MHz

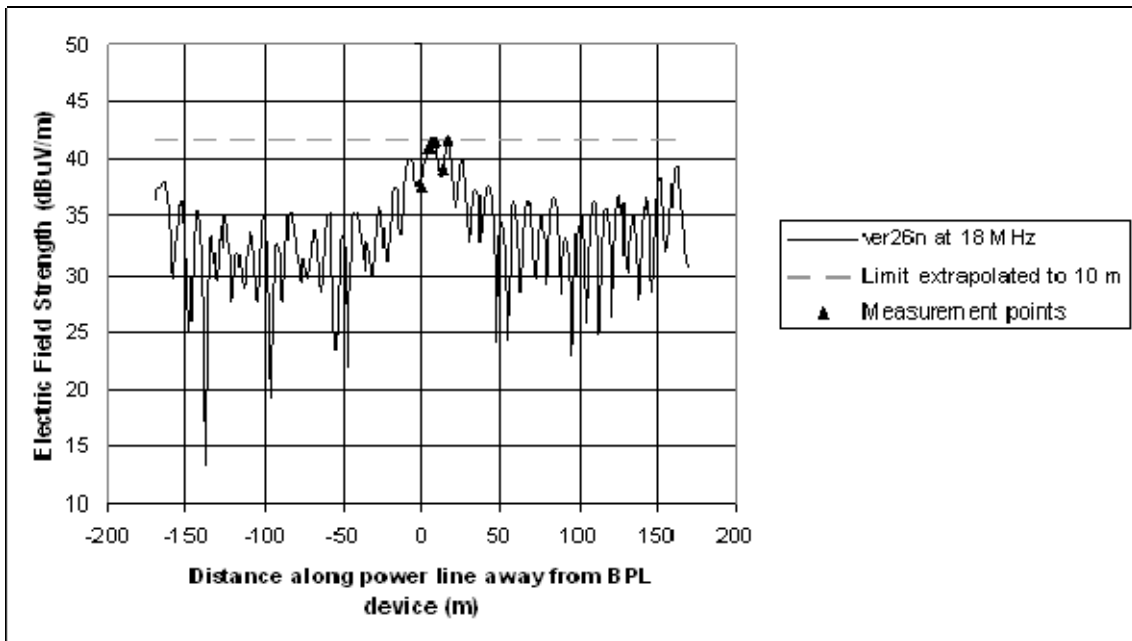


Figure 2-29: Vertical electric field strength along ver26n power line model at 18 MHz

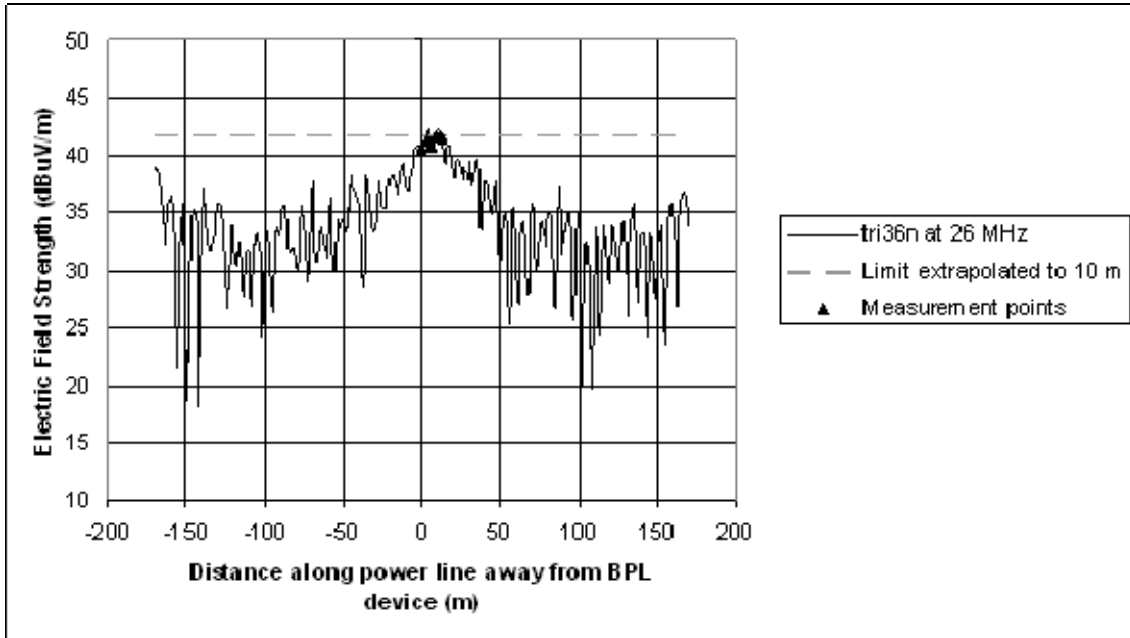


Figure 2-30: Vertical electric field strength along tri36n power line model at 26 MHz

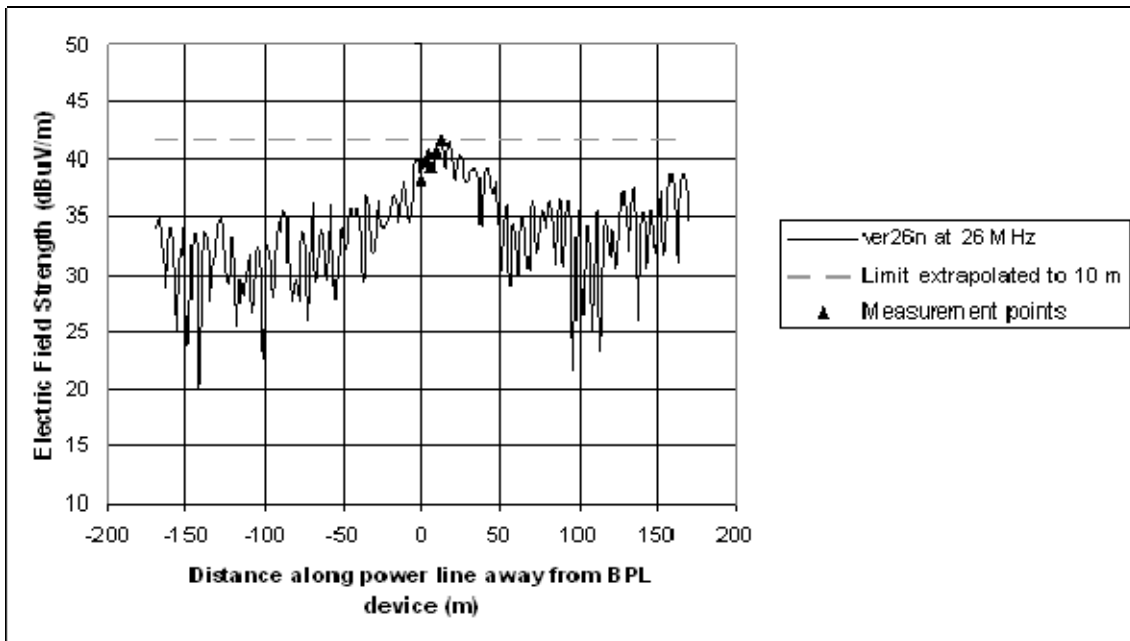


Figure 2-31: Vertical electric field strength along ver26n power line model at 26 MHz

The figures presented here, and those presented in Appendix B, reveal that there are some cases where the peak field strength may be underestimated by up to 5 dB. These cases generally occur at frequencies at or below 10 MHz. Where the results show occurrences of stronger field strength levels than the peak field strength levels seen at the Part 15 measurement locations specified for Access BPL systems, these occurrences are

spatially limited along the length of the power line. Based on the power line simulations considered in this analysis, the emissions from Access BPL devices can be characterized for demonstrating compliance with the Part 15 limits using a limited number of measurement points, as specified in the Commission's measurement guidelines.

## 2.5 MEASUREMENT DISTANCE EXTRAPOLATION

The distance extrapolation rules for Part 15 devices define a 40 dB per decade of distance roll-off factor from the equipment under test (EUT) for frequencies below 30 MHz, and a 20 dB per decade distance extrapolation factor above 30 MHz.<sup>[17]</sup> Distance from the EUT is described as the horizontal distance projected on the ground. NTIA's measurements of Access BPL systems, documented in its Phase 1 Study, shows that the roll-off of radiated emissions with increasing distance from the overhead MV power lines occurs at a slower rate than the distance extrapolation factors specified above.<sup>[18]</sup>

In the BPL Report and Order, the Commission modified the measurement guidelines as they apply to distance extrapolation for Access BPL systems on overhead MV power lines by replacing the horizontal distance between the Access BPL power lines and the measurement antenna with the slant range distance between them.<sup>[19]</sup> Prior to adoption of the measurement guidelines, NTIA analyzed the use of slant range distance to compare the Part 15 limits, extrapolated to other measurement distances, with the expected field strength decay of a variety of modeled power line structures. NTIA found that this modification to the rules for distance extrapolation resulted in good agreement between the extrapolated field strength limit and the rate in which field strength decays from the overhead MV power line.<sup>[20]</sup>

### 2.5.1 New Approach for Distance Extrapolation

When it is necessary to make field strength measurements for overhead Access BPL systems at distances other than the specified Part 15 measurement distance, the field strength measurements are extrapolated to the Part 15 measurement distance as described in Equations 2-2 and 2-3 below. Figure 2-32 illustrates the concept of distance extrapolation using the slant path distance between the antenna and the BPL power line.

$$d_{slant} = \sqrt{(h_{pwr\_line} - h_{ant})^2 + (d_h)^2} \quad \text{(Equation 2-2)}$$

where:

- $d_{slant}$  is the slant path distance, in meters;
- $d_h$  is the horizontal distance, in meters;
- $h_{pwr\_line}$  is the height of the power line wiring carrying BPL signals, in meters; and
- $h_{ant}$  is the measurement antenna height, in meters.

$$E_{extrap} = E_{meas} - N \cdot \text{Log}_{10} \left( \frac{d_{limit}}{d_{slant}} \right) \quad \text{(Equation 2-3)}$$

where:

$N$  is distance extrapolation factor: 40 for frequencies < 30 MHz, or 20 for frequencies  $\geq$  30 MHz;

$d_{limit}$  is the horizontal measurement distance corresponding to the Part 15 emissions limits: 30 meters, for frequencies < 30 MHz, or 10 meters, for frequencies  $\geq$  30 MHz;

$d_{slant}$  is the slant path distance, in meters;

$E_{meas}$  is the measured electric field strength at a horizontal distance,  $d_h$ , in dBV/m; and

$E_{extrap}$  is the electric field strength value after applying the distance extrapolation factor, in dBV/m.

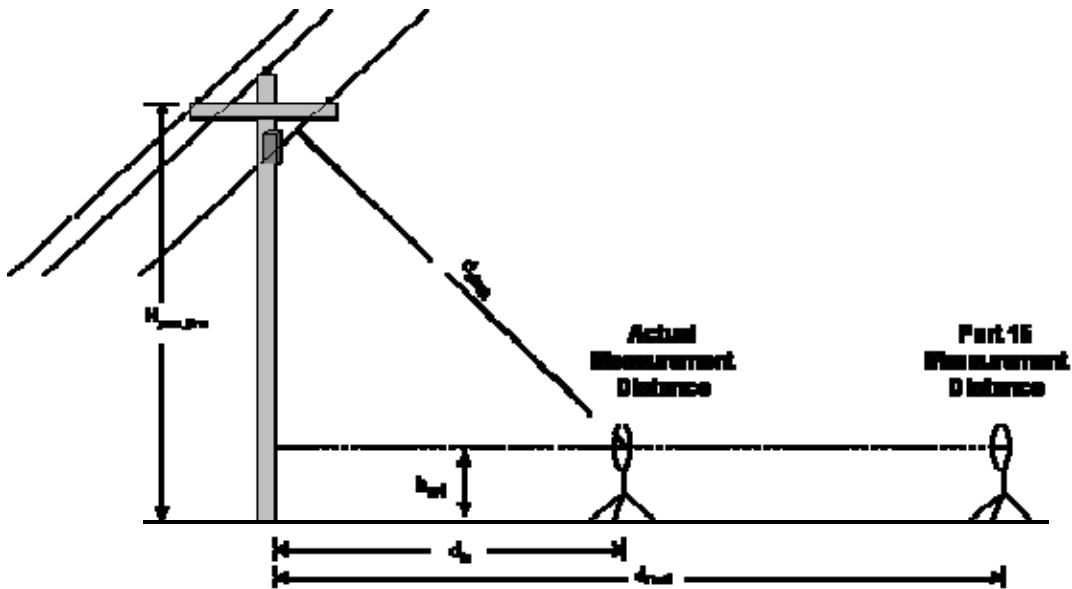


Figure 2-32: Slant path distance used for distance extrapolation of measurement limits

Table 2-2 shows the emissions levels at a measurement distance of 10 meters that satisfy the Part 15 limits for the distance extrapolation methodology based on horizontal distance and the slant-range methodology adopted in the BPL Report and Order. Figures 2-33 and 2-34 illustrate the electric field strength levels relative to the measurement distance for both distance extrapolation techniques.<sup>[21]</sup>

Table 2-2: An example of Access BPL emissions levels that meet Part 15 limits when extrapolated to a 10 meter measurement distance using horizontal and slant range extrapolation

Measurement Location
----------------------

Assumed power line height	12 meters	
Measurement height	1 meters	
Measurement distance	10 meters	
<b>Part 15 Limit &amp; Distance Extrapolation</b>		
< 30 MHz limit	29.5 dB $\mu$ V/m	30 meters
$\geq$ 30 MHz limit (Class A)	39.1 dB $\mu$ V/m	10 meters
Extrapolation < 30 MHz	40 dB/decade of distance	
Extrapolation $\geq$ 30 MHz (Class A)	20 dB/decade of distance	
<b>Extrapolated levels @ 10 m under 47 C.F.R. § 15.31(f)(1)-(2)</b>		
< 30 MHz limit	48.58 dB $\mu$ V/m	
$\geq$ 30 MHz limit (Class A)	39.10 dB $\mu$ V/m	
<b>Extrapolated levels @ 10 m using slant-range distance specified for BPL devices</b>		
< 30 MHz limit	41.70 dB $\mu$ V/m	
$\geq$ 30 MHz limit (Class A)	35.66 dB $\mu$ V/m	

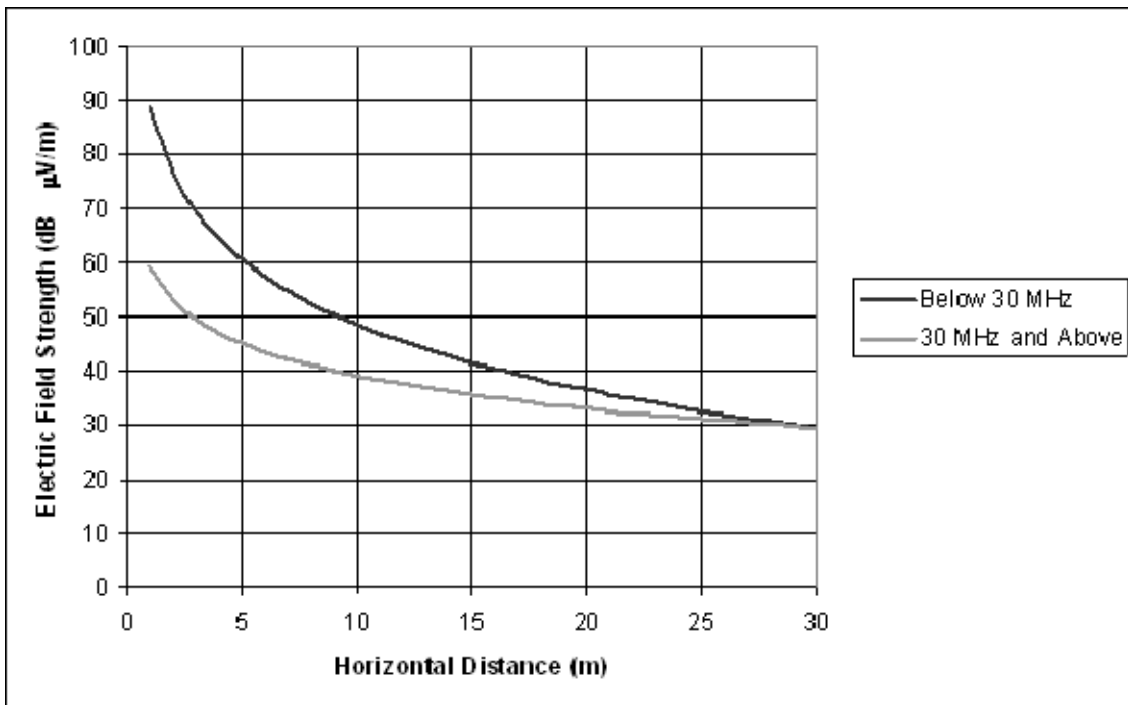
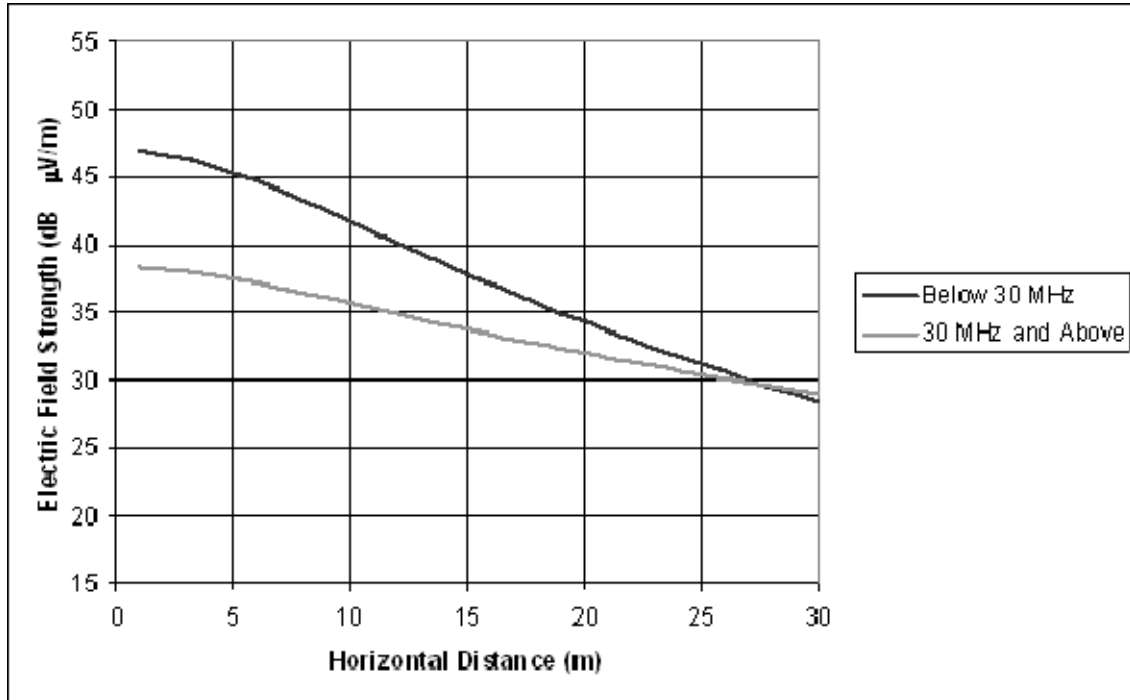


Figure 2-33: Extrapolated field strength levels meeting Part 15 emissions limits based on horizontal distance to a device under test, in accordance with 47 C.F.R. § 15.31(f)(1)-(2)





**Figure 2-34: Extrapolated field strength levels meeting Part 15 emissions limits based on slant-range distance to the BPL power line**

### 2.5.2 Calculated Electric Field Strength Decay for Distance Extrapolation

NTIA evaluated the field strength decay relative to the distance characteristics of the various power line models to evaluate the Commission’s slant-range distance extrapolation methodology. The signal source for each power line model was scaled such that the radiated field strength met the Part 15 emission limits extrapolated to the 10 meter measurement distance for the specified measurement points along the length of the power line. Figures 2-35 through 2-39 show the electric field strength of the modeled power lines and the extrapolated field strength levels meeting the Part 15 emissions limit for distances out to 30 meters from the power line for a subset of frequencies modeled below 30 MHz. Additional results are provided in Appendix C.

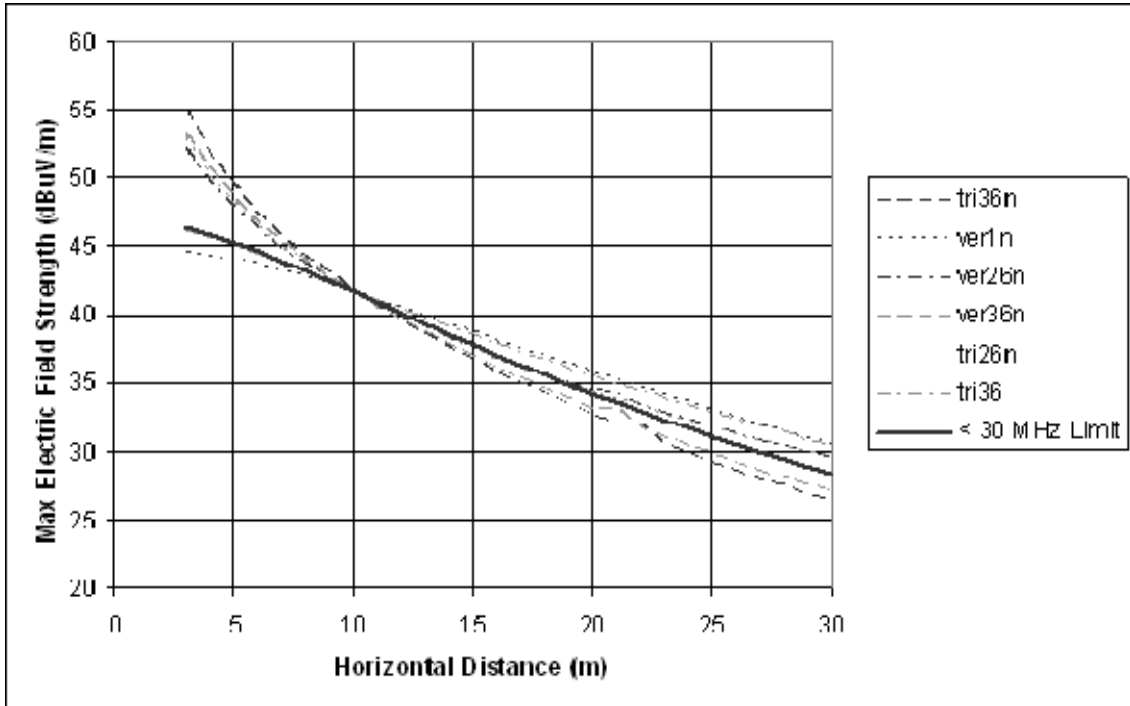


Figure 2-35: Electric field strength compared to emissions limit based on slant-range extrapolation for various power line models – 2 MHz

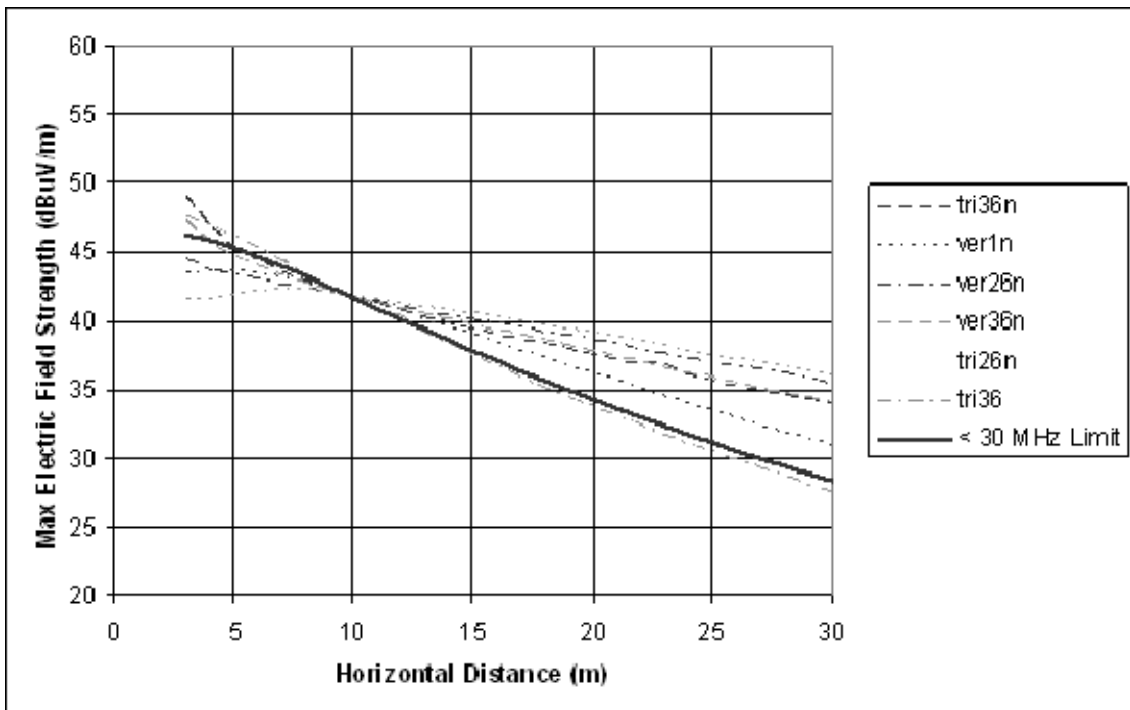


Figure 2-36: Electric field strength compared to emissions limit based on slant-range extrapolation for various power line models – 8 MHz

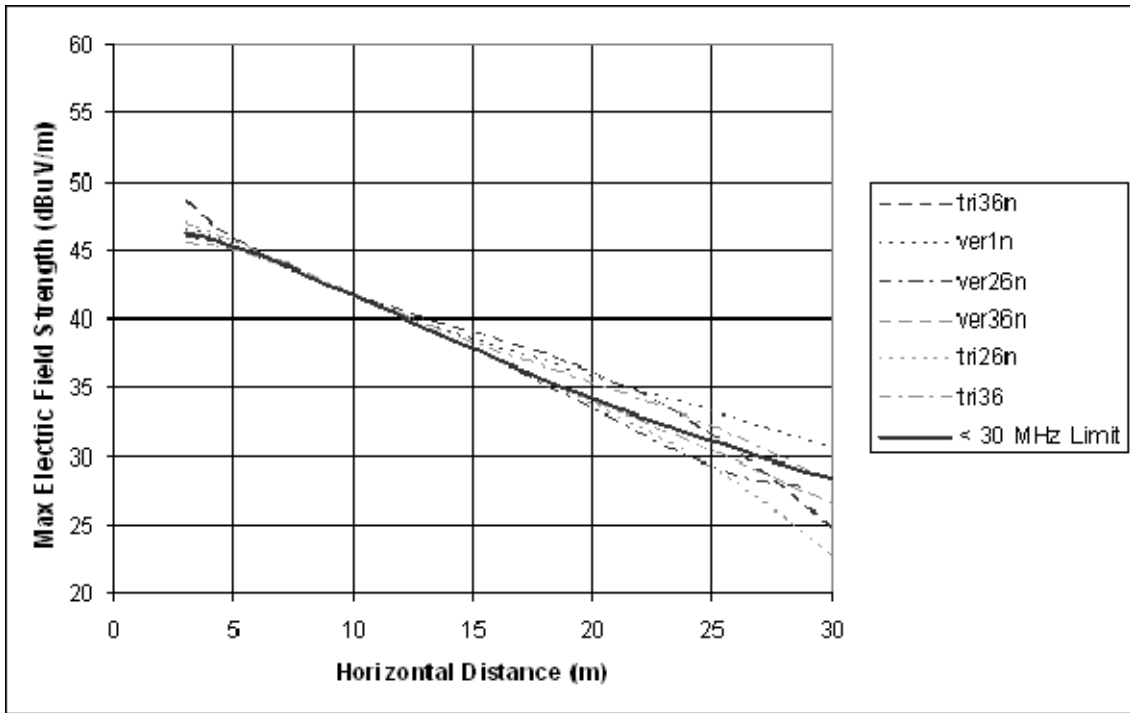


Figure 2-37: Electric field strength compared to emissions limit based on slant-range extrapolation for various power line models – 14 MHz

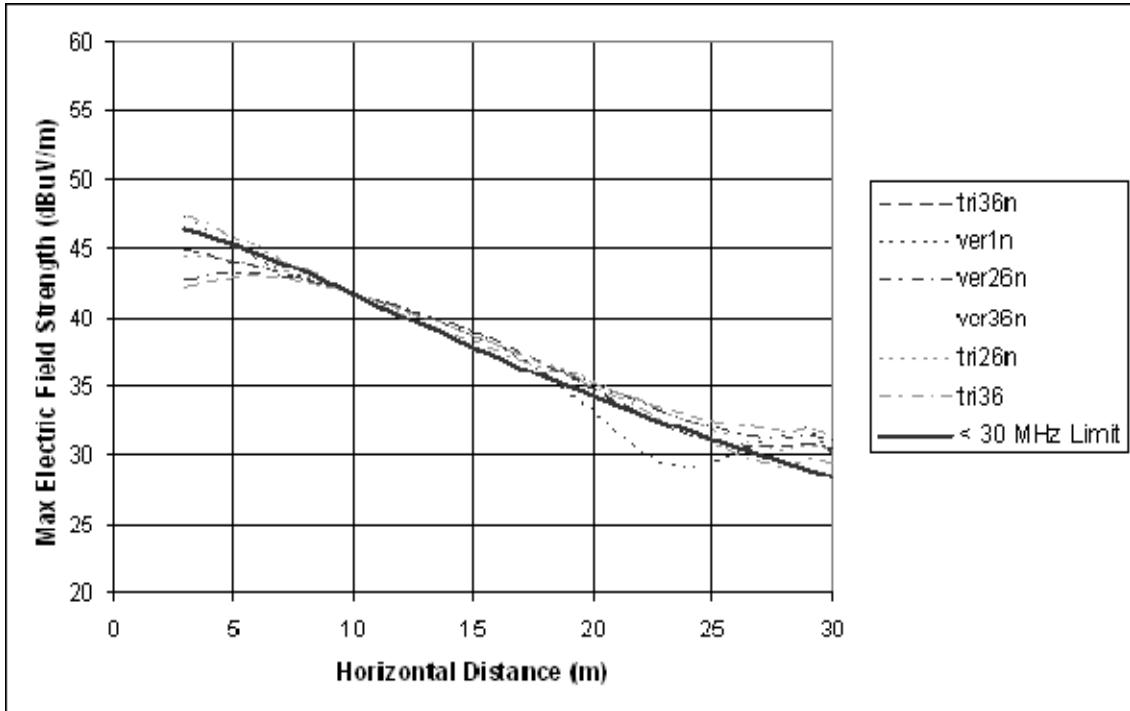


Figure 2-38: Electric field strength compared to emissions limit based on slant-range extrapolation for various power line models – 20 MHz

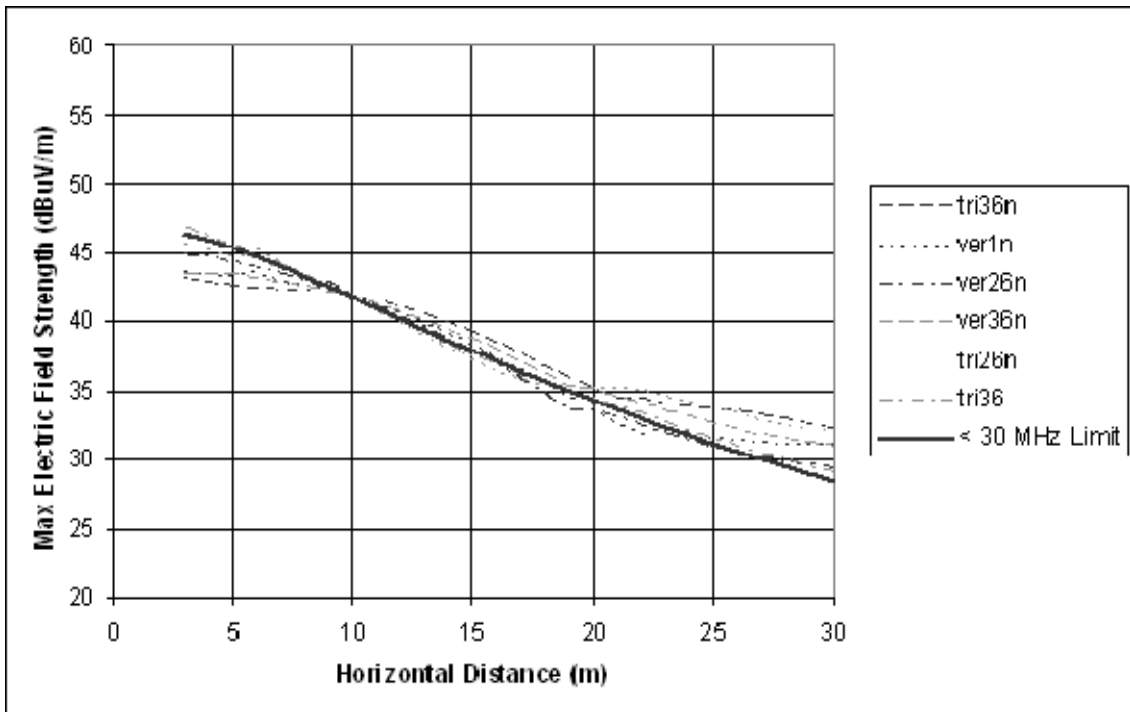


Figure 2-39: Electric field strength compared to emissions limit based on slant-range extrapolation for various power line models – 26 MHz

The simulation results in the 4 to 8 MHz frequency range showed that some of the power line models exhibited slower rates of field strength decay with distance than would be expected by the distance extrapolation rate in the Part 15 rules for Access BPL systems. This difference in the roll-off of field strength is as much as 6 dB less than the distance extrapolation rate.

At or above 10 MHz, the simulation results show good agreement between the rate that field strength decays and the distance extrapolation rate in the Part 15 rules, when slant path distance to the Access BPL device and power lines is used. The effect of the combination of direct and ground reflected rays at the simulated distances becomes more pronounced at frequencies above 14 MHz.

## 2.6 USE OF LOOP ANTENNA BELOW 30 MHz

Below 30 MHz, electric field strength is determined by measurement of the peak magnetic field in the horizontal plane using a loop antenna situated 1 meter above the ground. These measurements, conducted at a measurement distance of 10 meters from the power line, fall well within the near field region for many overhead MV power lines. To assess the validity of making measurements using the loop antenna below 30 MHz, NTIA evaluated the ratio of the peak vertical electric field to the peak magnitude of the horizontal magnetic field given by Equation 2-4 below:

$$\eta = \frac{E_z}{\sqrt{H_x^2 + H_y^2}} \quad \text{(Equation 2-4)}$$

where  $\eta$  is the wave impedance, in  $\Omega$ ;

$E_z$  is the vertically polarized electric field strength in  $\mu\text{V/m}$ ; and

$H_x, H_y$  are the x- and y-components of the horizontally polarized magnetic field strength in  $\mu\text{A/m}$ .

The value of  $\eta$  is nominally  $377 \Omega$  in the far field. The magnetic and electric field strength data were calculated at a distance of 10 meters from the various NEC power line models at a height of 1 meter. The peak vertical electric field was calculated for the entire length of the modeled power lines, in one-meter steps. The magnitude of the horizontal magnetic field was calculated as shown in the denominator of Equation 2-4 and its peak value along the length of the power line was determined. The ratio of these two values ( $\eta$ ) was then computed. Figure 2-40 illustrates the values of  $\eta$  determined for a variety of NEC power line models for the frequency range of 2 to 28 MHz. The calculated values of  $\eta$  tend to vary from approximately 200 to 400  $\Omega$ .

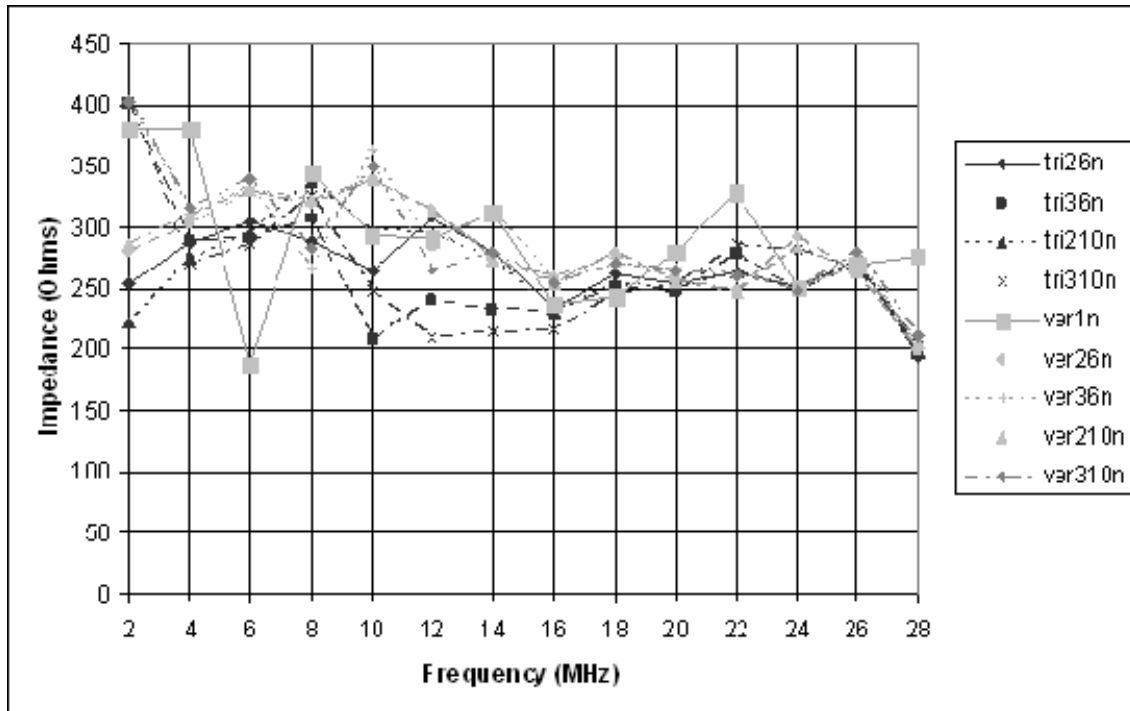


Figure 2-40: Ratio of peak electric to peak magnetic field strength at 10 meters from the power line

## 2.7 MEASUREMENT ANTENNA POLARIZATION

The Commission's measurement guidelines for Access BPL systems specify measurement with a loop antenna below 30 MHz, with the plane of the loop antenna oriented vertically at a height of 1 meter. The loop antenna is to be rotated 180° about its vertical axis to identify the maximum field strength. For frequencies above 30 MHz, the Commission specified measurements in both the vertical and horizontal polarizations using an electric field sensing antenna. The measurements at or above 30 MHz are made at antenna heights of 1 to 4 meters.

A vertically oriented loop antenna measures the horizontal magnetic field. This corresponds to the vertical component of the electric field. By rotating the antenna about its vertical axis, the peak horizontal magnetic field, and thus the peak vertical electric field, can be measured. This is ideally the case in the far field region where the electric and magnetic fields are orthogonal and their values differ by the wave impedance,  $377 \Omega$  (a reasonable assumption in the near field), as shown in Section 2.6.

Although the measurement guidelines specify that field strength measurements should address the horizontal magnetic field (vertical electric field) below 30 MHz, NTIA calculated both the horizontal and vertical polarizations of field strength from a number of NEC power line models. The calculations were performed from 2 to 30 MHz, in 2 MHz increments. The resulting field strength values were used to identify which electric field polarization corresponds to the overall peak at the 10 meter measurement

distance for each power line model. The vertical electric field polarization was consistently the strongest for the frequencies simulated below 30 MHz.

## 2.8 GUIDELINES FOR CHOOSING REPRESENTATIVE SYSTEMS

The Commission's measurement guidelines specify *in-situ* testing of three representative overhead, and three underground, BPL installations that include all Access BPL electronic devices such as couplers, injectors, extractors, repeaters, boosters and concentrators.<sup>[22]</sup> NTIA has shown in its field tests and NEC modeling of BPL power lines that, in addition to the BPL devices themselves, certain typical features of a MV power line give rise to the strongest levels of radiated emissions. These features include distribution transformers, risers connecting overhead and underground distribution circuits, distribution line endpoints and sharp direction changes.<sup>[23]</sup>

Other features to consider when picking representative sites for *in-situ* testing include power lines with asymmetrical features, stacked 3-phase conductors, transitions between three phases and one or two phases, and, where appropriate for the BPL equipment involved, multiple co-located BPL devices. Figures 2-41 through 2-45 provide examples of these characteristics.



Figure 2-41: Offset 3-phase power line conductors



**Figure 2-42: Offset 2-phase power line conductors**



**Figure 2-43: Stacked 3-phase power line conductors**





**Figure 2-44: Transition from 3-phase to 2-phase conductors**



**Figure 2-45: Multiple BPL devices located on the same utility pole**

## 2.9 SUMMARY

The FCC's BPL Report and Order specified the rules and measurement guidelines for Access BPL systems. These rules and measurement guidelines were applied in the analyses described in this section.

The results from NEC simulations of a number of power line structures indicate that the peak field strength seen in close proximity to a BPL energized overhead power line will occur at various heights, and often near the height of the power line. NTIA further analyzed the peak field strength at the specified measurement heights and found that use of the Commission's measurement guidelines effectively estimated the 80<sup>th</sup> percentile values of peak field strength at any height. As noted earlier, the 80<sup>th</sup> percentile values eliminate the localized peaks that are unlikely to be encountered by a radio receiver randomly located in close proximity to an Access BPL power line.

The Commission's measurement guidelines allow field strength measurements on overhead Access BPL power lines operating in the Very High Frequency (VHF) band to optionally be performed at a 1 meter height combined with application of a 5 dB height correction factor. This simplification of the measurement procedure substantially reduces the number of measurements to be performed. Results from NTIA's NEC simulations show that measurements at a 1 meter height tend to underestimate by anywhere from 2.5 to 7.5 dB the peak field strength that would be seen using a measurement height in the 1 to 4 meter range. The use of a 5 dB height correction factor improves the field strength estimate at the 1 meter measurement height to a reasonable level while greatly reducing the number of measurements taken.

The BPL Report and Order specifies measurement at a limited number of locations along the power line. When the electric field strength was scaled to be within the Part 15 limits using the Access BPL measurement guidelines, NTIA's NEC simulation results indicated that the percent of measurement points where the field strength exceeded the Part 15 limits was small.

NTIA evaluated the Commission's modification of the distance extrapolation rules, which replaced the use of the horizontal distance between the BPL device and the measurement antenna with the slant range distance between them. NTIA's NEC simulations in the 4 to 8 MHz frequency range exhibited somewhat slower rates of field strength decay with distance than would be expected by the distance extrapolation rate in the Part 15 rules for Access BPL systems. This difference was up to 6 dB less than the distance extrapolation rate. At or above 10 MHz, the simulation results show good agreement between the rate that field strength decays and the Part 15 distance extrapolation rate using the slant range distance to the Access BPL device and power lines. As noted earlier, the effect of the combination of ground and reflected rays at the simulated distances becomes more pronounced at frequencies above 14 MHz.

The use of slant range distance with the extrapolation rates (40 dB per decade of slant range distance below 30 MHz, and 20 dB per decade of slant range distance at or above 30 MHz) defined in the rules most accurately estimates electric field strength when

extrapolation is performed in close proximity to the BPL device and associated power lines. At great distances, the accuracy of this approach diminishes. At larger distances between the BPL device and measurement antenna, the slant range distance and the horizontal distance are approximately the same, and the extrapolation rate effectively becomes the same as if the horizontal distance was used. The Commission's rules state that measurements shall not be performed at distances greater than the specified measurement distance, or less, unless it is impractical to do so.<sup>[24]</sup>

Below 30 MHz, the electric field strength is determined by measuring the peak magnetic field strength in the horizontal plane using a loop antenna situated 1 meter above the ground, and applying a magnetic to electric field conversion factor of  $377 \Omega$ . These measurements, conducted at a distance of 10 meters from the BPL device and associated power lines, fall well within the near field region for many overhead MV power lines. NTIA evaluated the relationship between the magnetic and electric fields at 10 meters using a number of NEC power line models and determined that use of the loop antenna with this conversion factor provides a reasonable approximation at this distance. NTIA simulations investigating the field strength of both the vertical and horizontal polarizations showed that below 30 MHz, the vertical electric field (horizontal magnetic field) corresponds to the peak field strength when measured at 10 meters from the power line. This is consistent with the polarization specified by the Commission's measurement guidelines for Access BPL systems.

In Section 2.8, NTIA provided recommendations for choosing representative overhead MV Access BPL locations for *in-situ* testing. NTIA field tests and NEC modeling of BPL power lines identified that, in addition to the BPL devices themselves, many features of MV power lines give rise to the strongest levels of radiated emissions. NTIA suggests that a variety of these features should exist in power lines chosen as representative sites for compliance measurement testing.



## **SECTION 3**

### **SPECIAL PROVISIONS FOR PREVENTION OF INTERFERENCE FROM BPL SYSTEMS**

#### **3.1 INTRODUCTION**

NTIA's Phase 1 Study identified frequency bands in the 1.7 to 80 MHz frequency range for which radio operations have been specially protected in the FCC's rules or International Telecommunication Union (ITU) Radio Regulations.<sup>[25]</sup> NTIA's comments on the BPL NPRM recommended that the FCC adopt special mechanisms for preventing interference in addition to the baseline protection afforded by field strength limits, prohibition of harmful interference from BPL systems, and compliance measurement provisions.<sup>[26]</sup> The Commission adopted rules in its BPL Report and Order that delineated frequencies and areas in which these special provisions would apply.<sup>[27]</sup>

Aeronautical and maritime safety radiocommunications receivers, as well as radar and radioastronomy receivers operating at frequencies below 80 MHz may experience harmful interference from in-band emissions from relatively distant Access BPL systems. The Commission's BPL rules reduce the probability of BPL interference to such receivers by defining excluded frequency bands, exclusion zones, and consultation areas around the most sensitive federal radiocommunications facilities.<sup>[28]</sup> Within these areas, BPL systems are either prohibited outright or may be restricted from transmitting in specific frequency bands by mutual agreement between BPL service providers and federal radio operators. NTIA analyzed BPL emissions in these bands and confirmed the effectiveness of the protection radii adopted in these rules.

Excluded frequency bands (discussed in Section 3.4.1) place the greatest constraints on BPL deployment, including limitations on the flexibility for Access BPL systems to avoid other locally-used radio frequencies. Thus, frequency bands used for safety communications where co-channel emissions from numerous BPL devices may be received via line-of-sight and/or ionospheric interfering signal paths make up the excluded bands.

Exclusion zones (discussed in Section 3.4.2) are applied to protect reception at known receiver locations where safety communications must operate with weak desired signals and cooperation between BPL service providers and federal radio operators is unlikely to result in lesser constraints on BPL. Likewise, exclusion zones are applied around sensitive radio astronomy sites, which generally are located in remote, lightly populated areas (*i.e.*, little or no actual constraint on Access BPL market penetration).

Consultation areas (discussed in Section 3.4.3) are specified for receivers at known locations that must operate with very weak desired signals and where harmful interference must be prevented with a relatively high degree of certainty (rather than eliminated after discovery). Actual radio operating frequencies and other technical or

operational details (*e.g.*, manufacturer and type of BPL equipment, location of BPL service) should be considered during consultations.

Sections 3.4 and 3.5 provide the technical basis for these exclusion zone and consultation area distances. The underlying interference predictions demonstrate that Access BPL systems located beyond these distances would:

- be unlikely to cause substantial interference to receivers that are intended to be protected by these provisions, even given worst-case-oriented BPL deployment configurations; and
- present a very low probability of endangerment or actual harmful interference to safety communications and non-safety communications, respectively.

### **3.1.1 Background**

NTIA analyzed the BPL emissions levels that might be expected from MV overhead and underground power lines to determine the minimum radii of exclusion zones and consultation areas needed to meet the protection criteria for critical federal communication, radar and radioastronomy receivers. MV overhead lines are attached to utility poles at heights that typically range from 8 – 12 meters above ground. BPL signals are typically injected on one or more of the phase conductors at a utility pole. Underground power lines radiate the strongest emissions from above-ground segments, including mainly: pad mounted transformer enclosures; vertical risers where the power line emerges from underground and is routed up the side of a pole inside a metal, protective U-channel for connection with overhead power lines; and short line segments emerging from the ground and running through metal pipes for connections to the users' premises (low-voltage) or power substation (MV). The BPL signal typically is injected on the underground segment at one of the transformer pads.

NTIA's initial analyses of these distances employed a 5 dB height correction factor to account for stronger predicted levels of BPL emissions from the power line at heights other than that used for compliance measurements. In its Phase 1 Study and in the Technical Appendix to its Comments on the BPL NPRM, NTIA showed that the peak field strength typically occurs at heights greater than the 1 meter measurement height used for compliance testing, and is often found at or near the height of the power line. <sup>[29]</sup>

In the BPL Report and Order, the Commission adopted NTIA's recommended height correction factor, which may be optionally applied above 30 MHz when coupled with an antenna measurement height of 1 meter. The Commission indicated that BPL emissions above 30 MHz may be measured with an antenna height ranging from 1 to 4 meters. NTIA's revised analysis no longer assumes the 5 dB correction (reduction of BPL emissions) factor in calculating the size of these protection areas.

NTIA's earlier analysis also assumed that the receiver antenna gain for fixed/or mobile-base stations was 0 dBi in the direction of the power line carrying BPL signals.

This assumption was felt to be valid for many high-gain antennas operating in the near field of a BPL power line. However, NTIA conducted NEC simulations with a representative high-gain antenna (14 dBi maximum) to validate this assumption and found that the receiver antenna gain in the direction of the BPL power line may be as much as 5 dBi, depending on frequency. In response to these results, NTIA has revised its analysis to account for receiver antenna gain toward the power line.

Theory and limited NTIA measurements show that Access BPL using underground power lines poses very small, relatively localized interference risks, radiating potentially significant emissions only from above-ground segments. Each phase wire of MV underground power lines has a ground wire that is loosely, coaxially braided or wound around the insulation of the phase conductor. This ground wire suppresses radiation. Also, soil is a high-loss propagation medium in the 1.7-80 MHz frequency range. Above-ground segments of underground power line systems act as point radiators similar to other Part 15 devices.

The calculations to determine the exclusion zones and consultation radii consider only the effect of local co-frequency BPL devices on radio receivers over line-of-sight and diffracted interfering signal paths. Ionospheric propagation of distant BPL signals and ionospheric backscatter from local BPL devices are not considered in this section of the report.

## **3.2 POTENTIAL VICTIM RECEIVERS**

The NTIA Phase 1 Study included a characterization of Federal Government spectrum usage in the 1.7 to 80 MHz band, representative systems, and typical system parameters.<sup>[30]</sup> A number of these radiocommunication systems are considered particularly sensitive as they pertain to aeronautical and maritime safety-of-life services. Other federal systems that warrant protection include over-the-horizon radars and radioastronomy observatories. These potential victims of in-band emissions from Access BPL systems are described in the following sections.

### **3.2.1 Communications Receivers**

The United States Coast Guard operates high frequency (HF) systems for communications between shore stations and ships, and from ship-to-ship. These systems support command and control communications with cutters, aircraft, and shore facilities for various purposes including: off shore search and rescue; drug interdiction; enforcement of laws and treaties; and Arctic and Antarctic operations. The Coast Guard relies on the HF band for services such as distress and safety communications, broadcast of maritime safety information, emergency medical assistance communications, broadcast of weather observation reports, and receipt of vessel position reports for safety purposes. In addition, the Coast Guard has an HF network that ties its major bases together throughout the continental United States (CONUS), Alaska, Hawaii, Puerto

Rico, the U.S. Virgin Islands, and the trust territories of the Pacific Ocean. The typical technical characteristics for these maritime mobile base stations are described in Table 3-1.

**Table 3-1: Typical technical characteristics of Maritime Mobile base stations in the 1.7-30 MHz Band**

Bandwidth (kHz)	Ant. Gain (dBi)	Ant. Height (Ft)	Ant. Type/ Polarization	Modulations
2.8	0-2	Not available	Whip, Cone/V	Single sideband-suppressed carrier, single channel, analog, telephony

The United States Customs and Border Protection Customs Over the Horizon Enforcement Network (COTHEN) provides communications support for more than 235 aircraft, numerous maritime interdiction vessels, several command offices, and numerous allied agencies including the United States Coast Guard, Drug Enforcement Administration, Border Patrol, Army, Navy, and Joint Interagency Task Forces. The typical technical characteristics for the COTHEN fixed base stations are described in Table 3-2.

**Table 3-2: Typical technical characteristics of COTHEN base stations in the 1.7-80 MHz Band**

Bandwidth (kHz)	Ant. Gain (dBi)	Ant. Height (Ft)	Ant. Type/ Polarization	Modulations
2.8	0	30-100	Whip/V& H	Analog, single channel, suppressed carrier, telephony

The aeronautical mobile service is subdivided into two distinct radio services; namely, aeronautical mobile route (R) and aeronautical mobile off-route (OR) services. By definition, the aeronautical mobile (R) service is reserved for communications relating to safety and regularity of flight, primarily along national or international civil air routes; while the aeronautical mobile (OR) service is intended for other communications, including those relating to flight coordination, primarily outside national or international civil air routes. <sup>[31]</sup>

Table 3-3 shows typical technical characteristics of federal systems in the aeronautical mobile (R) service. Table 3-4 shows typical technical characteristics of federal aeronautical mobile (OR) service systems in the HF band.

**Table 3-3: Typical technical characteristics of Aeronautical Mobile (R) base stations (1.7-30 MHz Band)**

Bandwidth (kHz)	Ant. Gain (dBi)	Ant. Height (Ft)	Ant. Type/ Polarization	Modulations
2.8	0-3	Not available	Various /V	Analog, single channel, suppressed carrier, telephony

**Table 3-4: Typical technical characteristics of Aeronautical Mobile (OR) base stations (1.7-30 MHz Band)**

Bandwidth (kHz)	Ant. Gain (dBi)	Ant. Height (Ft)	Ant. Type/ Polarization	Modulations
-----------------	-----------------	------------------	-------------------------	-------------



3.5	0	6-32	Whip/V	Analog and digital, single channel, reduced or suppressed carrier, telephony and data
-----	---	------	--------	---

The size of the exclusion zones and consultation areas recommended by NTIA for base stations associated with the land mobile, maritime mobile, aeronautical mobile (R) and (OR) services result from analyzing the distances at which radiated emissions from an Access BPL source raises the noise floor by a certain amount.<sup>[32]</sup> The exclusion zone and consultation area radii were chosen to be the distance beyond which the probability that a communications receiver experiences a 1 dB increase in noise floor is negligible.

### 3.2.2 Radar Receivers

HF band over-the-horizon (OTH) radar systems are employed by the Department of Defense. The OTH radars use sky wave propagation to detect targets at long ranges from the radar transmitter site. The target return is a result of the backscatter signal traversing the path to the ionosphere and back to the original transmitter site (primary radar) or an alternative site (secondary site). OTH-HF radars are capable of detecting targets at distances beyond the horizon and therefore, targets located well beyond the range of the conventional microwave radar. This increased range is possible due to the ability of the HF signals to propagate well beyond the line-of-sight either by ground wave diffraction around the curvature of the Earth or by sky wave. The basic technical characteristics of the OTH radar receiver are shown in Table 3-5.

**Table 3-5: Technical characteristics of the OTH radar receiver (1.7-30 MHz Band)**

Bandwidth (kHz)	Ant. Gain (dBi)	Ant. Height (Ft)	Ant. Type/Polarization	Modulations
4.2-100	9-36 *	Not available	Phased Array/Vertical	FM/CW or angle-modulated, single channel, with analog or digital signals.

\* The 9 dBi and 36 dBi antenna gains are measured at 5 MHz to 28 MHz, respectively.

The protection requirement used to develop the exclusion zone for OTH radar receivers in the 1.7 to 30 MHz band is a spectral power flux density (PFD) threshold of -258 dBW/m<sup>2</sup>-Hz.<sup>[33]</sup> This analysis assumes that the interfering BPL signal is received through a 0 dBi side lobe of the radar antenna.

### 3.2.3 Radioastronomy Receivers

Radio astronomical measurements are made from the Earth's surface from 2 MHz to beyond 800 GHz. The sensitivity of radio astronomy receivers greatly exceeds the sensitivity of typical communications and radar equipment. The sensitivity is defined by the smallest power level change, ΔP, at the receiver input that can be detected and measured. The interfering signal threshold levels are defined as the interfering signal level which introduces an error of 10 percent in the measurement of ΔP.

The protection criterion applicable for terrestrial interference sources is based on reception of an interfering signal through 0 dBi side lobes of a radioastronomy antenna.

The International Telecommunication Union Radiocommunications Sector (ITU-R) protection level for radioastronomy is a spectral PFD of  $-258 \text{ dBW/m}^2\text{-Hz}$  in the 73.0-74.6 MHz frequency band.<sup>[34]</sup> This level is assumed for the radioastronomy exclusion zone radii analysis.

### **3.3 POTENTIAL SOURCES OF INTERFERENCE**

Using the NEC software, NTIA modeled the field strength of MV overhead and underground BPL power lines for this analysis. A description of these models follows below.

#### **3.3.1 Overhead Power Line Model**

NTIA modeled an overhead BPL power line as three horizontal parallel copper wires, each 340 meters long and 8.5 meters (27.9 feet) above ground having average characteristics (conductivity  $\sigma = .005 \text{ S/m}$ , relative permittivity  $\epsilon_r = 15$ ). Each wire had a diameter of 1 centimeter (approximating American Wire Gauge (AWG) gauge 4/0) and the wires were separated in the horizontal plane by 0.60 meter. The feed point was at the center of one of the outside wires, which ran parallel to the x axis ( $y = 0$ ). The equivalent of a BPL coupler was placed on the center segment of the wire and was modeled as a voltage source of 1 volt in series with a  $150 \Omega$  resistor that represented the source impedance. The other two phase wires ran parallel to the x axis at  $y = 0.6$  and  $y = 1.2$  meters. All wires were connected at the ends to one another through  $50 \Omega$  impedances to model the loads. The overhead power line was modeled at a number of discrete frequencies ranging from 4 MHz to 74 MHz.

#### **3.3.2 Underground Power Line Model**

NTIA created a NEC model of an Underground Residential Distribution (URD) cable and a shielded, pad-mounted transformer for the radioastronomy (Section 3.4.3) and aggregation (Section 5) analyses. The modeled cable consisted of a center copper conductor 1 centimeter in diameter, surrounded by simulated cross-linked polyethylene insulation (using NEC's Insulated Wire feature) having a thickness of 6 millimeters. Around the outside of the insulation were three 12 AWG multi-grounded neutral copper wires.

The URD cable in the NEC model spanned 340 meters (+/- 170 meters along the x-axis), 1 meter below ground level. Near the origin, the cable was routed up to ground level, breaking the surface inside a wire-grid rectangular structure one meter on a side and one-half meter high. This structure represented the pad-mounted transformer casing, and was given steel conductivity. The wires composing the transformer casing were 4 millimeters thick (Figure 3-1).

Inside the transformer casing, only the center conductor of the URD cable continued above ground. The simulated BPL device was placed on this short loop of wire, 0.2 meters off the ground.

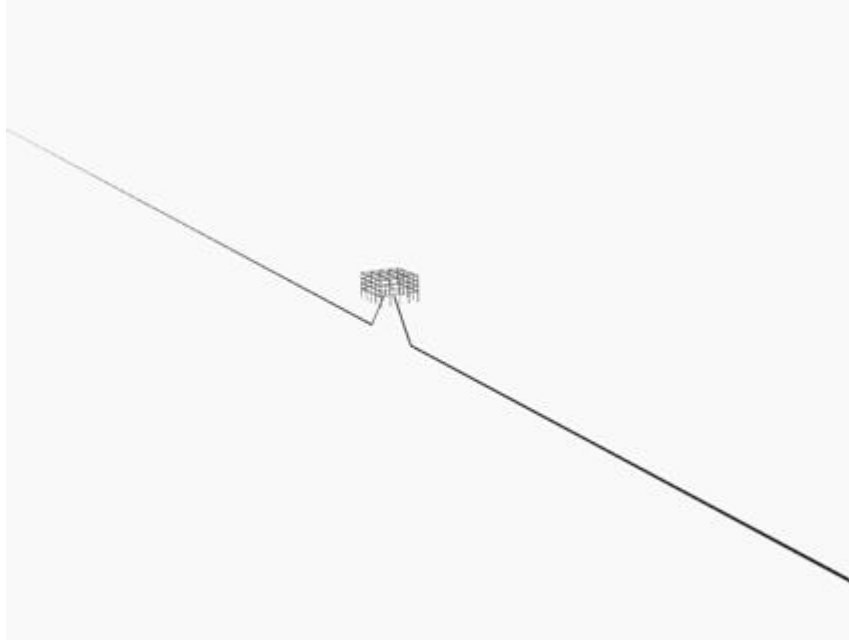


**Figure 3-1: Representation of a NEC model of an underground BPL power line and transformer pad**

### **3.3.3 Part 15 Scaling of Power Line Models**

NTIA computed electric field strength values for these NEC power line models using the measurement guidelines for Access BPL systems. Below 30 MHz, the measurement guidelines specify measurement of magnetic field with a loop antenna rotated about its vertical axis (horizontal magnetic field) at a height of 1 meter. Conversion to electric field strength resulted from application of Equation 2-1 (page 2-2).

Below 30 MHz, the FCC Part 15 radiated emissions limit is specified as 30  $\mu\text{V}/\text{m}$  at 30 meters horizontal distance.<sup>[35]</sup> To convert the limit to the 10 meter distance specified in the measurement guidelines for Access BPL systems, the slant range between an overhead power line and the measurement point must be used in conjunction with a 40 log correction factor. Application of Equations 2-2 (page 2-22) and 2-3 (page 2-23) with a modeled overhead power line height of 8.5 meters and measurement height of one meter, the slant range adjustment to the electric field strength limit results in an extrapolated value of the Part 15 limit at 10 meters as shown below. The peak value of  $E_v$  from the specified measurement locations along the power line was scaled to achieve the value of  $E_{10\text{m}}$  shown below. The specified measurement locations were at points  $1/4$ ,  $1/2$ ,  $3/4$ , and 1 wavelength down the line from the BPL source.

$$E_{10\text{m}} = E_{30\text{m}} \cdot 10^{\frac{40 \cdot \log_{10} \left( \frac{30\text{m}}{\sqrt{(8.5\text{m}-1\text{m})^2 + 10\text{m}^2}} \right)}{20}} \approx 72 \mu\text{V}/\text{m}$$

Above 30 MHz, the Part 15 Class A emission limit of 90  $\mu\text{V}/\text{m}$ , at a distance of 10 meters, applies and the measurement height ranges from 1 to 4 meters. The peak value of the horizontal and vertical electric field strength from the specified measurement locations along the overhead power line and at the specified measurement heights was scaled to the 90  $\mu\text{V}/\text{m}$  emissions limit.<sup>[36]</sup>

The underground BPL system was analyzed at 74 MHz in this study; therefore, the Class A emission limit of 90  $\mu\text{V}/\text{m}$ , 10 meter measurement distance, and the 1 to 4 meter measurement heights were applied. Instead of measurement points along the power line, as would be the case for overhead power lines, the underground system was measured at 16 evenly spaced radials surrounding the BPL signal source. The peak value of the horizontal and vertical electric field strength from the 16 radials surrounding the underground BPL source and at the specified measurement heights was scaled to the 90  $\mu\text{V}/\text{m}$  emissions limit.

With the Part 15 calibration completed, NTIA used NEC to calculate field strength values over a range of horizontal distances from the BPL device and elevation angles determined by the assumed receive antenna.

## **3.4 ANALYTICAL APPROACH**

### **3.4.1 Communications Receivers**

This analysis evaluates the protection radii needed around base station receivers for the various federal radiocommunication systems discussed in Section 3.2. The NEC software tool was used to model a representative radio receiver antenna. The model was initially patterned as a horizontal dipole at 42.7 meters above ground with a gain of 0 dBi in the direction of the power line.<sup>[37]</sup> NEC models were used to calculate the electric field strength values at points along and away from the power line at the assumed height of the receiver antenna, and then translate these values into received interfering signal power levels.

NTIA subsequently developed a second NEC model to address the typical gain in the direction of the power line for a high-gain receiver antenna. This high-gain antenna was patterned after a stacked log-periodic antenna used for aeronautical radiocommunications.<sup>[38]</sup> This antenna model has a maximum gain of approximately 14 dBi for frequencies between 4 to 30 MHz, with a gain in the direction of the power line of up to 5 dBi. In order to model more accurately the BPL signal power seen by a communications receiver with a high-gain antenna, NTIA utilized NEC's Maximum Coupling feature to determine the loss of power between the modeled BPL source and the modeled stacked log-periodic antenna receive point.

The use of exclusion zones and consultation areas is intended to reduce the risk of harmful interference at these protected receiver sites. Their radii are determined by noting the distance from the modeled power line where the radiated emissions from a BPL source raise the noise floor (*e.g.*,  $(I+N)/N$ ) by a certain amount. The radii chosen

were determined to be the distances beyond which the probability was negligible that a communications receiver would experience an increase in noise floor of 1 dB.

The BPL interfering signal power “I” was determined from NEC power line simulations. Calculations of electric field strength for the 0 dBi receiver antenna case were made along the length of the modeled power line in 0.5 meter steps. These calculations were performed at increasing distances away from the power line at a height of 42.7 meters, the height of the assumed communications receiver antenna. For the high-gain antenna case, the field strength calculations along the power line were performed at 5 meter steps along the power line to reduce computation time for the analysis.

The noise power “N” was assumed to be the median noise level for a quiet rural noise environment. This assumption is reasonable, as most of these protected receiver sites were selected because they exhibit very low background noise levels. In addition, personnel at these sites (where manned) actively work with local utilities to prevent or correct any increases in ambient noise due to power line noise sources. The noise levels used in this analysis are listed in Table 3-6.

**Table 3-6: Ambient noise level assumptions used in the communications receiver analysis<sup>[39]</sup>**

<b>Frequency</b>	<b>Bandwidth</b>	<b>Noise Power Level</b>
4 MHz	2.8 kHz	-135.3 dBW
10 MHz	2.8 kHz	-136.7 dBW
15 MHz	2.8 kHz	-144.7 dBW
20 MHz	2.8 kHz	-147.9 dBW
25 MHz	2.8 kHz	-150.2 dBW
30 MHz	16 kHz	-144.6 dBW
40 MHz	16 kHz	-147.5 dBW

NTIA calculated the percentage of simulation points that, at a given distance around the modeled power line, resulted in a 1 dB noise floor increase. These calculations were performed at increasing distances away from the modeled power line.

### **3.4.2 Radar Receivers**

In analyzing the protection radii for radar receivers, NTIA employed the NEC overhead power line model described in Section 3.3.1 and the Irregular Terrain Model (ITM) software to calculate the basic transmission loss due to the distance separation and diffraction of a radio frequency (RF) signal over a spherical earth.<sup>[40]</sup> The protection requirement used in this analysis for radar receivers in the 1.7 to 30 MHz band is a PFD threshold of  $-258 \text{ dBW/m}^2\text{-Hz}$ . This protection criterion assumes reception of a terrestrial interfering signal through a 0 dBi side lobe of a radar antenna.

NTIA used NEC to calculate the peak electric field strength at horizontal distances of 1 to 10 kilometers from the BPL device and an elevation of 42.7 meters, the

assumed height of the receiving antenna.<sup>[41]</sup> The electric field strength values computed by NEC were converted into PFD values using Equation 3-1 below:

$$PFD_{NEC}(dist) = 10 \cdot \log\left(\frac{(E(dist))^2}{120 \cdot r}\right) + 10 \cdot \log\left(\frac{1}{300 \cdot BW_{meas}}\right) + 10 \cdot \log(n_{equiv})$$

(Equation 3-1)

where

- $PFD_{NEC}$  is the power flux density computed by NEC, in dBW/m<sup>2</sup>-Hz;
- $dist$  is the distance separation between the BPL source and the radar receiver, in meters;
- $E$  is the electric field strength, scaled to meet Part 15 limits, in V/m;
- $BW_{meas}$  is the Part 15 measurement bandwidth, in Hz;<sup>[42]</sup> and
- $n_{equiv}$  is the number of equivalent-power BPL sources contributing to the PFD calculation.

PFD values are calculated based on the root mean square (RMS) value of electric field strength; therefore, the peak electric field strength values determined by the NEC simulation were adjusted downward by a factor of 6 dB.<sup>[43]</sup> The analysis assumes that the calculated PFD is based on the equivalent of four equal-power BPL signals ( $n_{equiv} = 4$ ) operating at the Part 15 limit, accounting for potential aggregation of multiple co-frequency emission sources beyond the protection radius surrounding the radar antenna. The four simulated power lines were assumed to be oriented broadside ( $\theta = 90^\circ$ ) to the receiving antenna. This assumption was used to provide a reasonable simplification of the analysis, where a widely deployed BPL system may encompass many more than four co-frequency BPL devices generating various field strength levels at or below the Part 15 limit with a variety of distances and orientations with respect to the receiving antenna.

Simulations using NEC were run to a distance of 10 km from the power line since NEC does not account for the diffraction losses that would be expected at greater distances. ITM transmission loss data was used to calculate PFD values from 10 km out to 50 km. The ITM results were based on use of the same ground parameters as NEC, and the same power line height of 8.5 meters and an assumed radar antenna height of 42.7 meters.<sup>[44]</sup> ITM input parameters are detailed in Table 3-7.

**Table 3-7: ITM input parameters**

Input Variable	Value
Frequency <sup>[45]</sup>	25 MHz

Antenna Heights	Transmitter – 8.5 m, Receiver – 42.7 m
Siting Criteria	Transmitter – Random, Receiver – Very Careful
Terrain Irregularity Factor, $\Delta h$	30 m
Polarization	Horizontal
Relative Permittivity	15
Ground Conductivity	0.005 S/m
Climate	Continental Temperate
Surface Refractivity	301 N-units
Percent Time	90.0%
Percent Location	50.0%
Percent Confidence	50.0%
Mode of Variability	Individual

To determine the PFD values accounting for diffraction losses that come into play at large distances from the power line, the transmission losses beyond 10 km calculated by ITM were scaled relative to the value that ITM computed at 10 km (Equation 3-2). Within 10 km of the power line, the adjusted PFD was the same as the PFD computed using NEC electric field strength directly (Equations 3-1 and 3-3a). Beyond 10 km, the scaled ITM loss values, at each distance, and the PFD computed at 10 km from NEC were used to compute the adjusted PFD (Equation 3-3b).

$$ScaledLoss_{ITM}(dist) = Loss_{ITM}(dist) - Loss_{ITM}(10 km), \text{ for } dist \geq 10 km$$

(Equation 3-2)

where

- $dist$  is the horizontal distance from the power line, in km;
- $Loss_{ITM}$  is the path loss at a distance, in dB; and
- $ScaledLoss_{ITM}$  is the path loss at a distance relative to the path loss at 10 km from the power line, in dB.

$$PFD_{Adjusted}(dist) = PFD_{NEC}(dist), \text{ for } 0 \leq dist < 10 km \quad (\text{Equation 3-3a})$$

$$PFD_{Adjusted}(dist) = PFD_{NEC}(10 km) - ScaledLoss_{ITM}(dist), \text{ for } dist \geq 10 km \quad (\text{Equation 3-3b})$$

where

- $PFD_{NEC}$  is the power flux density computed by NEC, in dBW/m<sup>2</sup>-Hz; and
- $PFD_{Adjusted}$  is power flux density, at a distance, adjusted by the relative path loss beyond 10 km, if applicable, in dBW/m<sup>2</sup>-Hz.

### 3.4.3 Radioastronomy Receivers

The methodology described in Section 3.4.2 was also used to analyze protection area requirements for radioastronomy receivers. The peak electric field strength, computed at any distance, was converted into PFD values at the receiver for comparison to the  $-258 \text{ dBW/m}^2\text{-Hz}$  interference threshold.<sup>[46]</sup> This protection criterion is applicable for terrestrial interference sources based on reception of the interfering signal through 0 dBi side lobes of a radioastronomy antenna.

NEC was used to calculate electric field strength values at horizontal distances of 1 to 10 kilometers from the BPL device and at an elevation of 20 meters, the assumed height of the radioastronomy antenna. These field strength values were converted into PFD values using Equation 3-1.

The calculated values of peak electric field strength were adjusted downward by a factor of 6 dB to approximate the RMS values required for determining PFD values. As in the radar receiver analysis, the calculated PFD is based on the assumption of an equivalent of four equal-power BPL signals ( $n_{\text{equiv}} = 4$ ), accounting for potential aggregation of multiple co-frequency emission sources beyond the protection radius surrounding the radar antenna. The four simulated power lines were assumed to be oriented broadside ( $\theta = 90^\circ$ ) to the receiving antenna. This assumption was used to provide a reasonable simplification of the analysis, where a widely deployed BPL system may encompass many more than four co-frequency BPL devices generating various field strength levels at or below the Part 15 limit with a variety of distances and orientations with respect to the receiving antenna.

As indicated above, electric field strength simulations using NEC were only run to a distance of 10 km from the power line, as NEC does not account for the diffraction losses that would be expected at greater distances. ITM transmission loss data was used to calculate PFD values from 10 km out to 50 km. The ITM input parameters remained the same as for the radar receiver case, with the exception that the radioastronomy receiver antenna was assumed to have a height of 20 meters and the analysis frequency was assumed to be 74 MHz.<sup>[47]</sup> To determine the PFD values accounting for diffraction losses that come into play at large distances from the power line, the transmission losses beyond 10 km calculated by ITM were scaled relative to the value that ITM computed at 10 km (Equation 3-2). Within 10 km of the power line, the adjusted PFD was the same as the PFD computed using NEC electric field strength directly (Equations 3-1 and 3-3a). Beyond 10 km, the scaled ITM loss values, at each distance, and the PFD computed at 10 km from NEC were used to compute the adjusted PFD (Equation 3-3b).

For the underground BPL analysis, the ITM input parameter for the transmitter antenna was set to 0.2 meter.<sup>[48]</sup> This is the height at which the BPL device protrudes above ground in the NEC underground power line model. In addition, the transition to ITM-computed transmission losses was made at a distance of 1 km, the minimum separation distance supported by ITM. Unlike the overhead BPL case, the far field region for the underground BPL case is close to the BPL device because the underground wiring only protrudes above ground for a length on the order of 1 meter. The extent of



the near field region for the underground case is only meters or tens of meters from the BPL device.

### 3.5 SIMULATION RESULTS

A summary of the simulation conditions described in Section 3.4 is provided in Table 3-8. The results for communications receivers based on limiting the noise floor increase to 1 dB are provided in Section 3.5.1. The results for limiting the PFD seen by radar and radioastronomy receivers to less than  $-258 \text{ dBW/m}^2\text{-Hz}$  are described in Sections 3.5.2 and 3.5.3, respectively.

**Table 3-8: Simulation Conditions**

<b>Power Line Models</b>	<b>Overhead</b>	<b>Underground</b>
Conductors	3 horizontal	1 power / 3 neutral
Conductor Material	Copper	Copper
Conductor Thickness	1 cm (approx. AWG 4/0)	1 cm (approx. AWG 4/0)
Conductor insulation	N/A	6 mm cross-linked polyethylene
Conductor spacing	0.6 m	-
Length	340 m	340 m
Height above ground	8.5 m	-1 m
Coupler location	Center conductor, center of span	Power conductor, 0.2 m above ground
Source	1 Volt in series with 150 $\Omega$	1 Volt
Load	50 $\Omega$ between conductors	-
Shield enclosure size	N/A	1 m x 1 m x 0.5 m high
Shield material	N/A	Steel
Shield thickness	N/A	4 mm (wire grid)
<b>Ground Conditions</b>		
Conductivity	$\sigma = 0.005 \text{ S/m}$	
Relative permittivity	$\epsilon_r = 15$	
<b>Simulation Frequencies</b>		
Communication Receiver	4, 10, 15, 20, 25, 30, 40 MHz	
OTH Radar	25 MHz	
Radioastronomy	74 MHz	
<b>Number of BPL emitters</b> (equal power, co-frequency, broadside orientation)		
Communication Receiver	1, 2	
Radar / Radioastronomy	4	
<b>Receiver Antenna</b>		
Communication Receiver	Low Gain	High Gain
Type	Horizontal dipole	Stacked log-periodic
Gain towards power line	0 dBi	5 dBi
Height	42.7 m	12.5m (average)

<b>OTH Radar</b>		
Gain towards power line	0 dBi	
Height	42.7 m	
<b>Radioastronomy</b>		
Gain towards power line	0 dBi	
Height	20 m	
<b>Noise Conditions</b>		
Quiet Rural, as per Table 3-6		
<b>ITM Conditions</b>		
Frequency	Radar – 25 MHz	Radioastronomy – 74 MHz
<b>Antenna Heights</b>		
Transmitter (Power line)	Overhead	Underground
Height	8.5 m	0.2 m
Receiver	Radar	Radioastronomy
Height	42.7 m	20 m
Siting Criteria	Transmitter – Random	Receiver – Very Careful
Terrain Irregularity Factor, $\Delta h$	30 meters	
Polarization	Horizontal	
Relative Permittivity	15	
Ground Conductivity	0.005 S/m	
Climate	Continental Temperate	
Surface Refractivity	301 N-units	
Percent Time	90.0%	
Percent Location	50.0%	
Percent Confidence	50.0%	
Mode of Variability	Individual	
<b>Interference Criteria</b>		
Communication Receiver	Noise Floor Increase $((I+N)/N) = 1$ dB	
Radar / Radioastronomy	PFD = -258 dBW/m <sup>2</sup> -Hz	

### 3.5.1 Communications Receivers

Figures 3-2 through 3-8 illustrate the percentage of points along a simulated BPL power line where the noise floor increase due to BPL emissions from 4 to 40 MHz exceeds 1 dB, in a receiver having antenna gain of 0 dBi towards the power line. These results are plotted relative to the horizontal distance away from the power line. Figures 3-9 through 3-11 show the simulation results at 4, 15 and 25 MHz for a 14 dBi gain receiving antenna having up to 5 dBi of gain in the direction of the power line. In these plots, the results are shown for the case of a single Access BPL device operating at the Part 15 limit, and for the assumed case of two equal-power co-frequency Access BPL devices operating at the Part 15 limit. This latter assumption may encompass more than two co-frequency BPL devices generating various field strength levels below the Part 15 limit. Figure 3-12 summarizes the minimum radii needed to limit the noise floor increase to 1 dB or less, assuming the presence of two equal-power co-frequency BPL devices

operating at the Part 15 limit. The minimum radii correspond to the horizontal distances at which 0 percent of the data points around the simulated power line result in a 1 dB noise floor increase.

Figure 3-12 shows that distances beyond which a 1 dB increase in noise are predicted to be possible increase slowly as frequency increases from 1.7 MHz to over 10 MHz, mainly as a result of decreasing median noise power levels. Between 15 MHz and 30 MHz, the greater radiation efficiency of the BPL power line significantly increases the distances where the noise floor can increase by 1 dB or more. The gain of the modeled high-gain antenna in the direction of the BPL power line is greatest between 15 MHz and 30 MHz as well.

Distance results for 4 MHz have been applied to establish the adopted 1 km exclusion zone dimension for the 2,173.5 to 2,190.5 kHz band used by coast stations.<sup>[49]</sup> Upward rounding of the 4 MHz distance of 895 meters to 1 km and application of that distance from the boundary of the coast station facility accommodates receiver antenna location flexibility, error tolerance in the reported antenna coordinates, and the possibility that other BPL power line configurations not evaluated herein may generate higher field strength.

Among the frequencies considered, the largest distance within which a 1 dB increase in noise is predicted occurs at 25 MHz (distance of about 3.9 km). Upward rounding of this distance to 4 km would accommodate error tolerance in the reported antenna coordinates and the possibility that other BPL power line configurations and BPL signal aggregation not evaluated herein may generate higher field strength.

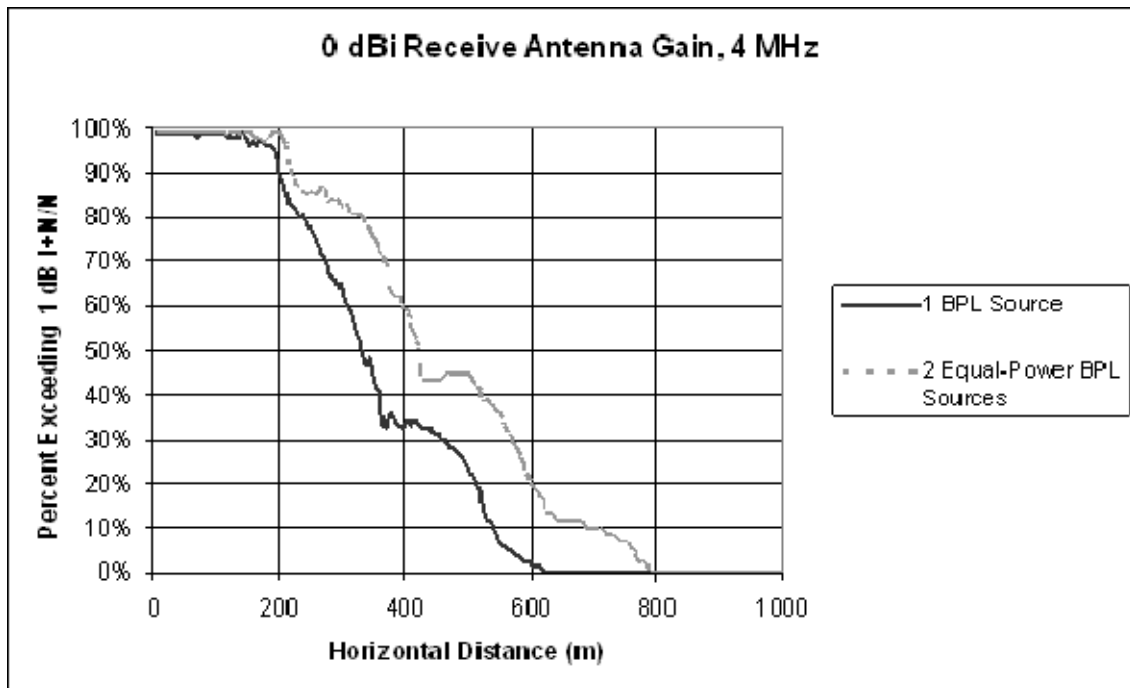


Figure 3-2: Percentage of points exceeding a 1 dB increase in noise floor as a function of distance from the power line

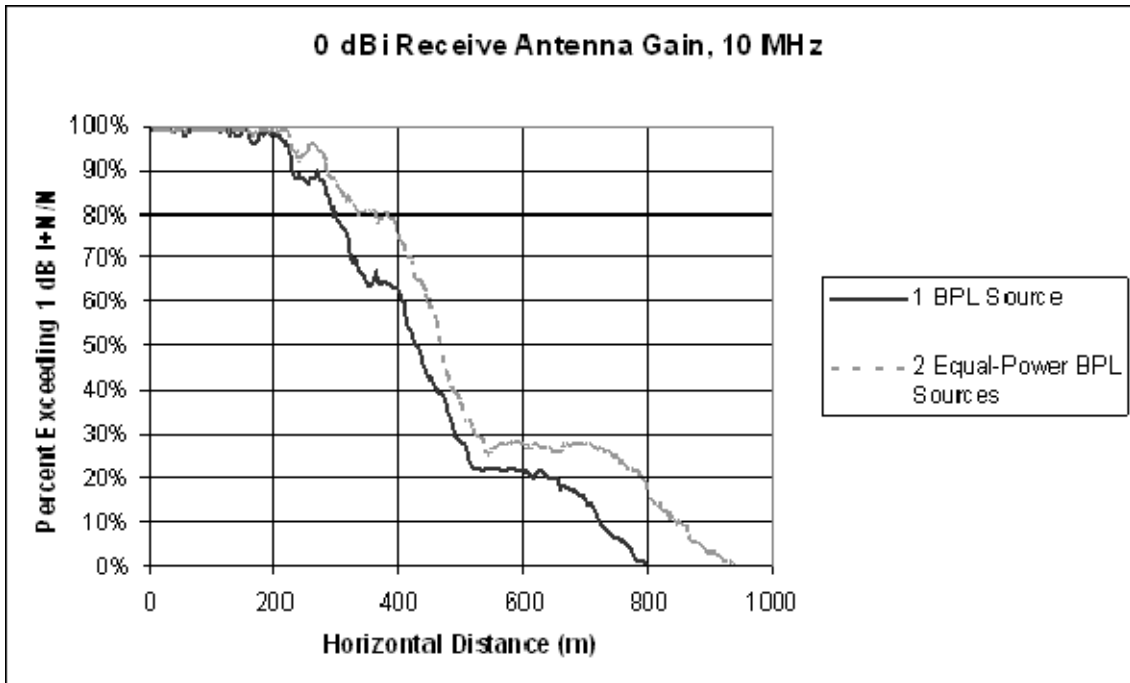


Figure 3-3: Percentage of points exceeding a 1 dB increase in noise floor as a function of distance from the power line

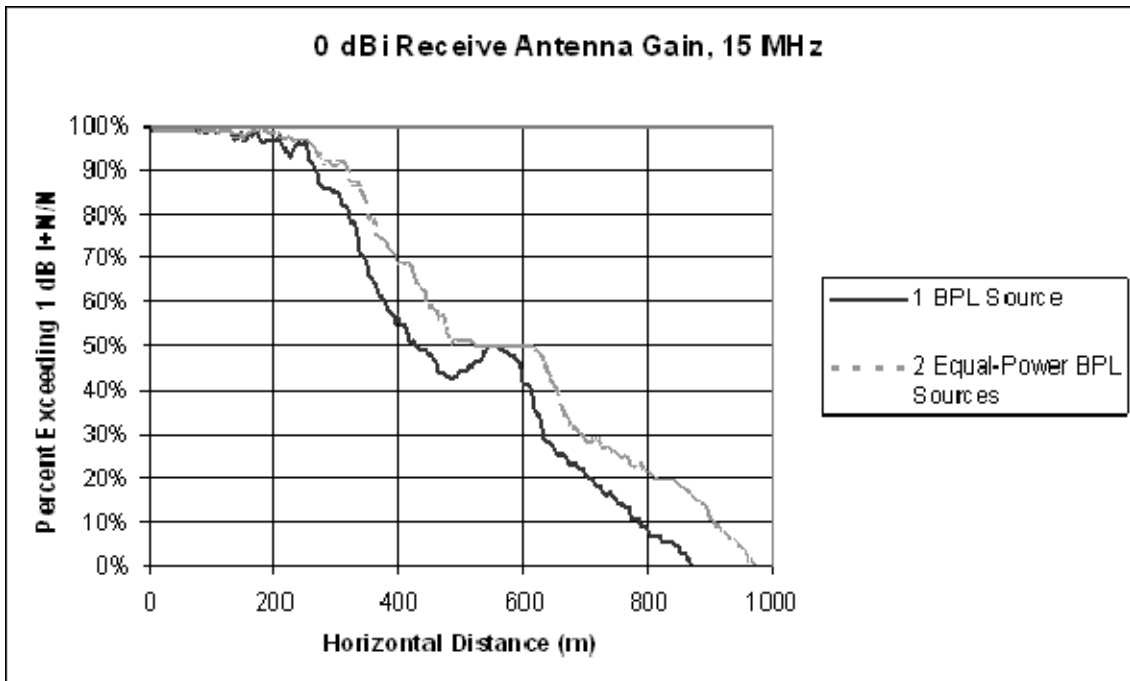
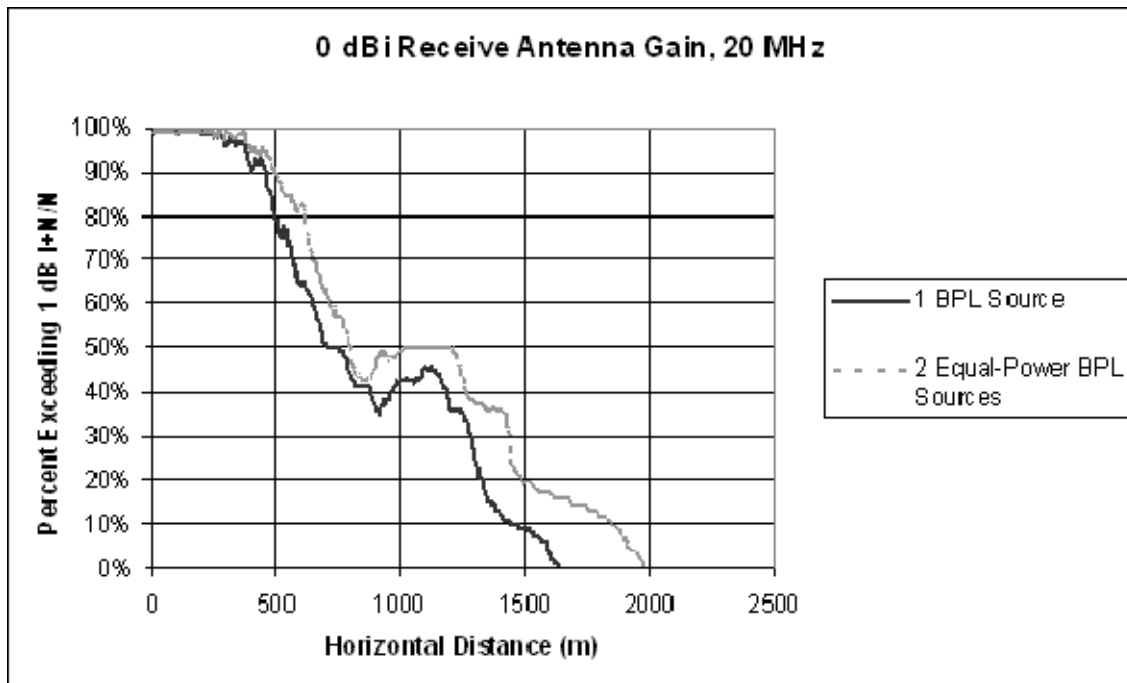
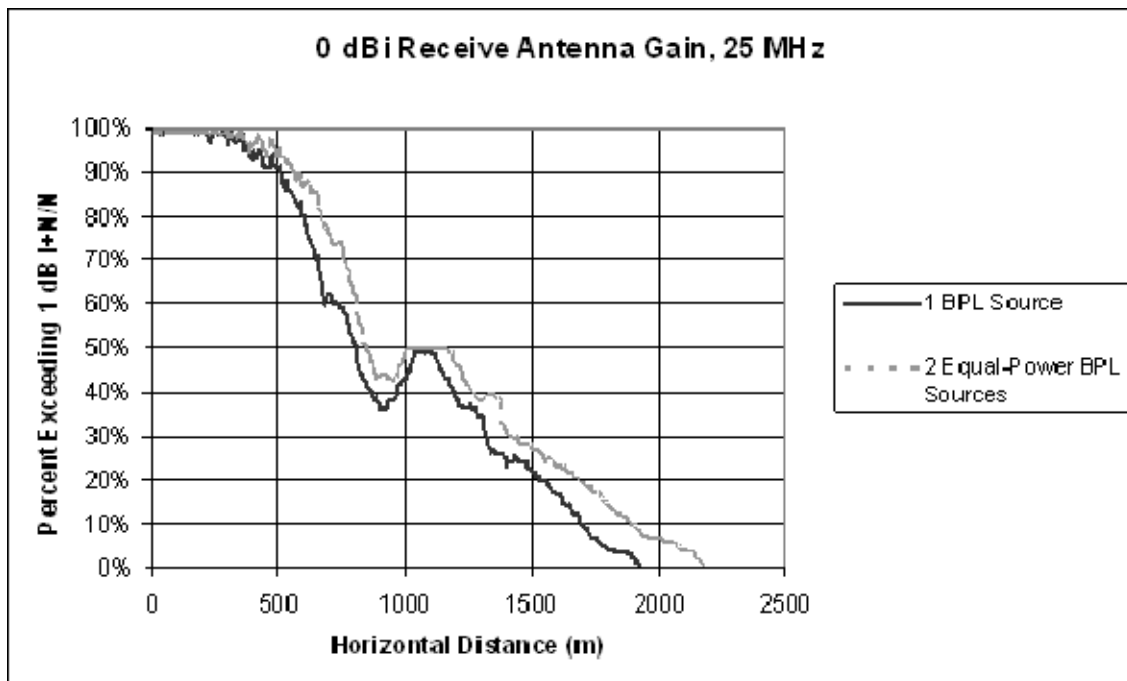


Figure 3-4: Percentage of points exceeding a 1 dB increase in noise floor as a function of distance from the power line



**Figure 3-5: Protection Percentage of points exceeding a 1 dB increase in noise floor as a function of distance from the power line**



**Figure 3-6: Percentage of points exceeding a 1 dB increase in noise floor as a function of distance from the power line**

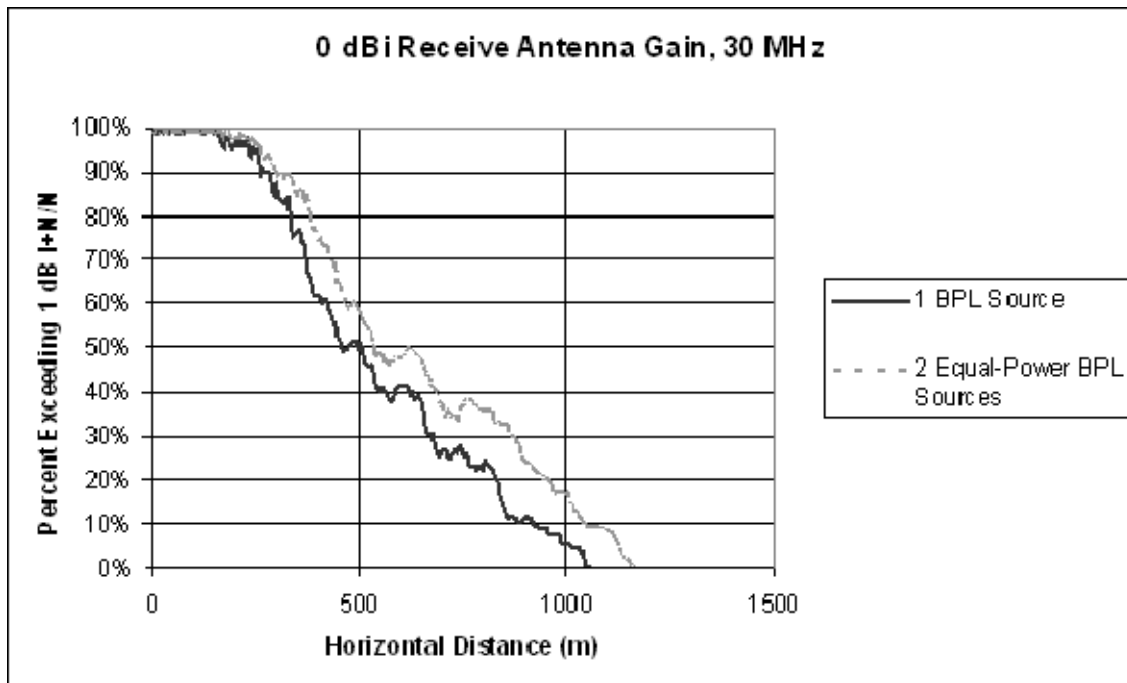


Figure 3-7: Percentage of points exceeding a 1 dB increase in noise floor as a function of distance from the power line

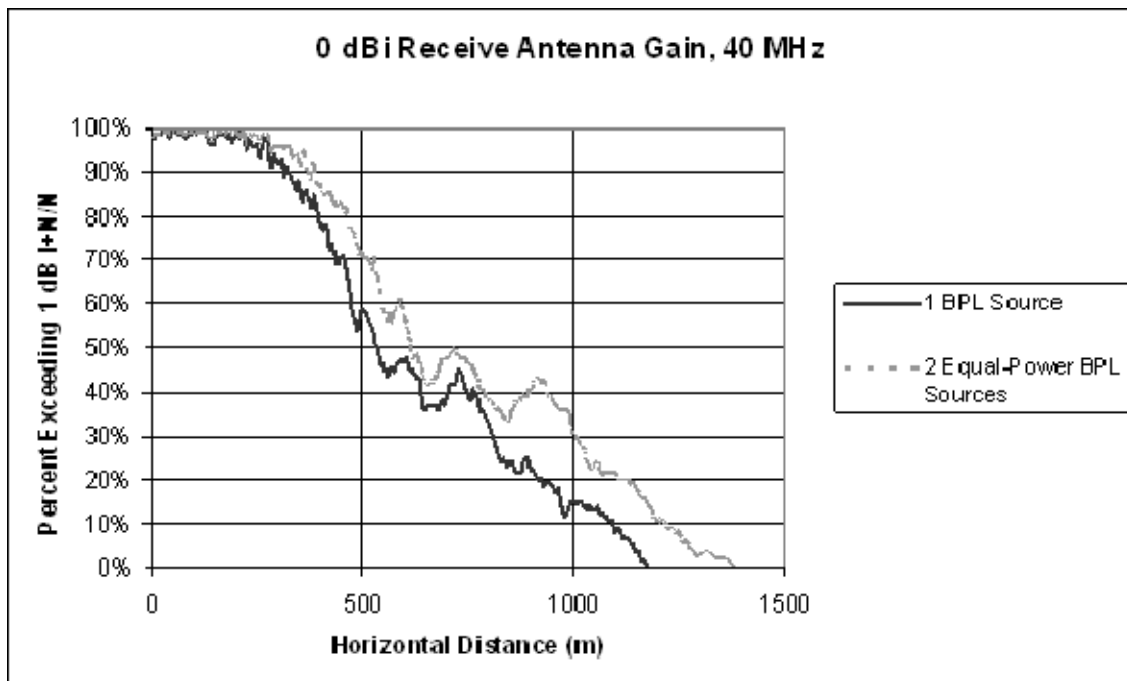


Figure 3-8: Percentage of points exceeding a 1 dB increase in noise floor as a function of distance from the power line

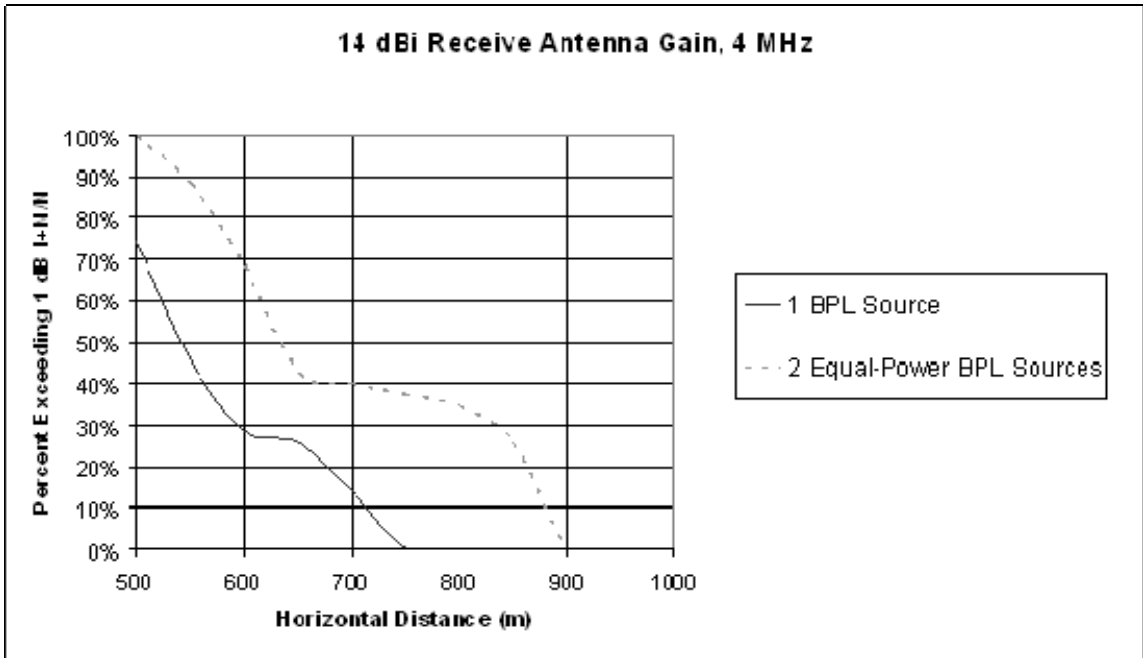


Figure 3-9: Percentage of points exceeding a 1 dB increase in noise floor as a function of distance from the power line

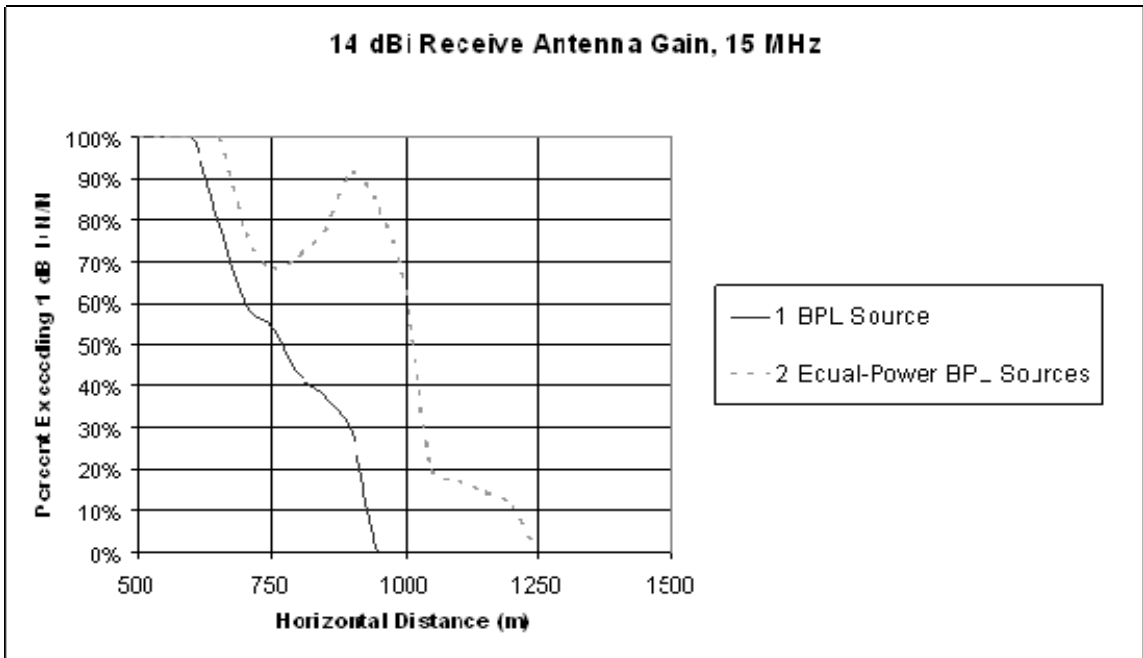


Figure 3-10: Percentage of points exceeding a 1 dB increase in noise floor as a function of distance from the power line

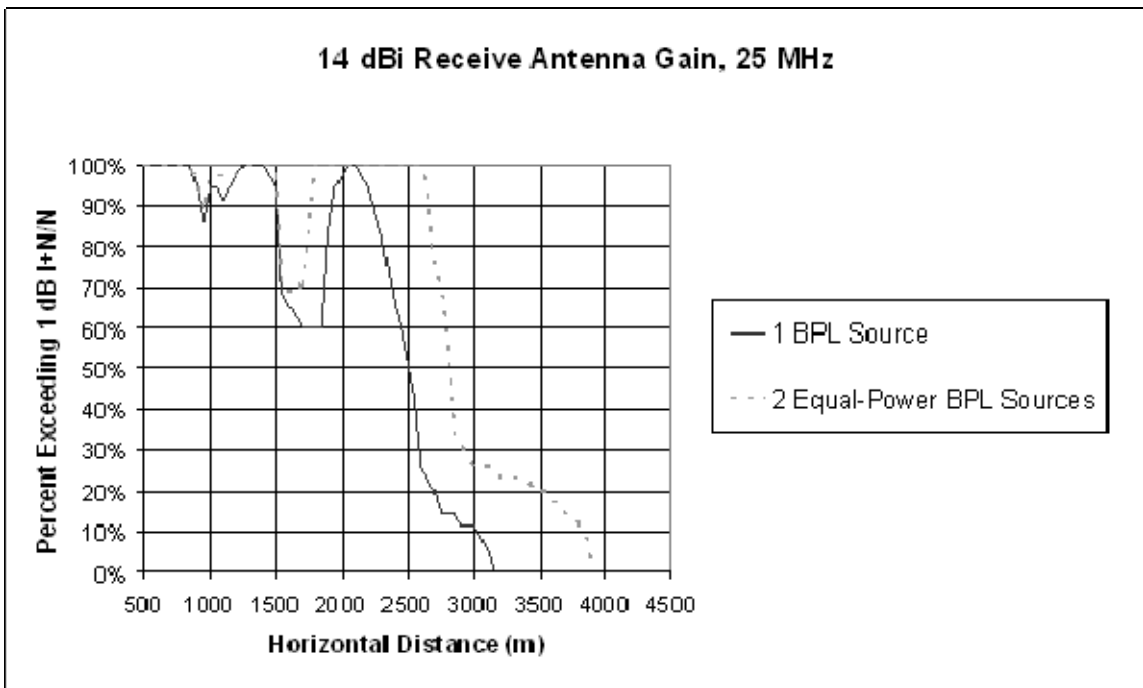


Figure 3-11: Percentage of points exceeding a 1 dB increase in noise floor as a function of distance from the power line

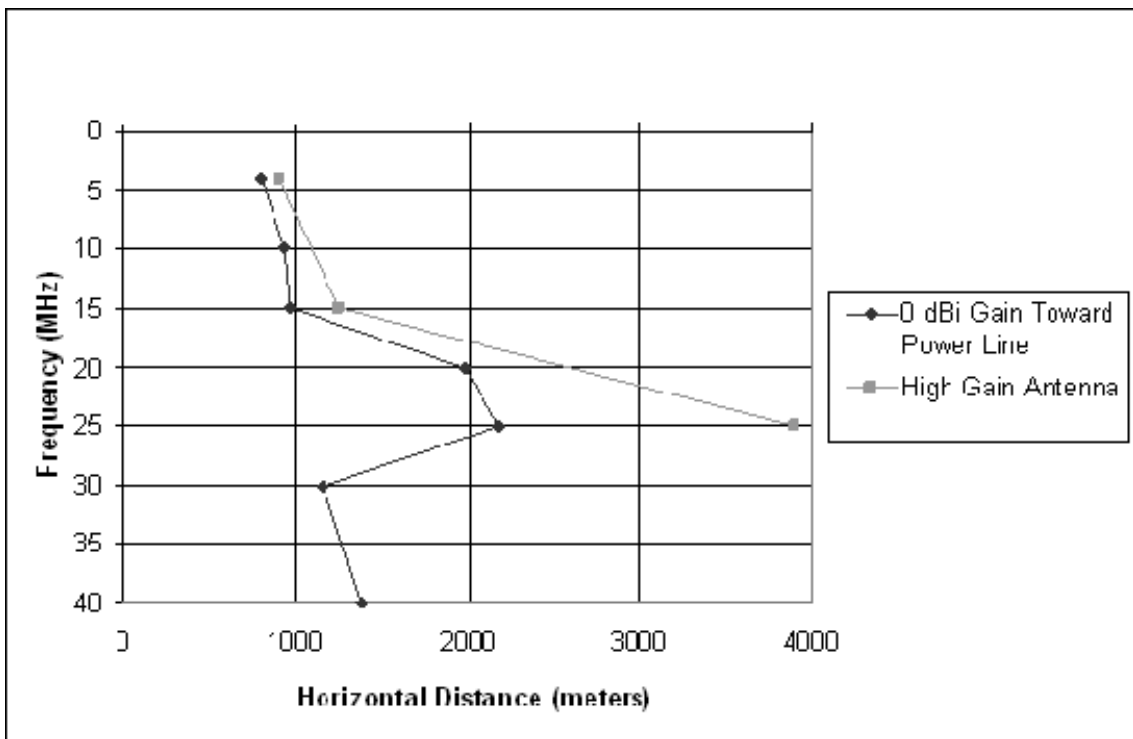


Figure 3-12: Summary of minimum protection area radii to limit noise floor increase to 1 dB or less



### 3.5.2 Radar Receivers

The calculated PFD at a radar receiving antenna located at various horizontal distances from multiple overhead BPL sources is shown in Figure 3-13. The results show the PFD at 25 MHz due to four equal-power co-frequency overhead BPL sources, positioned at a height of 8.5 meters above the ground and radiating at the Part 15 limit in the direction of the receiving antenna at the horizontal distances plotted below. As the results presented in Section 3.5.1 illustrate, the modeled overhead power line radiates most effectively at 25 MHz, and therefore, this frequency was chosen for evaluation in the radar receiver analysis.

Figure 3-13 shows that the maximum PFD levels begin to exceed the assumed threshold of  $-258 \text{ dBW/m}^2\text{-Hz}$  at horizontal distances of 36 km or less from the power line. The Commission, in its BPL Report and Order, adopted a radius of 37 km for consultation areas around a number of critical radar receiving facilities in the 1.7 to 30 MHz frequency range.<sup>[50]</sup>

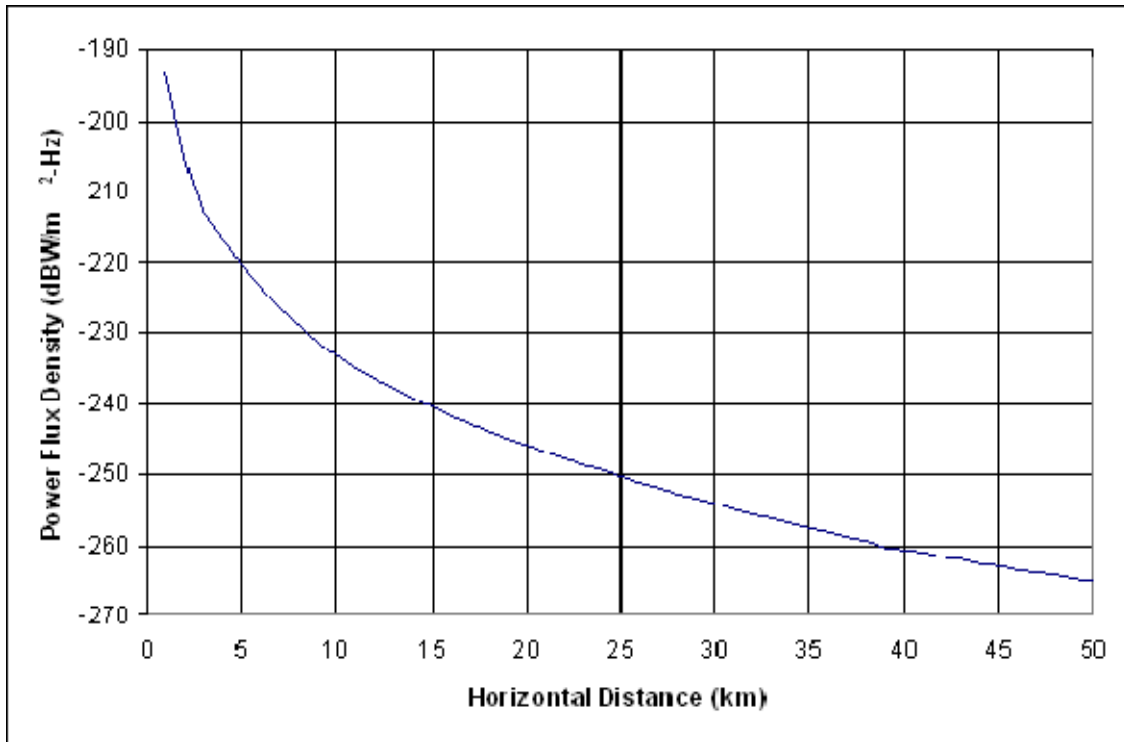
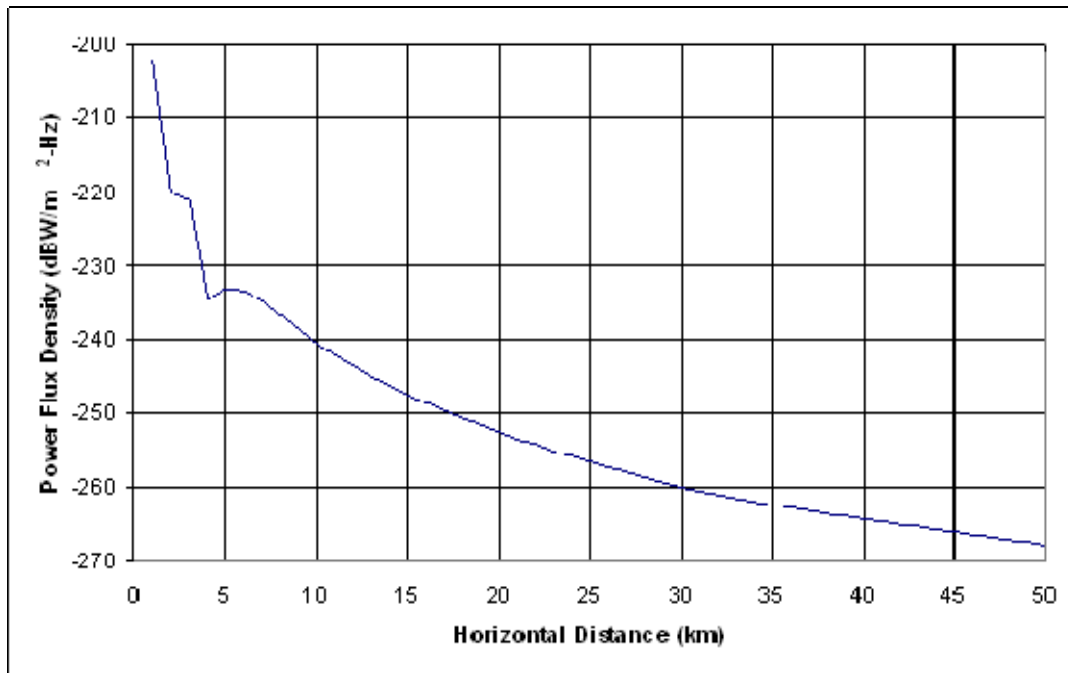


Figure 3-13: Power flux density relative to the distance from overhead BPL at 25 MHz (4 equal power co-frequency BPL signal sources)

### 3.5.3 Radioastronomy Receivers

The PFD levels expected at a radioastronomy antenna located at various horizontal distances from overhead and underground BPL sources are shown in the figures below. These analyses assumed that there were four equal-power co-frequency BPL sources radiating at the Part 15 limit in the direction of the receiving antenna.

For the overhead BPL power line case, the BPL sources were assumed to be positioned at a height of 8.5 meters off of the ground. In Figure 3-14, the PFD falls below the  $-258 \text{ dBW/m}^2\text{-Hz}$  threshold interference level at distances greater than 27 km from the overhead BPL sources. In a letter to the FCC, NTIA requested that the Commission adopt an exclusion zone of 29 km around the boundary of the Very Large Array (VLA) radioastronomy site located in Socorro, New Mexico.<sup>[51]</sup>



**Figure 3-14: Power flux density relative to the distance from overhead BPL at 74 MHz (4 equal-power co-frequency BPL signal sources)**

Figure 3-15 shows the results for the underground BPL case, assuming four equal-power co-frequency underground BPL sources radiating at the Part 15 limit in the direction of the receiving antenna.

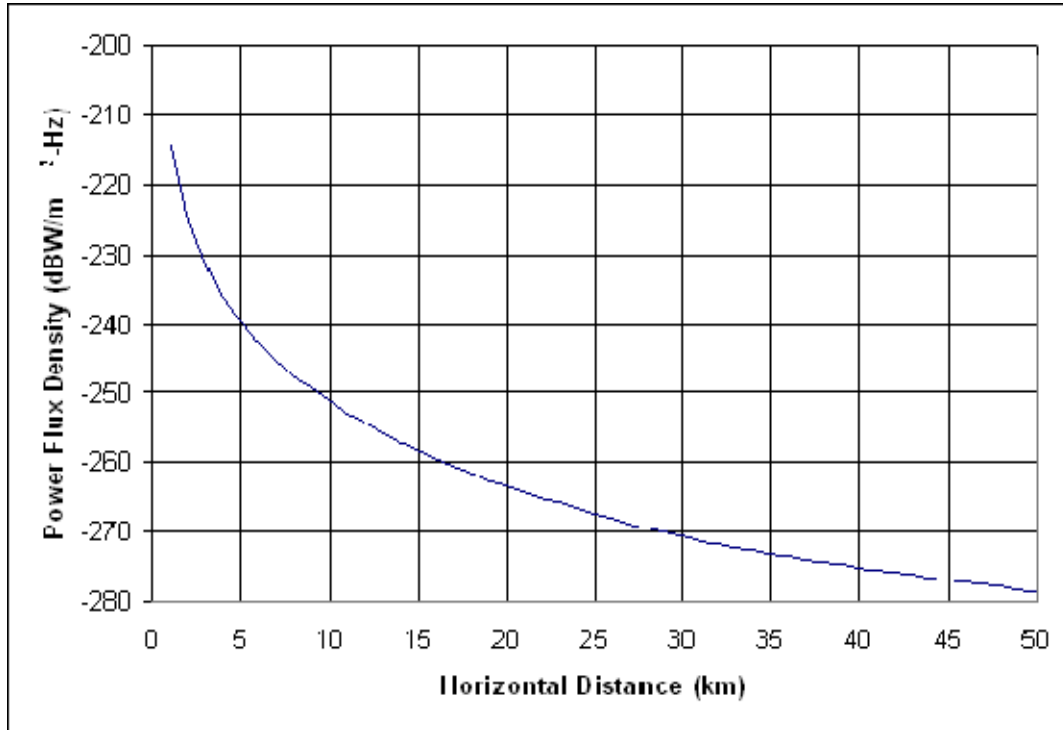


**Figure 3-15: Power flux density relative to the distance from underground BPL at 74 MHz (4 equal-power co-frequency BPL signal sources)**

For the underground BPL case, the power flux density falls below the threshold interference level at distances beyond 14 km from the underground MV power lines. This somewhat exceeds the 11 km protection radius associated with the 73.0-74.6 MHz exclusion zone around the boundary of the VLA radioastronomy location. From NTIA’s experience conducting field measurements on underground BPL systems, emissions levels are typically well below the Part 15 limits, and in many cases, the radiated BPL signal was not measurable. <sup>[52]</sup>

### 3.6 SUMMARY

Based on recommendations provided by NTIA resulting from these and earlier analyses, the Commission has specified excluded frequency bands, exclusion zones and consultation areas needed to prevent interference from BPL systems to certain federal radio operations in the 1.7 to 80 MHz frequency range. NTIA’s analysis shows that, at the distances corresponding to these protection area radii, BPL emissions are expected to result in only small increases in the noise floor of protected communications receivers, or PFD levels that fall below the interference protection requirement for sensitive radioastronomy or over-the-horizon radar receivers.

These special safeguards provide an additional measure of interference protection beyond that afforded by field strength limits, prohibition of harmful interference from BPL systems, and compliance measurement provisions. The special protection

provisions place only a minimal constraint on BPL deployment, as they impact only about two percent of the spectrum between 1.7 and 80 MHz. Additional special protection provisions may be needed if, at some time in the future, Access BPL devices are permitted to operate outside the 1.7 to 80 MHz frequency range.

## **SECTION 4**

### **CASE STUDY OF POTENTIAL INTERFERENCE USING ADOPTED BPL RULES**

#### **4.1 INTRODUCTION**

To examine the potential effectiveness of the rules for Access BPL, a case study was undertaken. The study modeled a residential neighborhood in which BPL devices had been installed on overhead power lines, with the radiation level from the BPL energized power line designed to meet FCC Part 15 rules and measurement guidelines adopted for Access BPL systems. Using this model, the potential noise floor increase seen by land mobile devices on roads adjacent to the line was determined. PFD levels resulting from BPL emissions that might be experienced at distant fixed receivers, such as for OTH radars, were also evaluated in this case study.

The modeling effort detailed herein is not intended to be representative of a typical residential neighborhood; however, the power line and nearby roads are modeled using an actual residential area in which BPL devices have been installed, and this study is therefore instructive regarding conditions that might be encountered by nearby land mobile receivers and by distant receivers under the adopted rules. It is an extension of NTIA's previous work that attempted to characterize typical interference potential due to BPL signals injected into a generic power line layout.

#### **4.2 METHODOLOGY**

The Commission's BPL Report and Order specified measurement guidelines to enable BPL providers to determine compliance of their systems with FCC Part 15 limits. The relevant measurement guidelines are as follows:

- For systems using data burst rates of at least 20 bursts per second, quasi-peak measurements are to be employed;
- For frequencies above 30 MHz, electric field sensing antennas are to be used, with the measurement height from 1 to 4 meters to maximize the measured field at the Part 15 reference distance of 10 meters. Alternatively, the measurement may be made at 1 meter height, with a correction factor of 5 dB added to the measured field;
- For frequencies below 30 MHz, a magnetic field sensing loop is to be employed at a measurement height of 1 meter, with the loop rotated about the vertical axis to maximize the measured field at the Part 15 reference distance of 30 meters;
- Measurements should normally be performed at a horizontal separation distance of 10 meters from the overhead line;

- For field strength measurements, the slant range distance between the overhead wiring carrying the BPL signals and the measurement antenna is used to compute a distance correction factor for adjusting the field strength measurement;
- For signals with a bandwidth that is less than the midband frequency, measurement points are to be at the device and at  $\frac{1}{4}$ -wavelength multiples of the midband frequency wavelength down the line, to a distance equal to one wavelength of the midband frequency;
- For signals with a bandwidth exceeding the midband frequency, measurement distance down the line are to be extended in  $\frac{1}{2}$ -wavelength of the midband frequency increments until the distance equals or exceeds  $\frac{1}{2}$  wavelength of the lowest in-band frequency.

A computer model was constructed based upon an actual power line structure where NTIA conducted measurements of BPL emissions. The model was created with the help of *in-situ* observations and measurements, and was designed for simulation using NEC-4.1. As closely as possible and within program constraints, this model was designed to conform to the actual features of the power grid, including the use of catenary wires, correct placement of transformers loads, wire height and placement on power poles, grounding wires, riser, pole placement and wire junctions. The overall extent of the model was approximately 328 meters in the x-axis direction, and 435 meters in the y-axis direction. The modeled power line height was 12 meters. All wires were 12.6 millimeters in diameter and given the conductivity of copper ( $5.8 \times 10^7$  S/m). The ground plane for the model (a flat earth structure beneath the wires) had characteristics typical of “good” ground (dielectric constant of 15.0, conductivity of 0.005 S/m). Due to the computational complexity of this model, the simulations were constrained to frequencies below 30 MHz.

Simulations were focused on wideband and narrowband cases, based upon the FCC testing methodology stipulated above. For the wideband case, the BPL signal was assumed to cover the frequency range of 4 to 22 MHz, with a midband frequency of 13 MHz. For the narrowband case, signals were assumed to occupy 4 MHz bandwidth, with midband frequencies ranging from 4 MHz to 28 MHz, in 4 MHz increments.

#### **4.2.1 Structure Injection Points**

NTIA’s elaborate overhead power line model has enough topological power-line features and sufficient geographic extent that simulations can be run for BPL devices placed at several points on the model. In this effort, three points in the power line structure were selected, as shown in Figure 4-1.

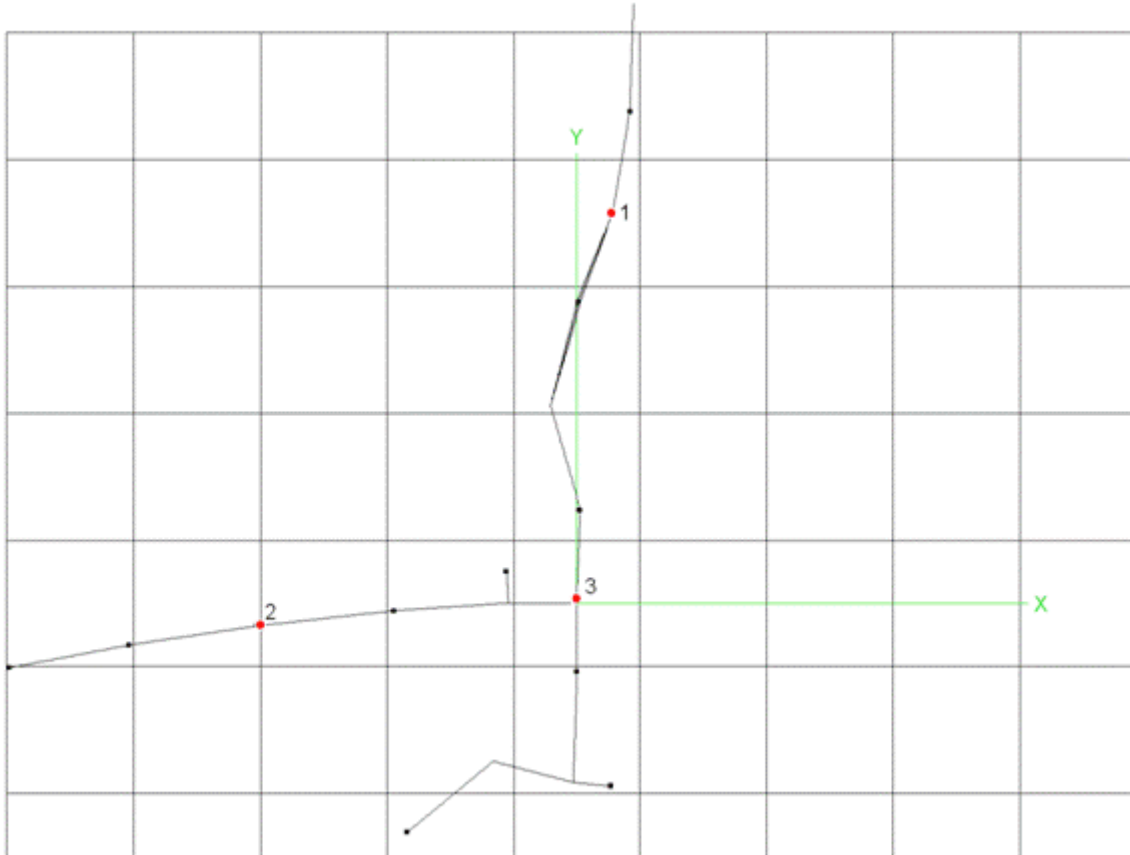


**Figure 4-1: Overhead view of the power line model depicting BPL injection points (red dots). Distribution transformers (impedance loads to neutral) are shown by black dots.**

In selecting the three points to be used, particular attention was paid to the magnitude and geographic extent of the radiated field around the power line structure by initial, wide-area NEC simulations of the magnetic field, as illustrated in Figure 4-2. In part, it may be assumed that the level of such radiation is influenced by the number and type of discontinuities (impedance and topological changes) encountered near each point. This methodology was used in order to better simulate expected radiation levels over a range of operating conditions and power line configurations.

#### **4.2.2 Simulation Frequencies**

For both narrowband and wideband cases, simulations were conducted at 2 MHz intervals including the lower and upper bounds of each band. The 4 MHz narrowband signals, centered at 4, 8, 12, 16, 20, 24 and 28 MHz, were simulated at three frequency points (lower bound, midband and higher bound), while wideband signals were simulated at 10 frequency points, from 4 to 22 MHz. The frequencies and midband points are detailed in Table 4-1.

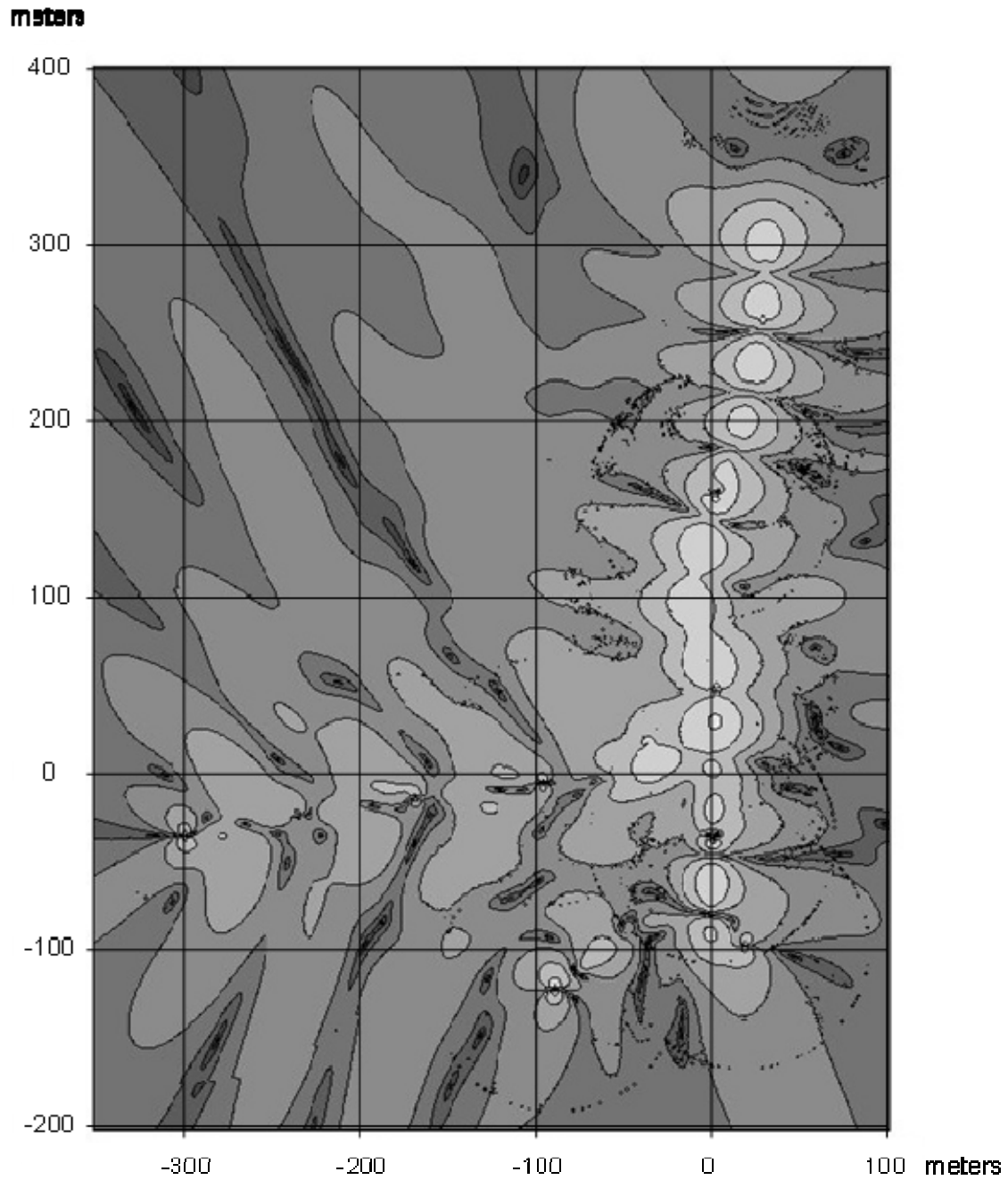


**Figure 4-2: X-axis (horizontal) magnetic field due to BPL-energized power line (4 MHz), one meter off the ground, excited at point “3” and depicted in overhead view. Lighter shades represent stronger fields.**



**Table 4-1: NEC simulation frequencies**

<b>Frequency Band (MHz)</b>	<b>Midband Frequency (MHz)</b>	<b>Simulation Frequencies (MHz)</b>
<b>Narrowband Case</b>		
2-6	4	2, 4, 6
6-10	8	6, 8, 10
10-14	12	10, 12, 14
14-18	16	14, 16, 18
18-22	20	18, 20, 22
22-26	24	22, 24, 26
26-30	28	26, 28, 30
<b>Wideband Case</b>		
4-22	13	4,6,8,10,12,14,16,18,20,22

### 4.2.3 Part 15 Scaling

#### 4.2.3.1 Measurement points

As discussed previously, the rules adopted by the FCC specify measurement locations along the power line under two broad conditions: narrowband signals and wideband signals. For the narrowband case, measurement points are defined at the BPL energizing device, and  $\frac{1}{4}$ ,  $\frac{1}{2}$ ,  $\frac{3}{4}$ , and 1 wavelength of the midband frequency away from the device down the power line. For the wideband case, the measurements are to continue down the power line at midband  $\frac{1}{2}$  wavelength intervals, until the total measurement distance exceeds  $\frac{1}{2}$  wavelength at the lowest frequency.

Lines parallel to and 10 meters away from, the power line segments were derived from the model layout, and measurement points along those lines were identified. For the wideband case, 4 MHz was assumed to be the lowest operating frequency (corresponding to a wavelength of 74.95 meters), with a midband frequency of 13 MHz (23.06 meter wavelength). As Table 4-2 illustrates, the measurement regime indicates measurements in this case should be made at points out to 2 wavelengths distant at the midband frequency from the BPL device.

**Table 4-2: Distances down the line from BPL device for wideband-case Part 15 measurement points**

<b>Wavelength from BPL Device</b>	0	1/4	1/2	3/4	1	1 1/2	2
<b>Distance Down Power Line (m)</b>	0	5.765	11.531	17.296	23.06	34.592	46.123

For the narrowband case, simulations were run at locations along the power line appropriate for each band's midband frequency (Table 4-3).

**Table 4-3: Distances down the line from BPL device for Part 15 measurement points in narrowband case, by frequency**

Narrowband Center Frequency (MHz)	Distance Down Power Line, by Wavelength (m)				
	0	1/4	1/2	3/4	1
4	0.000	18.738	37.475	56.213	74.950
8	0.000	9.369	18.738	28.106	37.475
12	0.000	6.246	12.492	18.738	24.983
16	0.000	4.684	9.369	14.053	18.738
20	0.000	3.748	7.495	11.243	14.990
24	0.000	3.123	6.246	9.369	12.492
28	0.000	2.677	5.354	8.030	10.707

Coordinates for points along the power line, 10 meters distant from the line (as specified in the BPL Report and Order, Appendix C) were calculated at the distances from the BPL injection device as specified above. Exceptions to this scheme were points at which a power line “T” branch or end caused a calculated point to be closer or farther than 10 meters from the power line. When these points were encountered, simulation results were not used.

**4.2.3.2 Scaling output power to meet FCC Part 15 limits**

Initial NEC simulations were used to determine the power output of each modeled BPL device that would meet Part 15 limits using the adopted BPL measurement guidelines. For the frequencies considered in this analysis (all below 30 MHz), the FCC Part 15 radiated emissions limit,  $E_{30m}$ , is specified as 30  $\mu\text{V/m}$  at 30 meters horizontal distance.<sup>[53]</sup> To adjust electric field strength levels computed at the 10 meter distance specified in the Access BPL measurement guidelines, the slant range between the power line and measurement point must be used in conjunction with a 40 log correction factor. With the modeled power line height of 12 meters and measurement point height of one meter, the slant range adjustment results in an extrapolated limit at 10 meters as shown below using Equations 2-2 and 2-3.

$$E_{10m} = E_{30m} \cdot 10^{\frac{40 \cdot \log_{10} \left( \frac{30m}{\sqrt{(12m-1m)^2 + 10m^2}} \right)}{20}} \approx 122.2 \mu\text{V/m}$$

For all frequencies below 30 MHz, the Part 15 measurement bandwidth is specified as 9 kHz.

The BPL energized power line radiation was simulated for the wideband case at the specified frequencies within the band (See Table 4-1). Magnetic field values at the geographic measurement points specified in the Part 15 measurement guidelines for Access BPL systems were calculated and converted to electric field values following Equation 2-1. The maximum of these electric field values calculated by NEC over all

measurement points and frequencies ( $E_{\max}$ ) was subsequently divided by  $E_{10m}$  to obtain a scaling factor, “A”, used to scale the electric field strength data in the wideband case.

$$A = \frac{E_{\max}}{E_{10m}} \quad (\text{Equation 4-1})$$

For the narrowband case, simulations were run for all specified frequencies within each band to determine the magnetic field values at the appropriate measurement points for each band (See Table 4-1). As with the wideband case, all values were converted to electric field values, and the maximum electric field value at any measurement point and frequency for each band was divided by  $E_{10m}$  to obtain the scaling factor, A, for each band.

#### **4.2.4 Simulation of Potential Interference**

After scaling the output power to meet the Part 15 limits for each frequency, bandwidth case, and BPL device location, the interference potential for each situation was simulated. Field-strength values were obtained from simulations both along and away from the modeled power line. From these results, noise floor level increases for a simulated land-mobile receiver located on a road next to the power line were calculated. Additionally, PFD calculations were carried out to determine the possible impact upon a radar receiver at a large distance from the power line.

##### **4.2.4.1 Ambient noise levels**

Noise levels calculated for this analysis were median values for the location in question over time of day and season. To simulate the local (*i.e.*, private residence) BPL operating conditions under which land mobile receivers might encounter BPL signals, the residential manmade noise conditions shown in Table 4-4 were used. As in the NTIA’s Phase 1 Study, ambient noise was calculated using the Institute for Telecommunication Sciences NOISEDAT computer program.<sup>[54]</sup> A bandwidth of 2.8 kHz was used consistent with that of a land mobile receiver.

**Table 4-4: Ambient noise power, by frequency, in a 2.8 kHz bandwidth**

<b>Frequency (MHz)</b>	<b>Noise Power, <math>N_{dBW}</math> (dBW)</b>
2	-104.28
4	-112.08
6	-116.98
8	-121.03
10	-124.13
12	-126.28
14	-128.28
16	-130.08
18	-131.63
20	-132.93
22	-134.13
24	-135.18
26	-136.13
28	-137.03
30	-137.83

#### **4.2.4.2 Simulation of increased noise levels along an overhead power line**

NTIA analyzed the noise floor increase that may be experienced by a land mobile radio operating in close proximity to a BPL-energized MV overhead power line. The analysis was undertaken to compute the percentage of points along the power line that experienced a given increase in the noise floor above the ambient level.<sup>[55]</sup> To accomplish this, NTIA ran NEC simulations to obtain electric field values around the modeled power line. The points at which the electric field was calculated were in the path of roads found along the actual power line upon which the model was based, as shown in Figure 4-3. Electric field strength values were computed at two meters off the ground to simulate the height of a vehicle-mounted land mobile radio antenna, and at one meter increments along the path. The land mobile radio system was assumed to be using a vertical whip antenna. Accordingly, only the z-axis (vertical) electric field values were used.

The path around the modeled power line along which electric field strength values were calculated varied in distance from the power line. Along one section of the modeled power line, the horizontal distance from the power line to the center of the road was approximately 3 meters, and ranged from 30 to 48 meters along another section. The path along which calculations were performed passed under a branch of the power line model at one point (Figure 4-3).

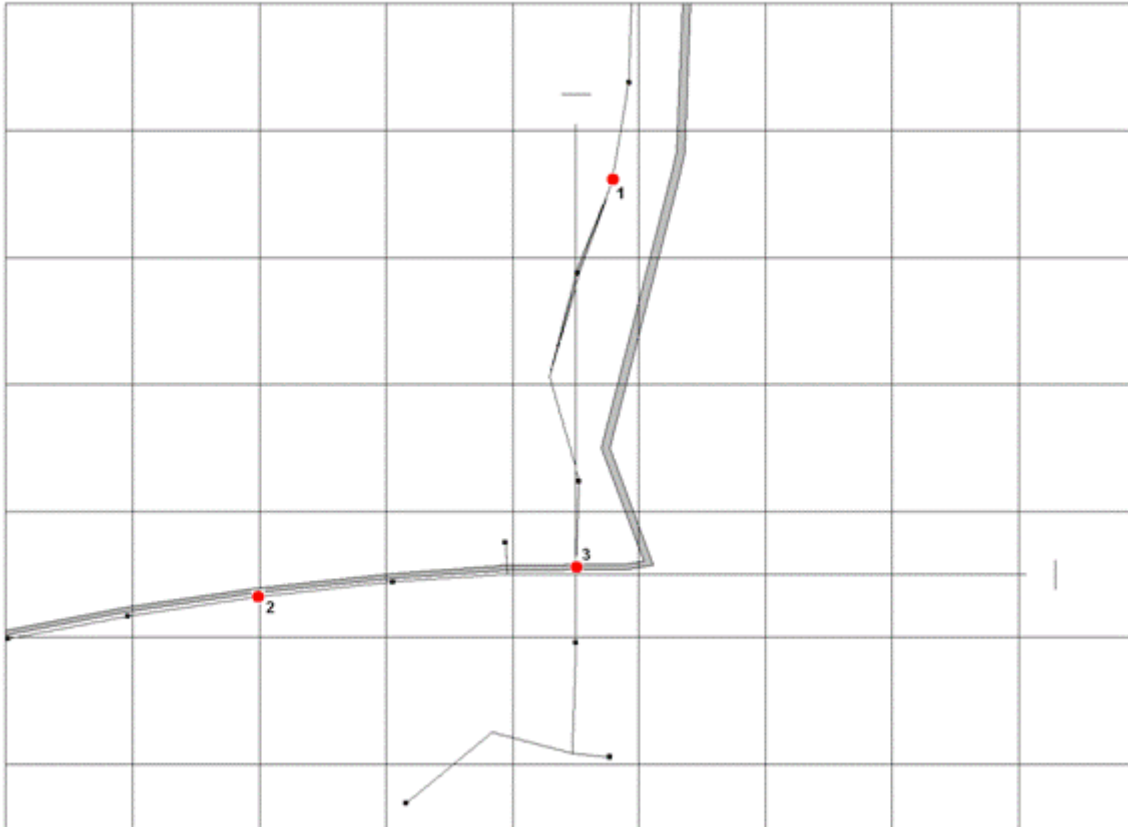


**Figure 4-3: Path of along-the-line land mobile simulations (thick grey line). This path corresponds to that followed by actual road next to the power that the model is based on, depicted in overhead view.**

Once derived, the electric field values were translated into received interfering signal power using Equation 4-2.

$$P = 20 \cdot \text{Log}_{10} \left( \frac{E}{A} \right) - 20 \cdot \text{Log}_{10}(F) + G_r + 10 \cdot \text{Log}_{10}(BW) + 10 \cdot \text{Log}_{10}(\phi) + \delta + 128 \quad (\text{Equation 4-2})$$

where

- $P$  is received BPL signal power, in dBW;
- $E$  is the calculated vertical electric field strength, in V/m;
- $A$  is the Part 15 electric field scaling factor determined for the narrowband case, and for the wideband case, as described in Section 4.2.3.2;
- $F$  is the measurement frequency, in MHz;
- $G_r$  is the gain of the receiving antenna, in dBi;
- $BW$  is the ratio of receiver to measurement bandwidth;
- $\phi$  is the average duty cycle; and
- $\delta$  is a quasi-peak to RMS measurement factor.

As in NTIA’s Phase 1 Study, the average duty cycle ( $\phi$ ) was taken to be 55 percent, which was midway between an always-on (100 percent) downstream signal and an intermittent (10 percent) upstream customer-to-internet signal. The gain ( $G_r$ ) of the receiving antenna was taken to be a constant 0 dBi across all frequencies, and the ratio of receiver bandwidth to measurement bandwidth (BW) was 2.8 kHz to 9 kHz, respectively. Finally, to compensate for differences between ambient noise levels expressed in RMS values and BPL signal radiation measured using quasi-peak detection, a measurement factor ( $\delta$ ) adjustment of -2 dB was applied to the calculated received BPL signal power.<sup>[56]</sup>

The increase in the noise floor due to BPL emissions, or  $(I+N)/N$ , was calculated using Equation 4-3.

$$\frac{(I+N)}{N} = 10 \cdot \text{Log}_{10} \left[ 1 + 10^{\frac{P-N}{10}} \right] \quad \text{(Equation 4-3)}$$

where

- $P$  is the received BPL signal power, in dB, from Equation 4-2;
- $N$  is the ambient noise power, in dB; and
- $I$  is the interfering signal, in dB.

The results of these calculations are used to determine the percentage of geographic locations that exceed given thresholds of noise floor increase.

#### 4.2.4.3 Simulation of PFD levels away from an overhead power line

NTIA analyzed the PFD levels due to BPL emissions that may be seen by fixed receivers, such as OTH radar receivers, at increasing distances from the power line structure used in this case study. Both NEC and ITM were used to derive PFD values at 1 km intervals on radials extending out from the power line injection points. The radials were spaced 1 degree apart, for a total of 360 radials, and extended from 1 to 50 km from the origin.

Electric field strength values were calculated first using Equation 4-4 along each radial at 42.7 meters height, the height of the assumed receiver antenna. NEC calculations were performed to a distance of 10 km from the origin, a distance chosen to minimize variations due to the large size of the power line layout and diffraction effects due to the curvature of the earth. Beyond 10 km, ITM was used to calculate the basic transmission loss due to distance separation and diffraction of the RF signal over a spherical earth.

$$E_{\text{max}}(r) = \sqrt{E_r^2 + E_\theta^2 + E_\phi^2} \quad \text{for } 1 \text{ km} \leq r \leq 10 \text{ km} \quad \text{(Equation 4-4)}$$

where

- $E_{SUM}$  is electric field strength vector, in V/m;
- $E_z$  is the z-axis (vertical) component of electric field, in V/m;
- $E_\phi$  is the phi-axis (perpendicular to radial and z-axis) component of electric field, in V/m; and
- $E_\rho$  is the rho-axis (along the radial) component of electric-field, in V/m.

The PFD was then derived from  $E_{SUM}$  using Equation 4-5.

$$PFD_{NEC}(\rho) = 10 \cdot \text{Log}_{10} \left[ \frac{\left( \frac{E_{SUM}(\rho)}{A} \right)^2}{120 \rho} \right] + 10 \cdot \text{Log}_{10} \left( \frac{1}{BW} \right) \quad \text{for } 1 \text{ km} \leq \rho \leq 10 \text{ km} \quad \text{(Equation 4-5)}$$

where

- $A$  is the Part 15 electric field scaling factor determined for the narrowband case, and for the wideband case, as described in Section 4.2.3.2;
- $BW$  is the specified Part 15 measurement bandwidth (9 kHz for signals below 30 MHz); and
- $PFD_{NEC}$  is the power flux density computed at various distances,  $\rho$ , along the radials, in dBW/m<sup>2</sup>-Hz.

ITM transmission loss data and the PFD values at 10 km were combined to calculate PFD values from 10 km out to 50 km. The ITM results used the same ground parameters as NEC, and the same power line height of 12 meters and an assumed receiver antenna height of 42.7 meters.<sup>[57]</sup> ITM input parameters are detailed in Table 4-5.

**Table 4-5: ITM input parameters**

<b>Input Variable</b>	<b>Value</b>
Frequency	2-30 MHz in 2 MHz steps
Antenna Heights	Transmitter – 12 m, Receiver – 42.7 m
Siting Criteria	Transmitter – Random, Receiver – Very Careful
Terrain Irregularity Factor, $\Delta h$	30 m
Polarization	Horizontal
Relative Permittivity	15
Ground Conductivity	0.005 S/m
Climate	Continental Temperate
Surface Refractivity	301 N-units
Percent Time	50.0%
Percent Location	50.0%
Percent Confidence	50.0%
Mode of Variability	Individual

To determine the PFD values accounting for diffraction losses that come into play at large distances from the power line, the transmission losses beyond 10 km calculated by ITM were scaled relative to the value that ITM computed at 10 km (Equation 4-6). Within 10 km of the power line, the adjusted PFD was the same as the PFD computed using NEC electric field strength directly (Equations 4-5 and 4-7a). Beyond 10 km, the scaled ITM loss values, at each distance, and the PFD computed at 10 km from NEC were used to compute the adjusted PFD (Equation 4-7b).

$$\text{ScaledLoss}_{ITM}(\rho) = \text{Loss}_{ITM}(\rho) - \text{Loss}_{ITM}(10 \text{ km}), \text{ for } \rho \geq 10 \text{ km}$$

(Equation 4-6)

$$\text{PFD}_{\text{Adjusted}}(\rho) = \text{PFD}_{\text{NEC}}(\rho), \text{ for } 0 \leq \rho < 10 \text{ km}$$

(Equation 4-7a)

$$\text{PFD}_{\text{Adjusted}}(\rho) = \text{PFD}_{\text{NEC}}(10 \text{ km}) - \text{ScaledLoss}_{ITM}(\rho), \text{ for } \rho \geq 10 \text{ km}$$

(Equation 4-7b)

### 4.3

## RESULTS

A summary of the simulation conditions described in Section 4.2 is provided in Table 4-6. The results for computing the receiver noise floor increase along the simulated power line are provided in Section 4.3.1. The results for analyzing the PFD the might be seen by a fixed receiver located at some distance away from the power line are described in Section 4.3.2.



**Table 4-6: Simulation conditions**

<b>Overhead Power Line Model</b>	
Conductors	3 power conductors, catenary wiring between simulated power pole locations. Multi-grounded neutral conductor. Primarily vertical orientation, switching to horizontal at one location. Four simulated risers connecting to simulated underground load.
Conductor Material	Copper
Conductor Thickness	12.6 mm (approx. AWG 4/0)
Conductor spacing	0.6 m with neutral conductor 1.2 m below
Model Size	328.2 m in the 'x' direction, 435 m in the 'y' direction
Height above ground	Power conductors at 12 m with neutral wire at 9.6m
Coupler location	A coupler was simulated roughly halfway down each of the two main branches and another at the junction of these branches
Source	1 Volt in series
Load	7 simulated transformer loads ( $3 \Omega + 5 \mu\text{H}$ ) between power conductors and neutral. Risers had simulated $30 \Omega$ loads between power conductors and ground.
BPL average duty cycle	55%
QP-to-RMS conversion	-2 dB
<b>Ground Conditions</b>	
Conductivity	$\sigma = 0.005 \text{ S/m}$
Relative permittivity	$\epsilon_r = 15$
<b>Simulation Frequencies</b>	
Land Mobile Receiver	2 -30 MHz
Fixed (e.g., OTH Radar)	2 - 30 MHz
<b>Receiver Antenna</b>	
Land Mobile	Vertical Whip
Gain towards power line	0 dBi
Height	2 m
Fixed (e.g., OTH Radar)	
Gain towards power line	0 dBi
Height	42.7 m
<b>Noise Conditions</b>	
Residential, as per Table 4-4	
<b>Land Mobile Simulation</b>	
For Noise Floor Increase ((I+N)/N) Analysis	
Victim Receiver Location	Center of simulated roadway
Power Line Branch	Parallel to x-axis
Dist. From Power Line	3 m
	Parallel to y-axis
	Ranging from 30 to 48 m

<b>ITM Conditions</b>	<b>For PFD Analysis</b>	
Frequency	2 – 30 MHz	
	Transmitter (Power line)	Receiver (Fixed)
Antenna Heights	12 m	42.7 m
Siting Criteria	Random	Very Careful
Terrain Irregularity Factor, $\Delta h$	30 meters	
Polarization	Horizontal	
Relative Permittivity	15	
Ground Conductivity	0.005 S/m	
Climate	Continental Temperate	
Surface Refractivity	301 N-units	
Percent Time	50.0%	
Percent Location	50.0%	
Percent Confidence	50.0%	
Mode of Variability	Individual	

### **4.3.1 Receiver Noise Floor Increase Along the Power Line**

Results were considered from simulations of potential interference to a land mobile receiver on roads next to the simulated power line for all three BPL device injection points across both narrowband and wideband systems, and across frequencies in the 2 to 30 MHz range. The results are presented in terms of the percentage of points along the BPL energized power line that increased the receiver noise floor by various levels.

#### **4.3.1.1 Receiver noise floor increase relative to the injection point**

The results shown in Figures 4-4 and 4-5 illustrate the percentage of simulated points along the modeled power line that result in a given level of noise floor increase for all simulation frequencies shown in Table 4-1 for narrowband and wideband BPL signals, respectively. These figures show that the percentage of locations resulting in a given increase in the noise floor varied somewhat by injection point.

The most notable feature of the data is the sharp divergence in the percentage of points for a noise floor increase of 30 dB or more seen by the three modeled injection points. The close proximity of Injection Point 2 to the road and to a modeled transformer load likely accounts for the highest percentages of locations exceeding a 30 dB increase in the noise floor. Injection Point 3 is positioned close to the intersection of three power lines, but at least one utility pole away from nearby transformer loads. This may also have resulted in the increase in the receiver noise floor associated with this point being greater than that of Injection Point 1. Injection Point 1 was located farthest away from the street in this model, and one or more utility poles away from any discontinuities such as transformer loads.

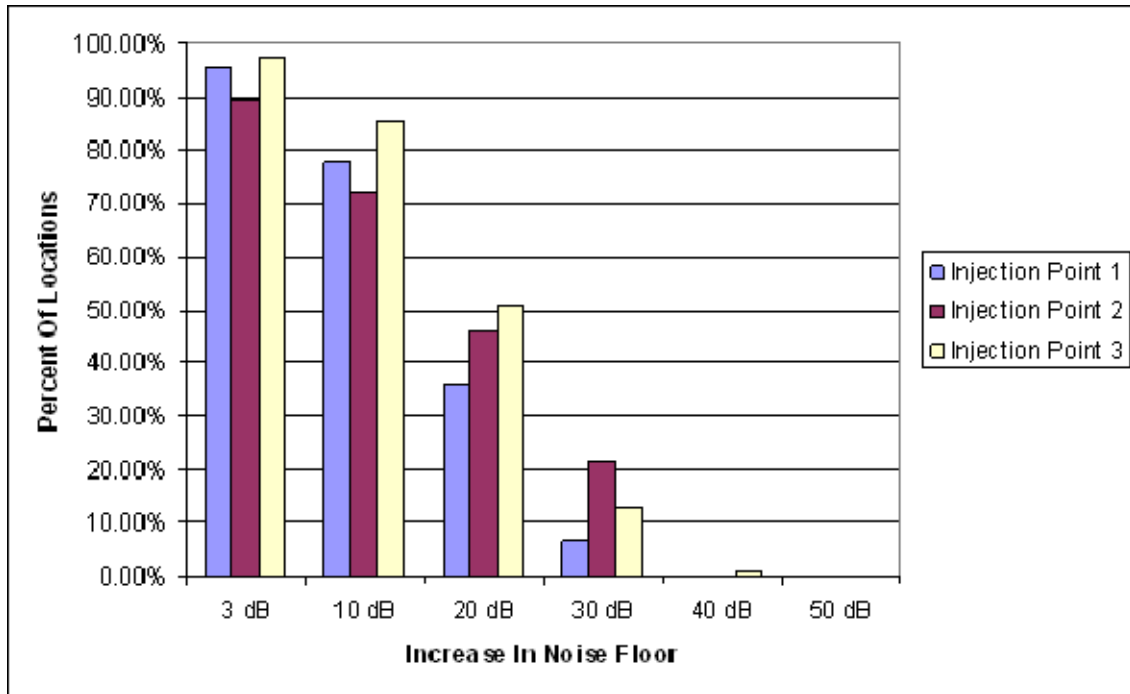


Figure 4-4: Increase in receiver noise floor  $[(I+N)/N]$  as a function of the percentage of measurement points around the power line for narrowband BPL signals

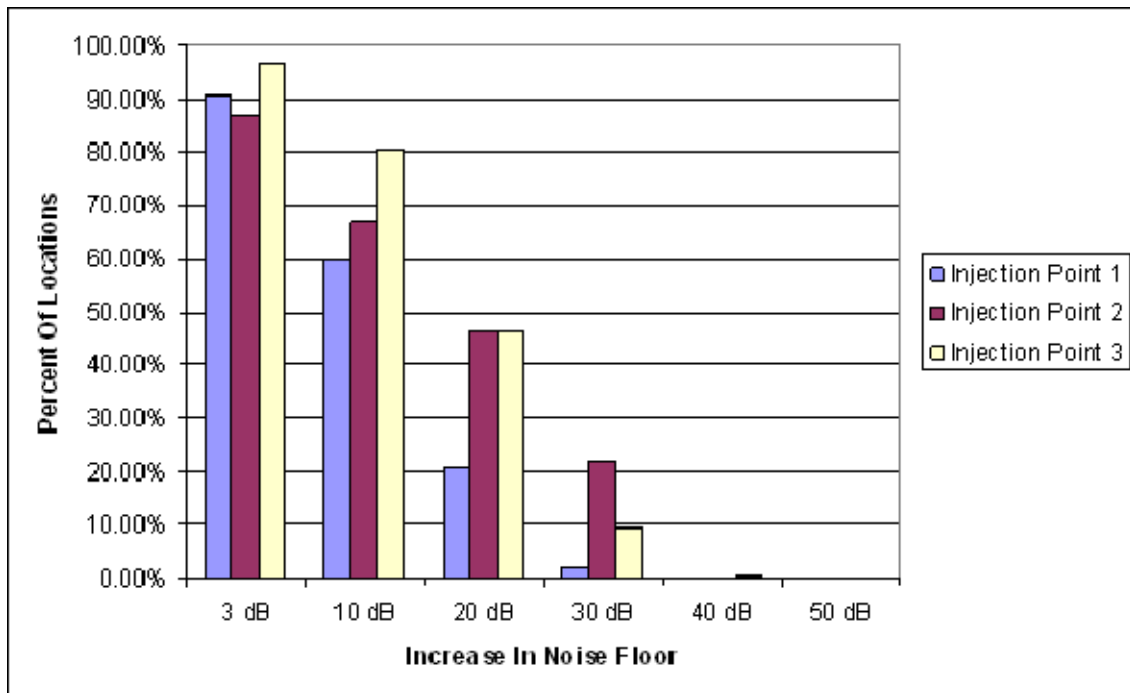


Figure 4-5: Increase in receiver noise floor  $[(I+N)/N]$  as a function of the percentage of measurement points around the power line for wideband BPL signals

#### 4.3.1.2 Receiver noise floor increase as a function of frequency

For both narrowband and wideband BPL signals, variation was noted in the calculated results over frequency. Table 4-6 shows the results for narrowband signals and Table 4-7 shows results for wideband signals based on simulations for Injection Point 3.

**Table 4-6: Percentage of simulated points along the power line at which the receiver noise floor was increased by at least the specified amount for narrowband BPL signals**

Frequency Band (MHz)	Noise Floor Increase (dB)					
	3	10	20	30	40	50
2-6	95.22%	67.97%	34.29%	9.50%	0.00%	0.00%
6-10	95.83%	80.59%	38.81%	4.78%	0.00%	0.00%
10-14	97.39%	82.30%	47.41%	12.57%	0.00%	0.00%
14-18	98.94%	87.53%	61.04%	20.97%	2.46%	0.00%
18-22	98.94%	92.86%	63.90%	20.76%	1.56%	0.00%
22-26	98.49%	90.60%	49.17%	5.68%	0.00%	0.00%
26-30	99.20%	95.22%	60.78%	14.98%	0.00%	0.00%

**Table 4-7: Percentage of simulated points along the power line at which the receiver noise floor was increased by at least the specified amount for wideband BPL signals**

Mid-band Frequency (MHz)	Noise Floor Increase (dB)					
	3	10	20	30	40	50
4	93.51%	56.71%	22.02%	1.81%	0.00%	0.00%
6	88.99%	60.94%	28.66%	0.00%	0.00%	0.00%
8	99.40%	87.03%	43.59%	3.62%	0.00%	0.00%
10	95.78%	81.75%	37.71%	3.17%	0.00%	0.00%
12	96.08%	79.49%	50.38%	7.69%	0.00%	0.00%
14	98.19%	78.58%	47.96%	14.78%	0.00%	0.00%
16	98.04%	82.20%	42.53%	0.60%	0.00%	0.00%
18	99.70%	97.89%	82.81%	39.06%	4.68%	0.00%
20	98.64%	92.91%	61.24%	11.46%	0.00%	0.00%
22	98.34%	86.73%	46.30%	10.86%	0.00%	0.00%

#### 4.3.2 Power Flux Density Away from the Power Line

The away-from-the-line analysis computed the PFD seen by a fixed receiver, such as an OTH radar receiver, as a function of distance of the receiver from the modeled Access BPL system. The PFD as a function of distance was determined for the three modeled BPL injection points and frequency bands for narrowband and wideband BPL signals. In considering these results, NTIA looked at median values for both narrowband and wideband BPL signals across radials leading away from the power line model and across the 2 to 30 MHz frequency band.

Figures 4-6 and 4-7 depict median PFD versus distance from the origin for all simulated in-band frequencies for the three BPL injection points described in Section

4.2.2. Variation in PFD as a function of horizontal distance for the different injection points on the structure was very small and did not exceed 3 dB at any given distance from the power line model.

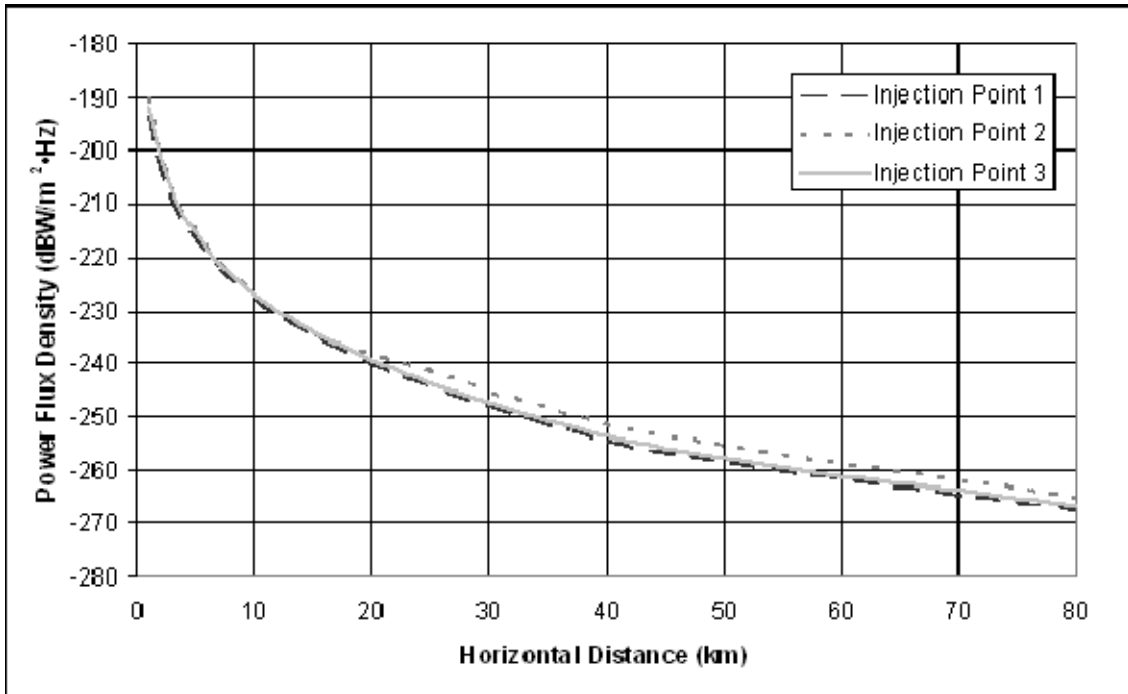
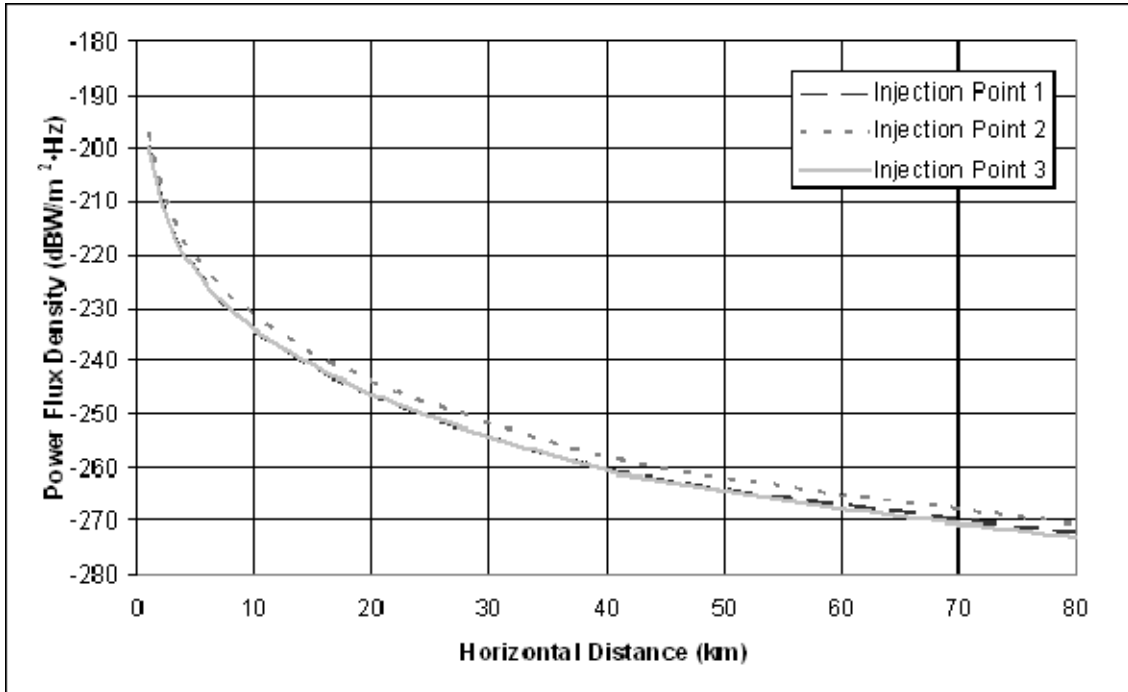


Figure 4-6: Power Flux Density as a function of distance from the origin for narrowband BPL signals across all simulated in-band frequencies



**Figure 4-7: Power Flux Density as a function of distance from the origin for wideband BPL signals across all simulated in-band frequencies**

When considering frequency as a factor, the median (with respect to azimuth) PFD results from Injection Point 3 as a function of distance take on more variation. As shown in Figures 4-8 and 4-9 for the narrowband and wideband BPL signals, respectively, the maximum variation as a function of frequency was approximately 13 dB at 1 km distance for narrowband BPL signals and nearly 15 dB at 4 km distance for wideband BPL signals.

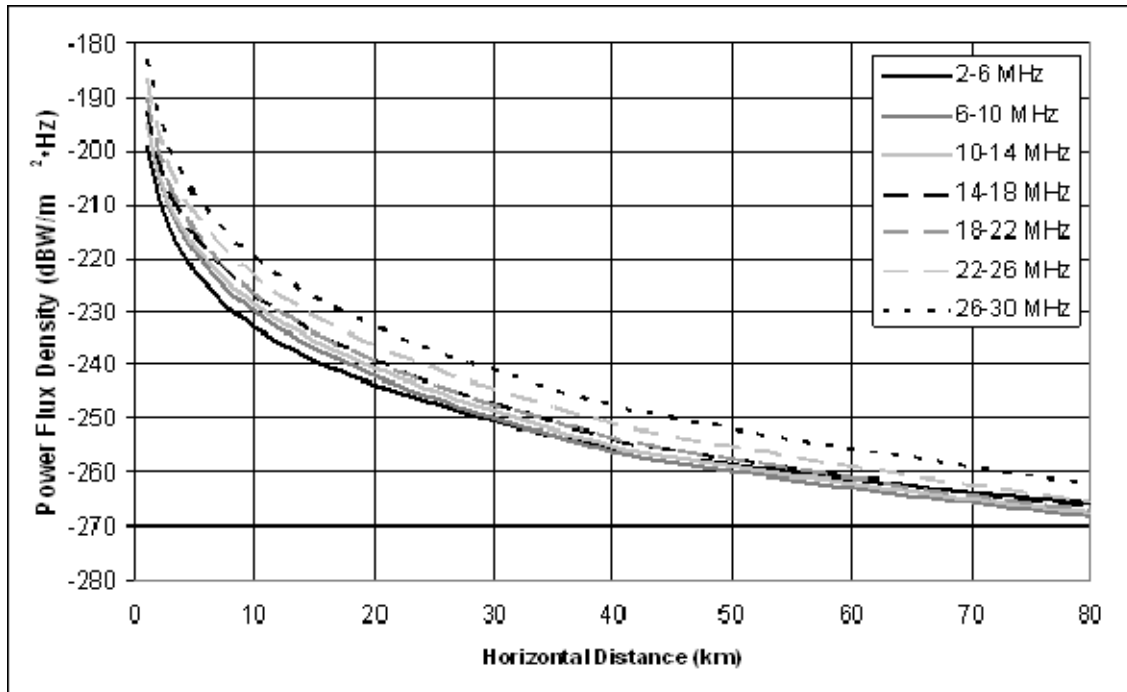


Figure 4-8: Power Flux Density as a function of distance from Injection Point 3 for narrowband BPL signals, organized by frequency band

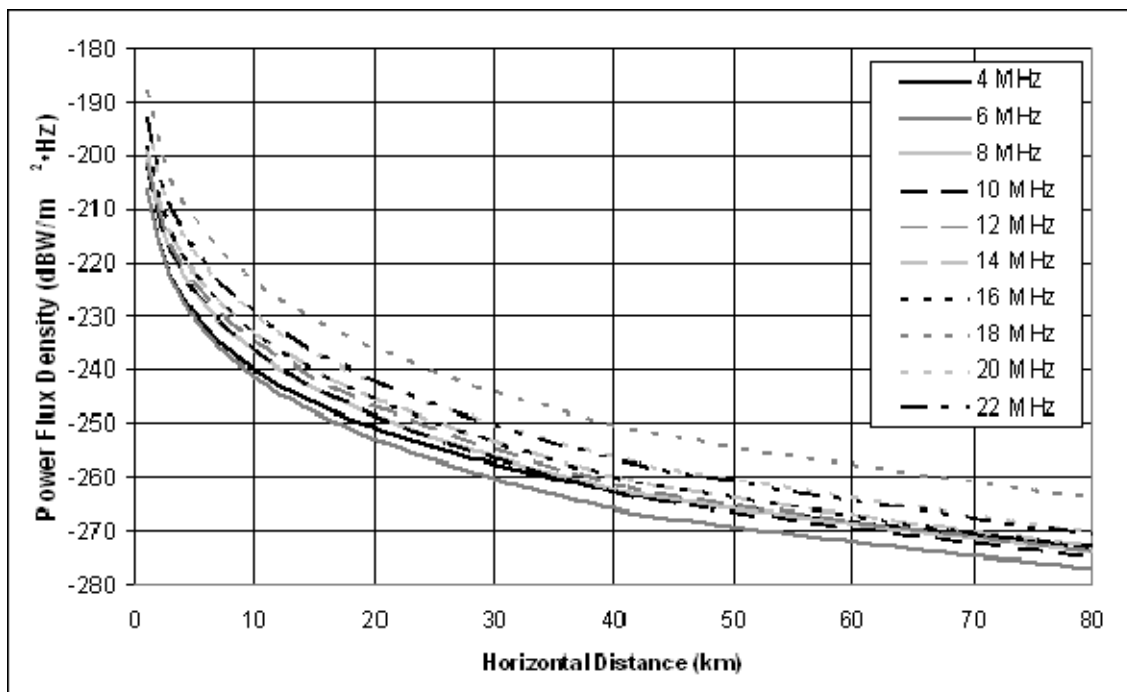


Figure 4-9: Power Flux Density as a function of distance from Injection Point 3 for wideband BPL signals, organized by frequency

For the narrowband BPL signals shown in Figure 4-8, the PFD level at any given distance tends to increase as the frequency band increases. This trend results primarily

from increasing radiated power as frequency increases. In other words, the total radiated power of this model tends to increase as frequency increases, while still meeting the Part 15 electric field strength limit as measured using the Commission's measurement guidelines. For wideband BPL signals, where Part 15 scaling relies on the measurement locations associated with the midband frequency (Table 4-2), the estimate of electric field strength for some individual frequencies may be somewhat less accurate. This may be observed in the variability of PFD levels for each frequency band shown in Figure 4-9, where the calculated PFD levels do not consistently increase with frequency.

#### **4.4 SUMMARY**

The NTIA case study illustrates application of the Commission's Part 15 rules and measurement guidelines for Access BPL systems. NTIA analyzed the potential impact on mobile radiocommunication systems close to an overhead BPL-energized power line emitting RF energy at the Part 15 limit, as well as to fixed radiocommunication systems, (such as OTH radars) at great distances from the line. While previous analyses made use of simple power line models, this case study employed an elaborate power line model that included a variety of features found in an actual MV power distribution system carrying BPL signals.

The results of this analysis are comparable to those found in NTIA's earlier investigations, and indicate that the Part 15 measurement procedures described in the BPL Report and Order appear to estimate adequately the electric field strength levels around the power line near ground level.<sup>[58]</sup>



## **SECTION 5**

# **IONOSPHERIC PROPAGATION AND AGGREGATION OF BPL EMISSIONS**

### **5.1 INTRODUCTION**

Thus far, NTIA's Phase 2 Study regarding BPL interference potential has focused on local interference due to a small quantity of co-frequency BPL devices. Of additional interest, however, is the potential effect of a large scale BPL deployment on aggregate noise levels over a national scale. An aggregate effect from BPL interference, if any, would occur due to ionospheric or "sky wave" propagation.

This sky wave phenomena, in which HF signals are refracted by charged particles in the ionosphere and returned to earth hundreds or thousands of miles away, is the same process through which short wave communications can be heard around the globe. Since current BPL systems make use of HF frequencies, and since modeling of BPL-energized power lines indicates much of the BPL emissions appear to radiate in an upward direction, these HF BPL emissions have the potential to travel many miles from their source. Moreover, because a given listening point may receive radiated BPL emissions from many sources, it is conceivable that an aggregation of signals could occur, raising the receiver noise floor level and rendering weak, desired signals unintelligible. In general, ionospheric propagation occurs for frequencies between 1.7 MHz and 30 MHz, as discussed in the NTIA Phase 1 Study.<sup>[59]</sup>

The analysis presented in this section expands upon and clarifies results presented in the NTIA Comments on the BPL NPRM.<sup>[60]</sup> These results have been augmented by additional modeling and application of the measurement guidelines released in the Commission's BPL Report and Order.

### **5.2 ANALYTICAL MODELING OF SKY WAVE PROPAGATION**

#### **5.2.1 Background**

In its BPL comments, NTIA detailed a preliminary analysis of aggregation of BPL emissions via ionospheric propagation. That analysis employed the VOACAP HF statistical propagation prediction software and overhead power line models using the NEC software. The goal of that effort was to obtain a preliminary determination as to whether noise-like BPL emissions, propagated by ionospheric refraction and aggregated at a point, could present a viable interference concern.

NTIA's initial ionospheric aggregation analysis consisted of two parts: an effort to determine probable "worst-case" conditions for aggregation, and a set of simulations

of widespread BPL deployments on overhead MV power lines and possible aggregation effects.

To estimate worst-case aggregation conditions, point-to-point VOACAP propagation calculations were used between several sites in North America over a wide range of times of day, months of the year and frequencies. NTIA then selected the conditions that produced the highest signal-to-noise levels at the various receive points to simulate widespread aggregation.

NTIA's aggregation simulation employed VOACAP in its "area" mode to calculate aggregate emissions received at multiple points from widespread BPL deployments. In the geographic center of every county in the United States, NTIA placed effective BPL emitters, each representing the total BPL emissions from its respective county. In the NTIA Comments, the power output of each effective BPL emitter was derived from NEC modeling of a simple overhead power line model described in the NTIA Phase 1 Study.<sup>[61]</sup> The model consisted of three 340-meter-long straight wires terminated together at the ends through impedances. In that report, NTIA calculated the radiated power output from the straight-wire power line model which would result in electric fields that met Part 15 limits, and the result was scaled by NTIA's deployment model and county population to arrive at the power output of each effective BPL emitter. The emitters were then given frequency-dependent, far-field radiation patterns based upon an elaborate overhead power line model developed using the NEC software.<sup>[62]</sup>

Propagation simulations were sequentially run for each emitter to a fixed grid of receive points covering CONUS, and the results were summed in the power domain. NTIA ran these simulations for the suspected worst-case sets of conditions derived from the point-to-point simulations described above.

This preliminary analysis led NTIA to conclude potential interference due to ionospheric aggregation of BPL signals was not a near-term challenge.

## **5.2.2 Approach**

### **5.2.2.1 Power Line Models**

For this report, NTIA determined new radiated power levels for each effective BPL emitter using the elaborate overhead power line model. Additionally, these power levels were calculated using the new measurement guidelines adopted in the BPL Report and Order.<sup>[63]</sup> Thus, the new simulations were based entirely upon the elaborate overhead power line model, rather than a combination of this model and the simplified power line model from NTIA's Phase I Study. This new approach resulted in different (but comparable) radiated power levels than those used in the NTIA Comments. Table 5-1 shows the values of radiated power as a function of frequency used in this study, along with the values previously presented in the Technical Appendix to the NTIA Comments.

NTIA created an additional NEC model of an underground BPL system (Figures 5-1 and 5-2). Similar propagation analyses were completed over a large sample of hours of the day, frequencies, months of the year and solar conditions (more than 1,300 sets of conditions), including the same conditions that resulted in the greatest aggregated interference-to-noise ratios using the overhead power line model as an emitter. As with the overhead model, NTIA used NEC to derive frequency-dependent directive-gain radiation patterns and radiated power necessary to meet Part 15 limits from the underground model. Radiated power calculations were again performed using the new BPL measurement guidelines in the BPL Report and Order.<sup>[64]</sup> The radiated power levels are listed in Table 5-1.

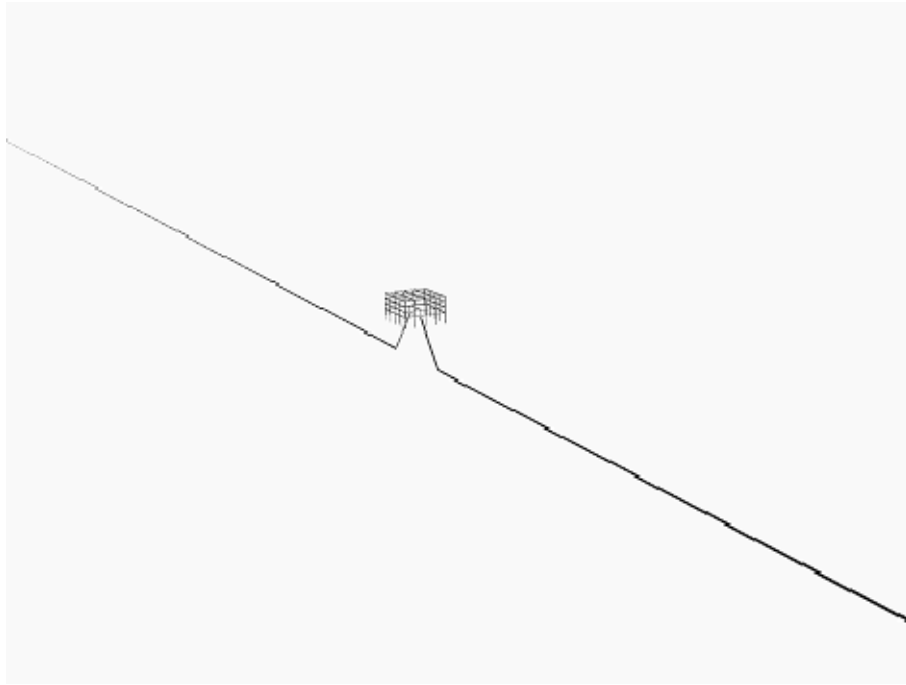


**Figure 5-1: Underground power line model with ground removed. The underground line, comprised of three neutral wires surrounding a dielectric-insulated central wire, extends 340 meters end to end**

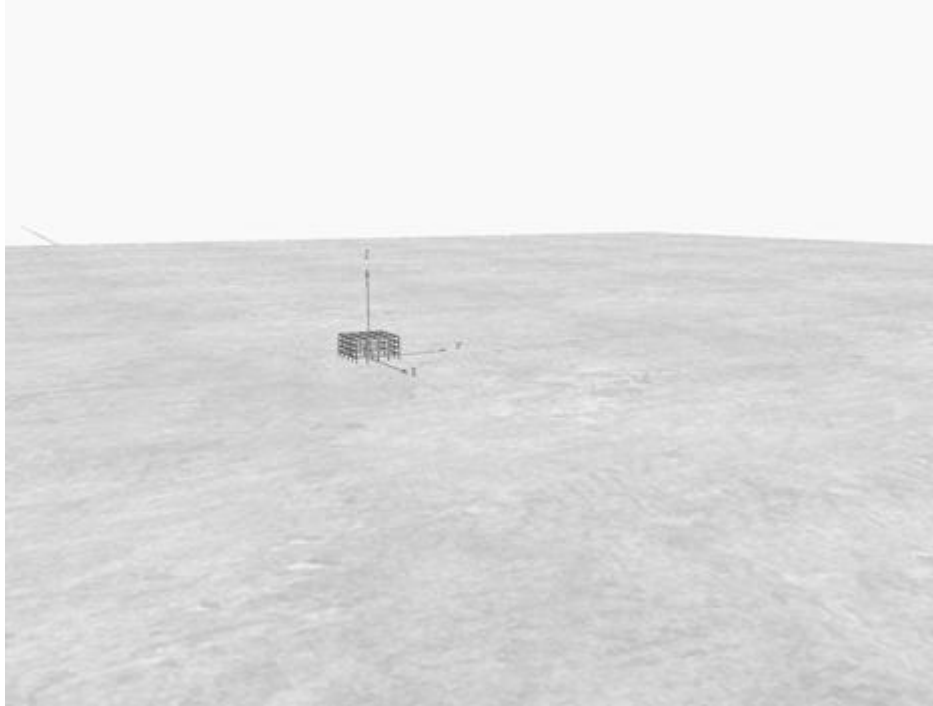


**Figure 5-2: Underground power line model with ground included. The visible wireframe box represents a pad-mounted transformer, in which the BPL source is installed.**

**Table 5-1: BPL structural radiated power at Part 15 limit**

<b>Frequency (MHz)</b>	<b>Radiated Power (dBW/Hz) Overhead (from Technical Appendix)</b>	<b>Radiated Power (dBW/Hz) Overhead</b>	<b>Radiated Power (dBW/Hz) Underground</b>
2	-105.49	-103.04	-94.26
4	-104.87	-106.71	-87.84
6	-104.27	-104.38	-84.66
8	-103.68	-102.99	-82.73
10	-103.11	-102.89	-83.29
12	-102.55	-102.93	-79.38
14	-102.01	-104.06	-78.43
16	-101.49	-106.32	-74.75
18	-100.98	-97.48	-75.16
20	-100.49	-103.48	-79.52
22	-100.01	-104.29	-81.67
24	-99.55	-101.04	-82.24
26	-99.11	-105.71	-82.45
28	-98.68	-100.98	-83.47
30	-98.27	-98.04	-84.28

Greater NEC-calculated radiated power from underground structures is not unexpected, as ground losses subsequently attenuate this power significantly. Thus, it is to be expected that NTIA’s underground model radiated significantly more power than overhead systems while meeting Part 15 limits. With both the overhead and underground

models, increased variability of radiated power with frequency is largely due to the vast increase in complexity of the model used over previous work.

The BPL Report and Order specified that compliance measurements should take place at  $\frac{1}{4}$  wavelength intervals down the power line from the BPL device, to a distance of one wavelength of the mid-band frequency, at a measurement height of one meter.<sup>[65]</sup> To derive the original Part 15 values used in the analysis presented in the NTIA Comments, field strength values were calculated at 0.5 meter intervals along the entire length of the power line. Thus, the new methodology makes use of far fewer points to find peak field strength values around the power line. Nonetheless, the derived radiated power is in remarkable agreement with the previously derived values reported in the Technical Appendix to the NTIA Comments.

The radiated power levels were derived by exciting the NEC models in question using a unit voltage source, finding the magnetic or electric field values through NEC simulation at appropriate points around the models as specified in the BPL measurement guidelines, and scaling all subsequent electric field values by the dividend of calculated electric field divided by the Part 15 limit. To translate the scaling to the power domain, NEC-calculated radiated power levels were scaled by the square of this factor.

#### **5.2.2.2 Use of Voice of America Coverage Analysis Program**

As in the NTIA Comments, NTIA calculated BPL interference and man made noise power values using VOACAP's area mode in a fixed  $31 \times 31$ -point grid of receiving points covering CONUS and centered on Kansas City, Missouri.<sup>[66]</sup> NTIA again assumed BPL deployment densities based in part on U.S. Census data to simulate effective BPL emitters in the geographic center of each county in the United States (including Alaska and Hawaii).<sup>[67]</sup> As before, these emitters were given frequency-dependent directive-gain radiation patterns calculated using the elaborate NEC overhead power line model and located in the geographic center of each county. The radiation patterns used were arithmetically averaged in azimuth to simulate the random orientation of multiple BPL-energized power lines represented by each effective emitter.

In this study, NTIA ran full ionospheric aggregation simulations over a comprehensive set of more than 8,500 sets of conditions (including all months of the year, hours of the day, low and high levels of solar activity and frequencies from 2 to 30 MHz in 2 MHz increments). NTIA used these simulations to calculate the Interference-plus-Noise-to-Noise ratio, or  $(I+N)/N$ , conditions due to large numbers of deployed BPL devices.<sup>[68]</sup> The results presented here were examined in terms of sets of conditions producing worst-case increases to the local receiver noise floor.

VOACAP reports results of propagation in terms of signal-to-noise ratio (SNR). Table 5-2 indicates how the SNR values reported by VOACAP translate into noise floor increases.

**Table 5-2: Noise floor increase [(I+N)/N] as a function of Signal-to-Noise Ratio**

Noise floor increase, (I+N)/N (dB)	SNR (dB)
3	0
1	-5.868
0.5	-9.135
0.1	-16.327
0.05	-19.363
0.01	-26.373
0.005	-29.386

### 5.3 SIMULATION CHARACTERISTICS

NTIA ran simulations both with the Smoothed Sunspot Number (SSN) parameter set to a high value (150) to simulate excellent propagation characteristics during the peak of the 11-year solar cycle, and to a low value (25) to simulate depressed propagation characteristics at the low point in the solar cycle. Because of software design, all receive points used VOACAP's quarter-wave vertical monopole antenna (type 22) over ground with dielectric constant  $\epsilon_r=15$  and conductivity  $\sigma$  set to 0.005 S/m.<sup>[69]</sup> In reality, ground characteristics vary in the United States, ranging from very poor ( $\epsilon_r=3$  and  $\sigma=0.001$  S/m) to excellent ( $\epsilon_r=20$  and  $\sigma=0.030$  S/m).

The manmade noise level was set to remote or quiet rural levels (-164 dBW/Hz at 3 MHz) at all receive points, to best address receiving conditions at many federal sites.<sup>[70]</sup> As with receive-point antennas, software design allows one manmade noise level to be assigned to all receive points in VOAAREA's calculation grid. Actual manmade noise levels in the United States can vary from quiet rural conditions to the very high noise levels that can be found in industrial areas. Furthermore, some preliminary studies now indicate that actual background noise levels at HF frequencies may have increased since benchmark noise studies were completed several decades ago.<sup>[71]</sup>

NTIA individually scaled the NEC-calculated radiated power levels by the number of active BPL devices expected to serve the urban households in each county in the United States. Urban households were used in this analysis as they present greater deployment densities than rural households, and as such, are more likely to be the bulk of early deployments of Access BPL service. As in the earlier analysis, NTIA assumed that a BPL injector had the data handling capacity to support an average of 30 customers, and 1 of 4 urban households was a BPL customer. In other words, one BPL injector was assumed per 120 urban households. With nearly 85 million urban households in the United States, this assumption resulted in a total of over 705,000 modeled BPL devices in this analysis.<sup>[72]</sup>

Several other factors were taken into consideration when predicting the receiver noise floor increase. First, NTIA considered that not all BPL devices will operate at the Part 15 limit; therefore, the average radiated signal was assumed to be 4 dB below the Part 15 limit. Second, the analysis was based on root-mean-square (RMS) values; therefore an adjustment was made to convert the quasi-peak BPL signal level to an RMS level.<sup>[73]</sup> Third, since the devices in the system do not all operate at the same frequency, an allowance of 6 dB was given (*i.e.*, 1 in 4 BPL injectors are assumed to be co-frequency). Finally, the assumed duty cycle of BPL devices was set at a mean of 55 percent. These adjustments to the BPL radiated power levels are listed in Table 5-3.

**Table 5-3: Adjustment Factors for Access BPL Devices**

Factor	Adjustment (dB)
Devices operating at levels below Part 15 limits	4
Quasi-Peak to RMS Conversion	3
Co-frequency distribution factor	6
Duty Cycle	2.6
Total	15.6

The receive points in the VOAAREA calculation grid used 1 Hz bandwidths (set by adjusting the radiated interfering BPL signal power of each transmitting point to the power in dBW/Hz). The noise power levels provided by VOAAREA were in dBW/Hz. The received signal power from all effective BPL emitters at a given receive point was summed in the power domain independent of the noise power level, and the resulting summed BPL interfering power and the noise power at that point were used to calculate interference-to-noise. Thus, the aggregate interference-to-noise ratio at a point was into a 1Hz bandwidth.

Simulations were run across frequencies from 2 to 28 MHz (in 2 MHz increments), for all months of the year and for all hours of the day (approximately 4300 simulations). Table 5-4 summarizes the assumptions listed above as they were applied to this simulation.

**Table 5-4: Simulation conditions**

Effective BPL emitters	Overhead	Underground
Excitation	Voltage source on single line, centrally located	Voltage source in pad-mounted transformer, centrally located
Far field pattern		
Source	NEC-4.1 overhead model	NEC-4.1 underground model
Variability	Averaged over azimuth, variable by elevation and frequency	
Type	Directive gain	
Power level		
Source	NEC-4.1 overhead model	NEC-4.1 underground model
Structure emissions limits	Limited by Part 15 limits, as measured using BPL measurement guidelines	
County-level scaling	Scaled by urban households in county	
Parameter used	NEC-4.1 “radiated power” value (specified as output power after	

	structure losses, but not ground losses, are considered)
Placement	Geographic centers of all counties in the United States
<b>Receive antennas</b>	
Antenna type	Quarter-wave monopole (VOACAP type 22)
Ground conditions	“Average” ground
Conductivity	0.005 S/m
Relative permittivity	15
Placement	31x31 grid of receive points throughout CONUS
Noise	“Quiet rural” noise conditions (-164 dBW/Hz)
<b>Simulation</b>	
Frequencies	From 2 to 30 MHz in 2 MHz steps
Times of day	From 0 to 23 hours UTC in 1-hour increments
Months of year	From January to December
Solar conditions	Smoothed Sunspot Numbers (SSN) 25 and 150
Primary path geometry	Short path
Calculation methodology	Short/long path smoothing
Calculated parameters	Received signal strength (SDBW), received noise (NDBW)
<b>Power Adjustment Factor</b>	-15.6 dB (detailed in Table 5-3)

## 5.4 SIMULATION RESULTS

In order to gauge whether a given aggregated BPL signal level presents a risk of harmful interference to a radiocommunication receiver, NTIA considered two threshold values of  $(I+N)/N$ , or receiver noise floor increase.<sup>[74]</sup> The lower threshold, a 1 dB increase in the noise floor (corresponding to a BPL interference-to-noise ratio of approximately -5.9 dB), was chosen as the level at which some harmful interference might occur. The higher threshold, increasing the noise floor by 3 dB (a BPL interference-to-noise ratio of 0 dB), was selected as a level at which harmful interference was considered to be a significant risk.

Analysis of the impact of BPL aggregation was done by combining the BPL signal levels of the modeled overhead and underground BPL systems with the background noise levels, such that the combination met the noise floor increase thresholds listed above. This analysis enabled NTIA to examine the ionospheric aggregation effects while varying the relative numbers of overhead and underground systems.

### 5.4.1 Comparison of Overhead and Underground Analysis Results

The simulations found overhead systems produced aggregated signal levels greatly in excess of underground systems, even when both classes of systems were adjusted to meet Part 15 limits. The median value for overhead aggregated BPL signal level was approximately 20 dB higher than that of an equal number of underground systems, given the same ionospheric propagation characteristics, over all the conditions modeled. This finding suggests that, where feasible, installation of BPL devices operating in the 1.7 to 30 MHz frequency range on underground wiring could have



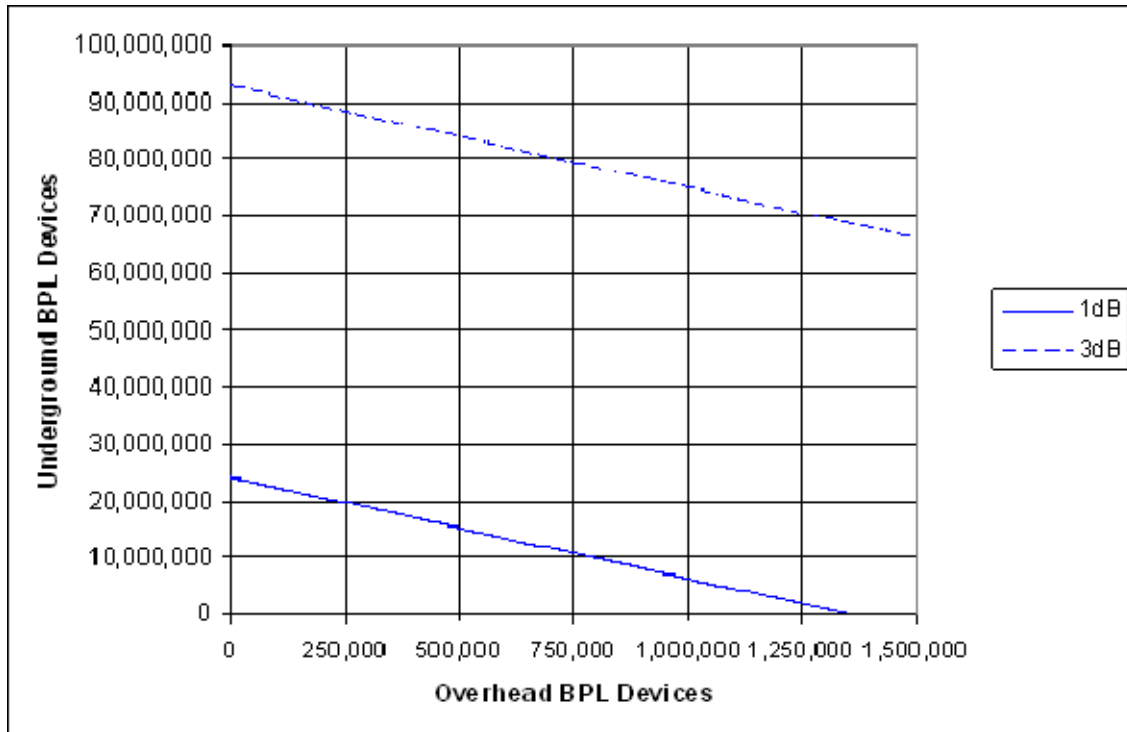
significant advantages over the same devices operating on overhead systems, from the standpoint of signal aggregation due to ionospheric propagation.

The relative impact of overhead and underground BPL aggregation can be seen graphically in the following results. Figures 5-3 and 5-4 illustrate the number of overhead plus underground devices needed to cause a worst-case 1 or 3 dB increase in the noise floor at any geographic location in the United States under best propagation and lowest local noise floor conditions.

For these graphs, ionospheric aggregation modeling was used to derive sets of conditions for both low and high solar activity during which the greatest ratios of signal-to-noise level due to aggregated BPL was produced. For all other sets of conditions and geographic locations, calculated aggregation resulted in less impact to the noise floor. Thus, for most calculated conditions, more BPL devices would be required to produce the same impact on the local noise floor as that illustrated in Figures 5-3 and 5-4.

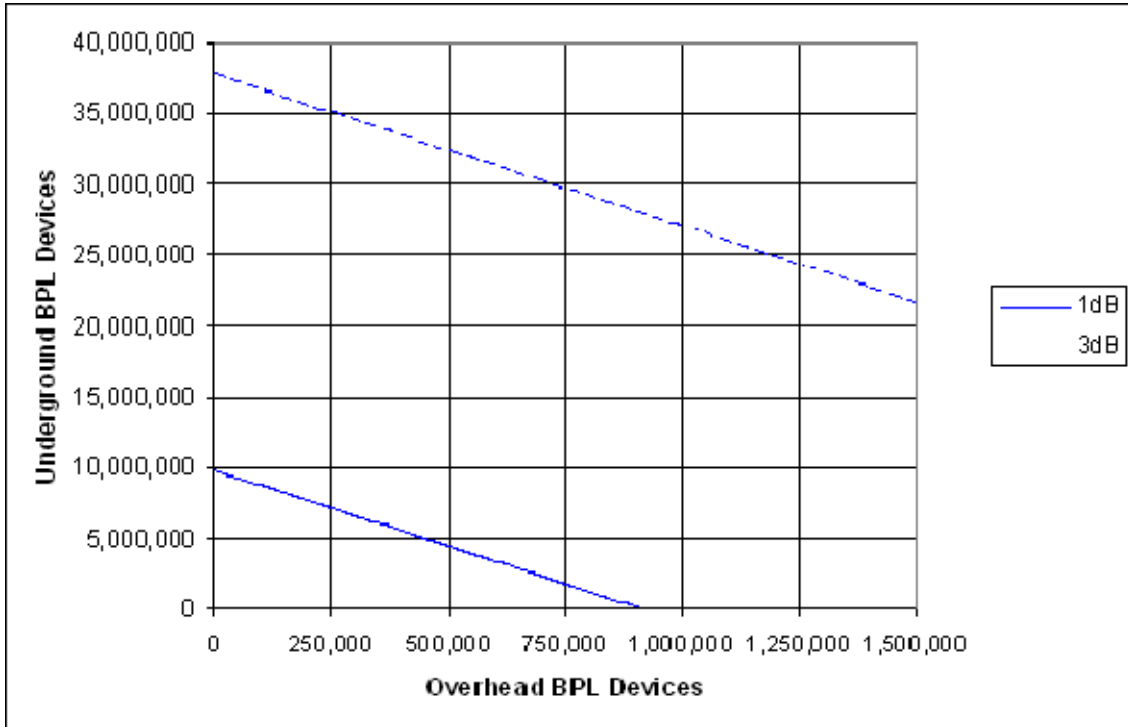
Calculations for periods of high solar activity indicated that maximum aggregated BPL signal levels occur primarily at higher frequencies in the HF band (18-30 MHz) during mid-to-late afternoon hours in the fall and winter. Calculations using low solar activity conditions found maximum aggregated BPL signal levels primarily at lower frequencies in the HF band (4-8 MHz). As was indicated by calculations assuming high solar activity conditions, maximum aggregated BPL signal levels were found during late afternoon hours during the fall and winter.

Figure 5-3 depicts combinations of underground and above-ground BPL devices that produce increases in the noise floor of 1dB (lower curve) and 3 dB (upper curve). This figure is generated for the combination of ionospheric propagation and noise conditions (15:00 UTC during November at 30 MHz, with high-level solar activity) that produce the highest aggregate BPL signal relative to the local noise floor at any geographic point. Under these conditions, more than 1.35 million overhead BPL devices alone could be deployed before realizing a 1 dB increase in the noise floor at any geographic location. This number increases to 5.23 million overhead BPL devices for a 3 dB aggregate noise floor increase. By reducing the number of overhead devices and adding underground BPL devices, the total number of deployed BPL devices can be greatly increased, while meeting the same levels of noise floor increase.



**Figure 5-3: Number of underground BPL devices compared to the number of overhead BPL devices required to meet specified increase in noise floor under high SSN conditions**

Figure 5-4 depicts numbers of overhead BPL devices compared to the number of underground BPL devices necessary to realize a 1 dB and 3 dB increase in the receiver noise floor under low solar cycle conditions. As with solar cycle maxima results, the fewest overall BPL devices necessary to meet the thresholds occurs when overhead BPL devices are used exclusively. For these conditions, approximately 916,000 overhead BPL devices would be required to raise the noise floor by 1 dB. By contrast, the exclusive use of underground BPL devices in the 1.7 to 30 MHz frequency range would allow nearly 10 million BPL devices to be deployed before producing a 1 dB noise floor increase.



**Figure 5-4: Number of underground BPL devices compared to the number of overhead BPL devices required to meet specified increase in noise floor under low SSN conditions**

### 5.4.2 Maps of Ionospheric Aggregation

Figures 5-6 through 5-17 depict aggregated BPL interference-to-noise ratio (labeled as “Signal-to-Noise”) contour maps across CONUS for a number of BPL deployment cases. These maps combine the aggregate power contributions of overhead and underground BPL devices distributed by population throughout the United States in various ratios such that the maximum aggregate BPL SNR encountered at any geographic point produces an approximate 1 dB or 3 dB increase in the noise floor.

Because of the way VOACAP produces output, only signal-to-noise ratios are indicated in the legends of the contour maps. To aid in interpreting Figures 5-6 through 5-17, a sample contour map is provided in Figure 5-5. Figure 5-5 illustrates the translation of the values in these legends to the respective increases in the noise floor. The lighter shaded regions correspond to greater levels of noise floor increase due aggregation of BPL emissions. The peak location or locations are identified on the contour maps by a circular symbol having a cross inside it.

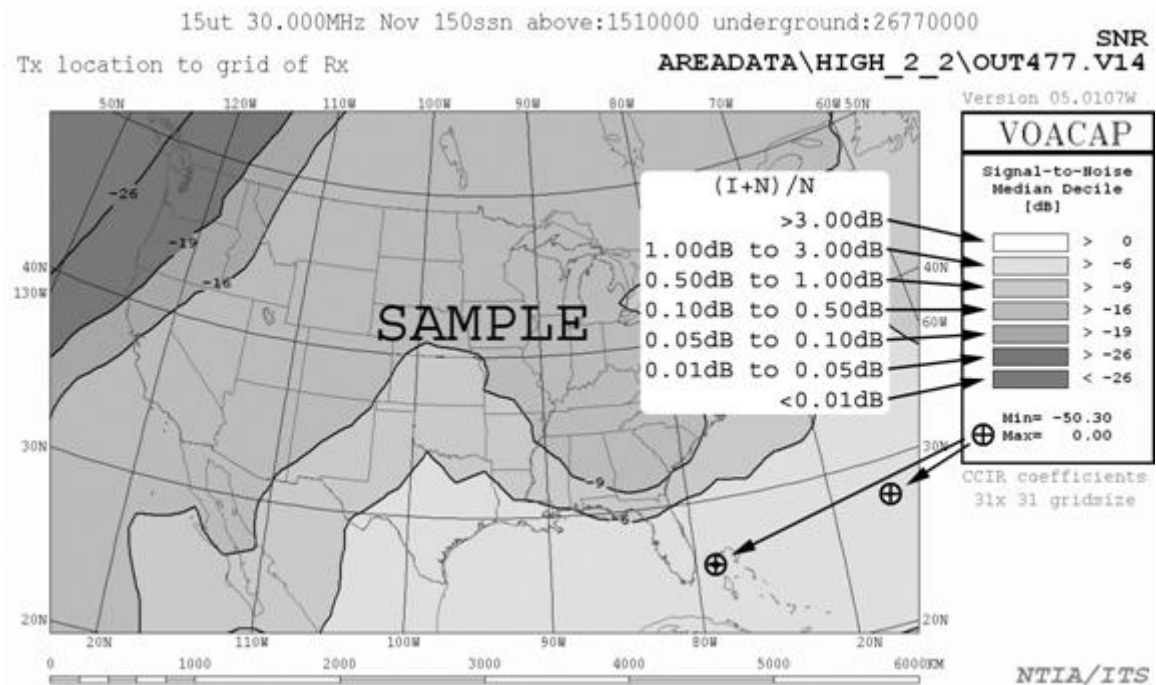


Figure 5-5: Sample VOAAREA output map detailing the increase in the noise floor for each signal-to-noise value in the map legend.

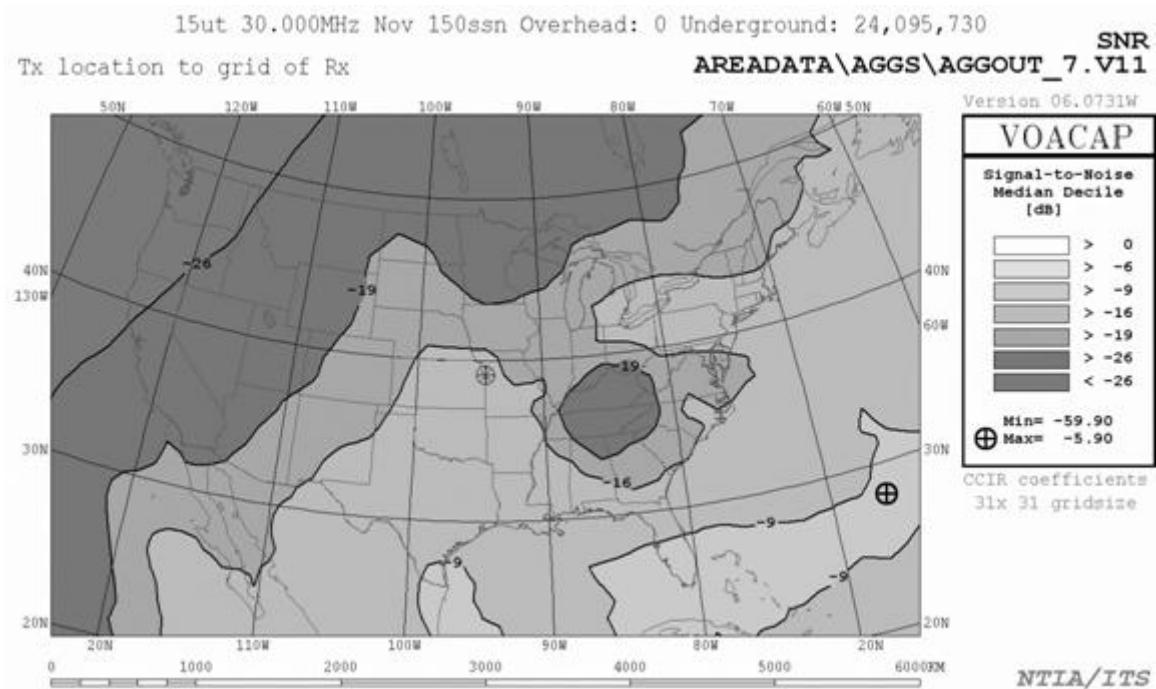


Figure 5-6: Aggregation under high SSN conditions due to 24,095,730 underground devices and no overhead devices with maximum noise floor increase of 1 dB

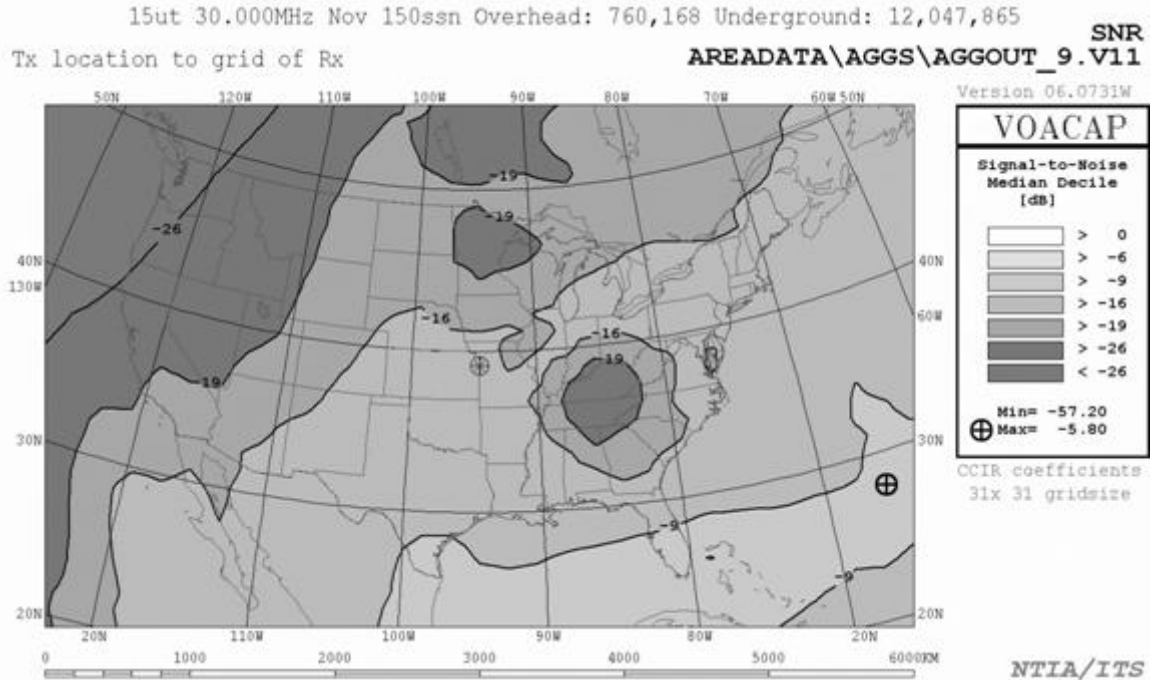


Figure 5-7: Aggregation under high SSN conditions due to 12,047,865 underground devices and 760,168 overhead devices with maximum noise floor increase of 1 dB

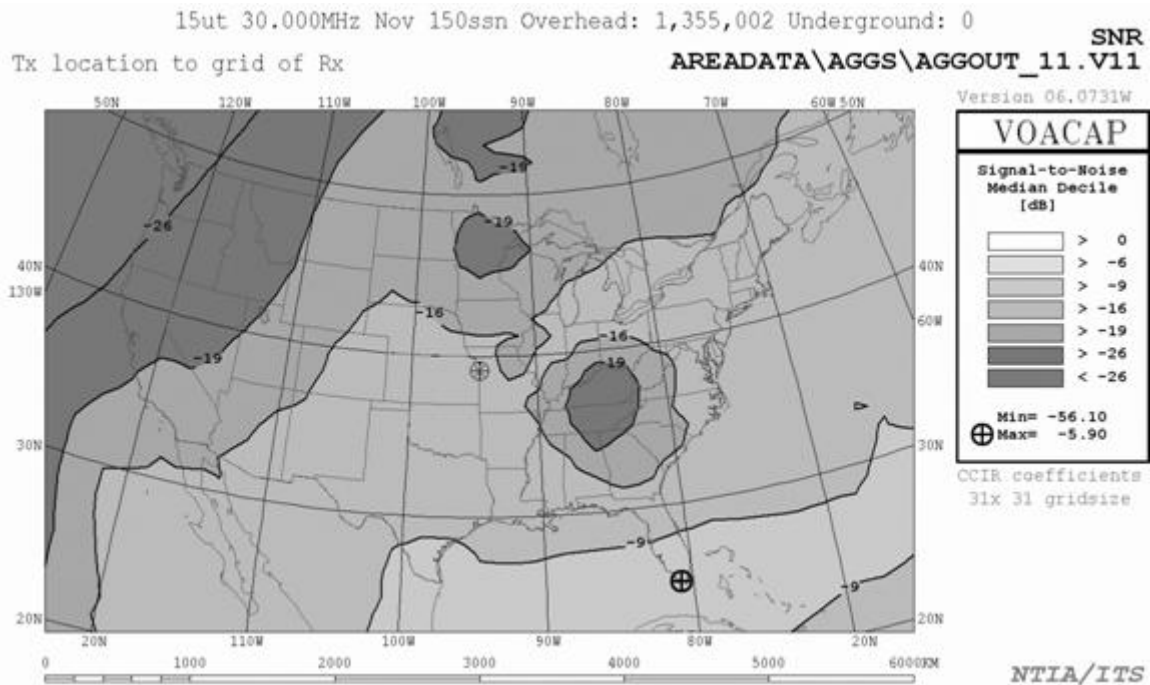


Figure 5-8: Aggregation example under high SSN conditions due to no underground devices and 1,355,002 overhead devices with maximum noise floor increase of 1 dB

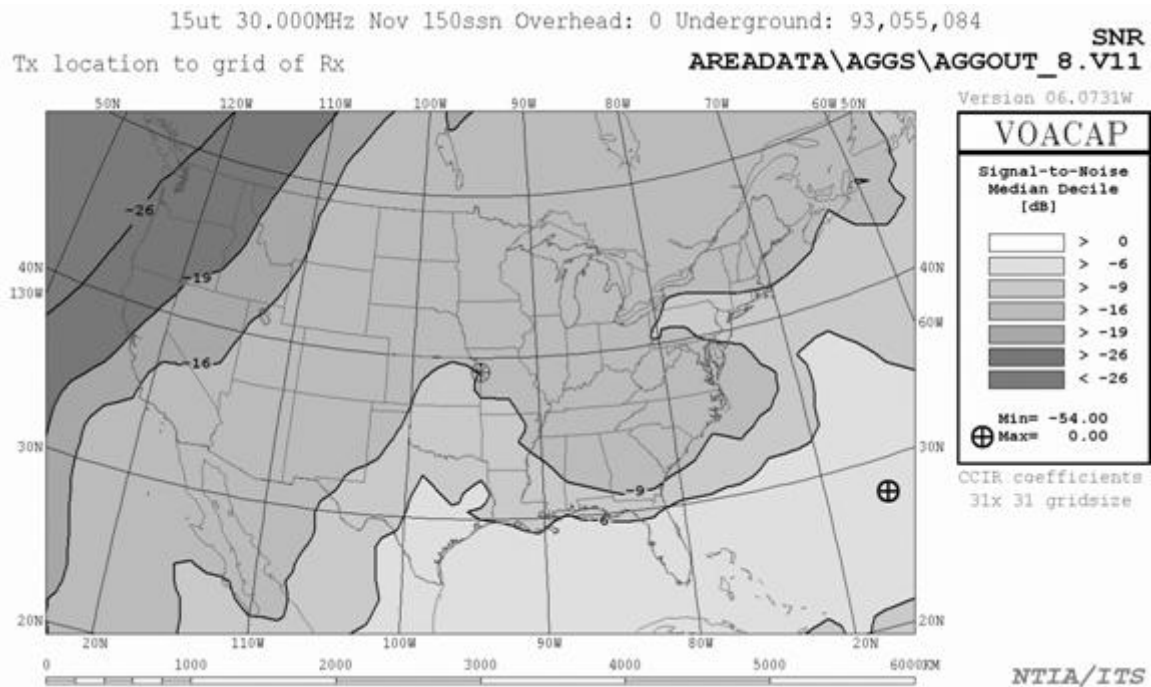


Figure 5-9: Aggregation example under high SSN conditions due to 93,055,084 underground devices and no overhead devices with maximum noise floor increase of 3 dB

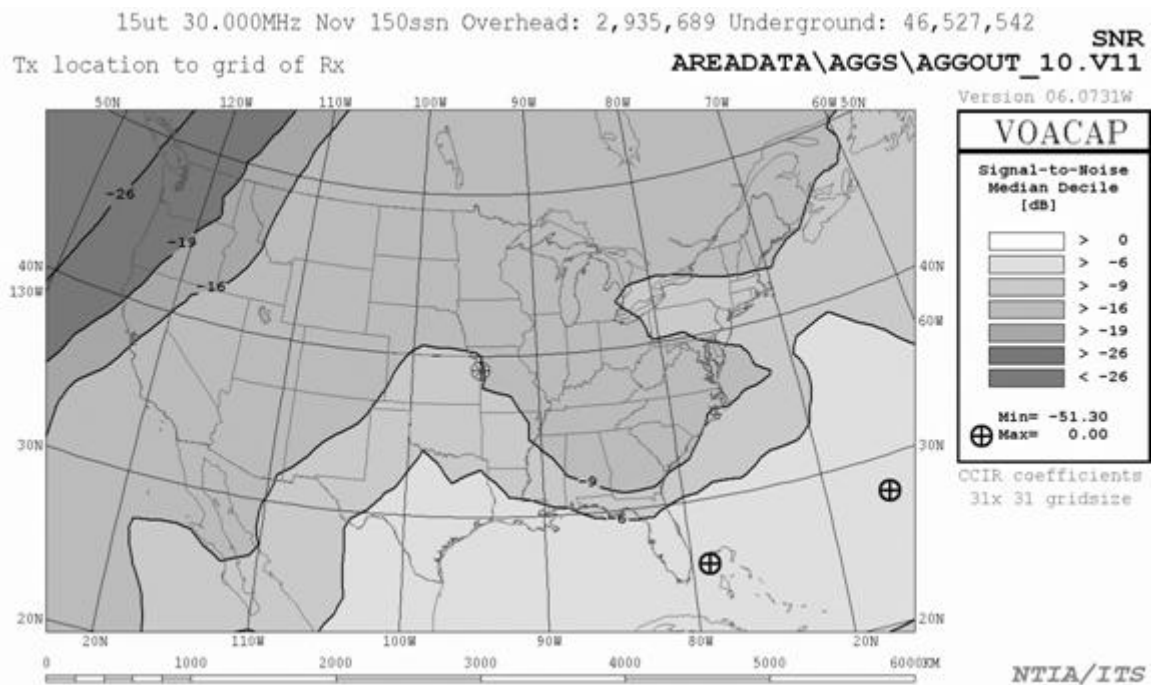


Figure 5-10: Aggregation example under high SSN conditions due to 46,527,542 underground devices and 2,935,689 overhead devices with maximum noise floor increase of 3 dB



Figure 5-11: Aggregation example under high SSN conditions due to no underground devices and 5,232,871 overhead devices with maximum noise floor increase of 3 dB

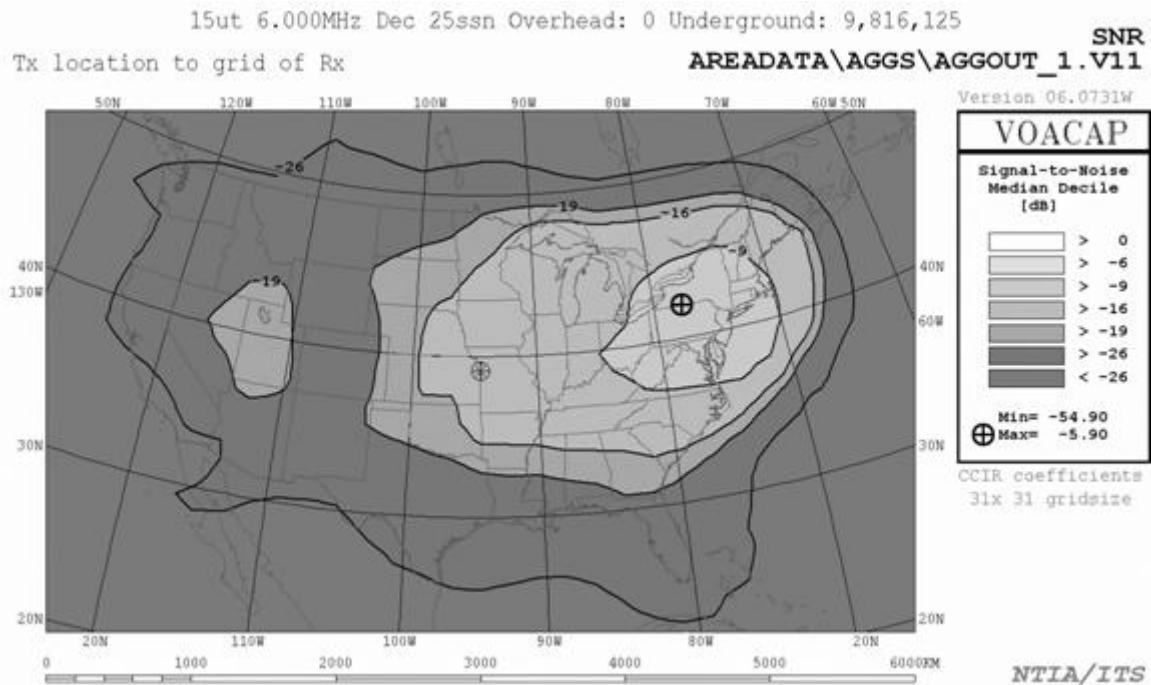


Figure 5-12: Aggregation example under low SSN conditions due to 9,816,125 underground devices and no overhead devices with maximum noise floor increase of 1 dB

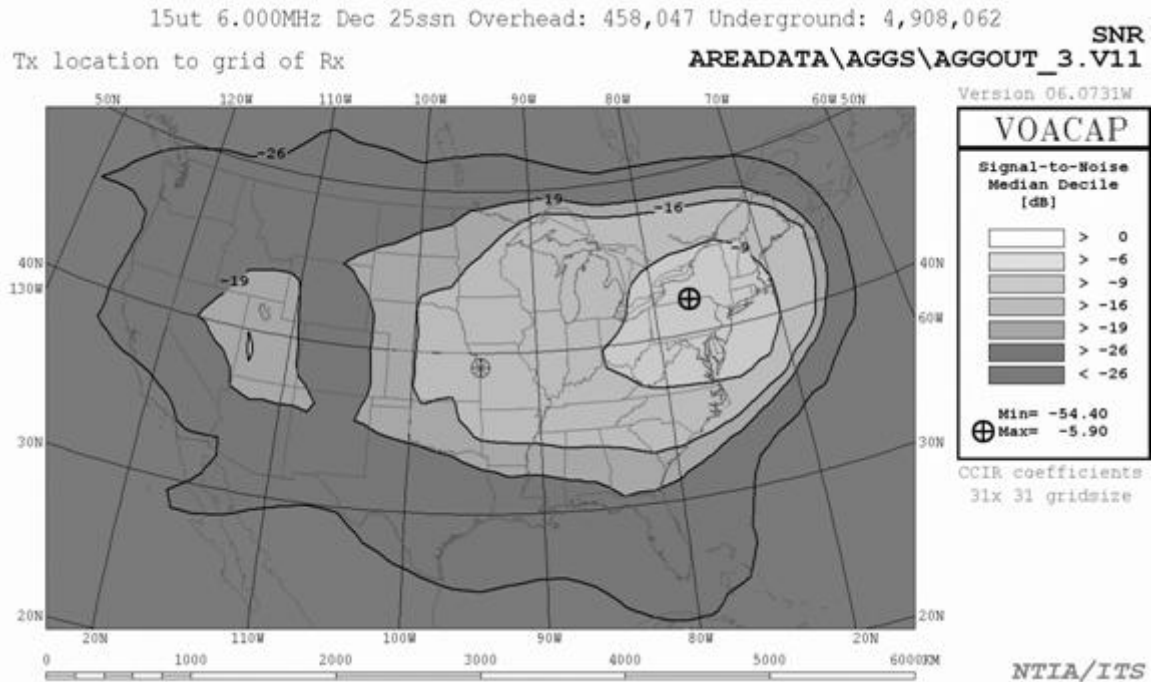


Figure 5-13: Aggregation example under low SSN conditions due to 4,908,062 underground devices and 458,047 overhead devices with maximum noise floor increase of 1 dB

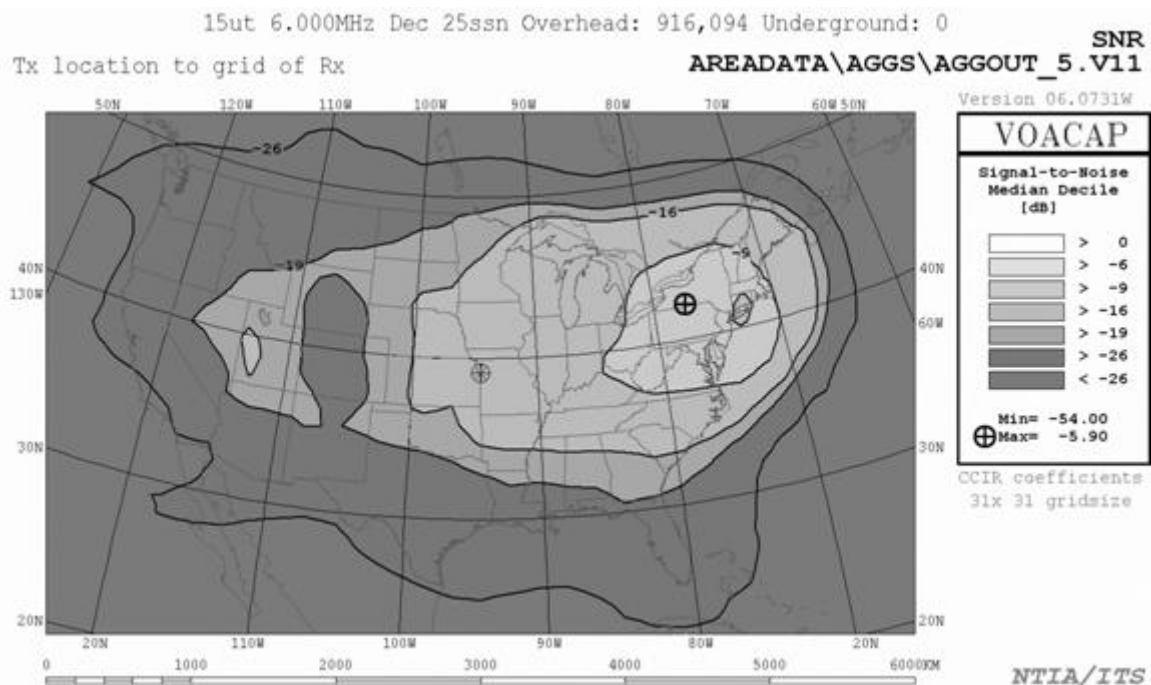


Figure 5-14: Aggregation example under low SSN conditions due to no underground devices and 916,094 overhead devices with maximum noise floor increase of 1 dB



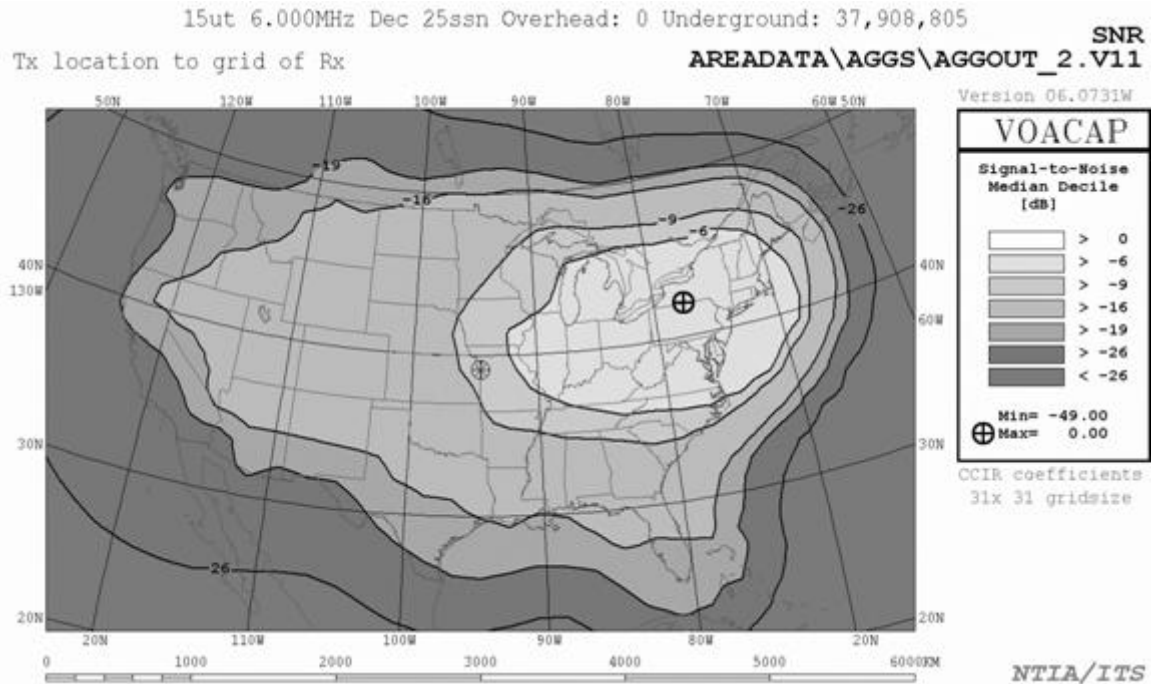


Figure 5-15: Aggregation example under low SSN conditions due to 37,908,805 underground devices and no overhead devices with maximum noise floor increase of 3 dB

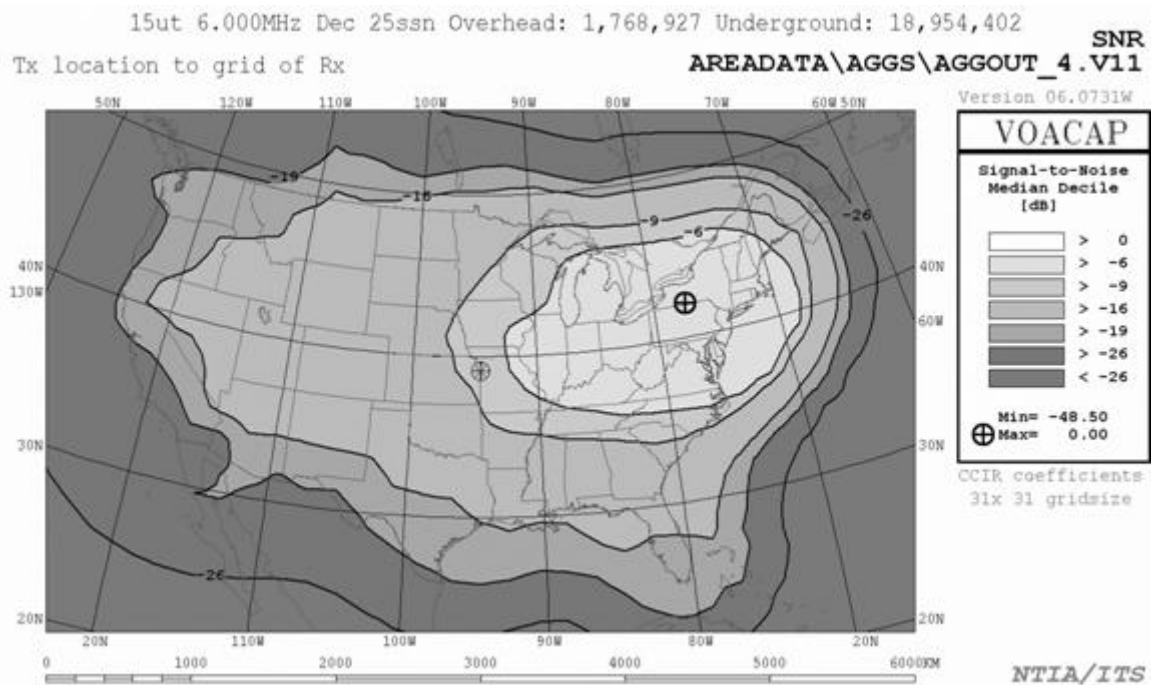
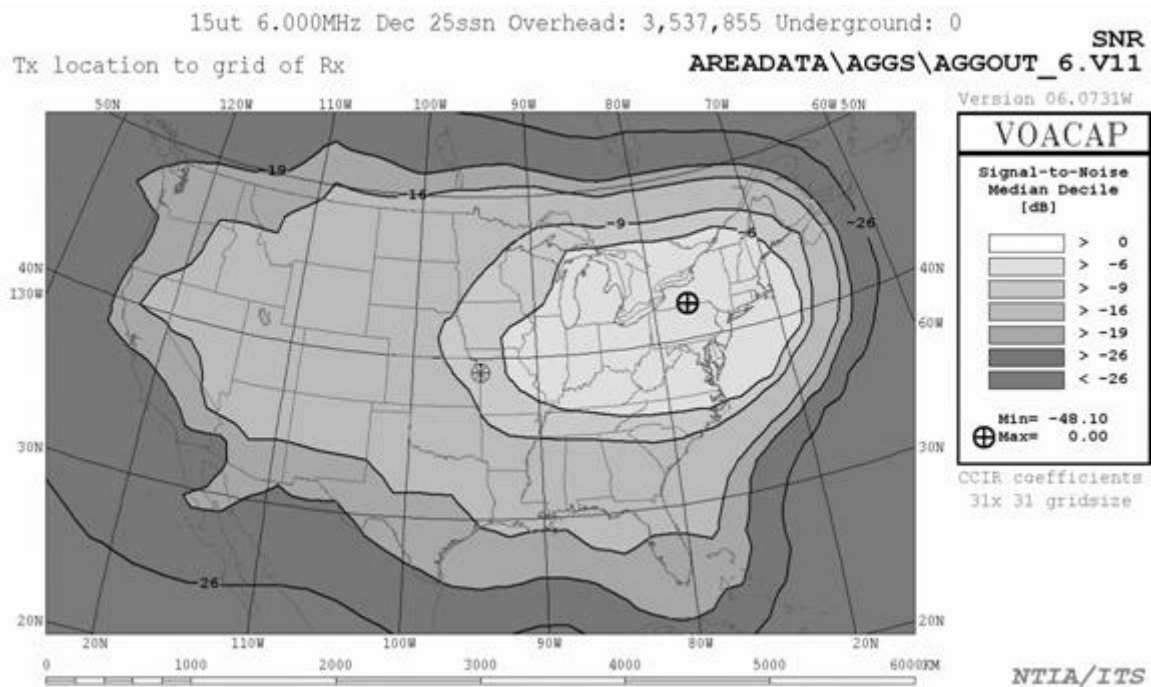


Figure 5-16: Aggregation example under low SSN conditions due to 18,954,402 underground devices and 1,768,927 overhead devices with maximum noise floor increase of 3 dB



**Figure 5-17: Aggregation example under low SSN conditions due to no underground devices and 3,537,855 overhead devices with maximum noise floor increase of 3 dB**

The aggregation examples of Figures 5-6 through 5-17 depict the two circumstances (one for low solar cycle activity and one for high) in which the fewest devices are needed to reach the thresholds indicated at any geographic point and across all conditions of time and frequency simulated. As can be seen from the figures, under these conditions of best propagation/lowest noise and using the assumptions developed in this study, more than 916,000 overhead BPL devices deployed nationwide would be necessary to produce increases in the noise floor of 1 dB at any geographic point—well above the 705,000 BPL devices expected in NTIA’s deployment model for passing 100 percent of the urban households in the United States. Far more devices could be deployed without reaching either 1 dB or 3 dB thresholds if a significant percentage are deployed on underground power lines.

In the vast majority of cases modeled (other times of day, months of the year and frequencies), many more devices, both underground and above ground, were required to produce the stipulated increases in the noise floor.

## 5.5 SUMMARY

NTIA modeled two power line structures and conducted comprehensive aggregation studies using VOAAREA propagation software to determine the potential for harmful interference to federal radiocommunication systems in the 1.7 to 30 MHz frequency range due to BPL signals propagated via the ionosphere. This analysis made use of several factors that differed from those used previously in the Technical Appendix

to the NTIA Comments. These factors included BPL transmitter characteristics based entirely on an elaborate power line model, the use of the Part 15 measurement methodology in the BPL Report and Order, a more comprehensive set of ionospheric aggregation simulations, and the use of an underground power line model to further characterize aggregated interference potential.

The simulation results for the deployment of Access BPL on MV overhead power lines operating in the 1.7 to 30 MHz band show that, for a wide scale deployment of overhead BPL devices (such that BPL services passes 100 percent of the urban households in the United States), the noise floor increase is expected to be less than 1 dB for the worst case propagation conditions. In reality, approximately 20 percent of the MV power lines are underground and many BPL systems operate in the VHF band. From these results, a widespread deployment of Access BPL systems in the United States is not expected to pose a problem for federal radiocommunication systems operating in the 1.7 to 30 MHz band.



## **SECTION 6 SUMMARY OF RESULTS**

### **6.1 INTRODUCTION**

The Commission's BPL Report and Order specified the rules and measurement guidelines for Access BPL systems. NTIA applied these rules and measurement guidelines in a number of analyses to evaluate their effectiveness at limiting the risk of interference to federal radiocommunication systems. The results of these analyses are summarized below.

### **6.2 PHASE 2 ANALYSES**

#### **6.2.1 Part 15 Rules and Measurement Guidelines**

In the NTIA Phase 1 Study, NTIA noted that adopting effective BPL measurement guidelines is critical to minimizing the risk of harmful interference to federal radiocommunications. NTIA further noted that emissions from Access BPL systems operating on overhead MV power lines were atypical of most Part 15 devices in that the peak field strength often occurs at heights significantly greater than 1 meter, and it may occur at various distances along the power line. The radiated field strength diminishes with distance from the source at a slower rate than that of a typical point source radiator. Measurements of BPL field strength are typically performed in the near field where the relationship between electric and magnetic field are not easily predicted. NTIA developed a number of power line models using the NEC software package to facilitate the analysis of these characteristics of BPL emissions when applying the new Access BPL measurement guidelines adopted by the Commission.

The results of NTIA's analysis of the characteristics of BPL emissions indicate that the peak field strength seen in close proximity to a BPL-energized overhead power line will occur at various heights, and often near the height of the power line. NTIA further analyzed the peak field strength using the specified measurement heights and found that at these measurement heights, the 80<sup>th</sup> percentile values of peak field strength at any height are effectively estimated by use of the Commission's measurement guidelines. As noted earlier, the 80<sup>th</sup> percentile values eliminate the localized peaks that are unlikely to be encountered by a radio receiver randomly located in close proximity to an Access BPL power line.

The measurement guidelines allow field strength measurements on overhead Access BPL power lines operating in the VHF band to be performed at a 1 meter height combined with application of a 5 dB height correction factor for BPL systems operating at or above 30 MHz. NTIA's analysis demonstrated that the peak field strength may be reasonably estimated after application of this height correction factor.

The FCC's measurement guidelines require field strength measurements to be performed at specific points along the power line within 1 wavelength of a BPL source.<sup>[75]</sup> When the electric field strength was scaled to be within the Part 15 limits using the Access BPL measurement guidelines, NTIA's NEC simulation results indicated that the percent of measurement points where the field strength exceeded the Part 15 limits was small.

NTIA evaluated the Commission's modification of the distance extrapolation rules, which replaced the use of the horizontal distance between the BPL device and the measurement antenna with the slant range distance between them. NTIA's NEC simulations in the 4 to 8 MHz frequency range exhibited somewhat slower rates of field strength decay with distance than would be expected by the distance extrapolation rate in the Part 15 rules for Access BPL systems. This difference was up to 6 dB less than the distance extrapolation rate. At or above 10 MHz, the simulation results show good agreement between the rate that field strength decays and the Part 15 distance extrapolation rate using the slant range distance to the Access BPL device and power lines. As noted earlier, the effect of the combination of direct and ground-reflected rays at the simulated distances becomes more pronounced at frequencies above 14 MHz.

One limitation with this methodology arises when measurements are to be performed at distances significantly beyond the specified 10 meter measurement distance called for in the Commission's measurement guidelines. In this case, the length of the slant range distance approaches that of the horizontal separation distance between the BPL device and measurement antenna, and the extrapolation rate effectively becomes the same as if the horizontal distance was used. The resulting extrapolation may overestimate the rate of field strength decay with distance and lead to the establishment of an operating level for the BPL device that exceeds Part 15 limits at 10 meters. It should also be noted that the Commission's rules state that measurements should not be performed at a distance greater than 30 meters unless it can be demonstrated that measurements at a distance of 30 meters or less are impractical.<sup>[76]</sup>

Below 30 MHz, electric field strength is determined by measurement of the peak magnetic field strength in the horizontal plane using a loop antenna situated 1 meter above the ground, and application of a magnetic to electric field conversion factor. As these measurements are performed at a distance of 10 meters from the BPL device and associated power lines, they fall well within the near field region where the relationship between magnetic and electric field strength is not easily predicted. NTIA's evaluation of the relationship between magnetic and electric field at this distance shows that use of the loop antenna with this conversion factor yields a reasonable approximation. NTIA simulations also show that, below 30 MHz, peak field strength consistently corresponded to the vertical electric field (horizontal magnetic field) polarization when measured at 10 meters from the power line. At or above 30 MHz, the guidelines specify that both the horizontal and vertical polarizations of electric field strength are to be measured. The simulations performed by NTIA indicate that the specified guidelines can be used to represent the electric field strength levels.

The measurement guidelines for Access BPL systems specify that *in-situ* testing shall be performed on three typical installations for both overhead and underground installations. NTIA field tests and NEC modeling of BPL power lines identified that, in addition to the BPL devices themselves, many features of MV power lines give rise to the strongest levels of radiated emissions. NTIA suggests that a variety of these features should exist in power lines chosen as representative sites for compliance measurement testing.

### **6.2.2 Special Protection Provisions**

As a result of NTIA's initial analysis, the Commission specified minimal sets of excluded frequency bands, exclusion zones and consultation areas needed to prevent BPL systems from interfering with critical federal radio operations in the 1.7 to 80 MHz frequency range.<sup>[77]</sup> NTIA extended the analyses for the recommended protection radii to include a more elaborate overhead power line model and a new underground power line model. NTIA analyzed the BPL emission levels that might be expected from MV overhead and underground power lines to determine the minimum radii of exclusion zones and consultation areas needed to meet the protection criteria for critical federal fixed and mobile radiocommunication systems, radar, and radioastronomy receivers.

These provisions provide an additional measure of protection beyond that afforded by field strength limits and compliance measurement provisions. These special exclusion zones and consultation areas place only a minimal constraint on BPL deployment, as they impact only about 2 percent of the spectrum between 1.7 to 80 MHz. Additional special protection provisions may be needed if, at some time in the future, Access BPL devices are permitted to operate outside the 1.7 to 80 MHz frequency range.

### **6.2.3 Case Study Applying the Access BPL Measurement Guidelines**

NTIA developed a simulation of an actual overhead MV Access BPL power line structure to illustrate application of the BPL measurement guidelines and assess the potential impact on nearby land mobile systems, as well as to fixed systems at greater distances from the power lines. The results of these simulations are consistent with those from NTIA's Phase 1 Study, and, as such, they indicate the Part 15 measurement procedures described in the BPL Report and Order appear to estimate adequately the peak field strength around the power line near ground level.<sup>[78]</sup>

### **6.2.4 Aggregation of Emissions Considering Ionospheric Propagation**

In its Comments on the BPL NPRM, NTIA presented a preliminary analysis of the aggregation of emissions via ionospheric (*i.e.*, "sky wave") propagation arising from a wide scale deployment of Access BPL devices on MV overhead power lines.<sup>[79]</sup> At that time, NTIA concluded that interference via this mechanism was not a near-term issue.

NTIA further developed its power line models to include an elaborate overhead power line model and an underground power line model. The radiation levels derived

from these models were scaled to Part 15 limits using the recently adopted compliance measurement methodology. Simulations of aggregation via ionospheric propagation were performed for high and low SSN conditions, with frequencies ranging from 2 to 30 MHz, and varying time of day and month of year.

### 6.3 CONCLUSION

The NTIA Phase 2 Study of Access BPL systems expanded upon the Phase 1 Study with additional modeling results and analyses that addressed the issues that had been identified as requiring further study. The Phase 2 Study applied the rules and measurement guidelines for Access BPL systems adopted by the FCC to evaluate their effectiveness in minimizing the potential for harmful interference to federal radiocommunication systems. The results of these analyses confirm that the Part 15 rules, measurement guidelines and special protection provisions applied to Access BPL deployment will limit the interference risks for federal radiocommunication systems.

---

<sup>[1]</sup> See *Potential Interference from Broadband over Power Line (BPL) Systems to Federal Government Radiocommunications at 1.7 – 80 MHz*, NTIA Report 04-413, April 2004 (“NTIA Phase 1 Study”). In 47 C.F.R. § 15.3(ff), an Access BPL system is defined as “[a] carrier current system installed and operated on an electric utility service as an unintentional radiator that sends radio frequency energy on frequencies between 1.705 MHz and 80 MHz over medium voltage lines or over low voltage lines to provide broadband communications and is located on the supply side of the utility service’s points of interconnection with customer premises. Access BPL does not include power line carrier systems as defined in Section 15.3(t) or In-House BPL systems as defined in Section 15.3(gg).”

<sup>[2]</sup> See Amendment of Part 15 regarding new requirements and measurement guidelines for Access Broadband over Power Line Systems, ET Docket 04-37, Notice of Proposed Rulemaking, FCC 04-29, released February 23, 2004, (“BPL NPRM”); Comments of the National Telecommunications and Information Administration (NTIA Comments) in ET Docket No. 04-37, June 4, 2004, (available at [www.ntia.doc.gov/ntiahome/fcc\\_filings/2004/BPLComments\\_06042004.pdf](http://www.ntia.doc.gov/ntiahome/fcc_filings/2004/BPLComments_06042004.pdf)) (“NTIA Comments”); Letter to Mr. Edmond J. Thomas, Chief, Office of Engineering and Technology, Federal Communications Commission, from Mr. Fredrick R. Wentland, Associate Administrator, Office of Spectrum Management, National Telecommunications and Information Administration, in ET Docket No. 04-37, September 13, 2004 (“NTIA September 13, 2004 Letter”); Letter to Mr. Edmond J. Thomas, Chief, Office of Engineering and Technology, Federal Communications Commission, from Mr. Fredrick R. Wentland, Associate Administrator, Office of Spectrum Management, National Telecommunications and Information Administration, in ET Docket No. 04-37, September 24, 2004 (“NTIA September 24, 2004 Letter”).

<sup>[3]</sup> See In the Matter of Amendment of Part 15 regarding new requirements and measurement guidelines for Access Broadband over Power Line Systems, ET Docket No. 04-37, Carrier Current Systems, including Broadband over Power Line Systems, ET Docket No. 03-104, Report and Order, adopted October 14, 2004 (“BPL Report and Order”).

<sup>[4]</sup> NEC version 4.1 software is available through Lawrence Livermore National Laboratory. URL: <http://www.llnl.gov/IPandC/technology/software/softwaretitles/nec.php>.

<sup>[5]</sup> VOACAP is an HF statistical propagation prediction software program developed by NTIA Institute of Telecommunication Sciences (ITS). VOACAP is available from the NTIA Institute for Telecommunication Sciences, URL: <http://elbert.its.bldrdoc.gov/hf.html>.



<sup>[6]</sup> See NTIA Phase 1 Study, Vol. I, at sec. 9.3.2.

<sup>[7]</sup> *Id.* Vol. I, at sec. 5, 6; *See also* NTIA Comments, Technical Appendix, at sec. 2; NTIA September 24, 2004 Letter.

<sup>[8]</sup> In actual systems, all transformer impedances vary widely based upon varying loads in the system. However, preliminary calculations found that changing transformer impedances had little impact on the results.

<sup>[9]</sup> See BPL Report and Order, at Appendix C, *Measurement Guidelines* ¶ 1.6.

<sup>[10]</sup> See BPL Report and Order, Appendix C, *Measurement Guidelines*.

<sup>[11]</sup> Below 30 MHz, the peak vertical electric field strength is calculated by scaling the peak horizontal magnetic field strength measured at a height of 1 meter by 377 ohms. Above 30 MHz, the peak electric field strength is calculated directly from the largest value in either the horizontal or vertical polarization at a measurement height of 1 to 4 meters. In both cases, the 80<sup>th</sup> percentile values are used as described above.

<sup>[12]</sup> See NTIA Comments, Technical Appendix, at pp. 2-18.

<sup>[13]</sup> See BPL Report and Order, Appendix C ¶ 2.b.2 (“Testing shall be performed at distances of 0, ¼, ½, ¾, and 1 wavelength down the line from the BPL injection point on the power line. Wavelength spacing is based on the mid-band frequency....”).

<sup>[14]</sup> See 47 C.F.R. § 15.31(g)-(k).

<sup>[15]</sup> See BPL Report and Order, at Appendix C, *Measurement Guidelines* ¶ 2.b.2.

<sup>[16]</sup> *Id.* ¶ 2.b.4 (describing the slant range distance extrapolation methodology).

<sup>[17]</sup> See 47 C.F.R. § 15.31(f)(1)-(2).

<sup>[18]</sup> See NTIA BPL Phase 1 Study, Vol. II, at sec. D.3.3.

<sup>[19]</sup> See BPL Report and Order, at Appendix C ¶ 2.b.4.

<sup>[20]</sup> See NTIA September 24, 2004 Letter.

<sup>[21]</sup> Note that the results at or above 30 MHz presented herein assume an antenna height of 1 meter for illustration purposes only. The Part 15 measurement guidelines specify that the measurements are to be performed at antenna heights of 1 to 4 meters.

<sup>[22]</sup> See BPL Report and Order, at Appendix C, *Measurement Guidelines* ¶ 2.a.

<sup>[23]</sup> See NTIA Phase 1 Study, Vol. I, at sec. 9.2.4; *id.*, Vol. II, at sec. D.3.2.

<sup>[24]</sup> See 47 C.F.R. § 15.31(f)(1)-(2).

<sup>[25]</sup> See NTIA Phase 1 Study, Vol. I, at Table 4-9.

<sup>[26]</sup> See NTIA Comments, at sec. III.

<sup>[27]</sup> See BPL Report and Order, at Appendix B (amending Part 15 to add a new Subpart G).

<sup>[28]</sup> See 47 C.F.R. § 15.615(f).

<sup>[29]</sup> NTIA Phase 1 Study, Vol. I, at sec. 5.3.6; NTIA Comments, at Technical Appendix sec. 2.3.

<sup>[30]</sup> See NTIA Phase 1 Study, Vol. II, at Appendix C.

<sup>[31]</sup> *Manual of Regulations and Procedures for Federal Radio Frequency Managers*, United States Department of Commerce, National Telecommunications and Information Administration, Washington, D.C., January 2004 Revision.

<sup>[32]</sup> In this description of noise floor increase, the term “I” is the interfering signal power at the receiver site associated with radiated BPL emissions, and the term “N” is the noise power that would be present at the receiver site in the absence of BPL emissions. The interference-plus-noise-to-noise [(I+N)/N] is used to determine the noise floor increase.

<sup>[33]</sup> For this analysis, the protection requirement for sensitive over-the-horizon (OTH) radar receivers was assumed to be the same as that used for the Very Large Array (VLA) radio astronomy receiver. Like radio astronomy receivers, radar receivers employ correlation techniques that enable reception of signals weaker than noise. The radioastronomy protection criterion is specified in Recommendation ITU-R RA.769-2, Table 1.

<sup>[34]</sup> See Recommendation ITU-R RA.769-2, Table 1 for the protection criteria in the 73.0-74.6 MHz frequency band. This frequency band is used at the Very Large Array (VLA) radioastronomy facility near Socorro, New Mexico.

<sup>[35]</sup> The Commission's rules specify an electric field strength limit of 30  $\mu\text{V}/\text{m}$  at a horizontal distance of 30 meters for radiated emissions in the 1.705 to 30 MHz band. 47 C.F.R. § 15.209(a).

<sup>[36]</sup> The modeled measurement heights ranged from 1 to 4 meters, in 0.5 meter increments.

<sup>[37]</sup> See NTIA Phase 1 Study, Vol. I, at Table 6-2.

<sup>[38]</sup> TCI Model 527, Super High Gain Log-Periodic Antenna data sheet.

<sup>[39]</sup> Noise power levels were determined using the NOISEDAT computer program, assuming a representative protected receiver location. NOISEDAT is available from the ITU website, url: <http://www.itu.int/ITU-R/software/study-groups/rsg3/databanks/ionosph/index.html>.

<sup>[40]</sup> *A Guide to the Use of the ITS Irregular Terrain Model in the Area Prediction Mode*, NTIA Report 82-100 (April 1982).

<sup>[41]</sup> See NTIA September 13, 2004 Letter, at Annex 1, sec. 2.2.

<sup>[42]</sup>  $BW_{\text{meas}}$  is 9 kHz for frequencies below 30 MHz, and 120 kHz for frequencies between 30 MHz and 80 MHz.

<sup>[43]</sup> See NTIA Phase 1 Study, Volume II, at pp. D-38 and D-39. The field measurements from the BPL Phase 1 Study indicated that 6 dB is an appropriate factor to convert between peak and RMS field strength for Access BPL systems.

<sup>[44]</sup> See NTIA September 13, 2004 Letter, at Annex 1, sec. 2.2.

<sup>[45]</sup> The frequency 25 MHz was chosen for this analysis due to simulation results showing that the power line may be a more efficient radiator at or near this frequency. See NTIA September 13, 2004 Letter, at 14.

<sup>[46]</sup> See Recommendation ITU-R RA.769-2, Table 1 for the protection criteria in the 73.0-74.6 MHz frequency band. This frequency band is used at the VLA radioastronomy facility near Socorro, New Mexico.

<sup>[47]</sup> See NTIA September 13, 2004 Letter, at Annex 1, sec. 2.2.

<sup>[48]</sup> The ITM program may yield inaccurate results due to ground clutter when an antenna height of less than 1 meter is used. When using a 0.2 meter antenna height, as was done for the underground BPL analysis, the results obtained by ITM can underestimate the path loss. In an actual underground BPL deployment, the values of path loss are expected to be greater, and the PFD at the boundary of the exclusion zones should be below the protection levels assumed in this analysis.

<sup>[49]</sup> See NTIA September 13, 2004 Letter, at Annex 1, sec. 3.1.

<sup>[50]</sup> See BPL Report and Order, at 71.

<sup>[51]</sup> Letter to Mr. Edmond J. Thomas, Chief, Office of Engineering and Technology, Federal Communications Commission, from Mr. Fredrick R. Wentland, Associate Administrator, Office of Spectrum Management, National Telecommunications and Information Administration in ET Docket No. 04-37, March 1, 2005 ("NTIA March 1, 2005 Letter"). For Access BPL on overhead MV power lines, NTIA requested a 65 km radius BPL exclusion zone centered at the coordinates of the VLA radioastronomy facility. This radius equates to 29 km beyond the 36 km radius of the antenna array. NTIA also requested a 47 km radius exclusion zone centered at the coordinates of the VLA for Access BPL systems operating on underground MV or overhead low voltage (LV) power lines.

<sup>[52]</sup> During its initial study of BPL systems, NTIA measured peak power emissions in close proximity to a transformer vault containing a BPL device. Most attempts to measure the peak power emanating from the underground BPL system resulted in levels below the minimum sensitivity of NTIA's Radio Spectrum Measurement System (RSMS-4). See NTIA Phase 1 Study, at Volume II, p. D-33.

<sup>[53]</sup> The Commission's rules specify an electric field strength limit of 30  $\mu\text{V}/\text{m}$  at a horizontal distance of 30 meters for radiated emissions in the 1.705 to 30 MHz band. 47 C.F.R. § 15.209(a).

<sup>[54]</sup> NOISEDAT is available from the ITU Website, URL: <http://www.itu.int/ITU-R/software/study-groups/rsg3/databanks/ionosph/index.html>.

<sup>[55]</sup> Noise floor increases of 3, 10, 20, 30, 40 and 50 dB were analyzed. This allows comparison with the results presented in the NTIA Phase 1 Study, Vol. I, at Table 6-1.

<sup>[56]</sup> The choice of quasi-peak-to-RMS measurement factor was based on the measurement data from the NTIA Phase 1 Study, which indicated that the BPL signal power measured using a quasi-peak detector typically exceeded the level measured using an average detector by 0 – 5 dB. *See* NTIA Phase 1 Study, Volume II, at sec. D.3.4.

<sup>[57]</sup> *See* NTIA September 13, 2004 Letter, at Annex 1, sec. 2.2.

<sup>[58]</sup> *See* NTIA Phase 1 Study, Vol. I, at pp. 6-11; NTIA September 13, 2004 Letter, at Annex 1.

<sup>[59]</sup> *See* NTIA Phase 1 Study, Vol. I, at sec. 5.2.2.

<sup>[60]</sup> *See* NTIA Comments, at Technical Appendix, sec. 4.

<sup>[61]</sup> *Id.* *See also* NTIA Phase 1 Study, Vol. I, at sec. 5.4.

<sup>[62]</sup> *See* NTIA Comments, at Technical Appendix, sec. 2.2.

<sup>[63]</sup> *See* BPL Report and Order, at Appendix C, *Measurement Guidelines* ¶ 2.b.

<sup>[64]</sup> *See* BPL Report and Order, at Appendix C, *Measurement Guidelines* ¶ 2.b.

<sup>[65]</sup> *See* BPL Report and Order, at Appendix C, *Measurement Guidelines* ¶ 2.b.2, for a description of additional measurements that may be required if the mid-band frequency of the BPL signal is two or more times greater than the lowest BPL signal injected onto the power line.

<sup>[66]</sup> *Id.*

<sup>[67]</sup> *See* NTIA Comments, at Technical Appendix, sec. 4.2. *See also* County and City Data Book: 2000, U.S. Census Bureau, National Data Summary File 1, Table P-15.

<sup>[68]</sup> In this report, (I+N)/N is also referred to as “noise floor increase.”

<sup>[69]</sup> VOAAREA allows one to set the length of the vertical antenna either to a fixed value in meters or to allow it to vary with frequency. In this analysis, it was assumed that a receiver subject to potential interference at any given frequency would make use of an antenna designed for that frequency; therefore, the antenna in this case was set to quarter-wave length for each frequency (*e.g.*, 7.5 meters at 10 MHz). VOACAP automatically adjusts this length such that the receive pattern stays the same regardless of frequency. As is appropriate for a monopole antenna, the maximum gain for the antenna at any height was set to 3 dB above that of a dipole.

<sup>[70]</sup> Noise level used in this analysis is based on Recommendation ITU-R P.372-8, “Radio Noise” implemented in VOACAP/VOAAREA.

<sup>[71]</sup> *See* ITU-R Chairman's report on the meeting of Working Party 1C, Geneva, 11-15 October 2004, document #54, Annex 2, “Noise Measurements.”

<sup>[72]</sup> *See* NTIA Comments, at Technical Appendix, sec. 4.

<sup>[73]</sup> The choice of quasi-peak-to-RMS conversion factor was based on the measurement data from the NTIA Phase 1 Study, which indicated that the BPL signal power measured using a quasi-peak detector typically exceeded the level measured using an average detector by 0 – 5 dB. *See* NTIA Phase 1 Study, at Volume II, sec. D.3.4.

<sup>[74]</sup> As previously noted in Section 3.2.3, the term “I” refers to the interfering signal power associated with radiated BPL emissions.

<sup>[75]</sup> For wide bandwidth BPL signals, where the center frequency exceeds the lowest in-band frequency by at least a factor of two, additional measurements beyond 1 wavelength are required. *See* BPL Report and Order, at Appendix C, *Measurement Guidelines* ¶ 2.b.2.

<sup>[76]</sup> *See* 47 C.F.R. § 15.31(f)(1) for operation at or above 30 MHz. Between 1.705 MHz and 30 MHz, 47 C.F.R. § 15.209(a) defines the field strength limit at a measurement distance of 30 meters.

<sup>[77]</sup> See NTIA September 13, 2004 Letter, at Annex 1.

<sup>[78]</sup> See NTIA Phase 1 Study, Vol. I, at pp. 6-11.

<sup>[79]</sup> See NTIA Comments, at Technical Appendix, at sec. 4.

**POTENTIAL INTERFERENCE FROM  
BROADBAND OVER POWER LINE (BPL)  
SYSTEMS TO FEDERAL GOVERNMENT  
RADIOCOMMUNICATION SYSTEMS  
AT 1.7 - 80 MHz**

**Phase 2 Study**

**VOLUME II**



*technical report*



NTIA Report 08-450

**POTENTIAL INTERFERENCE FROM BROADBAND OVER  
POWER LINE (BPL) SYSTEMS TO FEDERAL GOVERNMENT  
RADIOCOMMUNICATION SYSTEMS AT 1.7 - 80 MHz**

**Phase 2 Study**

**VOLUME II**

**James C. Richards  
Jonathan V. Williams**



**U.S. Department of Commerce  
Carlos M. Gutierrez, Secretary**

John M. R. Kneuer, Assistant Secretary  
for Communications and Information

**October 2007**





**VOLUME II**  
**TABLE OF CONTENTS**

**TECHNICAL APPENDICES**

TABLE OF CONTENTS .....	iii
GLOSSARY .....	iv
APPENDIX A     ANTENNA MEASUREMENT HEIGHT	
A.1         Introduction .....	A-1
A.2         Height of Peak Field Strength .....	A-1
A.3         Compliance Measurement Height for Operation Between 1.7 – 30 MHz .....	A-10
A.4         Compliance Measurement Height for Operation at 30 MHz and Above .....	A-53
A.5         Height Correction Factor Above 30 MHz .....	A-62
APPENDIX B     MEASUREMENT DISTANCE ALONG THE POWER LINE	
B.1         Introduction .....	B-1
B.2         Simulation Results .....	B-1
APPENDIX C     MEASUREMENT DISTANCE EXTRAPOLATION	
C.1         Introduction .....	C-1
C.2         BPL Field Strength Simulation Results .....	C-1
C.2.1     Extrapolated Field Strength Levels Meeting the Part 15 Limits ...	C-1
C.2.2     Simulation Results .....	C-2
APPENDIX D     SPECIAL PROTECTION PROVISIONS	
D.1         Excluded Frequency Bands .....	D-1
D.2         Exclusion Zones .....	D-2
D.2.1     Coast Stations .....	D-2
D.2.2     Radioastronomy Observatories .....	D-5
D.3         Consultation Areas .....	D-7

## GLOSSARY

AWG	American Wire Gauge
BPL	Broadband over Power Line(s)
BW	Bandwidth
CISPR	International Special Committee on Radio Interference
CONUS	Continental United States
COTHEN	Customs Over The Horizon Enforcement Network
dB	Decibel
dBi	Decibel referenced to an isotropic radiator
dBm	Decibel referenced to 1 milliwatt
dB $\mu$ V	Decibel referenced to 1 microvolt
dBW	Decibels referenced to 1 Watt
E	Electric Field Strength
EMC	Electromagnetic Compatibility
EUT	Equipment Under Test
FCC	Federal Communications Commission
G	Gain
GHz	Gigahertz
H	Magnetic Field Strength
HF	High Frequency
Hz	Hertz
I	Interference Power
ICAO	International Civil Aviation Organization
IRAC	Interdepartment Radio Advisory Committee
ITM	Irregular Terrain Model
ITS	Institute for Telecommunication Sciences
ITU	International Telecommunication Union
ITU-R	International Telecommunication Union Radiocommunication Sector
kHz	Kilohertz
km	Kilometer
LV	Low Voltage
m	Meter
MHz	Megahertz
mm	millimeter
mS	Siemens/meter
ms	Millisecond
MV	Medium Voltage
N	Noise Power
NEC	Numerical Electromagnetic Code
NOI	Notice of Inquiry
NPRM	Notice of Proposed Rulemaking
NTIA	National Telecommunications and Information Administration
OR	Off-Route

OTH	Over the Horizon
PFD	Power Flux Density
PLC	Power Line Communications
PLT	Power Line Telecommunications
R	Route
RF	Radio Frequency
RMS	Root Mean Square
RSMS	Radio Spectrum Measurement System
S	Signal Power
SNR	Signal-to-Noise Ratio
SSB	Single Sideband
SSN	Smoothed Sunspot Number
URD	Underground Residential Distribution
US&P	United States and Possessions
UTC	Universal Coordinated Time
VHF	Very High Frequency
VLA	Very Large Array
VOA	Voice of America
VOACAP	Voice of America Coverage Analysis Program
W	Watt
$\mu\text{A}$	Microampere
$\mu\text{V}$	Microvolt



# APPENDIX A

## MEASUREMENT ANTENNA HEIGHT

### A.1 INTRODUCTION

Section A.2 describes NTIA's Numerical Electromagnetics Code (NEC) simulation results showing the height where the peak field strength is expected in close proximity to an Access Broadband over Power Line (BPL) system operating on overhead Medium Voltage (MV) power lines. Section A.3 shows the effectiveness of the 1 meter measurement height in estimating the peak field strength at frequencies between 1.7 and 30 MHz. Section A.4 provides results from simulations performed in the 30 – 50 MHz range, using the 1 to 4 meter measurement height range defined in the compliance measurement guidelines for Access BPL systems operating above 30 MHz. In Section A.5, the optional 5-dB height correction factor for measurements at a 1 meter height is compared to the use of the 1 to 4 meter measurement height for the various power line simulations at frequencies above 30 MHz.

### A.2 HEIGHT OF PEAK FIELD STRENGTH

Figures A-1 through A-18 show the heights where the peak electric field strength occurred over the frequency range of 2 to 50 MHz for the NEC power line models described in Section 2.2. The height of the modeled power lines was 12 meters. These results assume field strength values are calculated at a horizontal distance of 10 meters.

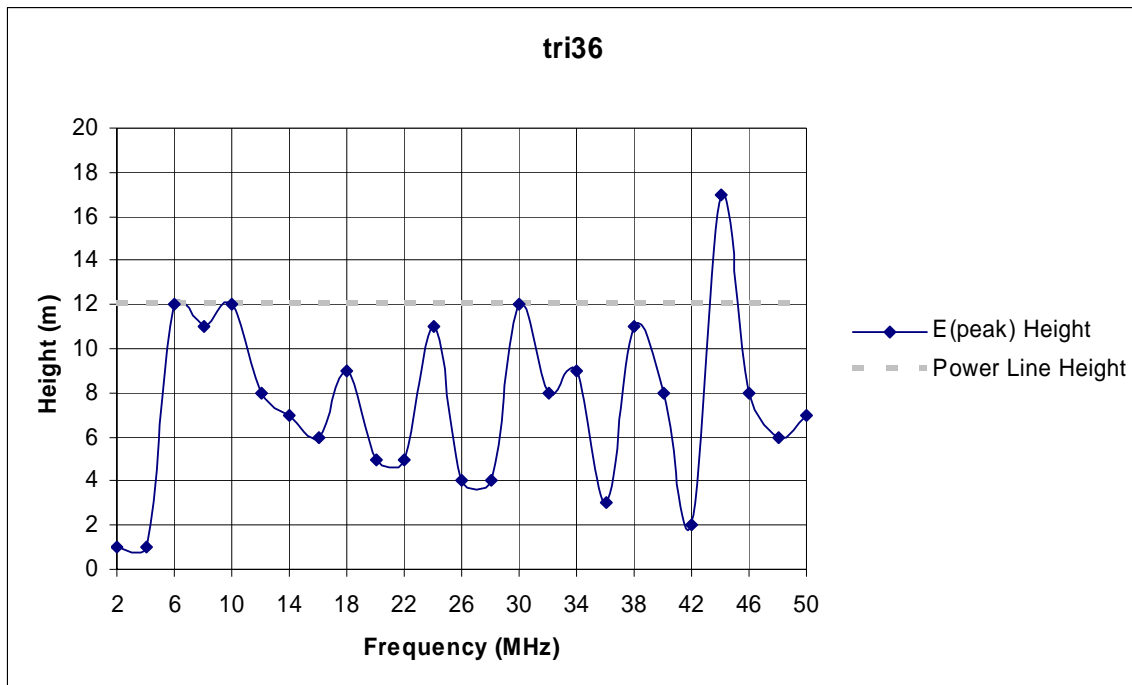
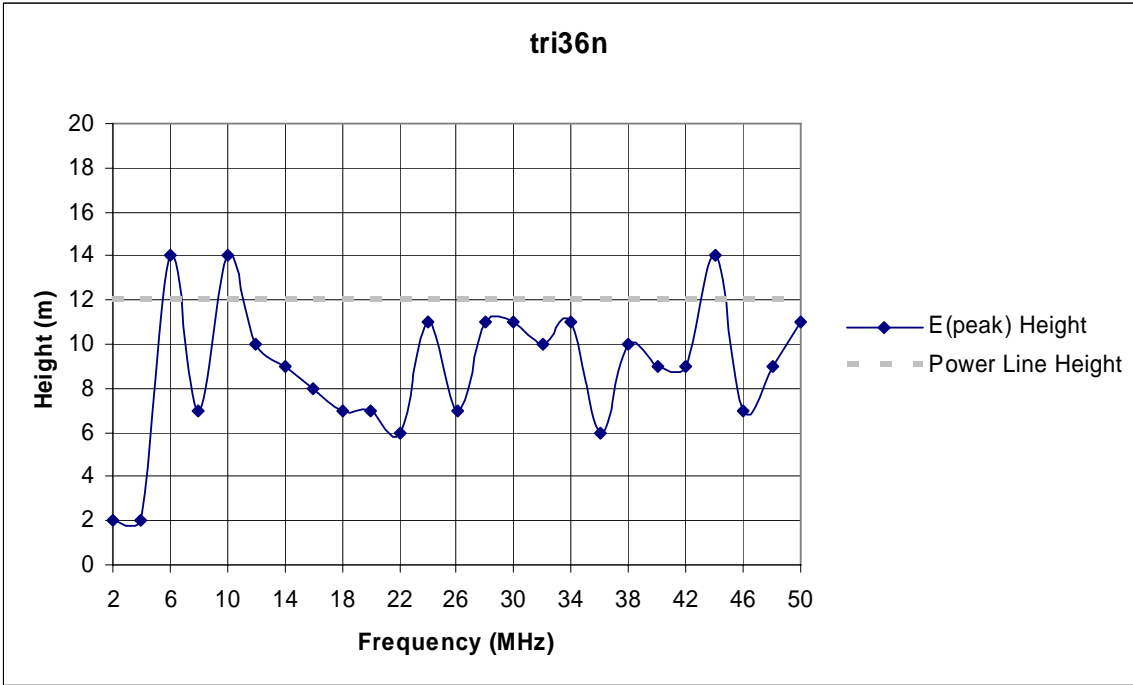
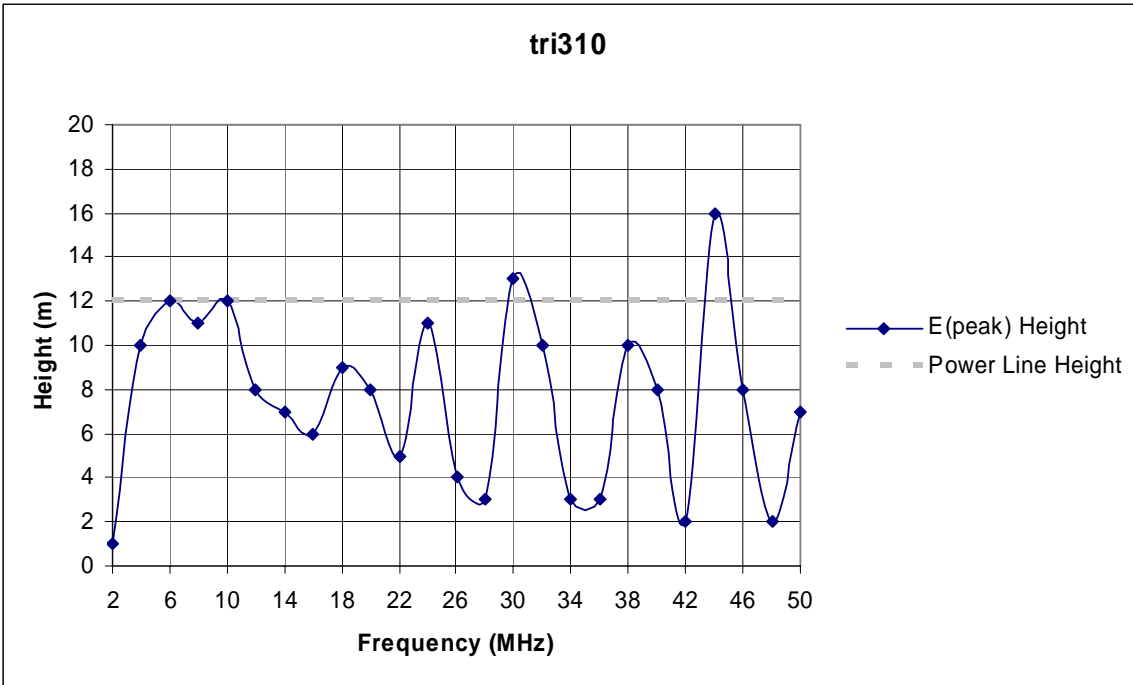


Figure A-1: Height corresponding to peak electric field strength as a function of frequency



**Figure A-2: Height corresponding to peak electric field strength as a function of frequency**



**Figure A-3: Height corresponding to peak electric field strength as a function of frequency**

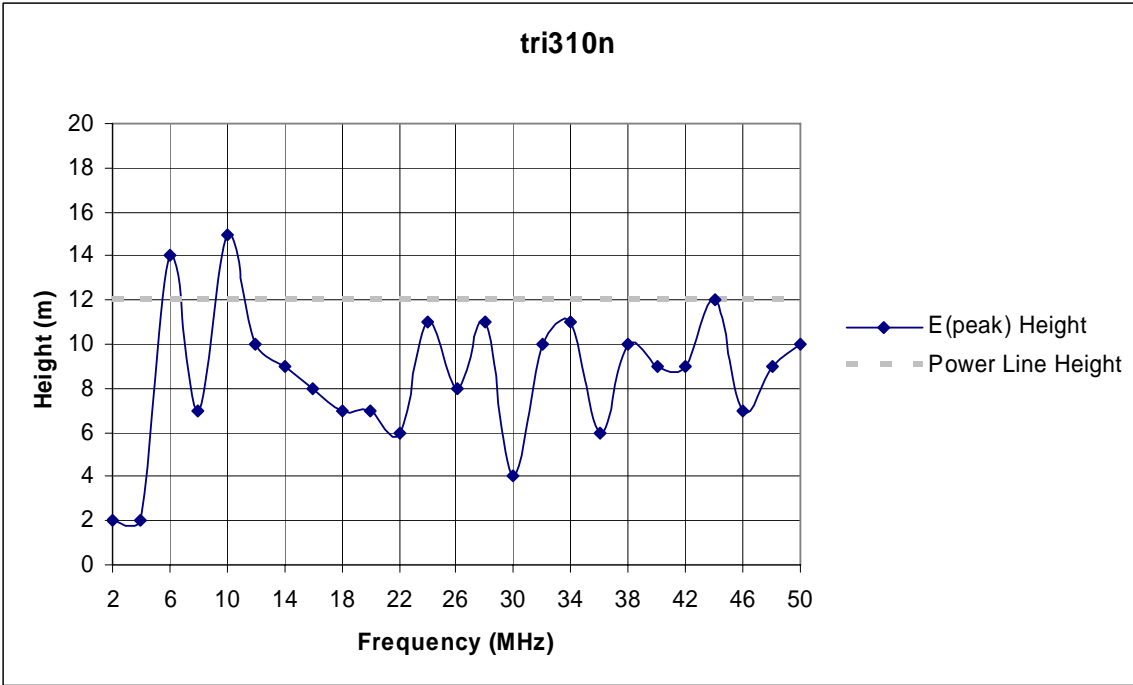


Figure A-4: Height corresponding to peak electric field strength as a function of frequency

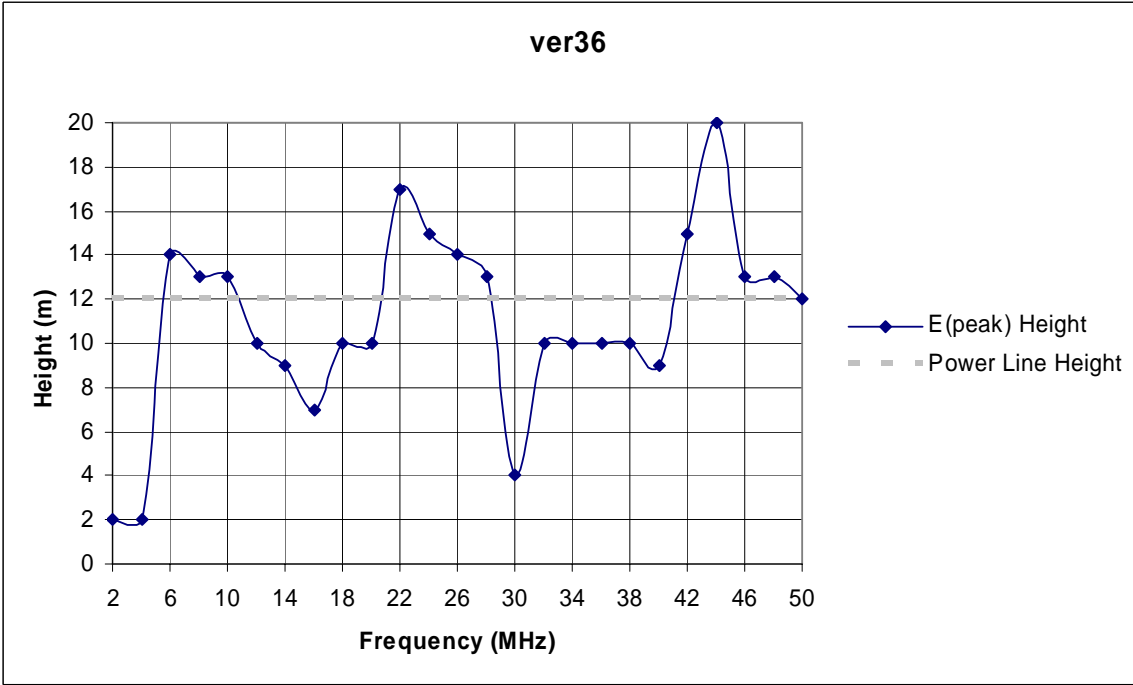


Figure A-5: Height corresponding to peak electric field strength as a function of frequency

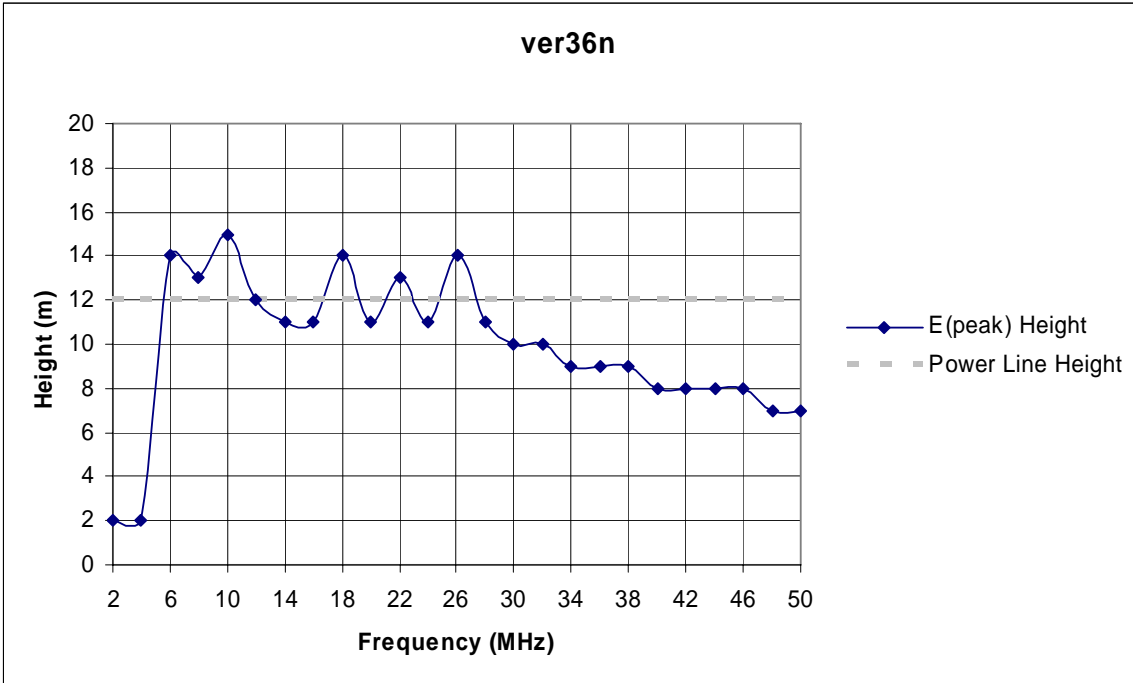


Figure A-6: Height corresponding to peak electric field strength as a function of frequency

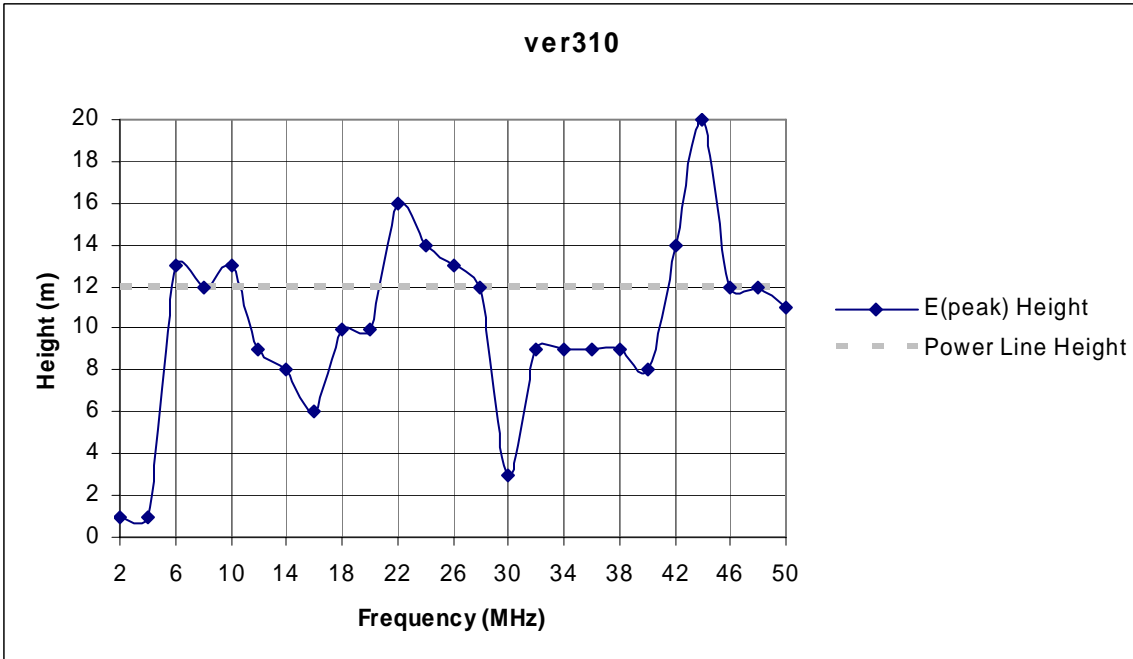


Figure A-7: Height corresponding to peak electric field strength as a function of frequency



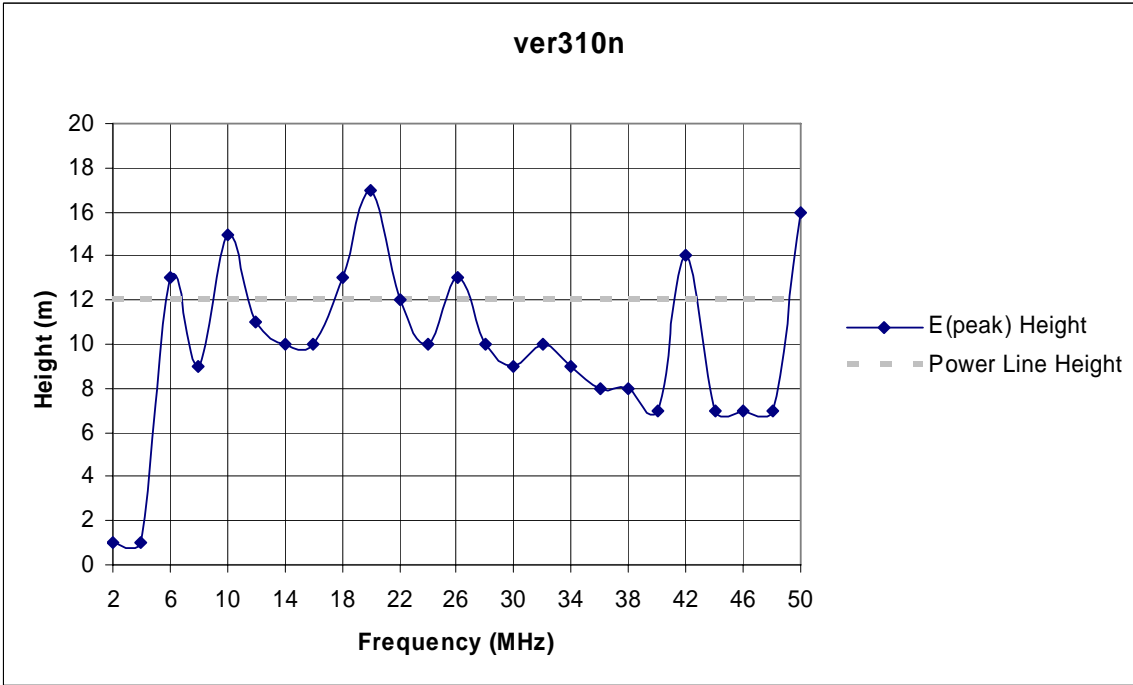


Figure A-8: Height corresponding to peak electric field strength as a function of frequency

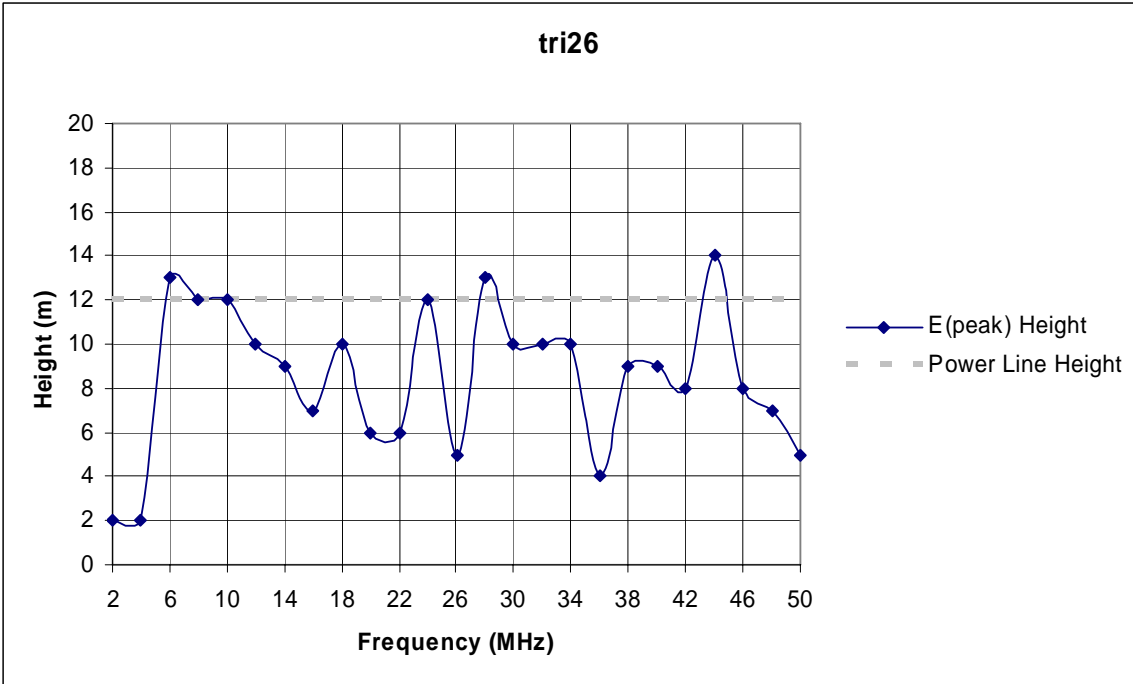


Figure A-9: Height corresponding to peak electric field strength as a function of frequency

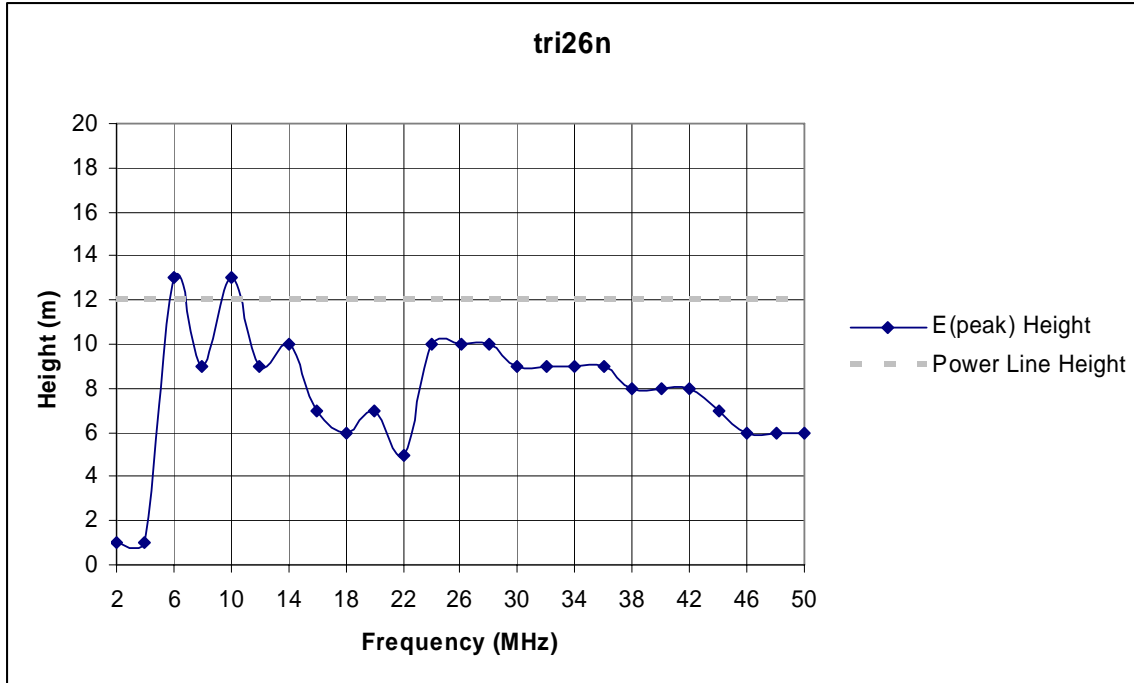


Figure A-10: Height corresponding to peak electric field strength as a function of frequency

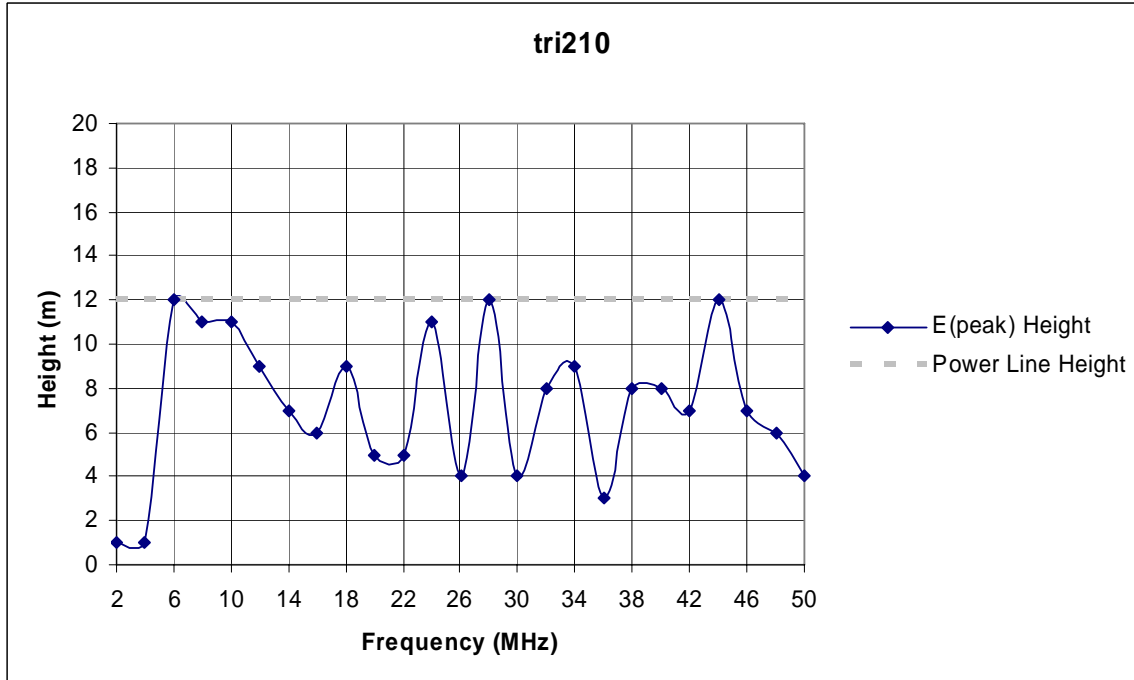


Figure A-11: Height corresponding to peak electric field strength as a function of frequency

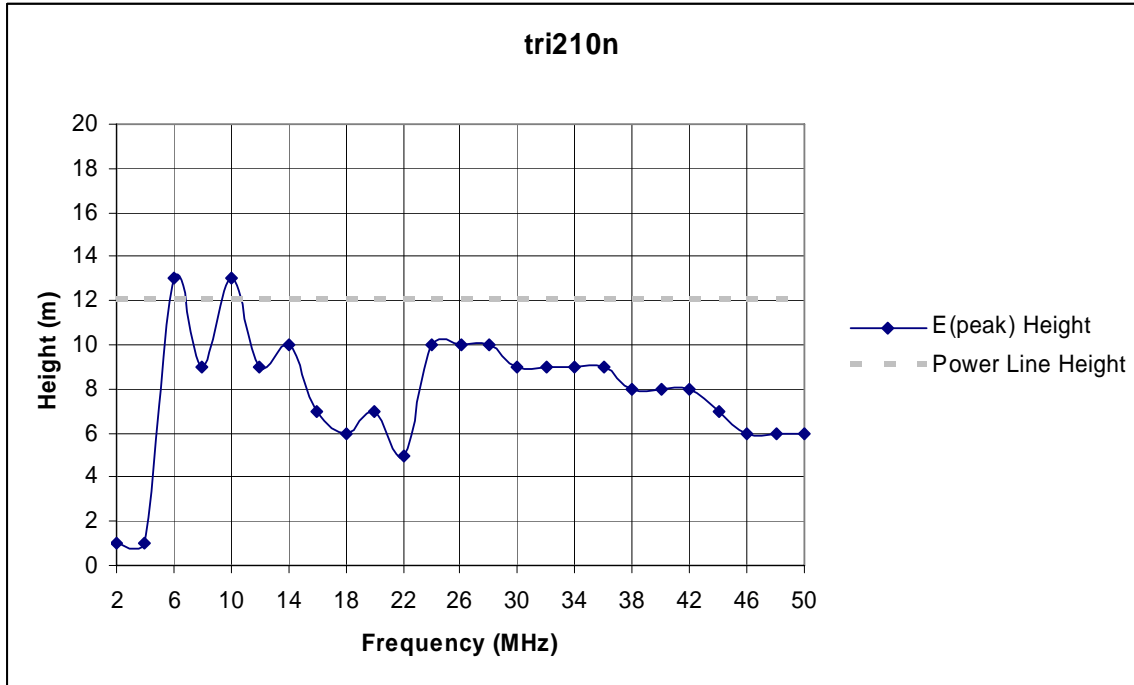


Figure A-12: Height corresponding to peak electric field strength as a function of frequency

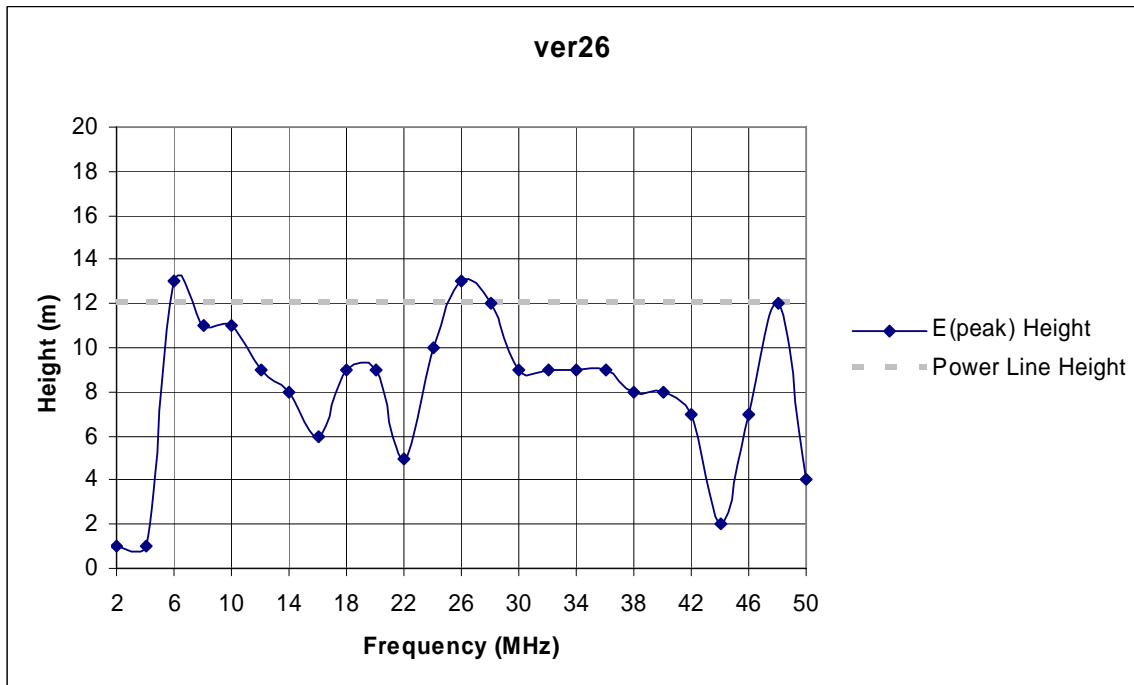


Figure A-13: Height corresponding to peak electric field strength as a function of frequency

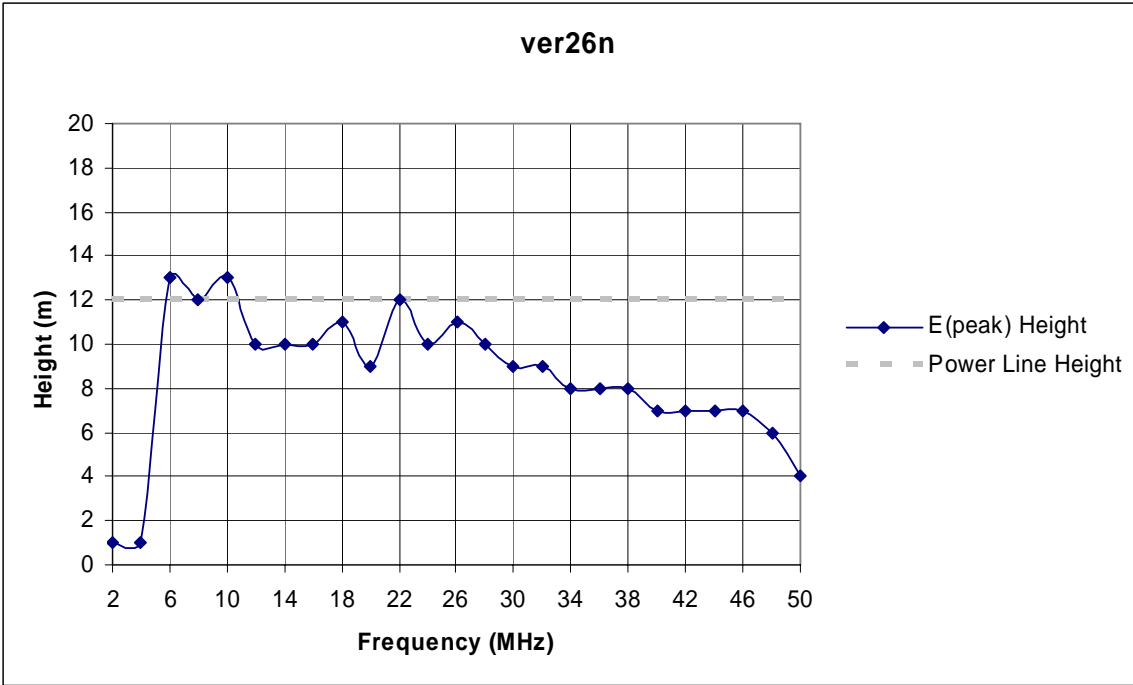


Figure A-14: Height corresponding to peak electric field strength as a function of frequency

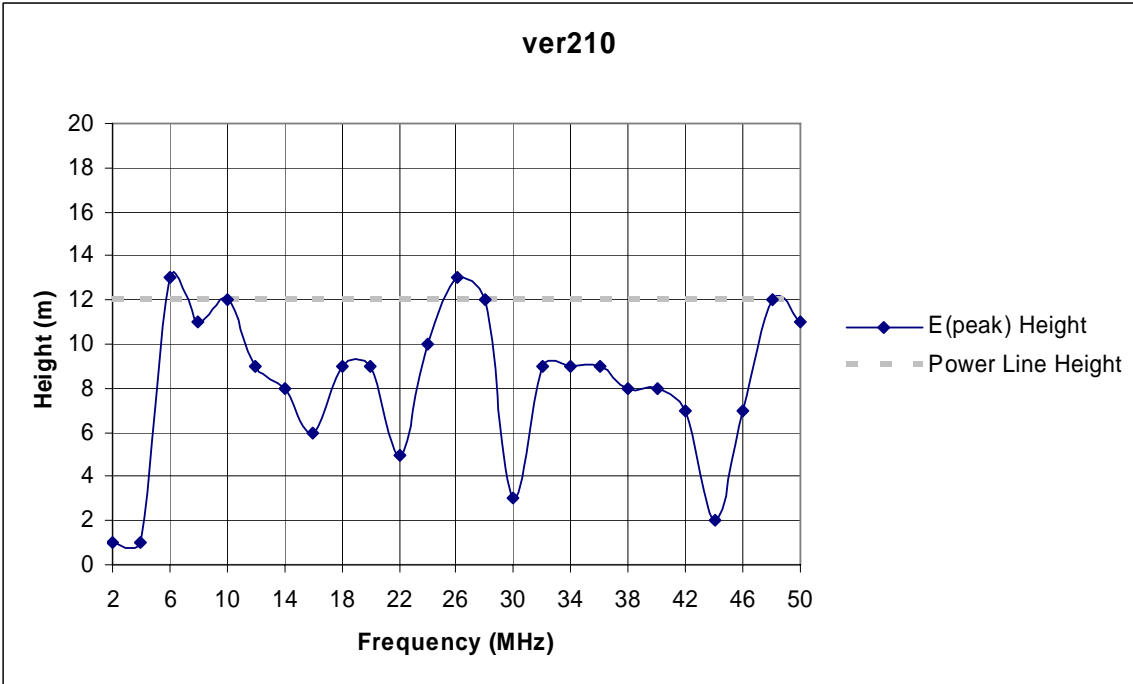


Figure A-15: Height corresponding to peak electric field strength as a function of frequency

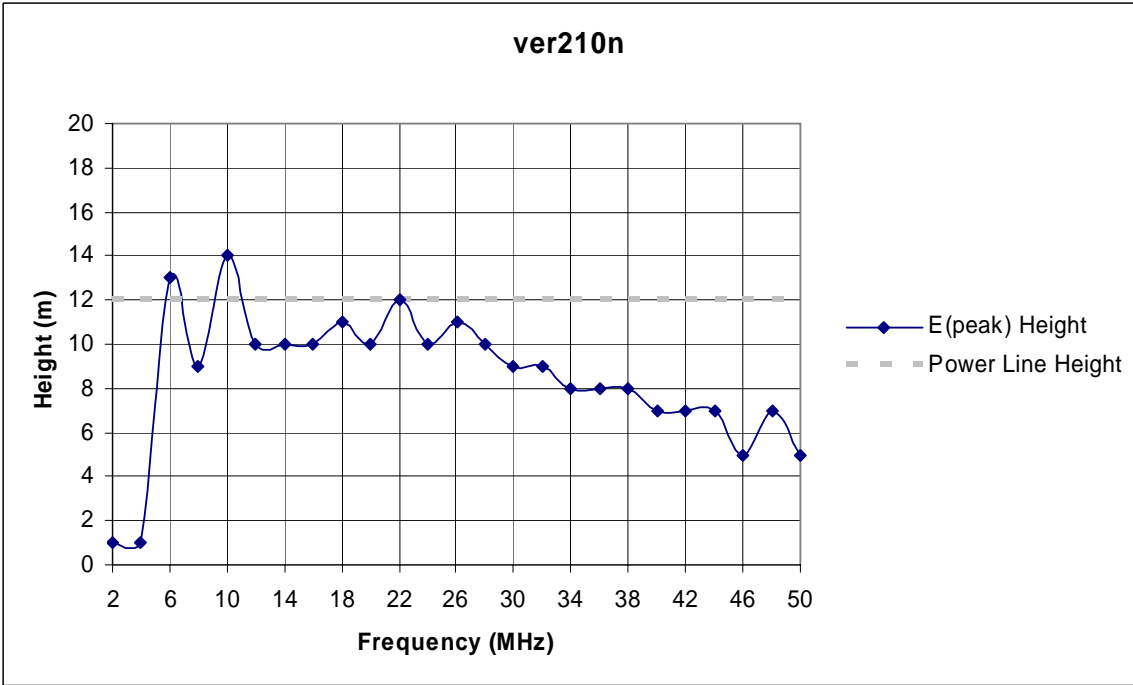


Figure A-16: Height corresponding to peak electric field strength as a function of frequency

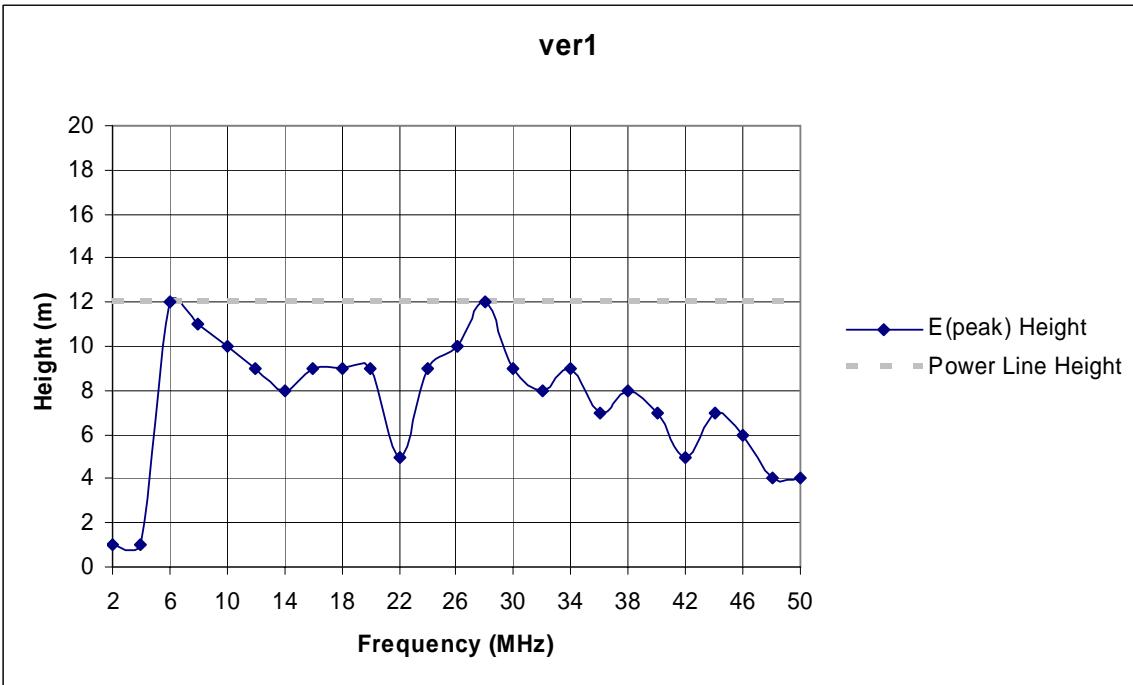


Figure A-17: Height corresponding to peak electric field strength as a function of frequency

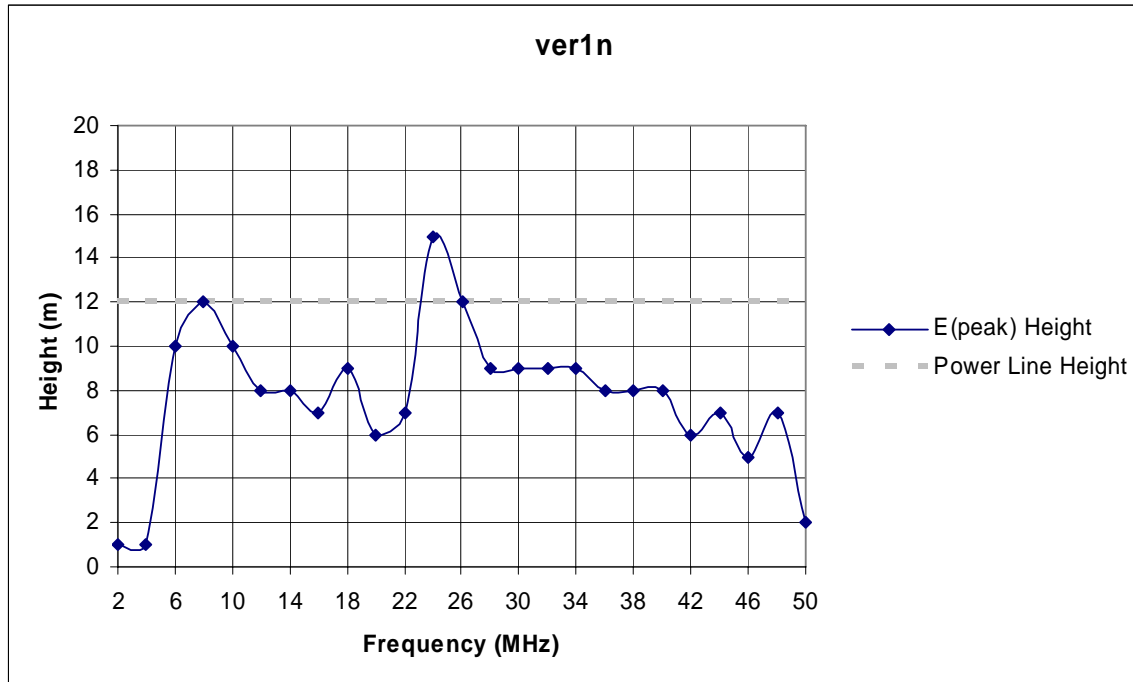


Figure A-18: Height corresponding to peak electric field strength as a function of frequency

### A.3 COMPLIANCE MEASUREMENT HEIGHT FOR OPERATION BETWEEN 1.7 - 30 MHz

The Federal Communication Commission (Commission or FCC) Part 15 measurement guidelines specify that below 30 MHz, measurements are to be made with the antenna positioned at a height of 1 meter. In Section A.2, the height corresponding to the peak field strength was often located well above the 1 meter measurement height. The following plots show a comparison between the peak field strength determined from the measurement guidelines and the 80<sup>th</sup> percentile of peak electric field strength at any height along the length of the power line. The 80<sup>th</sup> percentile values eliminate the localized peaks that are unlikely to be encountered by a radio receiver randomly located in close proximity to an Access BPL power line.<sup>1</sup> The plots are shown for a number of NEC power line models at frequencies from 2 to 28 MHz.

<sup>1</sup> See NTIA Comments, at Technical Appendix, pp. 2-18.

2 MHz Plots

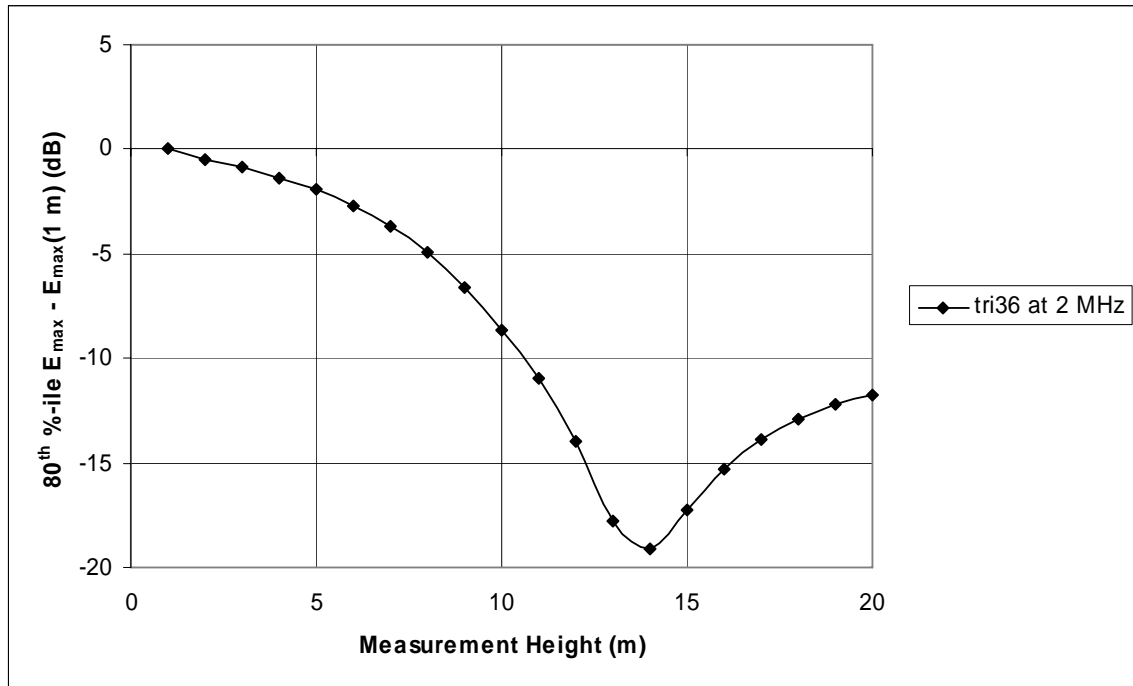


Figure A-19: 80<sup>th</sup> percentile of peak electric field strength along the power line relative to the peak electric field strength at a 1 meter measurement height

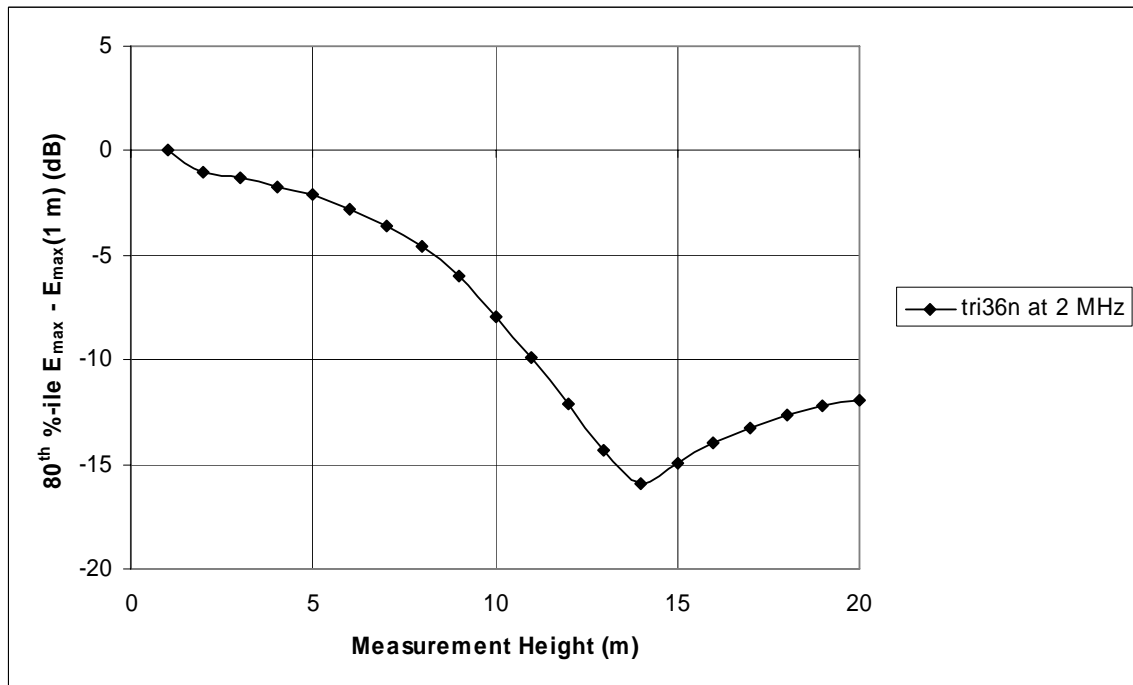


Figure A-20: 80<sup>th</sup> percentile of peak electric field strength along the power line relative to the peak electric field strength at a 1 meter measurement height

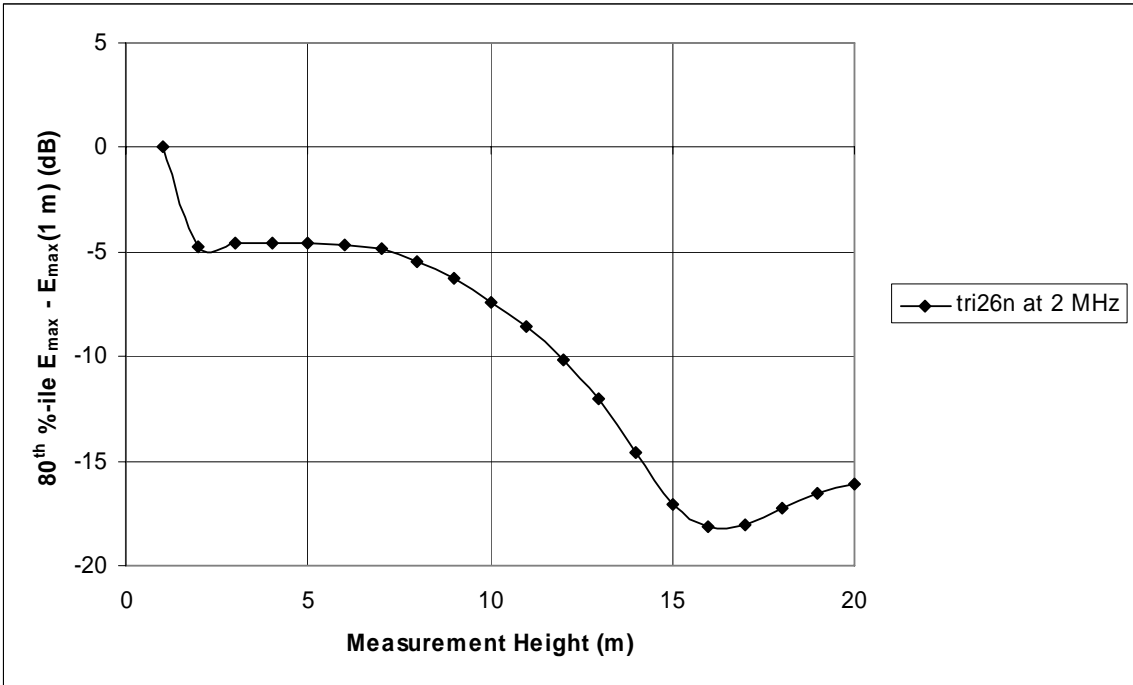


Figure A-21: 80<sup>th</sup> percentile of peak electric field strength along the power line relative to the peak electric field strength at a 1 meter measurement height

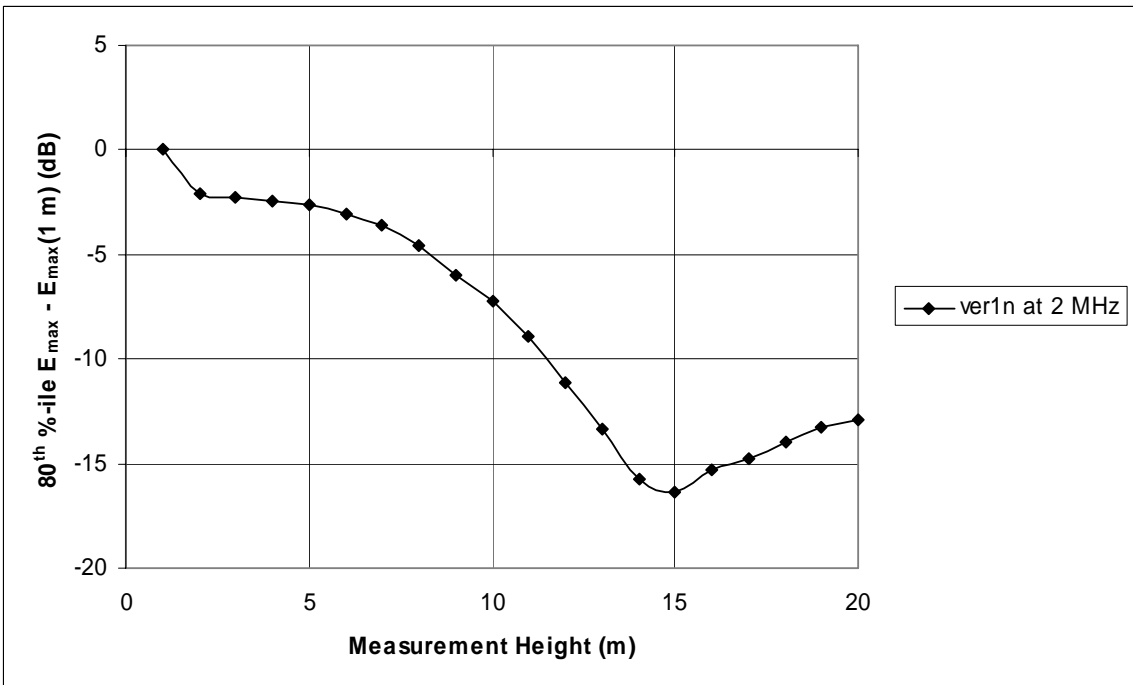


Figure A-22: 80<sup>th</sup> percentile of peak electric field strength along the power line relative to the peak electric field strength at a 1 meter measurement height



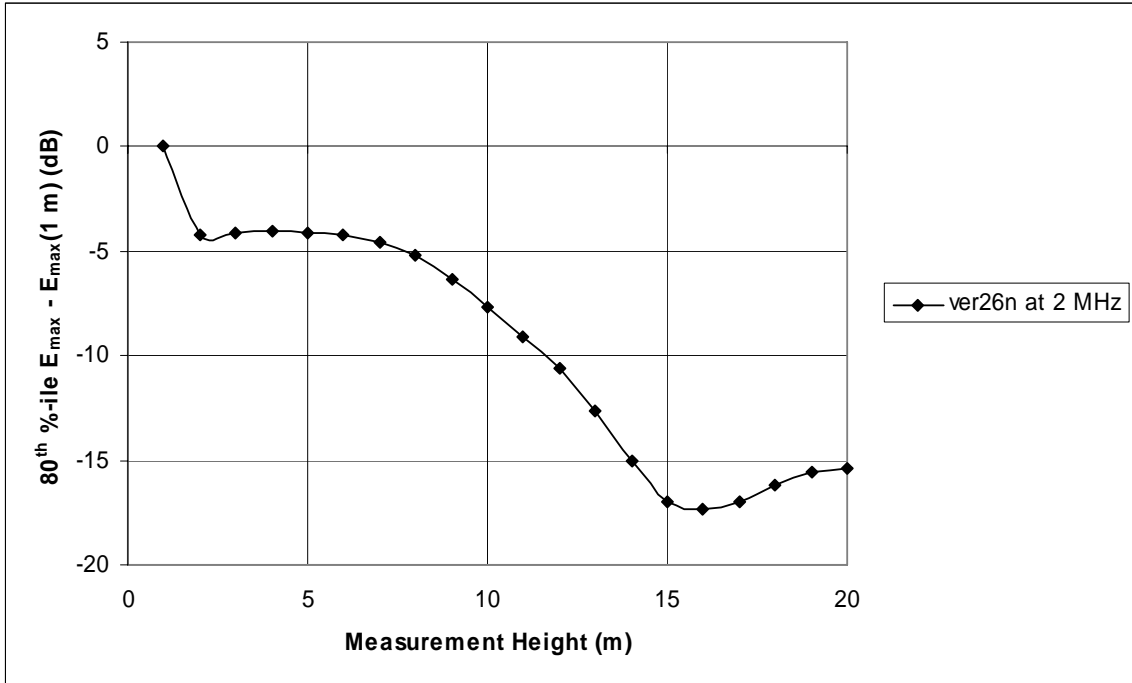


Figure A-23: 80<sup>th</sup> percentile of peak electric field strength along the power line relative to the peak electric field strength at a 1 meter measurement height

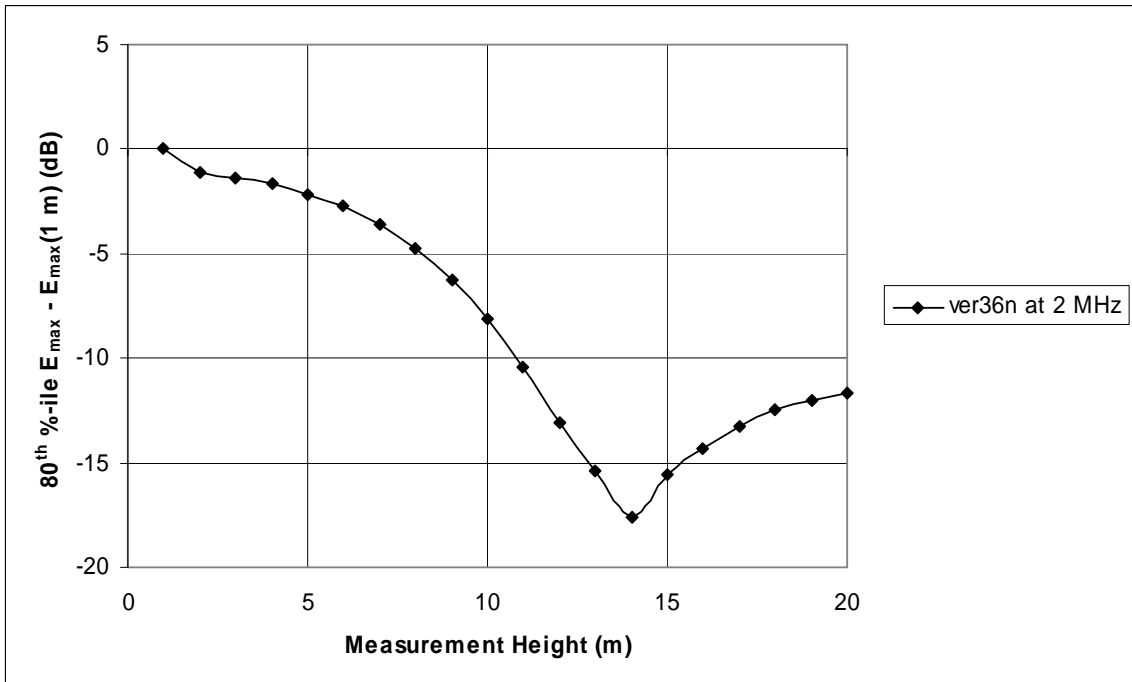


Figure A-24: 80<sup>th</sup> percentile of peak electric field strength along the power line relative to the peak electric field strength at a 1 meter measurement height

4 MHz Plots

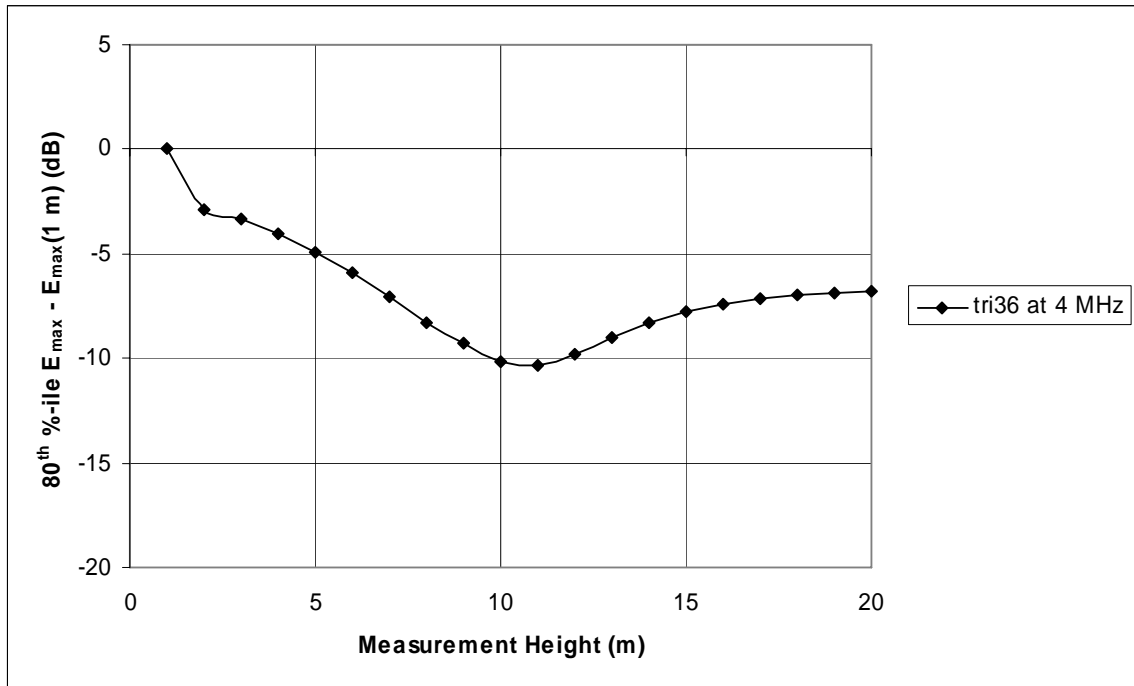


Figure A-25: 80<sup>th</sup> percentile of peak electric field strength along the power line relative to the peak electric field strength at a 1 meter measurement height

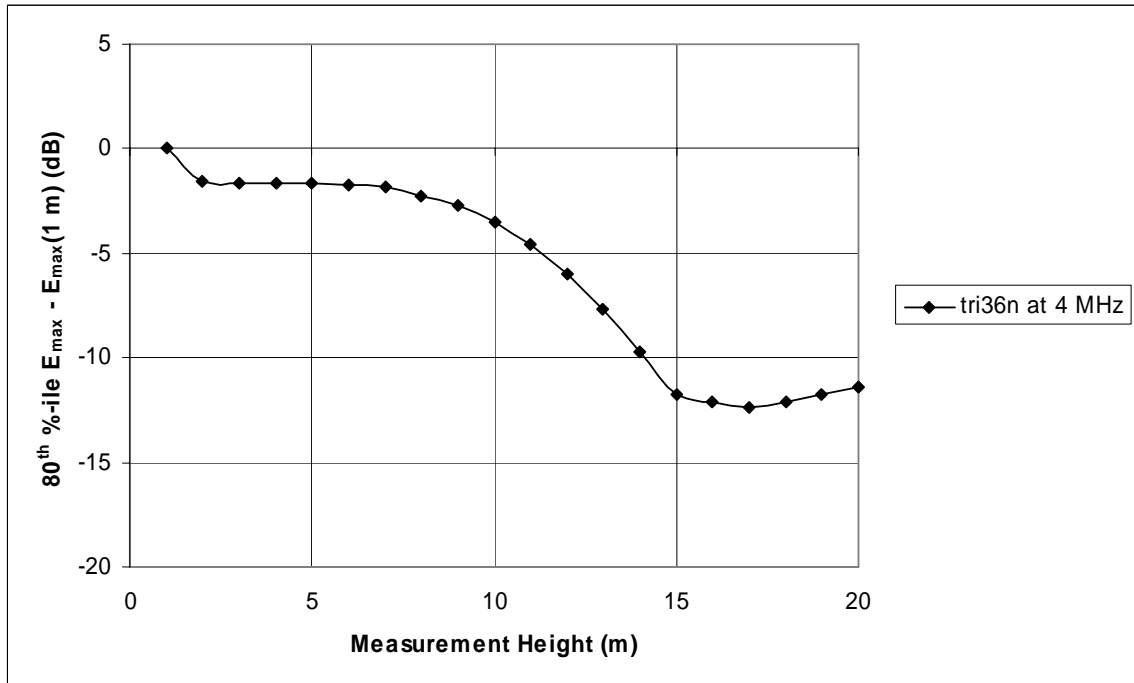


Figure A-26: 80<sup>th</sup> percentile of peak electric field strength along the power line relative to the peak electric field strength at a 1 meter measurement height

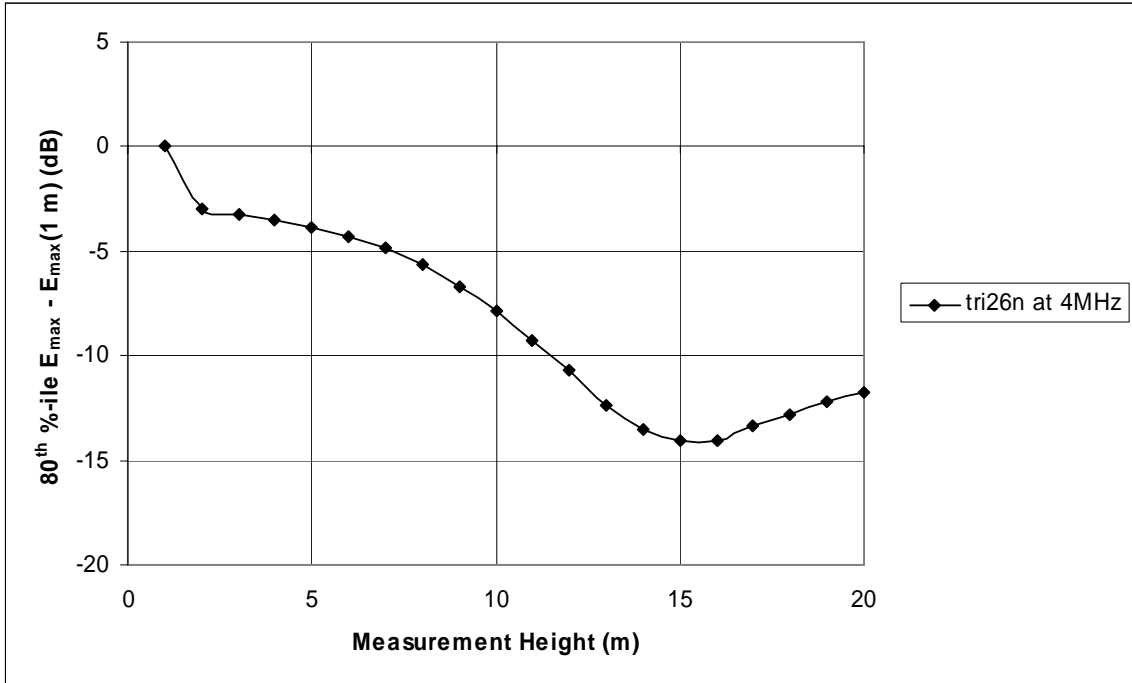


Figure A-27: 80<sup>th</sup> percentile of peak electric field strength along the power line relative to the peak electric field strength at a 1 meter measurement height

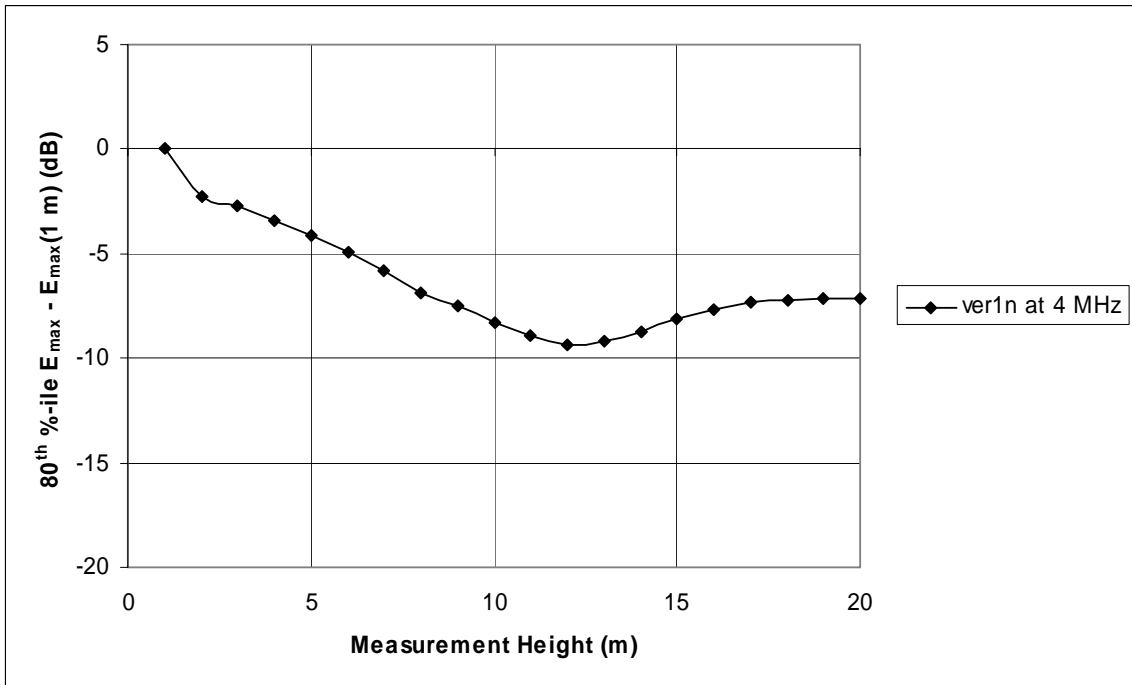


Figure A-28: 80<sup>th</sup> percentile of peak electric field strength along the power line relative to the peak electric field strength at a 1 meter measurement height

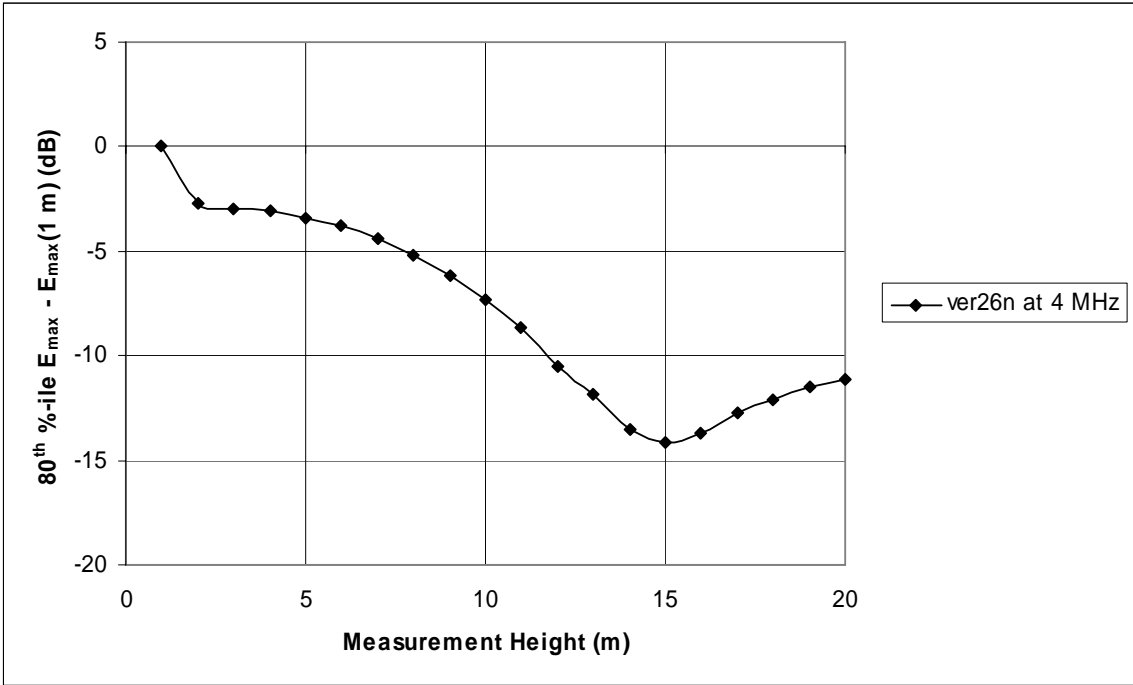


Figure A-29: 80<sup>th</sup> percentile of peak electric field strength along the power line relative to the peak electric field strength at a 1 meter measurement height

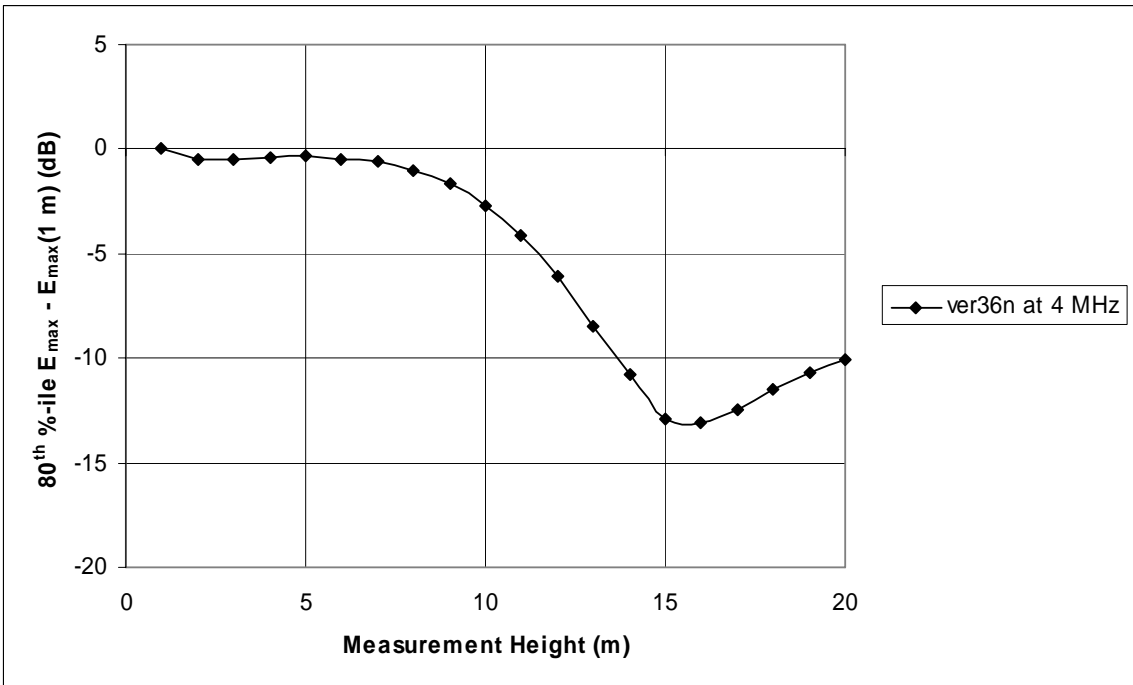


Figure A-30: 80<sup>th</sup> percentile of peak electric field strength along the power line relative to the peak electric field strength at a 1 meter measurement height

6 MHz Plots

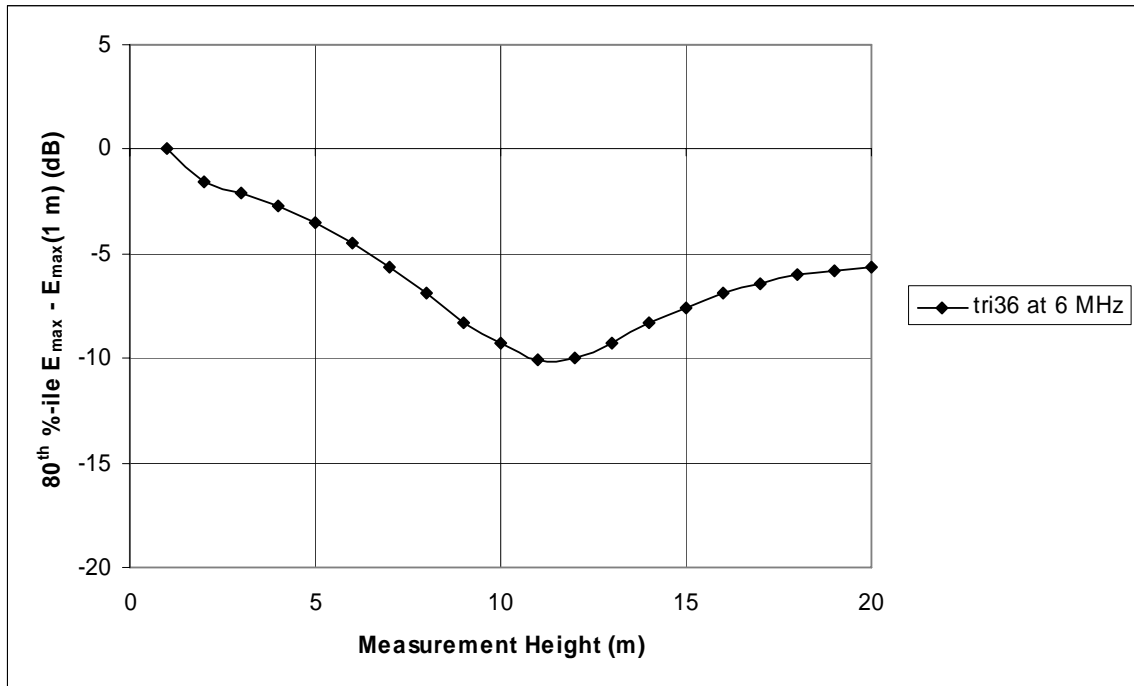


Figure A-31: 80<sup>th</sup> percentile of peak electric field strength along the power line relative to the peak electric field strength at a 1 meter measurement height

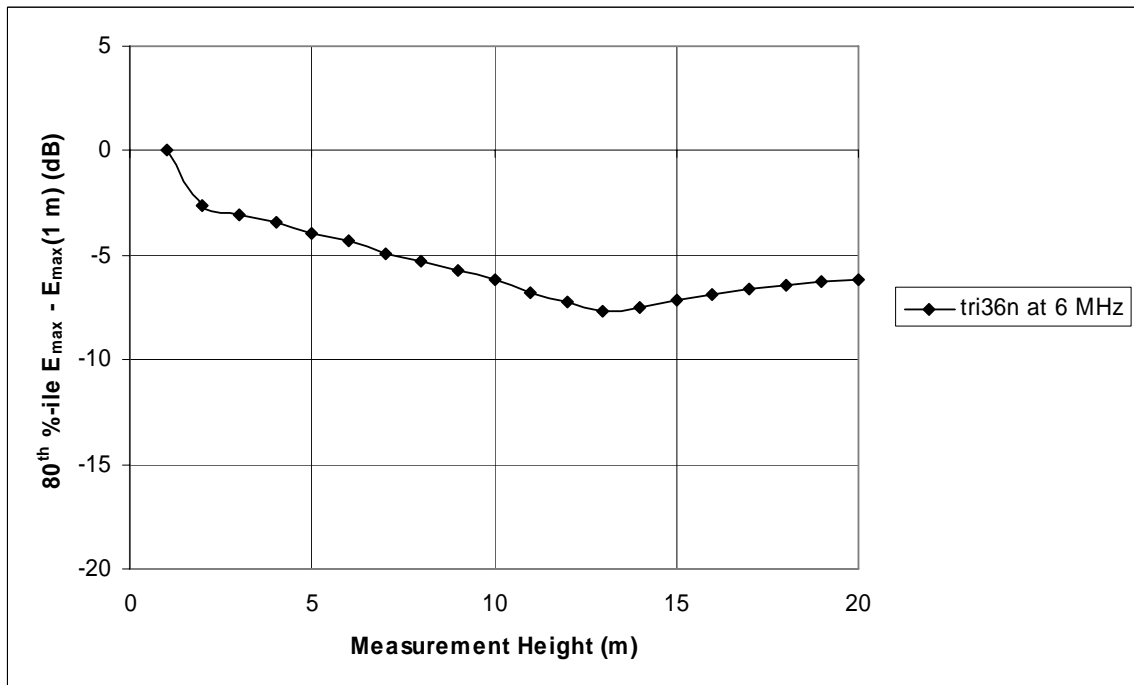


Figure A-32: 80<sup>th</sup> percentile of peak electric field strength along the power line relative to the peak electric field strength at a 1 meter measurement height

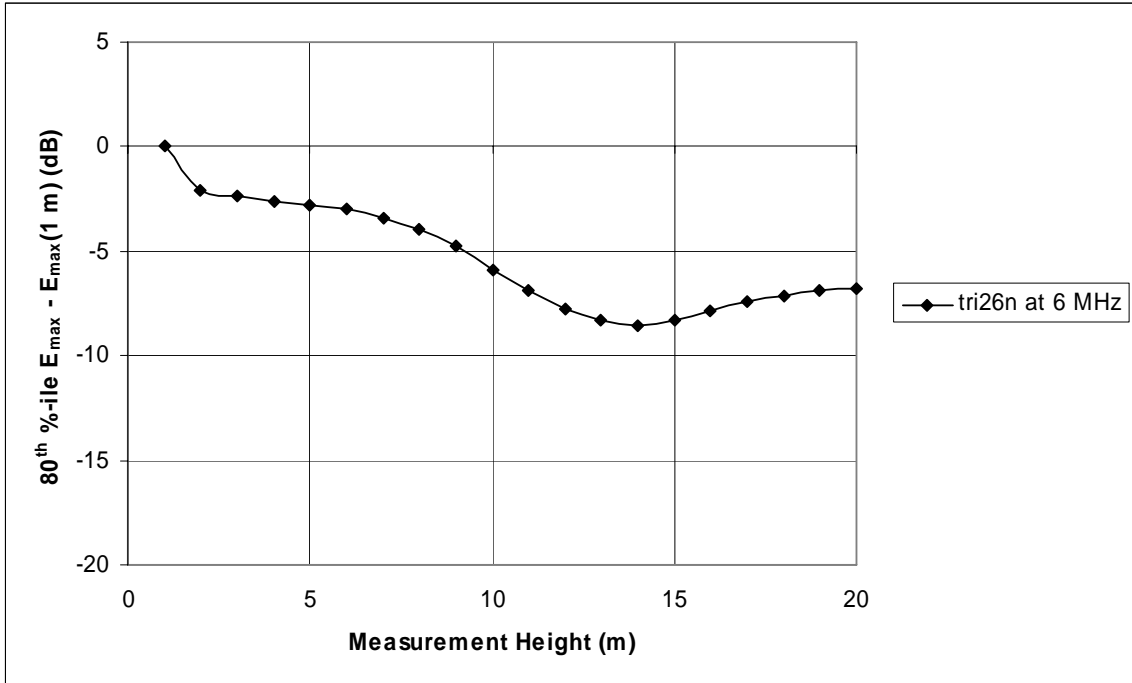


Figure A-33: 80<sup>th</sup> percentile of peak electric field strength along the power line relative to the peak electric field strength at a 1 meter measurement height

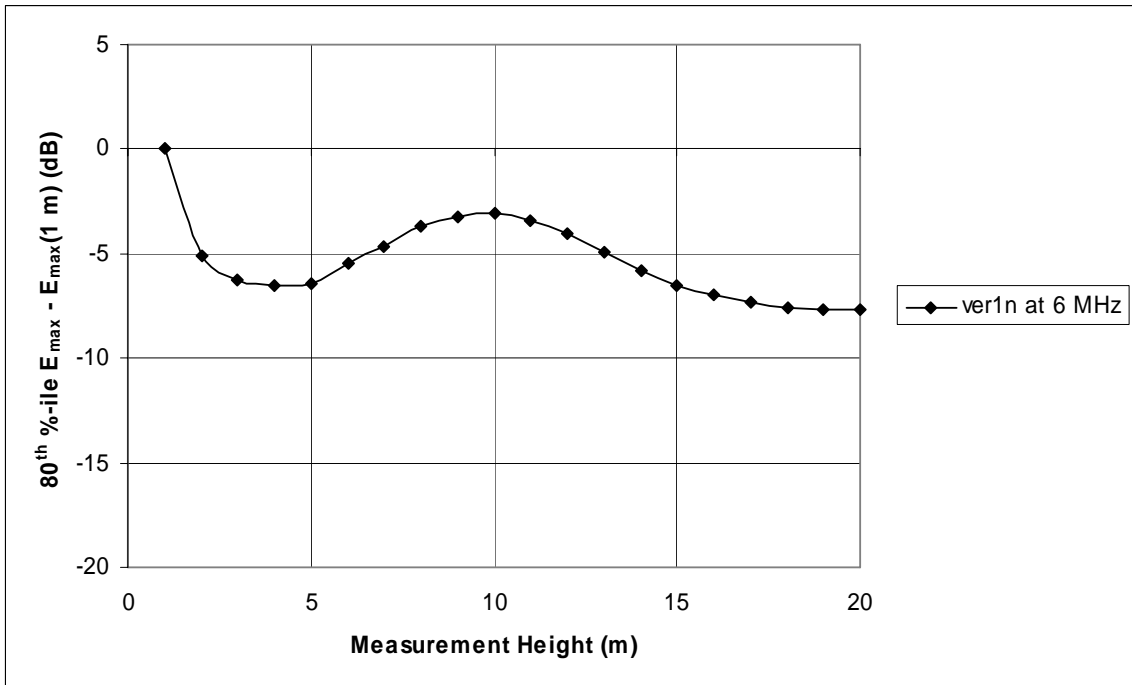


Figure A-34: 80<sup>th</sup> percentile of peak electric field strength along the power line relative to the peak electric field strength at a 1 meter measurement height

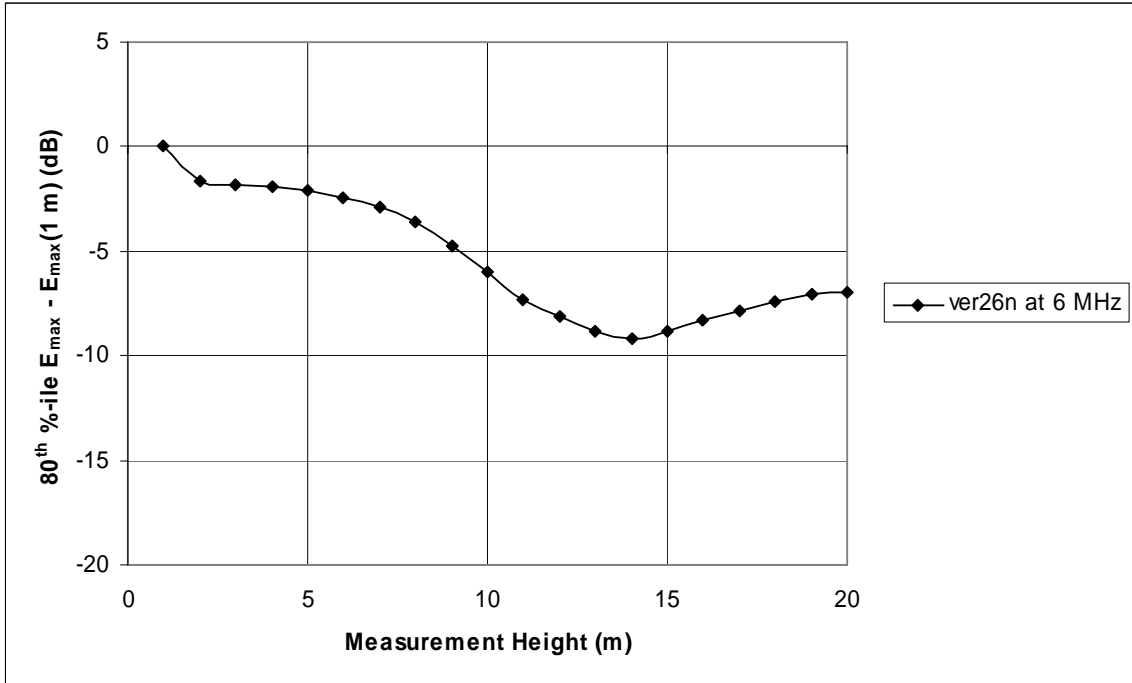


Figure A-35: 80<sup>th</sup> percentile of peak electric field strength along the power line relative to the peak electric field strength at a 1 meter measurement height

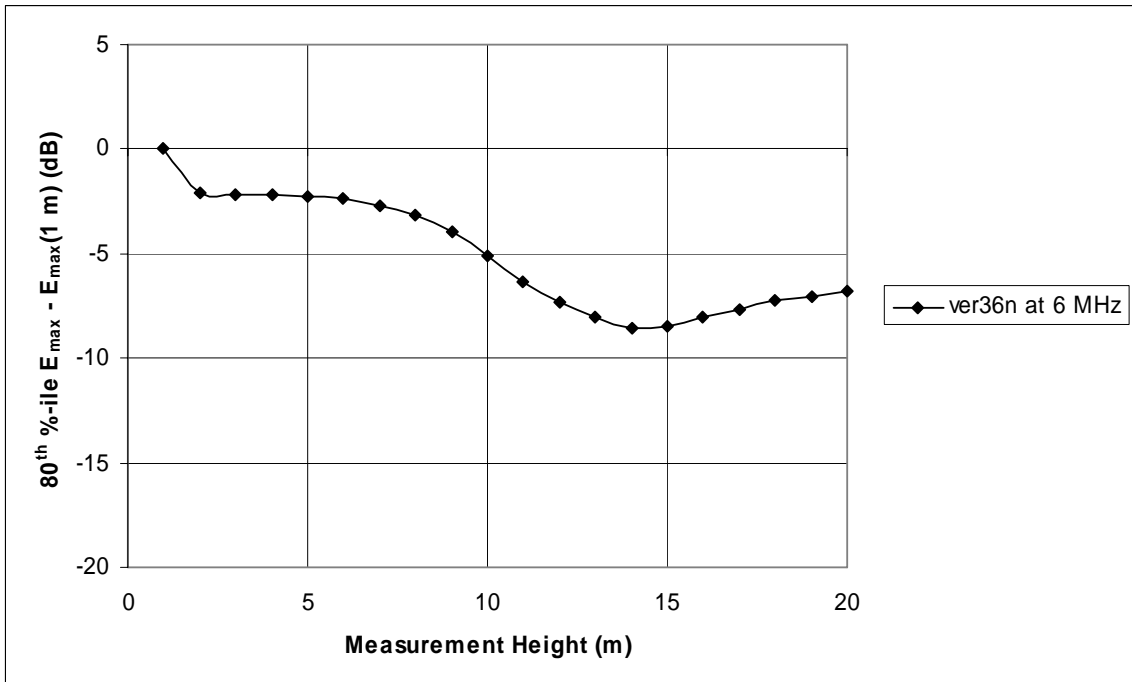


Figure A-36: 80<sup>th</sup> percentile of peak electric field strength along the power line relative to the peak electric field strength at a 1 meter measurement height

8 MHz Plots

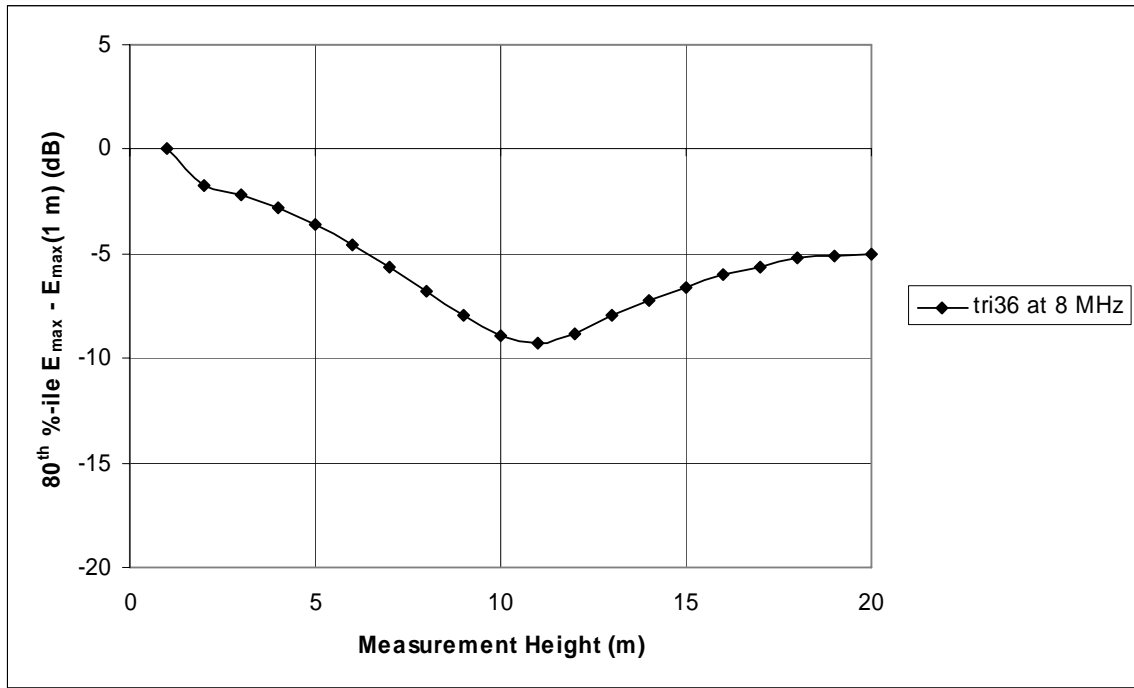


Figure A-37: 80<sup>th</sup> percentile of peak electric field strength along the power line relative to the peak electric field strength at a 1 meter measurement height

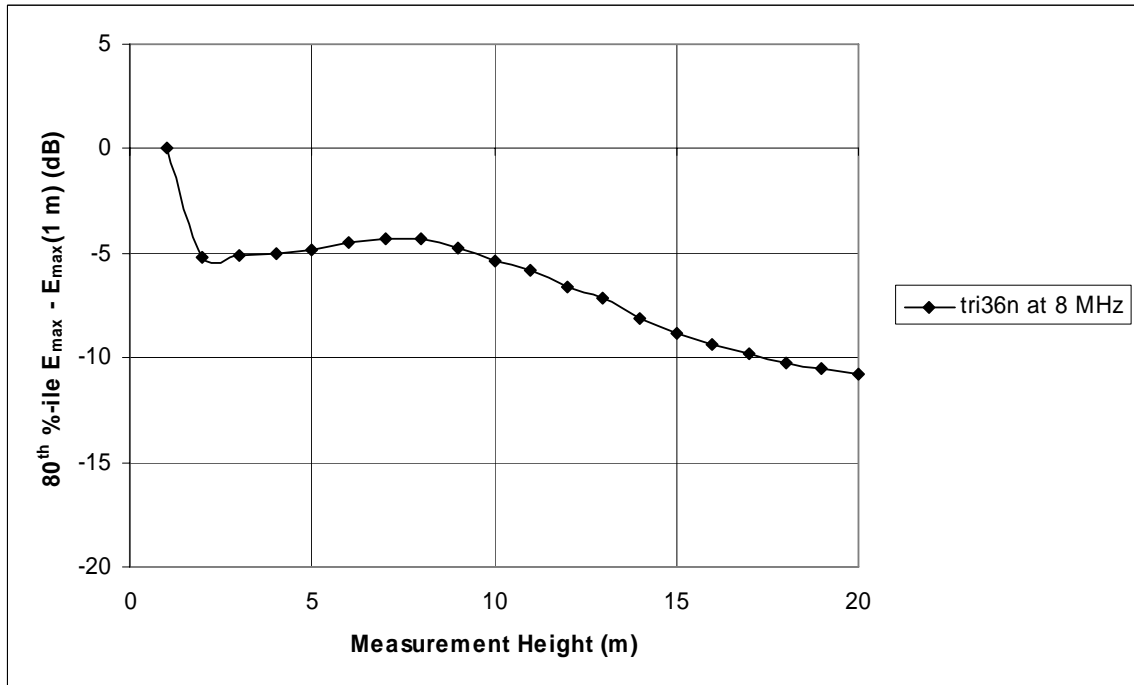


Figure A-38: 80<sup>th</sup> percentile of peak electric field strength along the power line relative to the peak electric field strength at a 1 meter measurement height



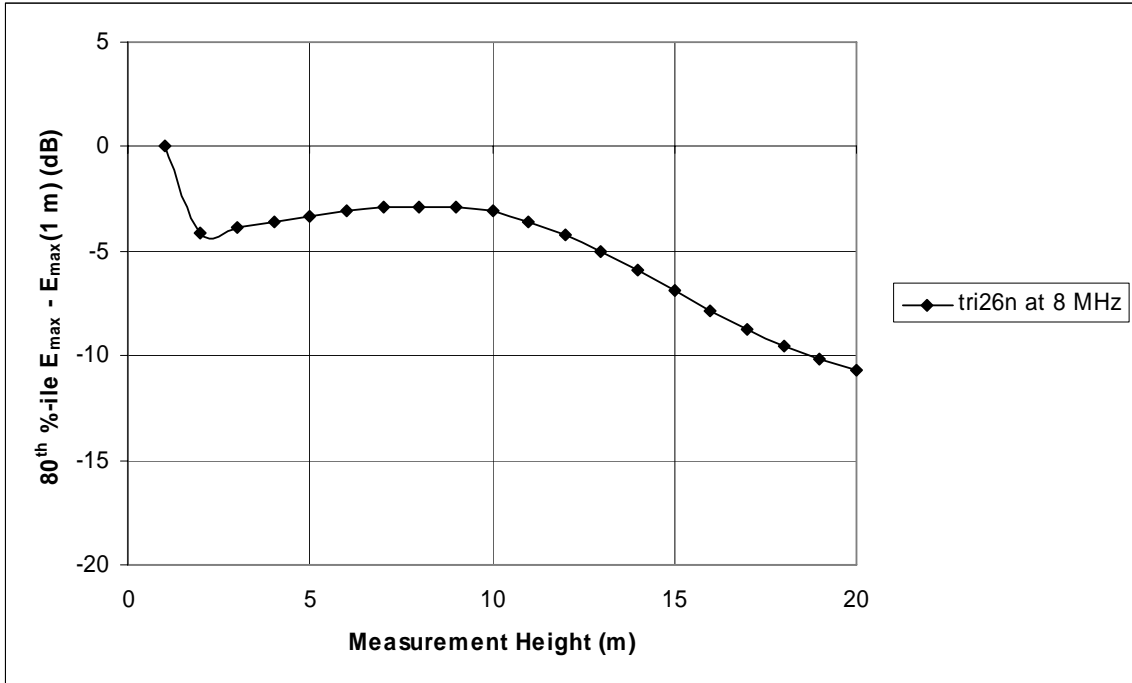


Figure A-39: 80<sup>th</sup> percentile of peak electric field strength along the power line relative to the peak electric field strength at a 1 meter measurement height

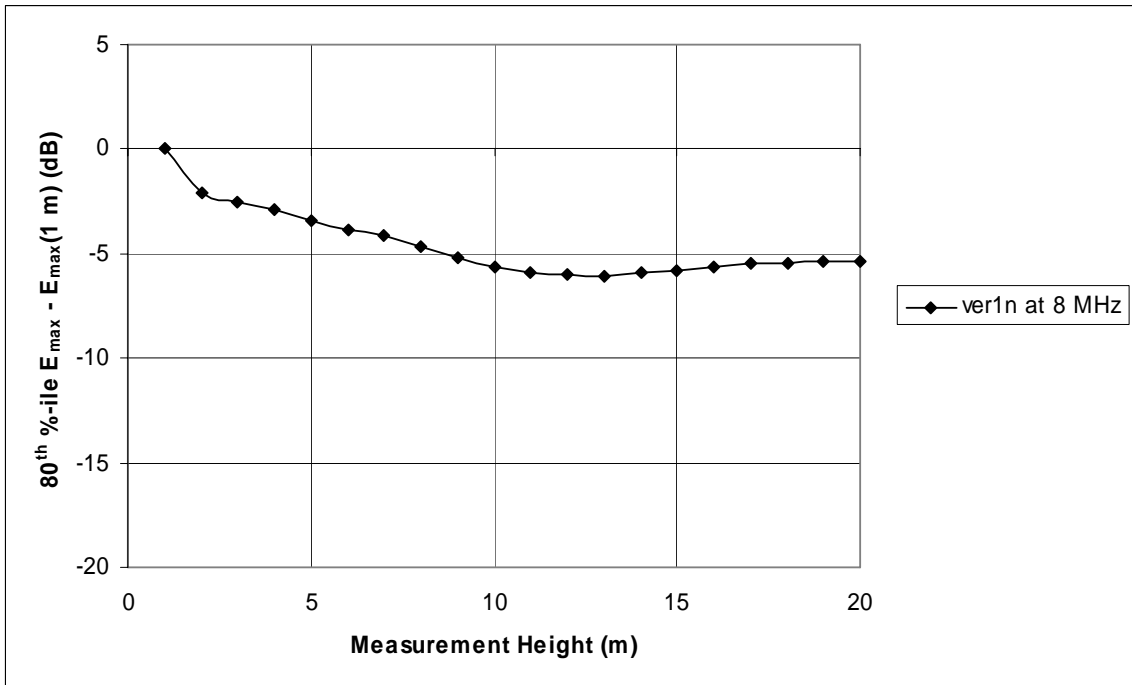


Figure A-40: 80<sup>th</sup> percentile of peak electric field strength along the power line relative to the peak electric field strength at a 1 meter measurement height

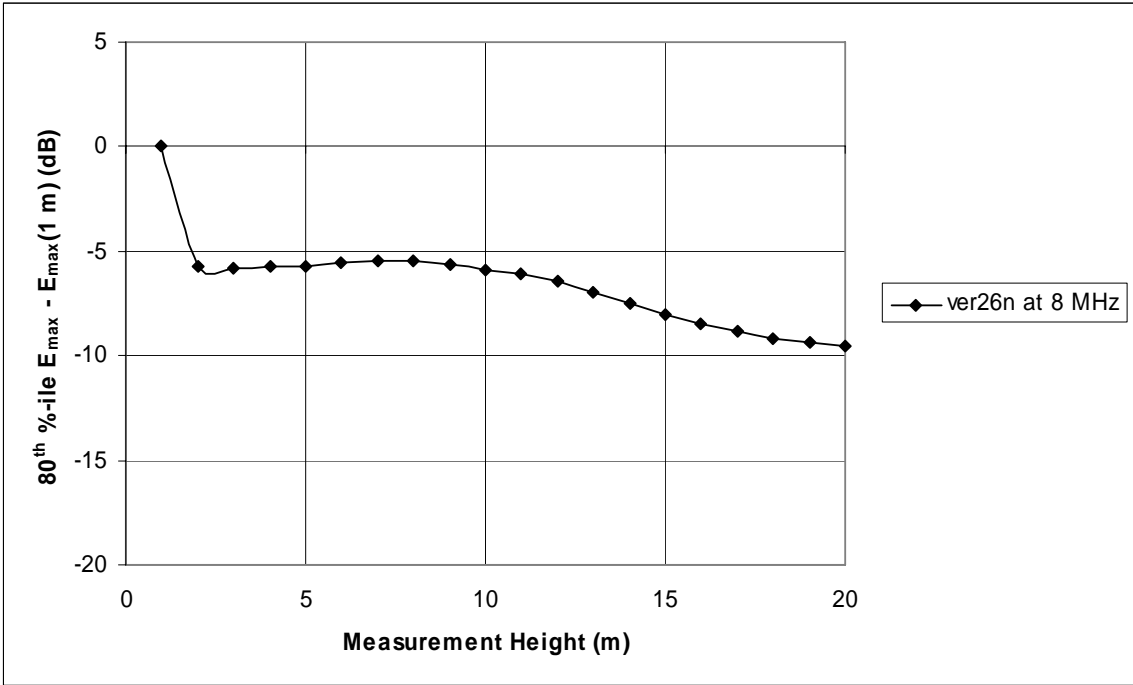


Figure A-41: 80<sup>th</sup> percentile of peak electric field strength along the power line relative to the peak electric field strength at a 1 meter measurement height

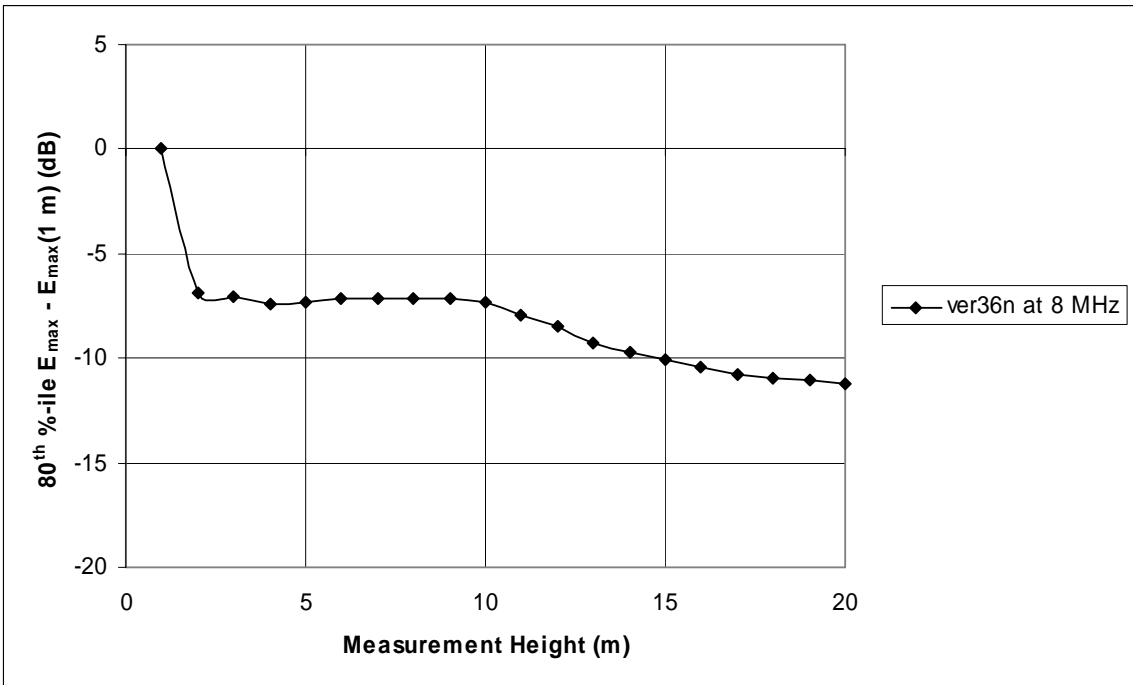


Figure A-42: 80<sup>th</sup> percentile of peak electric field strength along the power line relative to the peak electric field strength at a 1 meter measurement height

10 MHz Plots

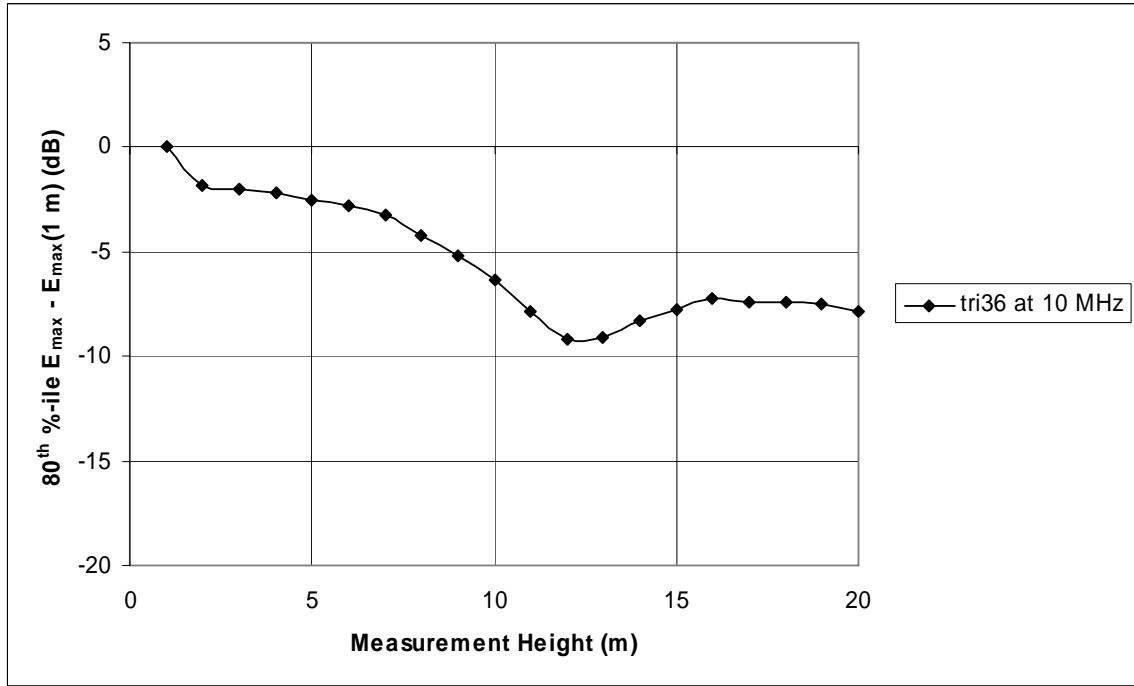


Figure A-43: 80<sup>th</sup> percentile of peak electric field strength along the power line relative to the peak electric field strength at a 1 meter measurement height

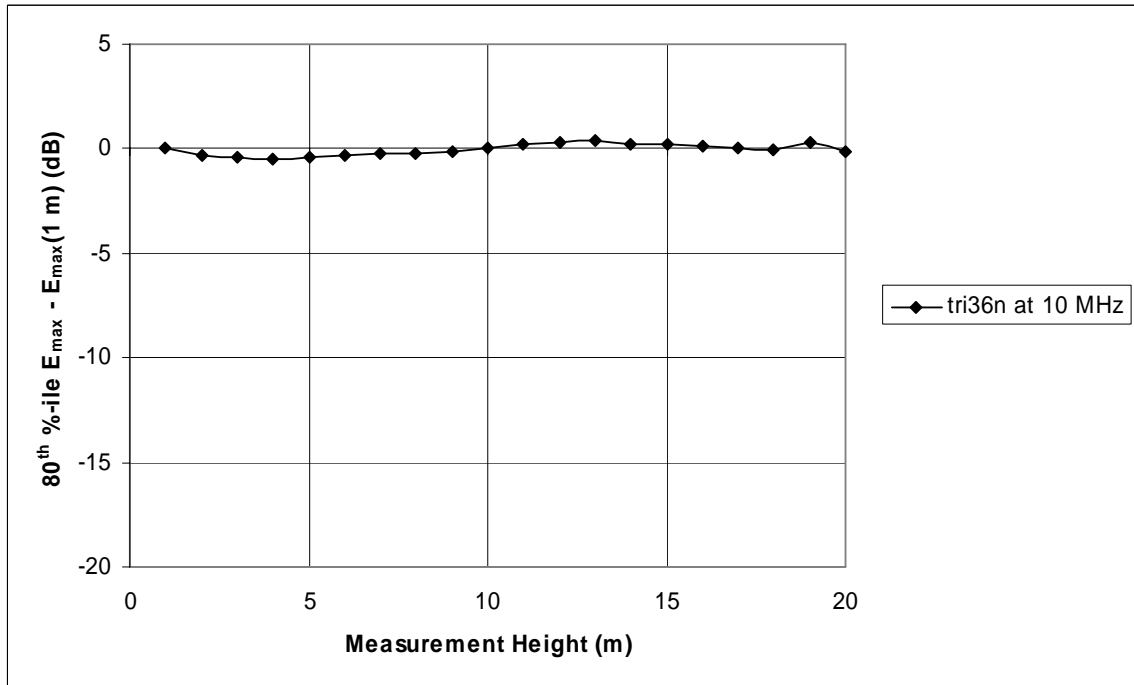


Figure A-44: 80<sup>th</sup> percentile of peak electric field strength along the power line relative to the peak electric field strength at a 1 meter measurement height

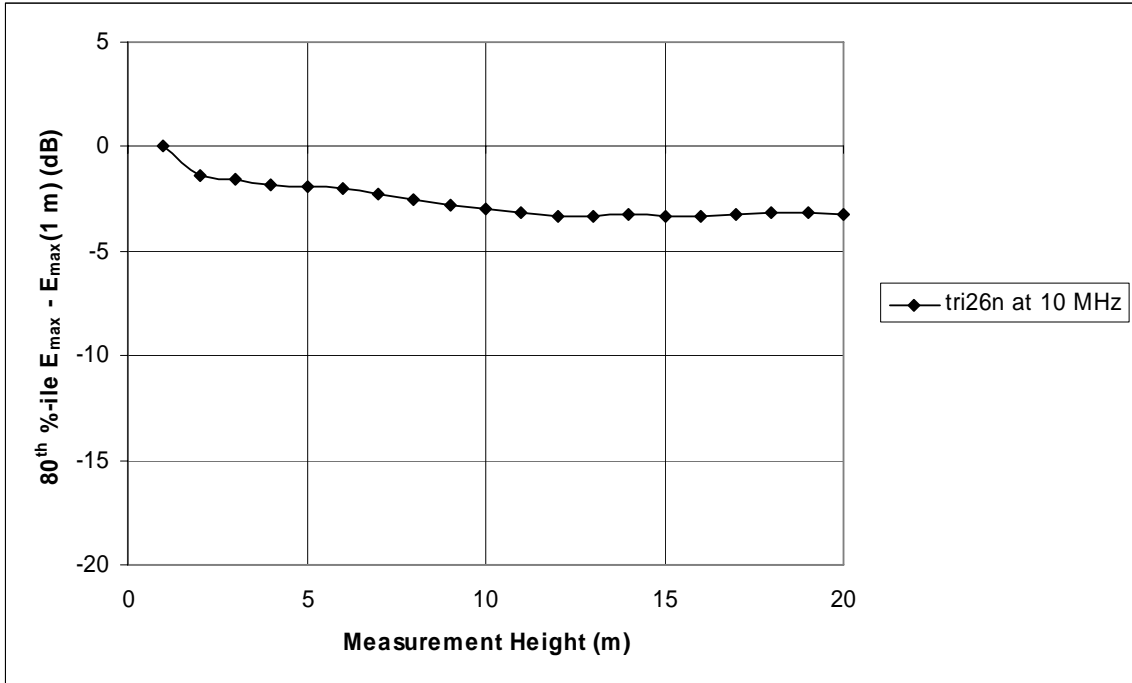


Figure A-45: 80<sup>th</sup> percentile of peak electric field strength along the power line relative to the peak electric field strength at a 1 meter measurement height

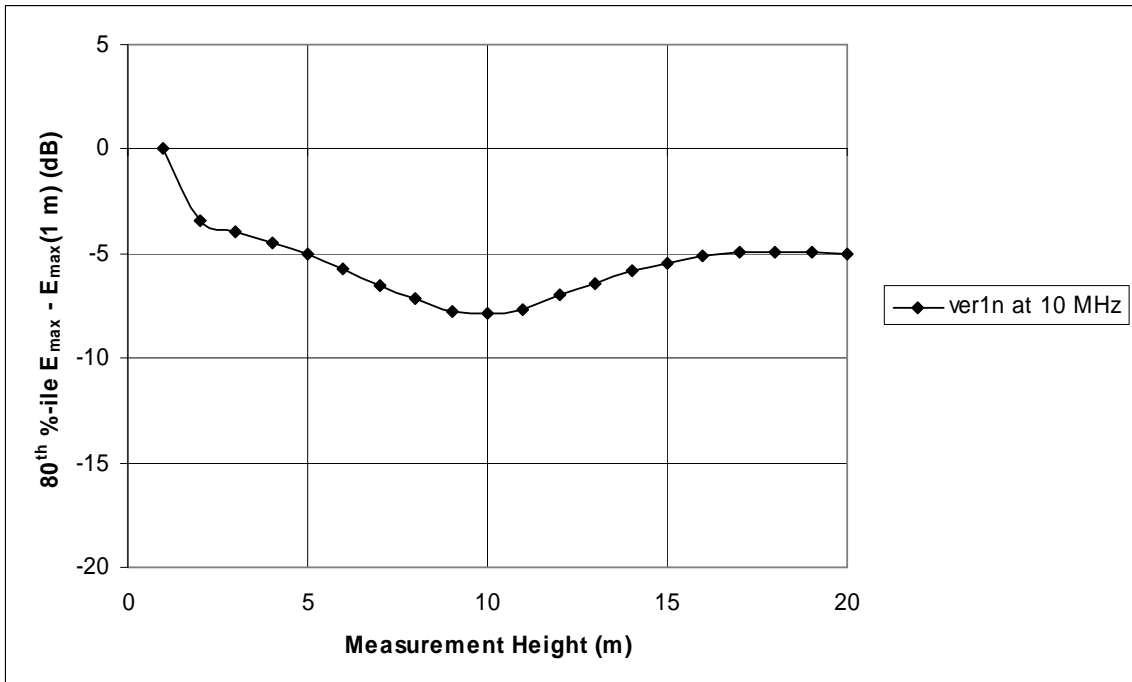


Figure A-46: 80<sup>th</sup> percentile of peak electric field strength along the power line relative to the peak electric field strength at a 1 meter measurement height

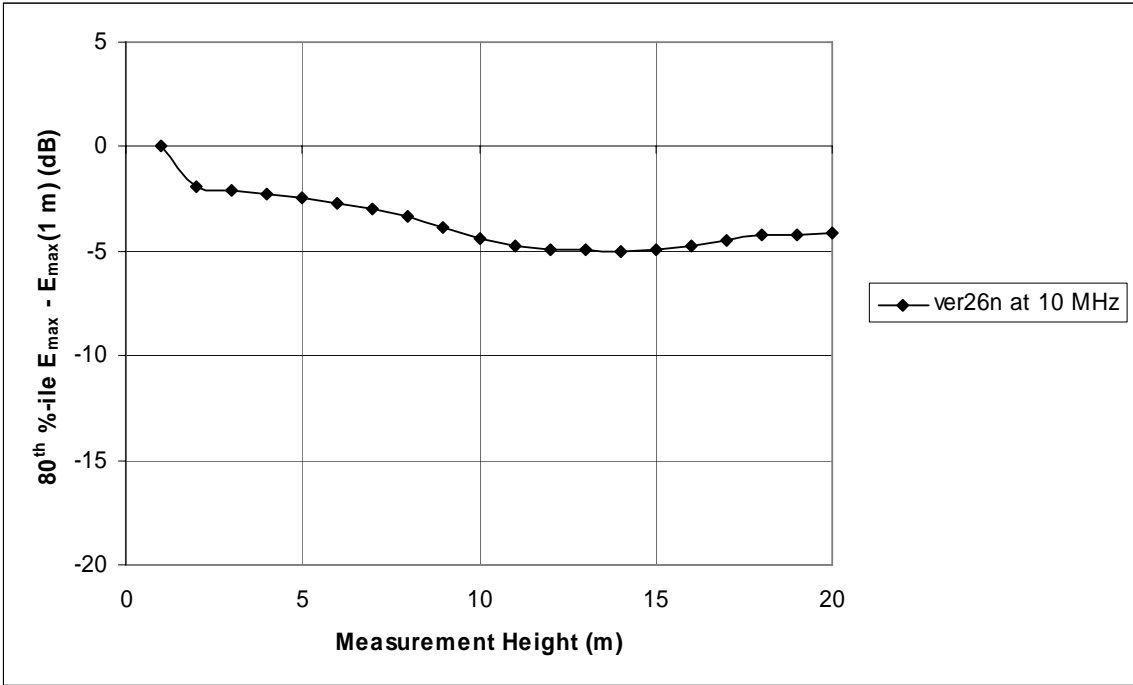


Figure A-47: 80<sup>th</sup> percentile of peak electric field strength along the power line relative to the peak electric field strength at a 1 meter measurement height

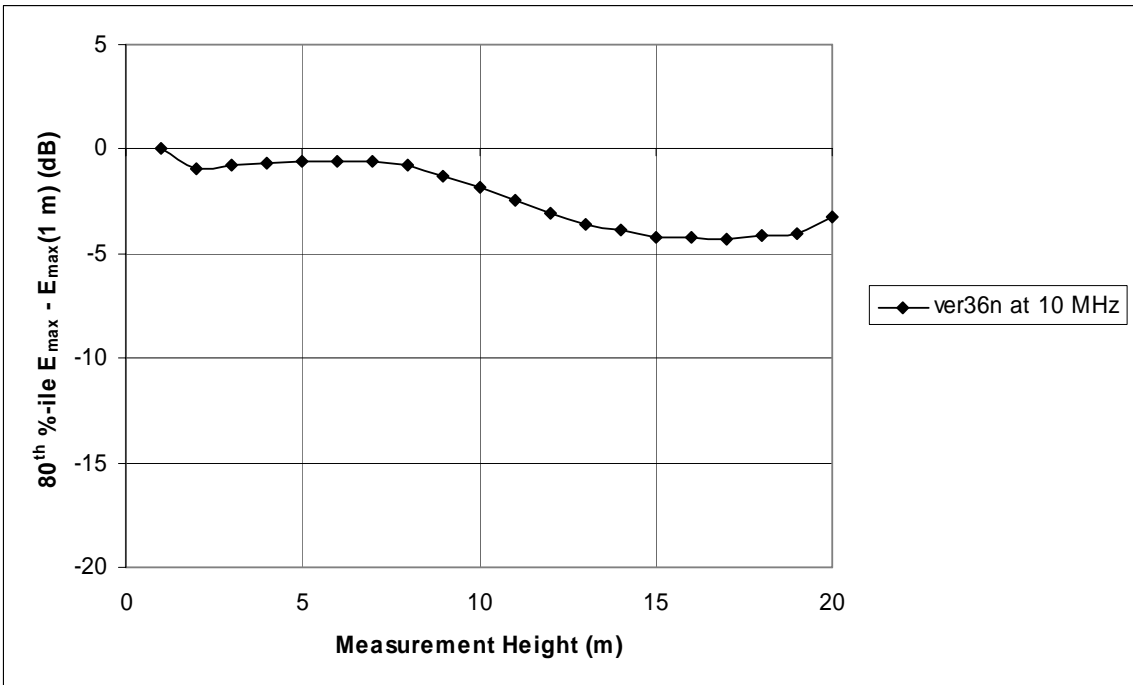


Figure A-48: 80<sup>th</sup> percentile of peak electric field strength along the power line relative to the peak electric field strength at a 1 meter measurement height

12 MHz Plots

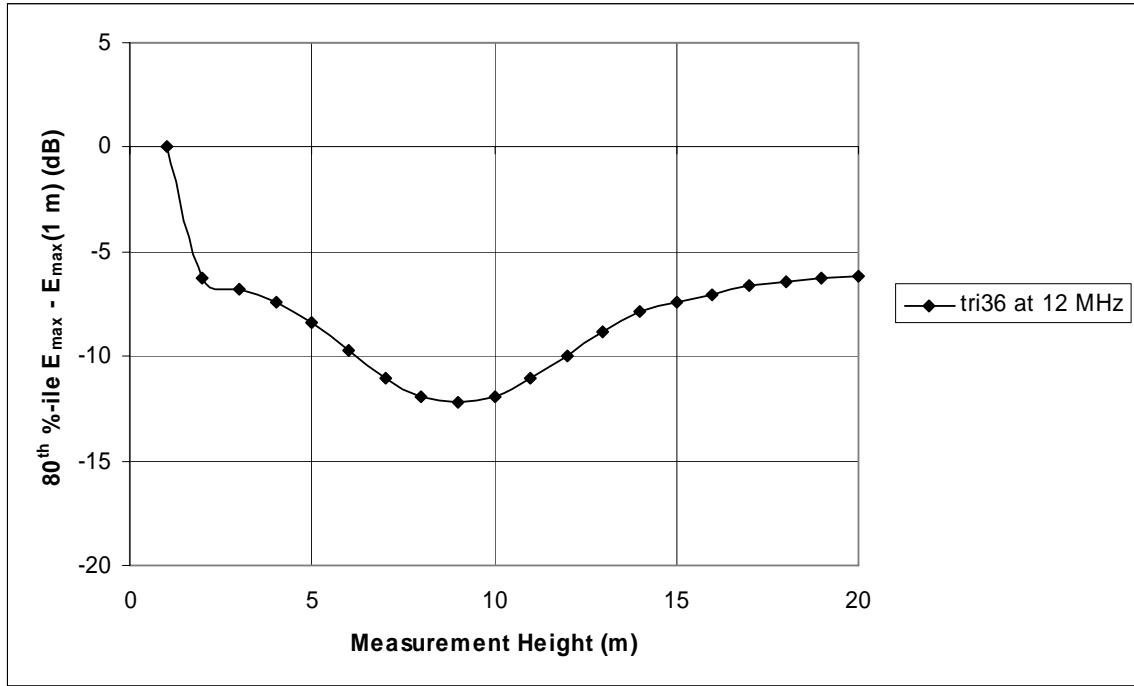


Figure A-49: 80<sup>th</sup> percentile of peak electric field strength along the power line relative to the peak electric field strength at a 1 meter measurement height

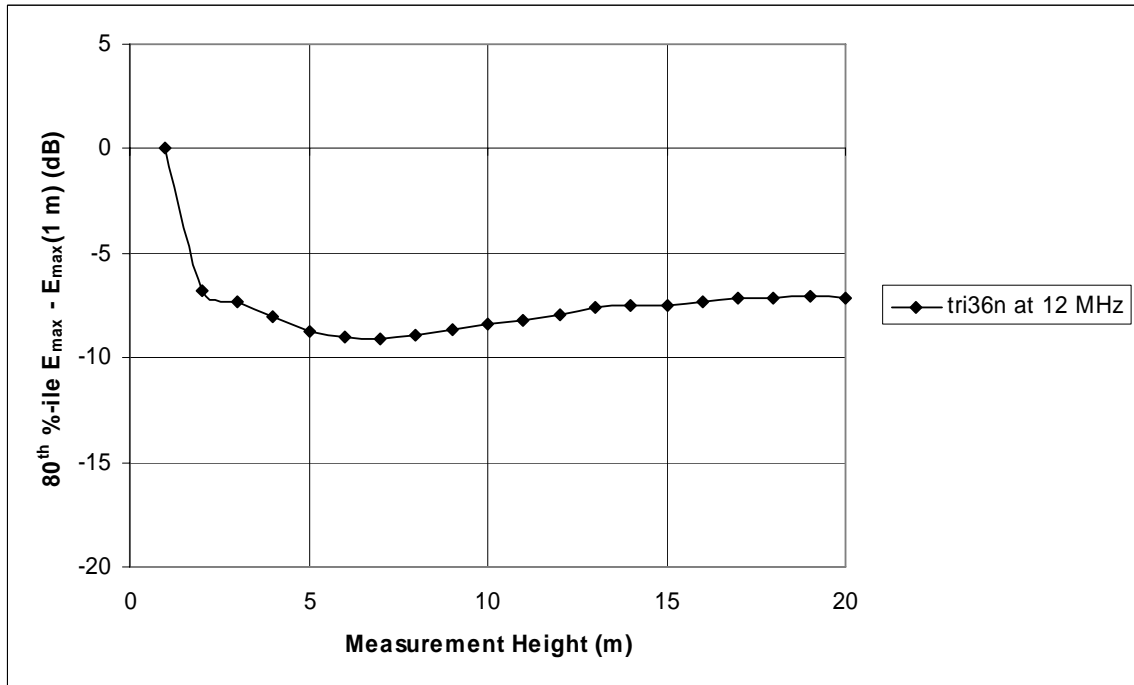


Figure A-50: 80<sup>th</sup> percentile of peak electric field strength along the power line relative to the peak electric field strength at a 1 meter measurement height

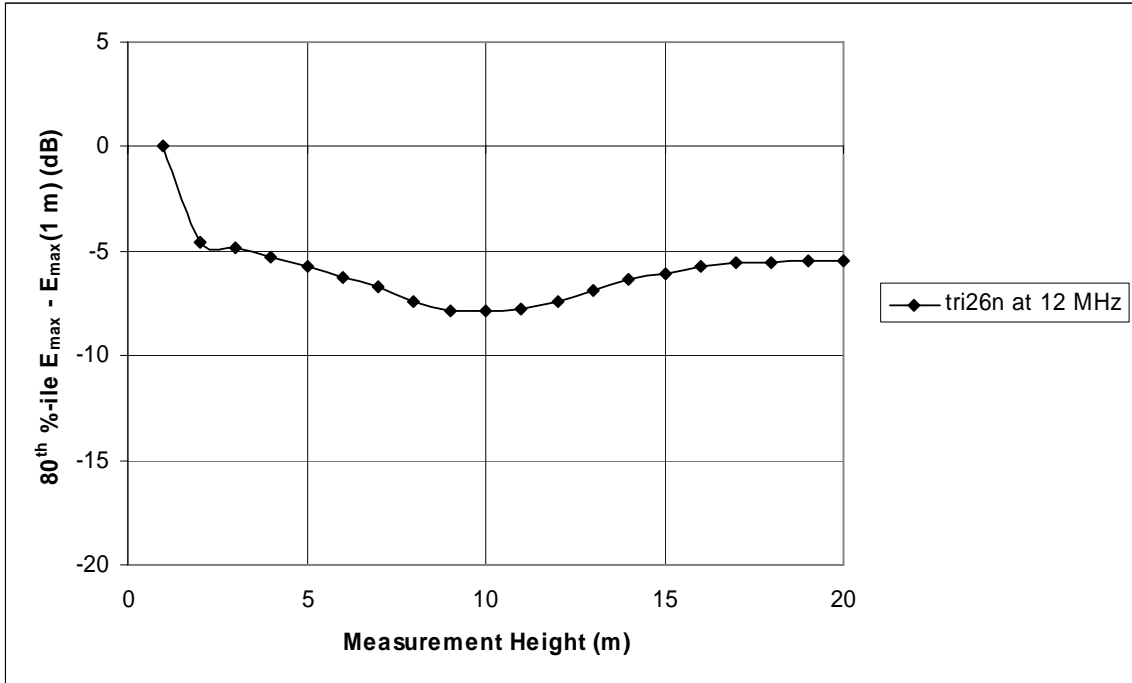


Figure A-51: 80<sup>th</sup> percentile of peak electric field strength along the power line relative to the peak electric field strength at a 1 meter measurement height

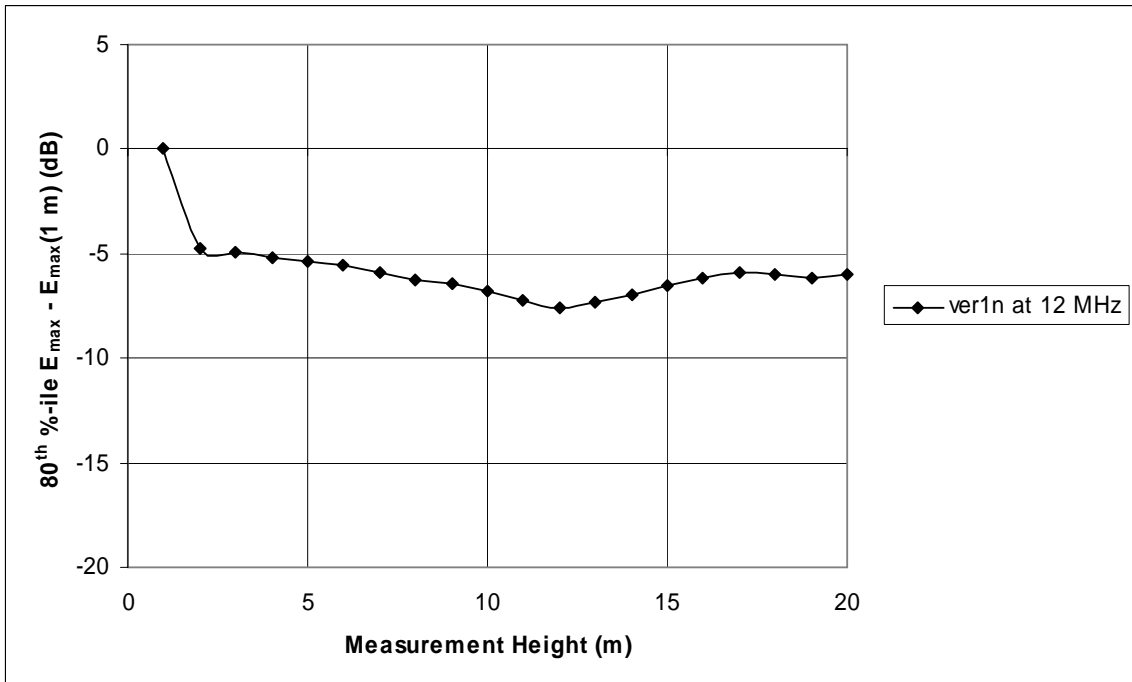


Figure A-52: 80<sup>th</sup> percentile of peak electric field strength along the power line relative to the peak electric field strength at a 1 meter measurement height

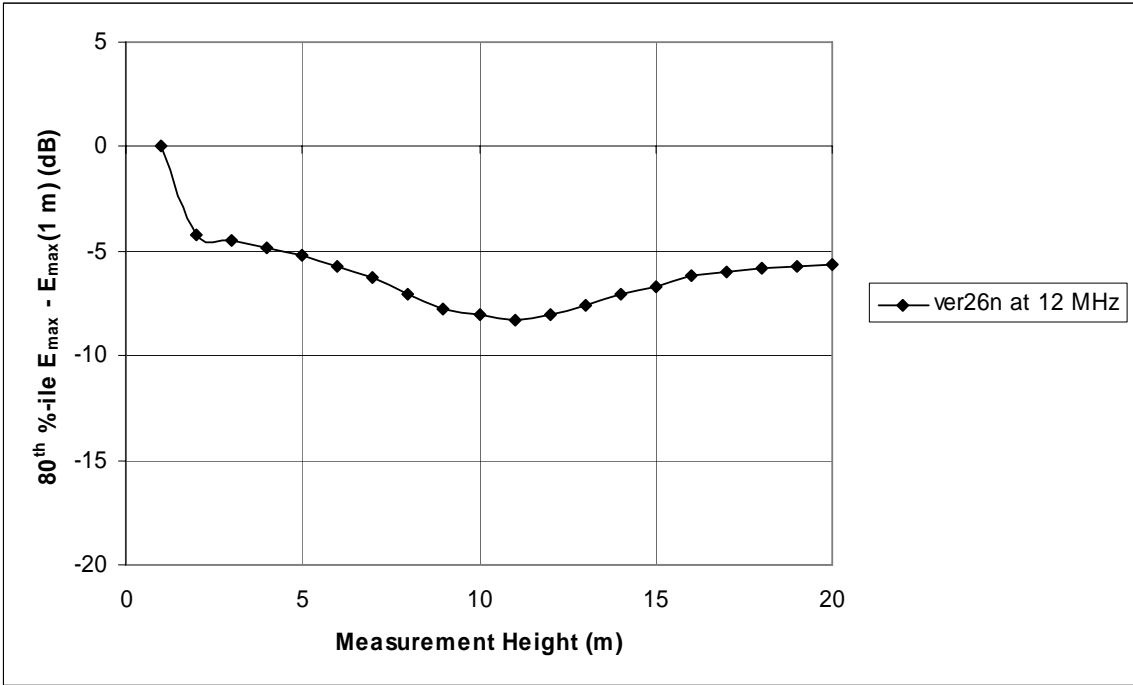


Figure A-53: 80<sup>th</sup> percentile of peak electric field strength along the power line relative to the peak electric field strength at a 1 meter measurement height

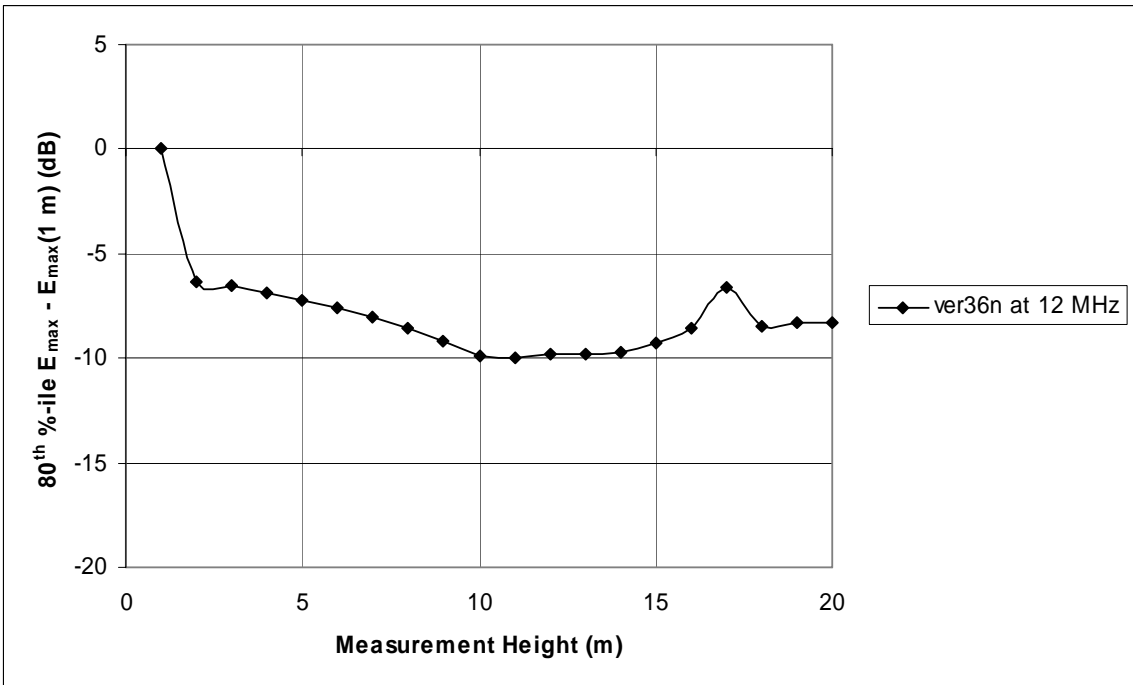


Figure A-54: 80<sup>th</sup> percentile of peak electric field strength along the power line relative to the peak electric field strength at a 1 meter measurement height



14 MHz Plots

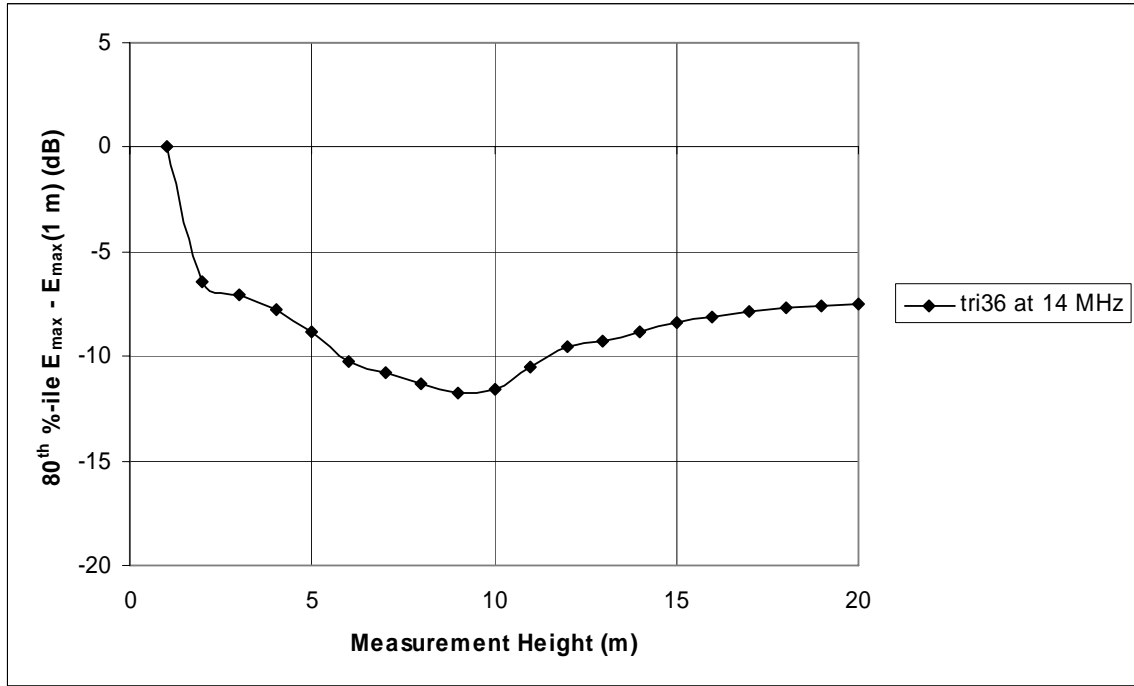


Figure A-55: 80<sup>th</sup> percentile of peak electric field strength along the power line relative to the peak electric field strength at a 1 meter measurement height

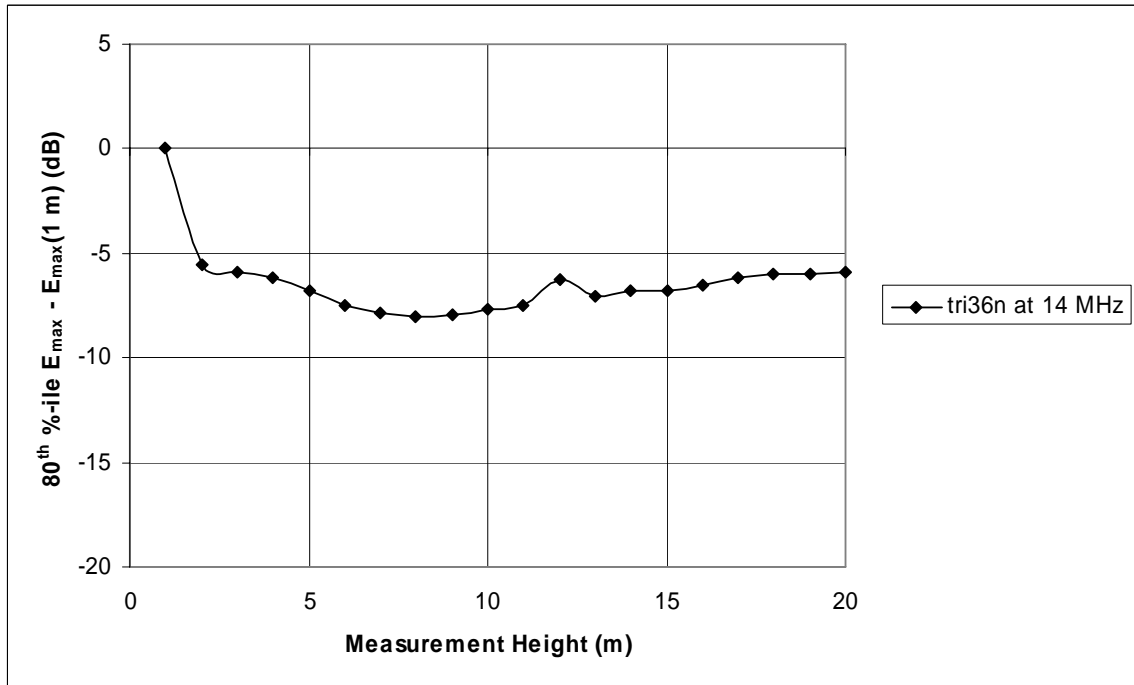


Figure A-56: 80<sup>th</sup> percentile of peak electric field strength along the power line relative to the peak electric field strength at a 1 meter measurement height

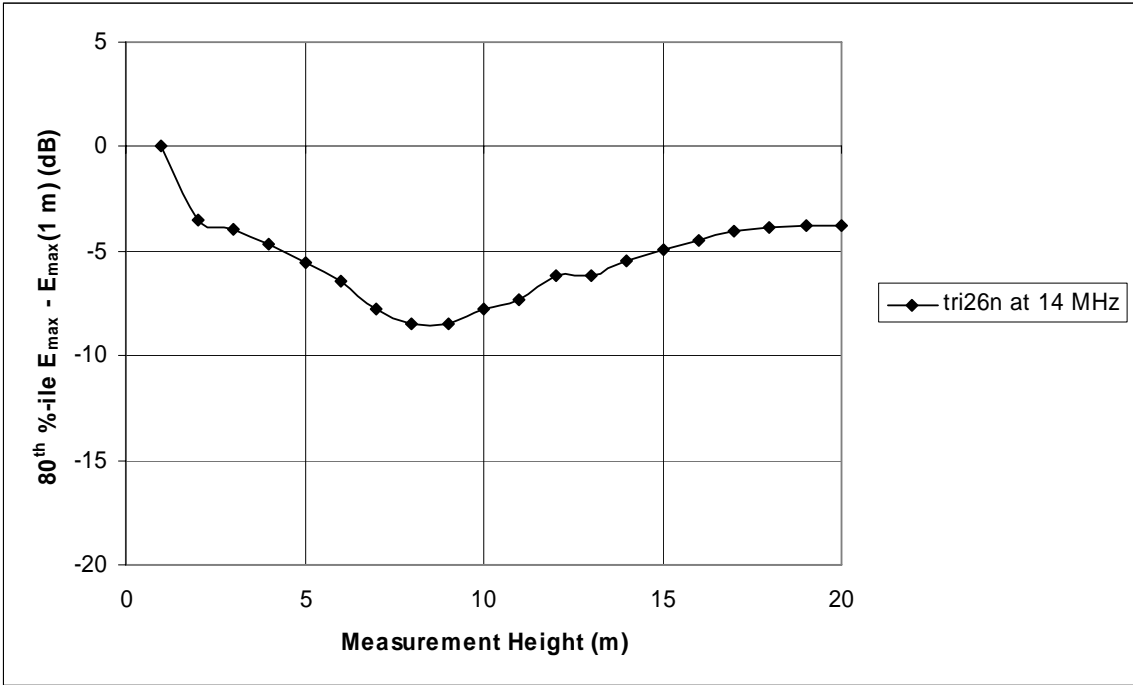


Figure A-57: 80<sup>th</sup> percentile of peak electric field strength along the power line relative to the peak electric field strength at a 1 meter measurement height

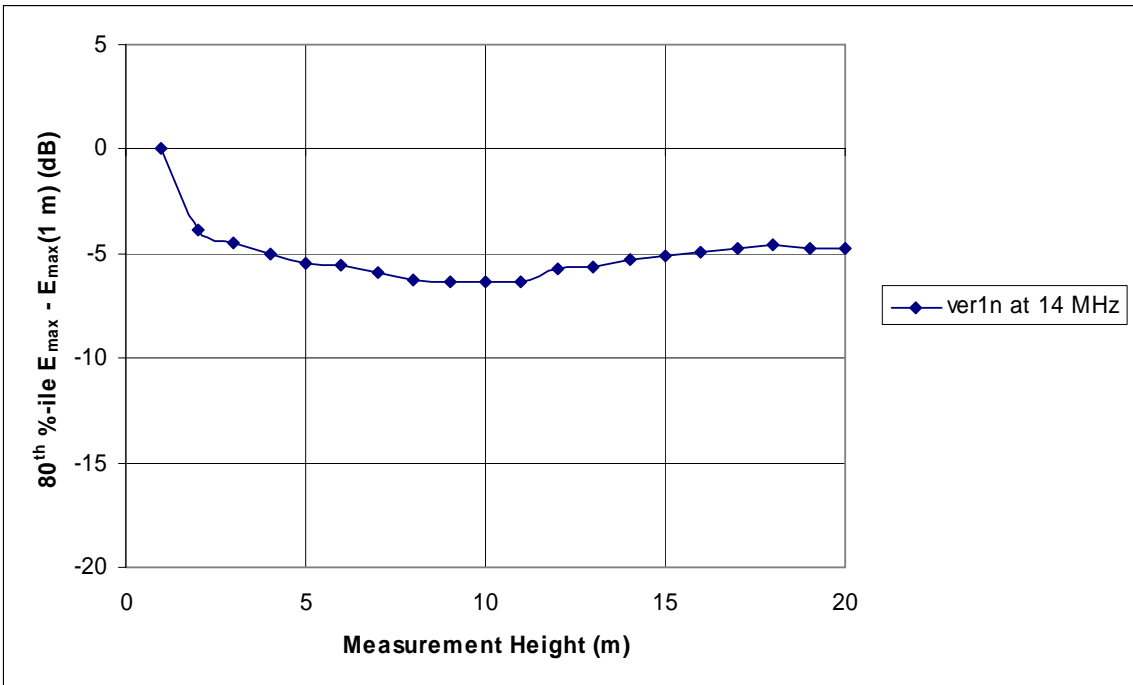


Figure A-58: 80<sup>th</sup> percentile of peak electric field strength along the power line relative to the peak electric field strength at a 1 meter measurement height

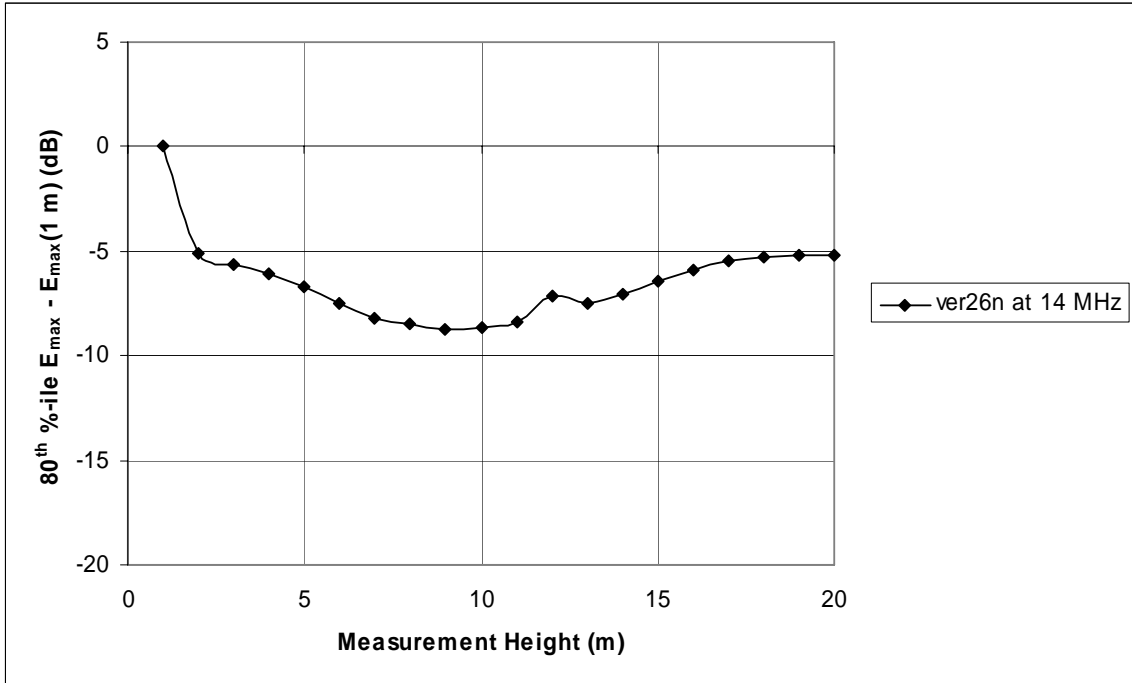


Figure A-59: 80<sup>th</sup> percentile of peak electric field strength along the power line relative to the peak electric field strength at a 1 meter measurement height

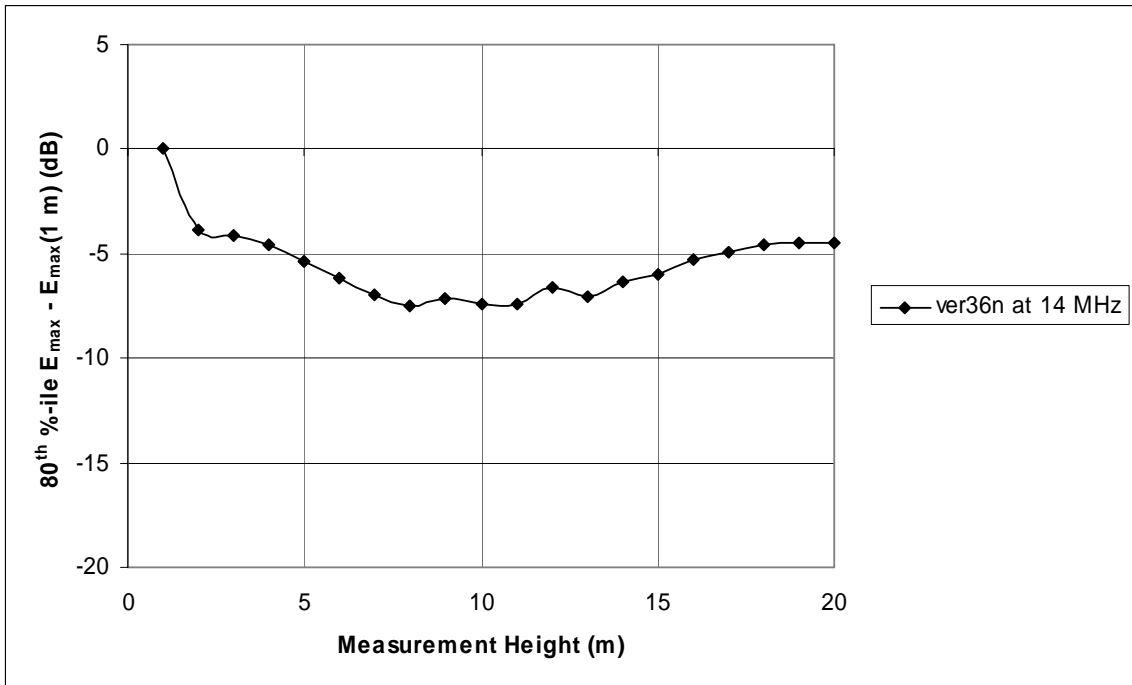


Figure A-60: 80<sup>th</sup> percentile of peak electric field strength along the power line relative to the peak electric field strength at a 1 meter measurement height

16 MHz Plots

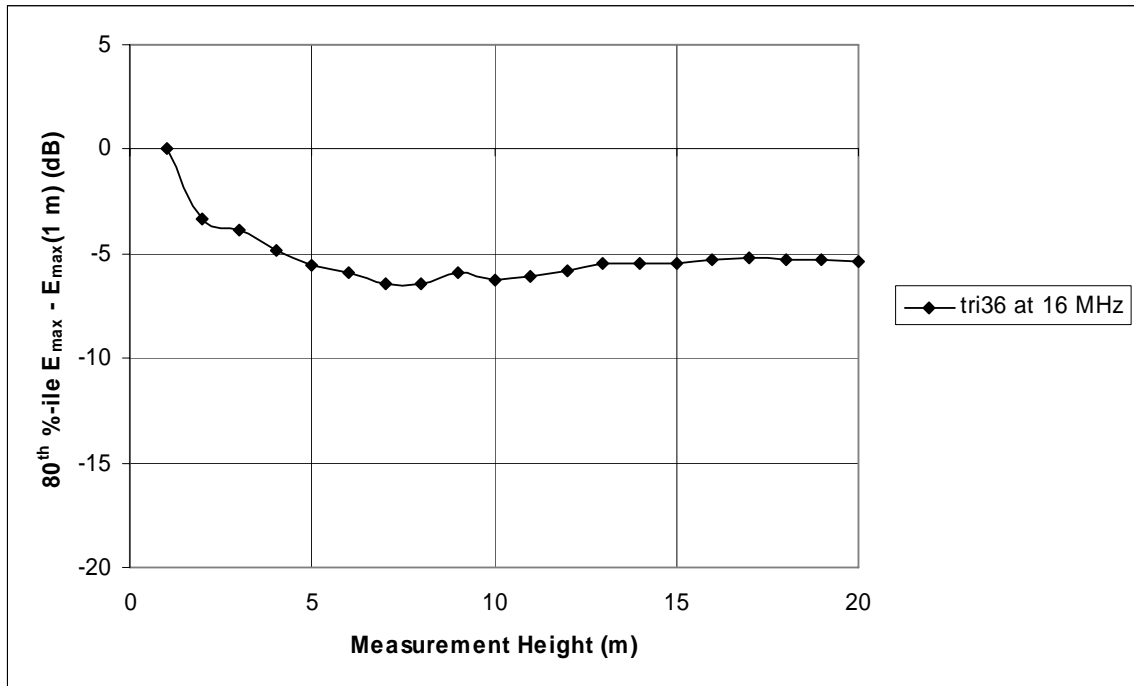


Figure A-61: 80<sup>th</sup> percentile of peak electric field strength along the power line relative to the peak electric field strength at a 1 meter measurement height

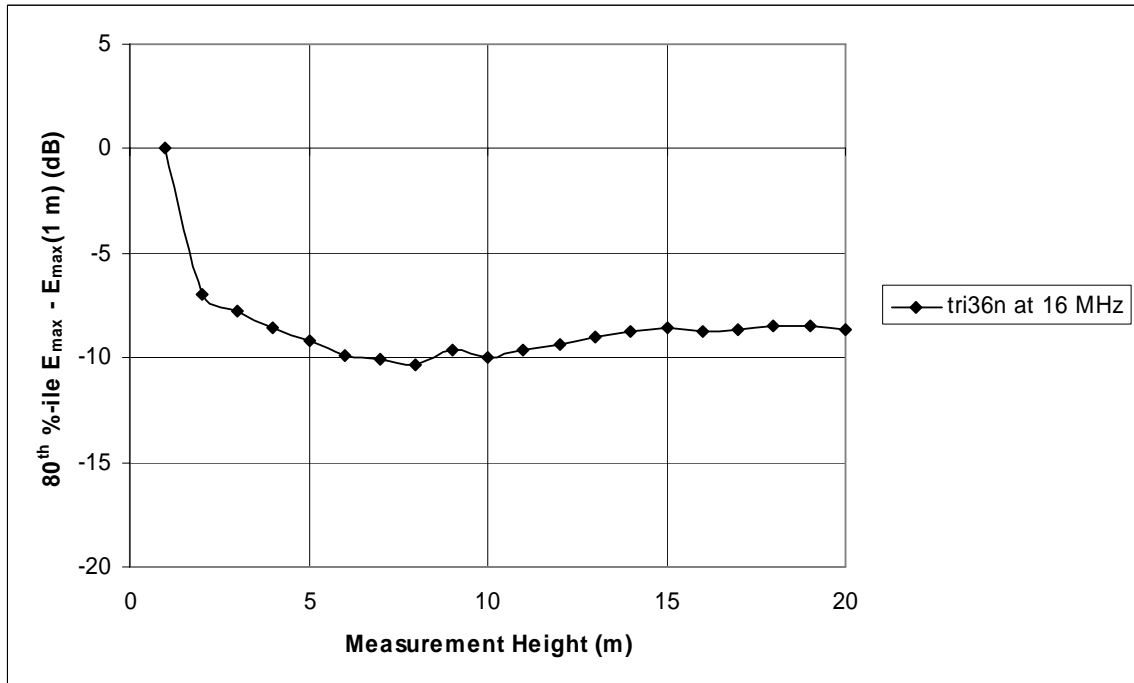


Figure A-62: 80<sup>th</sup> percentile of peak electric field strength along the power line relative to the peak electric field strength at a 1 meter measurement height

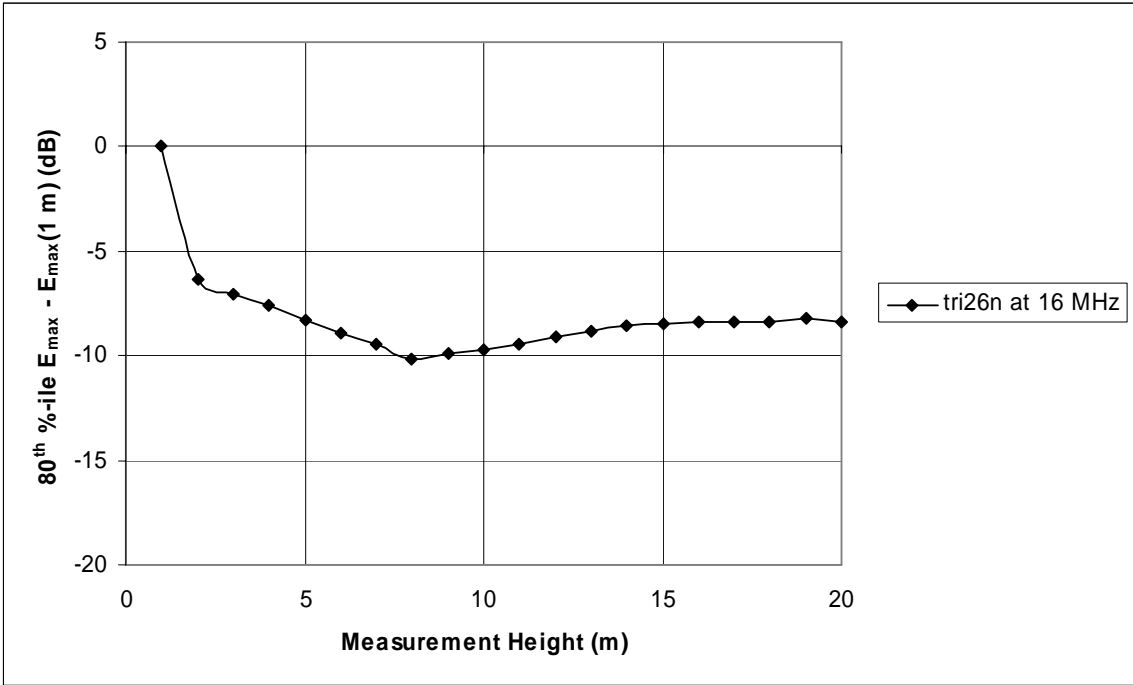


Figure A-63: 80<sup>th</sup> percentile of peak electric field strength along the power line relative to the peak electric field strength at a 1 meter measurement height

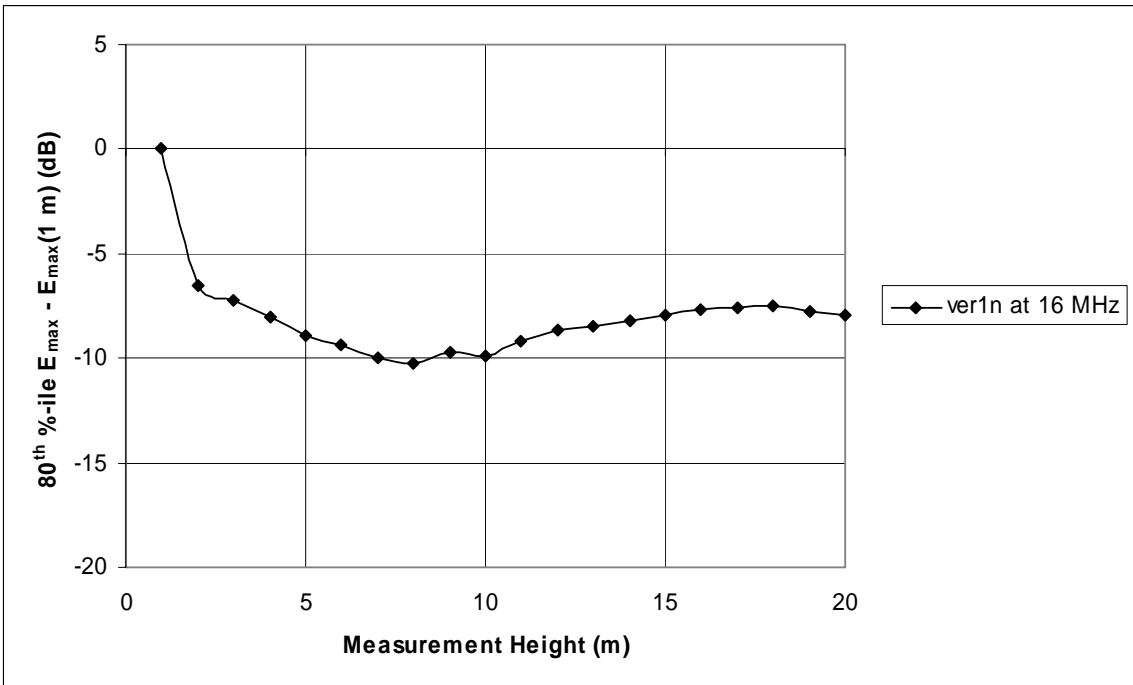


Figure A-64: 80<sup>th</sup> percentile of peak electric field strength along the power line relative to the peak electric field strength at a 1 meter measurement height

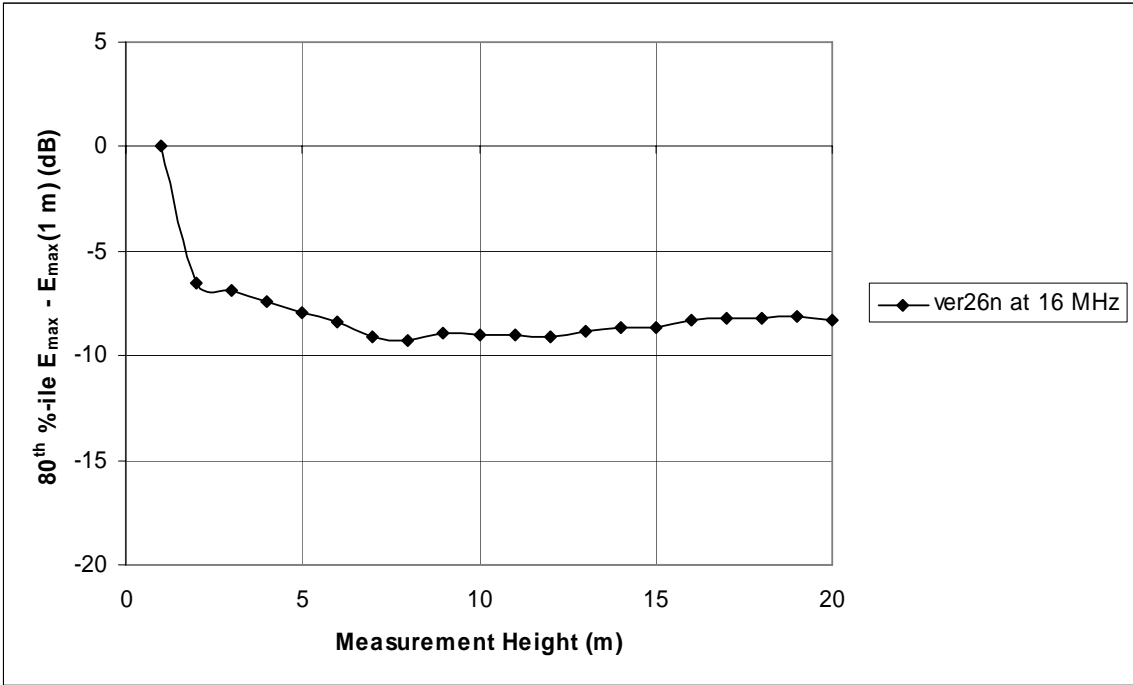


Figure A-65: 80<sup>th</sup> percentile of peak electric field strength along the power line relative to the peak electric field strength at a 1 meter measurement height

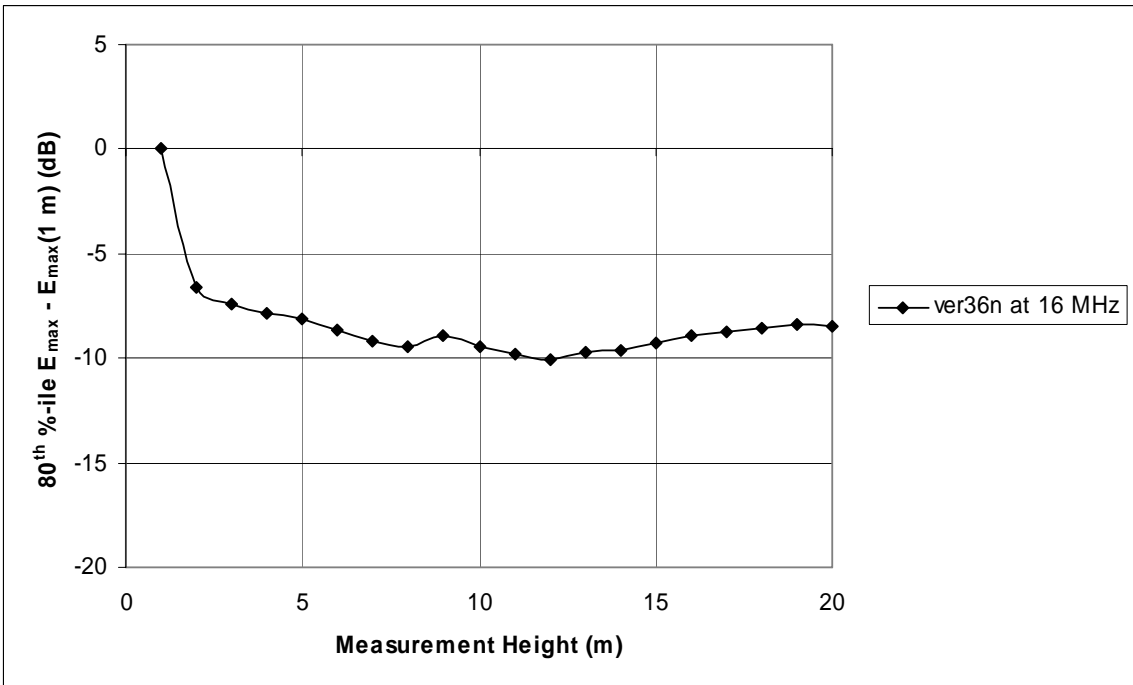


Figure A-66: 80<sup>th</sup> percentile of peak electric field strength along the power line relative to the peak electric field strength at a 1 meter measurement height

18 MHz Plots

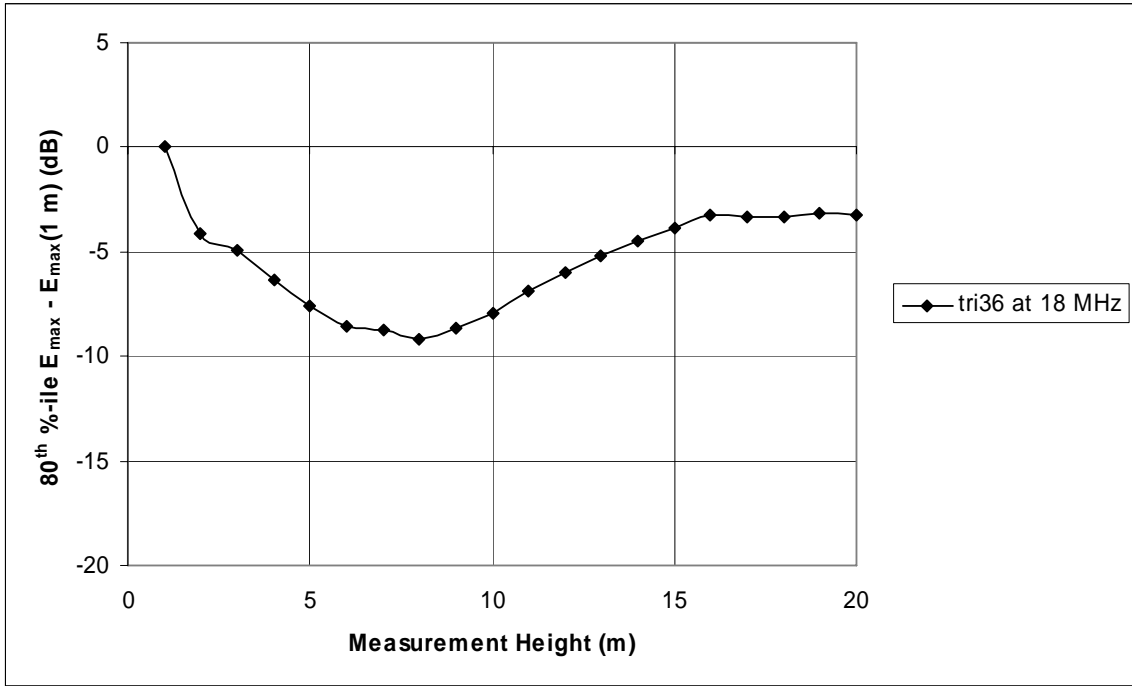


Figure A-67: 80<sup>th</sup> percentile of peak electric field strength along the power line relative to the peak electric field strength at a 1 meter measurement height

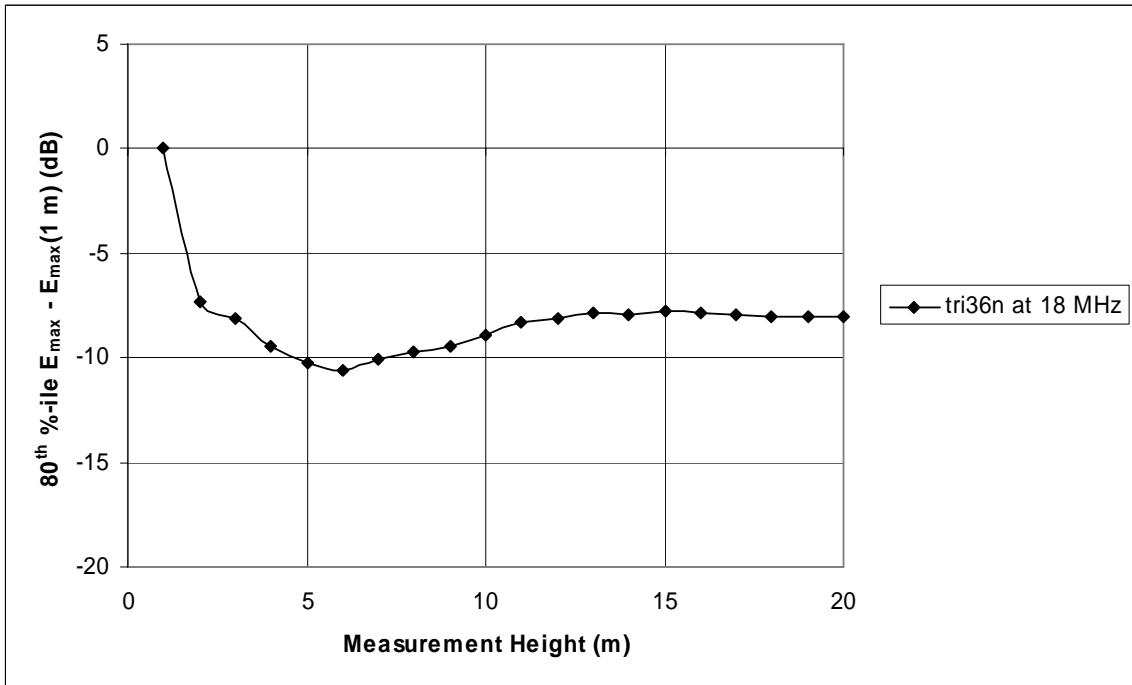


Figure A-68: 80<sup>th</sup> percentile of peak electric field strength along the power line relative to the peak electric field strength at a 1 meter measurement height

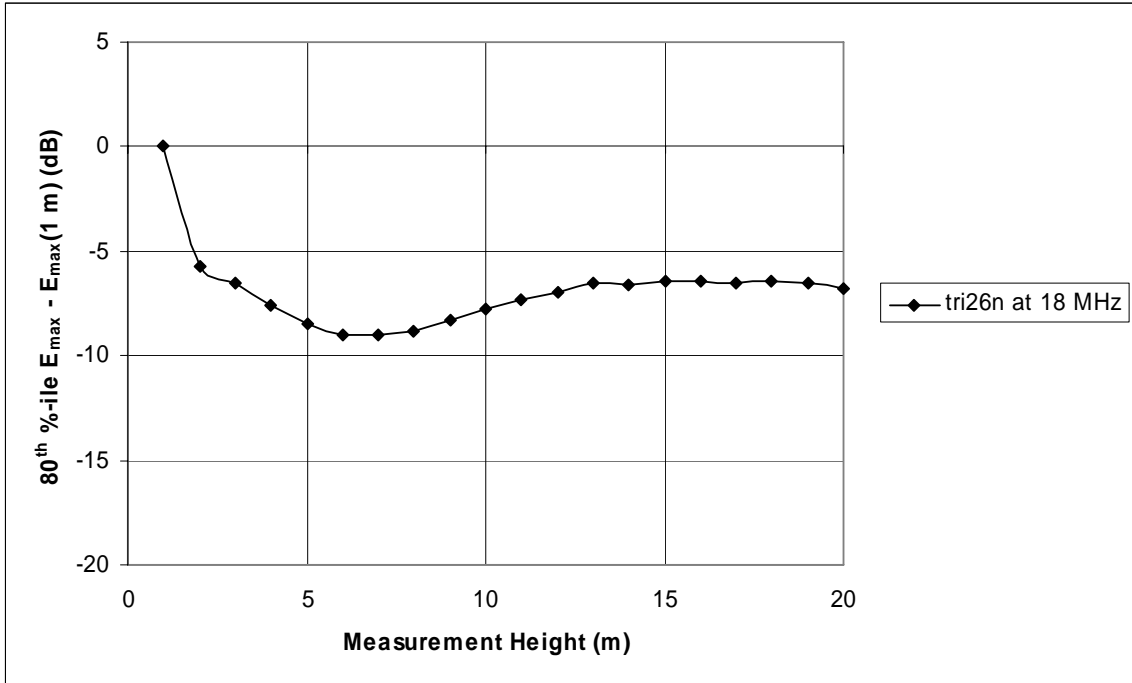


Figure A-69: 80<sup>th</sup> percentile of peak electric field strength along the power line relative to the peak electric field strength at a 1 meter measurement height

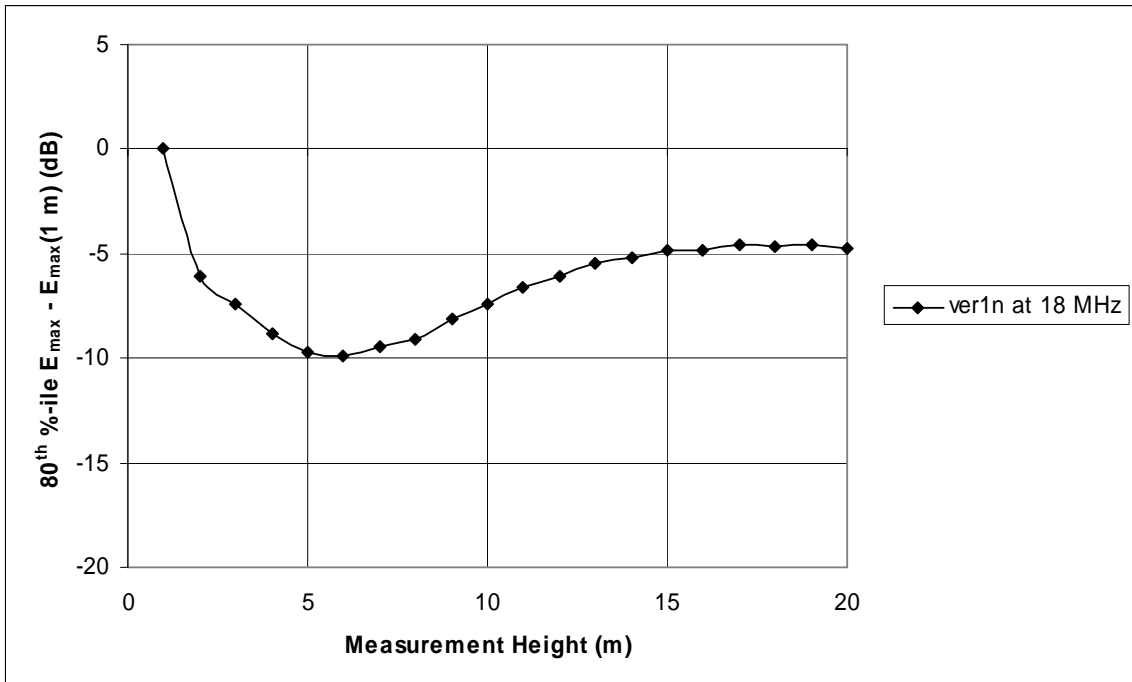


Figure A-70: 80<sup>th</sup> percentile of peak electric field strength along the power line relative to the peak electric field strength at a 1 meter measurement height



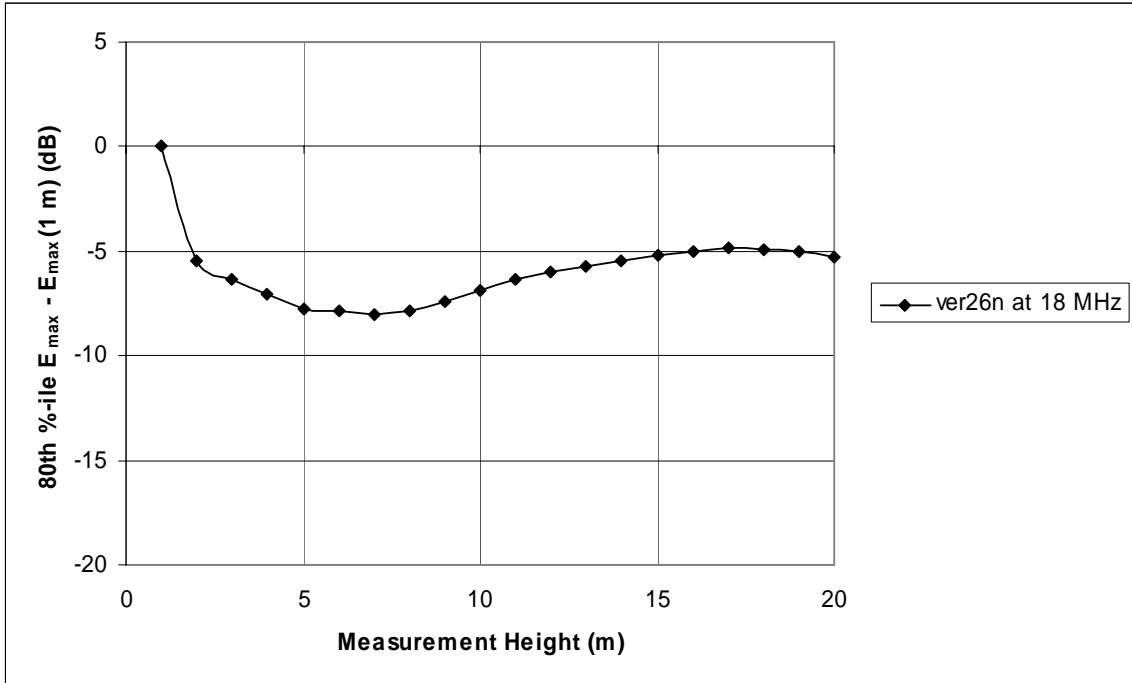


Figure A-71: 80<sup>th</sup> percentile of peak electric field strength along the power line relative to the peak electric field strength at a 1 meter measurement height

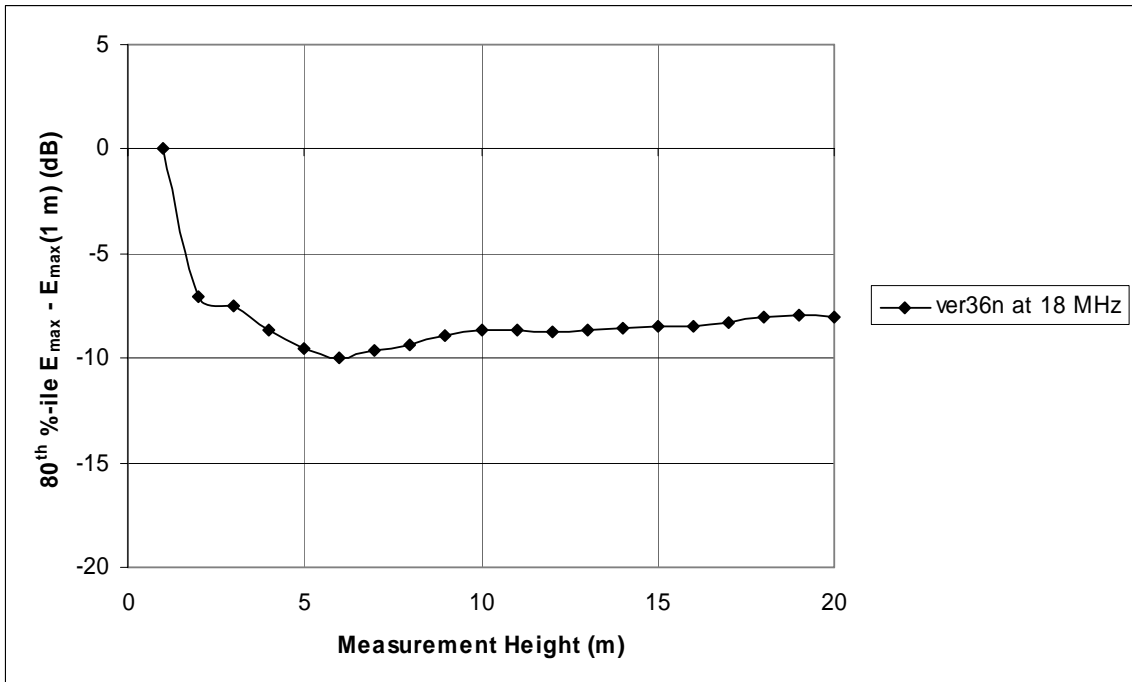


Figure A-72: 80<sup>th</sup> percentile of peak electric field strength along the power line relative to the peak electric field strength at a 1 meter measurement height

20 MHz Plots

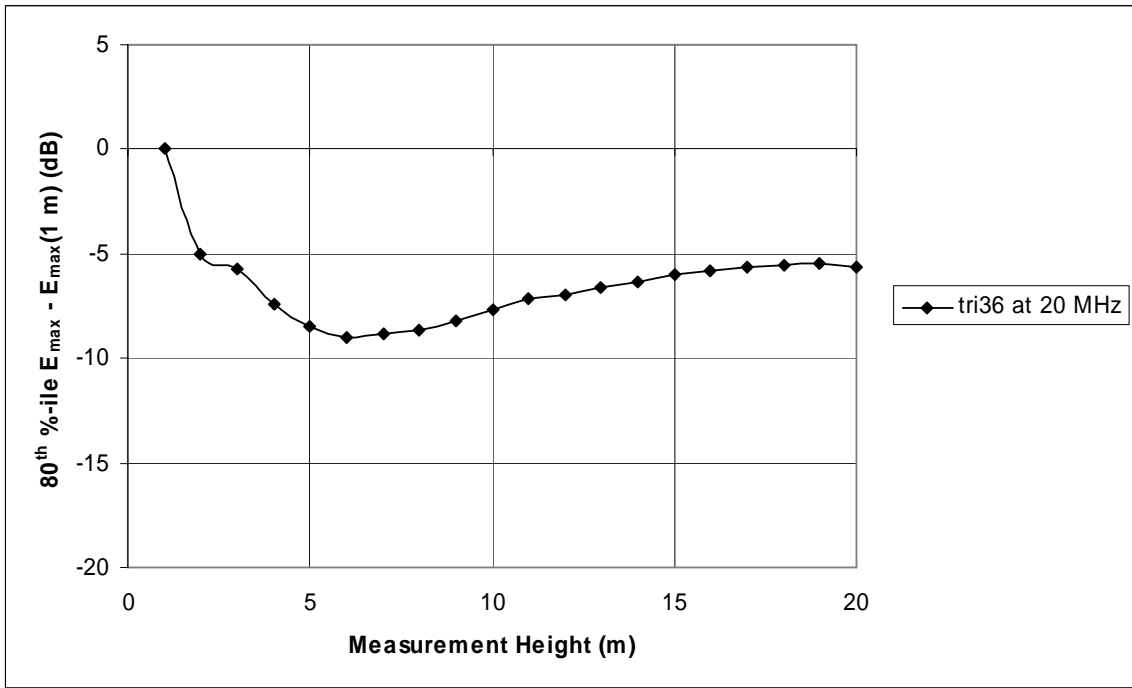


Figure A-73: 80<sup>th</sup> percentile of peak electric field strength along the power line relative to the peak electric field strength at a 1 meter measurement height

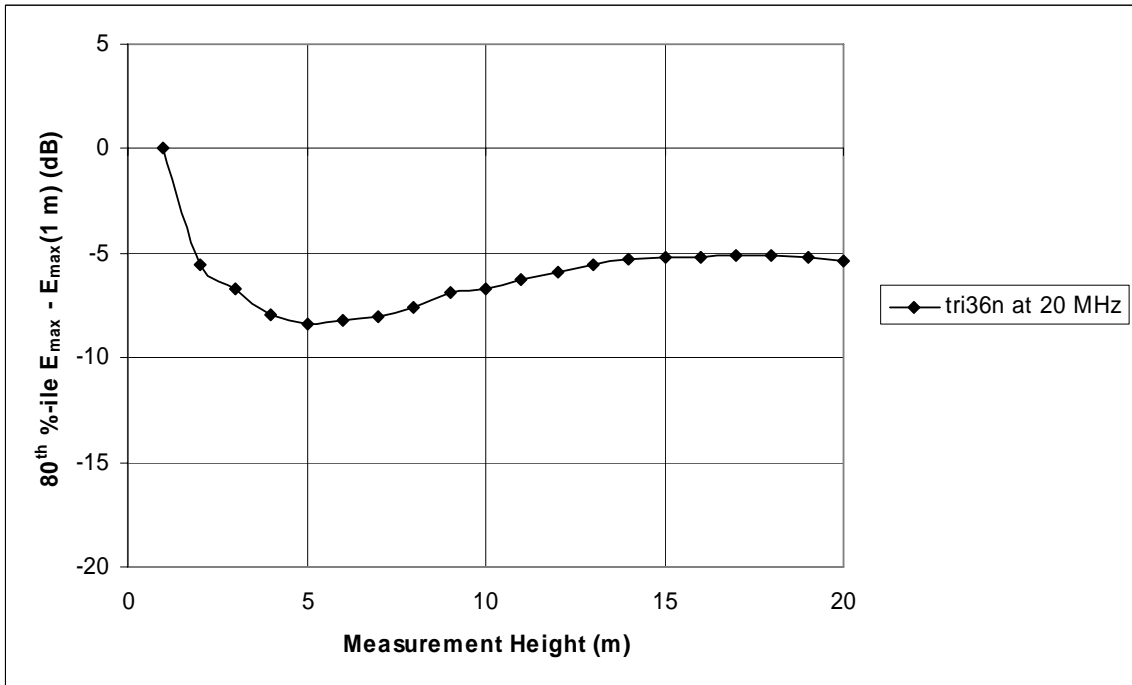


Figure A-74: 80<sup>th</sup> percentile of peak electric field strength along the power line relative to the peak electric field strength at a 1 meter measurement height

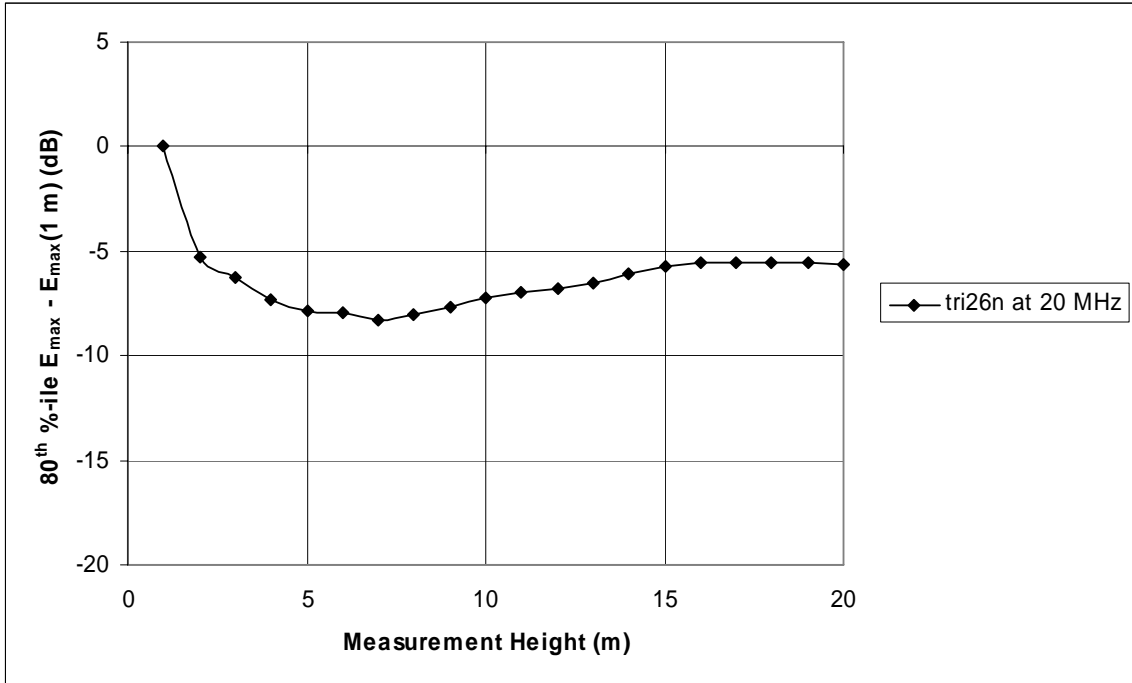


Figure A-75: 80<sup>th</sup> percentile of peak electric field strength along the power line relative to the peak electric field strength at a 1 meter measurement height

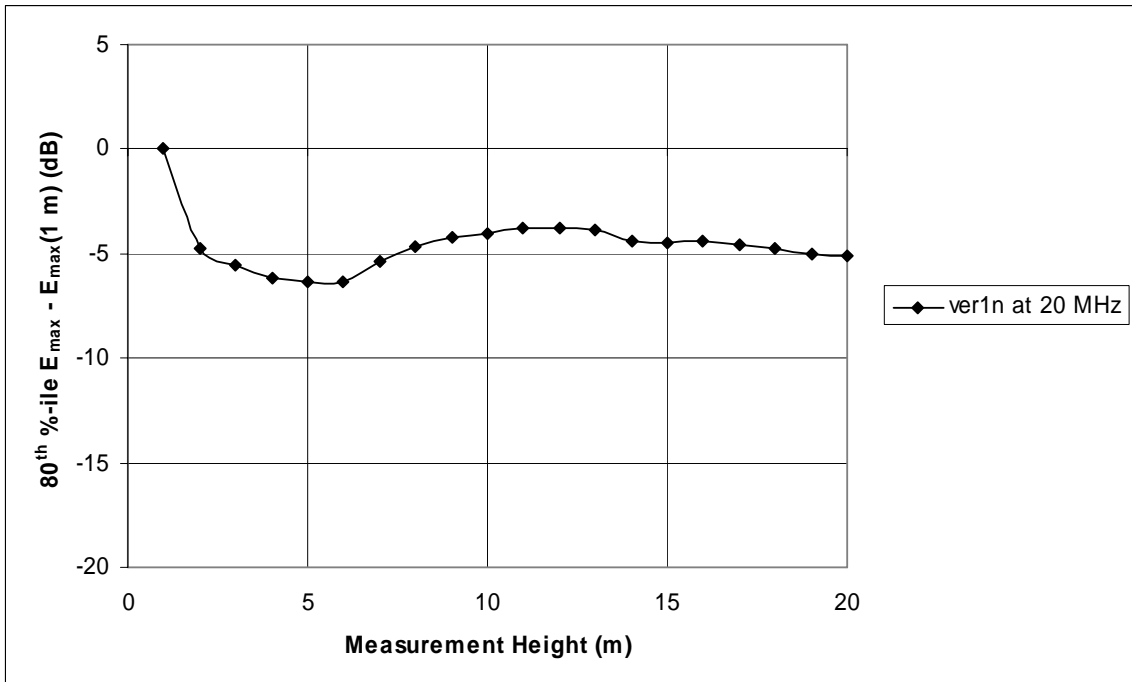


Figure A-76: 80<sup>th</sup> percentile of peak electric field strength along the power line relative to the peak electric field strength at a 1 meter measurement height

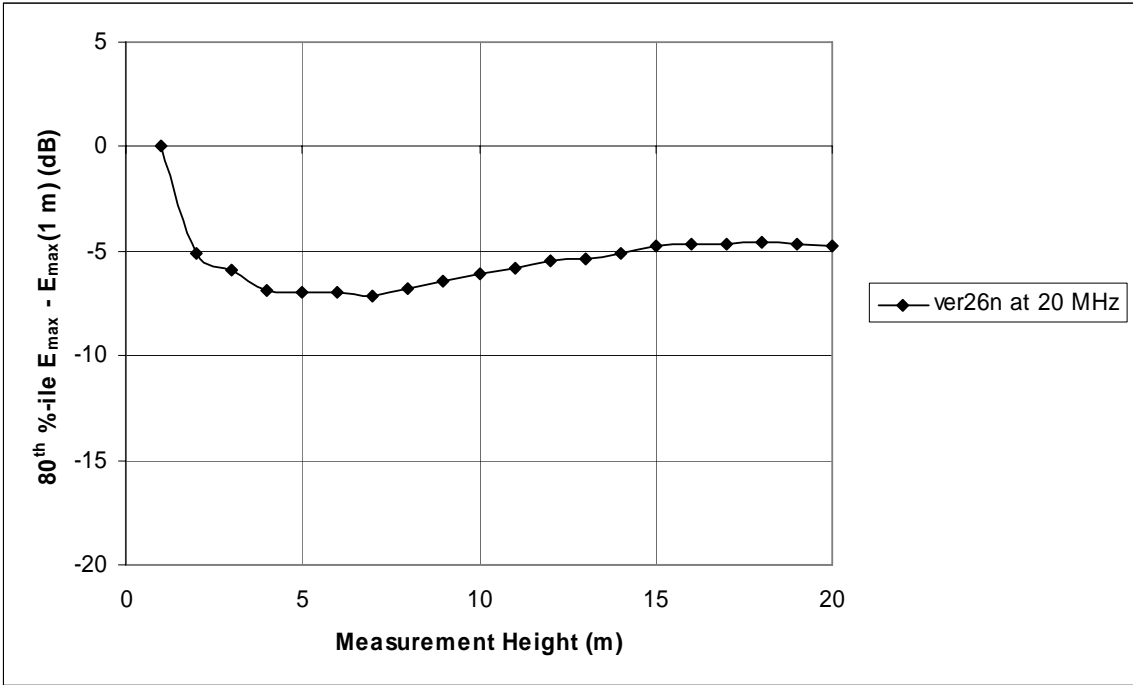


Figure A-77: 80<sup>th</sup> percentile of peak electric field strength along the power line relative to the peak electric field strength at a 1 meter measurement height

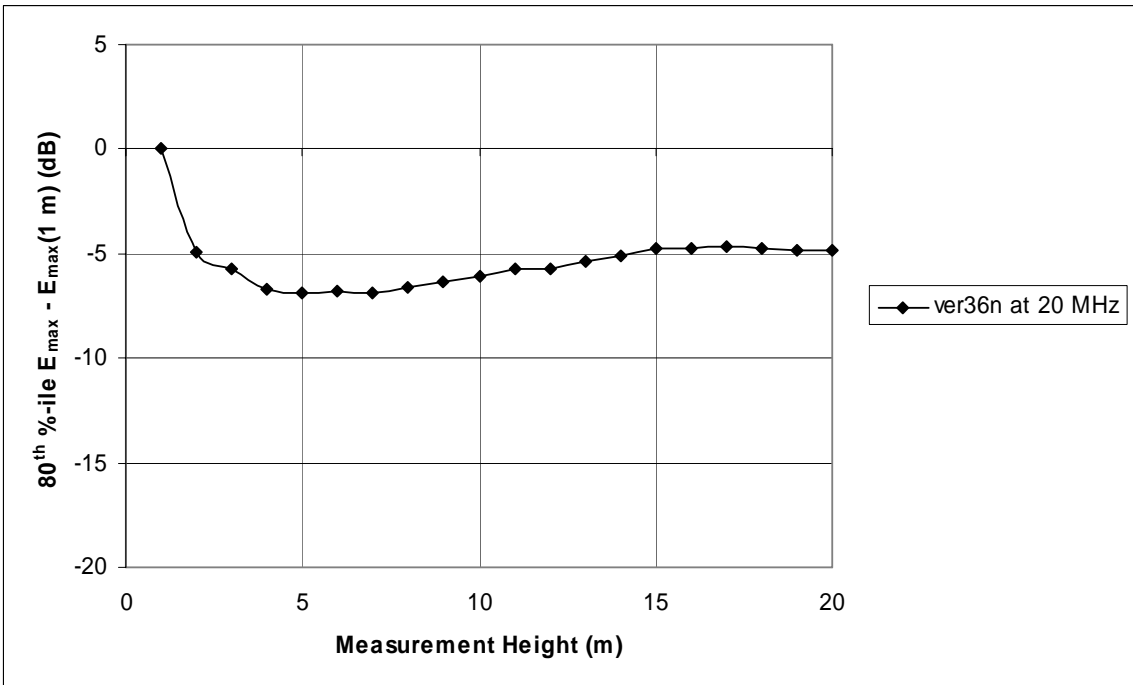


Figure A-78: 80<sup>th</sup> percentile of peak electric field strength along the power line relative to the peak electric field strength at a 1 meter measurement height

22 MHz Plots

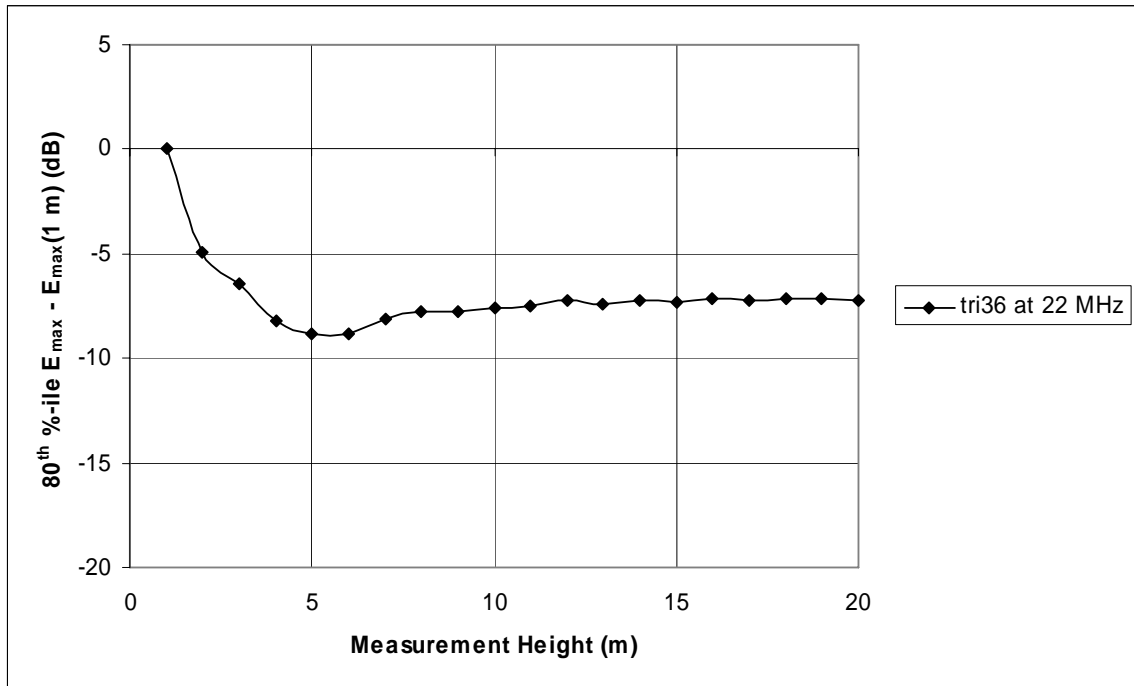


Figure A-79: 80<sup>th</sup> percentile of peak electric field strength along the power line relative to the peak electric field strength at a 1 meter measurement height

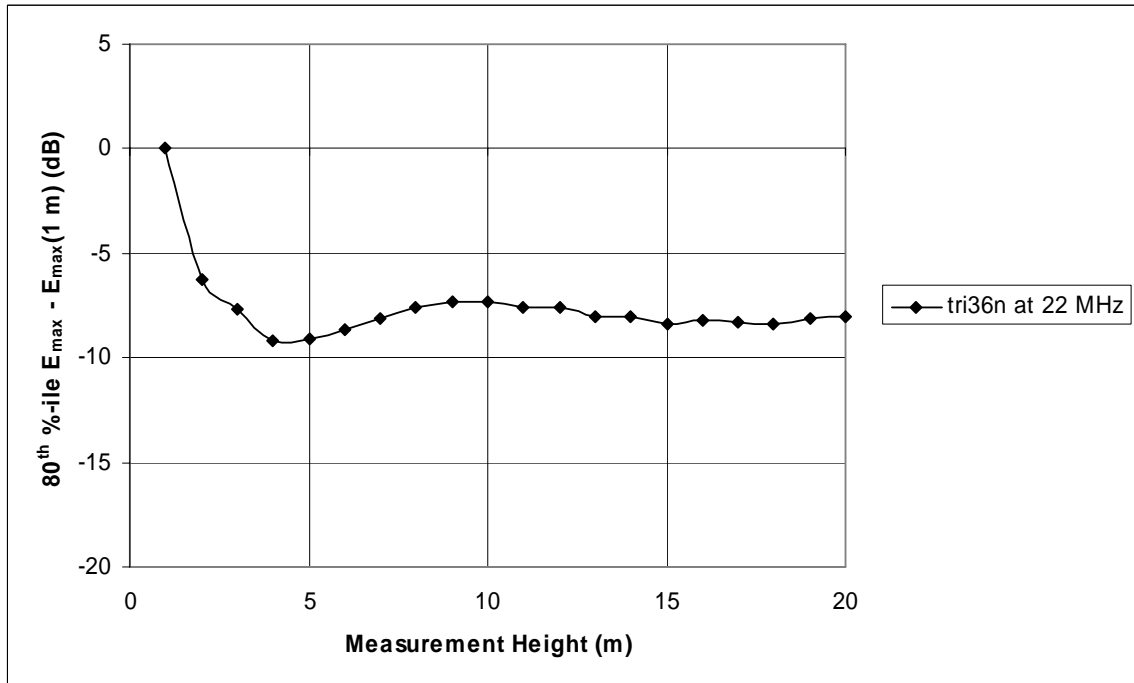


Figure A-80: 80<sup>th</sup> percentile of peak electric field strength along the power line relative to the peak electric field strength at a 1 meter measurement height

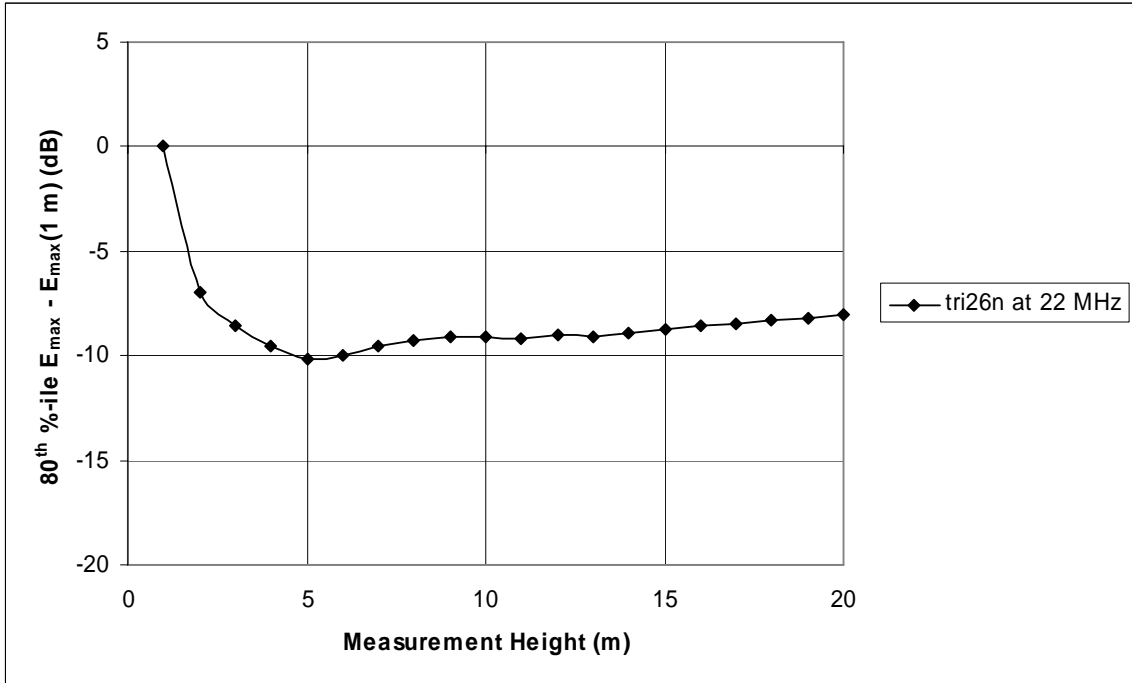


Figure A-81: 80<sup>th</sup> percentile of peak electric field strength along the power line relative to the peak electric field strength at a 1 meter measurement height

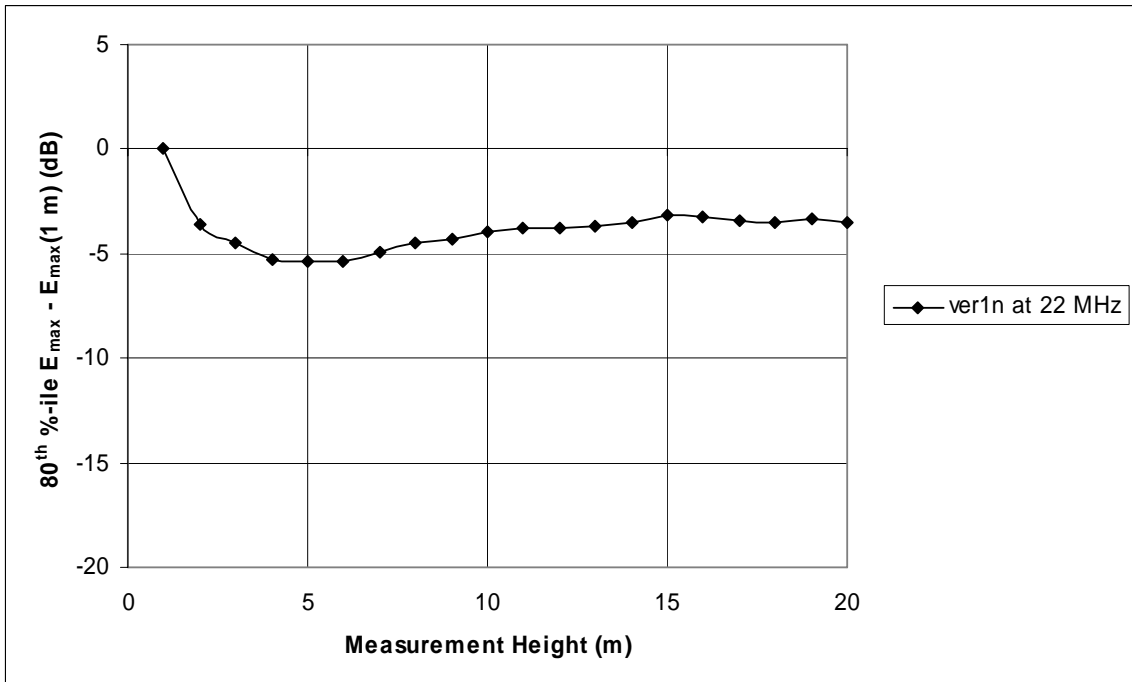


Figure A-82: 80<sup>th</sup> percentile of peak electric field strength along the power line relative to the peak electric field strength at a 1 meter measurement height

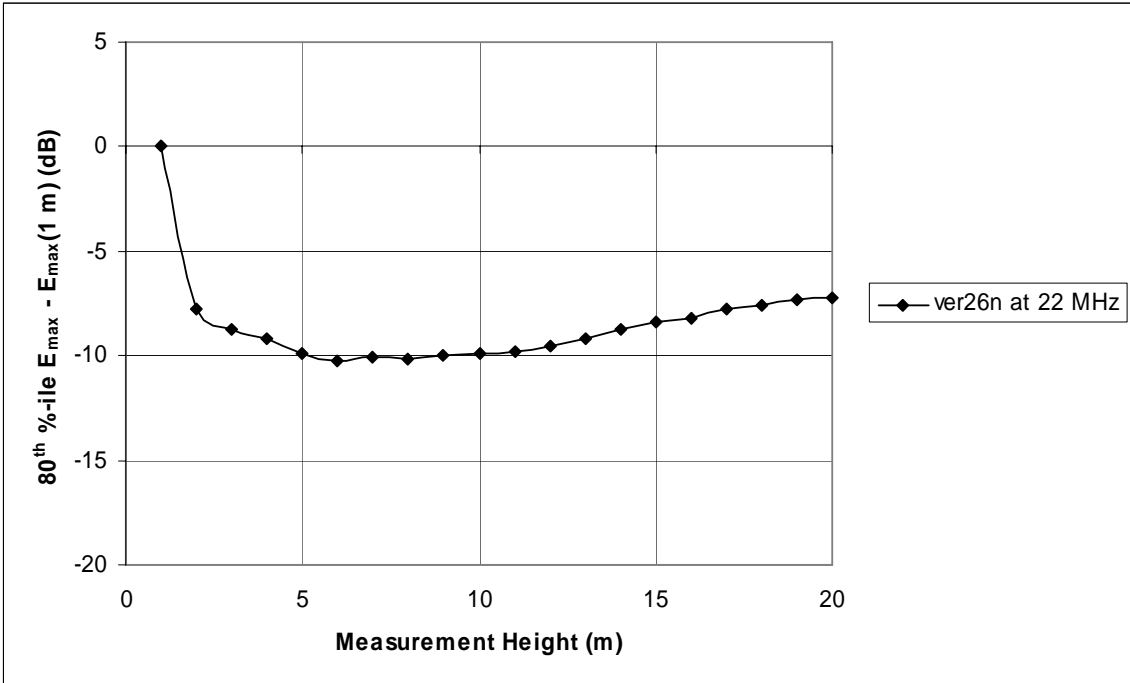


Figure A-83: 80<sup>th</sup> percentile of peak electric field strength along the power line relative to the peak electric field strength at a 1 meter measurement height

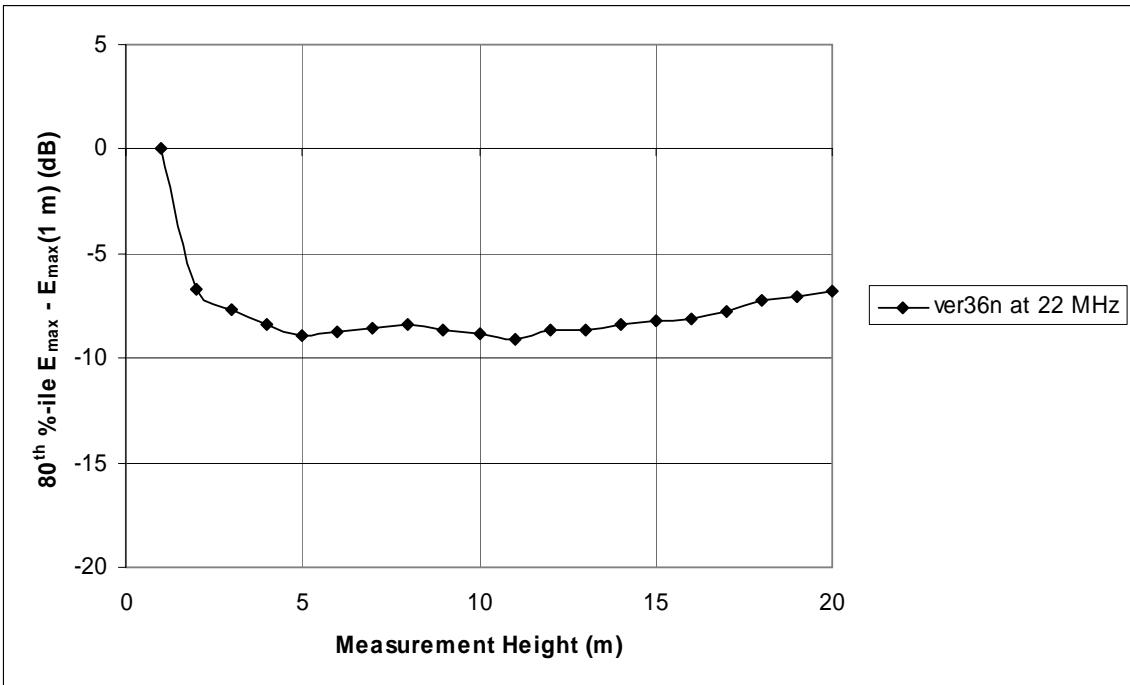


Figure A-84: 80<sup>th</sup> percentile of peak electric field strength along the power line relative to the peak electric field strength at a 1 meter measurement height

24 MHz Plots

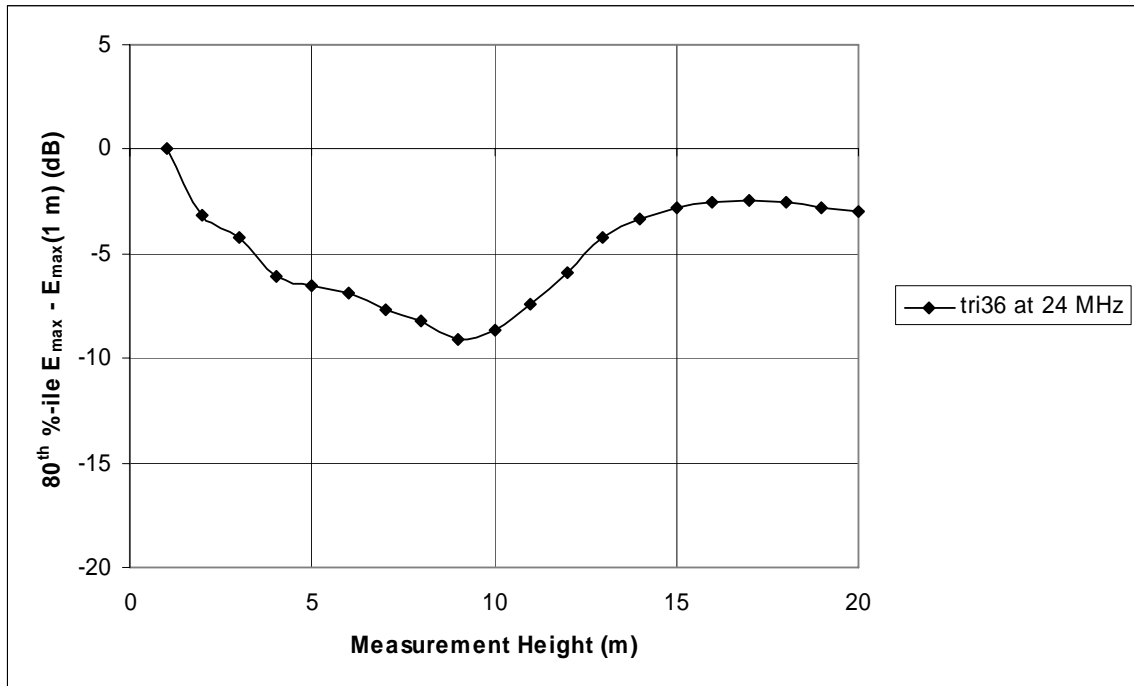


Figure A-85: 80<sup>th</sup> percentile of peak electric field strength along the power line relative to the peak electric field strength at a 1 meter measurement height

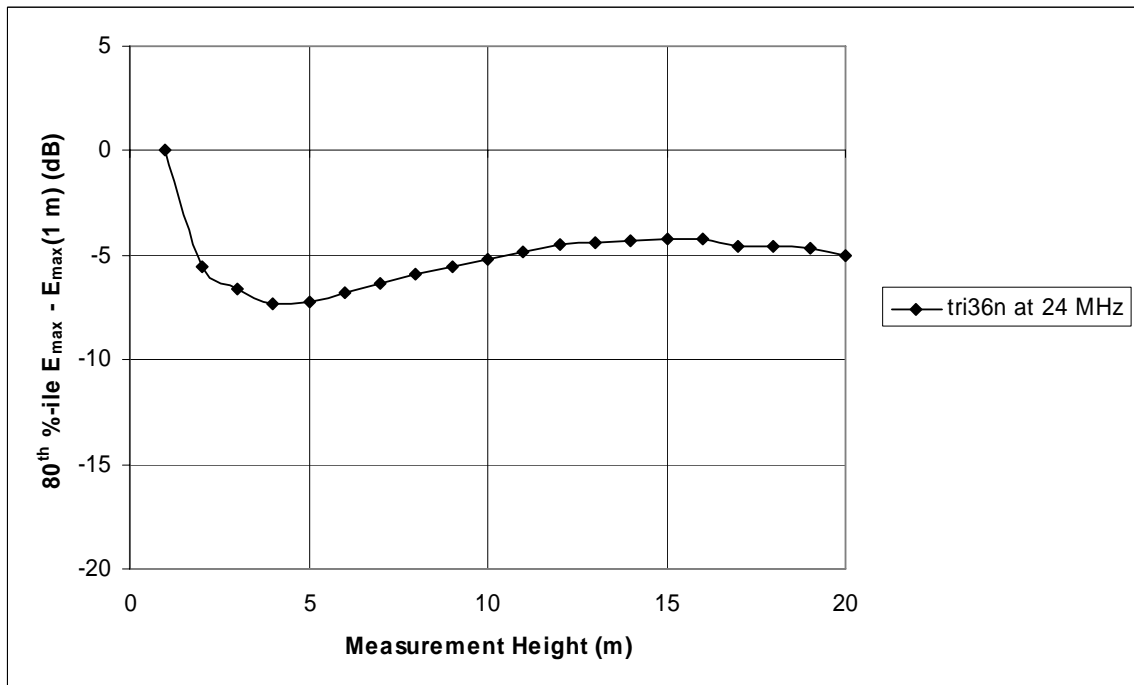


Figure A-86: 80<sup>th</sup> percentile of peak electric field strength along the power line relative to the peak electric field strength at a 1 meter measurement height



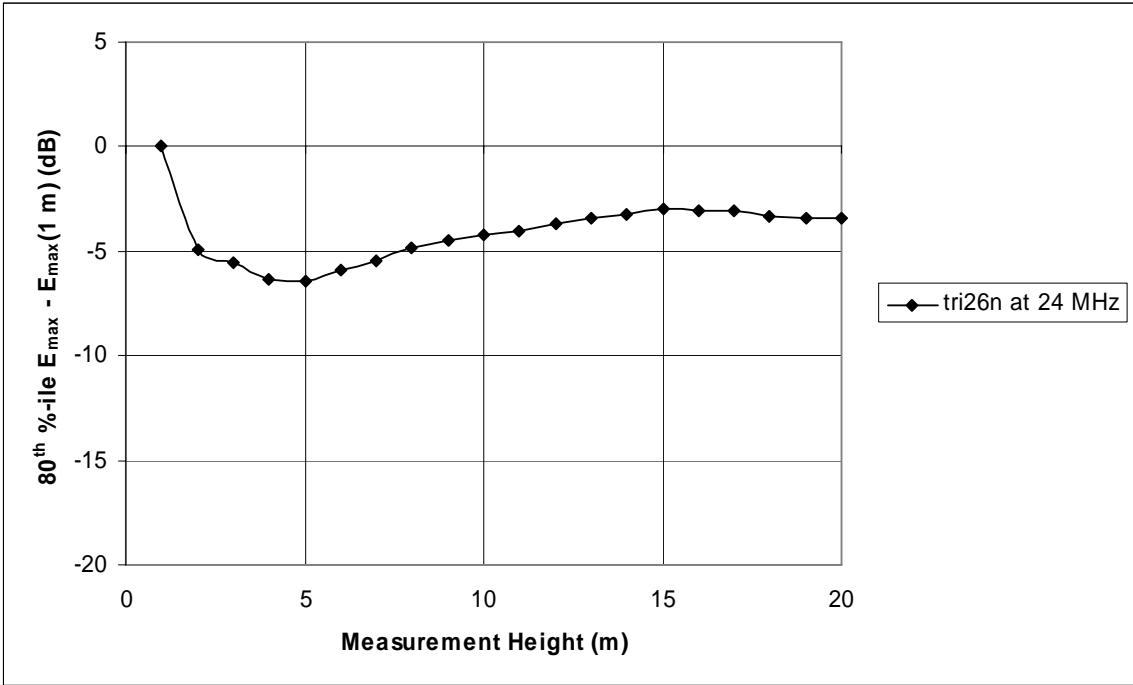


Figure A-87: 80<sup>th</sup> percentile of peak electric field strength along the power line relative to the peak electric field strength at a 1 meter measurement height

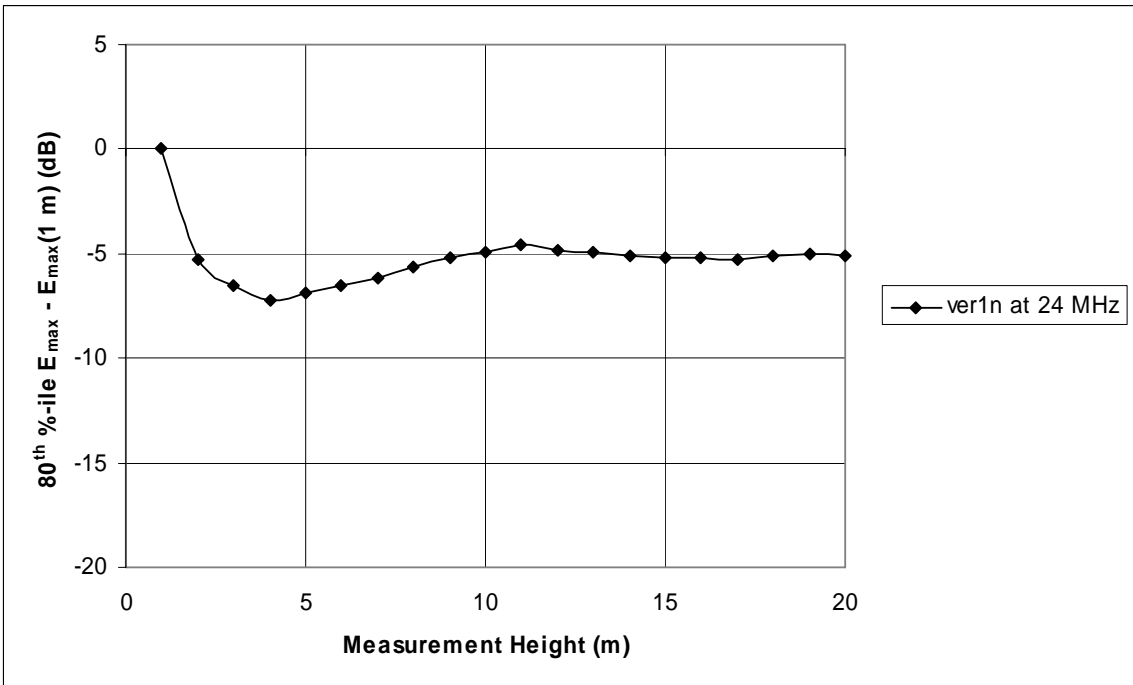


Figure A-88: 80<sup>th</sup> percentile of peak electric field strength along the power line relative to the peak electric field strength at a 1 meter measurement height

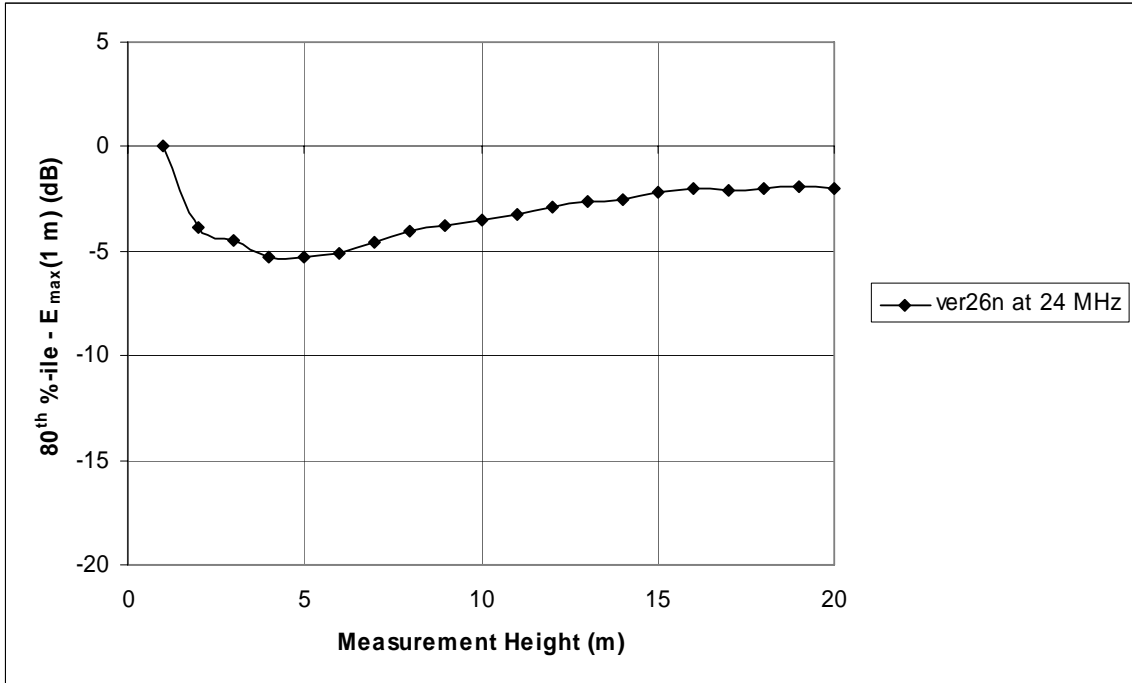


Figure A-89: 80<sup>th</sup> percentile of peak electric field strength along the power line relative to the peak electric field strength at a 1 meter measurement height

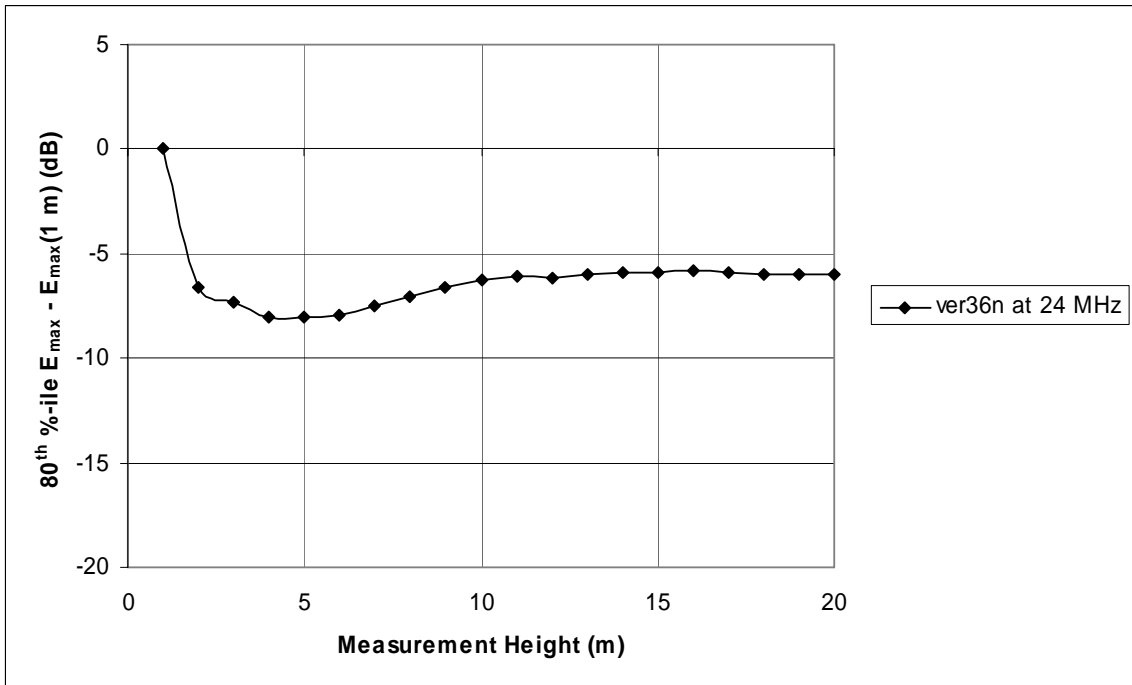


Figure A-90: 80<sup>th</sup> percentile of peak electric field strength along the power line relative to the peak electric field strength at a 1 meter measurement height

26 MHz Plots

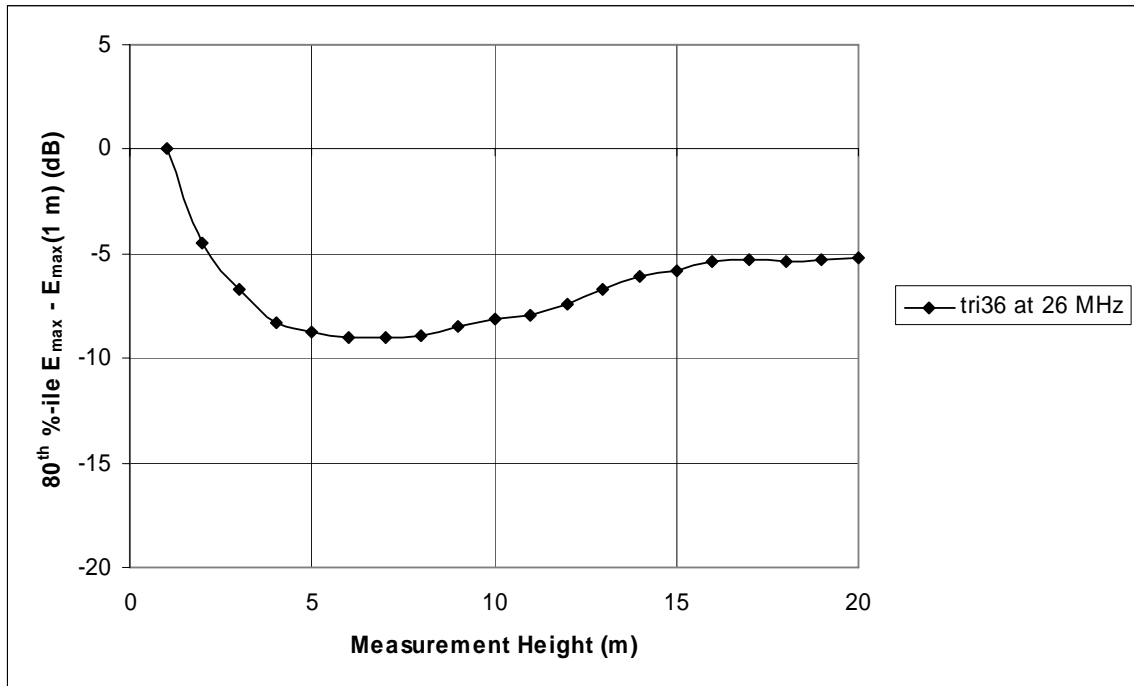


Figure A-91: 80<sup>th</sup> percentile of peak electric field strength along the power line relative to the peak electric field strength at a 1 meter measurement height

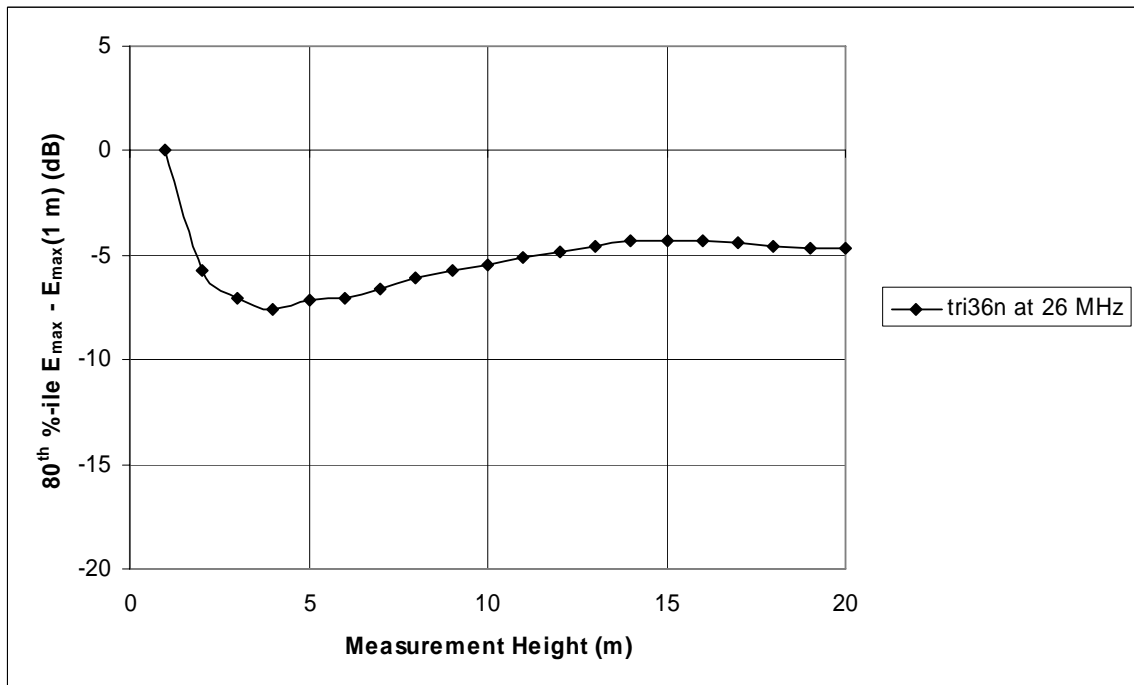


Figure A-92: 80<sup>th</sup> percentile of peak electric field strength along the power line relative to the peak electric field strength at a 1 meter measurement height

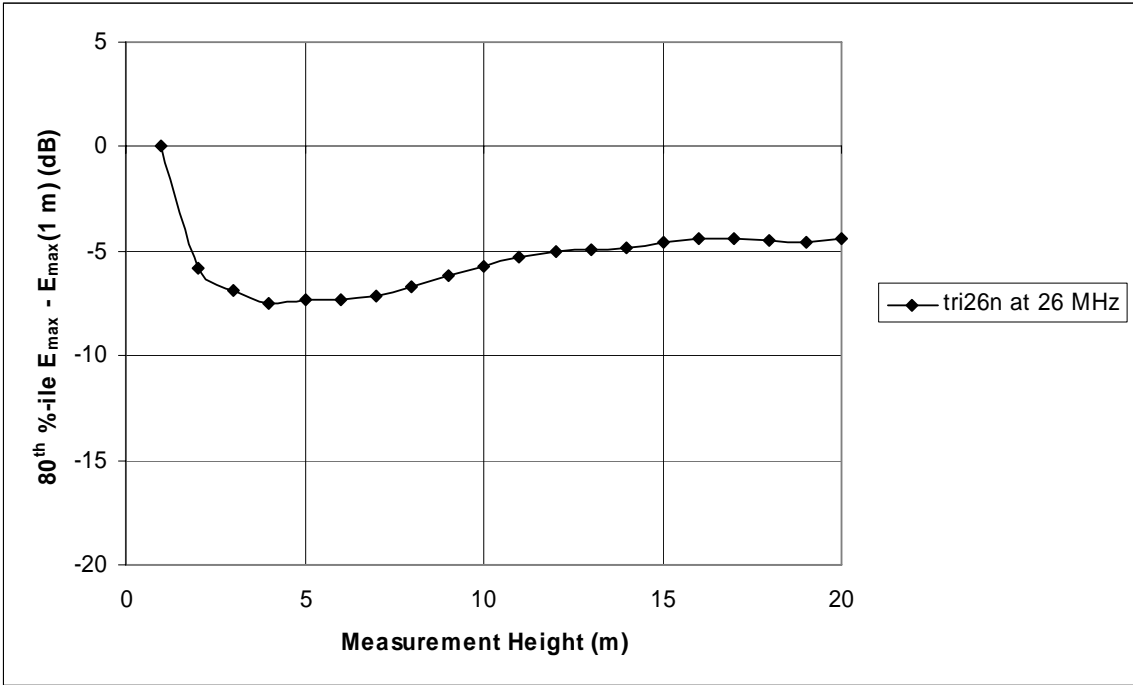


Figure A-93: 80<sup>th</sup> percentile of peak electric field strength along the power line relative to the peak electric field strength at a 1 meter measurement height

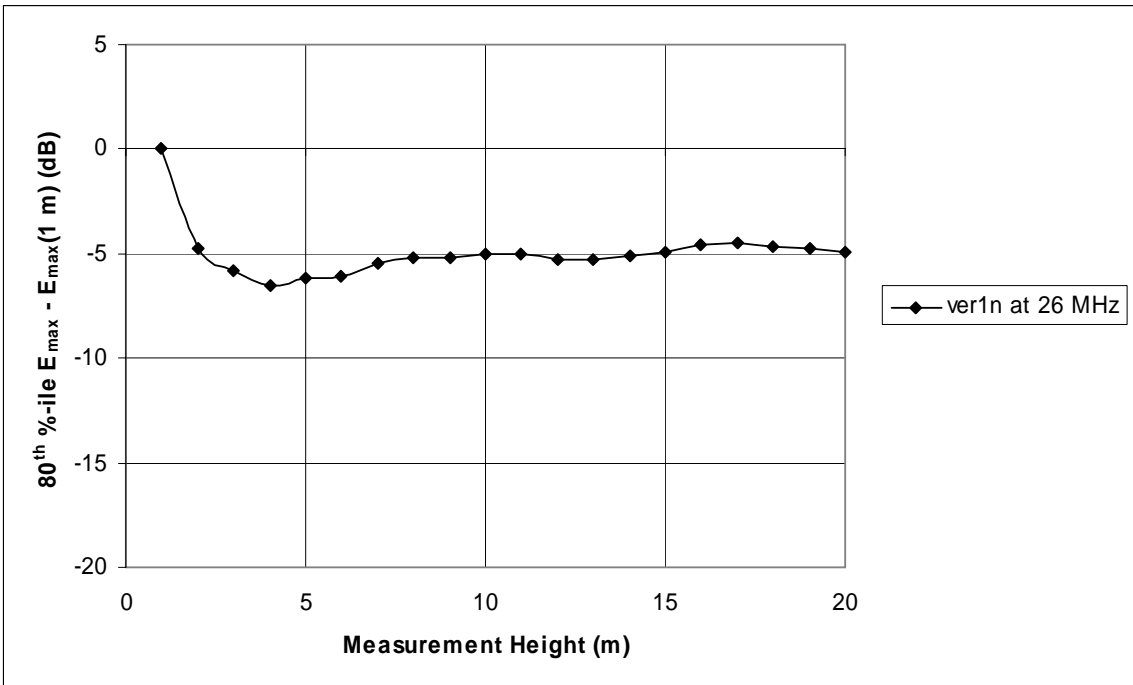


Figure A-94: 80<sup>th</sup> percentile of peak electric field strength along the power line relative to the peak electric field strength at a 1 meter measurement height

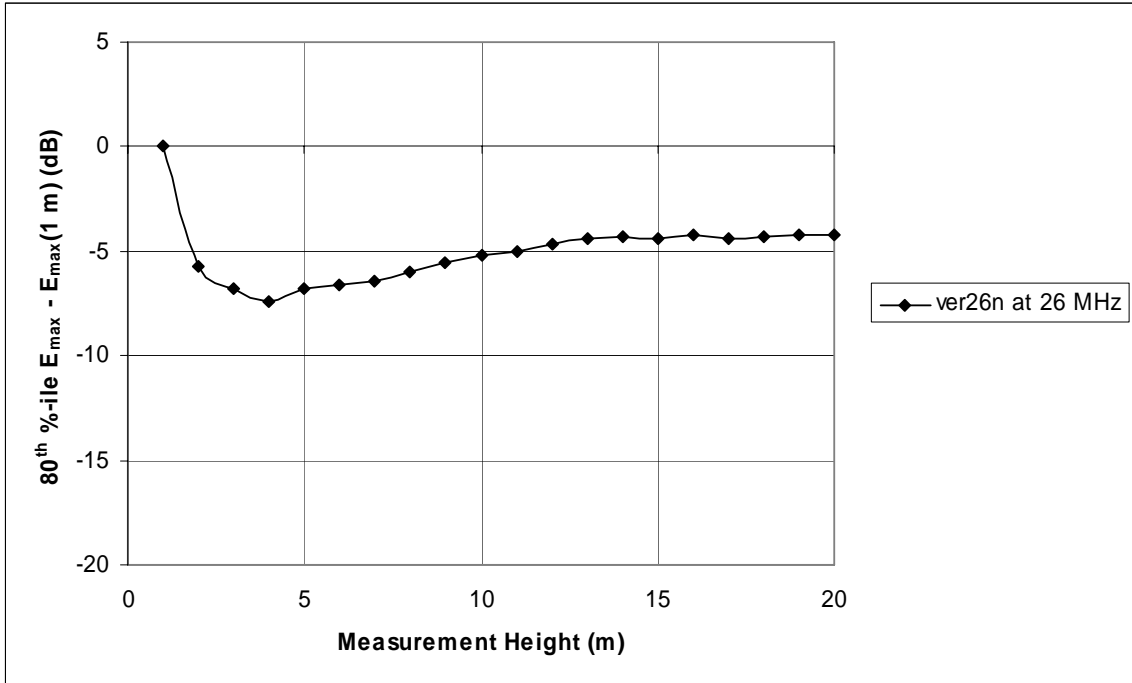


Figure A-95: 80<sup>th</sup> percentile of peak electric field strength along the power line relative to the peak electric field strength at a 1 meter measurement height

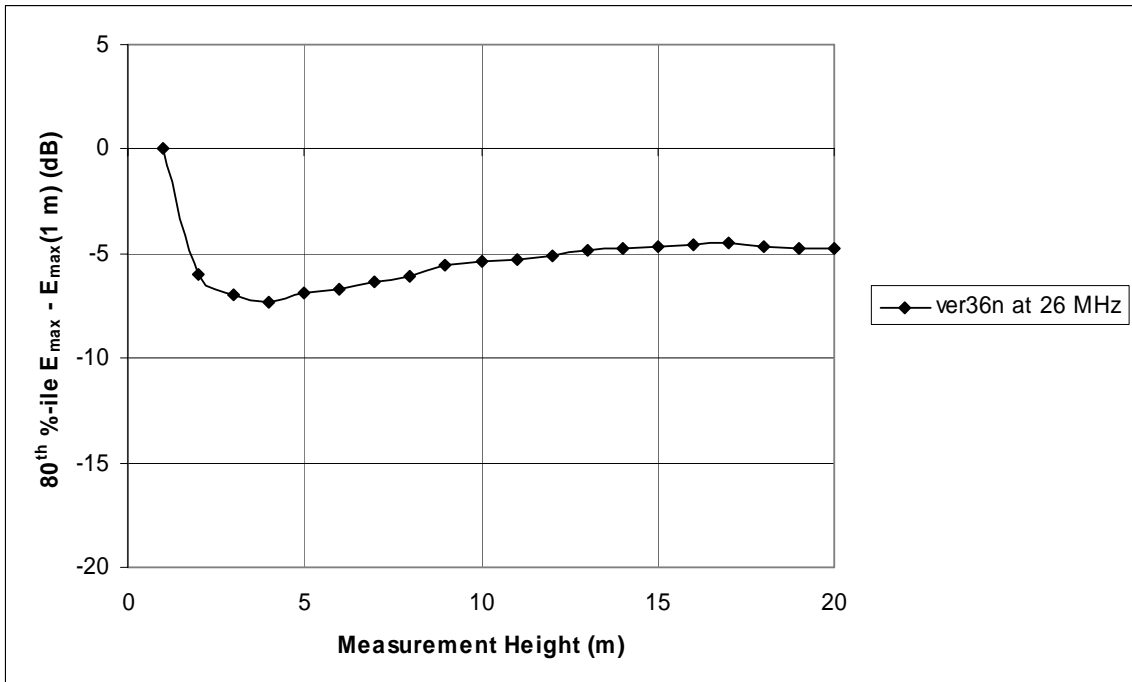


Figure A-96: 80<sup>th</sup> percentile of peak electric field strength along the power line relative to the peak electric field strength at a 1 meter measurement height

28 MHz Plots

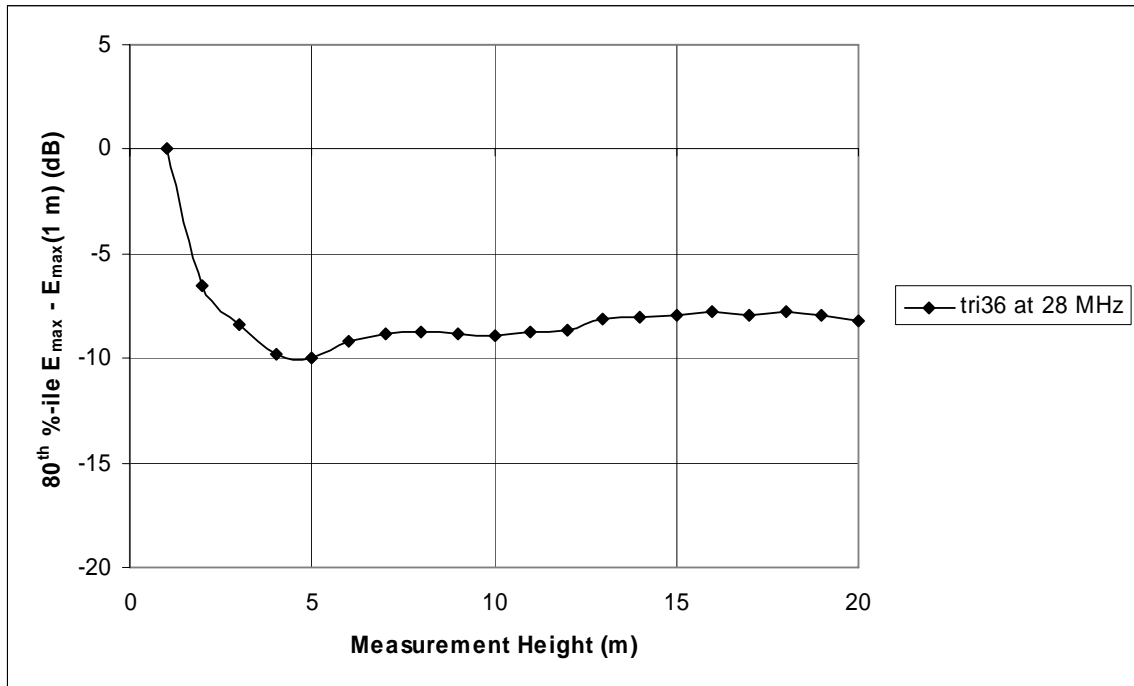


Figure A-97: 80<sup>th</sup> percentile of peak electric field strength along the power line relative to the peak electric field strength at a 1 meter measurement height

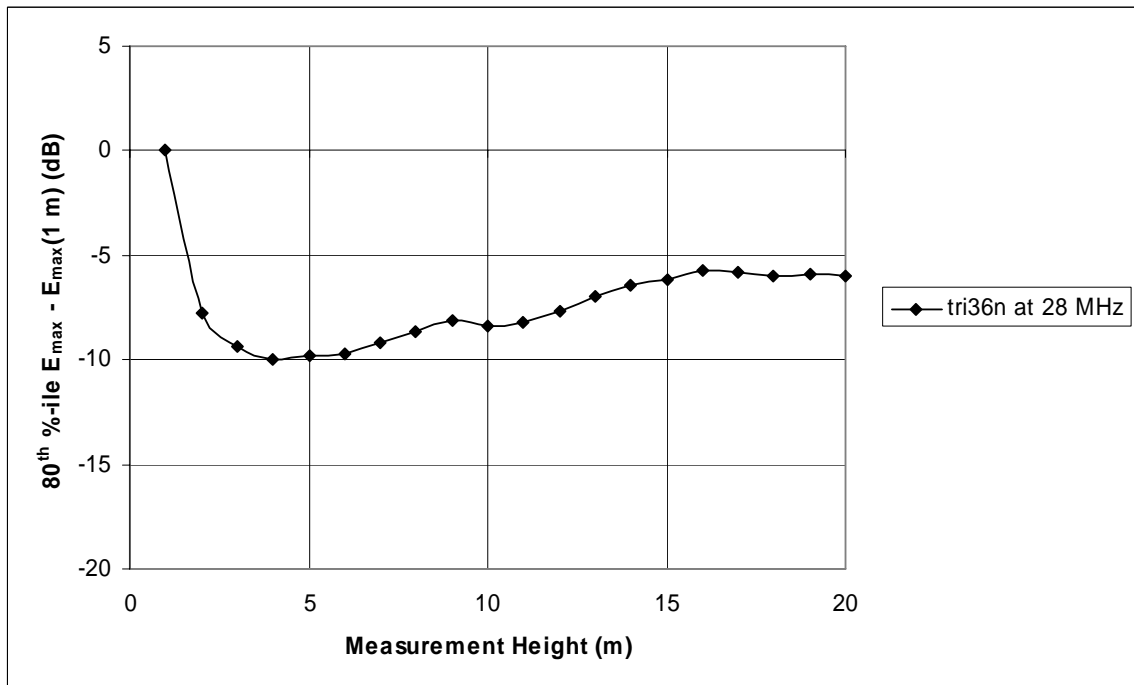


Figure A-98: 80<sup>th</sup> percentile of peak electric field strength along the power line relative to the peak electric field strength at a 1 meter measurement height

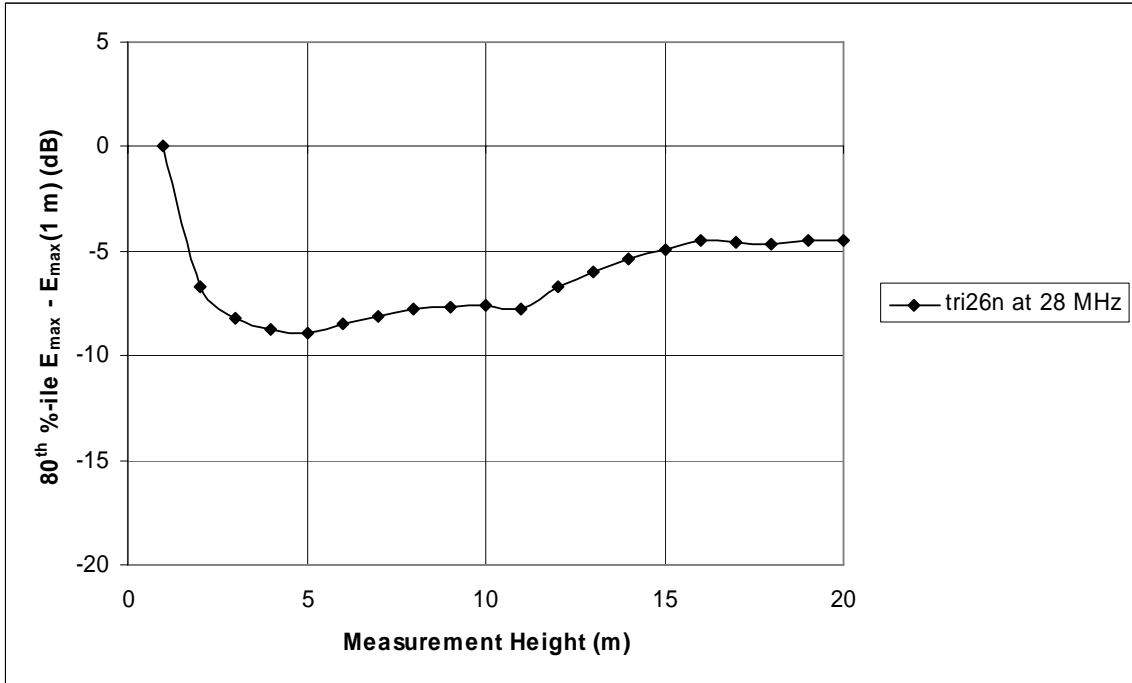


Figure A-99: 80<sup>th</sup> percentile of peak electric field strength along the power line relative to the peak electric field strength at a 1 meter measurement height

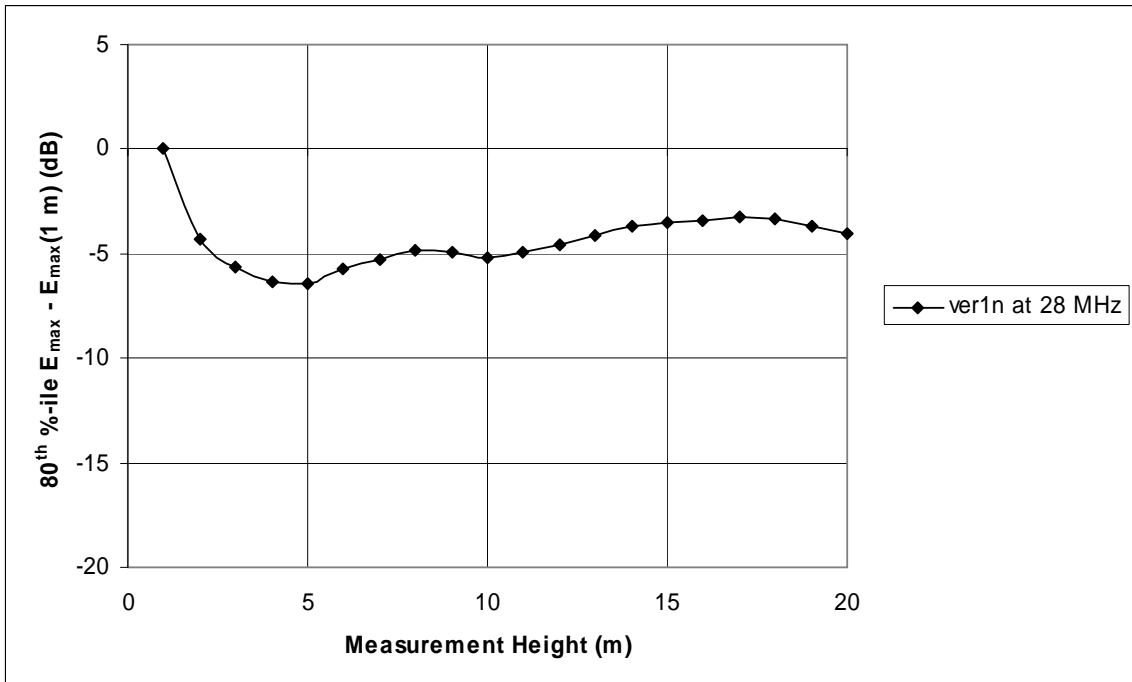


Figure A-100: 80<sup>th</sup> percentile of peak electric field strength along the power line relative to the peak electric field strength at a 1 meter measurement height

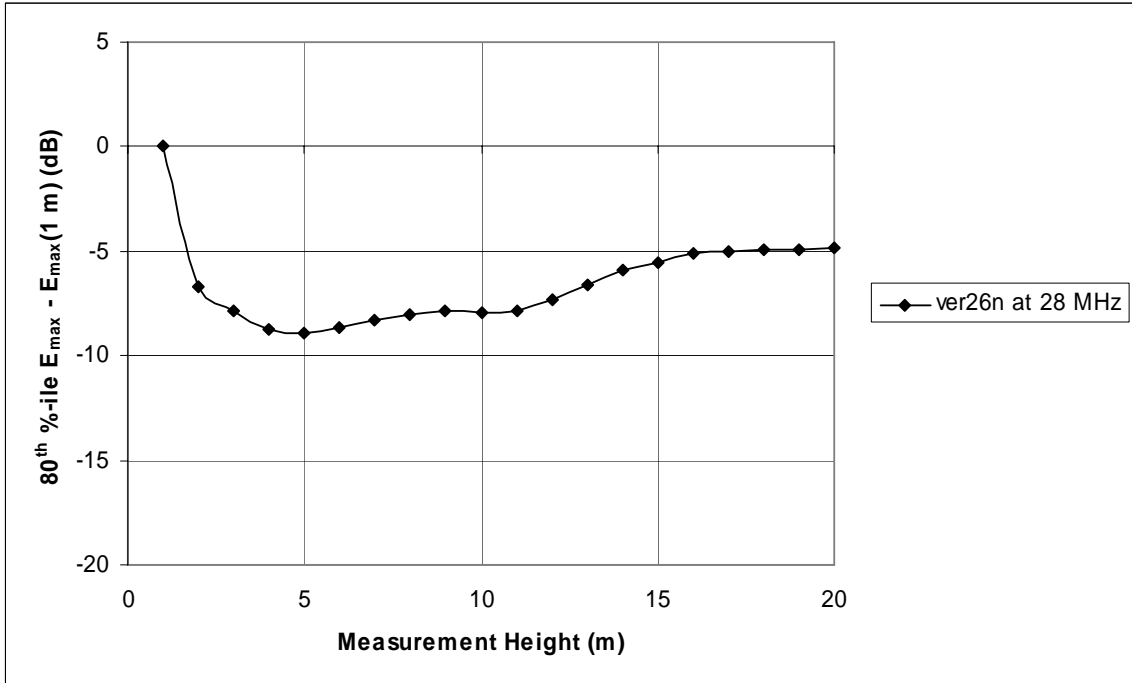


Figure A-101: 80<sup>th</sup> percentile of peak electric field strength along the power line relative to the peak electric field strength at a 1 meter measurement height

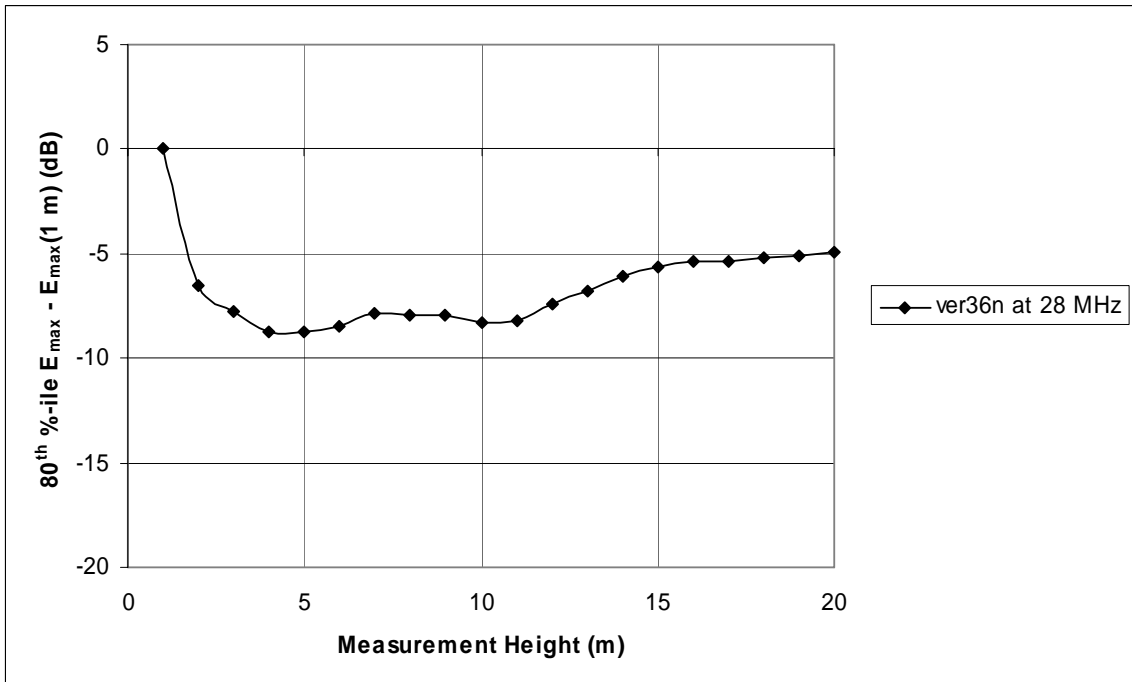


Figure A-102: 80<sup>th</sup> percentile of peak electric field strength along the power line relative to the peak electric field strength at a 1 meter measurement height



## A.4 COMPLIANCE MEASUREMENT HEIGHT FOR OPERATION AT 30 MHz AND ABOVE

The Commission's Part 15 measurement guidelines specify that at or above 30 MHz, measurements are to be made with the antenna positioned at a height ranging from 1 to 4 meters. The electric field strength should be measured in both the horizontal and vertical planes. The following plots show a comparison between the peak field strength determined from applying the measurement guidelines to the power line simulations to compute the 80<sup>th</sup> percentile of peak field strength at any height along the length of the power line. The rationale for use of 80<sup>th</sup> percentile values was previously addressed in Section A.3. The plots are shown for a number of NEC power line models at the frequencies of 30, 40 and 50 MHz.

### 30 MHz Plots

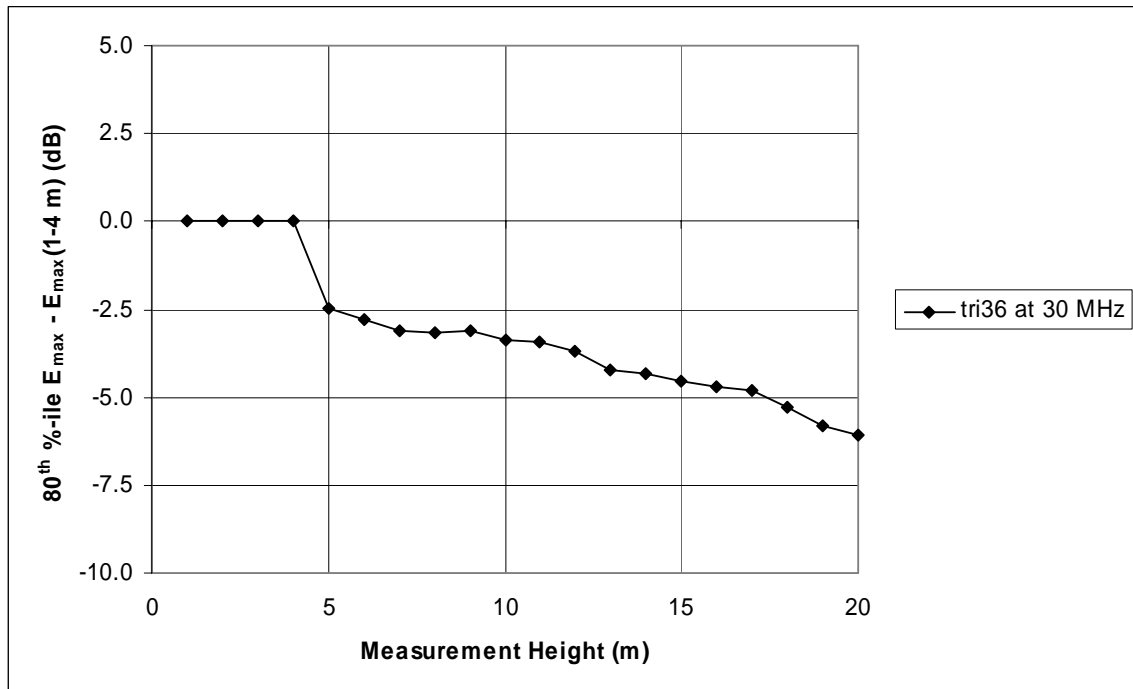


Figure A-103: 80<sup>th</sup> percentile of peak electric field strength along the power line relative to the peak electric field strength at the 1 to 4 meter measurement height

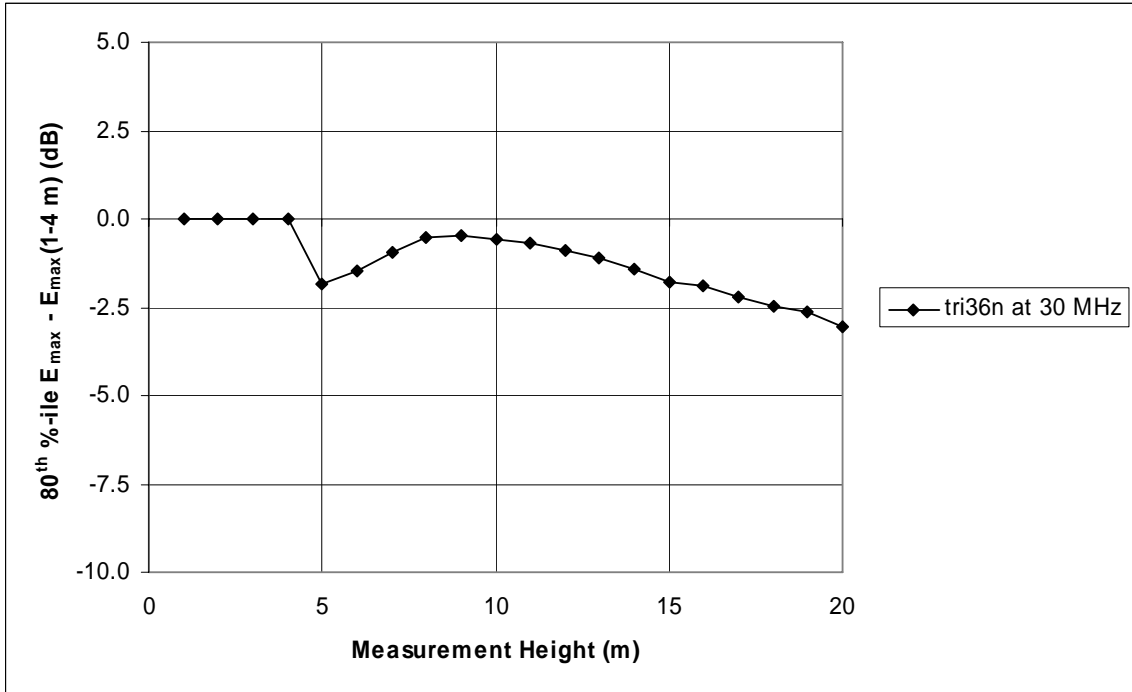


Figure A-104: 80<sup>th</sup> percentile of peak electric field strength along the power line relative to the peak electric field strength at the 1 to 4 meter measurement height

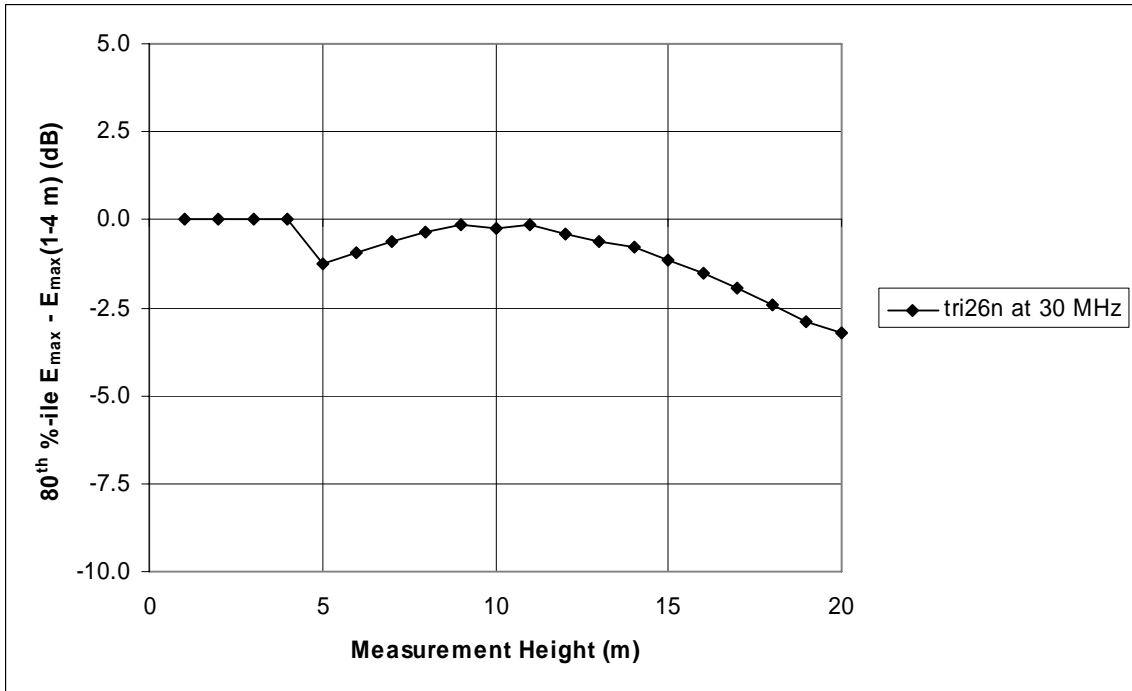


Figure A-105: 80<sup>th</sup> percentile of peak electric field strength along the power line relative to the peak electric field strength at the 1 to 4 meter measurement height

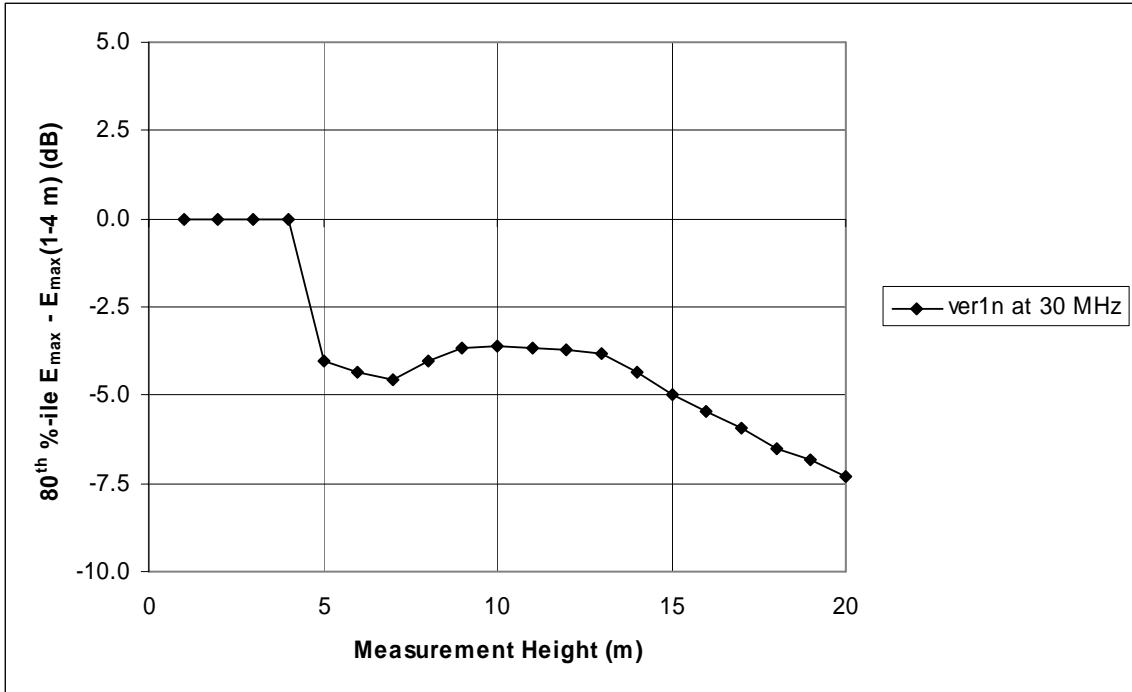


Figure A-106: 80<sup>th</sup> percentile of peak electric field strength along the power line relative to the peak electric field strength at the 1 to 4 meter measurement height

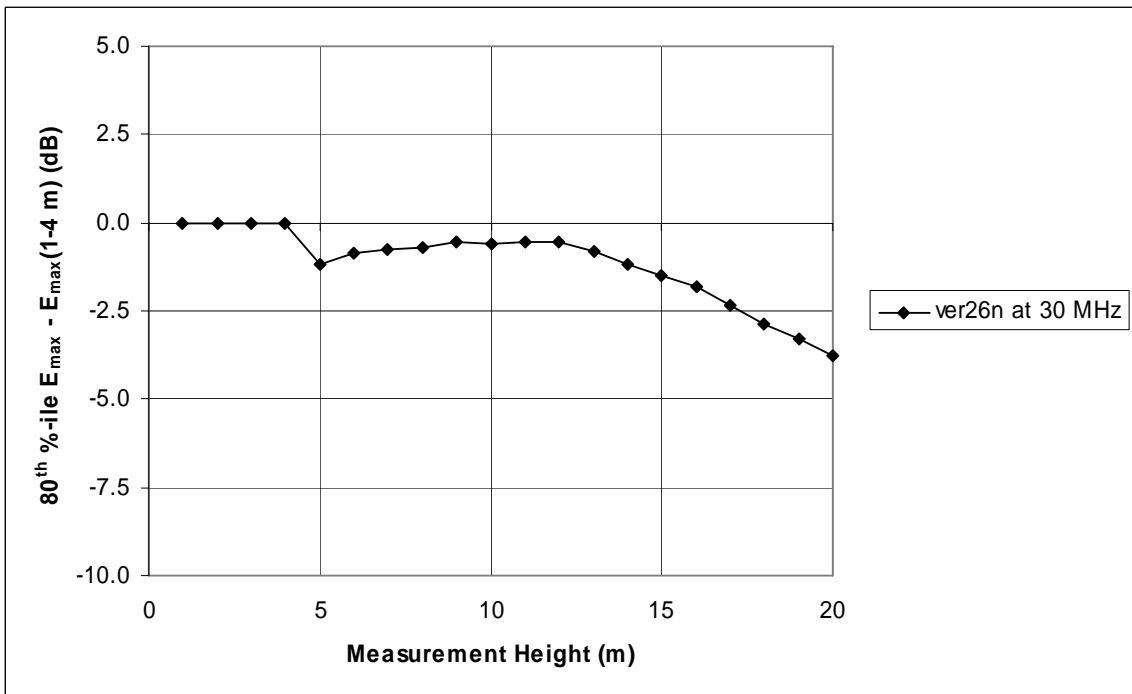


Figure A-107: 80<sup>th</sup> percentile of peak electric field strength along the power line relative to the peak electric field strength at the 1 to 4 meter measurement height

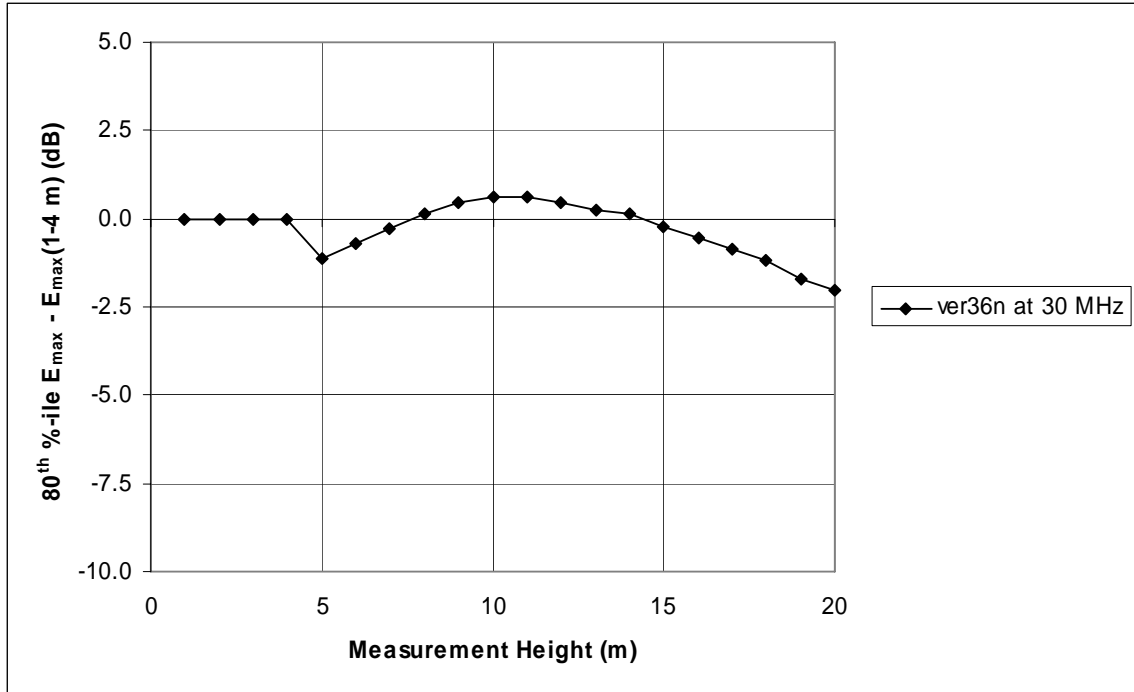


Figure A-108: 80<sup>th</sup> percentile of peak electric field strength along the power line relative to the peak electric field strength at the 1 to 4 meter measurement height

40 MHz Plots

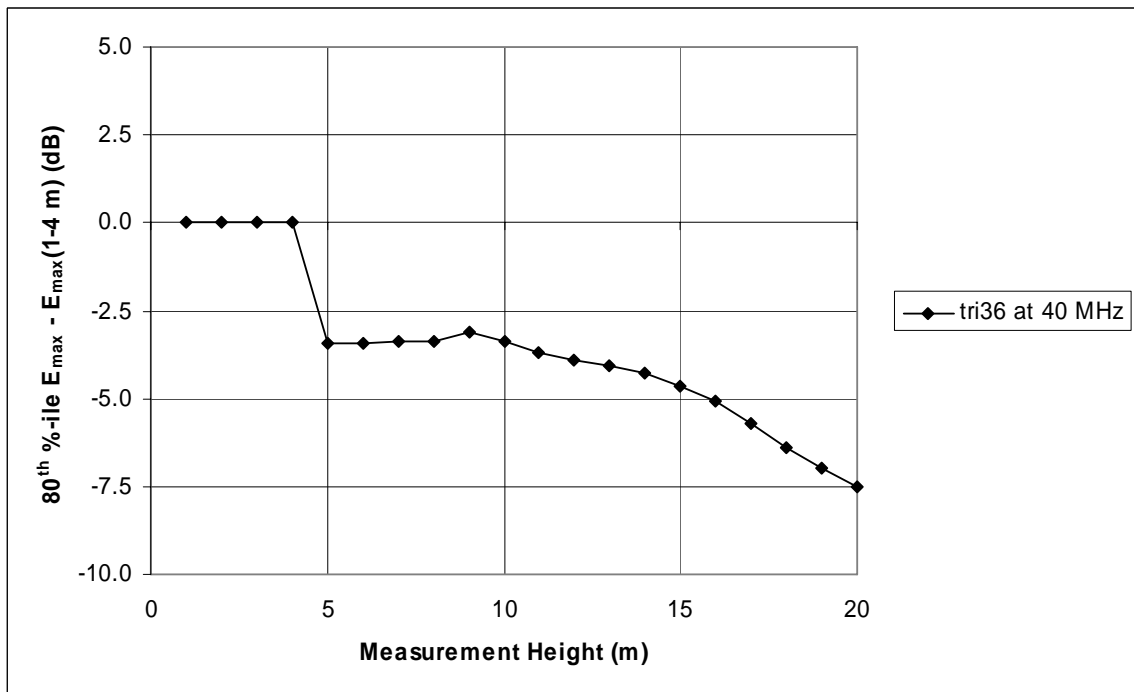


Figure A-109: 80<sup>th</sup> percentile of peak electric field strength along the power line relative to the peak electric field strength at the 1 to 4 meter measurement height

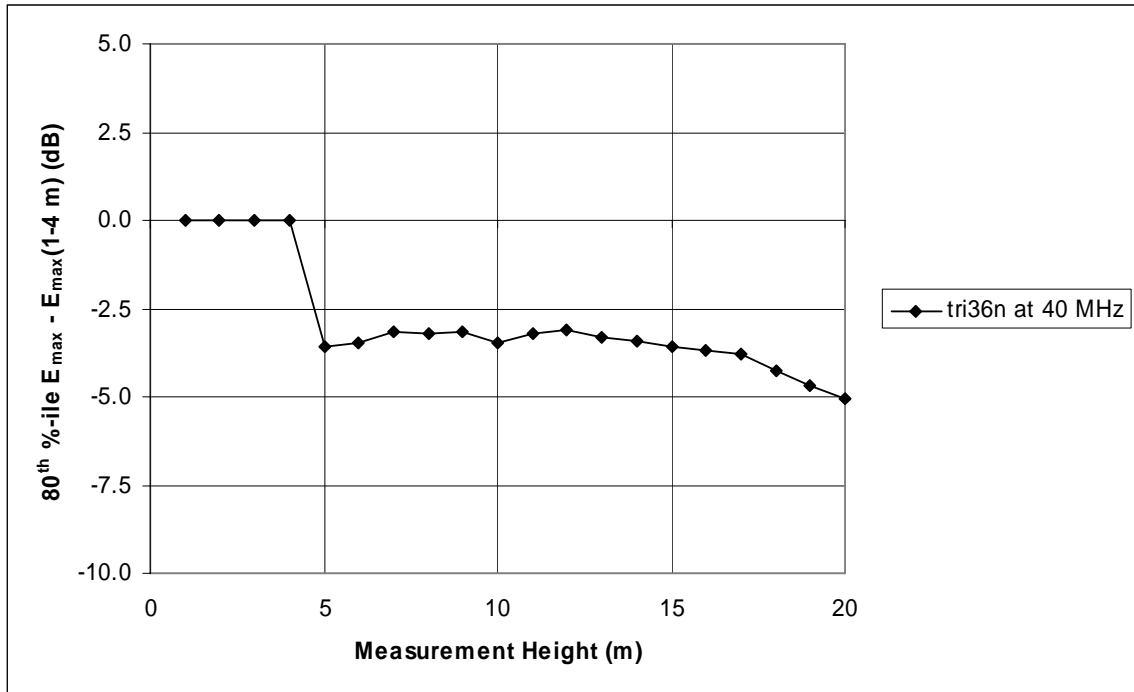


Figure A-110: 80<sup>th</sup> percentile of peak electric field strength along the power line relative to the peak electric field strength at the 1 to 4 meter measurement height

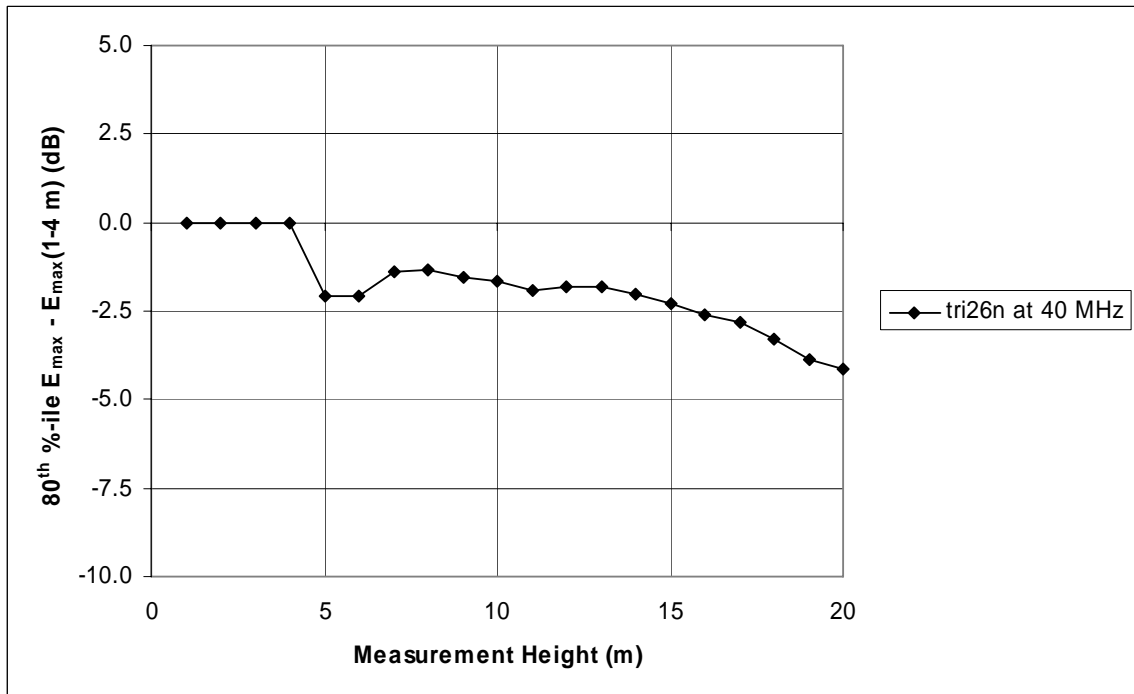


Figure A-111: 80<sup>th</sup> percentile of peak electric field strength along the power line relative to the peak electric field strength at the 1 to 4 meter measurement height

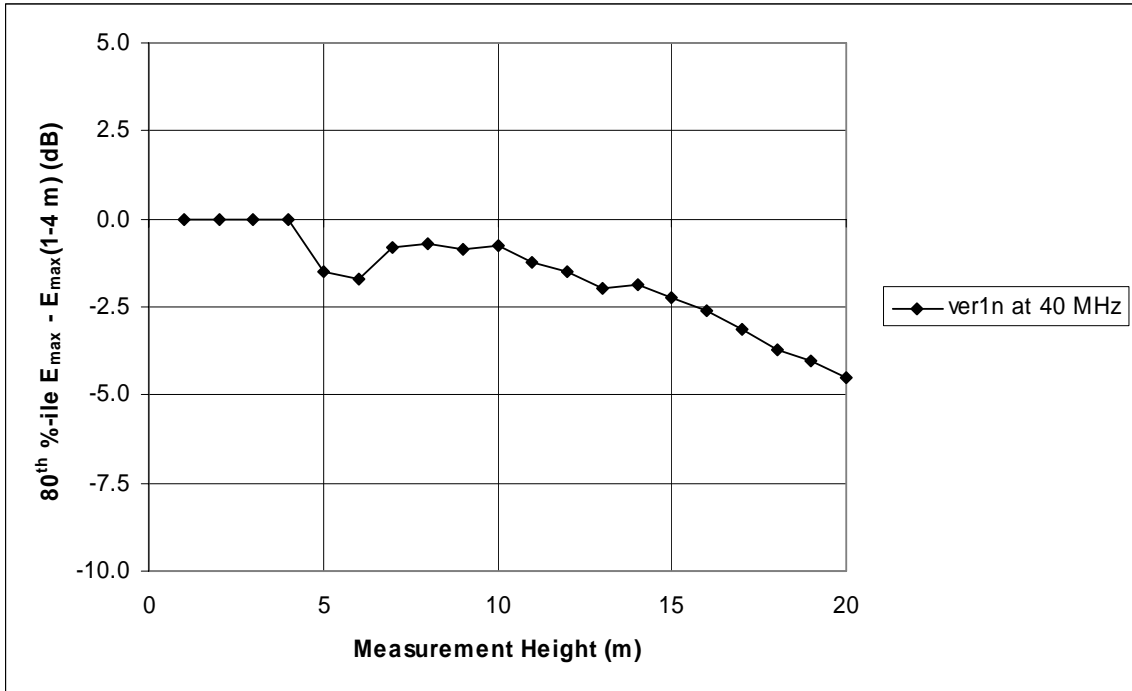


Figure A-112: 80<sup>th</sup> percentile of peak electric field strength along the power line relative to the peak electric field strength at the 1 to 4 meter measurement height

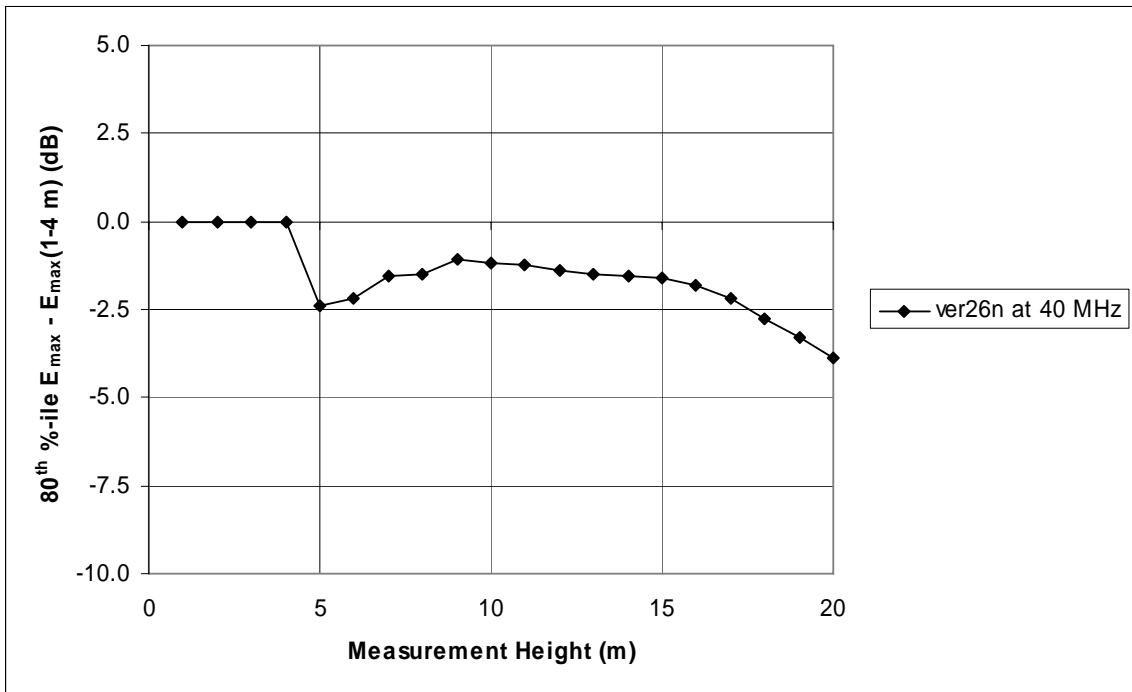


Figure A-113: 80<sup>th</sup> percentile of peak electric field strength along the power line relative to the peak electric field strength at the 1 to 4 meter measurement height

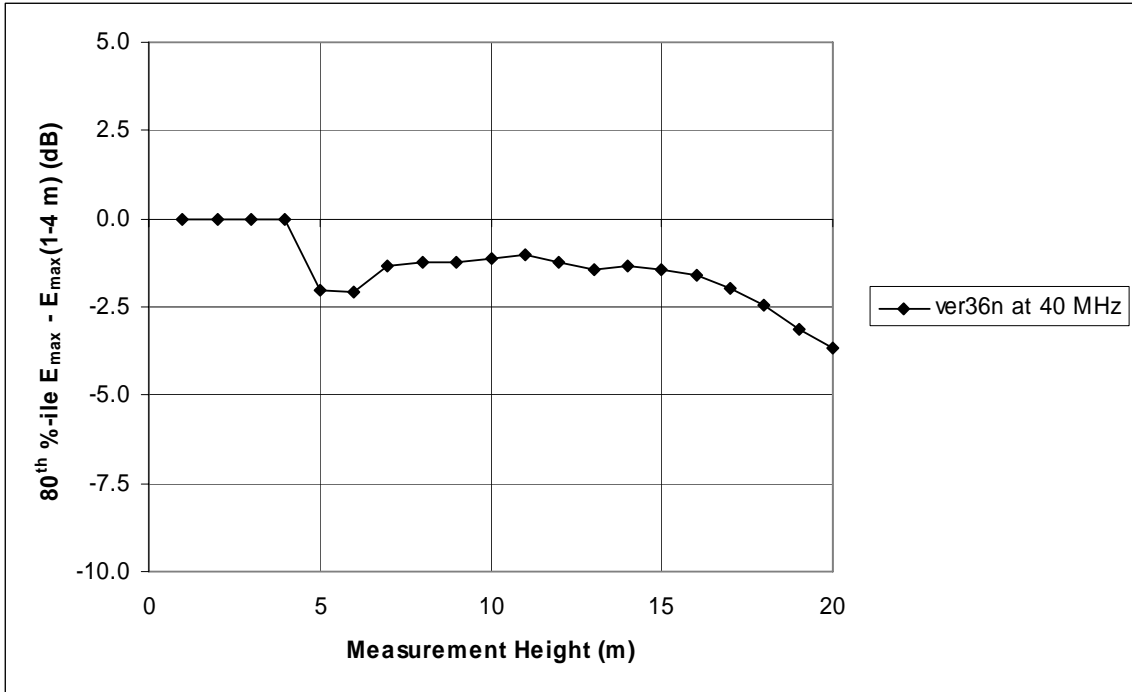


Figure A-114: 80<sup>th</sup> percentile of peak electric field strength along the power line relative to the peak electric field strength at the 1 to 4 meter measurement height

50 MHz Plots

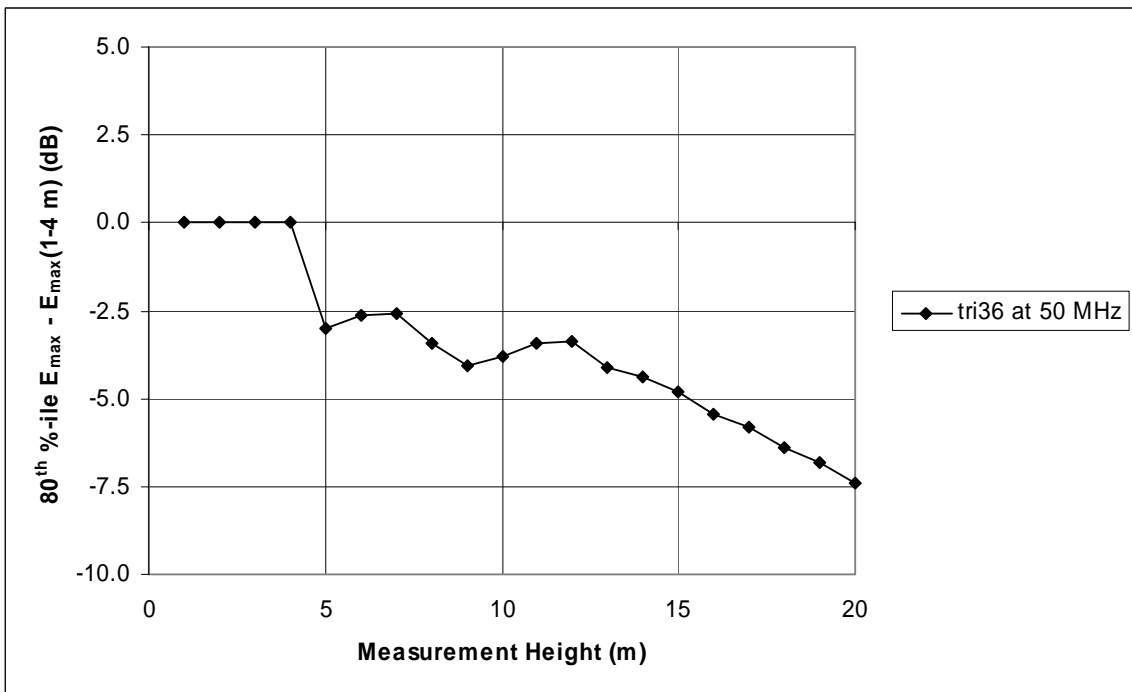


Figure A-115: 80<sup>th</sup> percentile of peak electric field strength along the power line relative to the peak electric field strength at the 1 to 4 meter measurement height

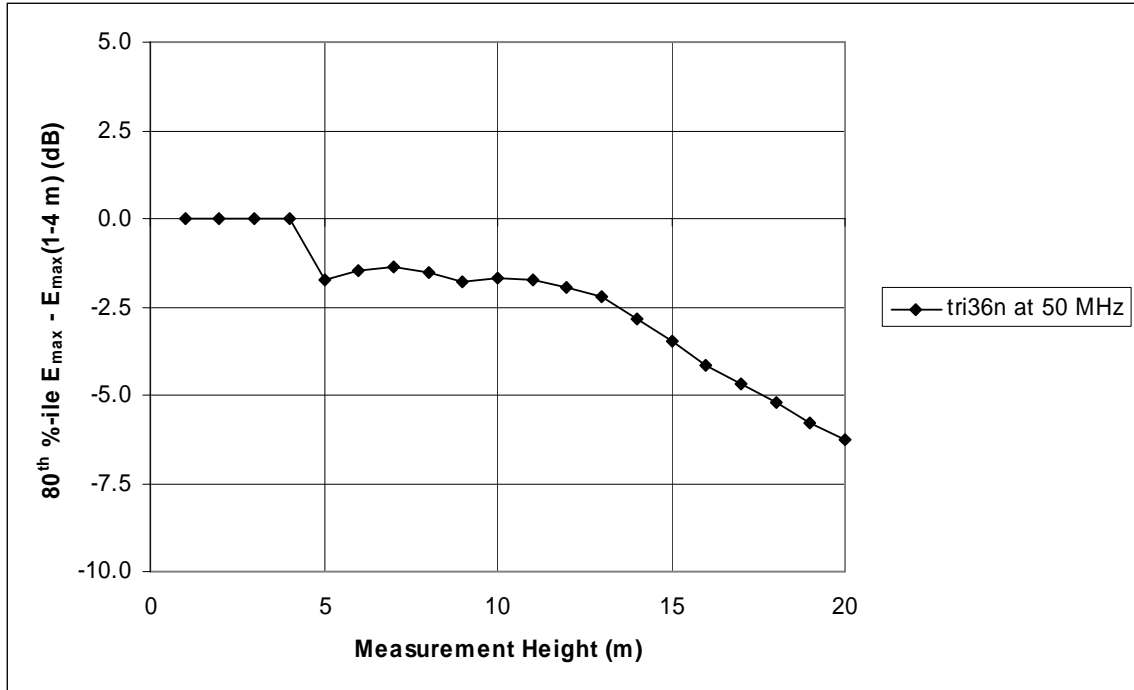


Figure A-116: 80<sup>th</sup> percentile of peak electric field strength along the power line relative to the peak electric field strength at the 1 to 4 meter measurement height

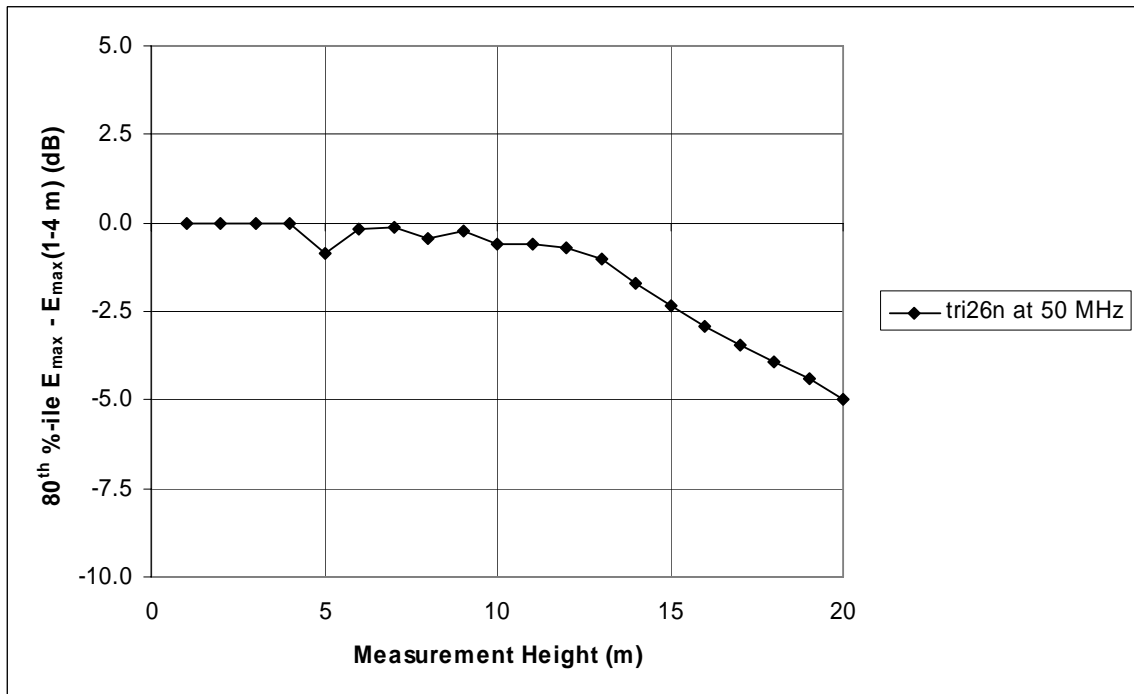


Figure A-117: 80<sup>th</sup> percentile of peak electric field strength along the power line relative to the peak electric field strength at the 1 to 4 meter measurement height



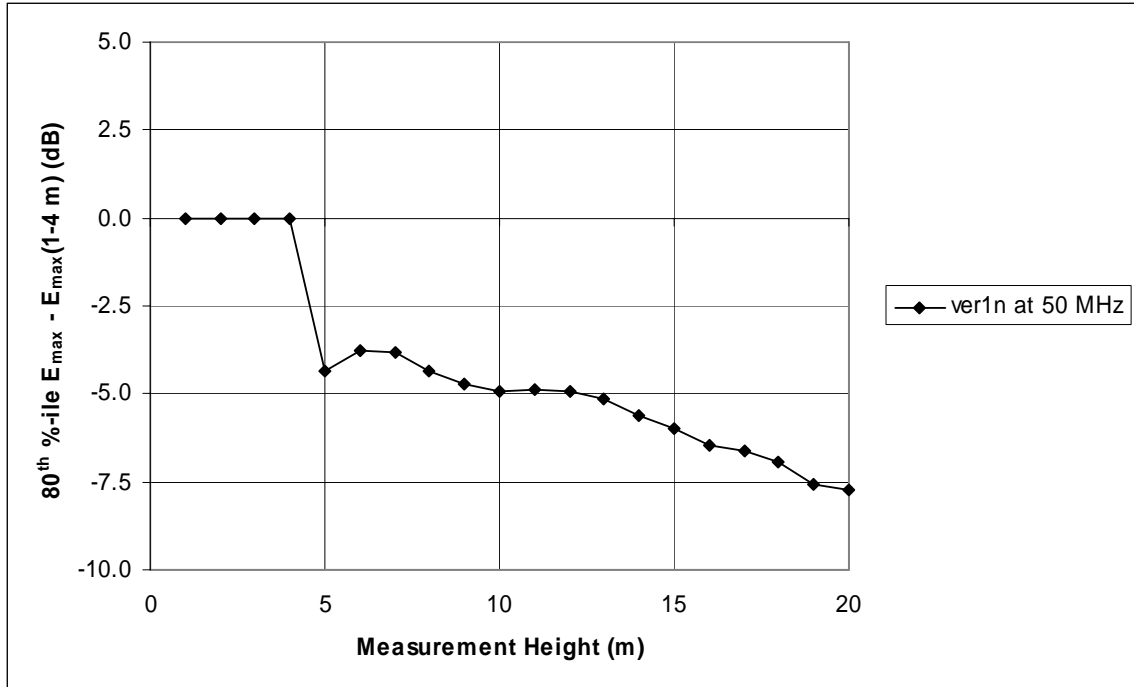


Figure A-118: 80<sup>th</sup> percentile of peak electric field strength along the power line relative to the peak electric field strength at the 1 to 4 meter measurement height

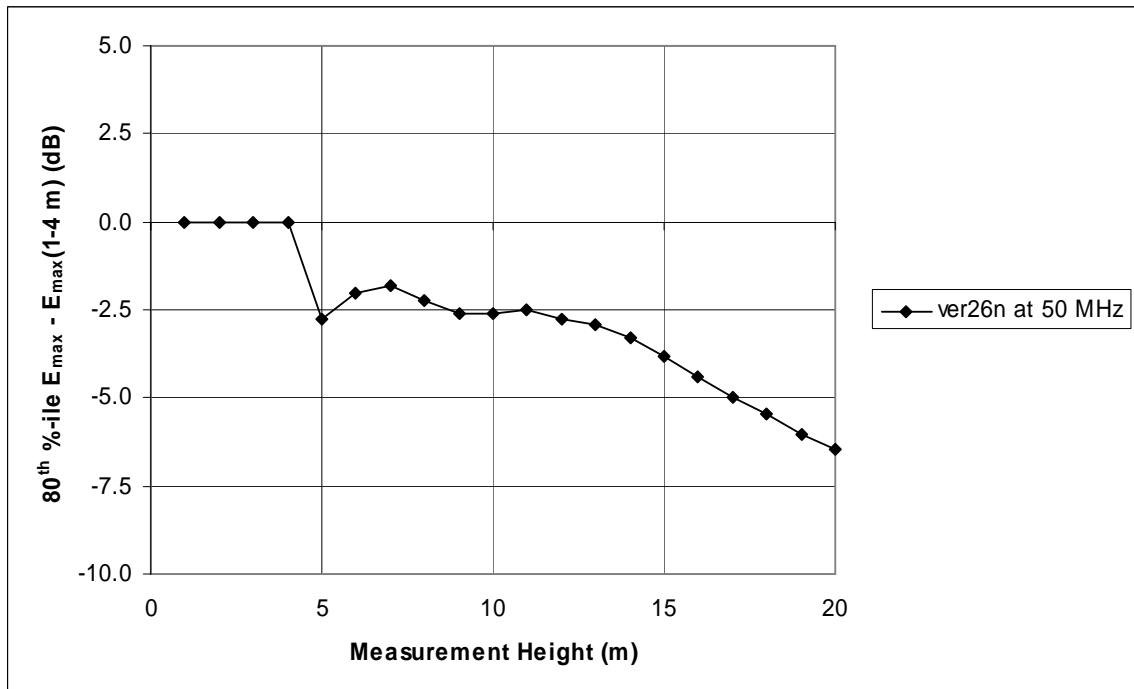


Figure A-119: 80<sup>th</sup> percentile of peak electric field strength along the power line relative to the peak electric field strength at the 1 to 4 meter measurement height

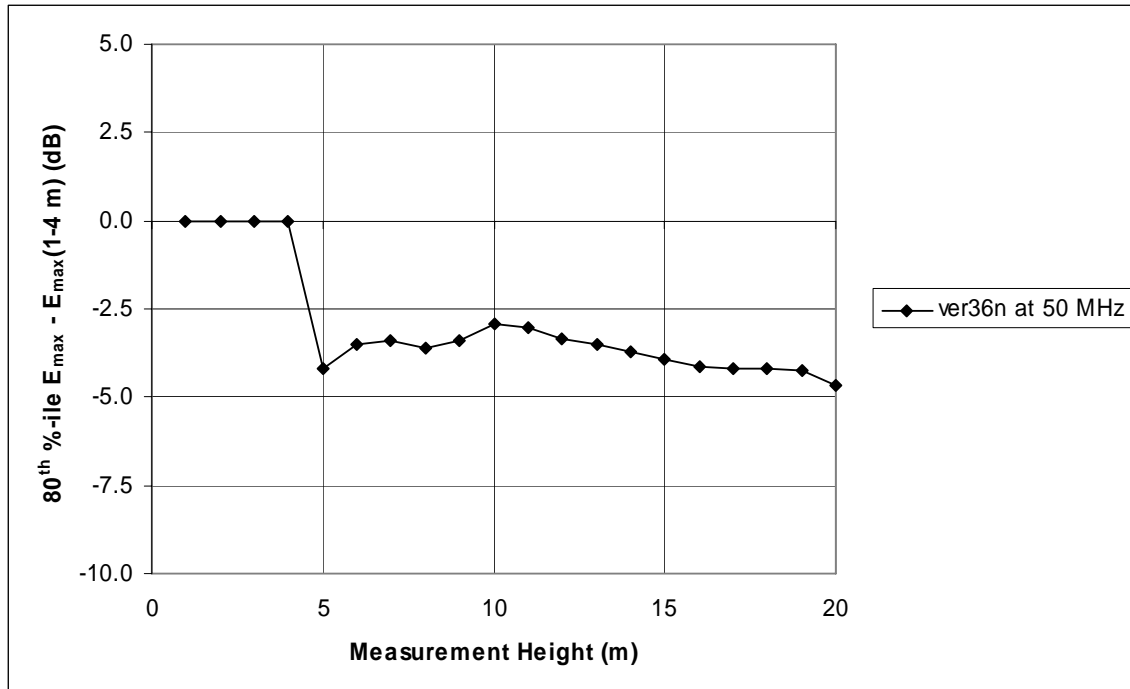


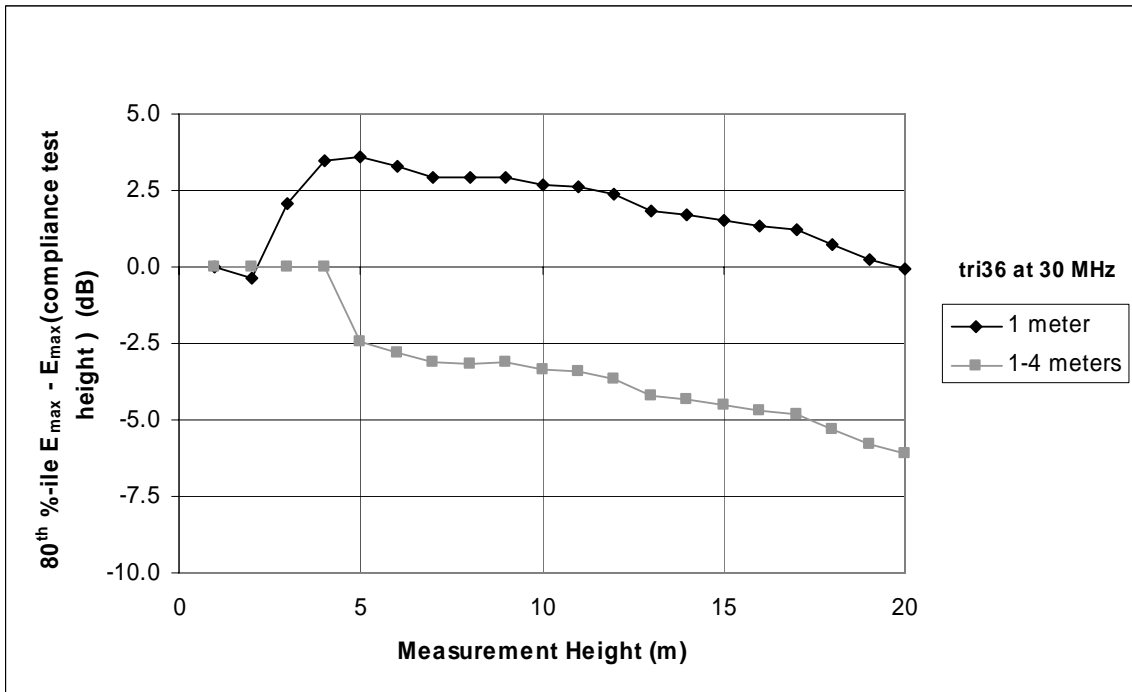
Figure A-120: 80<sup>th</sup> percentile of peak electric field strength along the power line relative to the peak electric field strength at the 1 to 4 meter measurement height

## A.5 HEIGHT CORRECTION FACTOR ABOVE 30 MHz

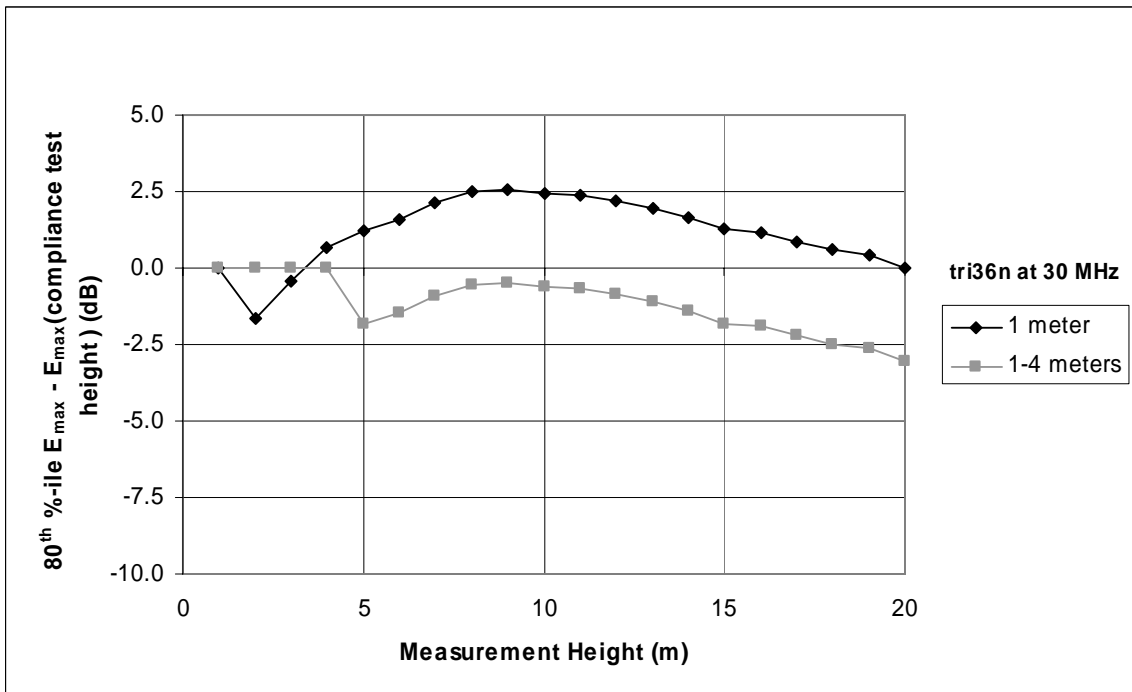
Above 30 MHz, the option to perform compliance measurements at a 1 meter measurement height coupled with a 5 dB height correction factor provides a much simpler measurement approach than to perform measurements over a 1 to 4 meter range of measurement antenna heights. Figures A-121 through A-138 show the comparison between use of a 1 to 4 meter measurement height and the optional use of a 1 meter measurement height.

The results shown in these figures indicate that use of the optional 1 meter measurement height tends to underestimate the peak electric field strength by 2.5 to 7.5 dB. Thus, the use of the optional 1 meter measurement height coupled with a 5 dB correction factor will, in general, provide similar results to measurements performed using a 1 to 4 meter measurement height.

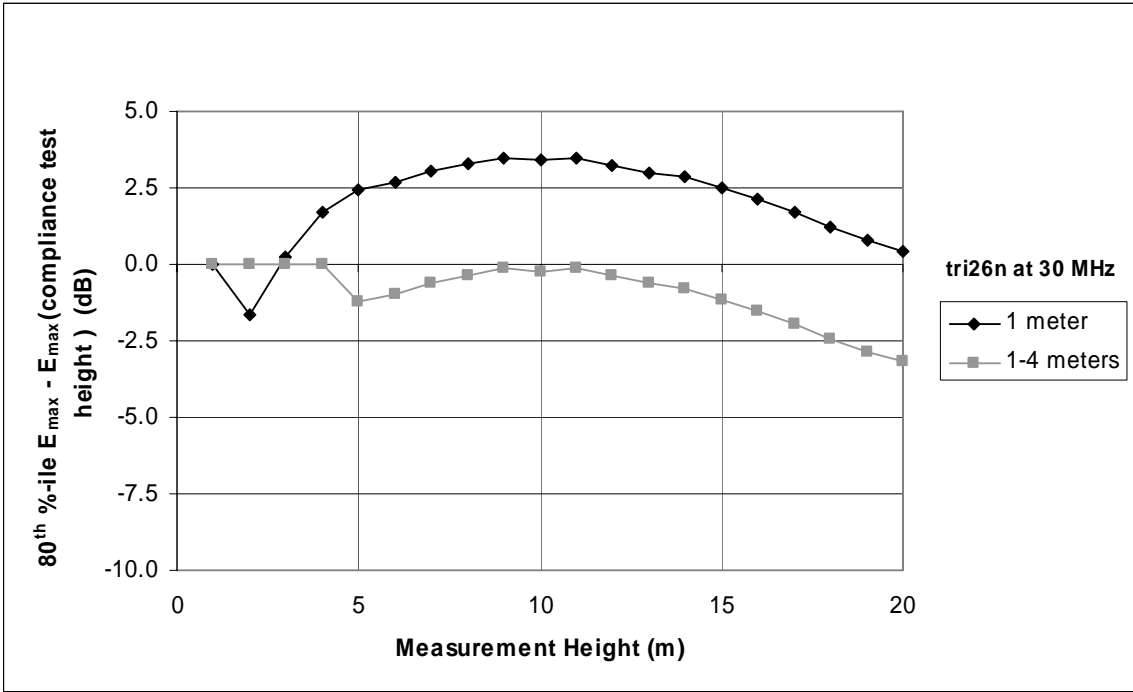
30 MHz Plots



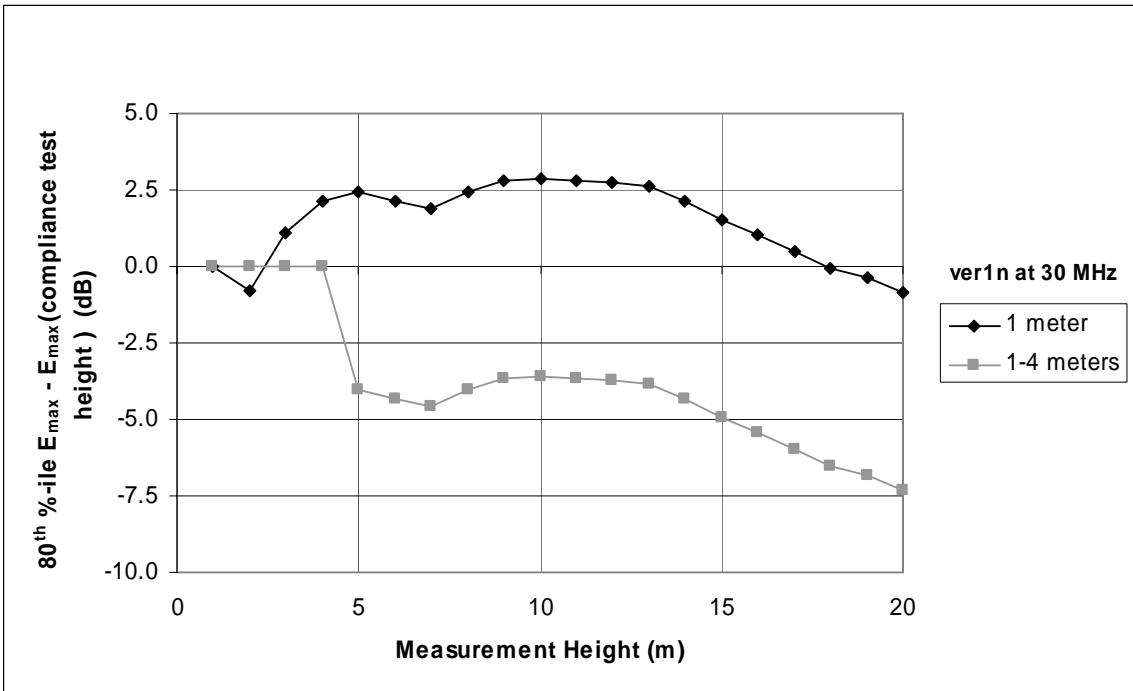
A-121: Comparison of electric field strength as a function of measurement height, if compliance measurements were performed at heights of 1 meter, or at 1 to 4 meters



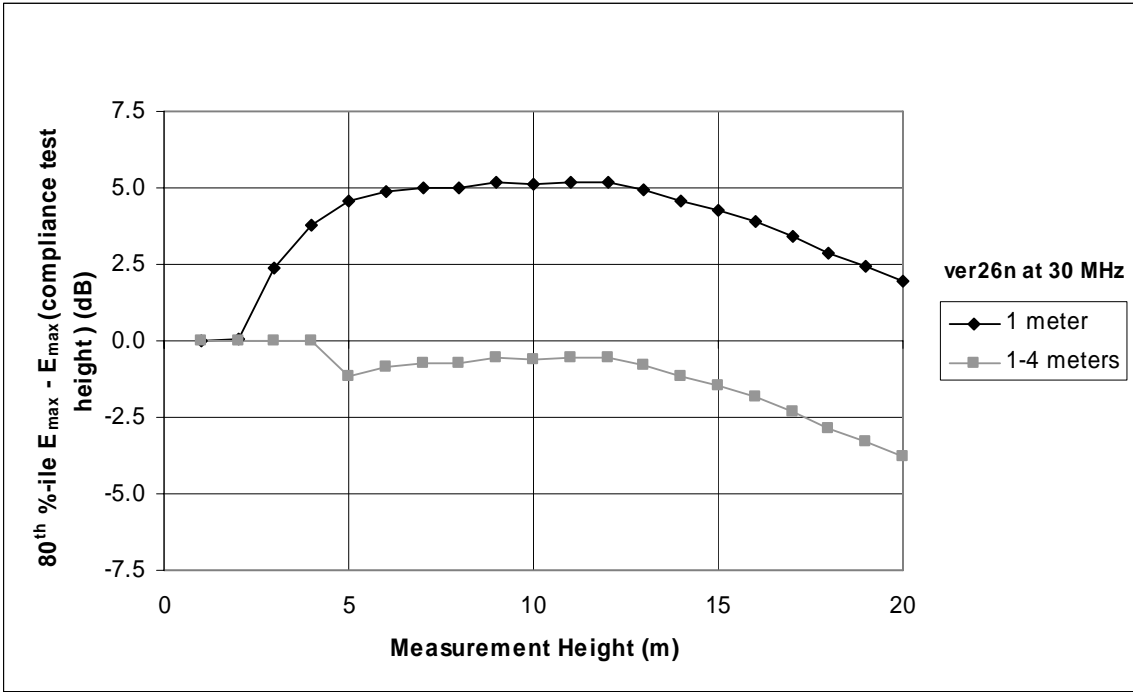
A-122: Comparison of electric field strength as a function of measurement height, if compliance measurements were performed at heights of 1 meter, or at 1 to 4 meters



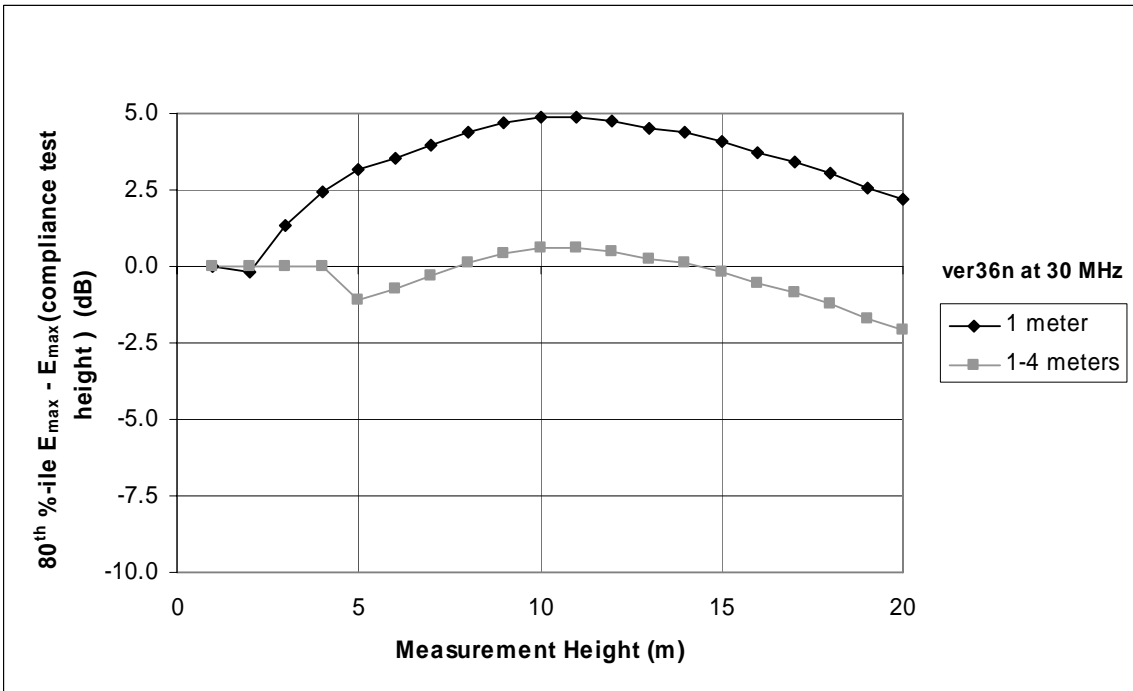
A-123: Comparison of electric field strength as a function of measurement height, if compliance measurements were performed at heights of 1 meter, or at 1 to 4 meters



A-124: Comparison of electric field strength as a function of measurement height, if compliance measurements were performed at heights of 1 meter, or at 1 to 4 meters

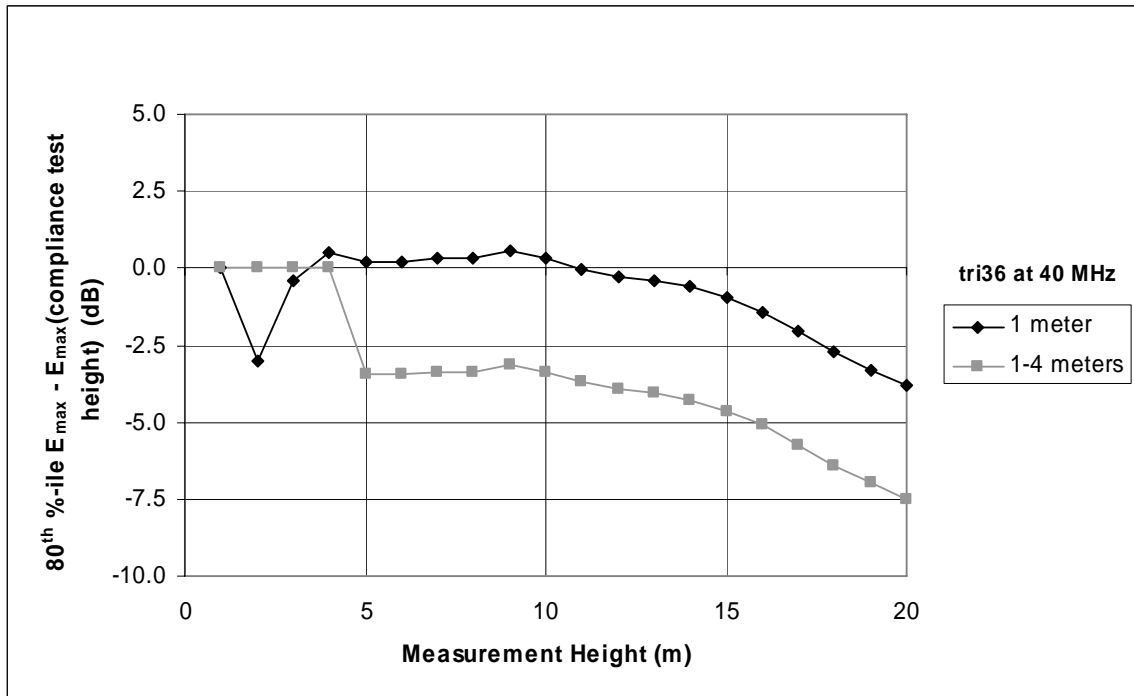


A-125: Comparison of electric field strength as a function of measurement height, if compliance measurements were performed at heights of 1 meter, or at 1 to 4 meters

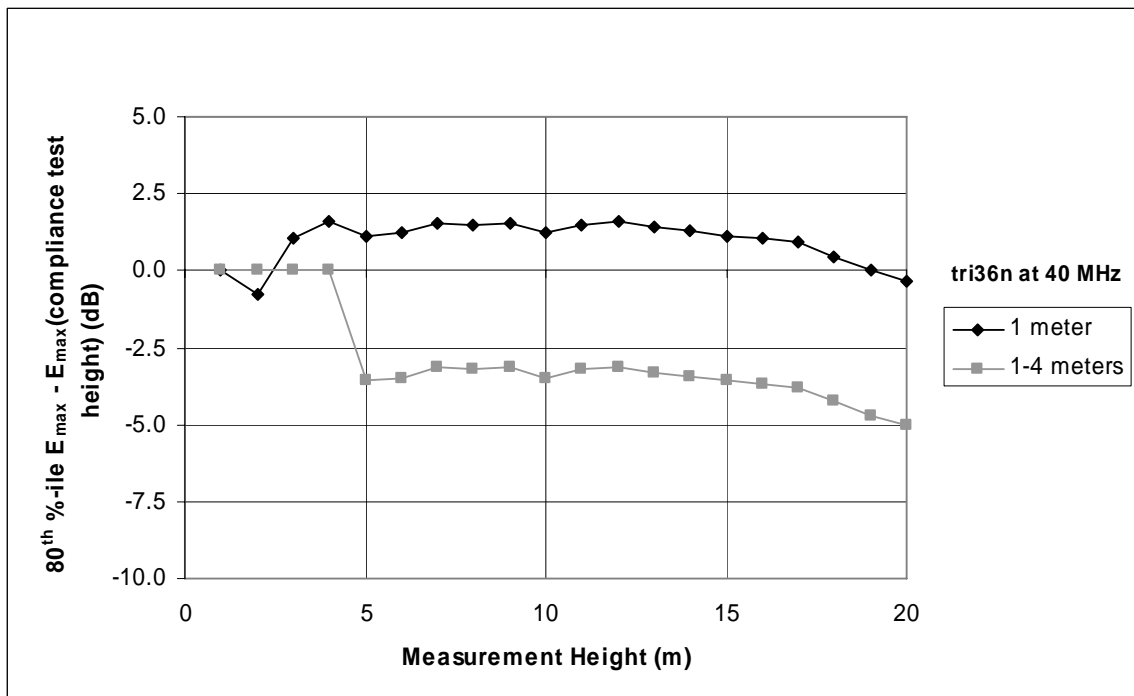


A-126: Comparison of electric field strength as a function of measurement height, if compliance measurements were performed at heights of 1 meter, or at 1 to 4 meters

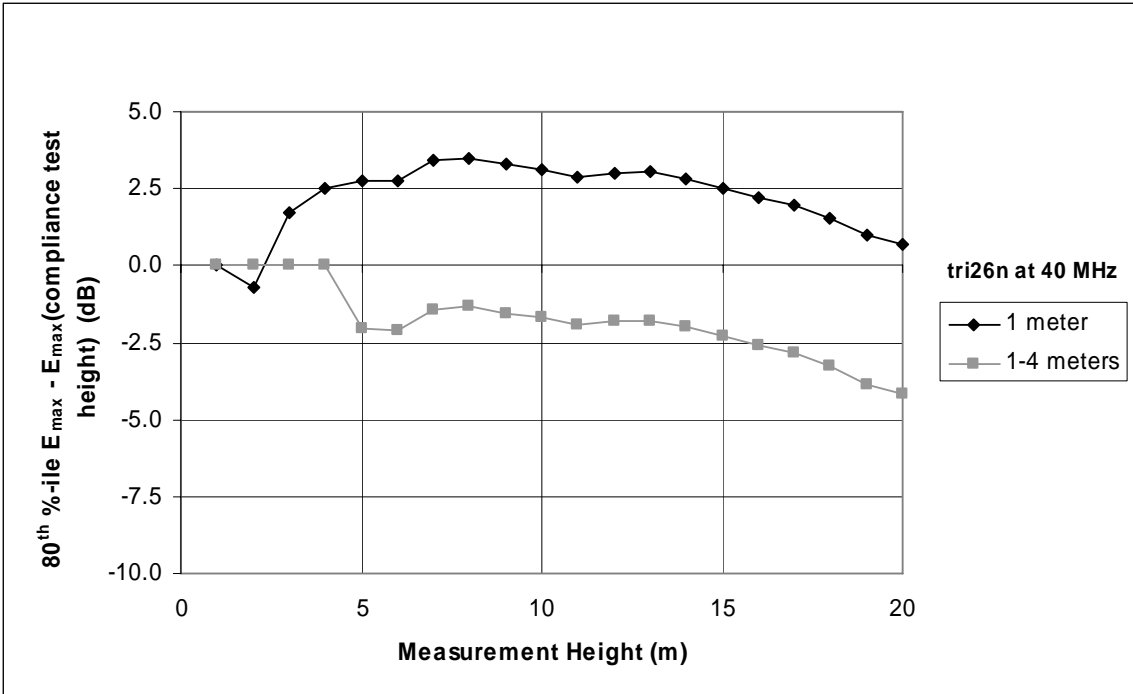
40 MHz Plots



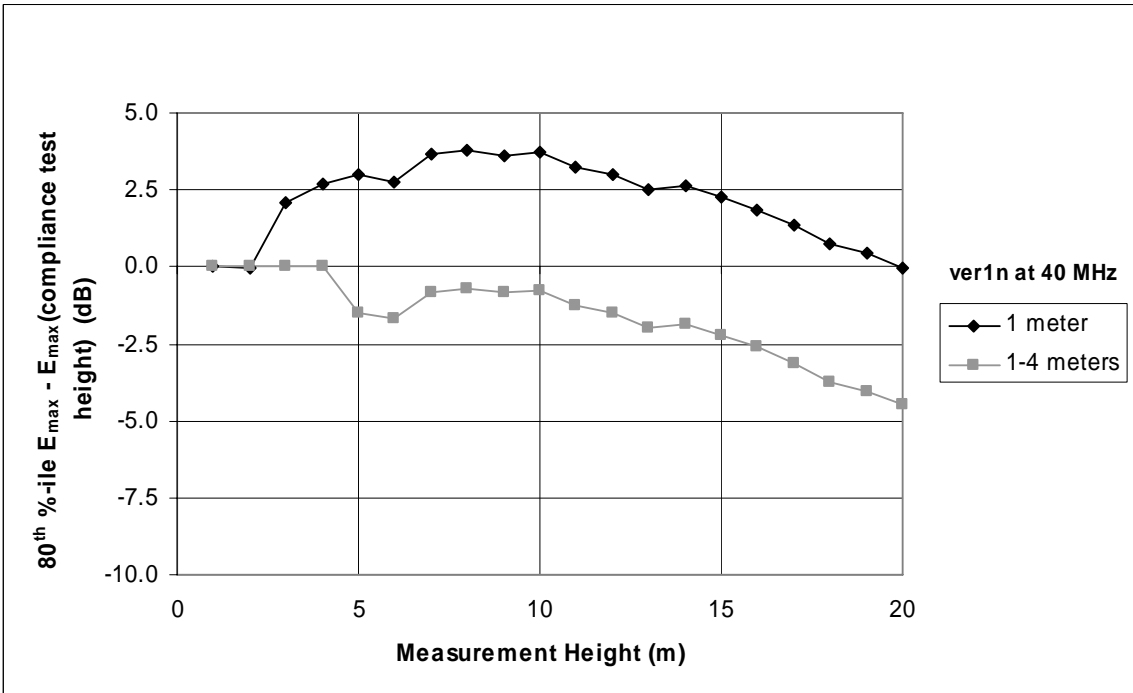
A-127: Comparison of electric field strength as a function of measurement height, if compliance measurements were performed at heights of 1 meter, or at 1 to 4 meters



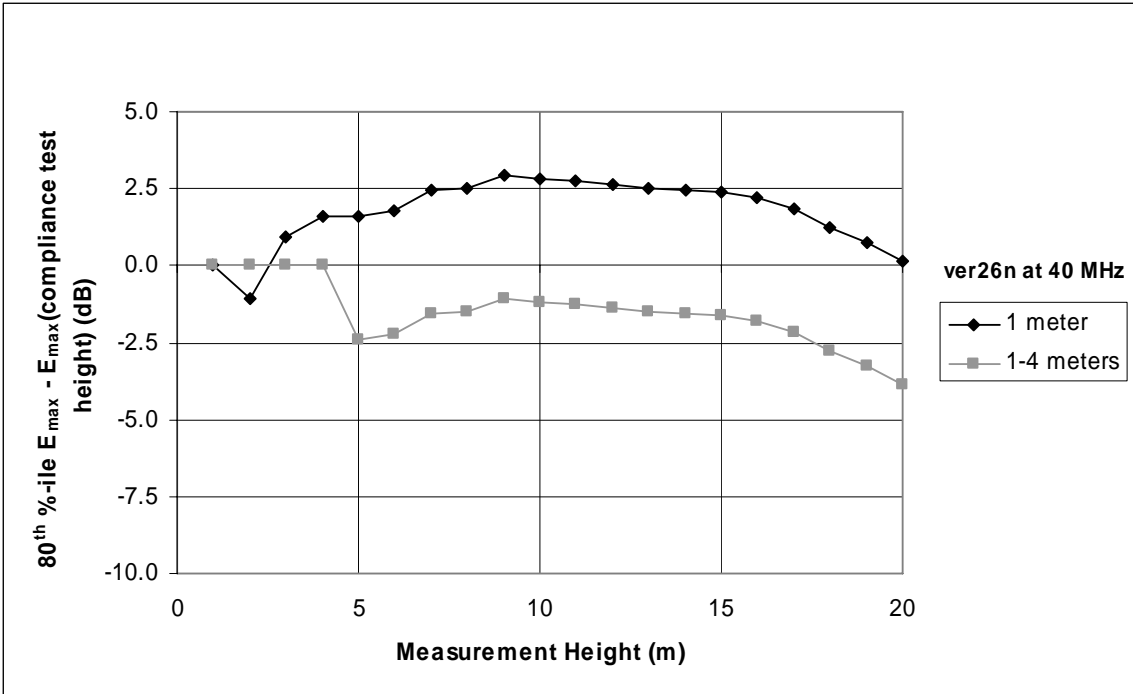
A-128: Comparison of electric field strength as a function of measurement height, if compliance measurements were performed at heights of 1 meter, or at 1 to 4 meters



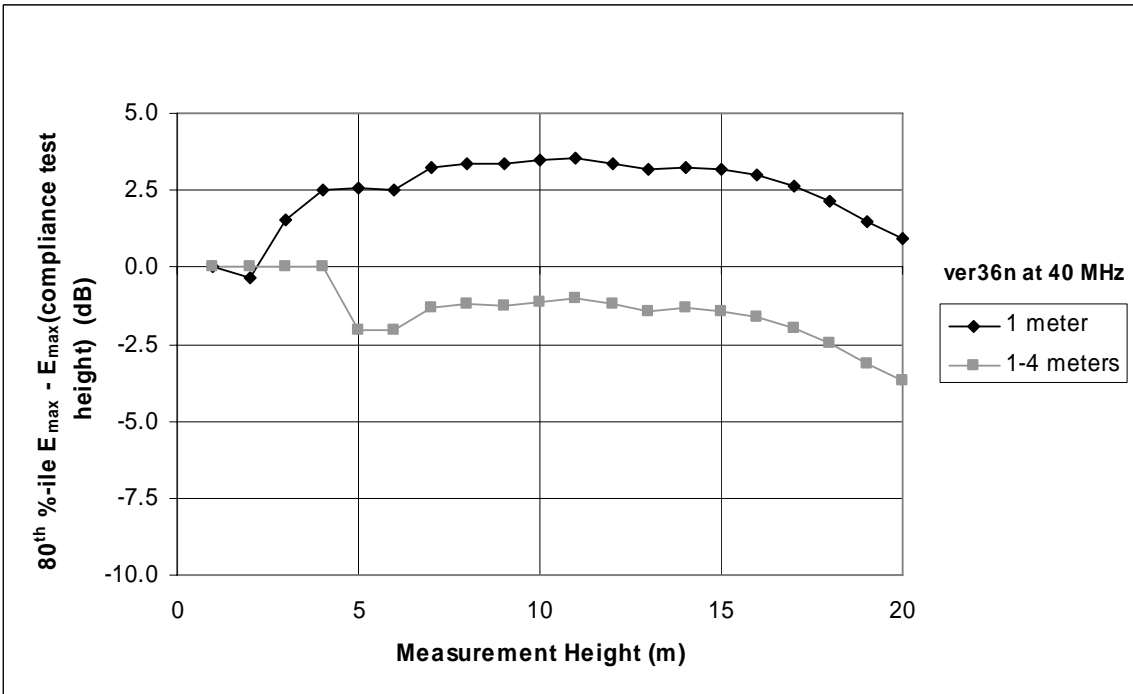
A-129: Comparison of electric field strength as a function of measurement height, if compliance measurements were performed at heights of 1 meter, or at 1 to 4 meters



A-130: Comparison of electric field strength as a function of measurement height, if compliance measurements were performed at heights of 1 meter, or at 1 to 4 meters



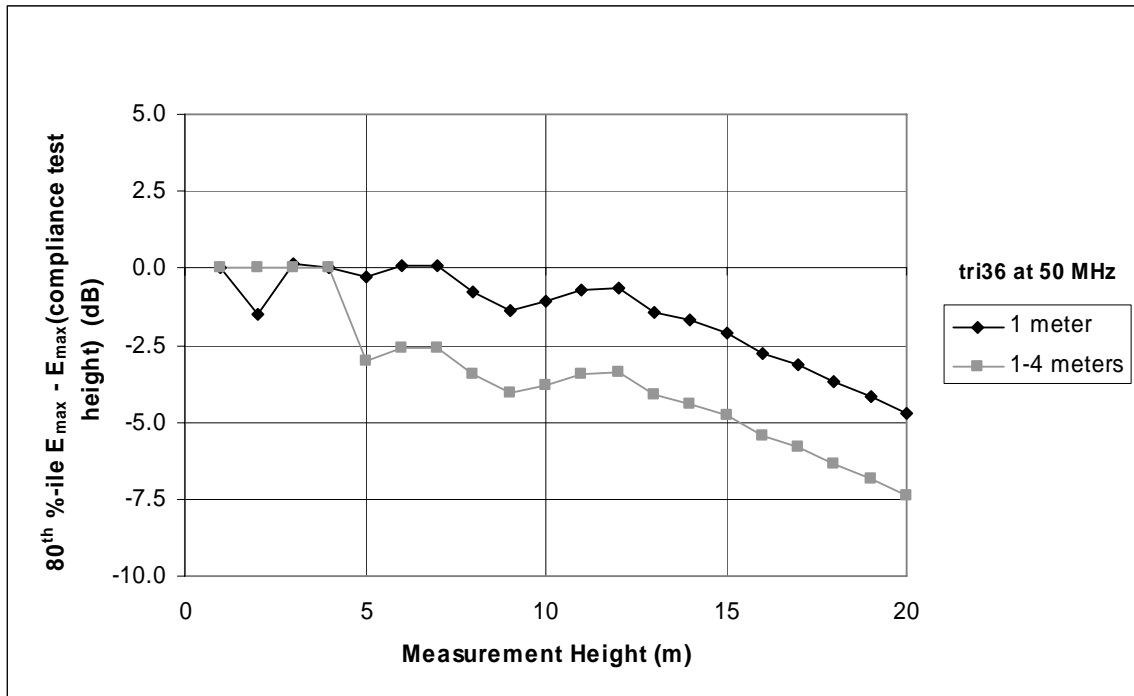
A-131: Comparison of electric field strength as a function of measurement height, if compliance measurements were performed at heights of 1 meter, or at 1 to 4 meters



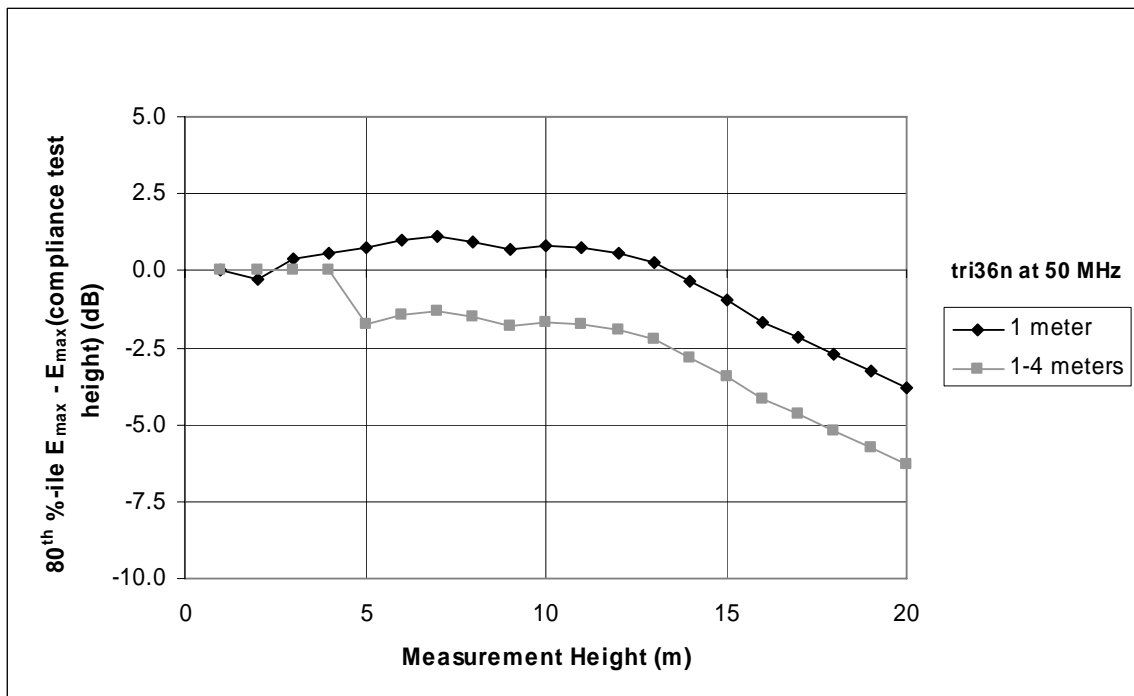
A-132: Comparison of electric field strength as a function of measurement height, if compliance measurements were performed at heights of 1 meter, or at 1 to 4 meters



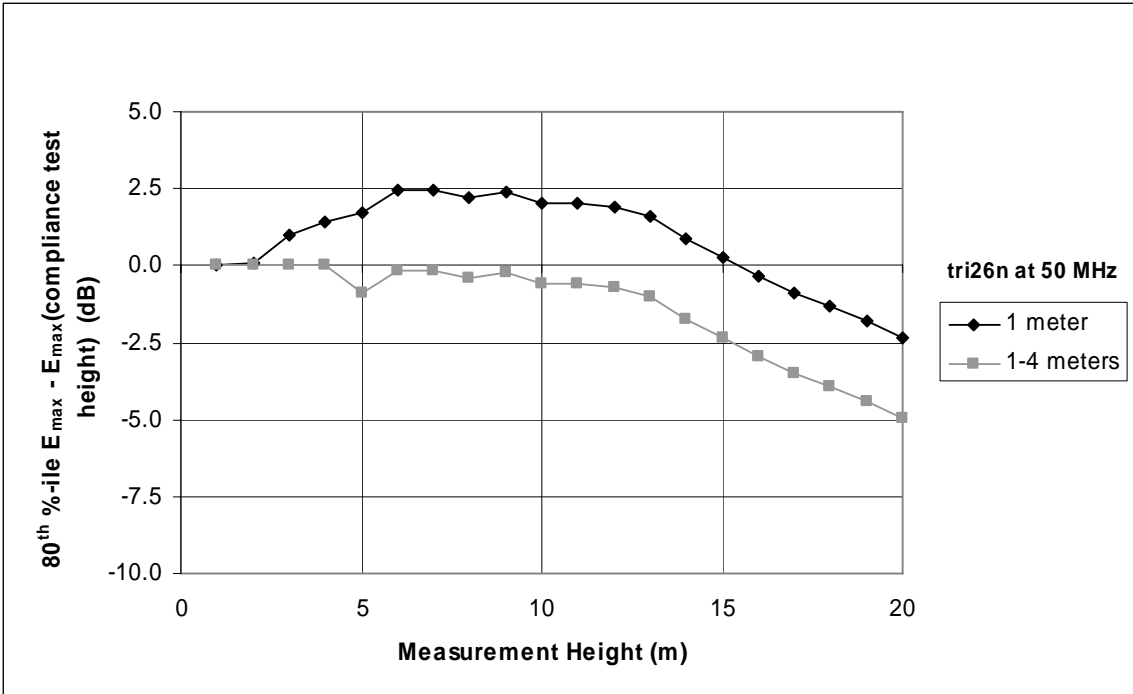
50 MHz Plots



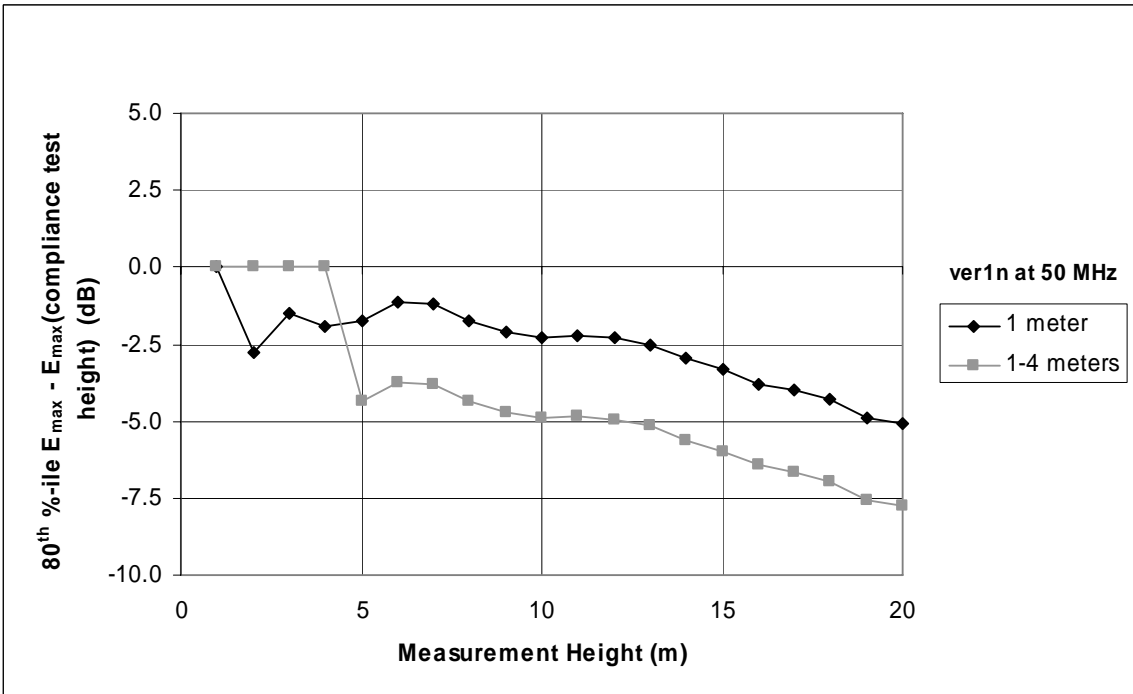
A-133: Comparison of electric field strength as a function of measurement height, if compliance measurements were performed at heights of 1 meter, or at 1 to 4 meters



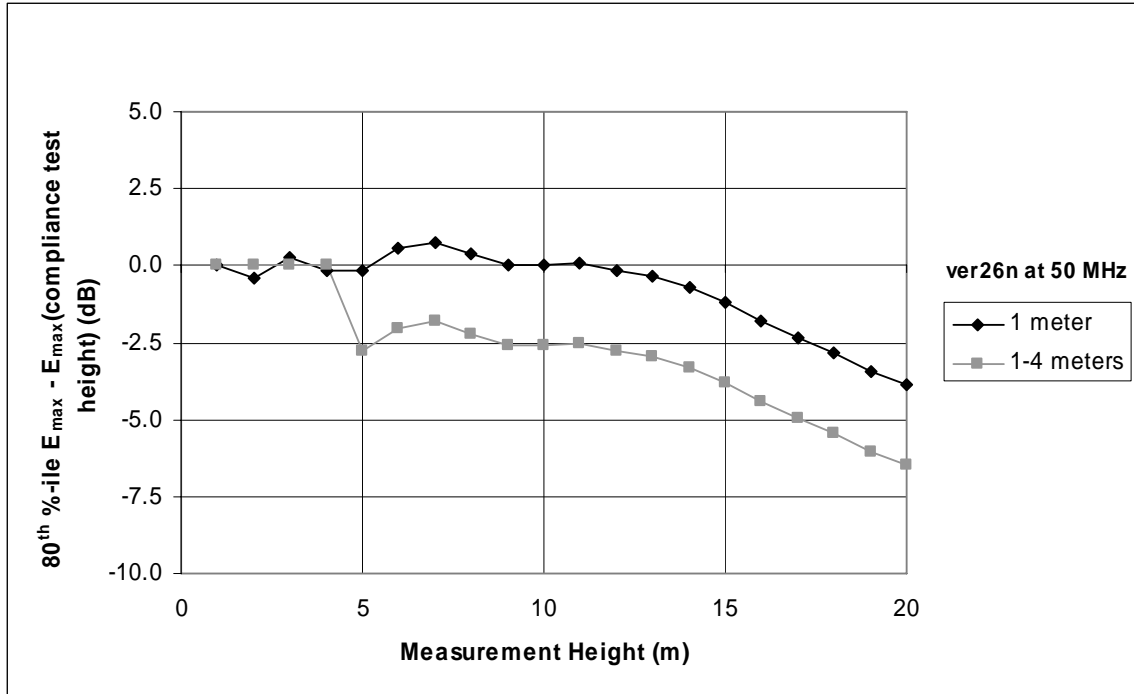
A-134: Comparison of electric field strength as a function of measurement height, if compliance measurements were performed at heights of 1 meter, or at 1 to 4 meters



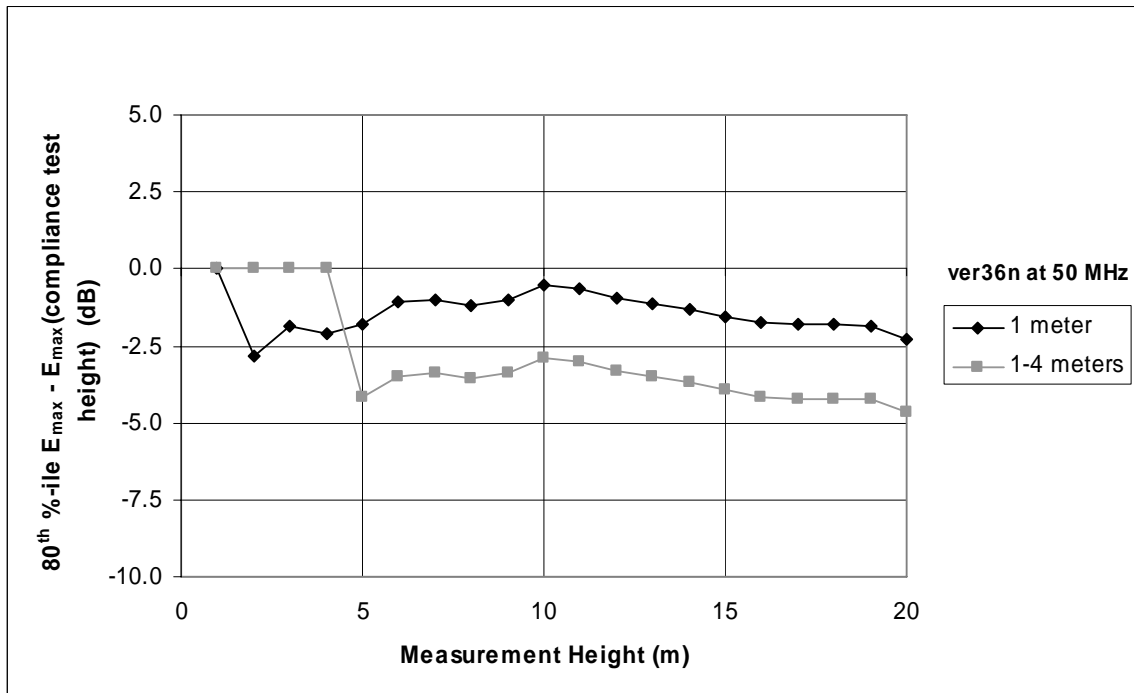
A-135: Comparison of electric field strength as a function of measurement height, if compliance measurements were performed at heights of 1 meter, or at 1 to 4 meters



A-136: Comparison of electric field strength as a function of measurement height, if compliance measurements were performed at heights of 1 meter, or at 1 to 4 meters



A-137: Comparison of electric field strength as a function of measurement height, if compliance measurements were performed at heights of 1 meter, or at 1 to 4 meters



A-138: Comparison of electric field strength as a function of measurement height, if compliance measurements were performed at heights of 1 meter, or at 1 to 4 meters



## **APPENDIX B MEASUREMENT DISTANCE ALONG THE POWER LINE**

### **B.1 INTRODUCTION**

As noted in the NTIA Phase 1 Study, compliance measurement testing commissioned by BPL equipment vendors and service providers has generally focused on radiated emissions measured on radials from the BPL device under test. However, FCC rules state that Part 15 devices and all attached wiring should be considered when measuring radiated emissions.<sup>2</sup> The Commission's BPL measurement guidelines specify the locations along the power line away from a BPL device where field strength measurements are to be taken.<sup>3</sup> This Appendix provides NTIA's results from evaluating the field strength along the length of the power line and comparing this to the field strength levels at the prescribed measurement locations.

### **B.2 SIMULATION RESULTS**

Figures B-1 through B-84 show the electric field strength level along the power line for a variety of simulated power line configurations, and over the frequency range of 2 to 28 MHz. Each figure includes the Part 15 radiated emissions limit extrapolated to a measurement distance of 10 meters assuming the power line height is 12 meters.<sup>4</sup> In addition, these figures show the measurement points specified in the measurement guidelines. The peak value of these points was used to scale the signal source level so that the power line model satisfies the Part 15 limit, as extrapolate to the 10 meter measurement distance. Electric field strength values were determined from NEC magnetic field strength simulations of the power line models using the methodology described in Section 2.2.

---

<sup>2</sup> See 47 C.F.R. §15.31(g)-(k).

<sup>3</sup> See BPL Report and Order, at Appendix C ¶ 2.b.2 (“Testing shall be performed at distances of 0, ¼, ½, ¾, and 1 wavelength down the line from the BPL injection point on the power line. Wavelength spacing is based on the mid-band frequency...”).

<sup>4</sup> *Id.* ¶ 2.b.4 (describing the slant range distance extrapolation methodology).

2 MHz Plots

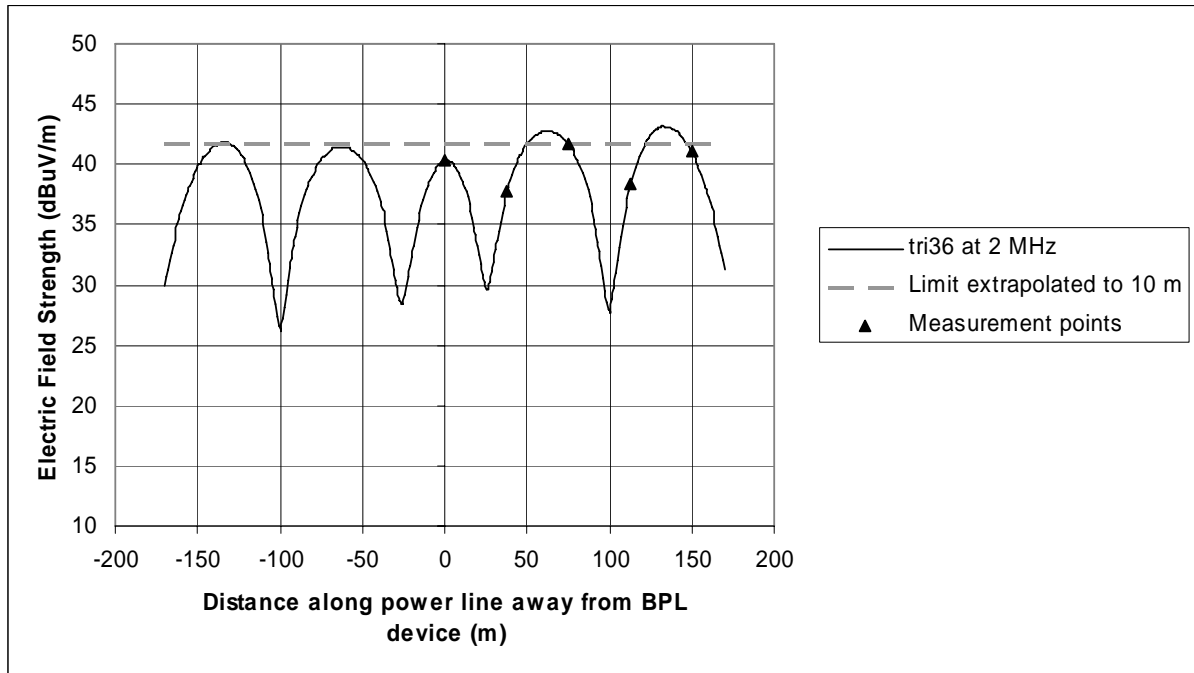


**Figure B-1: Vertical electric field strength along power line for tri36 topology**

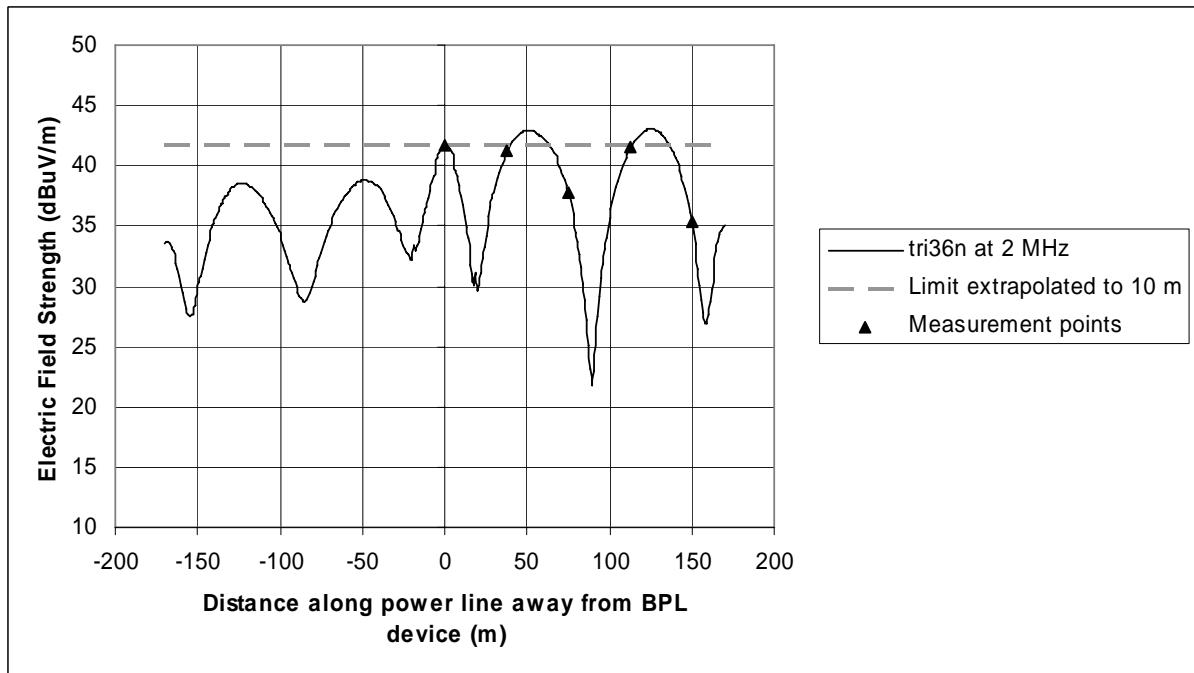


**Figure B-2: Vertical electric field strength along power line for tri36n topology**

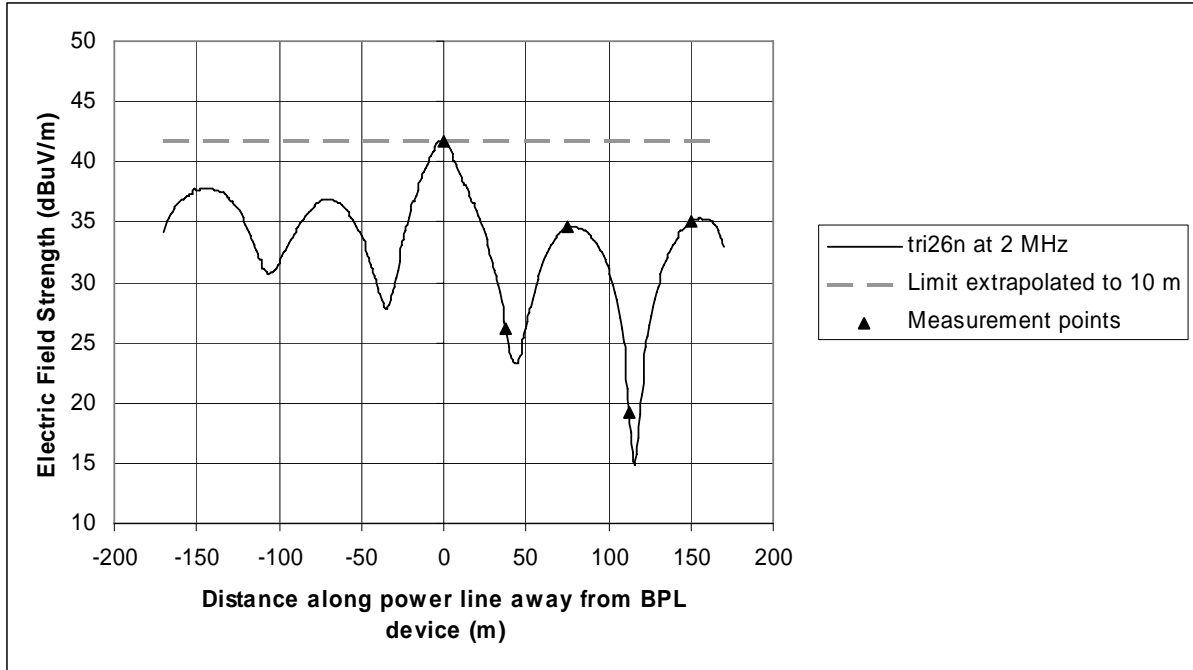


Figure B-3: Vertical electric field strength along power line for tri26n topology

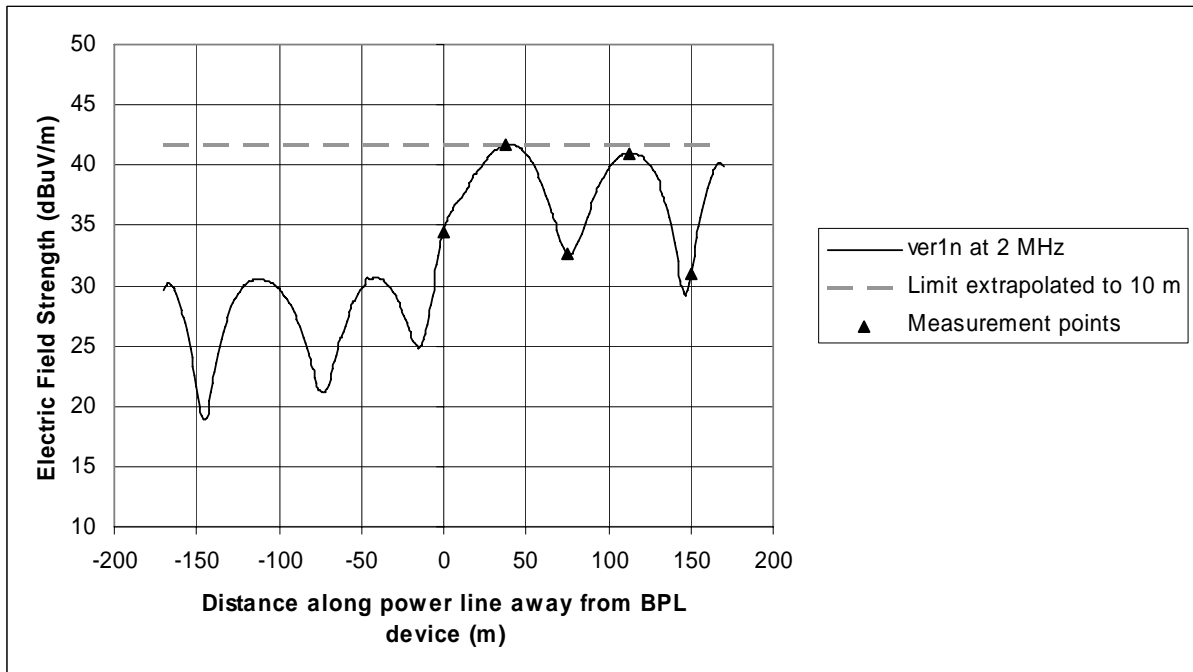
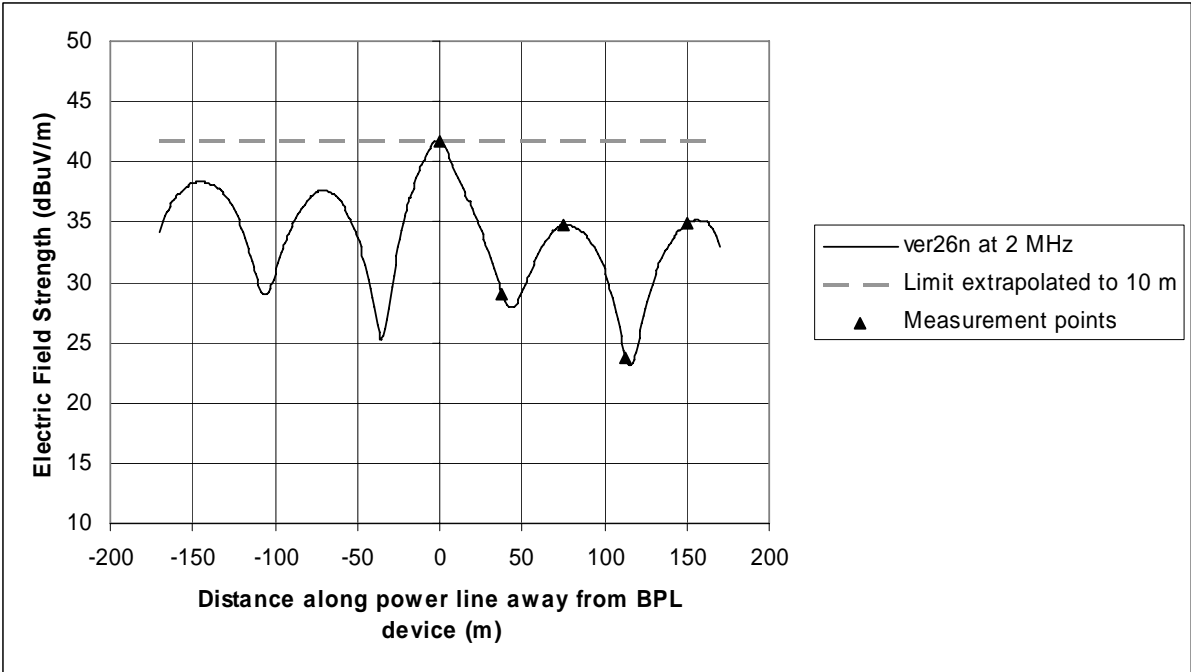
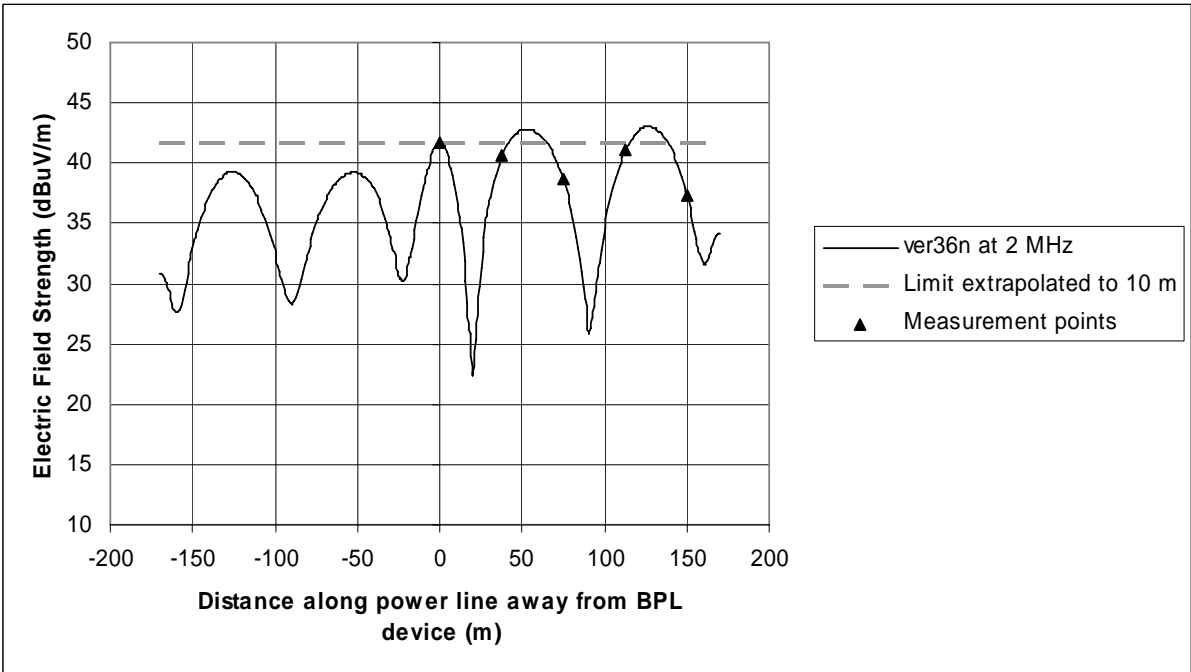


Figure B-4: Vertical electric field strength along power line for ver1n topology



**Figure B-5: Vertical electric field strength along power line for ver26n topology**



**Figure B-6: Vertical electric field strength along power line for ver36n topology**



4 MHz Plots

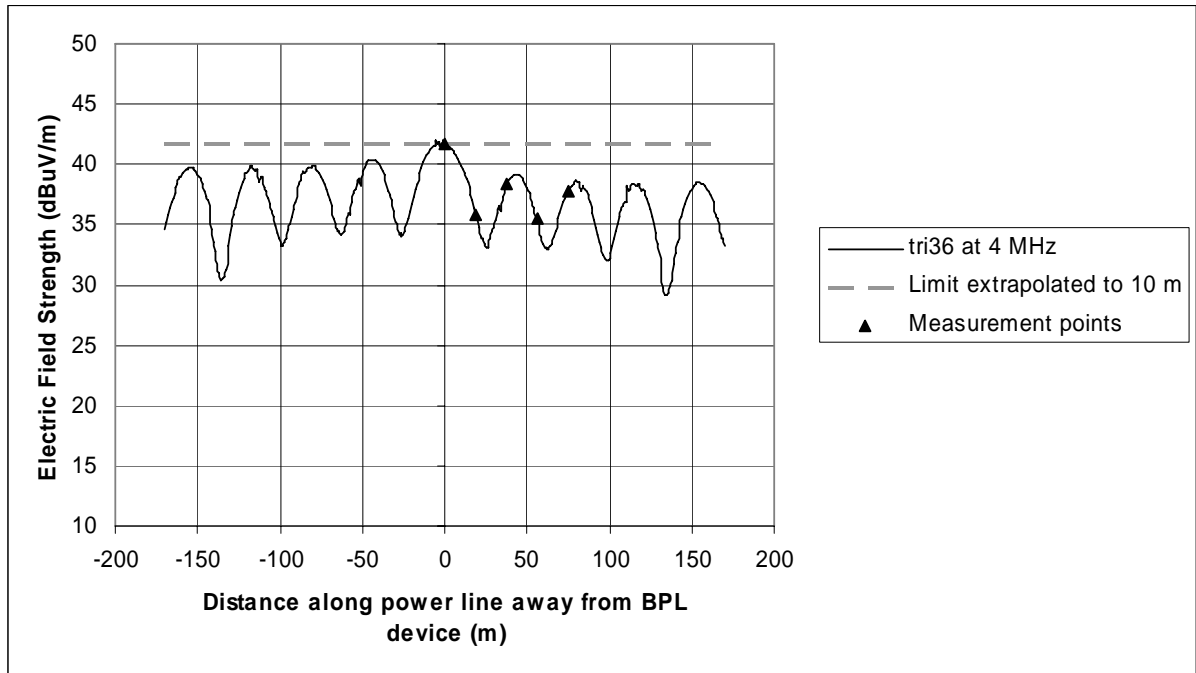


**Figure B-7: Vertical electric field strength along power line for tri36 topology**

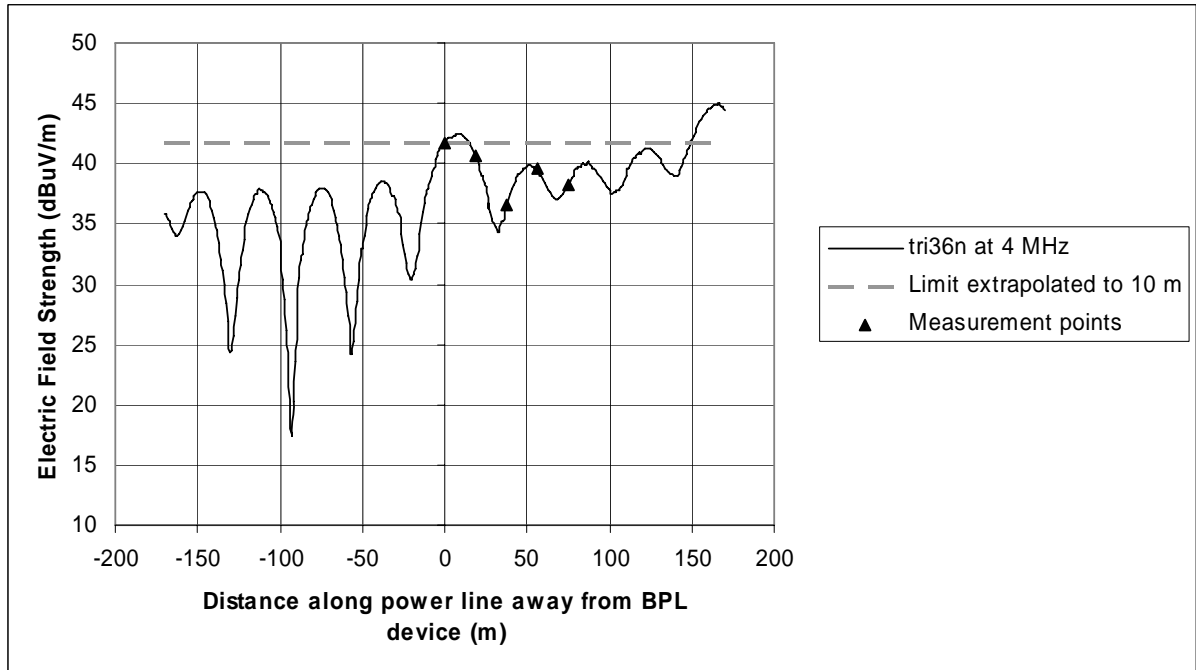


**Figure B-8: Vertical electric field strength along power line for tri36n topology**

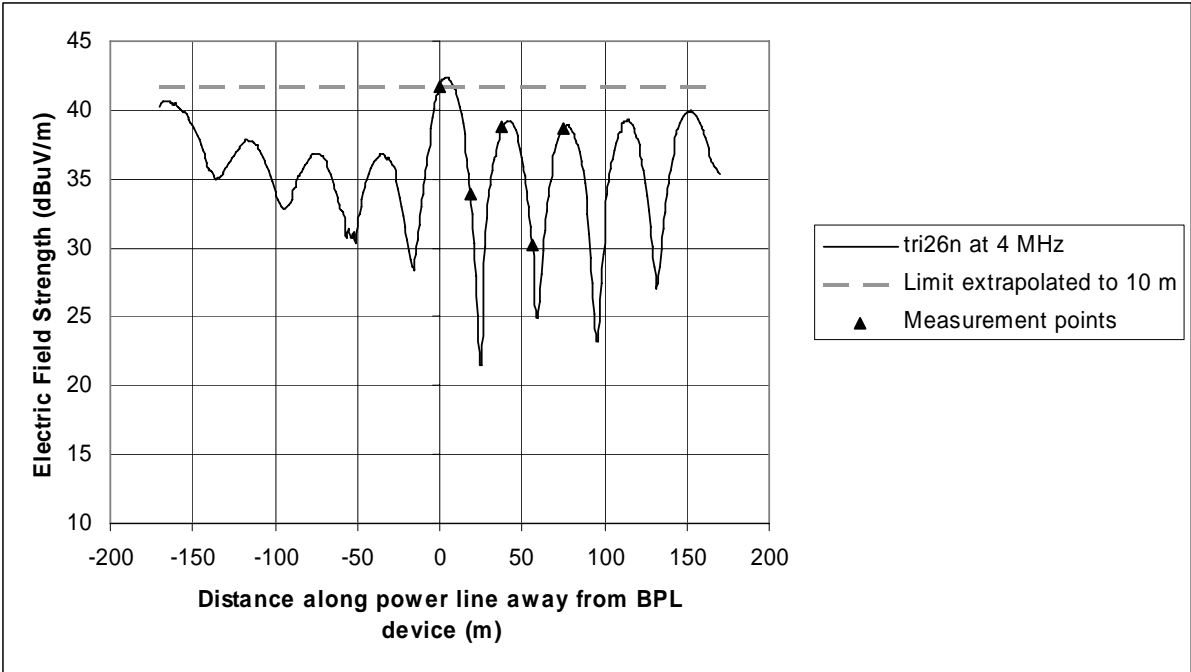


Figure B-9: Vertical electric field strength along power line for tri26n topology

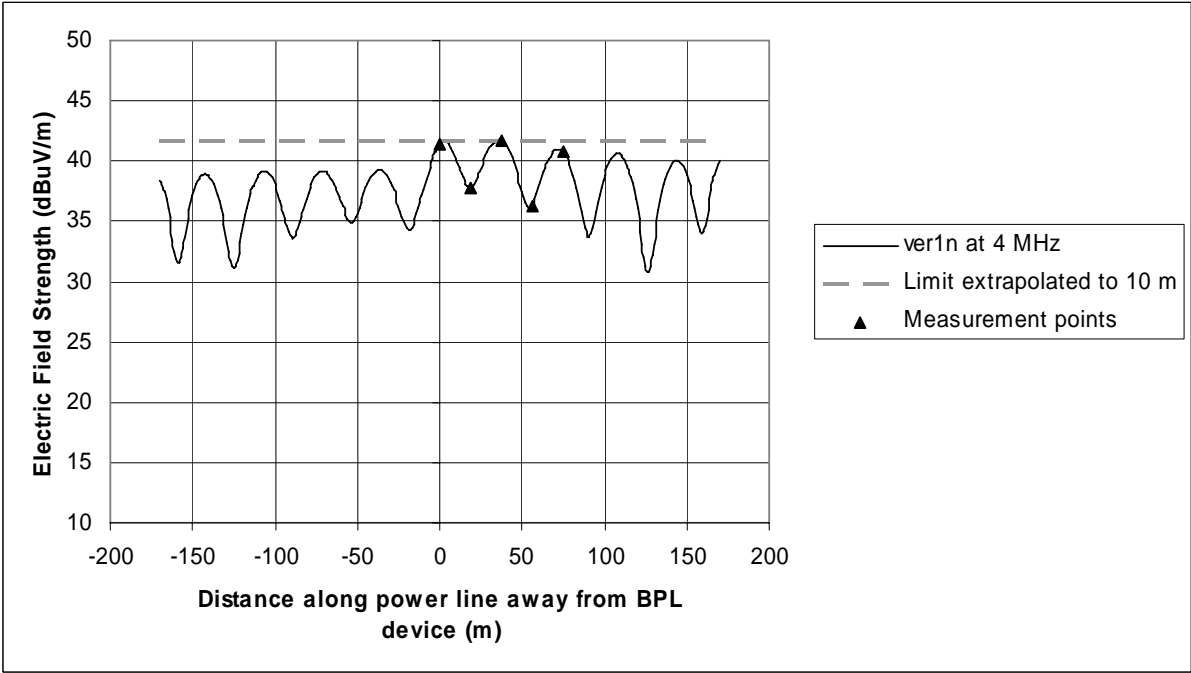
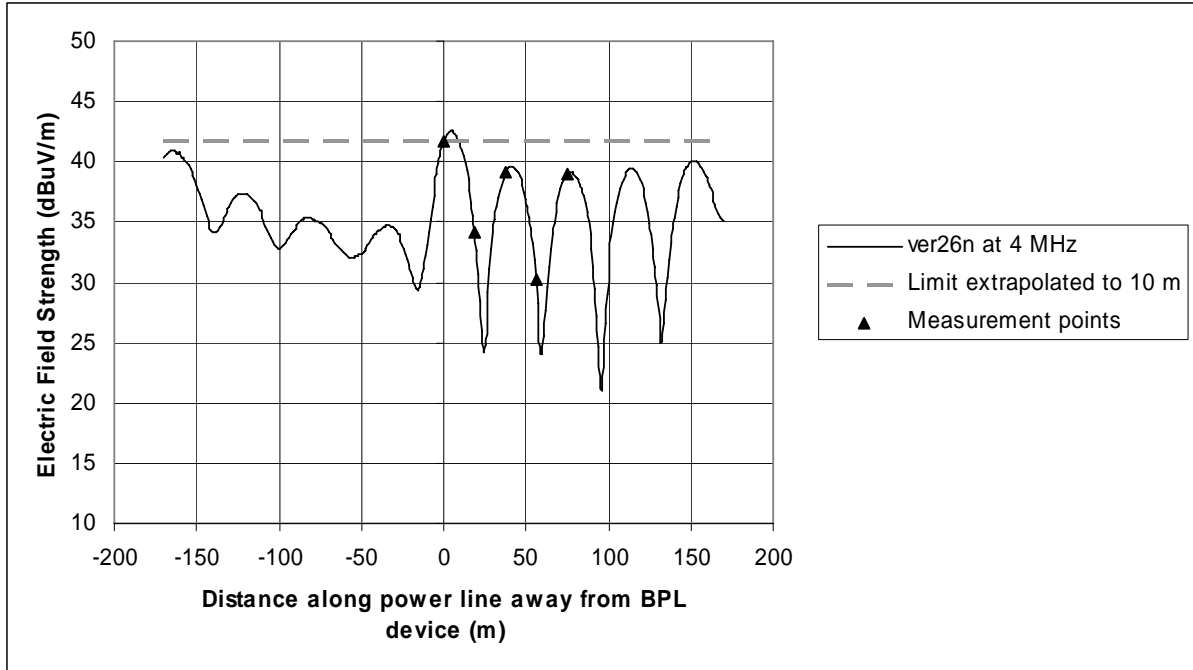
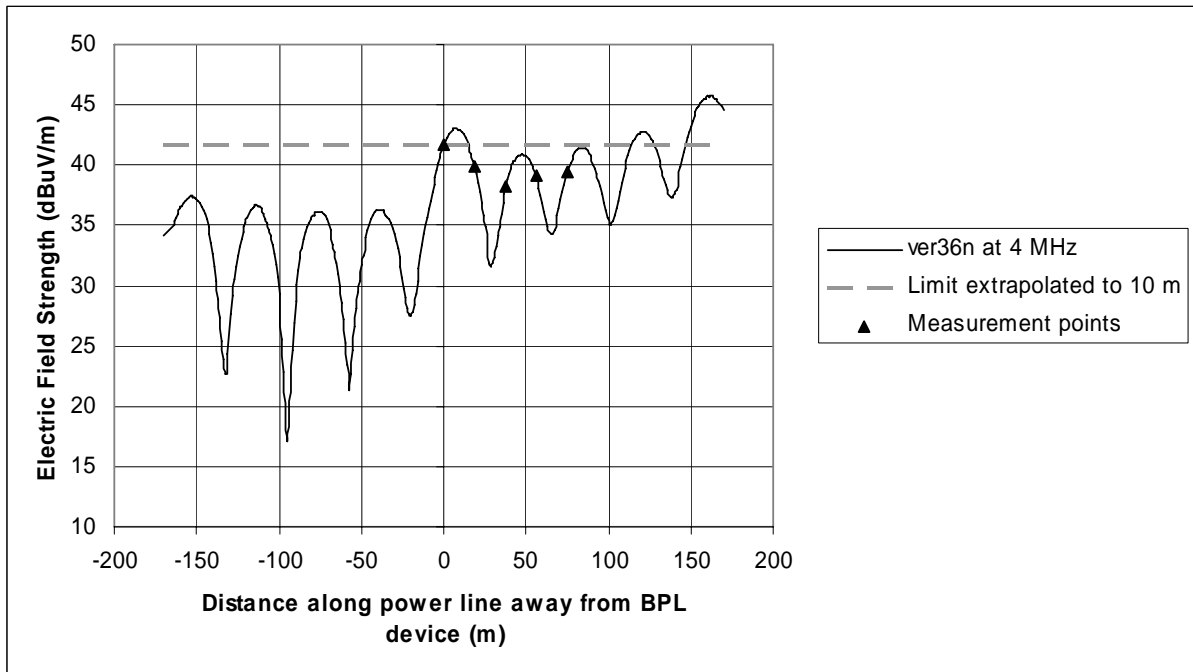


Figure B-10: Vertical electric field strength along power line for ver1n topology



**Figure B-11: Vertical electric field strength along power line for ver26n topology**



**Figure B-12: Vertical electric field strength along power line for ver36n topology**

6 MHz Plots

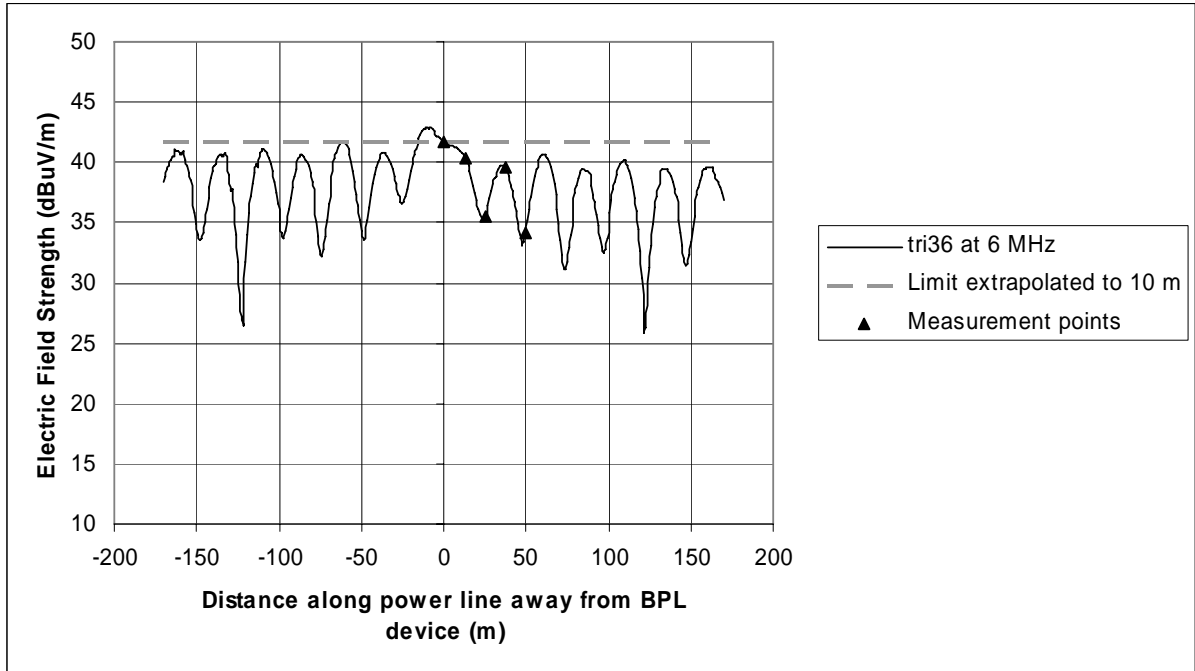


**Figure B-13: Vertical electric field strength along power line for tri36 topology**

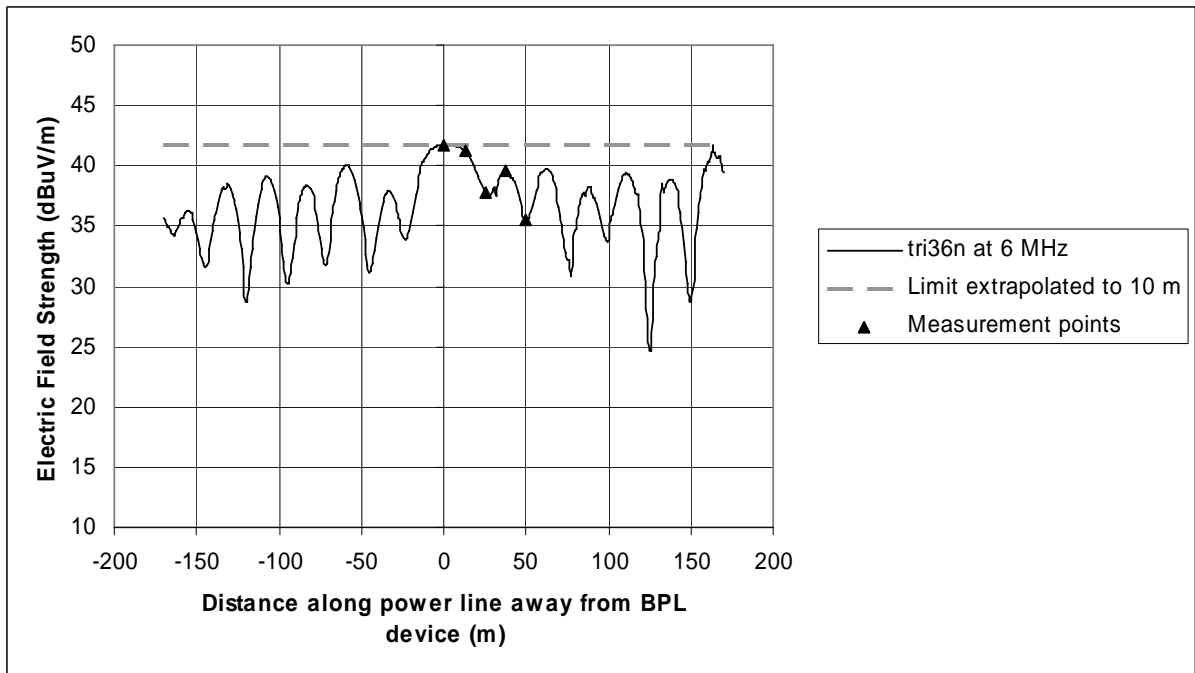


**Figure B-14: Vertical electric field strength along power line for tri36n topology**

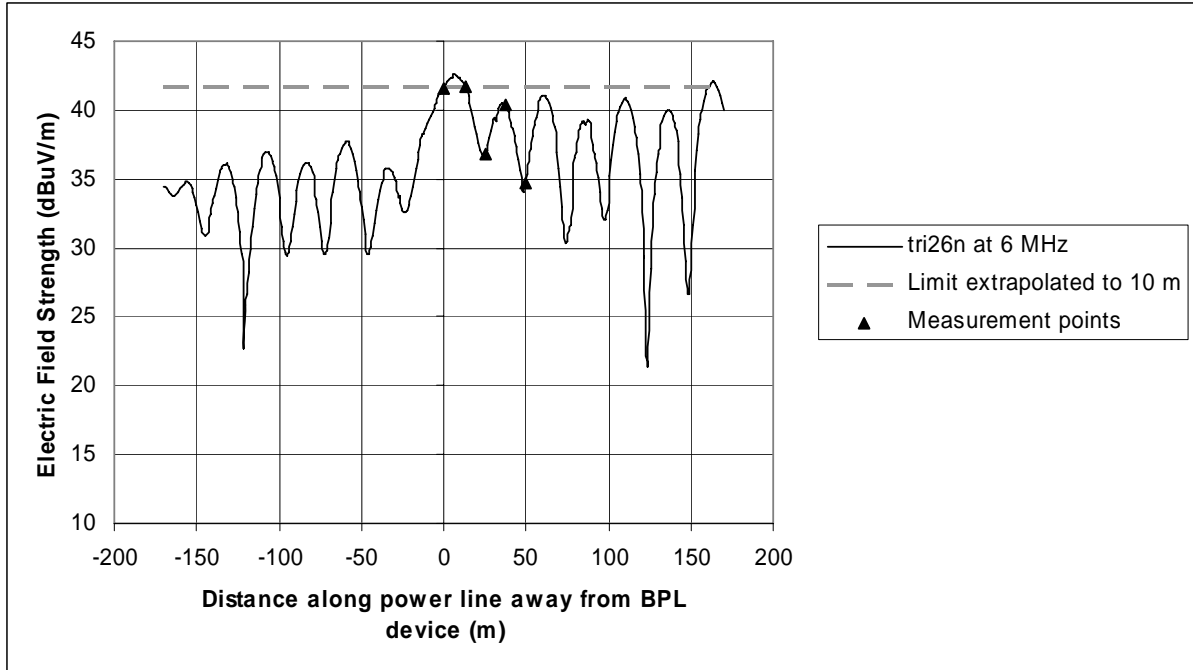


**Figure B-15: Vertical electric field strength along power line for tri26n topology**

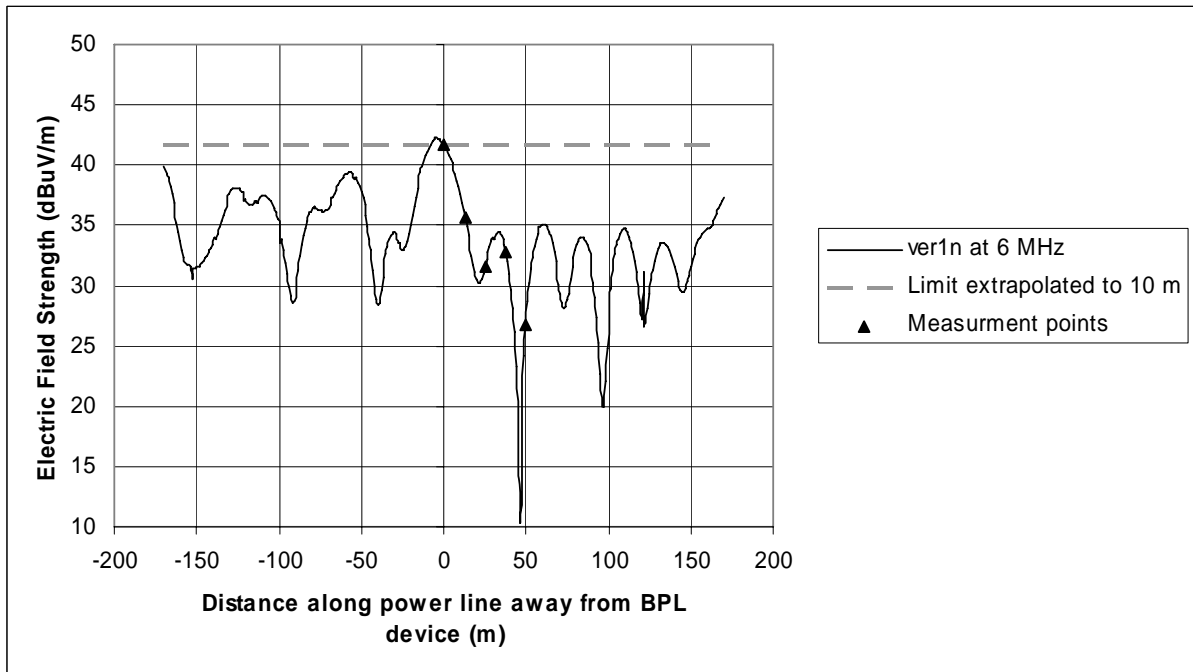


**Figure B-16: Vertical electric field strength along power line for ver1n topology**

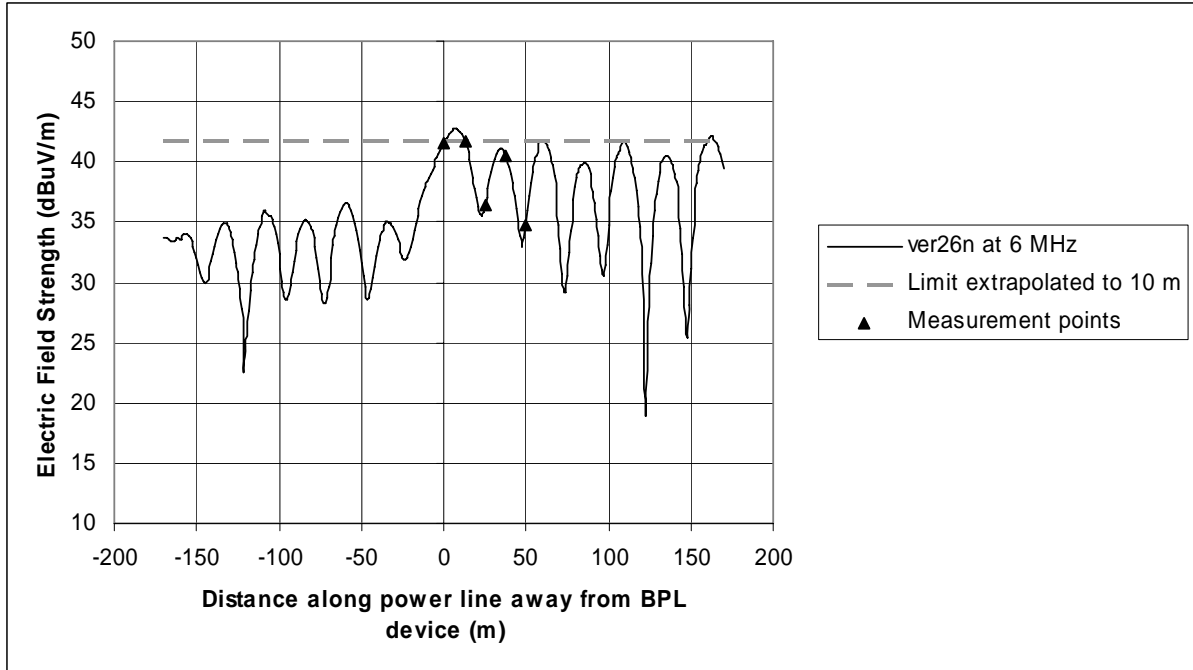


**Figure B-17: Vertical electric field strength along power line for ver26n topology**

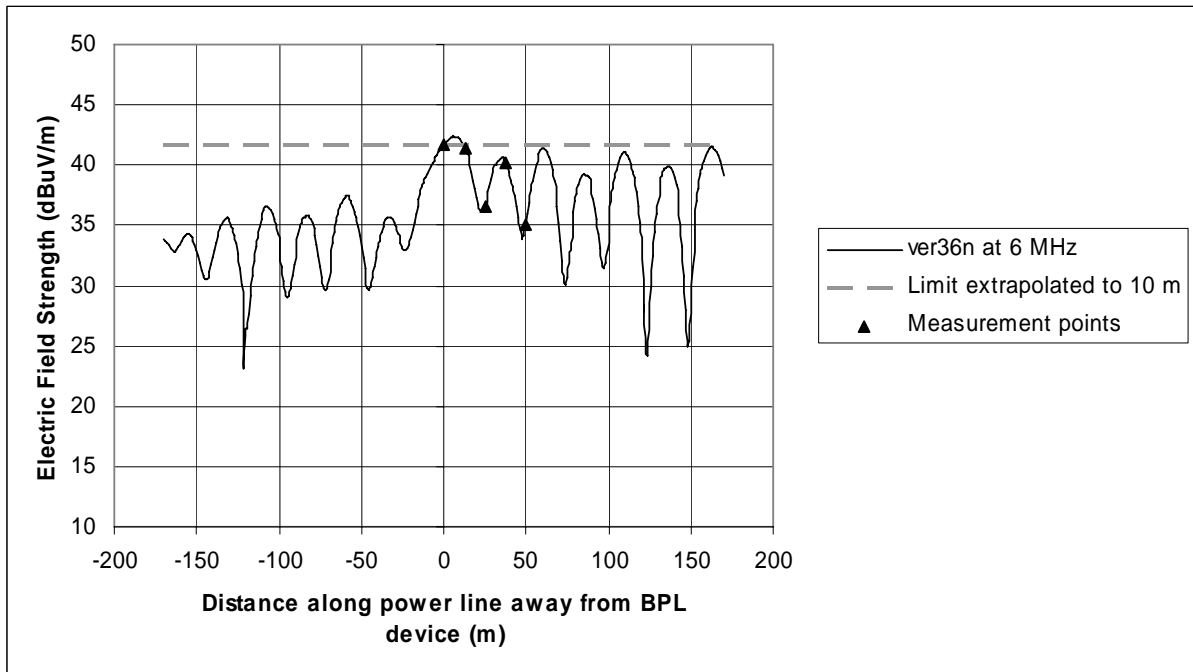


**Figure B-18: Vertical electric field strength along power line for ver36n topology**

8 MHz Plots

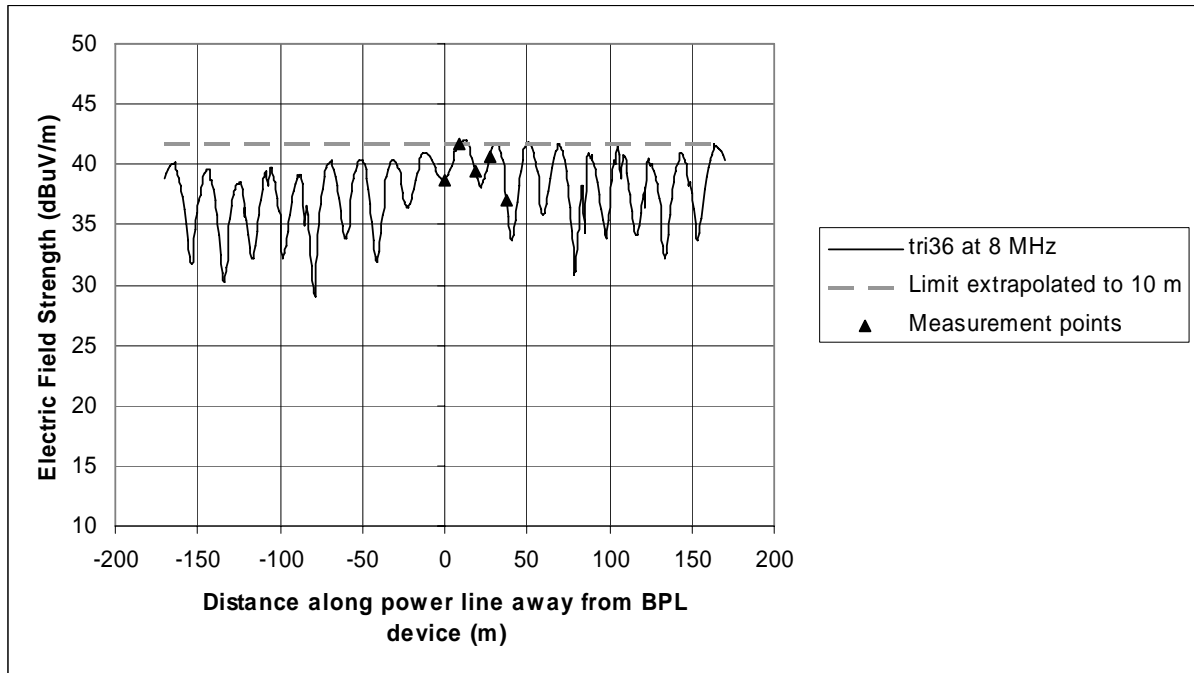


**Figure B-19: Vertical electric field strength along power line for tri36 topology**

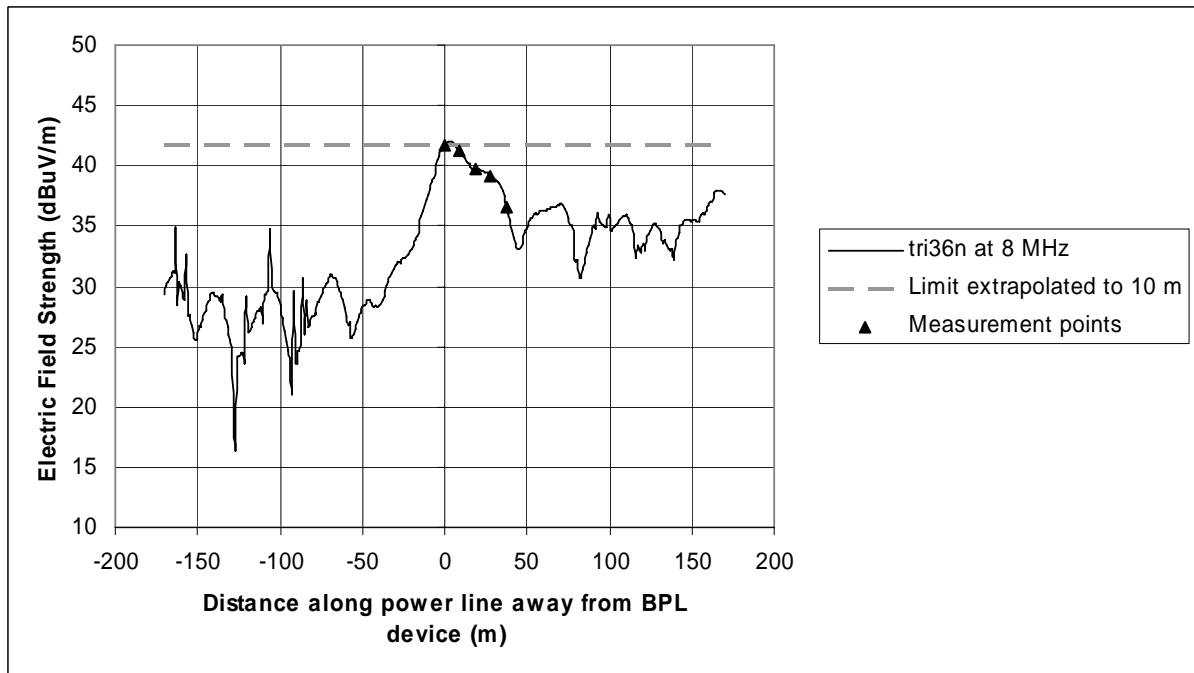


**Figure B-20: Vertical electric field strength along power line for tri36n topology**

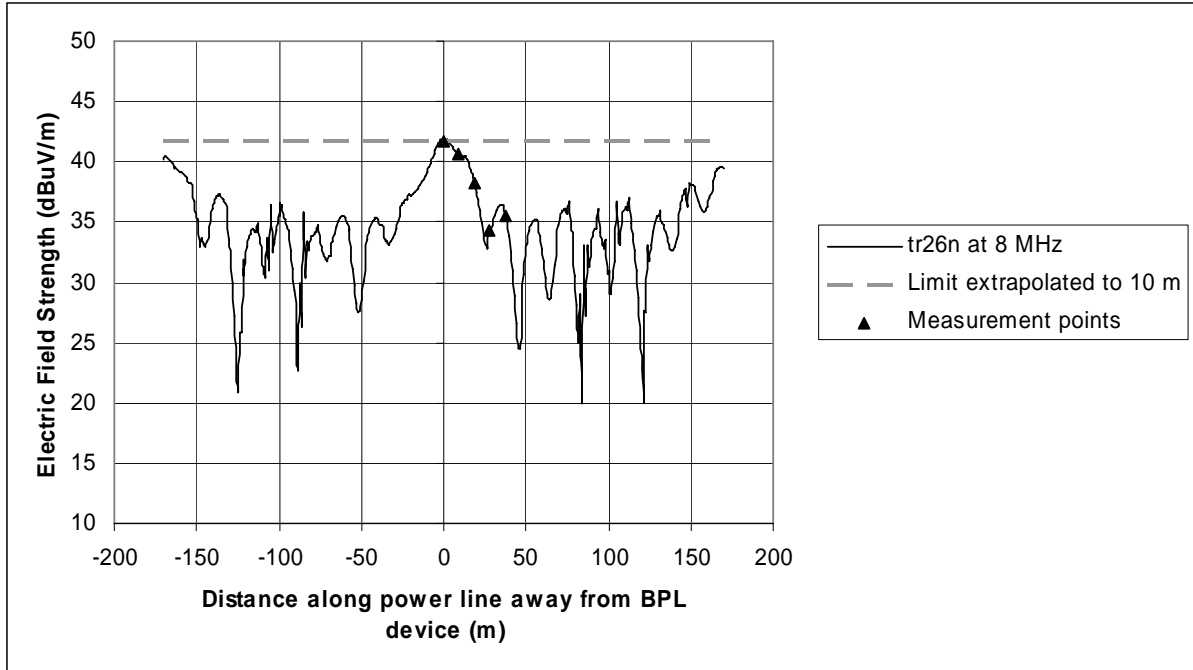


**Figure B-21: Vertical electric field strength along power line for tri26n topology**

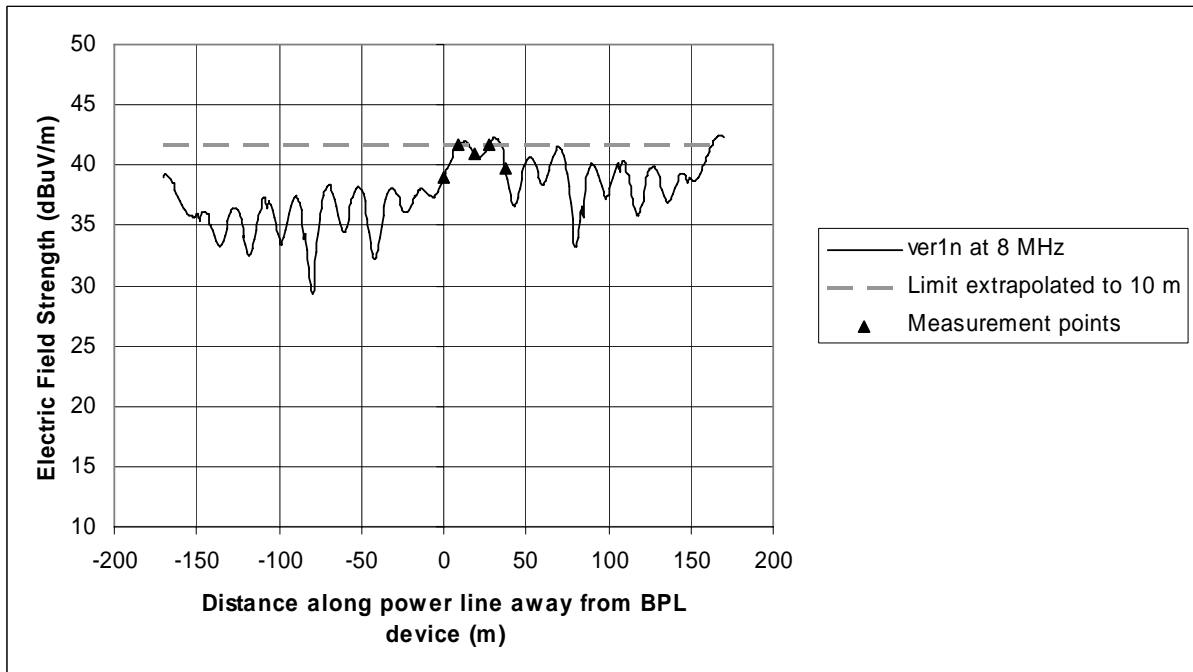


**Figure B-22: Vertical electric field strength along power line for ver1n topology**



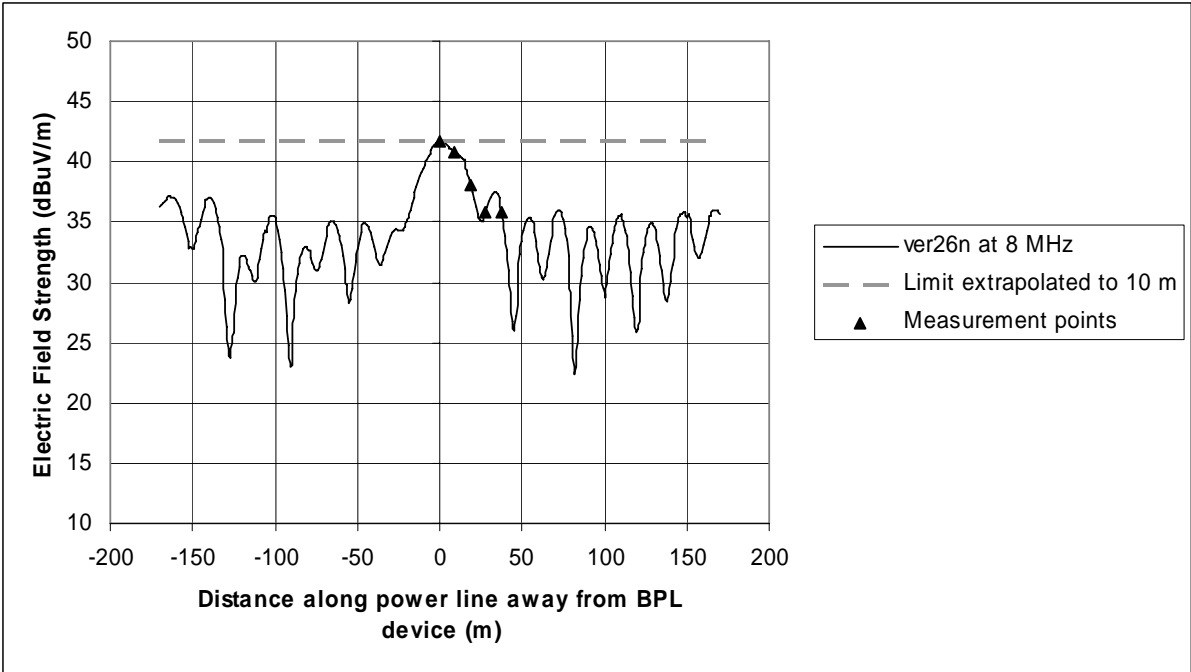


Figure B-23: Vertical electric field strength along power line for ver26n topology

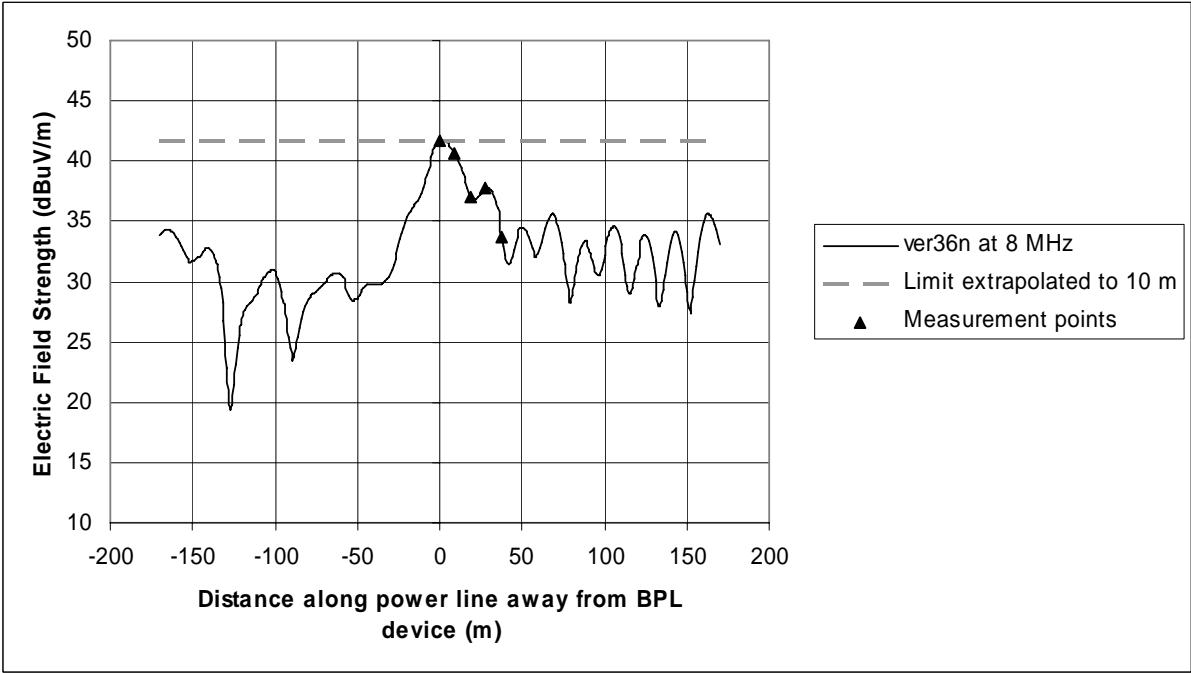
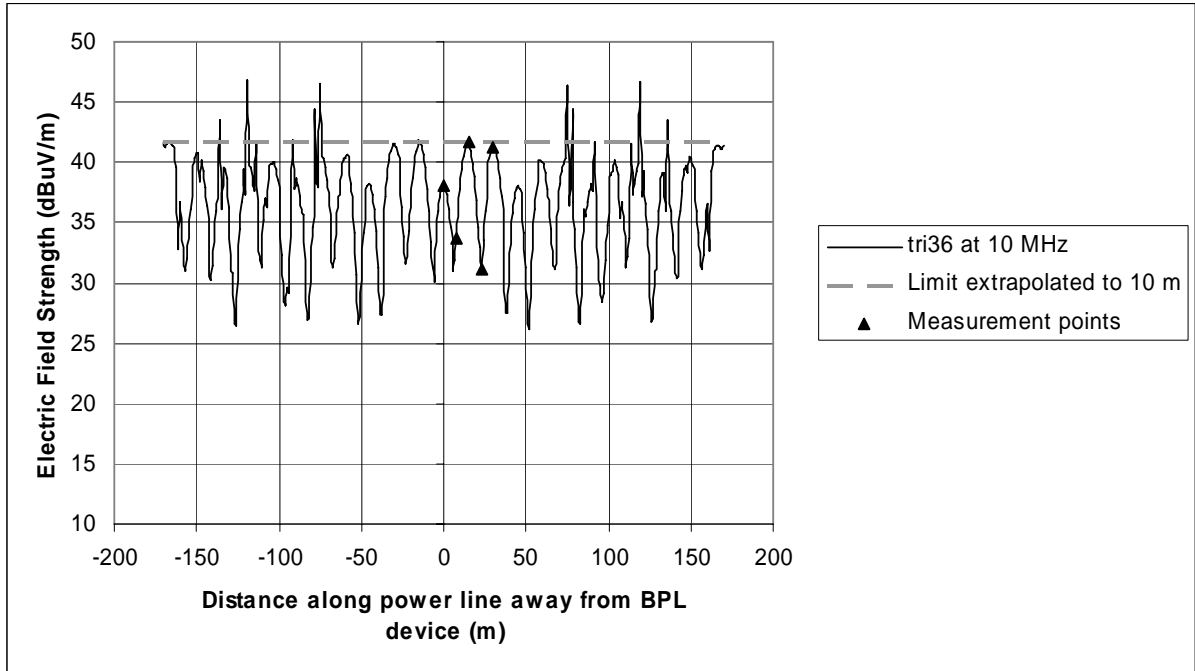
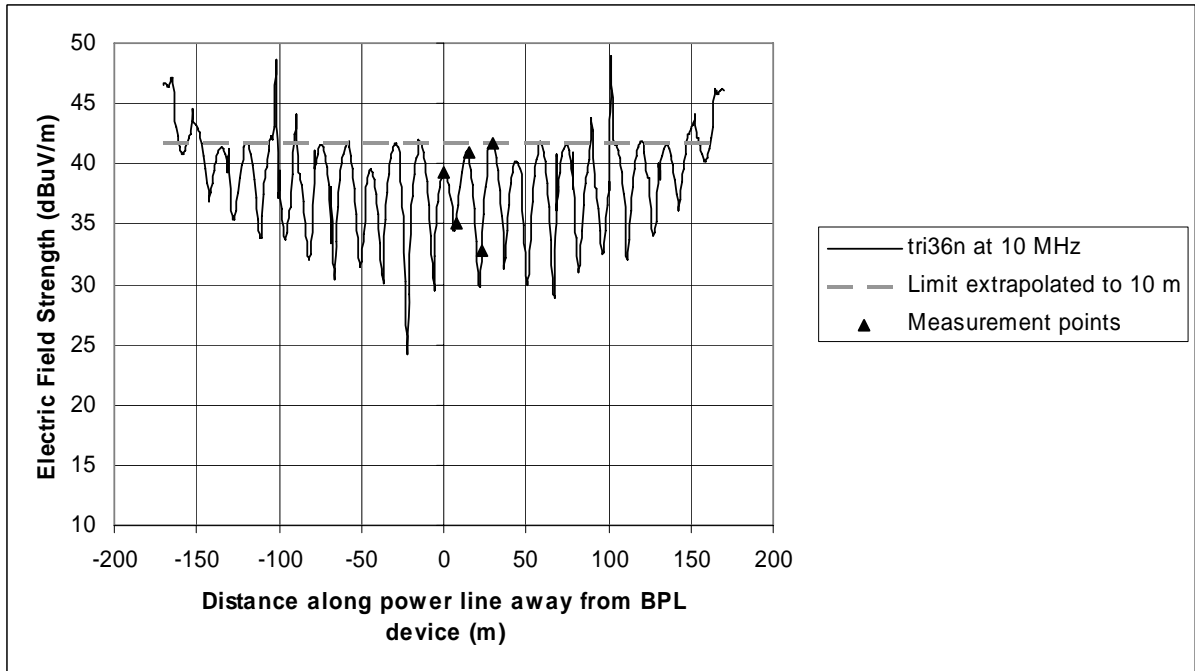


Figure B-24: Vertical electric field strength along power line for ver36n topology

10 MHz Plots



**Figure B-25: Vertical electric field strength along power line for tri36 topology**



**Figure B-26: Vertical electric field strength along power line for tri36n topology**

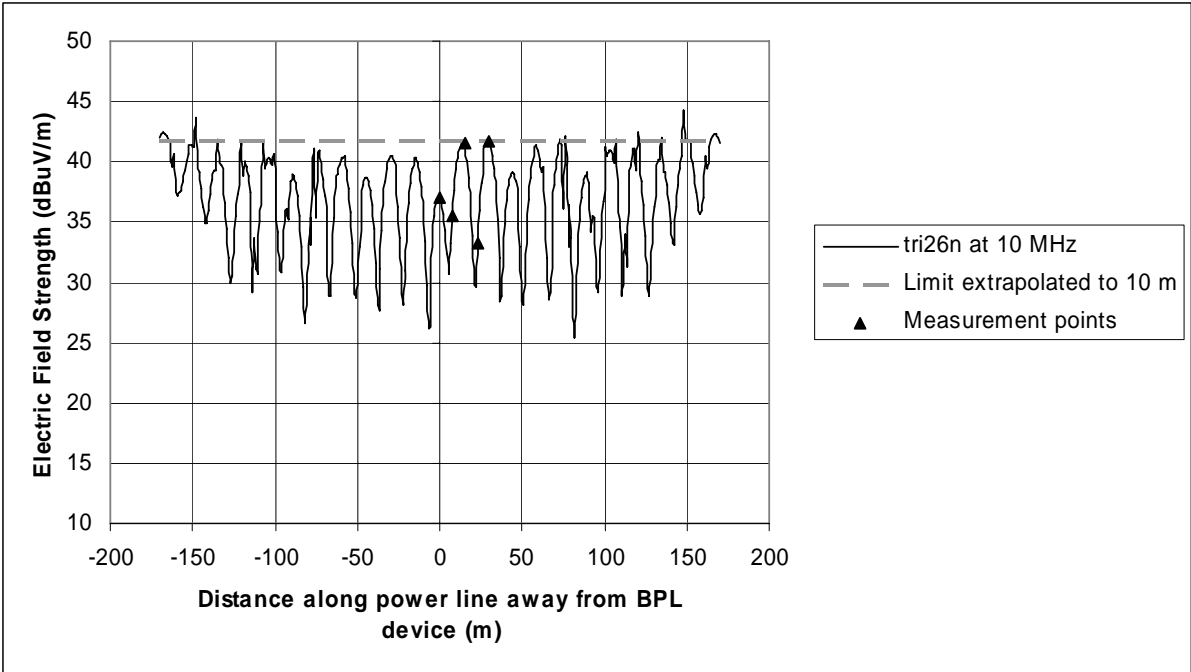


**Figure B-27: Vertical electric field strength along power line for tri26n topology**

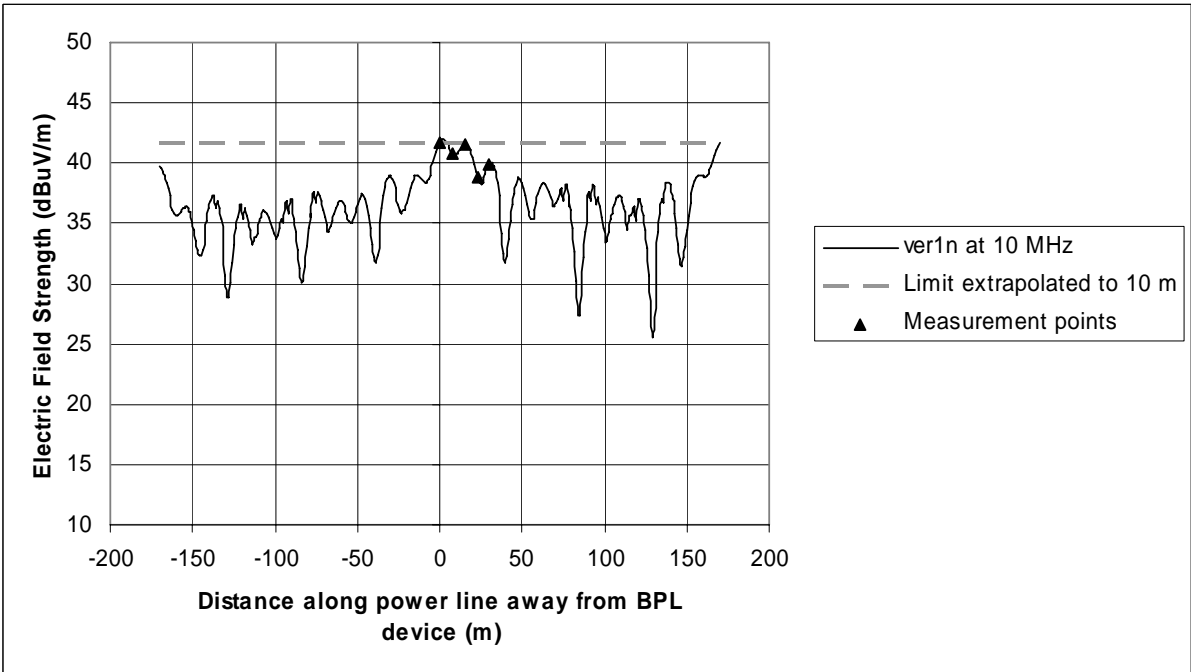


**Figure B-28: Vertical electric field strength along power line for ver1n topology**

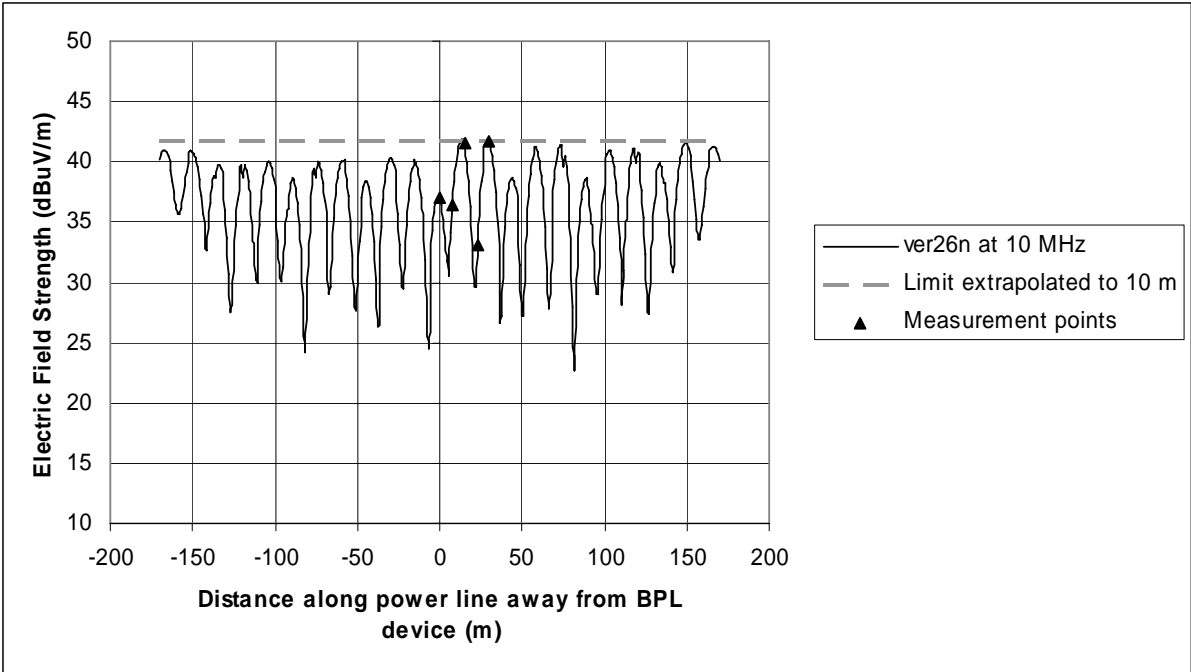


Figure B-29: Vertical electric field strength along power line for ver26n topology

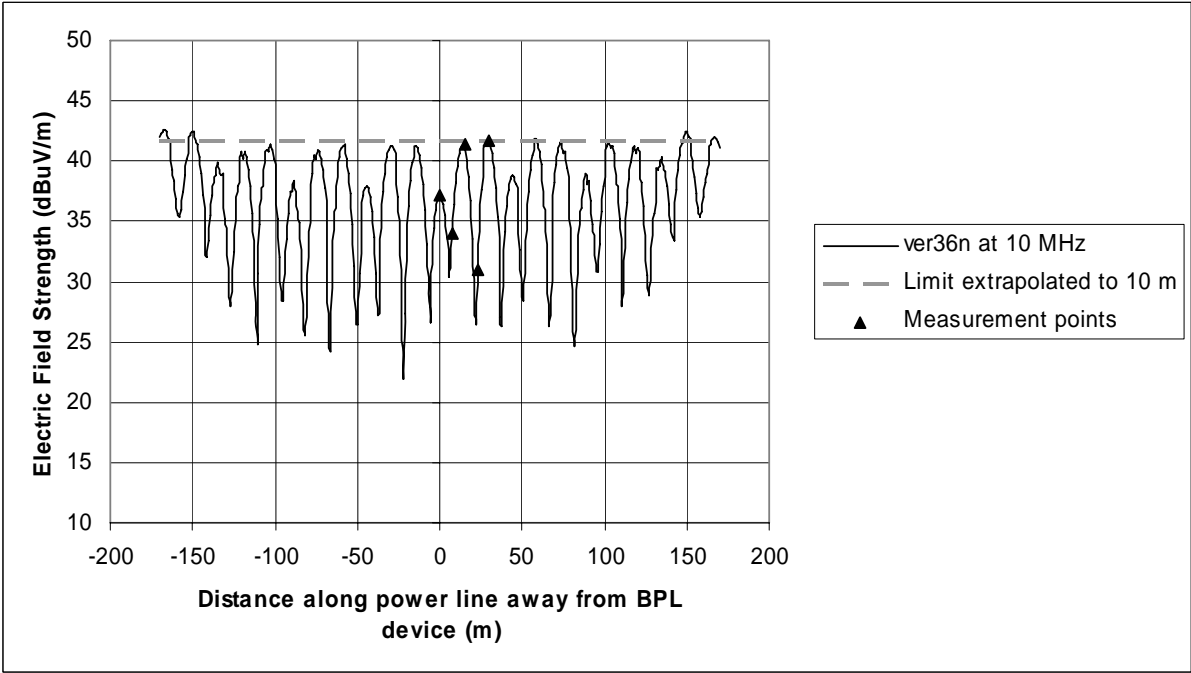
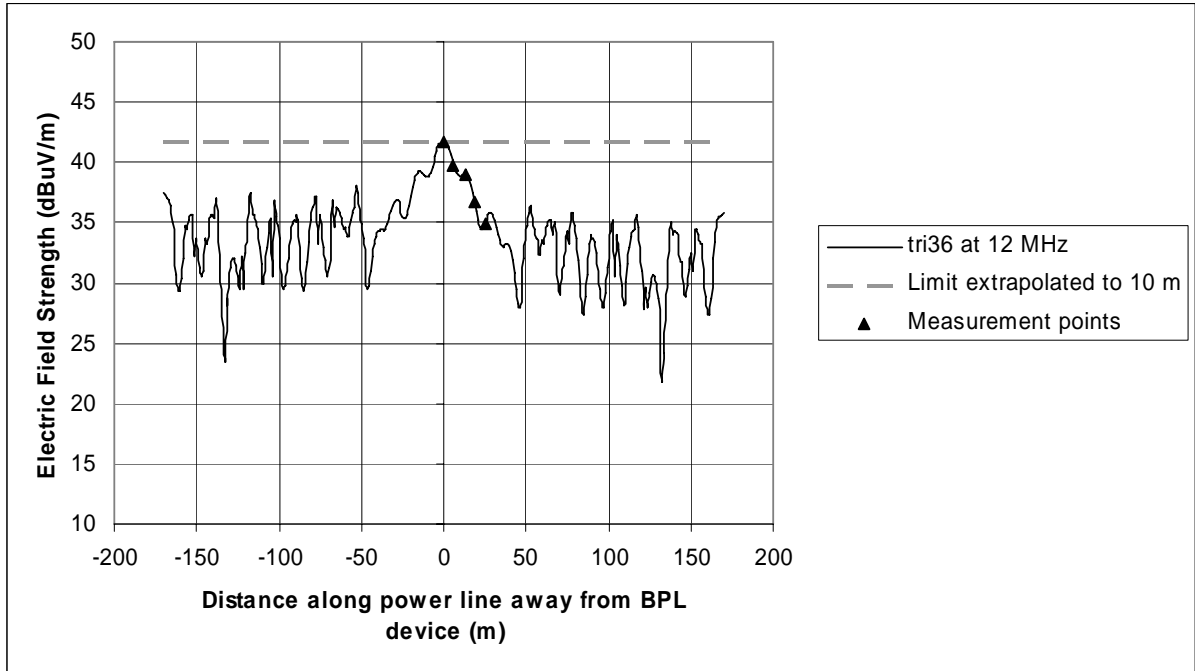
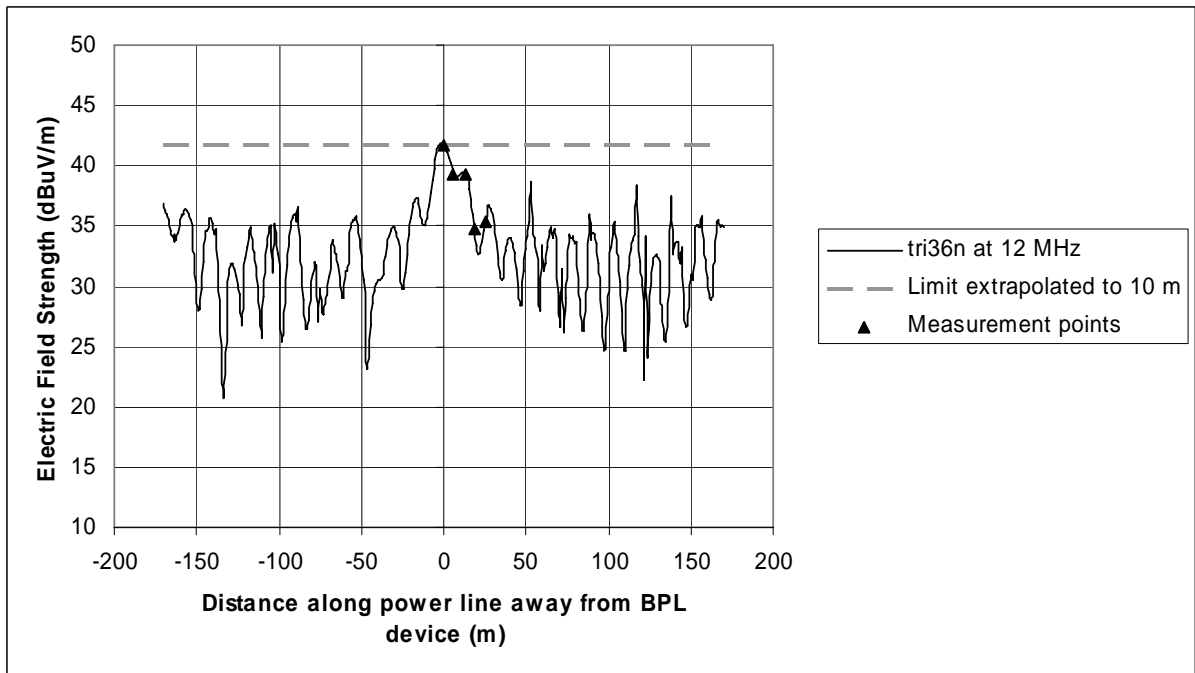


Figure B-30: Vertical electric field strength along power line for ver36n topology

12 MHz Plots



**Figure B-31: Vertical electric field strength along power line for tri36 topology**



**Figure B-32: Vertical electric field strength along power line for tri36n topology**

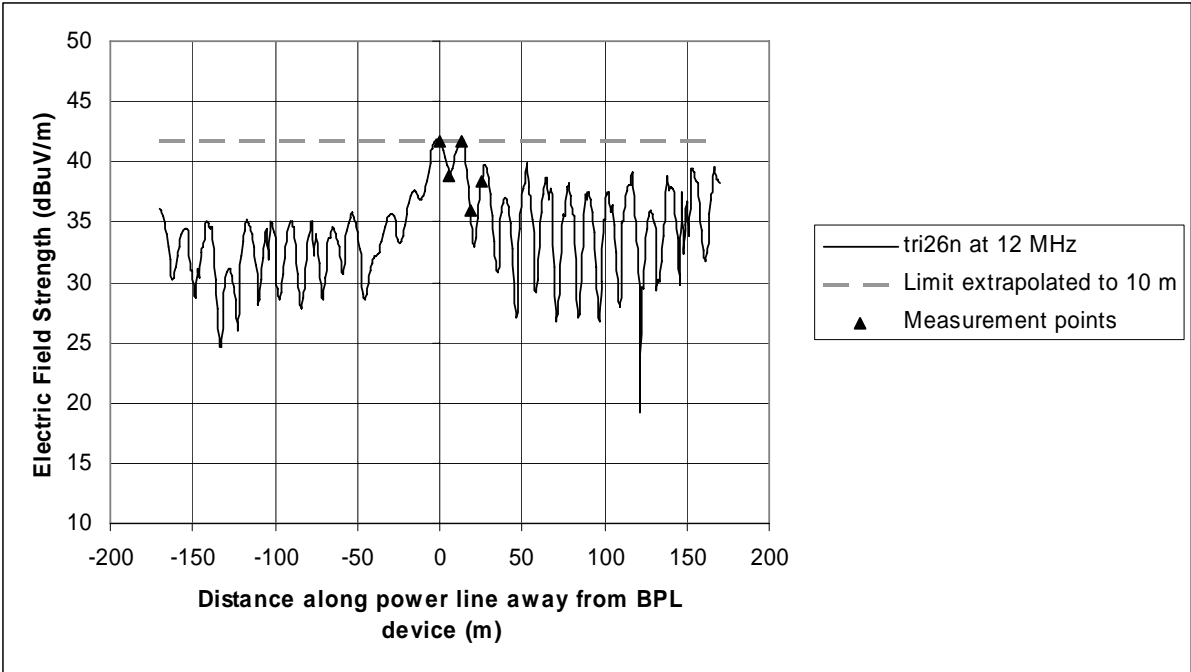


**Figure B-33: Vertical electric field strength along power line for tri26n topology**

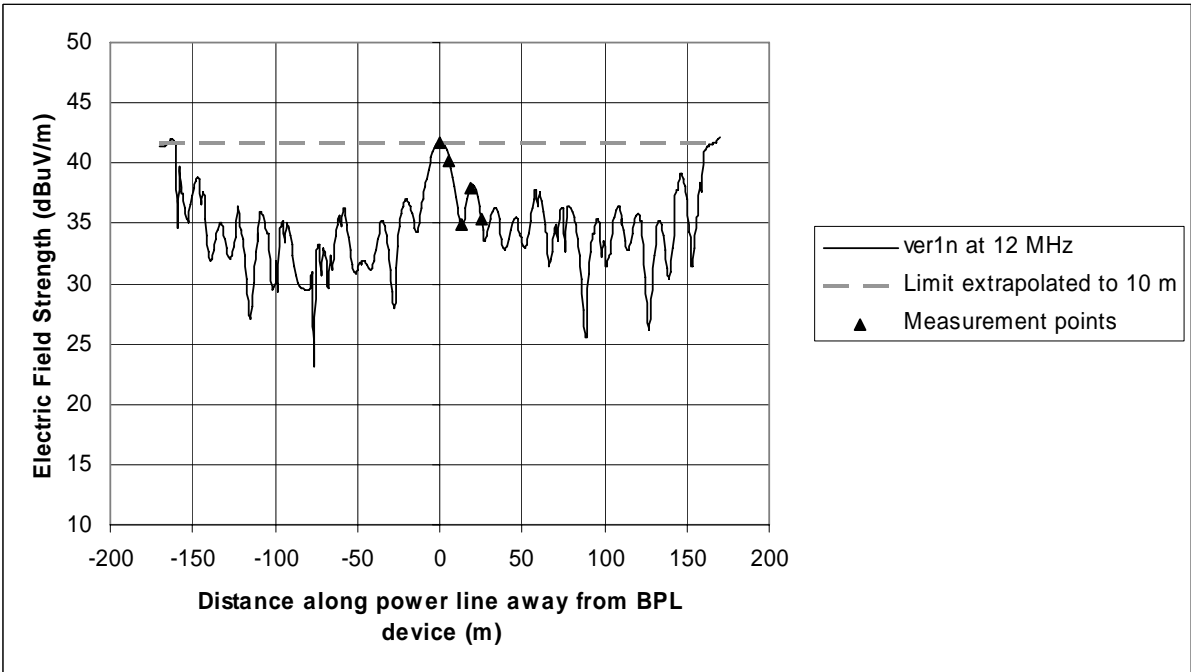


**Figure B-34: Vertical electric field strength along power line for ver1n topology**

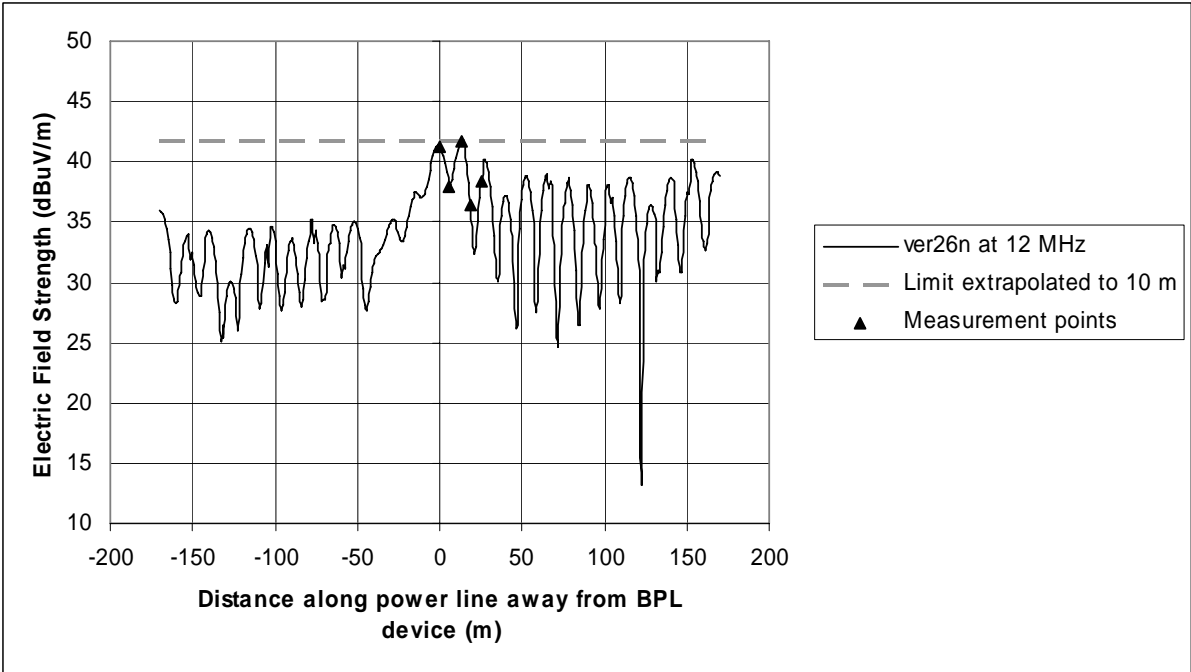


Figure B-35: Vertical electric field strength along power line for ver26n topology

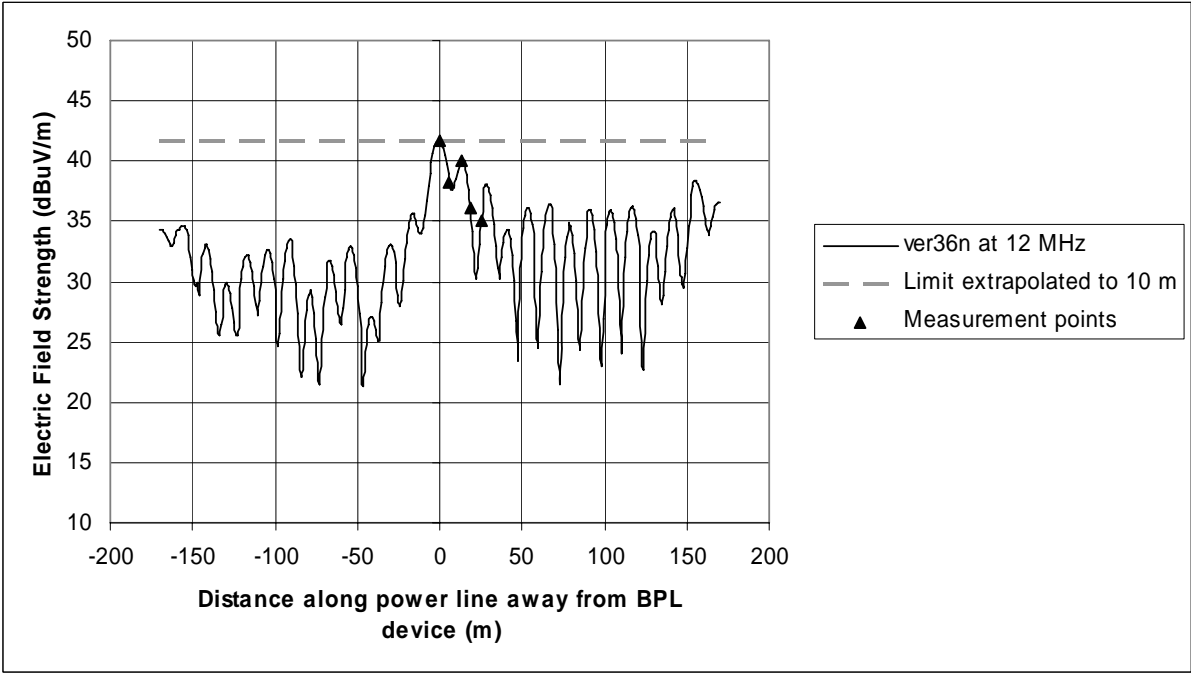
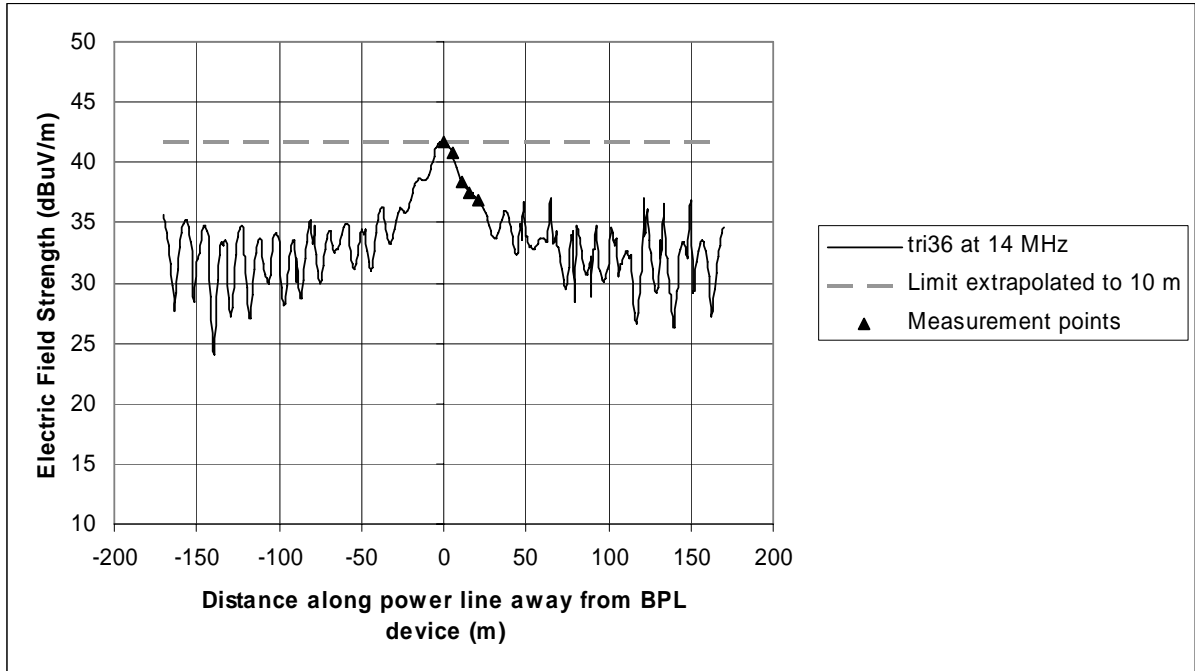
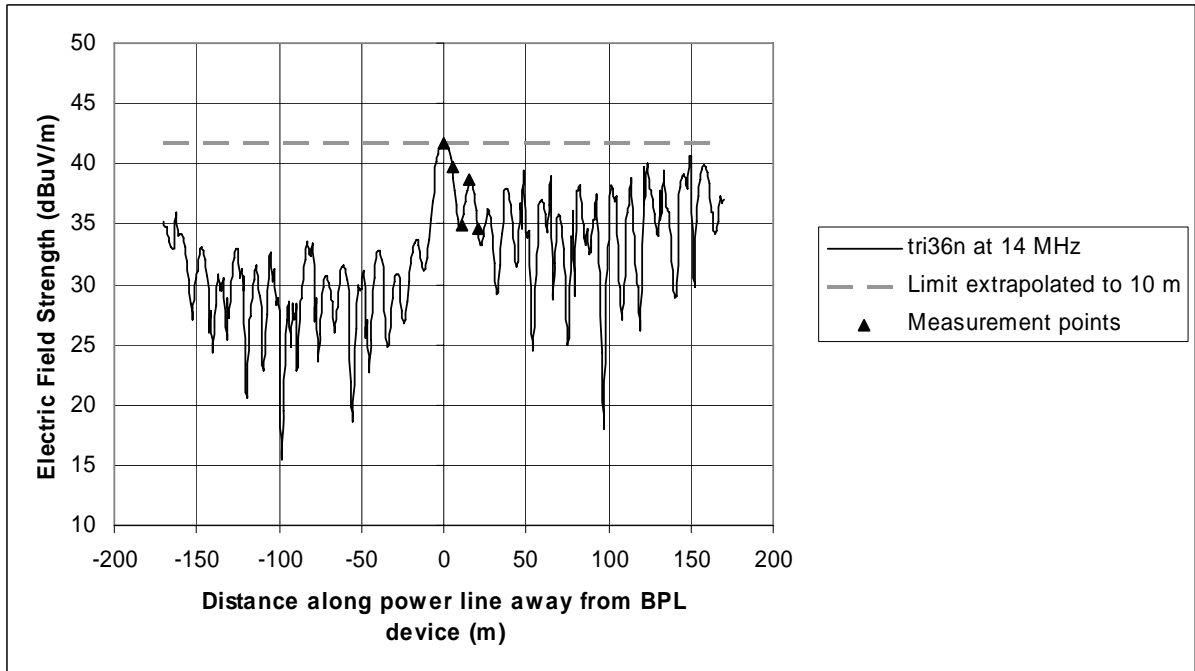


Figure B-36: Vertical electric field strength along power line for ver36n topology

*14 MHz Plots*



**Figure B-37: Vertical electric field strength along power line for tri36 topology**



**Figure B-38: Vertical electric field strength along power line for tri36n topology**



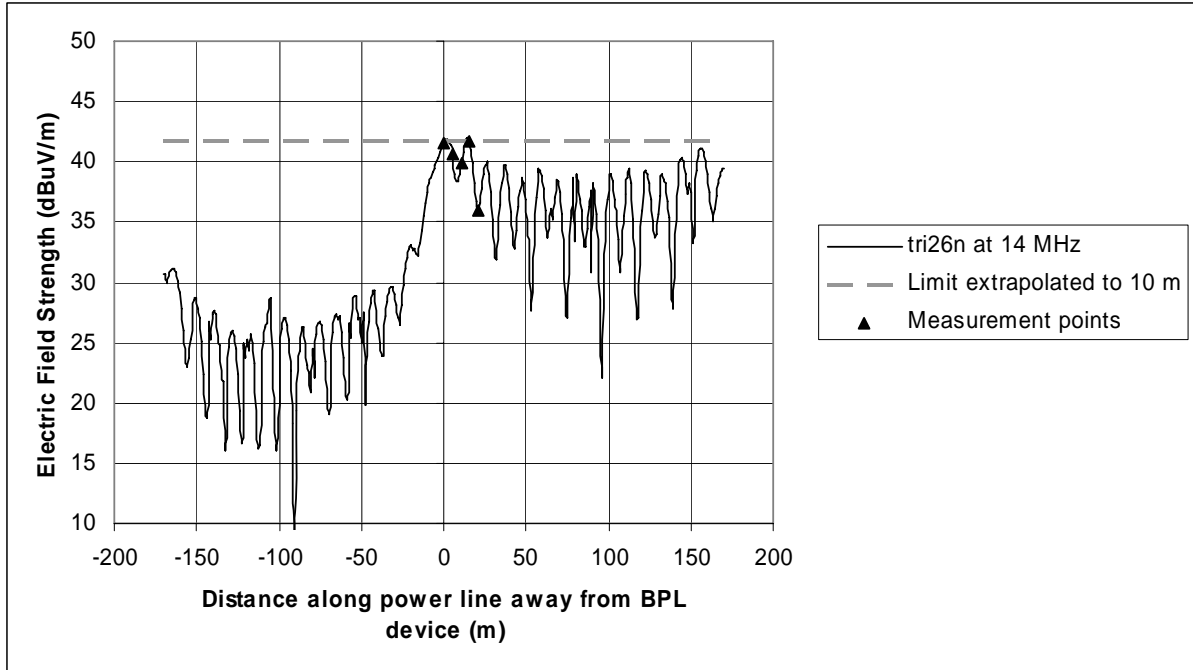


**Figure B-39: Vertical electric field strength along power line for tri26n topology**

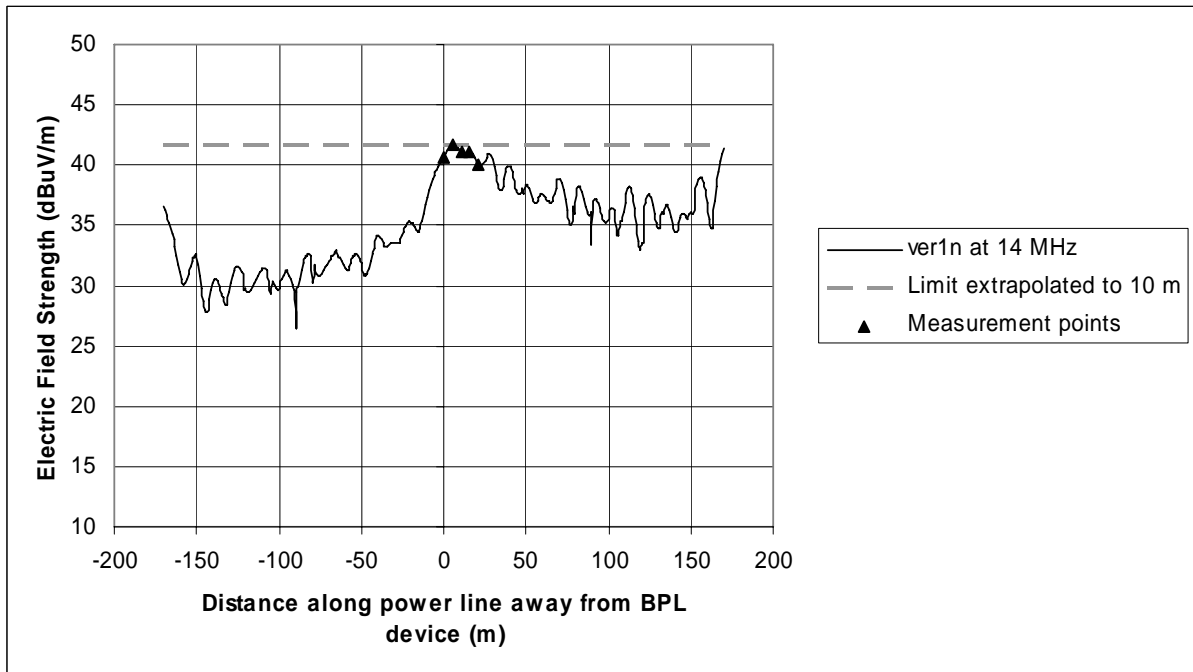


**Figure B-40: Vertical electric field strength along power line for ver1n topology**

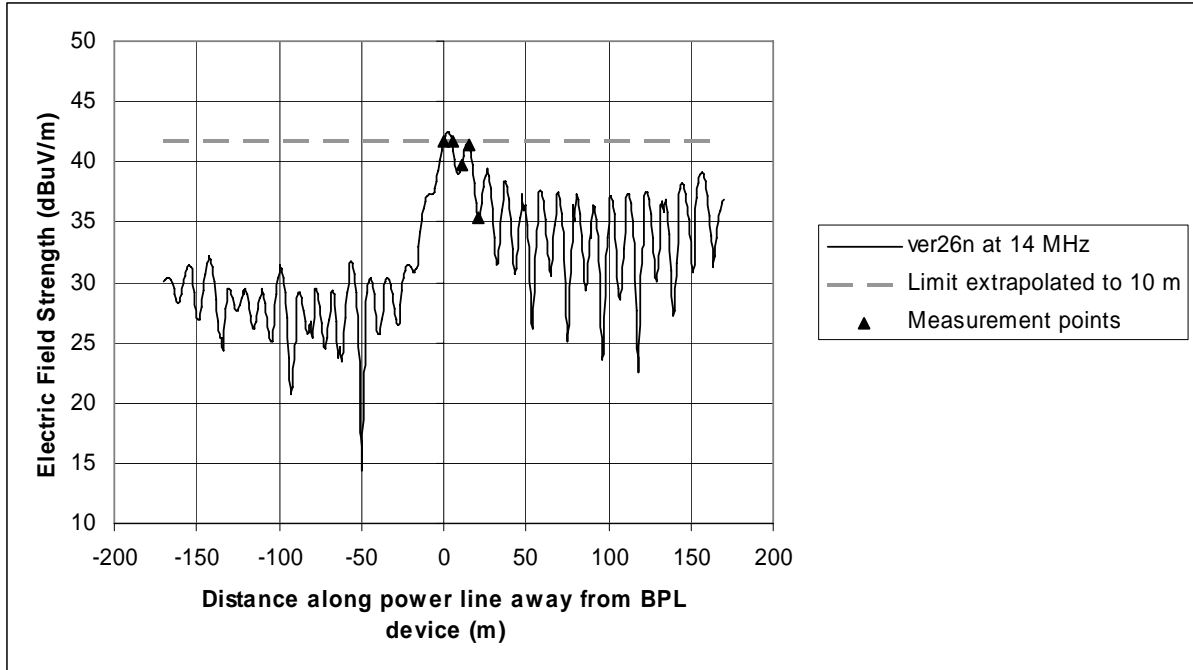


**Figure B-41: Vertical electric field strength along power line for ver26n topology**

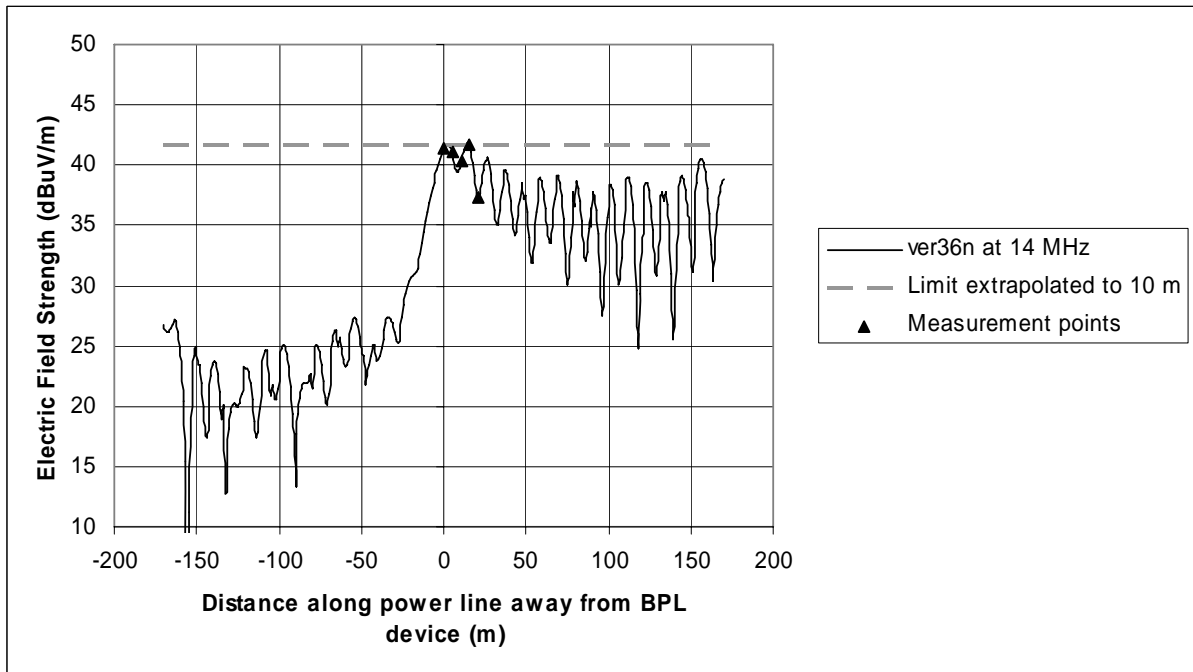


**Figure B-42: Vertical electric field strength along power line for ver36n topology**

*16 MHz Plots*

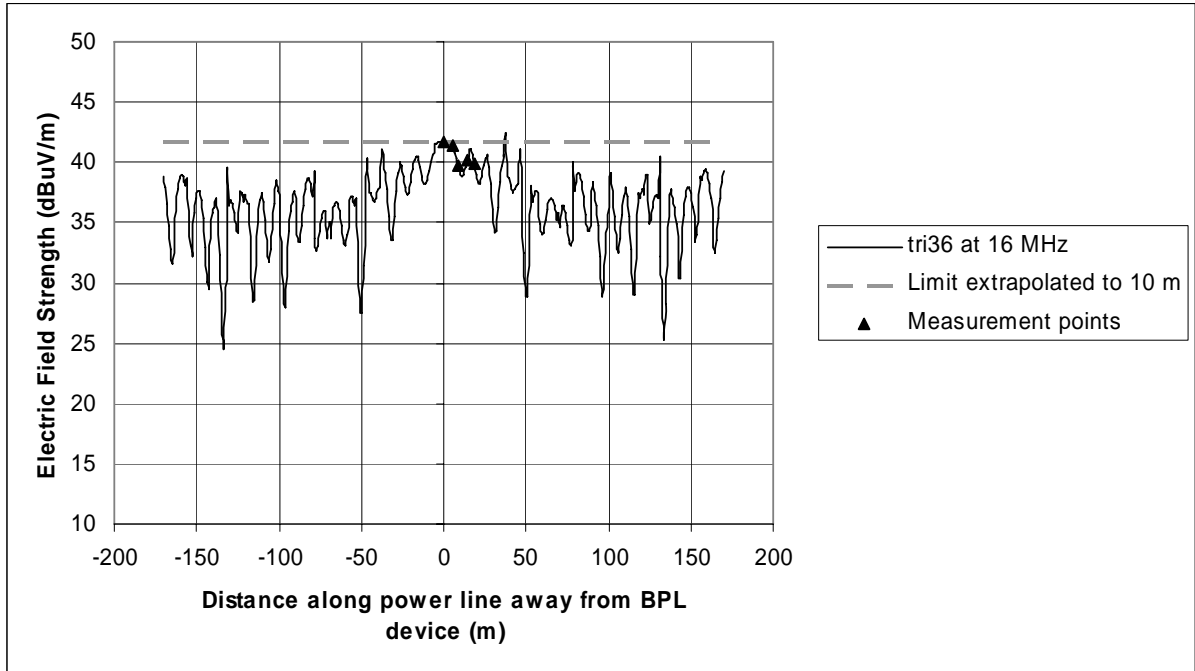


**Figure B-43: Vertical electric field strength along power line for tri36 topology**

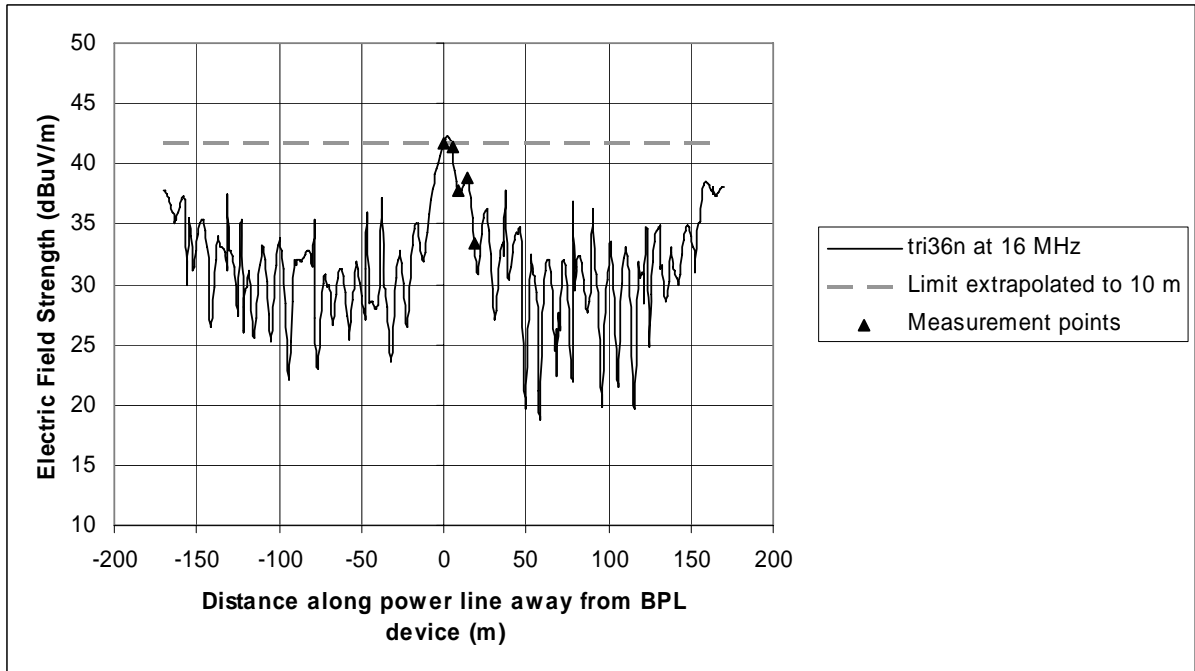


**Figure B-44: Vertical electric field strength along power line for tri36n topology**

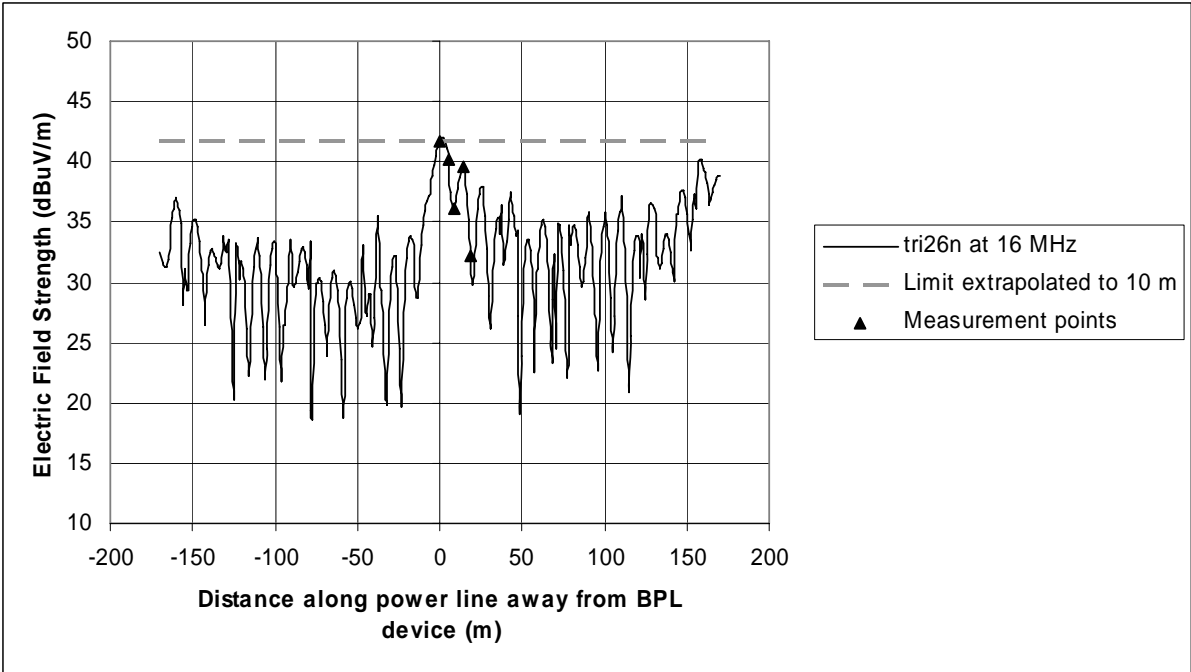


**Figure B-45: Vertical electric field strength along power line for tri26n topology**

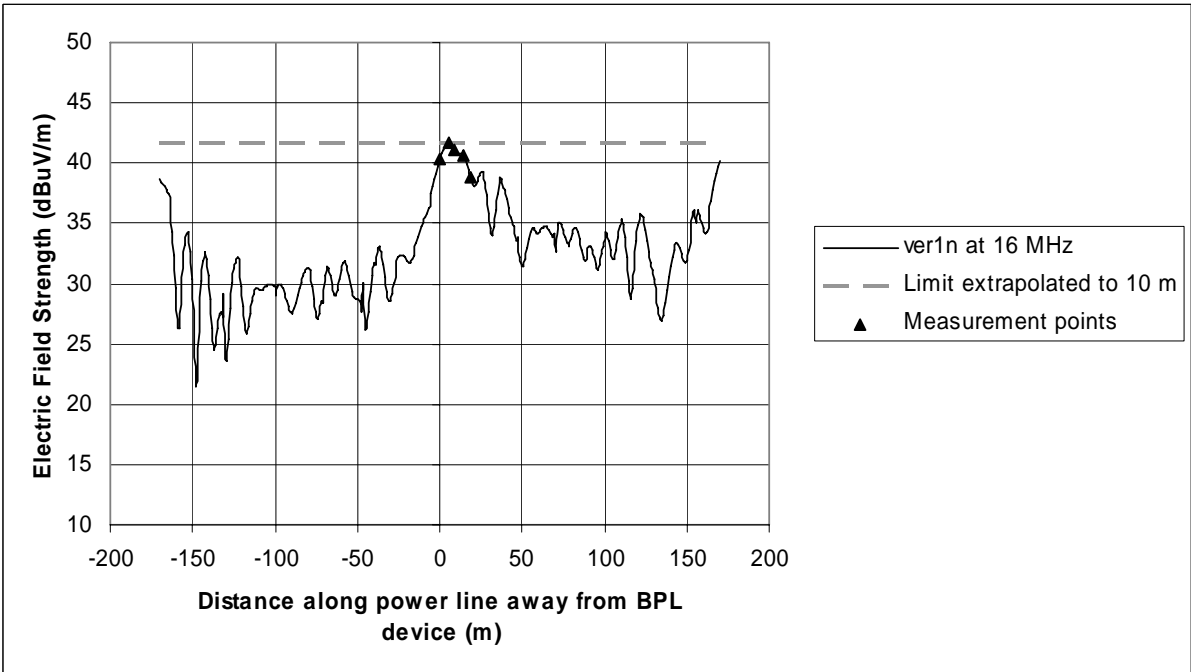


**Figure B-46: Vertical electric field strength along power line for ver1n topology**

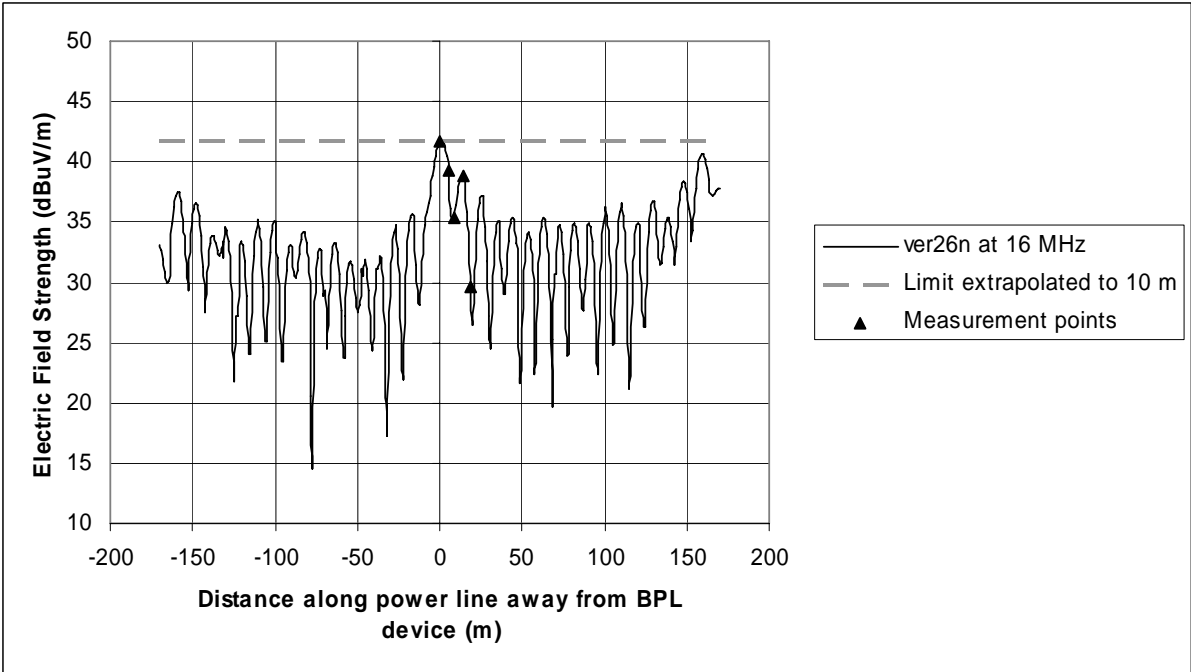


**Figure B-47: Vertical electric field strength along power line for ver26n topology**

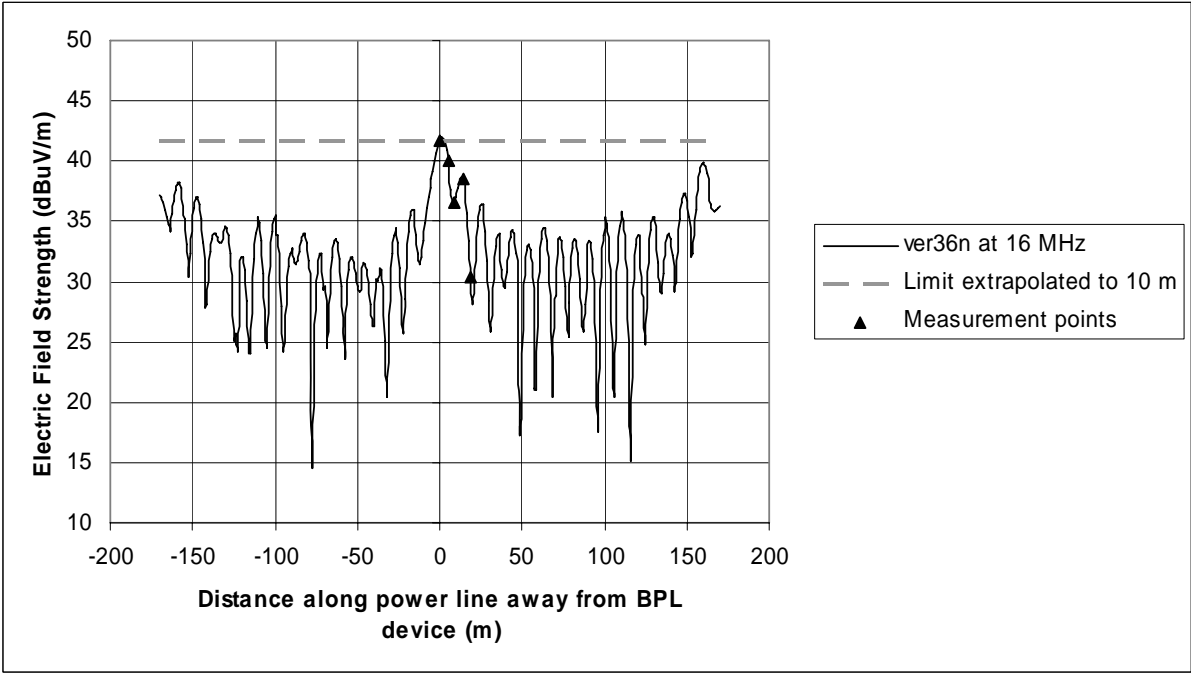


**Figure B-48: Vertical electric field strength along power line for ver36n topology**

*18 MHz Plots*

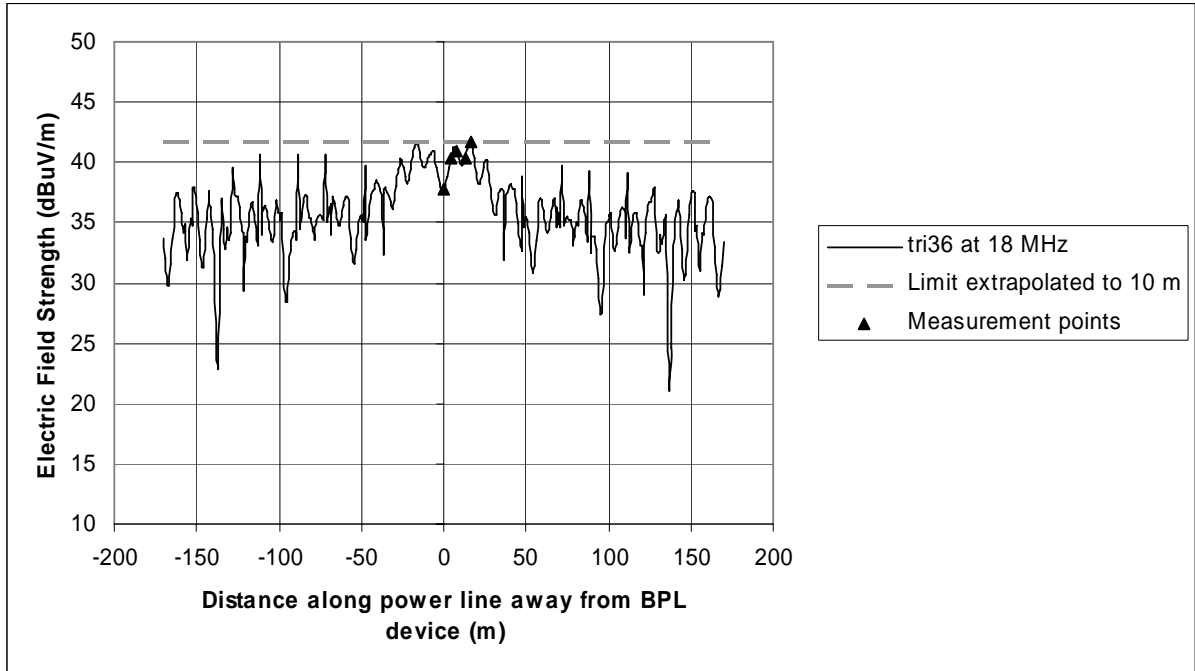


**Figure B-49: Vertical electric field strength along power line for tri36 topology**

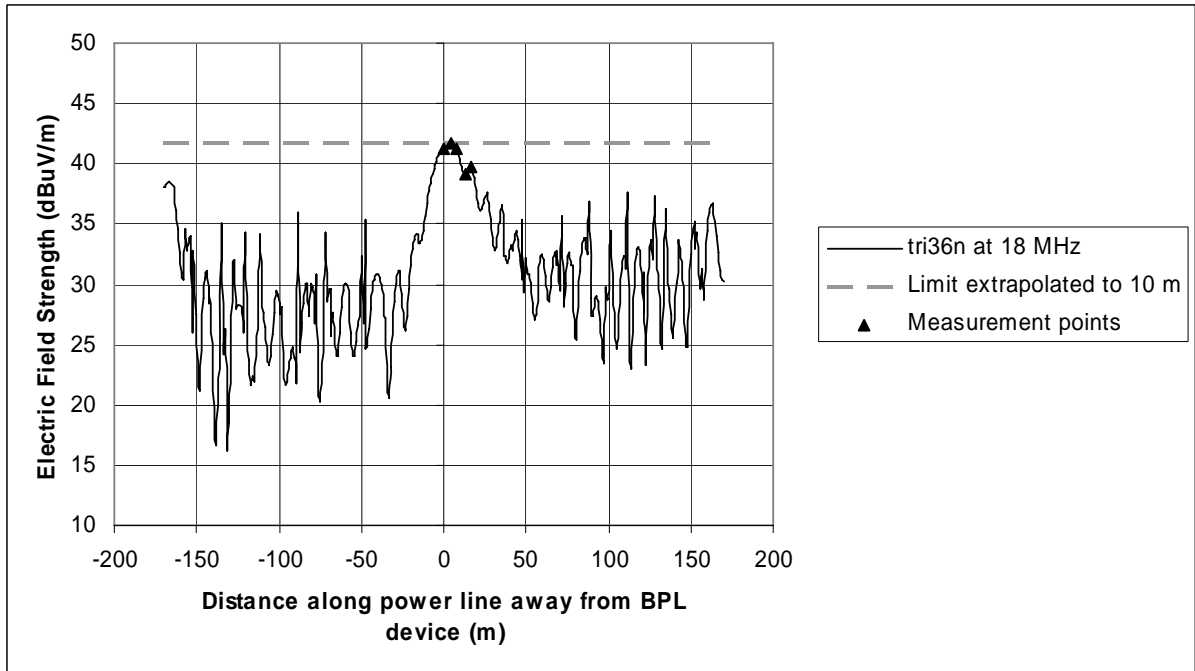


**Figure B-50: Vertical electric field strength along power line for tri36n topology**

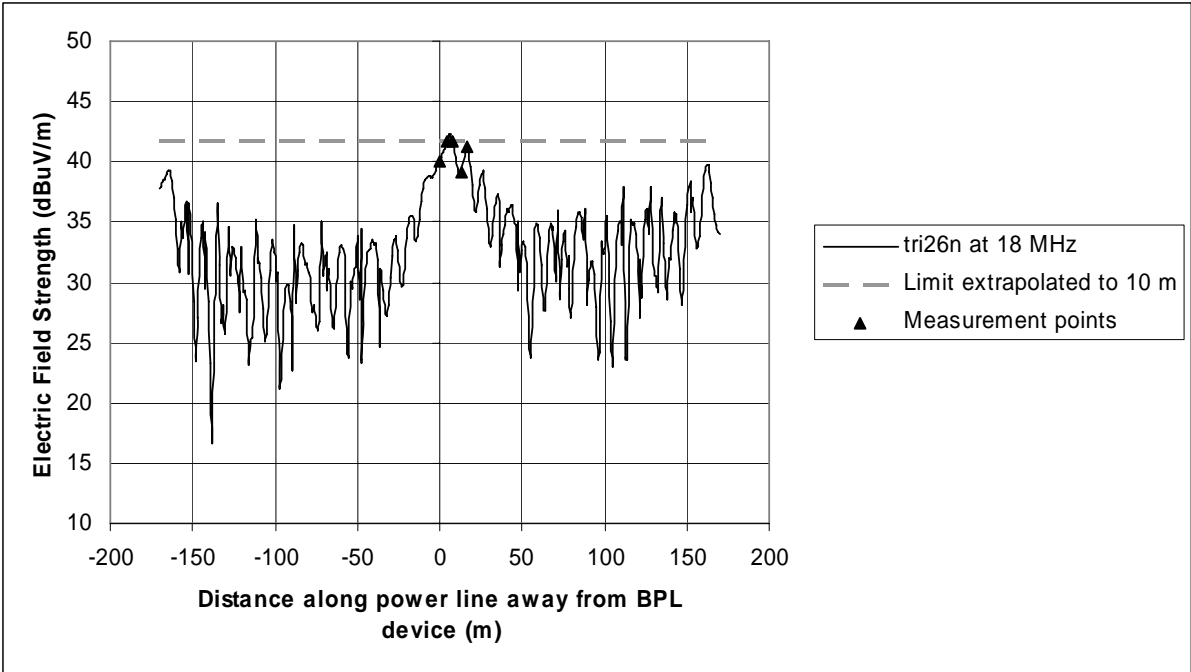


**Figure B-51: Vertical electric field strength along power line for tri26n topology**

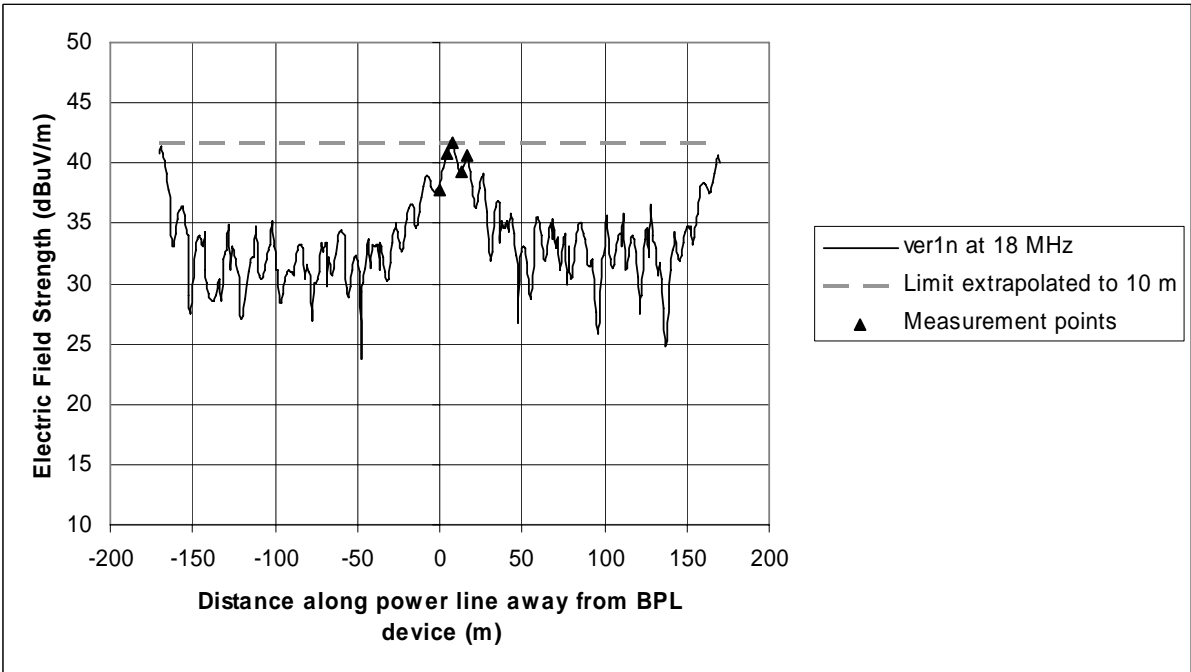


**Figure B-52: Vertical electric field strength along power line for ver1n topology**

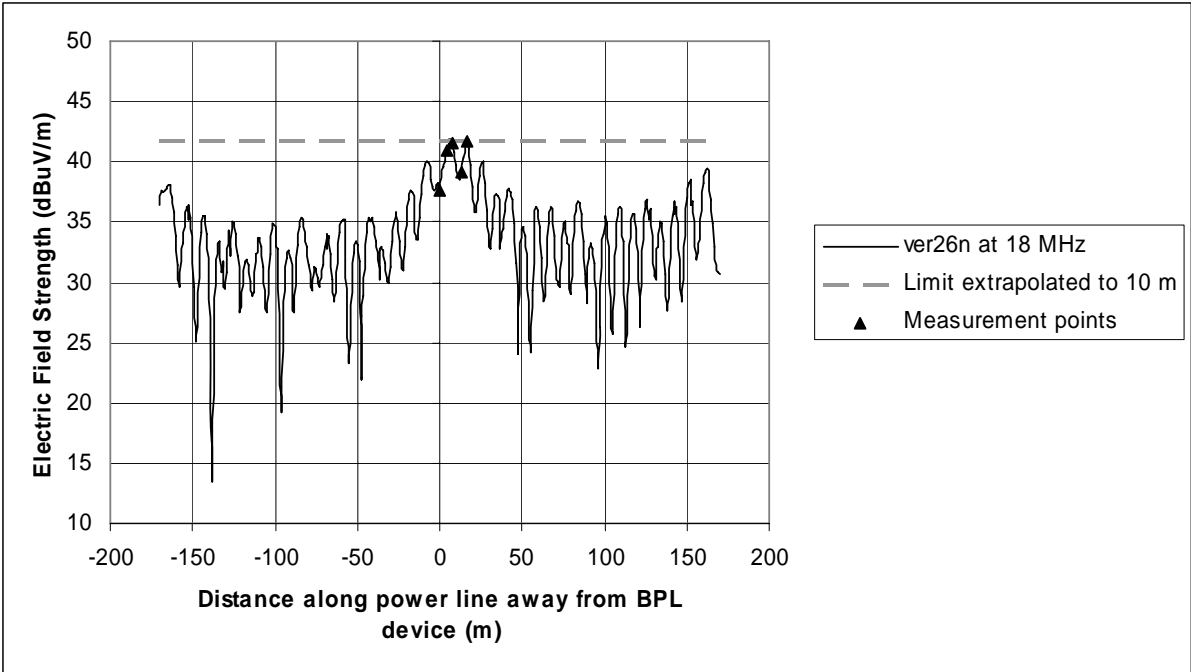


Figure B-53: Vertical electric field strength along power line for ver26n topology

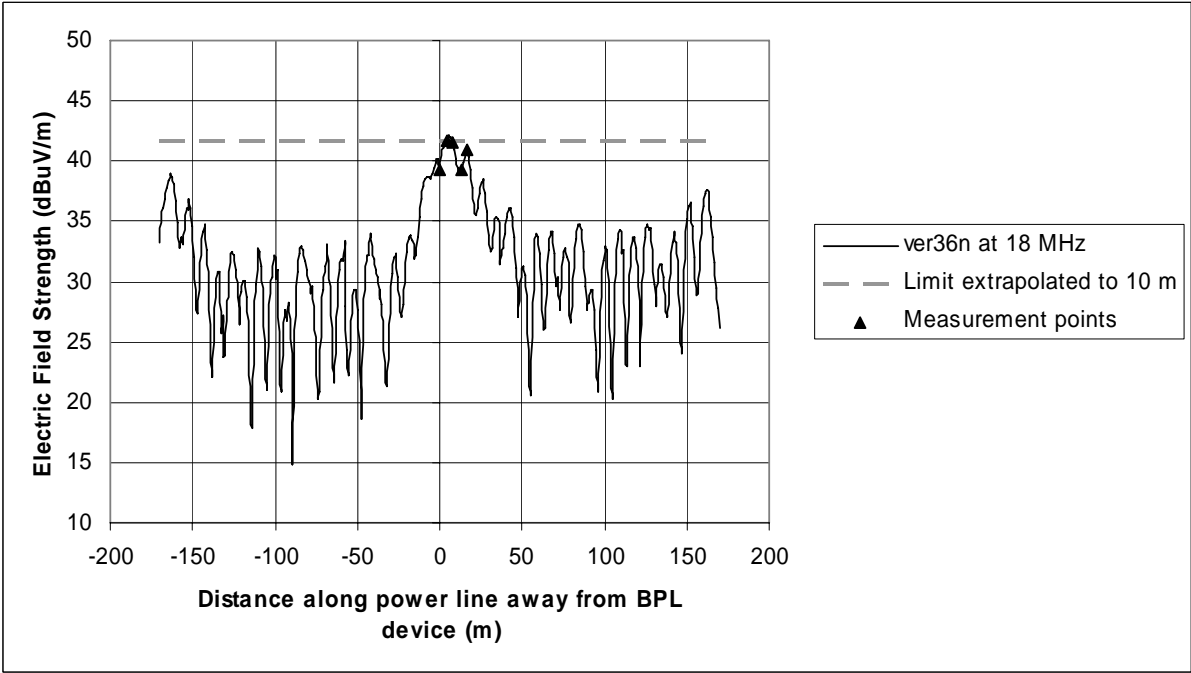
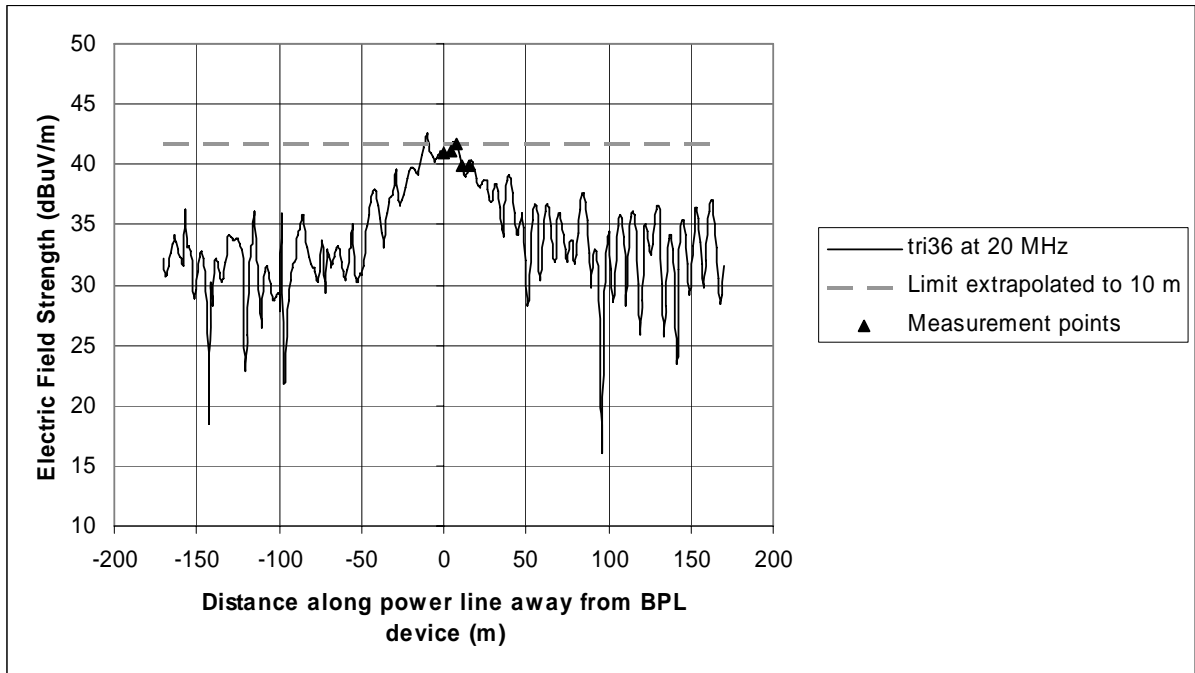


Figure B-54: Vertical electric field strength along power line for ver3n topology



20 MHz Plots



**Figure B-55: Vertical electric field strength along power line for tri36 topology**

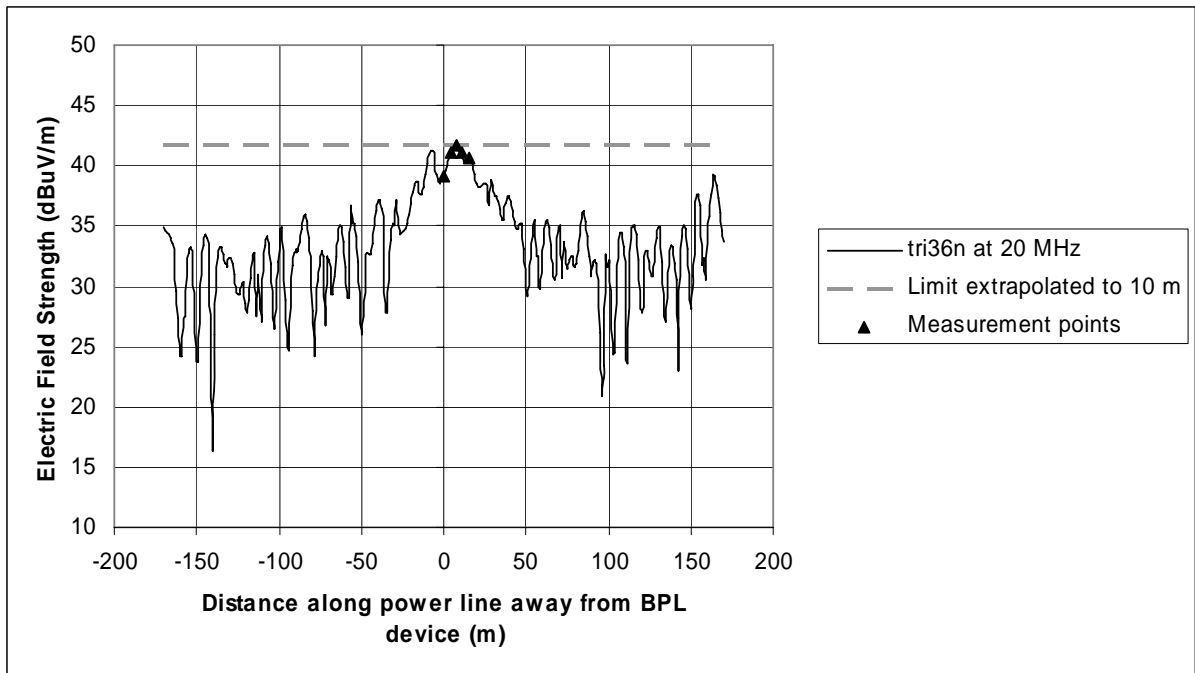


**Figure B-56: Vertical electric field strength along power line for tri36n topology**

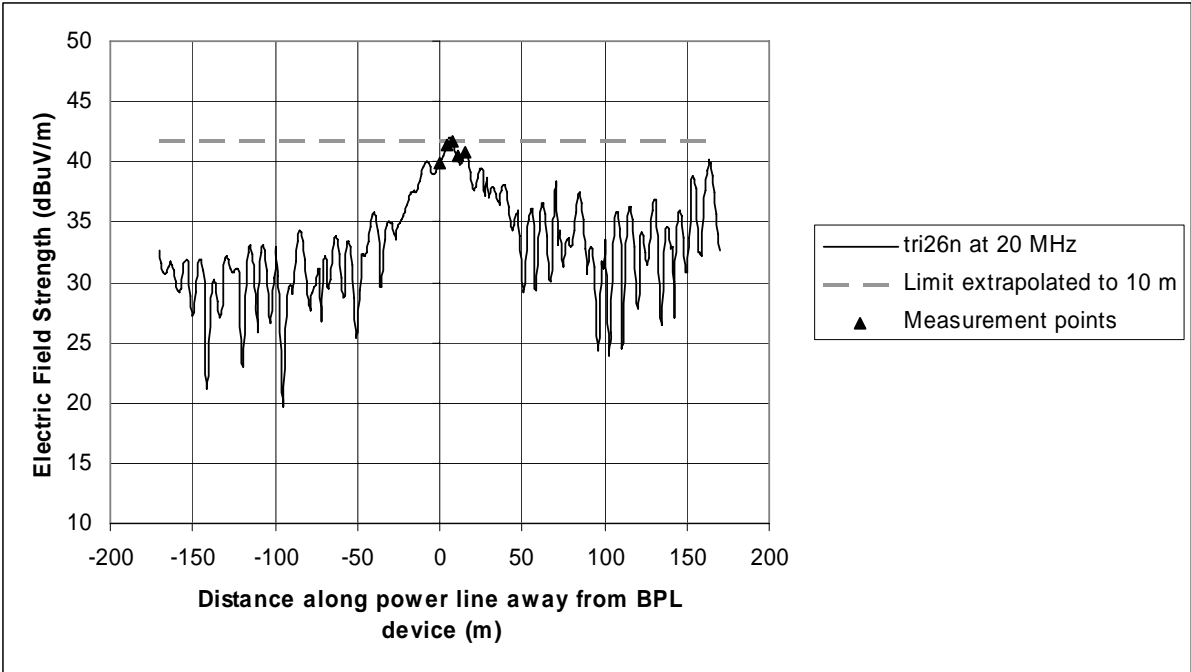


**Figure B-57: Vertical electric field strength along power line for tri26n topology**

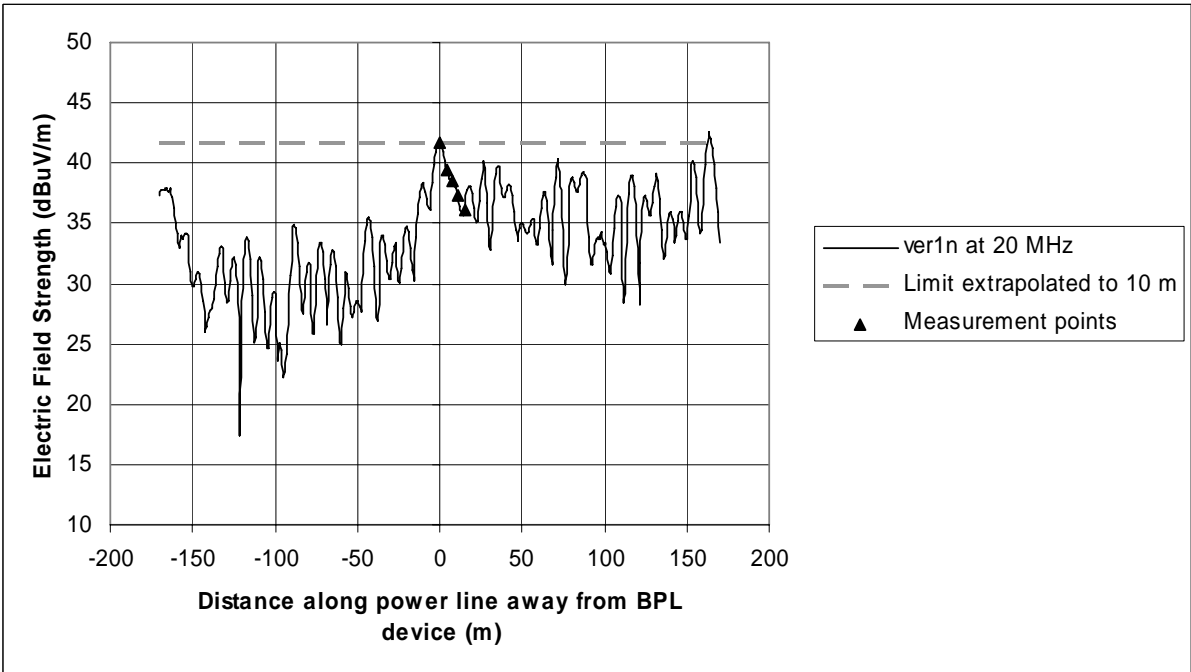


**Figure B-58: Vertical electric field strength along power line for ver1n topology**

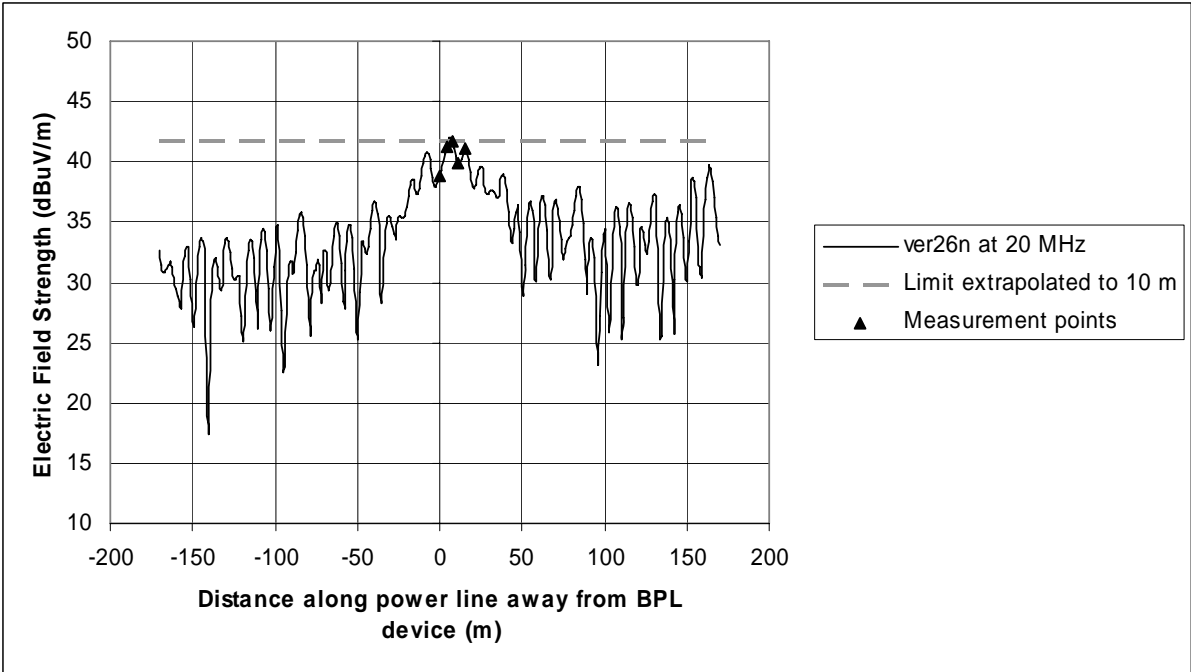


**Figure B-59: Vertical electric field strength along power line for ver26n topology**

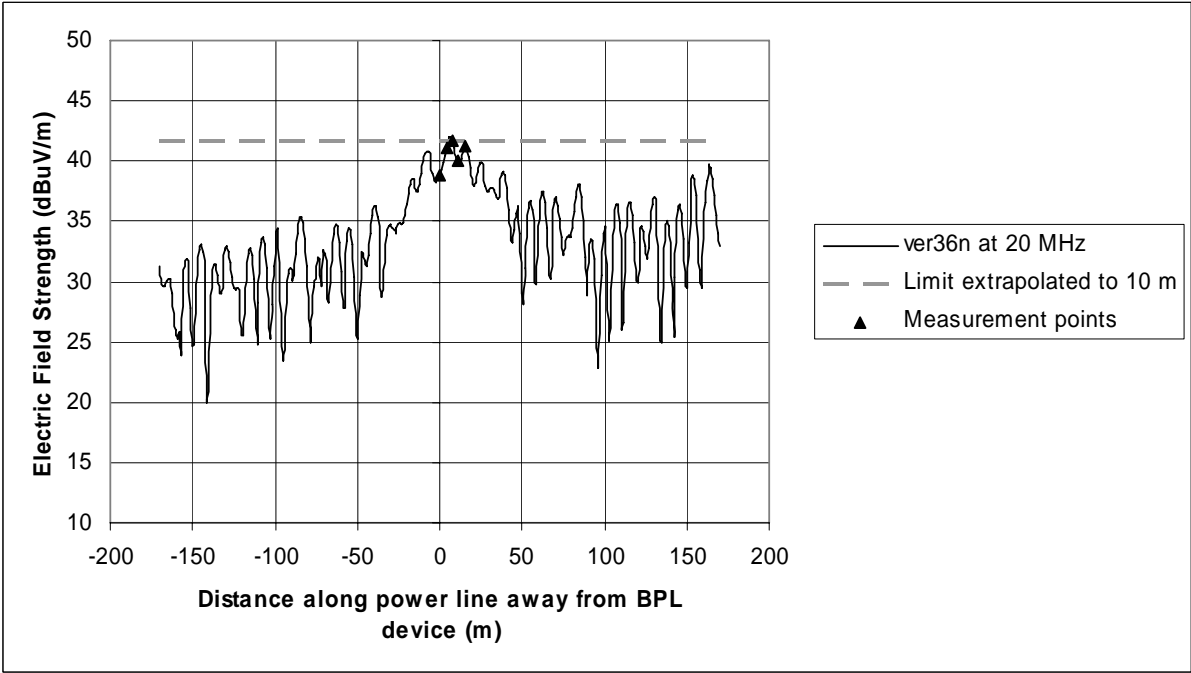


**Figure B-60: Vertical electric field strength along power line for ver36n topology**

22 MHz Plots

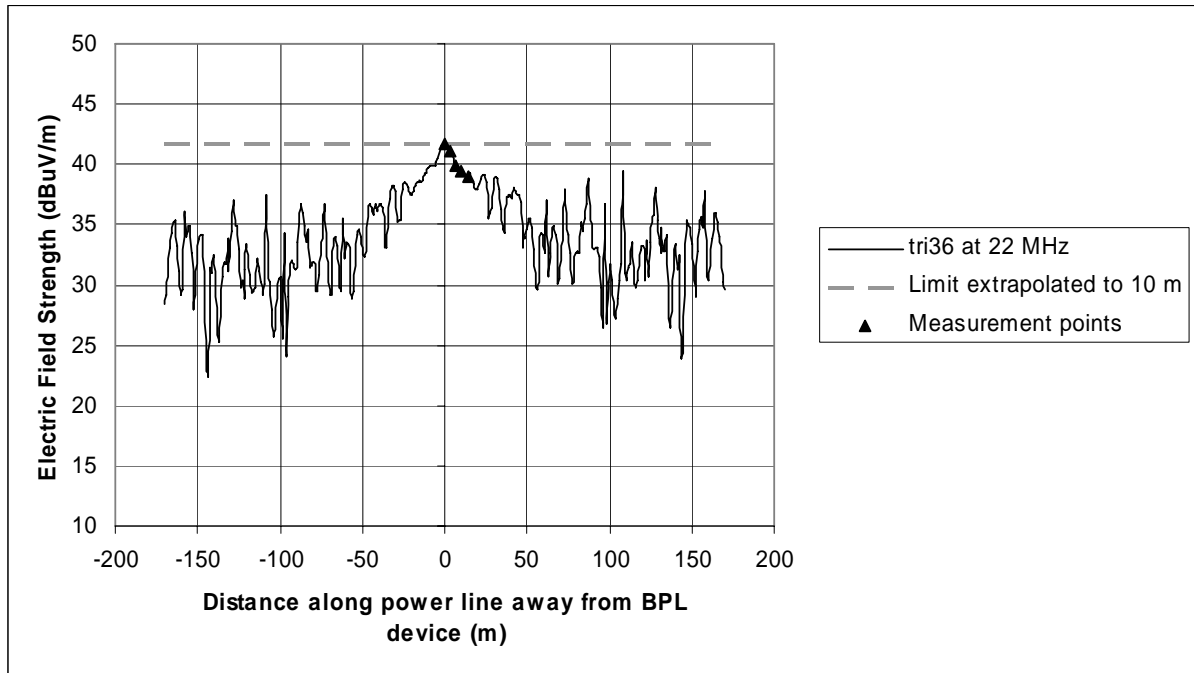


**Figure B-61: Vertical electric field strength along power line for tri36 topology**

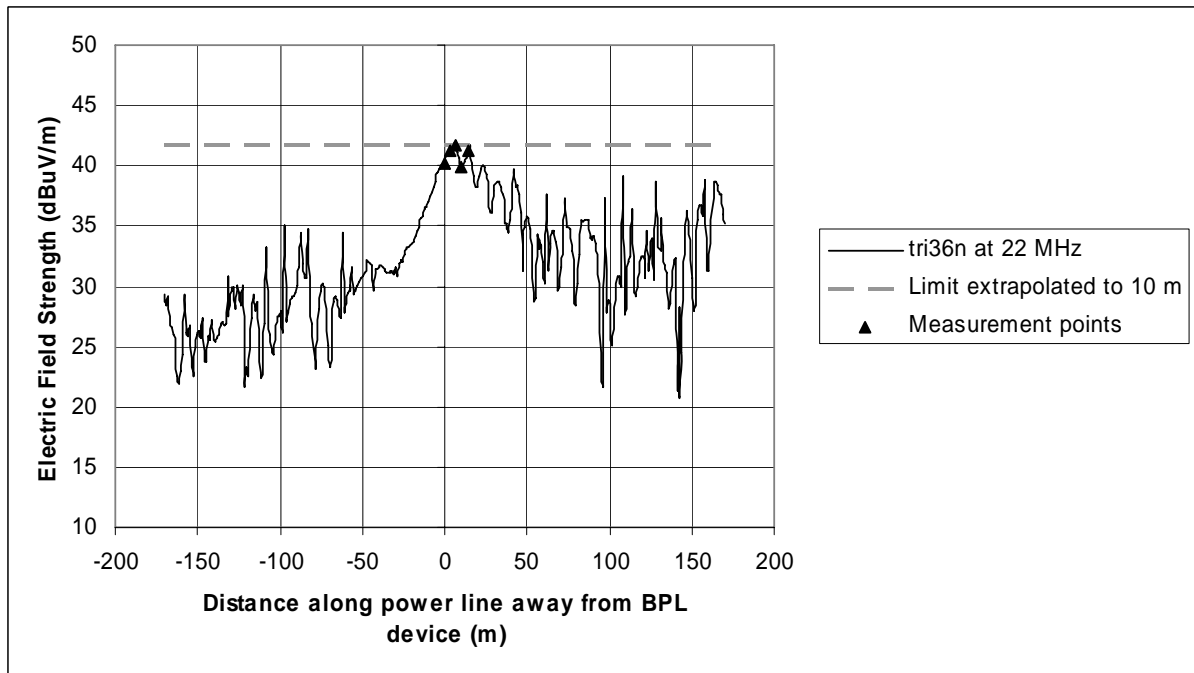


**Figure B-62: Vertical electric field strength along power line for tri36n topology**

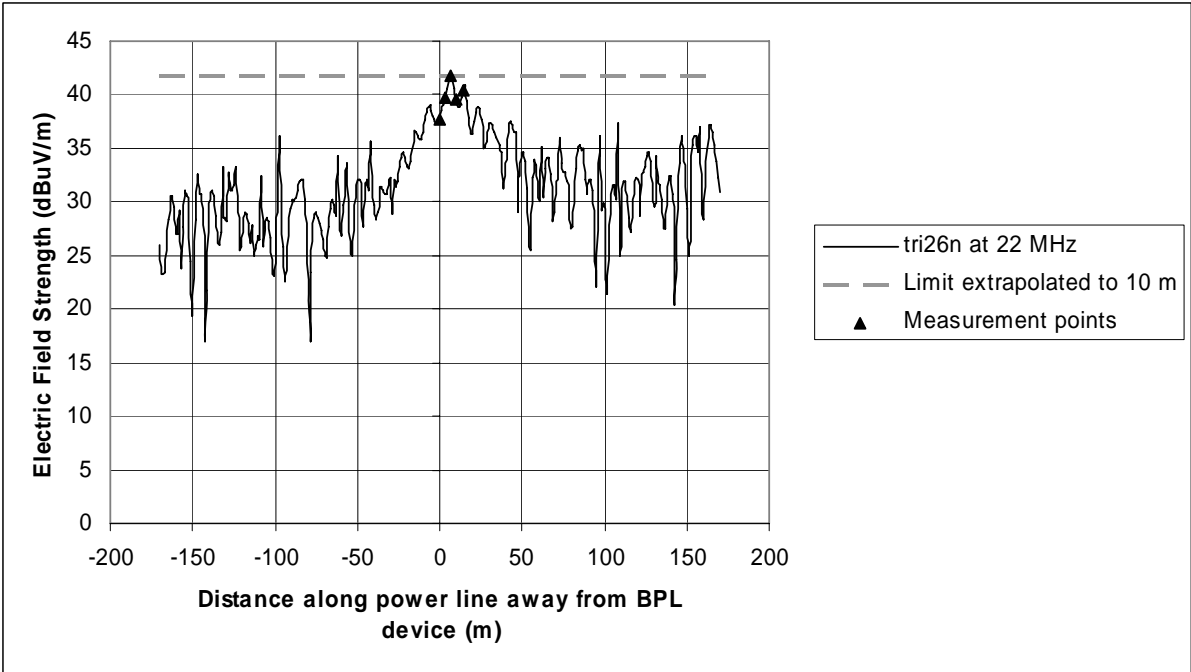


**Figure B-63: Vertical electric field strength along power line for tri26n topology**

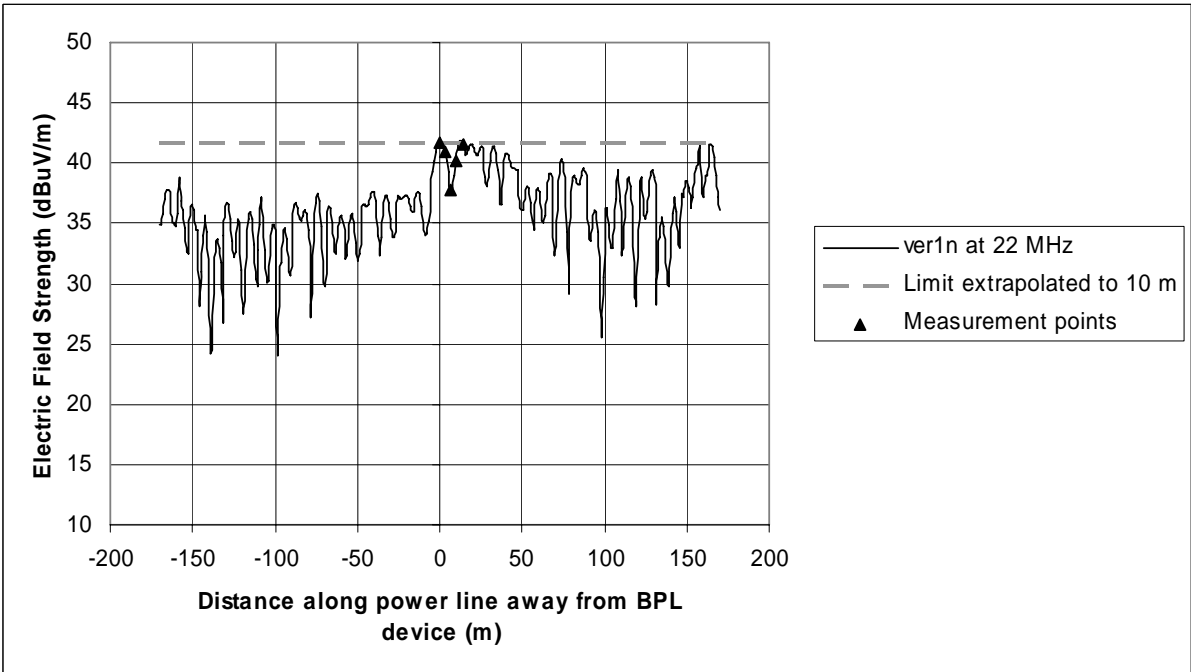


**Figure B-64: Vertical electric field strength along power line for ver1n topology**

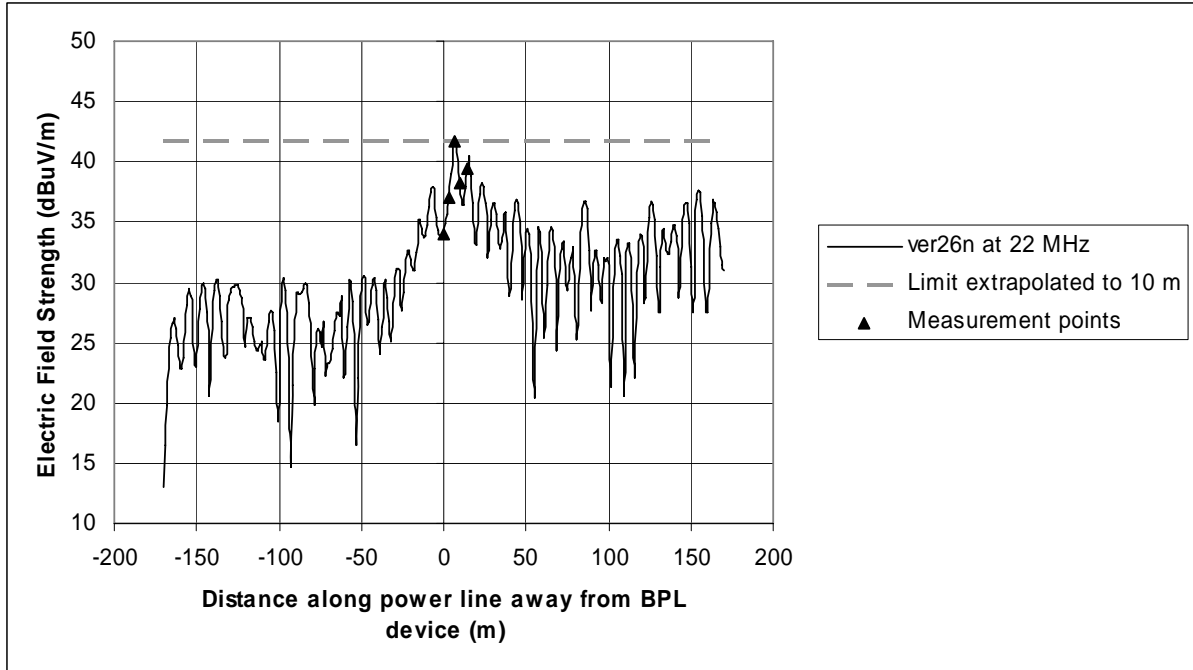


**Figure B-65: Vertical electric field strength along power line for ver26n topology**

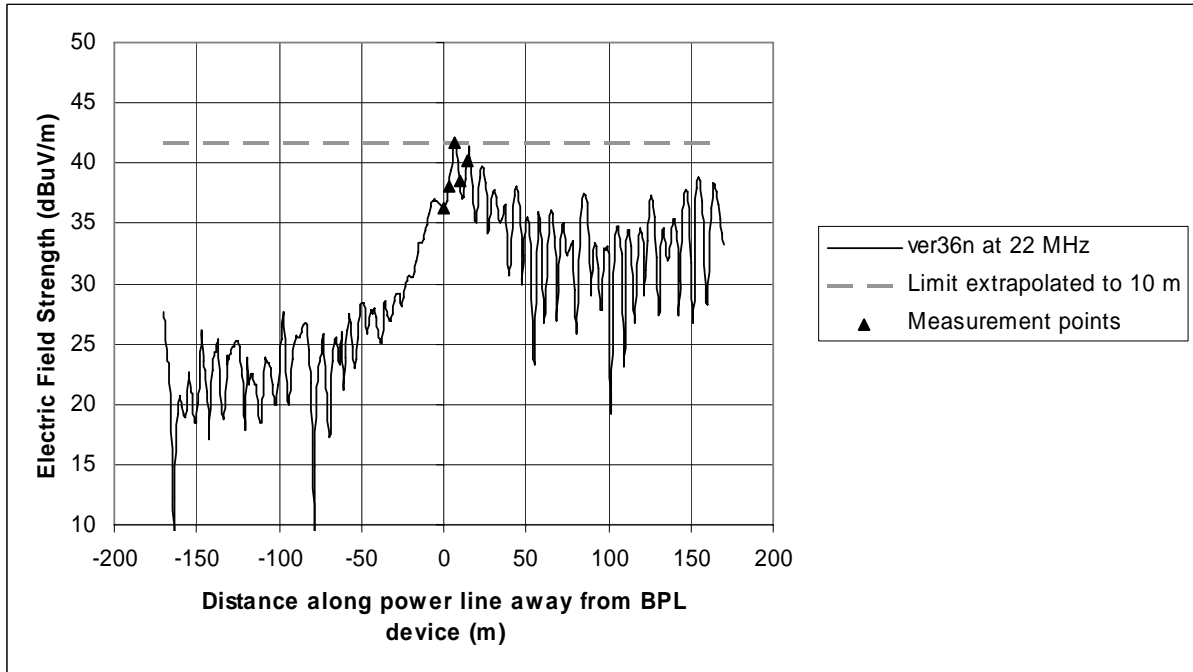


**Figure B-66: Vertical electric field strength along power line for ver36n topology**

*24 MHz Plots*

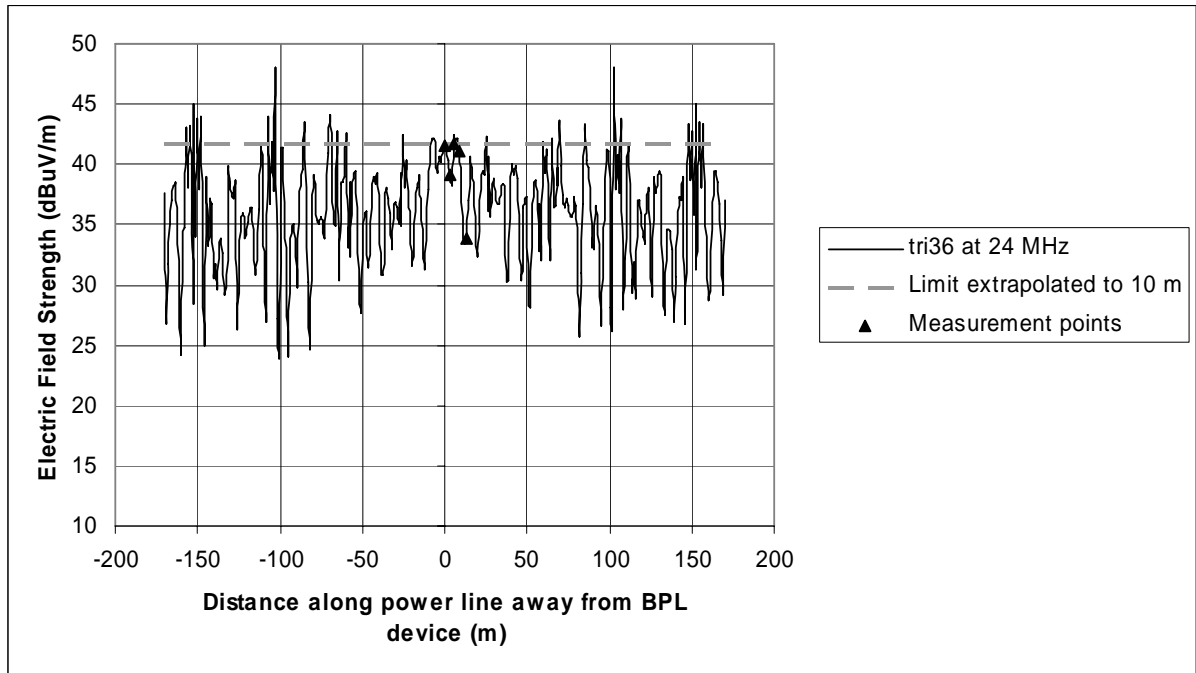


**Figure B-67: Vertical electric field strength along power line for tri36 topology**

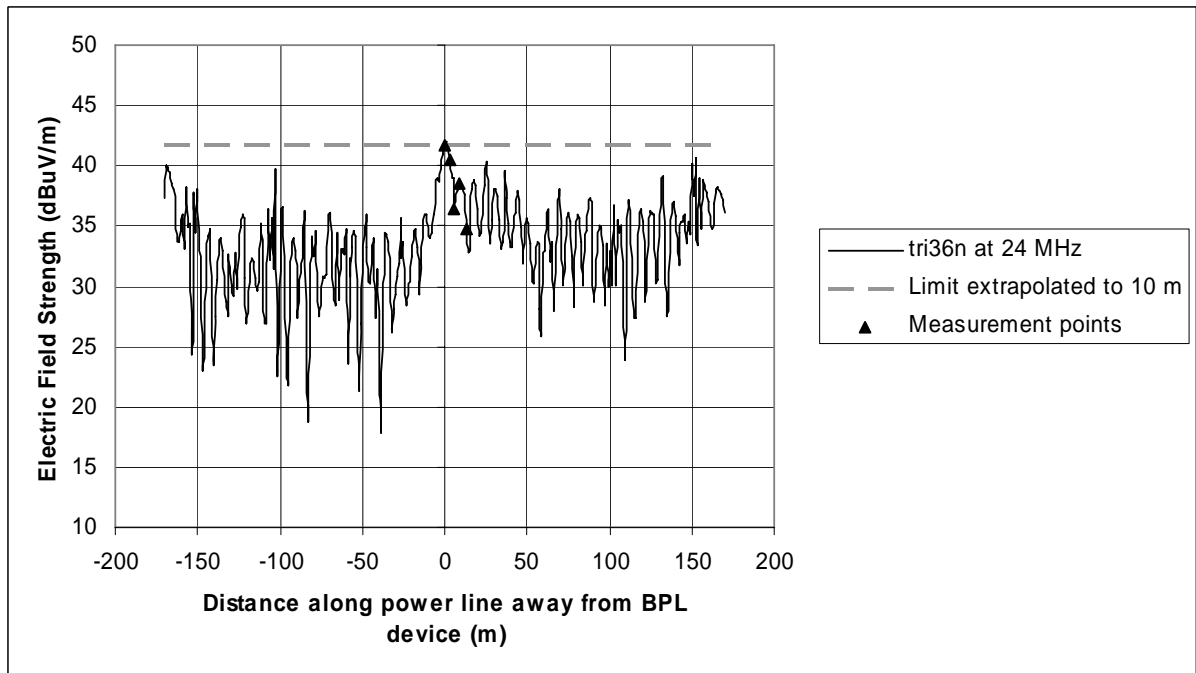


**Figure B-68: Vertical electric field strength along power line for tri36n topology**

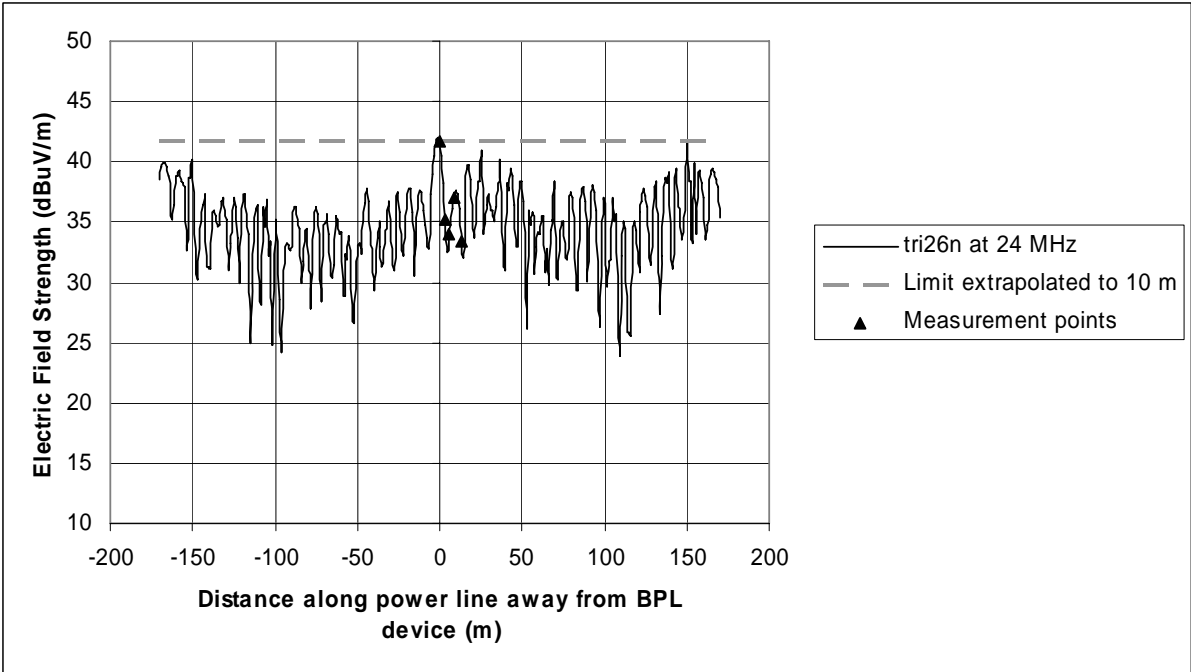


**Figure B-69: Vertical electric field strength along power line for tri26n topology**

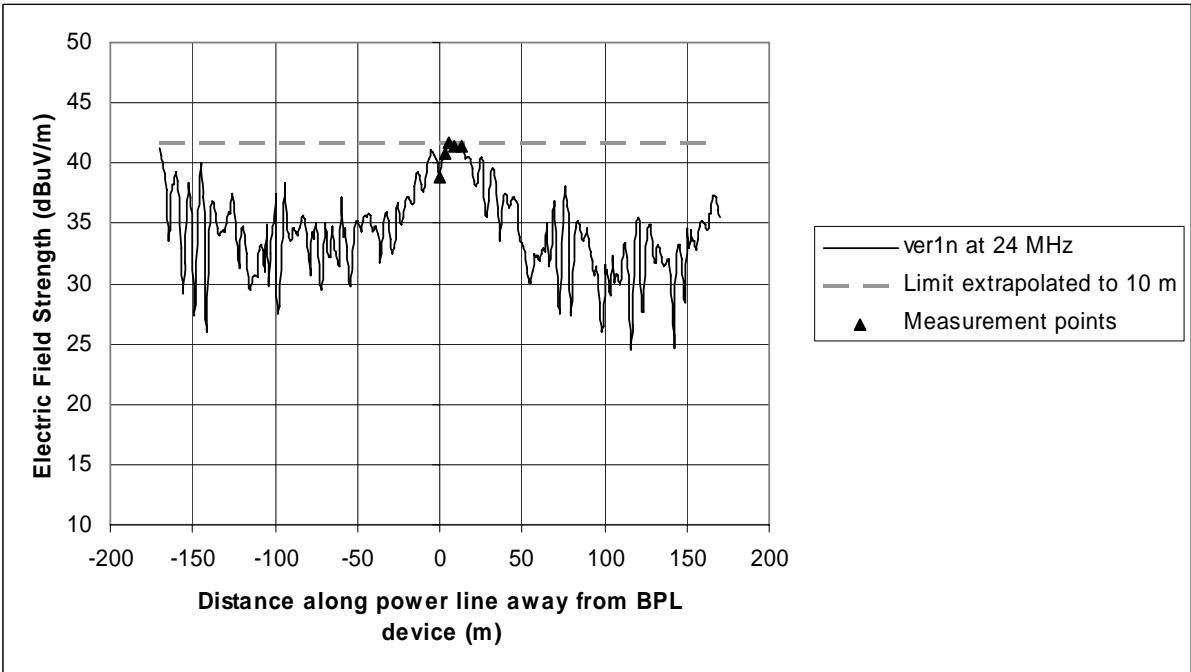


**Figure B-70: Vertical electric field strength along power line for ver1n topology**



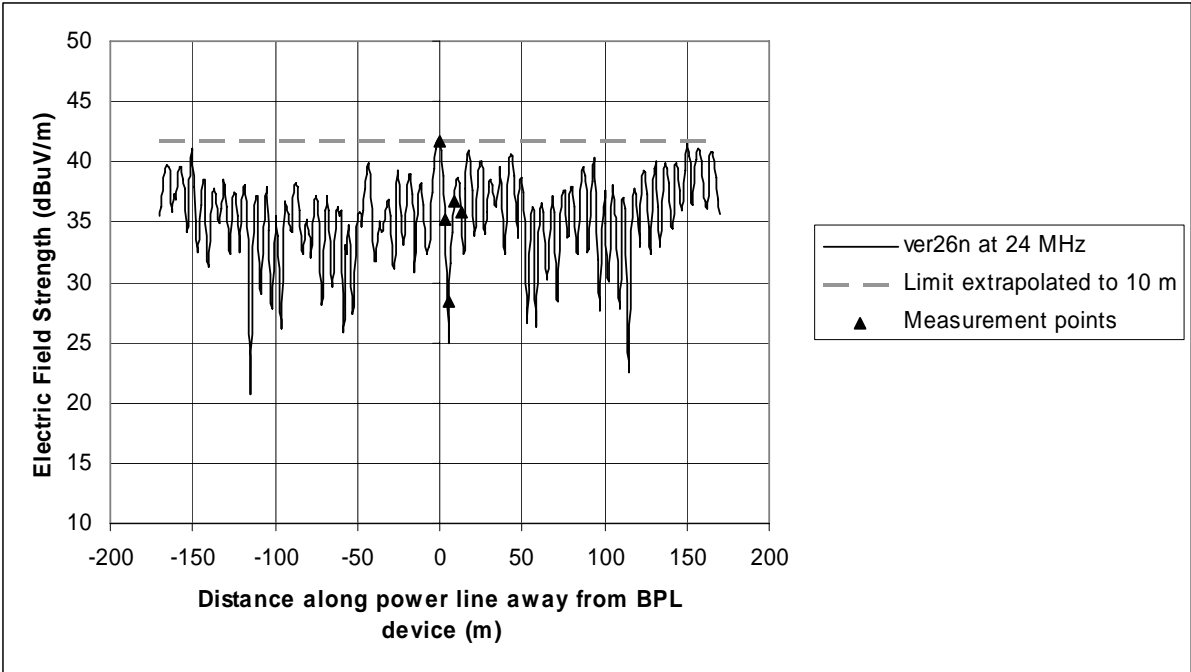


**Figure B-71: Vertical electric field strength along power line for ver26n topology**

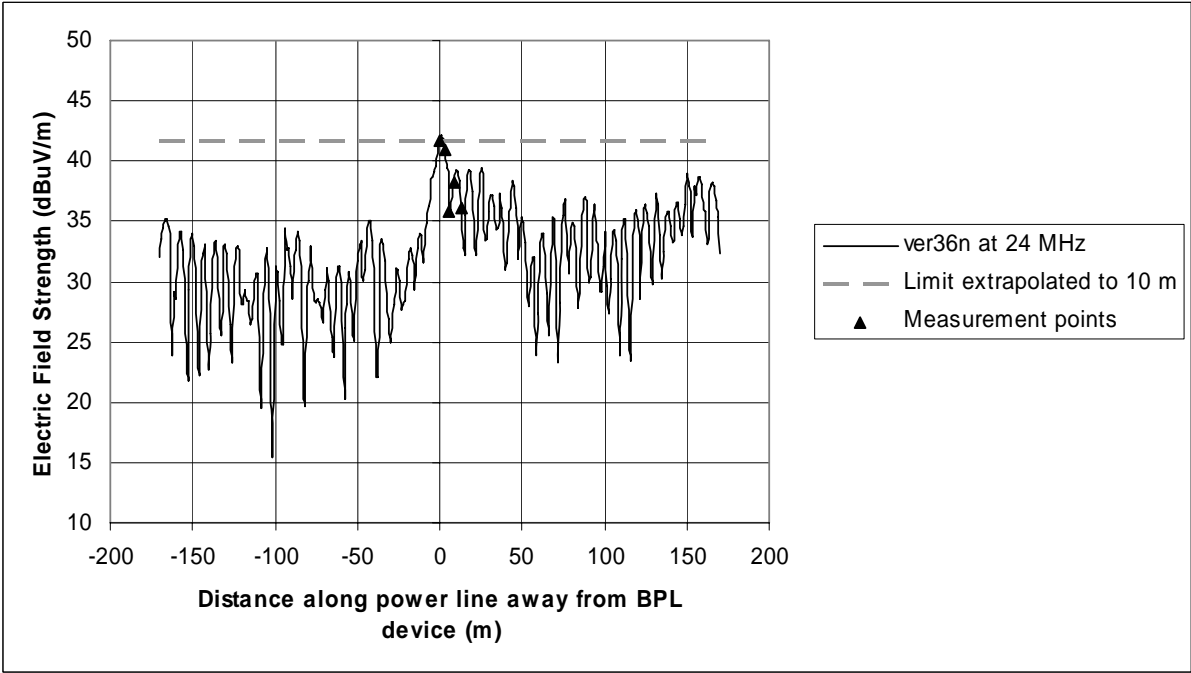


**Figure B-72: Vertical electric field strength along power line for ver36n topology**

26 MHz Plots

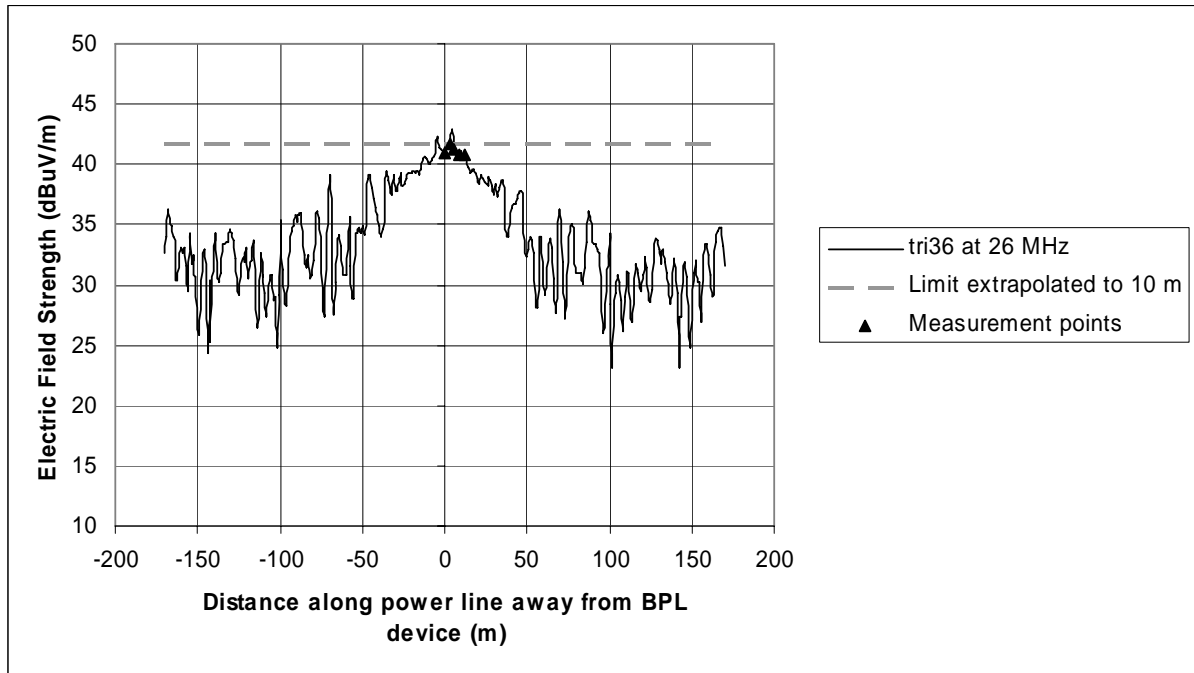


**Figure B-73: Vertical electric field strength along power line for tri36 topology**

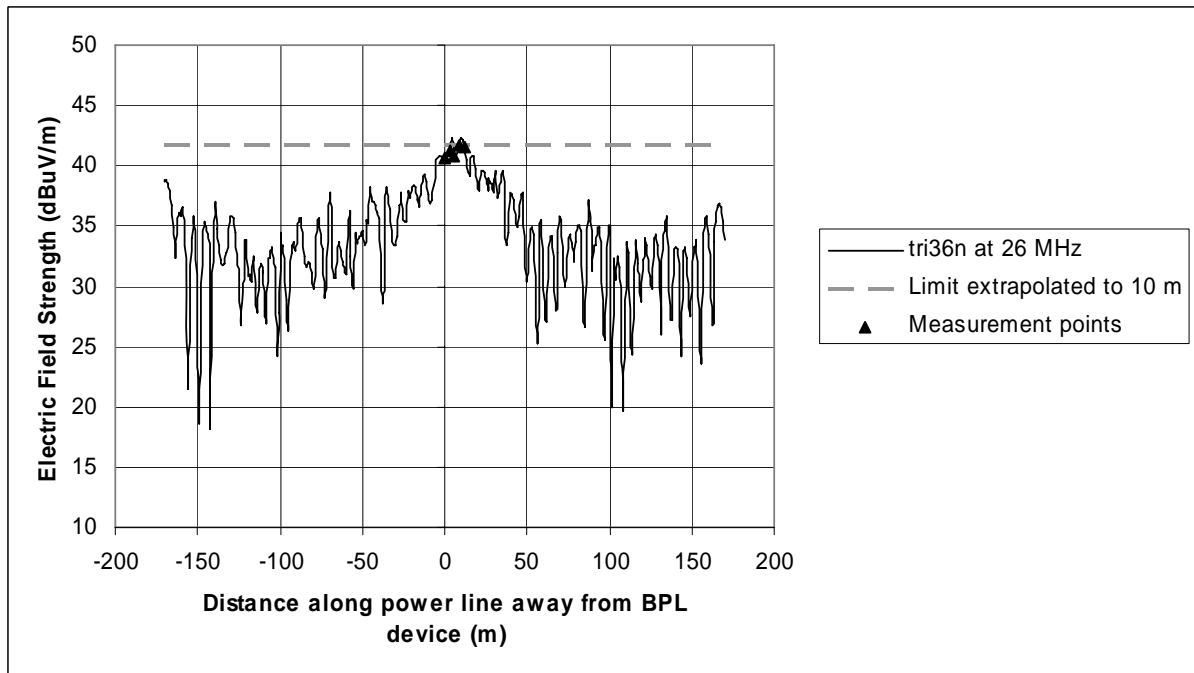


**Figure B-74: Vertical electric field strength along power line for tri36n topology**

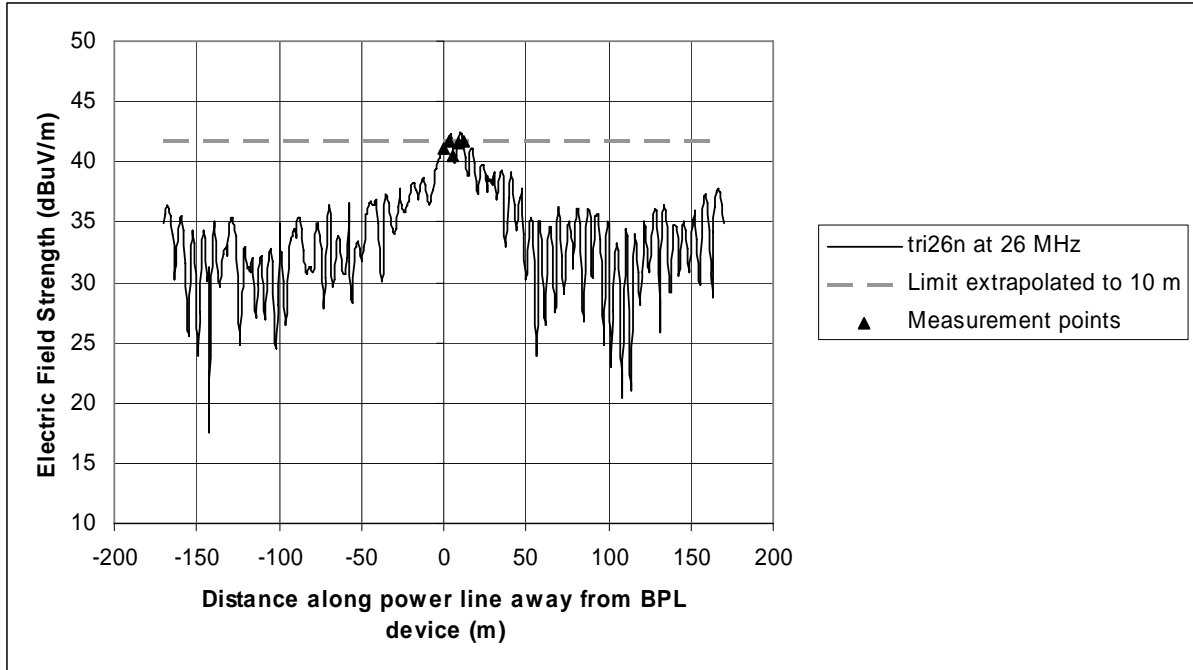


**Figure B-75: Vertical electric field strength along power line for tri26n topology**

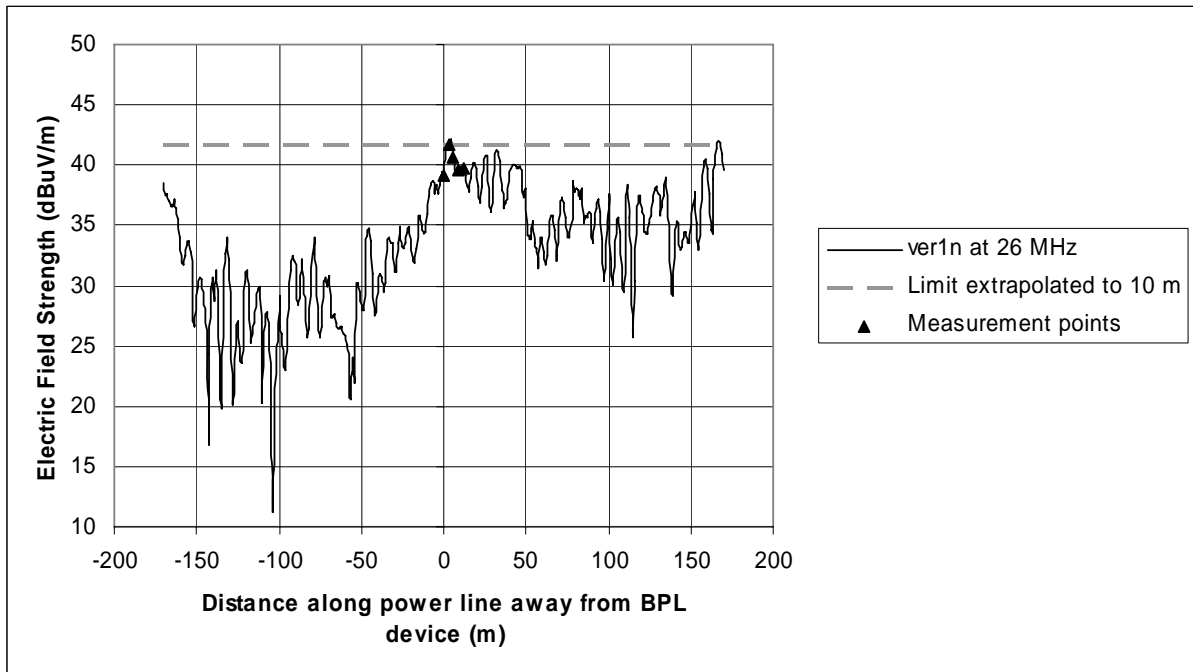


**Figure B-76: Vertical electric field strength along power line for ver1n topology**

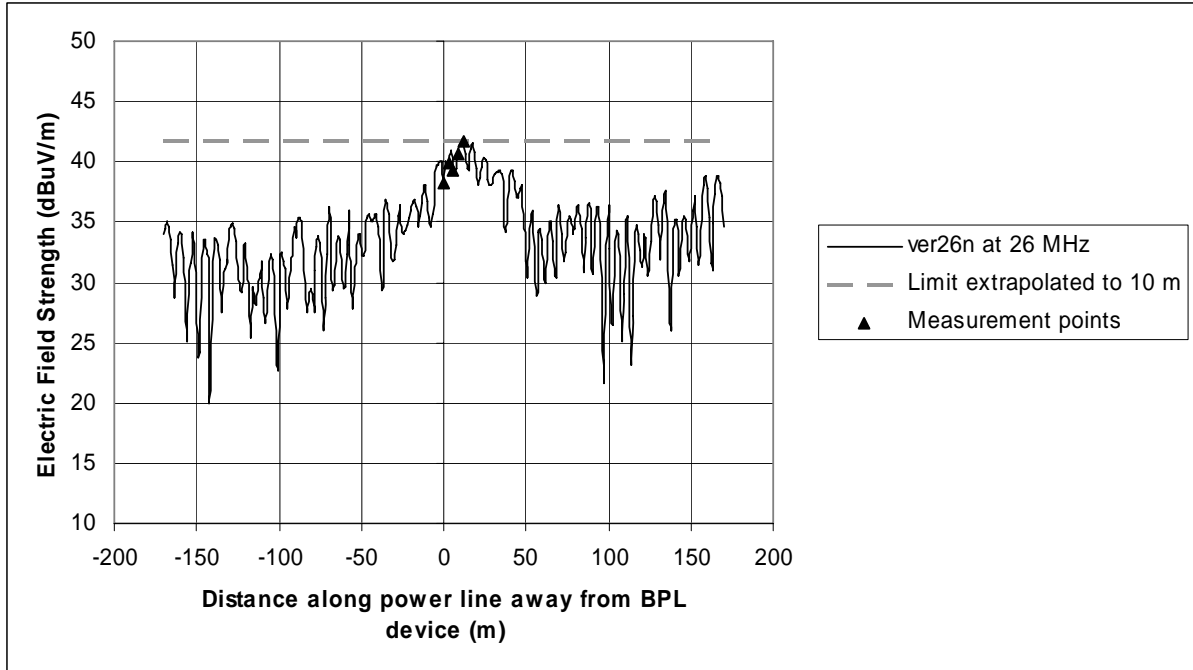


**Figure B-77: Vertical electric field strength along power line for ver26n topology**

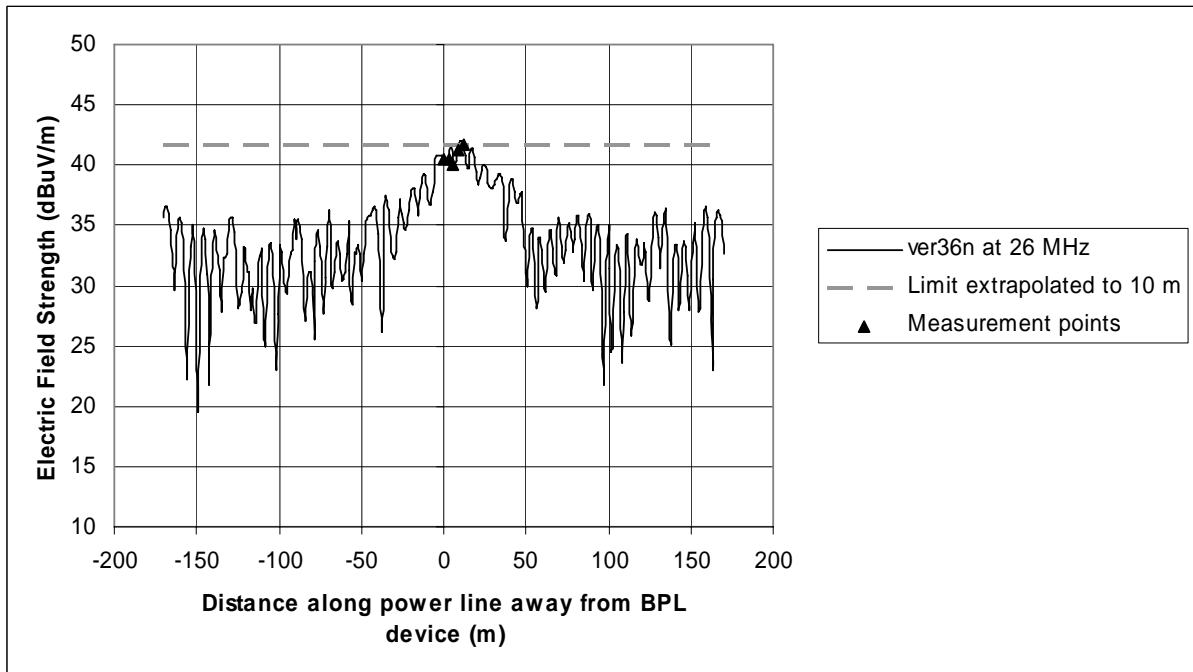


**Figure B-78: Vertical electric field strength along power line for ver36n topology**

28 MHz Plots

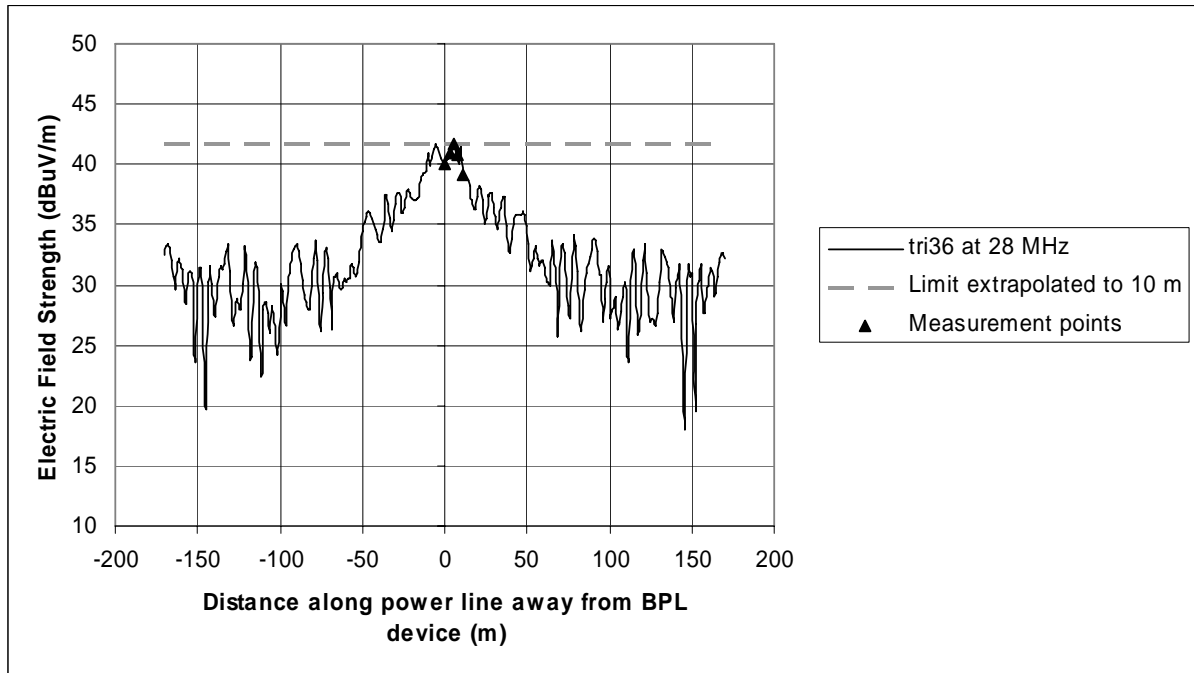


**Figure B-79: Vertical electric field strength along power line for tri36 topology**

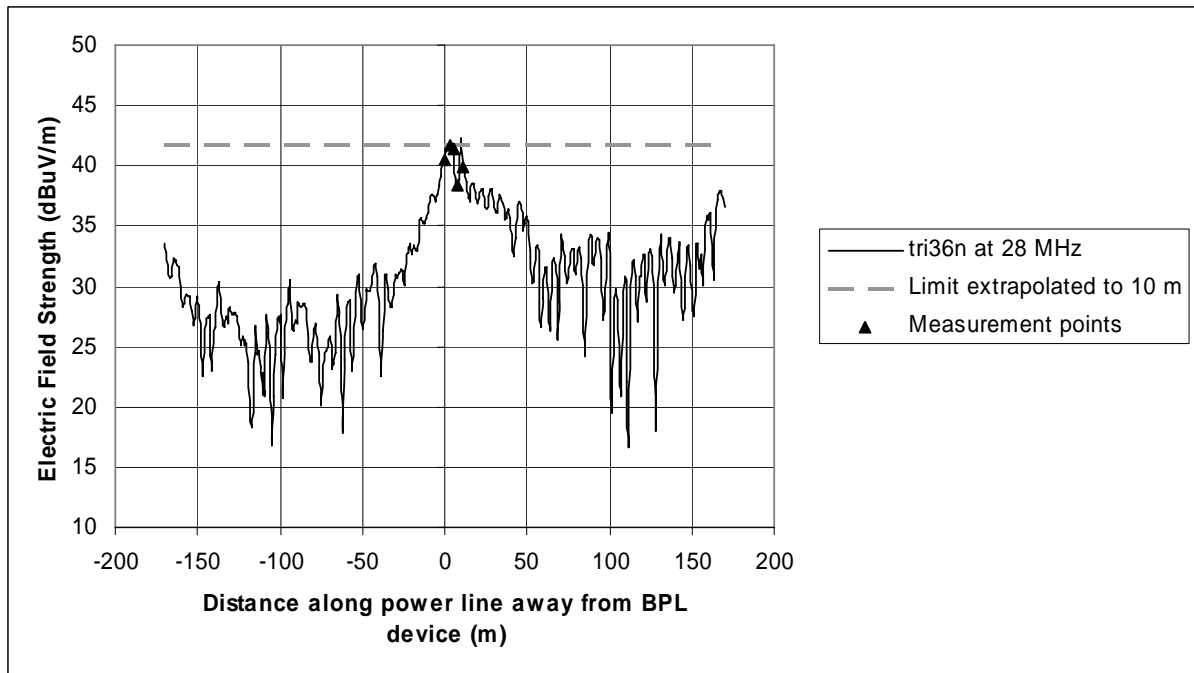


**Figure B-80: Vertical electric field strength along power line for tri36n topology**

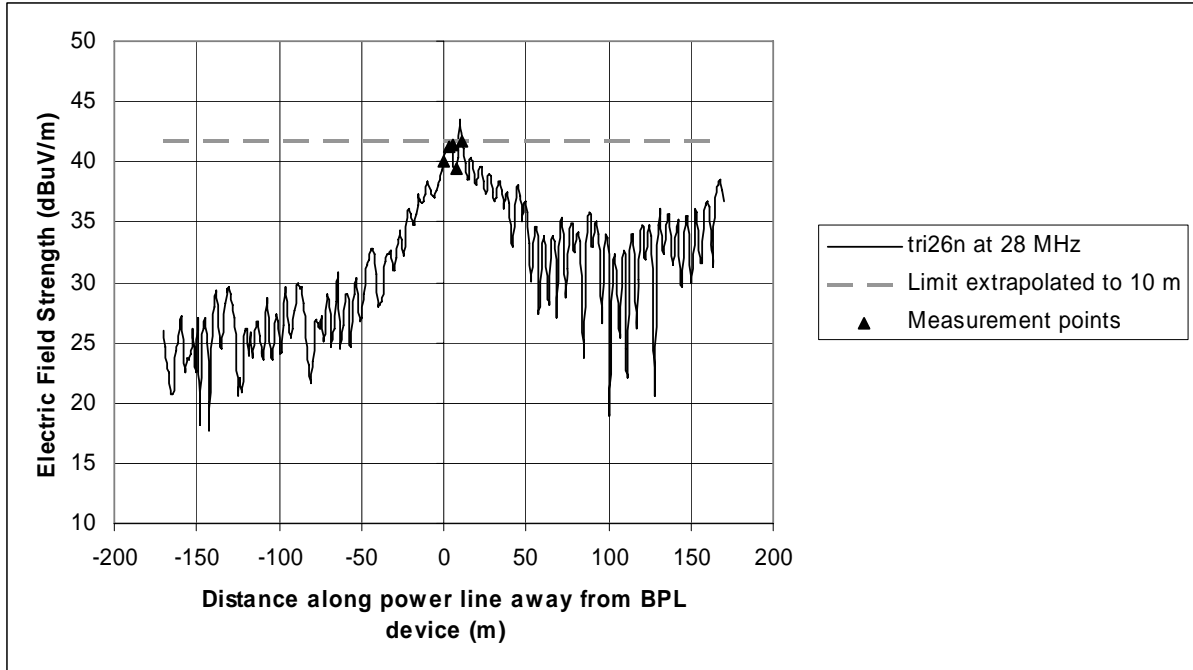


**Figure B-81: Vertical electric field strength along power line for tri26 topology**

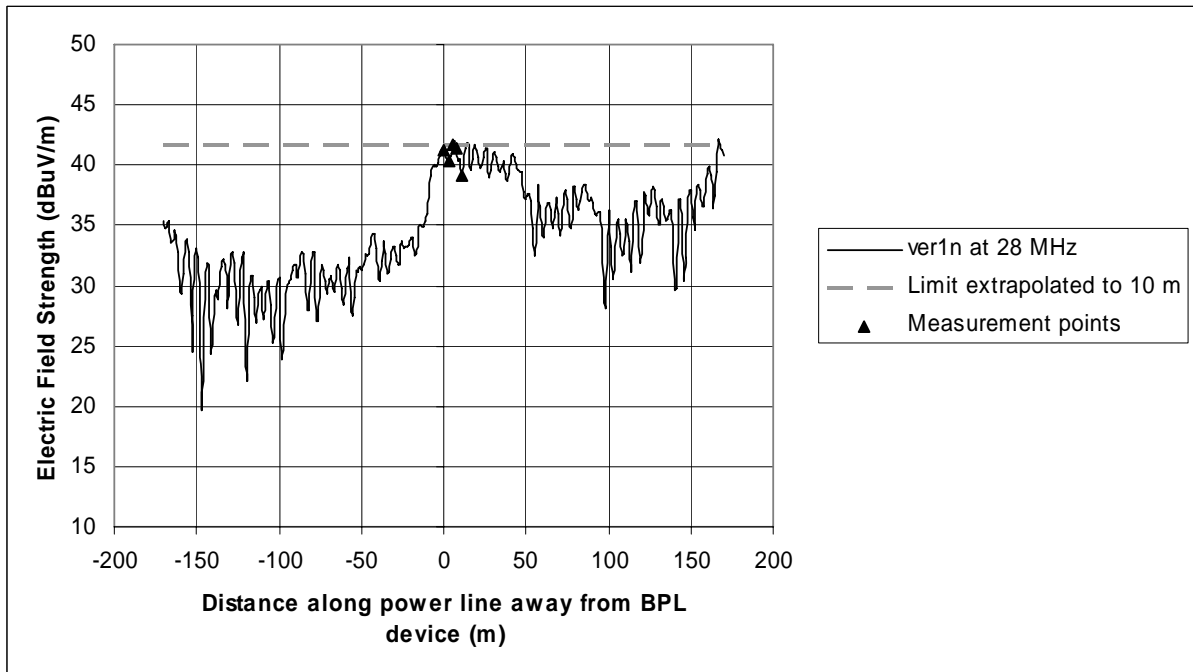


**Figure B-82: Vertical electric field strength along power line for ver1n topology**

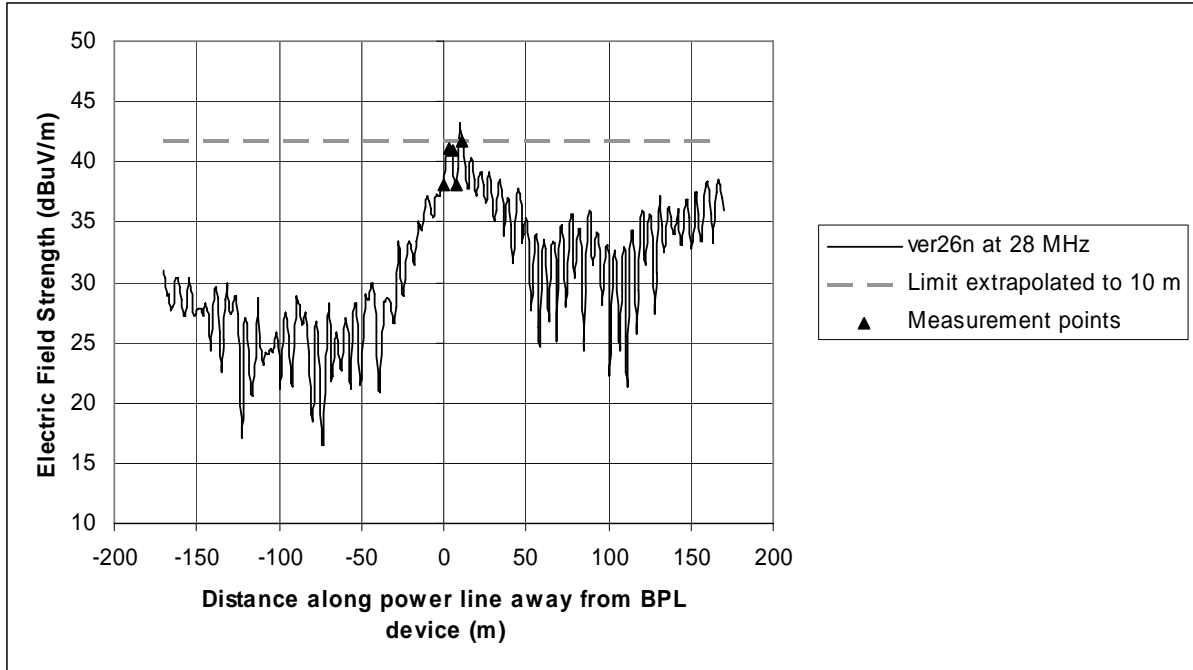


**Figure B-83: Vertical electric field strength along power line for ver26n topology**

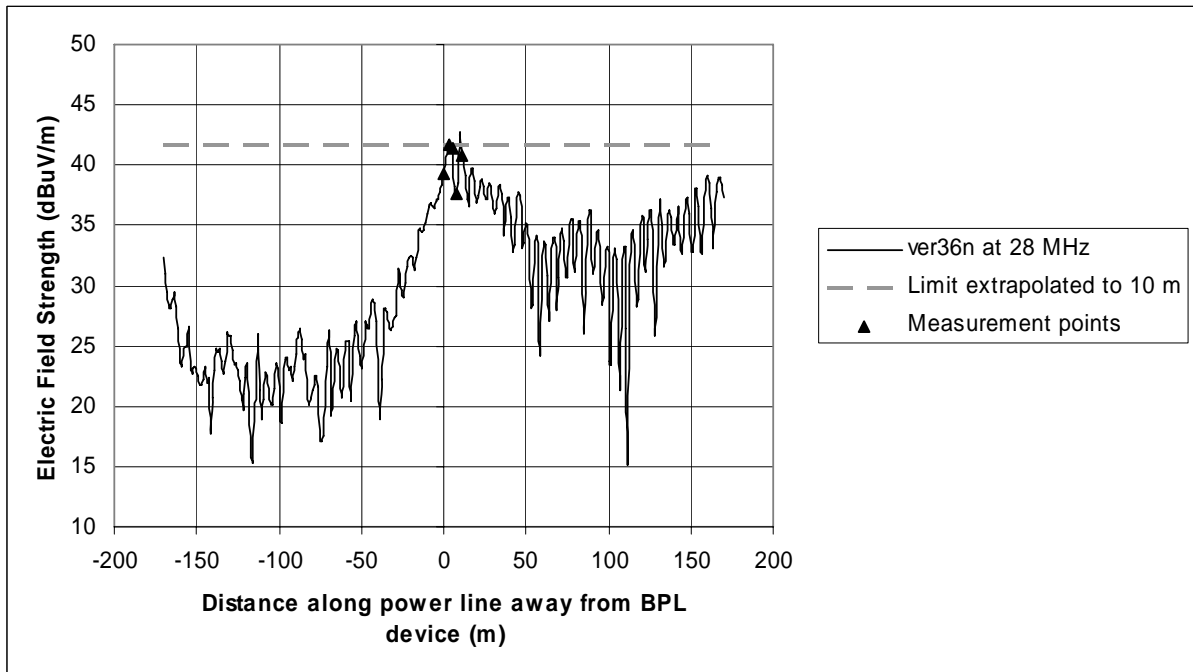


**Figure B-84: Vertical electric field strength along power line for ver36n topology**





# APPENDIX C

## MEASUREMENT DISTANCE EXTRAPOLATION

### C.1 INTRODUCTION

The distance extrapolation calculation based on use of the slant path distance from the BPL device and power lines under test and the measurement antenna was discussed in Section 2.5 of the report. Some of the resulting plots from NTIA's NEC power line model simulations were reported in that section. The remaining plots are included in this appendix.

### C.2 BPL FIELD STRENGTH SIMULATION RESULTS

#### C.2.1 Extrapolated Field Strength Levels Meeting the Part 15 Limits

Figure C-1 shows the extrapolated electric field strength levels that satisfy the Part 15 limits using slant range distance extrapolation, assuming a power line height of 12 meters. The simulated measurement antenna height is assumed to be 1 meter.

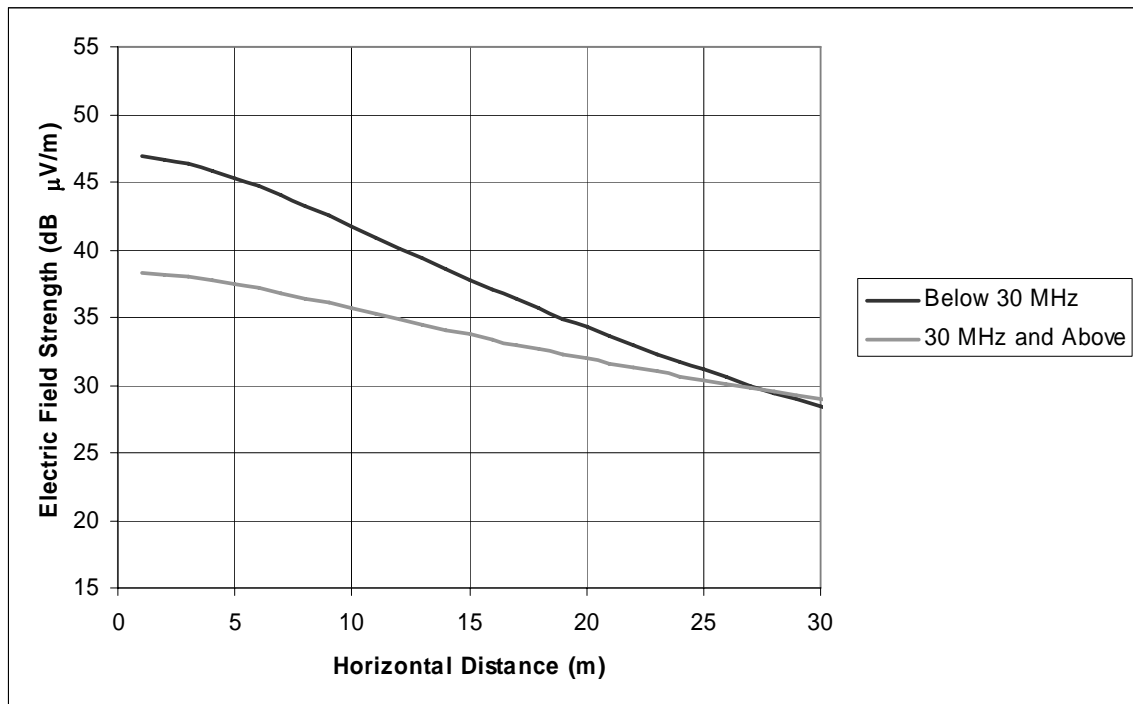


Figure C.1 - Extrapolated field strength levels meeting Part 15 emissions limits based on slant-range distance to the BPL device under test

## C.2.2 Simulation Results

Figures C-2 through C-15 shows the simulated electric field strength moving away from the power line for a number of power line structures that were previously defined in Section 2.2 of the BPL Phase 2 Study. The extrapolated field strength levels meeting the Part 15 emissions limit below 30 MHz are displayed on each figure for comparison. The simulations determined the vertical electric field strength from the horizontal magnetic field strength using the methodology for compliance testing in the Part 15 rules for Access BPL and assuming the electric field strength is related to the magnetic field strength by  $\eta = 377$  ohms ( $\Omega$ ). The peak field strength value was chosen from among the values calculated at points along the line, as defined in the measurement guidelines, at a distance of 10 meters away from the line. The plots of field strength relative to distance are taken from this corresponding location for each case.

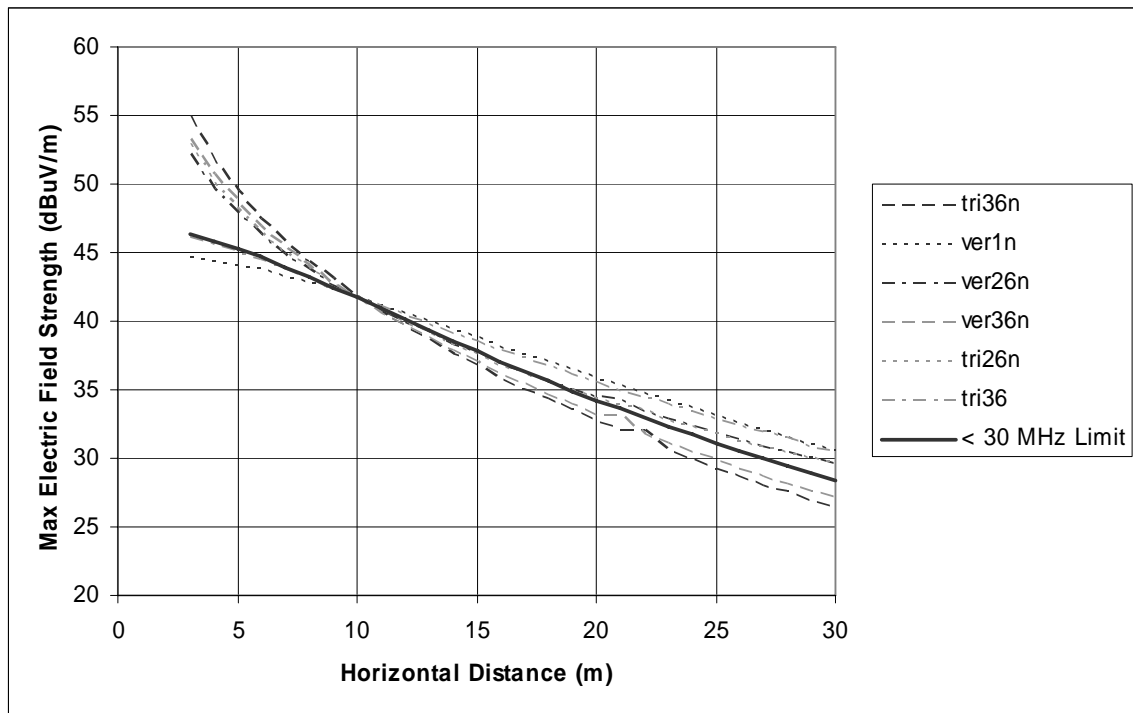
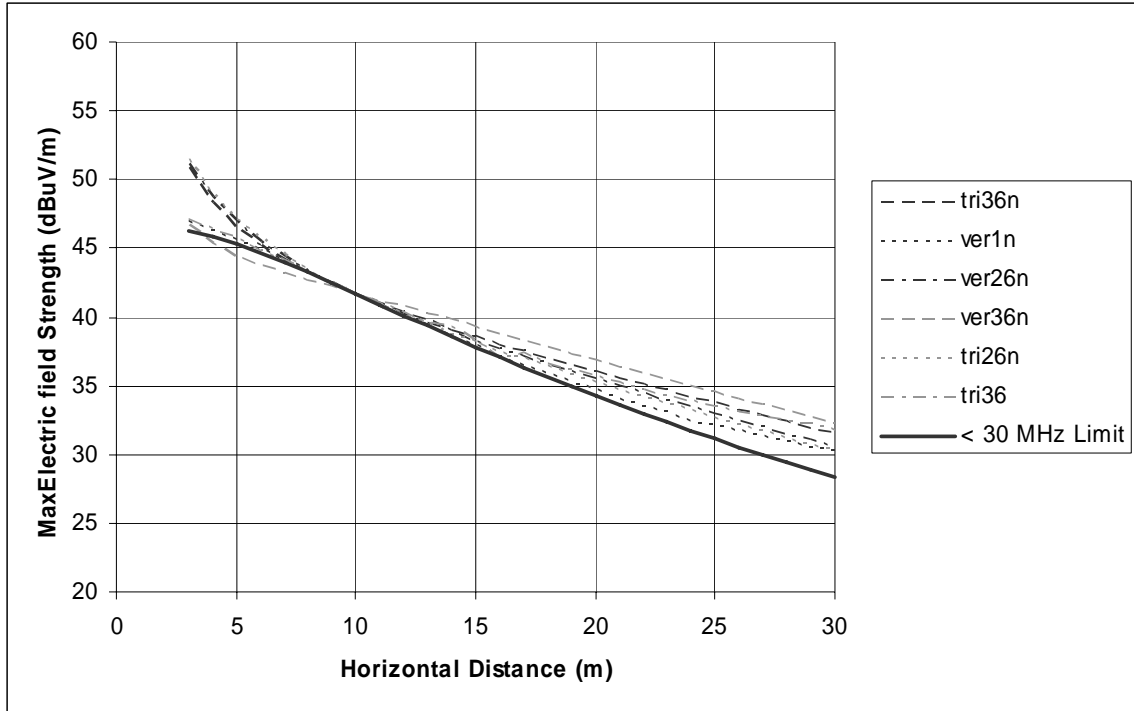
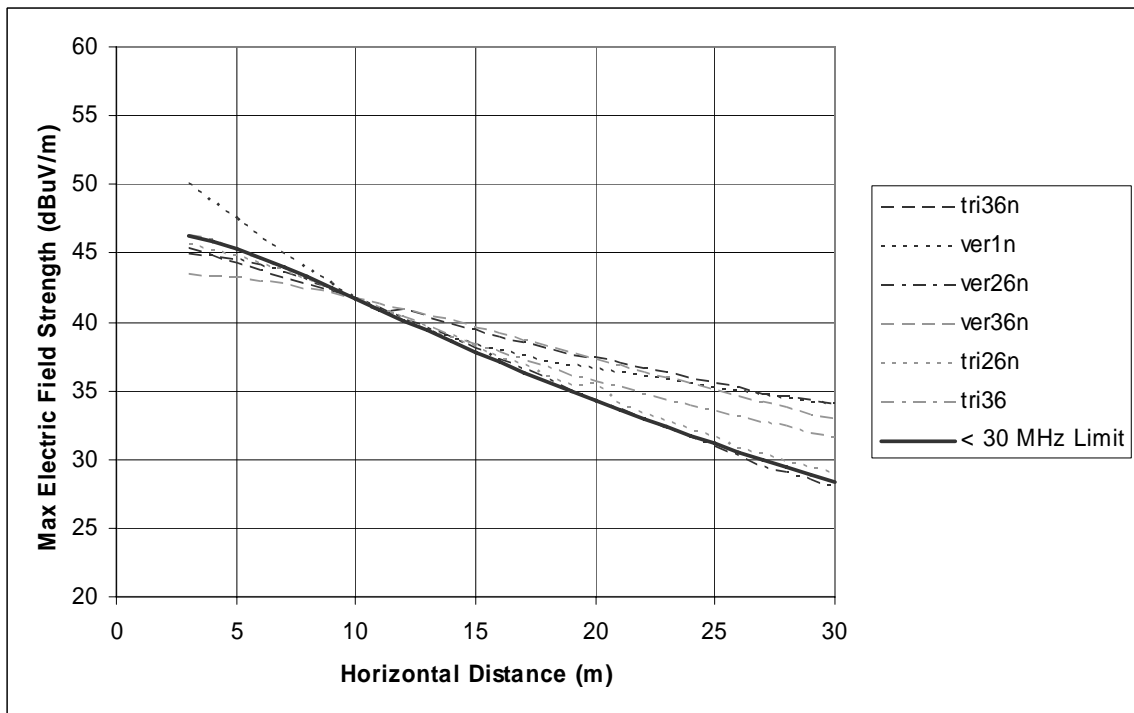


Figure C-2: Electric field strength compared to emissions limit based on slant-range extrapolation for various power line models – 2 MHz



**Figure C-3: Electric field strength compared to emissions limit based on slant-range extrapolation for various power line models – 4 MHz**



**Figure C-4: Electric field strength compared to emissions limit based on slant-range extrapolation for various power line models – 6 MHz**

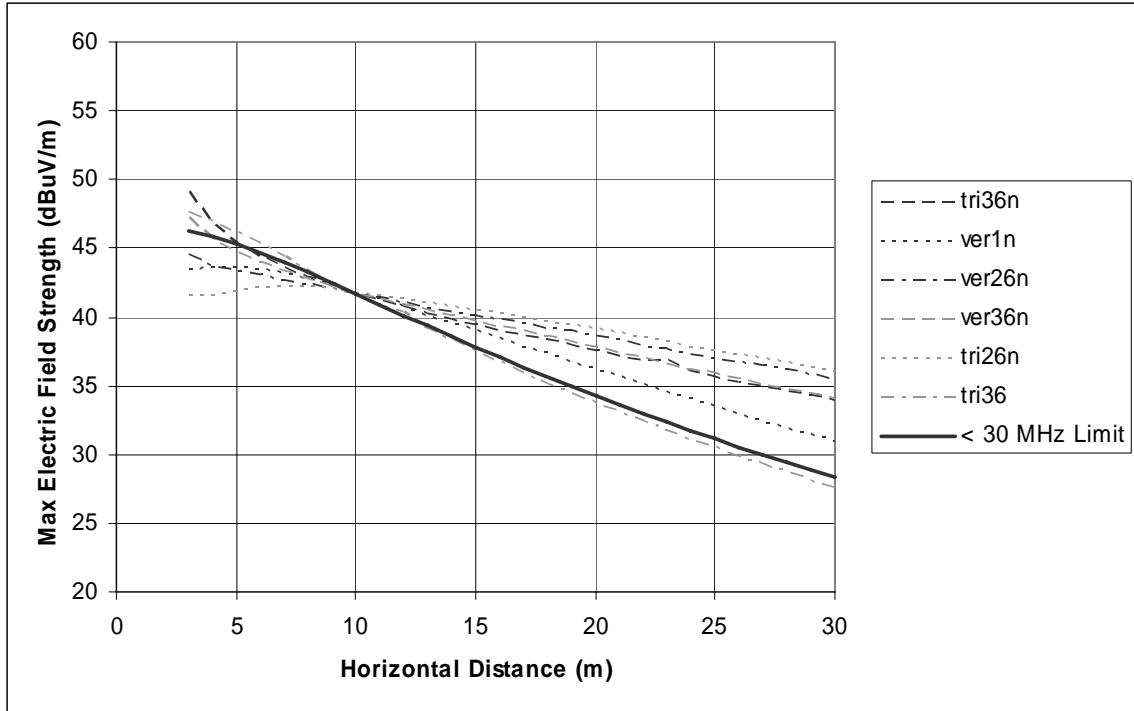


**Figure C-5: Electric field strength compared to emissions limit based on slant-range extrapolation for various power line models – 8 MHz**

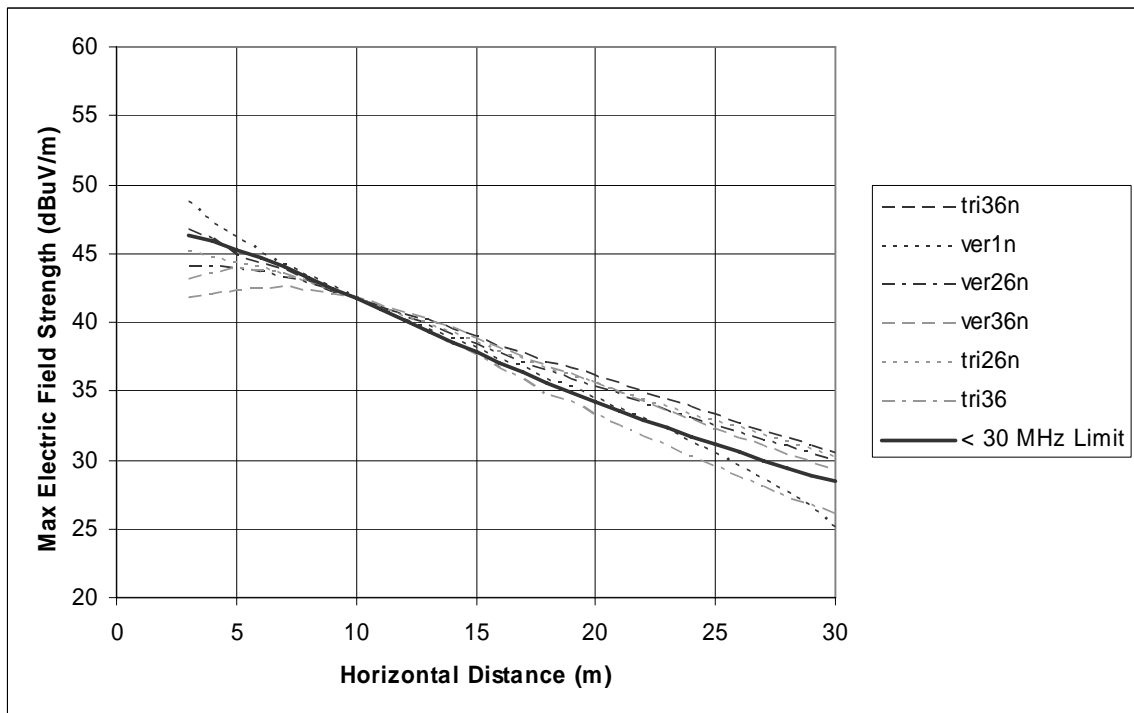


**Figure C-6: Electric field strength compared to emissions limit based on slant-range extrapolation for various power line models – 10 MHz**

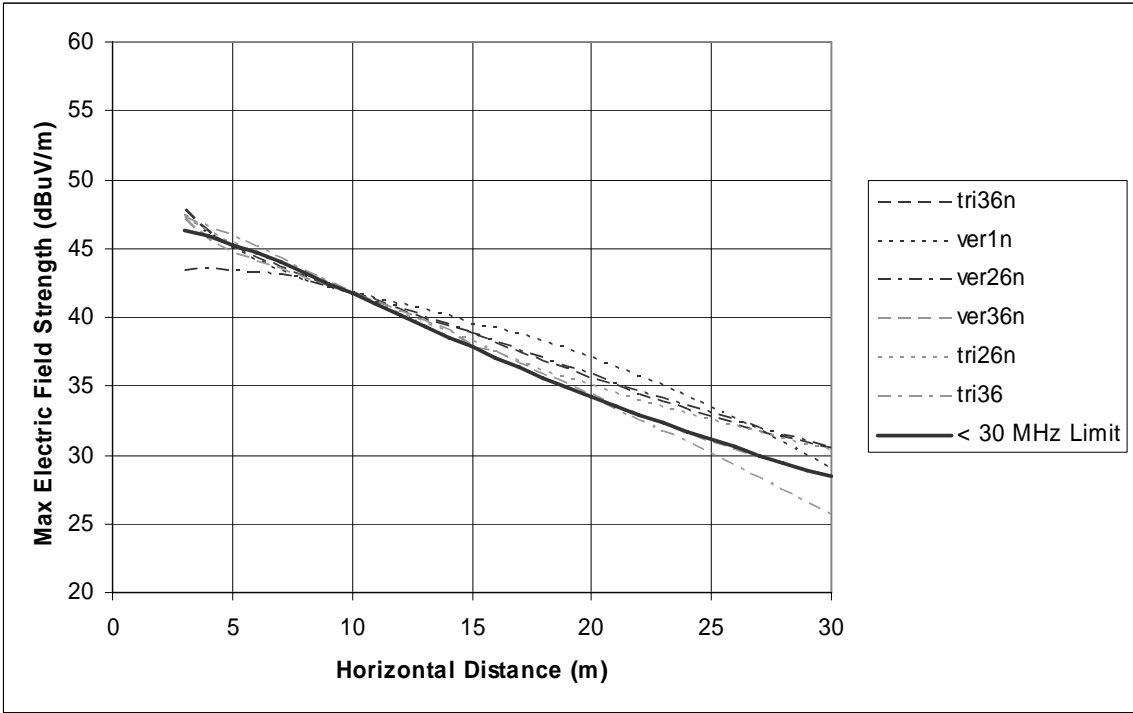


**Figure C-7: Electric field strength compared to emissions limit based on slant-range extrapolation for various power line models – 12 MHz**

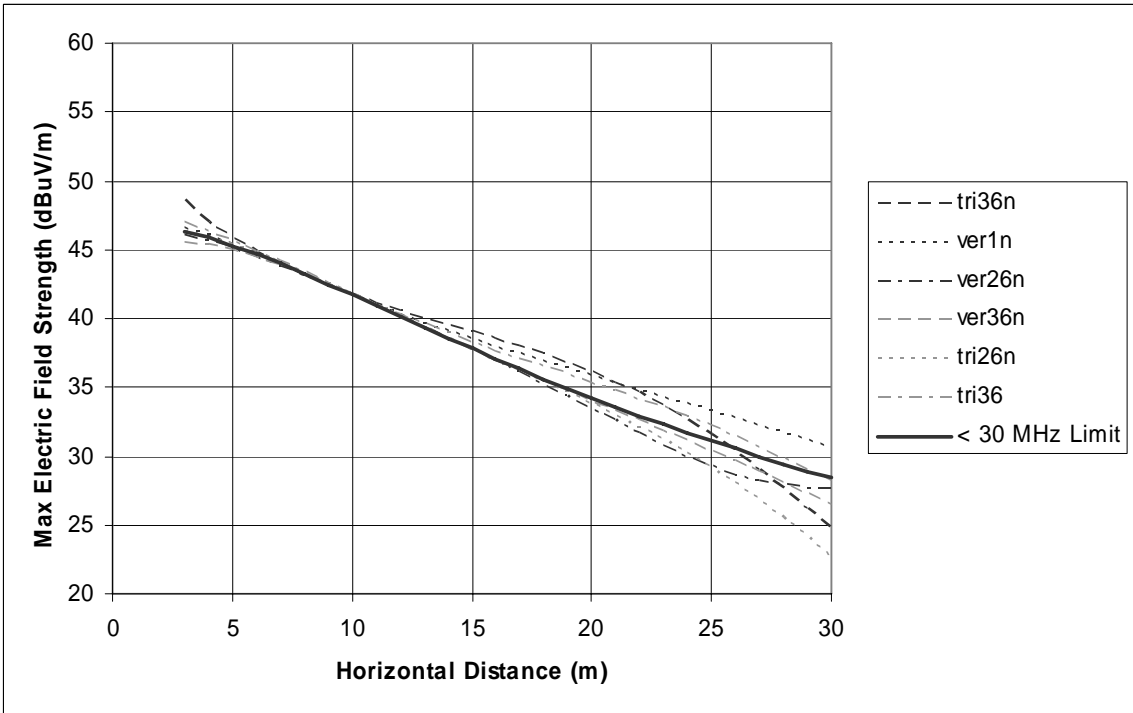


**Figure C-8: Electric field strength compared to emissions limit based on slant-range extrapolation for various power line models – 14 MHz**

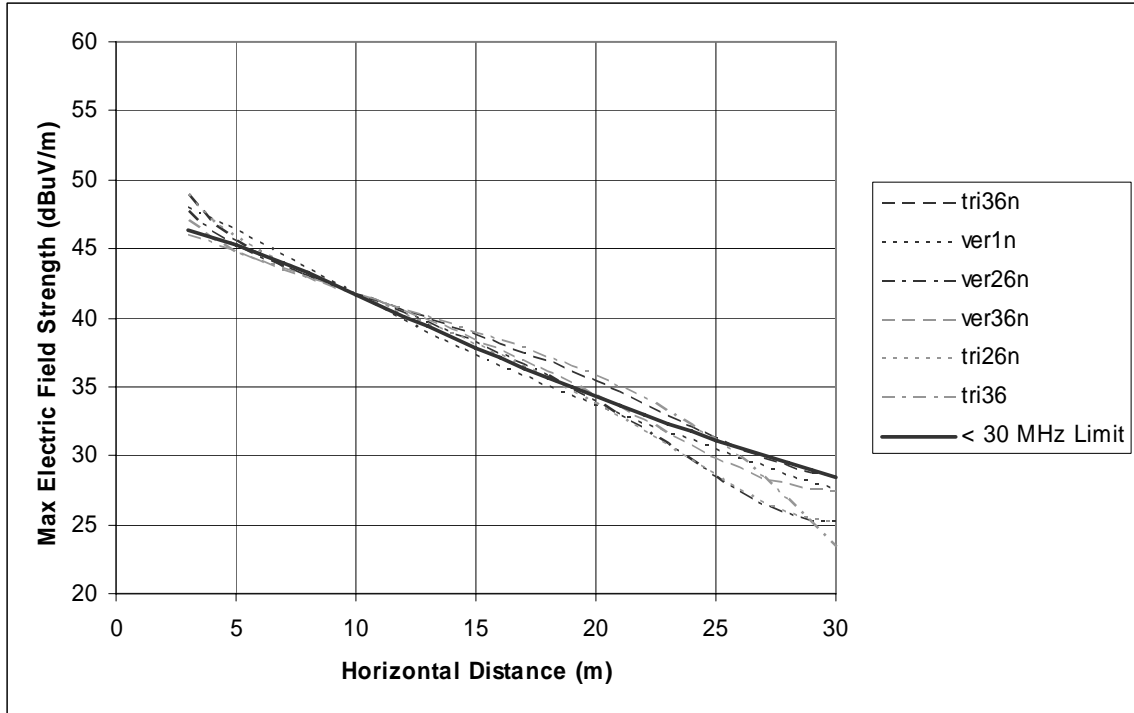


**Figure C-9: Electric field strength compared to emissions limit based on slant-range extrapolation for various power line models – 16 MHz**

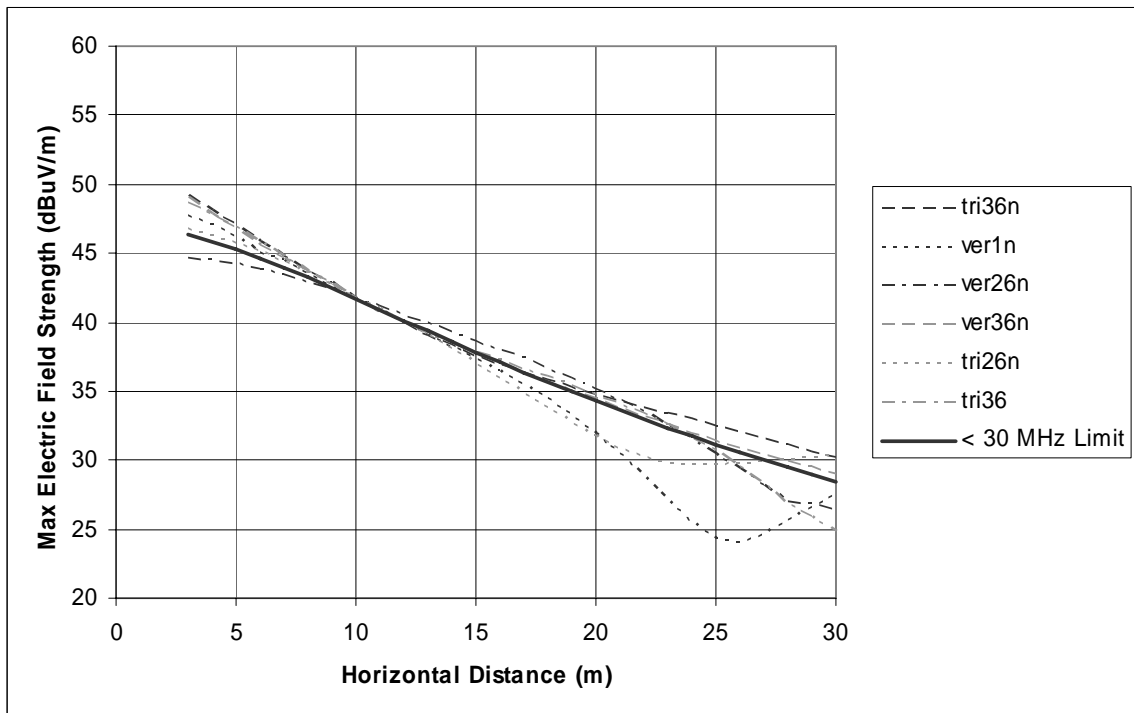


**Figure C-10: Electric field strength compared to emissions limit based on slant-range extrapolation for various power line models – 18 MHz**

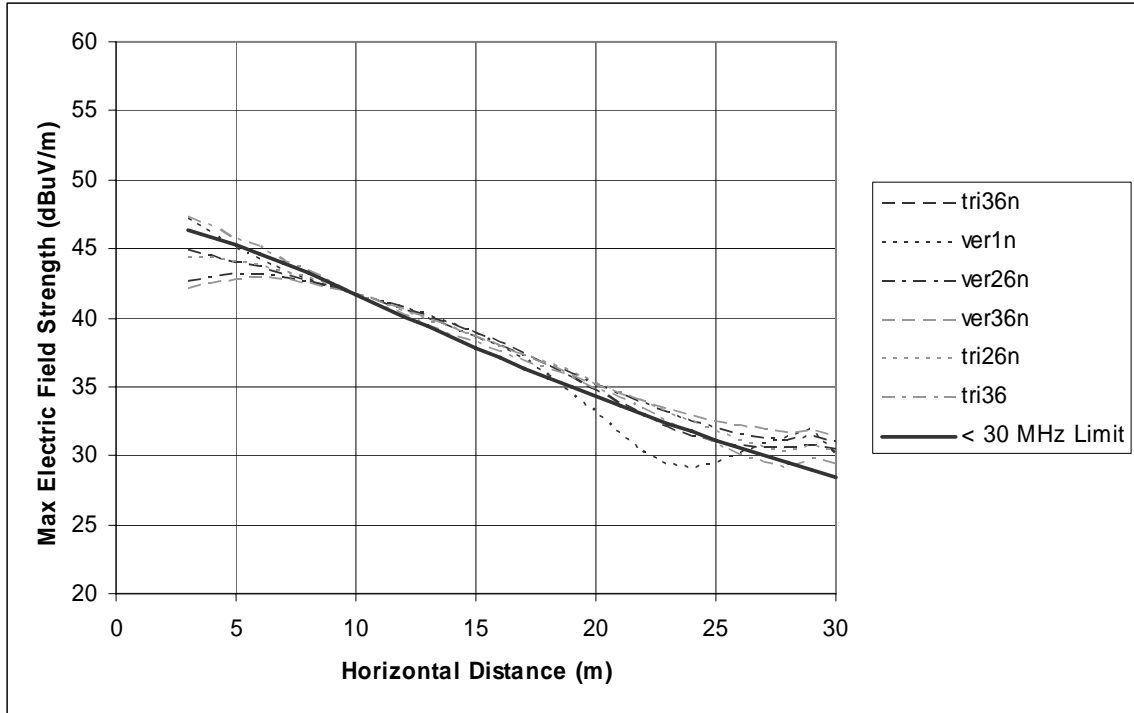


Figure C-11: Electric field strength compared to emissions limit based on slant-range extrapolation for various power line models – 20 MHz

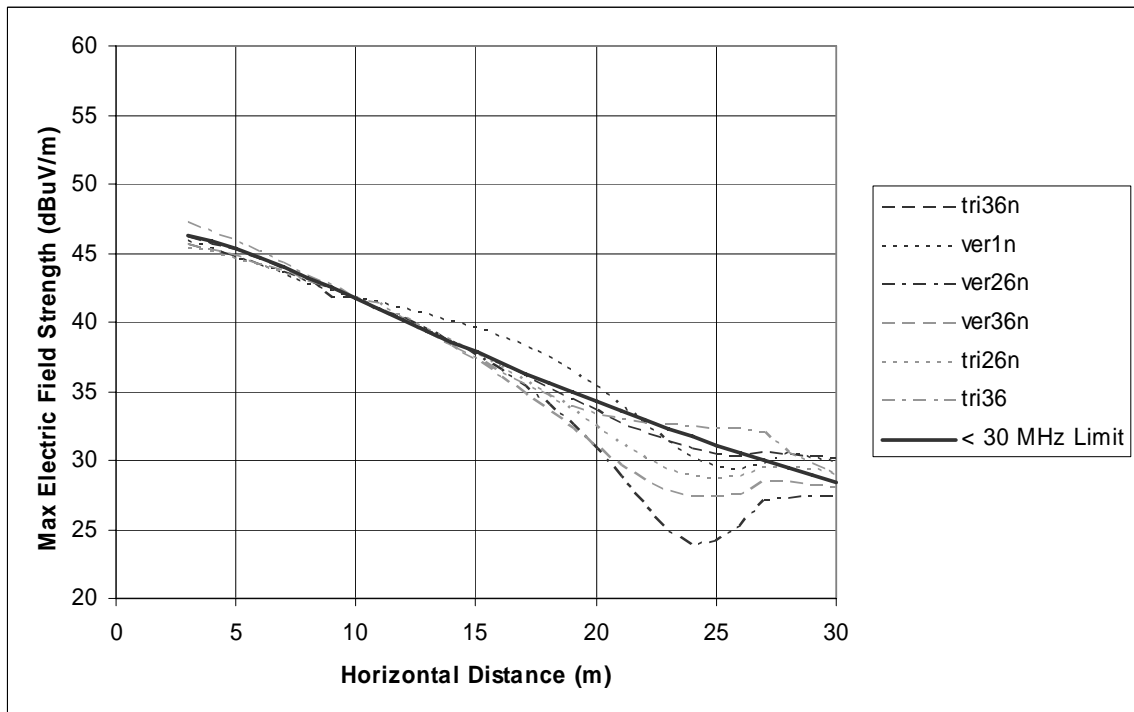
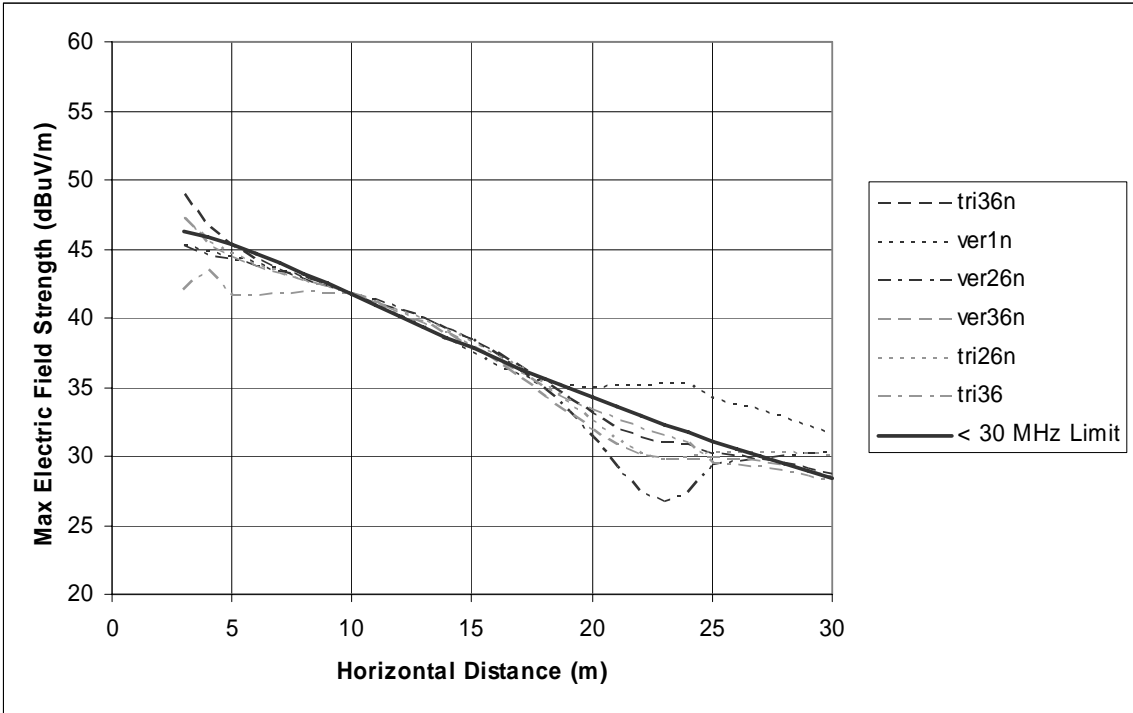
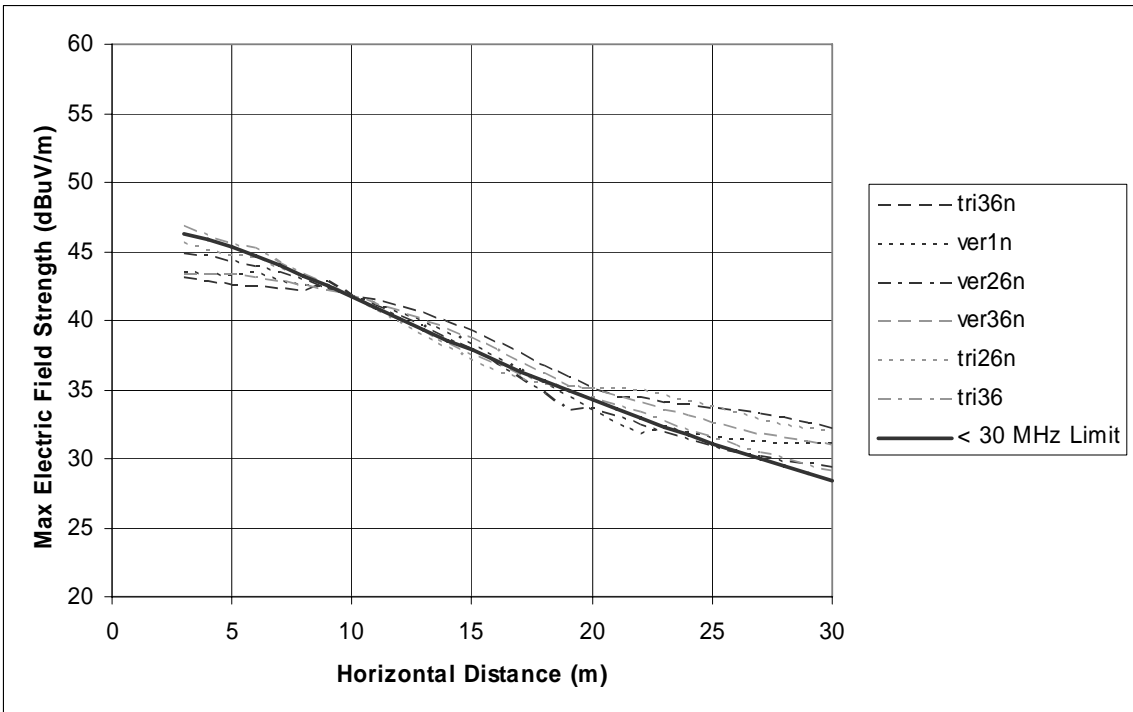


Figure C-12: Electric field strength compared to emissions limit based on slant-range extrapolation for various power line models – 22 MHz



**Figure C-13: Electric field strength compared to emissions limit based on slant-range extrapolation for various power line models – 24 MHz**



**Figure C-14: Electric field strength compared to emissions limit based on slant-range extrapolation for various power line models – 26 MHz**



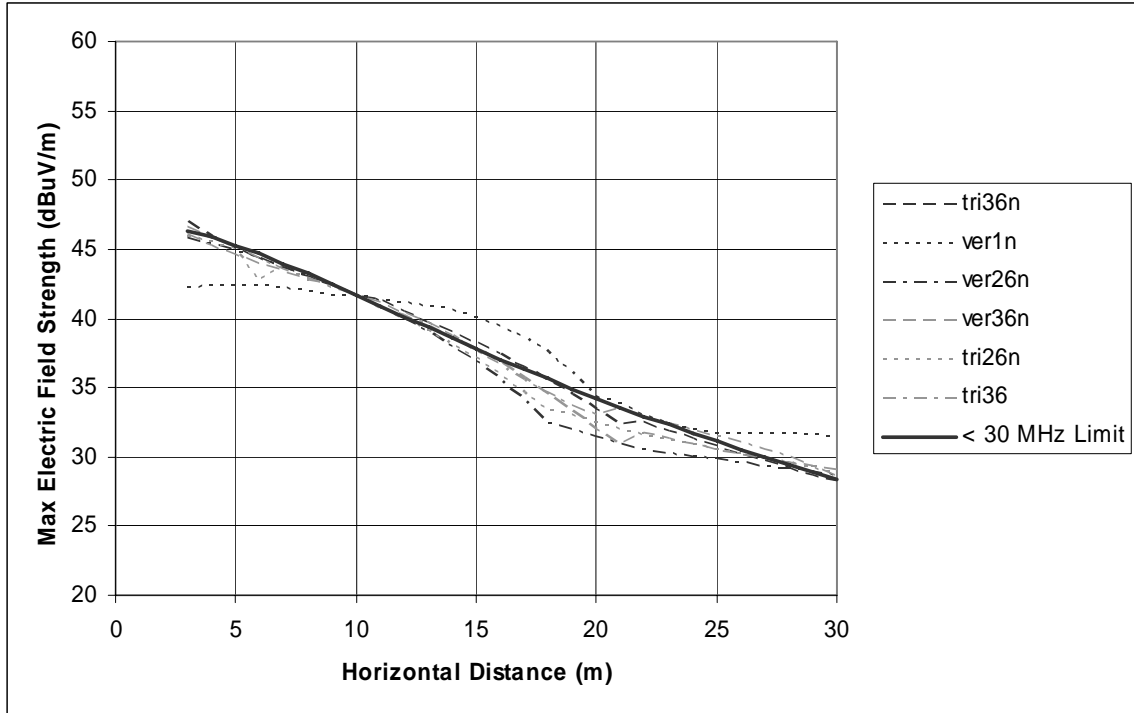


**Figure C-15: Electric field strength compared to emissions limit based on slant-range extrapolation for various power line models – 28 MHz**



## APPENDIX D SPECIAL PROTECTION PROVISIONS

### D.1 EXCLUDED FREQUENCY BANDS

As adopted in the BPL Report and Order, Access BPL emissions from overhead MV power lines are excluded from aeronautical (R) mobile allocations in the 1.7 – 30 MHz frequency range and the 74.8 – 75.2 MHz aeronautical radionavigation band, as delineated in Table D-1. Otherwise, with mature deployments of BPL devices: (1) reception of aeronautical safety communications by aeronautical (land or “base”) stations would be endangered; (2) reception of aeronautical safety communications by aircraft would be endangered; and (3) at some aeronautical station or aircraft locations, emissions from In-House BPL devices at these frequencies will increase receiver noise levels such that additional interfering signals from Access BPL devices cannot be risked. This exclusion amounts to less than 2.18 percent of national spectrum resource between 1.7 MHz and 80 MHz.

**Table D-1: Bands in Which Access BPL Emissions Are Prohibited**

Frequency Band	Total Spectrum (kHz)
2,850 – 3,025 kHz	175
3,400 – 3,500 kHz	100
4,650 – 4,700 kHz	50
5,450 – 5,680 kHz	230
6,525 – 6,685 kHz	160
8,815 – 8,965 kHz	150
10,005 – 10,100 kHz	95
11,275 – 11,400 kHz	100
13,260 – 13,360 kHz	100
17,900 – 17,970 kHz	70
21,924 – 22,000 kHz	76
74.8 – 75.2 MHz	400
TOTAL BANDWIDTH	1,706
U.S. AREA FACTOR	1.0
PORTION OF NATIONAL SPECTRUM RESOURCE AT 1.7 – 80 MHz	< 2.18% (area factor x bandwidth factor)

### D.2 EXCLUSION ZONES

#### D.2.1 Coast Stations

The analytical results of Section 3.3.1 lead to a requirement to define exclusion zones in the 2,173.5-2,190.5 kHz band within 1 km of coast station facilities, whose coordinates are listed in Tables D-2 and D-3. This amounts to 0.022 percent of the

bandwidth between 1.7 MHz and 80 MHz and less than 0.004 percent of U.S. territorial area, or less than 0.0000008 percent of national spectrum resource between 1.7 MHz and 80 MHz. This special protection requirement will prevent substantial endangerment of distress alerting by ships and aircraft in oceanic areas. In the event that an Access BPL operator plans to deploy numerous Access BPL devices at these frequencies in areas near these exclusion zones, consult with the following point of contact may best ensure that harmful interference is prevented at these facilities:

Commandant (CG 622)  
 U.S. Coast Guard  
 2100 2<sup>nd</sup> Street, S.W.  
 Washington, DC 20593 – 0001  
 Telephone: (202) 267 – 2860  
 E-Mail: cgcomms@comdt.uscg.mil

**Table D-2: Exclusion zones for U.S. Coast Guard Coast Stations**

<b>Locale</b>	<b>Latitude</b>	<b>Longitude</b>
Group Guam	13° 35' 23" N	144° 50' 24" E
GANTSEC	18° 18' 00" N	65° 46' 59" W
Puerto Rico	18° 28' 11" N	66° 07' 47" W
Honolulu	21° 18' 21" N	157° 53' 23" W
Group Key West	24° 33' 35" N	81° 47' 59" W
Trumbo Point CG Base	24° 33' 58" N	81° 47' 57" W
Miami	25° 37' 28" N	80° 23' 07" W
Everglades Park	25° 50' 10" N	81° 23' 13" W
Group Saint Petersburg (Everglades)	25° 51' 00" N	81° 23' 24" W
Station Ft. Lauderdale	26° 05' 21" N	80° 06' 40" W
Station Ft. Myers Beach	26° 27' 34" N	81° 57' 15" W
Group Miami (Ft. Pierce)	27° 27' 36" N	80° 18' 36" W
Station Ft. Pierce	27° 27' 50" N	80° 18' 27" W
Group Corpus Christi	27° 42' 01" N	97° 16' 11" W
Group Corpus Christi	27° 42' 06" N	97° 16' 45" W
ESD Saint Petersburg	27° 45' 21" N	82° 37' 32" W
Group Saint Petersburg	27° 46' 11" N	82° 37' 47" W
Station Port O'Connor	28° 26' 03" N	96° 25' 39" W
S. Padre Island	28° 26' 22" N	97° 09' 56" W
Freeport	28° 55' 59" N	95° 16' 59" W
Group Galveston (Freeport)	28° 56' 24" N	95° 17' 59" W
Station YANKEETOWN	29° 01' 51" N	82° 43' 39" W
Station Ponce De Leon Inlet	29° 03' 50" N	81° 55' 01" W
Group New Orleans (Grand Isle)	29° 15' 53" N	89° 57' 26" W
Galveston	29° 19' 59" N	94° 46' 18" W
Kapalan	29° 20' 04" N	94° 47' 17" W
Sabine	29° 43' 42" N	93° 52' 14" W
New Orleans	30° 01' 17" N	90° 07' 24" W
Panama City	30° 10' 01" N	85° 45' 04" W
Group Mobile (Panama City)	30° 10' 12" N	85° 45' 36" W

<b>Locale</b>	<b>Latitude</b>	<b>Longitude</b>
ANT Jacksonville Beach	30° 17' 16" N	81° 24' 10" W
Pensacola	30° 20' 24" N	87° 18' 17" W
Group Mayport	30° 23' 10" N	81° 26' 01" W
Group Mayport	30° 23' 24" N	81° 25' 48" W
Ft. Morgan	30° 39' 07" N	88° 03' 12" W
Tybee Lighthouse	32° 01' 15" N	80° 50' 39" W
Point Loma Lighthouse	32° 39' 56" N	117° 14' 34" W
Point Loma	32° 40' 07" N	117° 14' 14" W
Activities San Diego	32° 43' 59" N	117° 11' 13" W
Group Charleston (Sullivan's Island)	32° 45' 00" N	79° 49' 47" W
Sullivan's Island Lights	32° 45' 02" N	79° 50' 03" W
Group Charleston	32° 46' 25" N	79° 56' 37" W
Group San Diego	32° 52' 48" N	118° 26' 23" W
San Pedro	33° 45' 00" N	118° 15' 58" W
Group Fort Macon	33° 53' 24" N	78° 01' 48" W
Point Mugu	33° 59' 32" N	119° 07' 18" W
Group LA / Long Beach	34° 07' 11" N	119° 06' 35" W
Channel Island	34° 09' 17" N	119° 13' 11" W
Station Oxnard Channel Island	34° 09' 43" N	119° 13' 19" W
Group Ft. Macon	34° 41' 48" N	76° 40' 59" W
Group Cape Hatteras	35° 13' 59" N	75° 31' 59" W
Group Cape Hatteras	35° 15' 35" N	75° 31' 48" W
Morro Bay (Cambria)	35° 31' 21" N	121° 03' 21" W
San Clemente Island	32° 50' 24" N	118° 23' 15" W
Point Pinos	36° 38' 12" N	121° 56' 06" W
CAMSLANT	36° 43' 47" N	76° 01' 11" W
Group Hampton Roads	36° 53' 01" N	76° 21' 10" W
Point Montara	37° 31' 23" N	122° 30' 47" W
Point Montara Lighthouse	37° 32' 09" N	122° 31' 08" W
Group San Francisco	37° 32' 23" N	122° 31' 11" W
Group San Francisco	37° 48' 34" N	122° 21' 55" W
Point Bonita	37° 49' 00" N	122° 31' 41" W
Group Eastern Shores	37° 55' 47" N	75° 22' 47" W
Group Eastern Shore	37° 55' 50" N	75° 22' 58" W
CAMPSPAC	38° 06' 00" N	122° 55' 48" W
Point Arena Lighthouse	38° 57' 18" N	124° 44' 28" W
Point Arena	38° 57' 36" N	123° 44' 23" W
Group Atlantic City	39° 20' 59" N	74° 27' 42" W
Activities New York	40° 36' 06" N	74° 03' 36" W
Activities New York	40° 37' 11" N	74° 04' 11" W
ESD Moriches Hut	40° 47' 19" N	72° 44' 53" W
Group Moriches	40° 47' 23" N	72° 45' 00" W
Group Humboldt Bay	40° 58' 41" N	124° 06' 31" W
Group Humboldt Bay	40° 58' 47" N	124° 06' 35" W
Trinidad Head	41° 03' 15" N	124° 09' 02" W
Group Long Island Sound	41° 16' 12" N	72° 54' 00" W
Station New Haven	41° 16' 12" N	72° 54' 06" W

<b>Locale</b>	<b>Latitude</b>	<b>Longitude</b>
Station Brant Point	41° 17' 21" N	70° 05' 31" W
Group Woods Hole	41° 17' 23" N	70° 04' 47" W
Station Castle Hill	41° 27' 46" N	71° 21' 42" W
Group Woods Hole	41° 30' 30" N	70° 41' 42" W
Boston Area	41° 40' 12" N	70° 31' 48" W
Station Provincetown	42° 01' 48" N	70° 12' 42" W
Eastern Point	42° 36' 24" N	70° 39' 26" W
Cape Blanco	42° 50' 16" N	124° 33' 52" W
Group North Bend	43° 24' 16" N	124° 13' 22" W
Group North Bend	43° 24' 35" N	124° 14' 23" W
Cape Elizabeth	43° 33' 28" N	70° 12' 00" W
Group South Portland	43° 38' 24" N	70° 15' 00" W
Group South Portland	43° 38' 45" N	70° 14' 51" W
Group SW Harbor	44° 16' 19" N	68° 18' 27" W
Group Southwest Harbor	44° 16' 48" N	68° 18' 36" W
Fort Stevens, Oregon	46° 09' 14" N	123° 53' 07" W
Group Astoria	46° 09' 29" N	123° 31' 48" W
Group Astoria	46° 09' 35" N	123° 53' 24" W
La Push	47° 49' 00" N	124° 37' 59" W
Station Quillayute River	47° 54' 49" N	124° 38' 01" W
Port Angeles	48° 07' 59" N	123° 25' 59" W
Group Port Angeles	48° 08' 24" N	123° 24' 35" W
Juneau (Sitka)	57° 05' 24" N	135° 15' 35" W
Kodiak	57° 40' 47" N	152° 28' 47" W
Valdez (Cape Hinchinbrook)	60° 26' 23" N	146° 25' 48" W

**Table D-3: Exclusion zones for Maritime Public Coast Stations**

<b>Licensee Name</b>	<b>Location</b>	<b>Latitude</b>	<b>Longitude</b>
Shipcom LLC	Marina Del Ray, CA	33° 56' 21" N	118° 27' 14" W
Globe Wireless	Rio Vista, CA	38° 11' 55" N	121° 48' 34" W
Avalon Communications Corp	St. Thomas, VI	18° 21' 19" N	64° 56' 48" W
Globe Wireless	Bishopville, MD	38° 24' 10" N	75° 12' 59" W
Shipcom LLC	Mobile, AL	30° 40' 07" N	88° 10' 23" W
Shipcom, LLC	Coden, AL	30° 22' 35" N	88° 12' 20" W
Globe Wireless	Pearl River, LA	30° 22' 13" N	89° 47' 26" W
Globe Wireless	Kahalelani, HI	21° 10' 33" N	157° 10' 39" W
Globe Wireless	Palo Alto, CA	37° 26' 44" N	122° 06' 48" W
Globe Wireless	Agana, GU	13° 29' 22" N	144° 49' 39" E

### **D.2.2 Radioastronomy Observatories**

Using correlation techniques, the Very Large Array (VLA) receivers operate with desired signal levels that are well below ambient noise levels and rely on the protection

criteria specified by the International Telecommunication Union Radiocommunication Sector (ITU-R) for radioastronomy observatories. Figure D-1 illustrates the antenna array at this facility near Socorro, New Mexico. The BPL Memorandum Opinion and Order defined an exclusion zone where Access BPL systems operating on overhead MV power lines in the 73.0 – 74.6 MHz band should be no closer than 65 km from the coordinates of the VLA facility.<sup>5</sup> The coordinate at the center of the VLA is 34° 04' 43.50"N, 107° 37' 03.82"W. Figure D-2 shows the specified protection radii within the National Radio Astronomy Observatory. The BPL rules also state that Access BPL using LV power lines or underground power lines using the 73.0 – 74.6 MHz band should be excluded within 47 km from the coordinates of the VLA facility. The analyses in Section 3.3.3 confirmed that these exclusion zone radii are reasonable to limit the power flux density (PFD) to levels defined for this frequency band by the ITU-R. This amounts to 2.04 percent of the bandwidth between 1.7 MHz and 80 MHz and less than 0.028 percent of U.S. territorial area, or less than 0.0006 percent of national spectrum resource between 1.7 MHz and 80 MHz.



**Figure D-1: Very Large Array (VLA) radioastronomy observatory**

---

<sup>5</sup> See Amendment of Part 15 regarding new requirements and measurement guidelines for Access Broadband over Power Line Systems, ET Docket No. 04-37, Memorandum Opinion and Order, released August 7, 2006, (“BPL Memorandum Opinion and Order”), at ¶¶ 57 - 59.

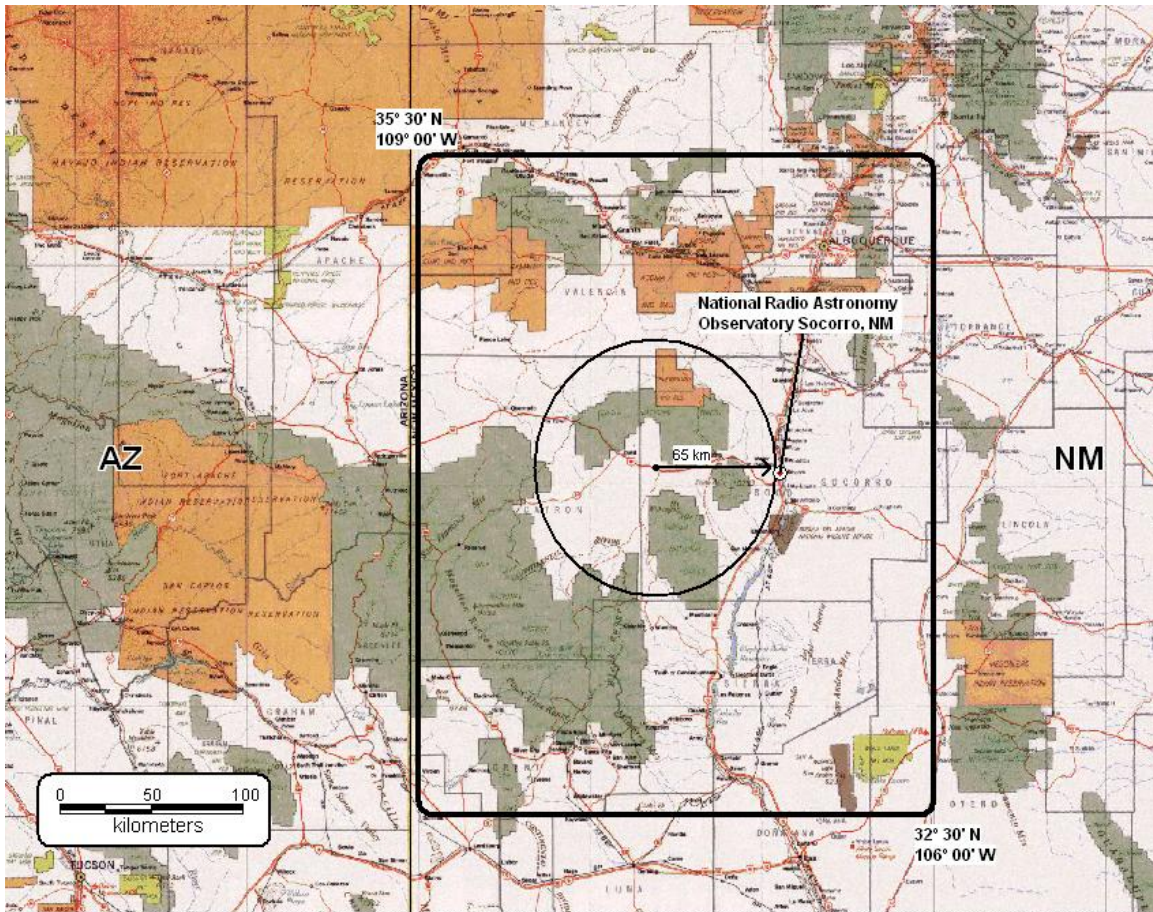


**Figure D-2: VLA protection radii for overhead Access BPL shown within the National Radio Astronomy Observatory near Socorro, New Mexico.**

### **D.3 CONSULTATION AREAS**

Part 15 of the Commission’s rules for carrier current systems apply the same field strength limits for wanted and unwanted emissions, and so, consultation between BPL service providers and radio operators should not be limited to the fundamental frequencies intentionally used in Access BPL systems. Moreover, frequencies used by many communications receivers in the 1.7 – 30 MHz frequency range are subject to change in the long-term and over hourly or shorter time frames. In light of these factors and given that the consultation areas needed for BPL systems are small, consultation should be required for all planned Access BPL operations at all frequencies of potential concern in these consultation areas. These consultation areas are:

- For frequencies in the 1.7 – 30 MHz frequency range, the areas within 4 km of facilities located at the following coordinates:
  - the Commission’s protected field offices listed in 47 C.F.R. § 0.121, the point-of-contact for which is specified in that section;
  - the aeronautical stations listed in Tables D-4 and D-5;
  - the land stations listed in Tables D-6 and D-7;



- For frequencies in the 1.7 – 80 MHz frequency range, the areas within 4 km of facilities located at the coordinates specified for radio astronomy facilities in US 311.
- For frequencies in the 1.7 – 80 MHz frequency range, the area within 1 km of the Table Mountain Radio Receiving Zone, the coordinates and point of contact for which are specified in 47 C.F.R. § 21.113(b).
- For frequencies in the 1.7 – 30 MHz frequency range, the areas within 37 km of radar receiver facilities located at the coordinates specified in Table D-8.

Point of contact  
 U.S. Coast Guard HQ  
 Division of Spectrum Management CG-622  
 2100 Second St., SW. Rm. 6611  
 Washington, DC 20593  
 Tel: 202-267-6036  
 Fax: 202-267-4106  
 Email: [jtaboada@comdt.uscg.mil](mailto:jtaboada@comdt.uscg.mil)

**Table D-4: Consultation Area Coordinates for Aeronautical (OR) Stations (1.7 – 30 MHz)**

<b>Command Name</b>	<b>Location</b>	<b>Latitude</b>	<b>Longitude</b>
Washington	Arlington, VA	38° 51' 07" N	77° 02' 15" W
Cape Cod	Cape Cod, MA	41° 42' 00" N	70° 30' 00" W
Atlantic City	Atlantic City, NJ	39° 20' 59" N	74° 27' 42" W
Elizabeth City	Elizabeth City, NC	36° 15' 53" N	76° 10' 32" W
Savannah	Savannah, GA	32° 01' 30" N	81° 08' 30" W
Miami	Opa Locka, FL	25° 54' 22" N	80° 16' 01" W
Clearwater	Clearwater, FL	27° 54' 27" N	82° 41' 29" W
Borinquen	Aguadilla, PR	18° 18' 36" N	67° 04' 48" W
New Orleans	New Orleans, LA	29° 49' 31" N	90° 02' 06" W
Traverse City	Traverse City, MI	44° 44' 24" N	85° 34' 54" W
San Diego	San Diego, CA	32° 43' 33" N	117° 10' 15" W
Sacramento	McClellan AFB, CA	38° 40' 06" N	121° 24' 04" W
Astoria	Warrenton, OR	46° 25' 18" N	123° 47' 46" W
North Bend	North Bend, OR	43° 24' 39" N	124° 14' 35" W
Barbers Point	Kapolei, HI	21° 18' 01" N	158° 04' 15" W
Kodiak	Kodiak, AK	57° 44' 19" N	152° 30' 18" W
Houston	Houston, TX	29° 45' 00" N	95° 22' 00" W
Detroit	Mt. Clemens, MI	42° 36' 05" N	82° 50' 12" W
San Francisco	San Francisco, CA	37° 37' 58" N	122° 23' 20" W
Los Angeles	Los Angeles, CA	33° 56' 36" N	118° 23' 48" W

Command Name	Location	Latitude	Longitude
Humboldt Bay	McKinleyville, CA	40° 58' 39" N	124° 06' 45" W
Port Angeles	Port Angeles, WA	48° 08' 25" N	123° 24' 48" W
Sitka	Sitka, AK	57° 05' 50" N	135° 21' 58" W

Point of contact  
 ARINC  
 2551 Riva Road  
 Annapolis, MD 21401  
 Tel: 1-800-633-6882  
 Fax: 410-266-2329  
 Email: [bplnotifications@arinc.com](mailto:bplnotifications@arinc.com)  
[www.arinc.com](http://www.arinc.com)

**Table D-5: Consultation Area Coordinates for Aeronautical Receive Stations (1.7 – 30 MHz)**

Locale	Latitude	Longitude
Southampton, NY	40° 55' 15" N	72° 23' 41" W
Molokai, HI	21° 12' 23" N	157° 12' 30" W
Oahu, HI	21° 22' 27" N	158° 05' 56" W
Half Moon Bay, CA	37° 39' 64" N	122° 24' 44" W
Pt. Reyes, CA	38° 06' 00" N	122° 56' 00" W
Barrow, AK	71° 17' 24" N	156° 40' 12" W
Guam	13° 25' 12" N	144° 48' 00" E (note: Eastern Hemisphere)
NY Comm Center, NY	40° 46' 48" N	73° 05' 46" W
Cedar Rapids, IA	42° 02' 05.0" N	91° 38' 37.6" W
Beaumont, CA	33° 54' 27.1" N	116° 59' 49.1" W
Fairfield, TX	31° 47' 02.6" N	96° 47' 03.0" W
Houston, TX	29° 36' 35.8" N	95° 16' 54.8" W
Miami, FL	25° 49' 05" N	80° 18' 28" W

Point Of Contact  
 U.S. Coast Guard HQ  
 Division of Spectrum Management CG-622  
 2100 Second St., SW. Rm. 6611  
 Washington, DC 20593  
 Tel: 202-267-6036  
 Fax: 202-267-4106  
 Email: [jtaboada@comdt.uscg.mil](mailto:jtaboada@comdt.uscg.mil)

**Table D-6: Consultation Area Coordinates for Land Stations, Set 1 (1.7–30 MHz)**

Command Name	Location	Latitude	Longitude
COMMSTA Boston	Maspee, MA	41° 24' 00" N	70° 18' 57" W
Camslant	Chesapeake, VA	36° 33' 59" N	76° 15' 23" W
COMMSTA Miami	Miami, FL	25° 36' 58" N	80° 23' 04" W

<b>Command Name</b>	<b>Location</b>	<b>Latitude</b>	<b>Longitude</b>
COMMSTA New Orleans	Belle Chasse, IA	29° 52' 40" N	89° 54' 46" W
Campac	Pt. Reyes Sta, CA	38° 06' 00" N	122° 55' 48" W
COMMSTA Honolulu	Wahiawa, HI	21° 31' 08" N	157° 59' 28" W
COMMSTA Kodiak	Kodiak, AK	57° 04' 26" N	152° 28' 20" W
Guam	Finegayan, GU	13° 53' 08" N	144° 50' 20" E

Point of contact  
 COTHEN Technical Support Center  
 COTHEN Program Manager  
 Tel: (800) 829-6336

**Table D-7: Consultation Area Coordinates for Land Stations, Set 2 (1.7 – 30 MHz)**

<b>Site Name</b>	<b>Latitude</b>	<b>Longitude</b>
Albuquerque, NM	35° 05' 02" N	105° 34' 23" W
Arecibo, PR	18° 17' 26" N	66° 22' 33" W
Atlanta, GA	32° 33' 06" N	84° 23' 35" W
Beaufort, SC	34° 34' 22" N	76° 09' 48" W
Cape Charles, VA	37° 05' 37" N	75° 58' 06" W
Cedar Rapids, IA	42° 00' 09" N	91° 17' 39" W
Denver, CO	39° 15' 45" N	103° 34' 23" W
Fort Myers, FL	81° 31' 20" N	26° 20' 01" W
Kansas City, MO	38° 22' 10" N	93° 21' 48" W
Las Vegas, NV	36° 21' 15" N	114° 17' 33" W
Lovelock, NV	40° 03' 07" N	118° 18' 56" W
Memphis, TN	34° 21' 57" N	90° 02' 43" W
Miami, FL	25° 46' 20" N	80° 28' 48" W
Morehead City, NC	34° 34' 50" N	78° 13' 59" W
Oklahoma City, OK	34° 30' 52" N	97° 30' 52" W
Orlando, FL	28° 31' 30" N	80° 48' 58" W
Reno, NV	38° 31' 12" N	119° 14' 37" W
Sarasota, FL	27° 12' 41" N	81° 31' 20" W
Wilmington, NC	34° 29' 24" N	78° 04' 31" W

Point Of Contact  
 ROTH Deputy Program Manager  
 (540) 653-3624

**Table D-8: Consultation Area Coordinates for Radar Receiver Stations (1.7 – 30 MHz)**

<b>Latitude/Longitude</b>
18° 01' N / 66° 30' W
28° 05' N / 98° 43' W
36° 34' N / 76° 18' W

Powerline30.nec

CM Complex Power Line Model  
CM Excitation Point 1  
CM 30 MHZ  
CM NTIA 2004  
CE

CW 1 119 -298 -34 12 -235 -22 12 0.0063 3 64.90226708  
CW 2 125 -235 -22 12 -168 -12 12 0.0063 3 68.55506412  
CW 3 135 -168 -12 12 -96 -4 12 0.0063 3 73.31239808  
CW 4 111 -96 -4 12 -36 0 12 0.0063 3 60.85478374  
CW 5 67 -36 0 12 0 0 12 0.0063 3 36.432  
CW 6 67 0 0 12 0 -36 12 0.0063 3 36.432  
CW 7 107 0 -36 12 -2 -94 12 0.0063 3 58.73088618  
CW 8 81 -2 -94 12 -44 -83 12 0.0063 3 43.93758573  
CW 9 109 -44 -83 12 -89 -120 12 0.0063 3 58.95714321  
CW 10 37 -2 -94 12 18 -96 12 0.0063 3 20.34094826  
CW 11 91 0 0 12 2 49 12 0.0063 3 49.62928893  
CW 12 107 2 49 12 -14 104 12 0.0063 3 57.96737413  
CW 13 105 -14 104 12 1 158 12 0.0063 3 56.71716058  
CW 14 93 1 158 12 19 205 12 0.0063 3 50.93286515  
CW 15 99 19 205 12 28 258 12 0.0063 3 54.40382487  
CW 16 105 28 258 12 30 315 12 0.0063 3 57.71949785  
CW 17 119 -298 -34 11.4 -235 -22 11.4 0.0063 3 64.90226708  
CW 18 125 -235 -22 11.4 -168 -12 11.4 0.0063 3 68.55506412  
CW 19 135 -168 -12 11.4 -96 -4 11.4 0.0063 3 73.31239808  
CW 20 111 -96 -4 11.4 -36 0 11.4 0.0063 3 60.85478374  
CW 21 67 -36 0 11.4 0 0 11.4 0.0063 3 36.432  
CW 22 67 0 0 11.4 0 -36 11.4 0.0063 3 36.432  
CW 23 107 0 -36 11.4 -2 -94 11.4 0.0063 3 58.73088618  
CW 24 81 -2 -94 11.4 -44 -83 11.4 0.0063 3 43.93758573  
CW 25 109 -44 -83 11.4 -89 -120 11.4 0.0063 3 58.95714321  
CW 26 37 -2 -94 11.4 18 -96 11.4 0.0063 3 20.34094826  
CW 27 91 0 0 11.4 2 49 11.4 0.0063 3 49.62928893  
CW 28 107 2 49 11.4 -14 104 11.4 0.0063 3 57.96737413  
CW 29 105 -14 104 11.4 0.04829 158.31 11.7 0.0063 3 56.77149123  
CW 30 93 0.04829 158.31 11.7 19 205 11.4 0.0063 3 50.99529567  
CW 31 99 19 205 11.4 28 258 11.4 0.0063 3 54.40382487  
CW 32 105 28 258 11.4 30 315 11.4 0.0063 3 57.71949785  
CW 33 119 -298 -34 10.8 -235 -22 10.8 0.0063 3 64.90226708  
CW 34 125 -235 -22 10.8 -168 -12 10.8 0.0063 3 68.55506412  
CW 35 135 -168 -12 10.8 -96 -4 10.8 0.0063 3 73.31239808  
CW 36 111 -96 -4 10.8 -36 0 10.8 0.0063 3 60.85478374  
CW 37 33 -36 0 10.8 -37 17 10.85 0.0063 3 17.23381329  
CW 38 67 -36 0 10.8 0 0 10.8 0.0063 3 36.432  
CW 39 67 0 0 10.8 0 -36 10.8 0.0063 3 36.432  
CW 40 107 0 -36 10.8 -2 -94 10.8 0.0063 3 58.73088618  
CW 41 81 -2 -94 10.8 -44 -83 10.8 0.0063 3 43.93758573  
CW 42 109 -44 -83 10.8 -89 -120 10.8 0.0063 3 58.95714321  
CW 43 37 -2 -94 10.8 18 -96 10.8 0.0063 3 20.34094826  
CW 44 91 0 0 10.8 2 49 10.8 0.0063 3 49.62928893  
CW 45 107 2 49 10.8 -14 104 10.8 0.0063 3 57.96737413  
CW 46 105 -14 104 10.8 1.9517 157.69 11.7 0.0063 3 56.68901019  
CW 47 93 1.9517 157.69 11.7 19 205 10.8 0.0063 3 50.89958235  
CW 48 99 19 205 10.8 28 258 10.8 0.0063 3 54.40382487  
CW 49 105 28 258 10.8 30 315 10.8 0.0063 3 57.71949785  
CW 50 119 -298 -34 9.6 -235 -22 9.6 0.0063 3 64.90226708  
CW 51 125 -235 -22 9.6 -168 -12 9.6 0.0063 3 68.55506412  
CW 52 135 -168 -12 9.6 -96 -4 9.6 0.0063 3 73.31239808  
CW 53 111 -96 -4 9.6 -36 0 9.6 0.0063 3 60.85478374  
CW 54 33 -36 0 9.6 -37 17 7.5 0.0063 3 17.36428044  
CW 55 67 -36 0 9.6 0 0 9.6 0.0063 3 36.432  
CW 56 67 0 0 9.6 0 -36 9.6 0.0063 3 36.432  
CW 57 107 0 -36 9.6 -2 -94 9.6 0.0063 3 58.73088618  
CW 58 81 -2 -94 9.6 -44 -83 9.6 0.0063 3 43.93758573

Powerline30.nec

CW 59 109 -44 -83 9.6 -89 -120 9.6 0.0063 3 58.95714321  
CW 60 37 -2 -94 9.6 18 -96 9.6 0.0063 3 20.34094826  
CW 61 91 0 0 9.6 2 49 9.6 0.0063 3 49.62928893  
CW 62 107 2 49 9.6 -14 104 9.6 0.0063 3 57.96737413  
CW 63 105 -14 104 9.6 1 158 9.6 0.0063 3 56.71716058  
CW 64 93 1 158 9.6 19 205 9.6 0.0063 3 50.93286515  
CW 65 99 19 205 9.6 28 258 9.6 0.0063 3 54.40382487  
CW 66 105 28 258 9.6 30 315 9.6 0.0063 3 57.71949785  
GW 67 19 -235 -22 9.6 -235 -22 0 0.0063  
GW 68 19 -168 -12 9.6 -168 -12 0 0.0063  
GW 69 19 -96 -4 9.6 -96 -4 0 0.0063  
GW 70 15 -37 17 7.5 -37 17 0 0.0063  
GW 71 19 2 49 9.6 2 49 0 0.0063  
GW 72 19 28 258 9.6 28 258 0 0.0063  
GW 73 19 -89 -120 9.6 -89 -120 0 0.0063  
GW 74 7 -235 -22 0 -235 -22 -3 0.0063  
GW 75 7 -168 -12 0 -168 -12 -3 0.0063  
GW 76 7 -96 -4 0 -96 -4 -3 0.0063  
GW 77 7 -37 17 0 -37 17 -3 0.0063  
GW 78 7 2 49 0 2 49 -3 0.0063  
GW 79 7 28 258 0 28 258 -3 0.0063  
GW 80 7 -89 -120 0 -89 -120 -3 0.0063  
GW 81 7 1.02 158.04 0 1.02 158.04 3 0.0063  
GW 82 7 0.97 158.04 0 0.97 158.04 3 0.0063  
GW 83 7 0.945 158 0 0.945 158 3 0.0063  
GW 84 7 0.97 157.95 0 0.97 157.95 3 0.0063  
GW 85 7 1.02 157.95 0 1.02 157.95 3 0.0063  
GW 86 7 1.045 158 0 1.045 158 3 0.0063  
GW 87 7 1.02 158.04 3 1.02 158.04 6 0.0063  
GW 88 7 0.97 158.04 3 0.97 158.04 6 0.0063  
GW 89 7 0.945 158 3 0.945 158 6 0.0063  
GW 90 7 0.97 157.95 3 0.97 157.95 6 0.0063  
GW 91 7 1.02 157.95 3 1.02 157.95 6 0.0063  
GW 92 7 1.045 158 3 1.045 158 6 0.0063  
GW 93 7 1.02 158.04 6 1.02 158.04 9 0.0063  
GW 94 7 0.97 158.04 6 0.97 158.04 9 0.0063  
GW 95 7 0.945 158 6 0.945 158 9 0.0063  
GW 96 7 0.97 157.95 6 0.97 157.95 9 0.0063  
GW 97 7 1.02 157.95 6 1.02 157.95 9 0.0063  
GW 98 7 1.045 158 6 1.045 158 9 0.0063  
GW 99 7 1.02 158.04 0 1.02 158.04 -3 0.0063  
GW 100 7 0.97 158.04 0 0.97 158.04 -3 0.0063  
GW 101 7 0.945 158 0 0.945 158 -3 0.0063  
GW 102 7 0.97 157.95 0 0.97 157.95 -3 0.0063  
GW 103 7 1.02 157.95 0 1.02 157.95 -3 0.0063  
GW 104 7 1.045 158 0 1.045 158 -3 0.0063  
GW 105 7 0.02 -35.96 0 0.02 -35.96 3 0.0063  
GW 106 7 -0.03 -35.96 0 -0.03 -35.96 3 0.0063  
GW 107 7 -0.055 -36 0 -0.055 -36 3 0.0063  
GW 108 7 -0.03 -36.05 0 -0.03 -36.05 3 0.0063  
GW 109 7 0.02 -36.05 0 0.02 -36.05 3 0.0063  
GW 110 7 0.045 -36 0 0.045 -36 3 0.0063  
GW 111 7 0.02 -35.96 3 0.02 -35.96 6 0.0063  
GW 112 7 -0.03 -35.96 3 -0.03 -35.96 6 0.0063  
GW 113 7 -0.055 -36 3 -0.055 -36 6 0.0063  
GW 114 7 -0.03 -36.05 3 -0.03 -36.05 6 0.0063  
GW 115 7 0.02 -36.05 3 0.02 -36.05 6 0.0063  
GW 116 7 0.045 -36 3 0.045 -36 6 0.0063  
GW 117 7 0.02 -35.96 6 0.02 -35.96 9 0.0063  
GW 118 7 -0.03 -35.96 6 -0.03 -35.96 9 0.0063  
GW 119 7 -0.03 -36.05 6 -0.03 -36.05 9 0.0063  
GW 120 7 0.02 -36.05 6 0.02 -36.05 9 0.0063  
GW 121 7 0.045 -36 6 0.045 -36 9 0.0063

Powerline30.nec

GW 122 7 0.02 -35.96 0 0.02 -35.96 -3 0.0063  
GW 123 7 -0.03 -35.96 0 -0.03 -35.96 -3 0.0063  
GW 124 7 -0.055 -36 0 -0.055 -36 -3 0.0063  
GW 125 7 -0.03 -36.05 0 -0.03 -36.05 -3 0.0063  
GW 126 7 0.02 -36.05 0 0.02 -36.05 -3 0.0063  
GW 127 7 0.045 -36 0 0.045 -36 -3 0.0063  
GW 128 7 18.2 -95.96 6 18.2 -95.96 9 0.0063  
GW 129 7 18.15 -95.96 6 18.15 -95.96 9 0.0063  
GW 130 7 18.125 -96 6 18.125 -96 9 0.0063  
GW 131 7 18.15 -96.05 6 18.15 -96.05 9 0.0063  
GW 132 7 18.2 -96.05 6 18.2 -96.05 9 0.0063  
GW 133 7 18.225 -96 6 18.225 -96 9 0.0063  
GW 134 7 18.2 -95.96 3 18.2 -95.96 6 0.0063  
GW 135 7 18.15 -95.96 3 18.15 -95.96 6 0.0063  
GW 136 7 18.125 -96 3 18.125 -96 6 0.0063  
GW 137 7 18.15 -96.05 3 18.15 -96.05 6 0.0063  
GW 138 7 18.2 -96.05 3 18.2 -96.05 6 0.0063  
GW 139 7 18.225 -96 3 18.225 -96 6 0.0063  
GW 140 7 18.2 -95.96 0 18.2 -95.96 3 0.0063  
GW 141 7 18.15 -95.96 0 18.15 -95.96 3 0.0063  
GW 142 7 18.125 -96 0 18.125 -96 3 0.0063  
GW 143 7 18.15 -96.05 0 18.15 -96.05 3 0.0063  
GW 144 7 18.2 -96.05 0 18.2 -96.05 3 0.0063  
GW 145 7 18.225 -96 0 18.225 -96 3 0.0063  
GW 146 7 18.15 -95.96 0 18.15 -95.96 -3 0.0063  
GW 147 7 18.125 -96 0 18.125 -96 -3 0.0063  
GW 148 7 18.15 -96.05 0 18.15 -96.05 -3 0.0063  
GW 149 7 18.2 -96.05 0 18.2 -96.05 -3 0.0063  
GW 150 7 18.225 -96 0 18.225 -96 -3 0.0063  
GW 151 7 18.2 -95.96 0 18.2 -95.96 -3 0.0063  
GW 152 7 18.175 -96 0 18.175 -96 -3 0.0063  
GW 153 7 0 -36 0 0 -36 3 0.0063  
GW 154 7 0 -36 3 0 -36 6 0.0063  
GW 155 7 0 -36 6 0 -36.005 9 0.0063  
GW 156 7 0 -36 0 0 -36 -3 0.0063  
GW 157 7 0.9983 158 0 0.9983 158 3 0.0063  
GW 158 7 0.9983 158 3 0.9983 158 6 0.0063  
GW 159 7 0.9983 158 6 0.9983 158 9 0.0063  
GW 160 7 0.9983 158 0 0.9983 158 -3 0.0063  
GW 161 7 18.175 -96 6 18.175 -96 9 0.0063  
GW 162 7 18.175 -96 3 18.175 -96 6 0.0063  
GW 163 7 18.175 -96 0 18.175 -96 3 0.0063  
GW 164 7 -298.125 -33.975 6 -298.125 -33.975 9 0.0063  
GW 165 7 -298.175 -33.975 6 -298.175 -33.975 9 0.0063  
GW 166 7 -298.2 -34.015 6 -298.2 -34.015 9 0.0063  
GW 167 7 -298.175 -34.065 6 -298.175 -34.065 9 0.0063  
GW 168 7 -298.125 -34.065 6 -298.125 -34.065 9 0.0063  
GW 169 7 -298.1 -34.015 6 -298.1 -34.015 9 0.0063  
GW 170 7 -298.125 -33.975 3 -298.125 -33.975 6 0.0063  
GW 171 7 -298.175 -33.975 3 -298.175 -33.975 6 0.0063  
GW 172 7 -298.2 -34.015 3 -298.2 -34.015 6 0.0063  
GW 173 7 -298.175 -34.065 3 -298.175 -34.065 6 0.0063  
GW 174 7 -298.125 -34.065 3 -298.125 -34.065 6 0.0063  
GW 175 7 -298.1 -34.015 3 -298.1 -34.015 6 0.0063  
GW 176 7 -298.125 -33.975 0 -298.125 -33.975 3 0.0063  
GW 177 7 -298.175 -33.975 0 -298.175 -33.975 3 0.0063  
GW 178 7 -298.2 -34.015 0 -298.2 -34.015 3 0.0063  
GW 179 7 -298.175 -34.065 0 -298.175 -34.065 3 0.0063  
GW 180 7 -298.125 -34.065 0 -298.125 -34.065 3 0.0063  
GW 181 7 -298.1 -34.015 0 -298.1 -34.015 3 0.0063  
GW 182 7 -298.175 -33.975 0 -298.175 -33.975 -3 0.0063  
GW 183 7 -298.2 -34.015 0 -298.2 -34.015 -3 0.0063  
GW 184 7 -298.175 -34.065 0 -298.175 -34.065 -3 0.0063

Powerline30.nec

GW 185 7 -298.125 -34.065 0 -298.125 -34.065 -3 0.0063  
GW 186 7 -298.1 -34.015 0 -298.1 -34.015 -3 0.0063  
GW 187 7 -298.125 -33.975 0 -298.125 -33.975 -3 0.0063  
GW 188 7 -298.15 -34.015 0 -298.15 -34.015 -3 0.0063  
GW 189 7 -298.15 -34.015 6 -298.15 -34.015 9 0.0063  
GW 190 7 -298.15 -34.015 3 -298.15 -34.015 6 0.0063  
GW 191 7 -298.15 -34.015 0 -298.15 -34.015 3 0.0063  
GW 192 7 -37 17 7.5 -37 17 10.85 0.0063  
GW 193 3 -96 -4 9.6 -96 -4.55 10.8 0.0063  
GW 194 3 -96 -4 11.4 -96 -4.55 10.8 0.0063  
GW 195 3 -168 -12 9.6 -168 -12.5 10.75 0.0063  
GW 196 3 -168 -12 12 -168 -12.5 10.75 0.0063  
GW 197 3 -235 -22 9.6 -235 -22 10.8 0.0063  
GW 198 3 -89 -120 11.4 -89.25 -120.25 10.5 0.0063  
GW 199 3 -89 -120 9.6 -89.25 -120.25 10.5 0.0063  
GW 200 3 2 49 10.8 2 49 9.6 0.0063  
GW 201 3 28 258 9.6 28.5 258 10.75 0.0063  
GW 202 3 28 258 12 28.5 258 10.75 0.0063  
GW 203 7 -0.055 -36 6 -0.055 -36 9 0.0063  
GW 204 3 1.75 157.75 10.8 1.9517 157.69 11.7 0.0063  
GW 205 7 0.5102 157.65 10.8 0.04829 158.31 11.7 0.0063  
GW 206 13 1 158 12 0.95 158.25 9.6 0.0063  
GW 207 3 0.95 158.25 9.6 0.9983 158 9 0.0063  
GW 208 11 0.5102 157.65 10.8 0.9983 158 9 0.0063  
GW 209 11 1.75 157.75 10.8 0.9983 158 9 0.0063  
GW 210 3 0 -36 10.8 0.32 -35.7 10.3 0.0063  
GW 211 7 0 -36 12 0.35 -36.3 10.35 0.0063  
GW 212 5 0 -36 11.4 -0.35 -36 10.35 0.0063  
GW 213 7 0.32 -35.7 10.3 0 -36.005 9 0.0063  
GW 214 7 0.35 -36.3 10.35 0 -36.005 9 0.0063  
GW 215 7 -0.35 -36 10.35 0 -36.005 9 0.0063  
GW 216 3 18.125 -96 9 18 -96 9.6 0.0063  
GW 217 7 18 -96 10.8 18.1 -95.75 9.6 0.0063  
GW 218 9 18 -96 11.4 18.35 -96 9.6 0.0063  
GW 219 3 18.35 -96 9.6 18.175 -96 9 0.0063  
GW 220 13 18 -96 12 18.125 -96.25 9.6 0.0063  
GW 221 3 18.125 -96.25 9.6 18.175 -96 9 0.0063  
GW 222 3 -298.1 -34.015 9 -298 -34 9.6 0.0063  
GW 223 7 -298 -34 10.8 -298.075 -34.15 9.6 0.0063  
GW 224 9 -298 -34 11.4 -298.25 -34 9.6 0.0063  
GW 225 13 -298 -34 12 -298.075 -33.875 9.6 0.0063  
GW 226 3 -298.075 -34.15 9.6 -298.15 -34.015 9 0.0063  
GW 227 3 -298.25 -34 9.6 -298.15 -34.015 9 0.0063  
GW 228 3 -298.075 -33.875 9.6 -298.15 -34.015 9 0.0063  
GW 229 3 18.175 -96 9 18.1 -95.75 9.6 0.0063

GE -1  
LD 0 192 1 1 3 0.005  
LD 0 193 1 1 3 0.005  
LD 0 195 1 1 3 0.005  
LD 0 197 1 1 3 0.005  
LD 0 199 1 1 3 0.005  
LD 0 200 1 1 3 0.005  
LD 0 201 1 1 3 0.005  
LD 0 213 6 6 30 0  
LD 0 214 6 6 30 0  
LD 0 215 6 6 30 0  
LD 0 207 2 2 30 0  
LD 0 208 10 10 30 0  
LD 0 209 10 10 30 0  
LD 0 219 2 2 30 0  
LD 0 221 2 2 30 0  
LD 0 226 2 2 30 0  
LD 0 227 2 2 30 0

Powerline30.nec

LD 0 228 2 2 30 0  
LD 0 229 2 2 30 0  
LD 5 0 0 0 58000000  
GN 2 0 0 0 15 0.005  
FR 0 1 0 0 30.000 0  
EX 0 15 1 0 1 0  
EN  
CM Complex Power Line Model  
CM Excitation Point 2  
CM 30 MHz  
CM NTIA 2004  
CE  
CW 1 119 -298 -34 12 -235 -22 12 0.0063 3 64.90226708  
CW 2 125 -235 -22 12 -168 -12 12 0.0063 3 68.55506412  
CW 3 135 -168 -12 12 -96 -4 12 0.0063 3 73.31239808  
CW 4 111 -96 -4 12 -36 0 12 0.0063 3 60.85478374  
CW 5 67 -36 0 12 0 0 12 0.0063 3 36.432  
CW 6 67 0 0 12 0 -36 12 0.0063 3 36.432  
CW 7 107 0 -36 12 -2 -94 12 0.0063 3 58.73088618  
CW 8 81 -2 -94 12 -44 -83 12 0.0063 3 43.93758573  
CW 9 109 -44 -83 12 -89 -120 12 0.0063 3 58.95714321  
CW 10 37 -2 -94 12 18 -96 12 0.0063 3 20.34094826  
CW 11 91 0 0 12 2 49 12 0.0063 3 49.62928893  
CW 12 107 2 49 12 -14 104 12 0.0063 3 57.96737413  
CW 13 105 -14 104 12 1 158 12 0.0063 3 56.71716058  
CW 14 93 1 158 12 19 205 12 0.0063 3 50.93286515  
CW 15 99 19 205 12 28 258 12 0.0063 3 54.40382487  
CW 16 105 28 258 12 30 315 12 0.0063 3 57.71949785  
CW 17 119 -298 -34 11.4 -235 -22 11.4 0.0063 3 64.90226708  
CW 18 125 -235 -22 11.4 -168 -12 11.4 0.0063 3 68.55506412  
CW 19 135 -168 -12 11.4 -96 -4 11.4 0.0063 3 73.31239808  
CW 20 111 -96 -4 11.4 -36 0 11.4 0.0063 3 60.85478374  
CW 21 67 -36 0 11.4 0 0 11.4 0.0063 3 36.432  
CW 22 67 0 0 11.4 0 -36 11.4 0.0063 3 36.432  
CW 23 107 0 -36 11.4 -2 -94 11.4 0.0063 3 58.73088618  
CW 24 81 -2 -94 11.4 -44 -83 11.4 0.0063 3 43.93758573  
CW 25 109 -44 -83 11.4 -89 -120 11.4 0.0063 3 58.95714321  
CW 26 37 -2 -94 11.4 18 -96 11.4 0.0063 3 20.34094826  
CW 27 91 0 0 11.4 2 49 11.4 0.0063 3 49.62928893  
CW 28 107 2 49 11.4 -14 104 11.4 0.0063 3 57.96737413  
CW 29 105 -14 104 11.4 0.04829 158.31 11.7 0.0063 3 56.77149123  
CW 30 93 0.04829 158.31 11.7 19 205 11.4 0.0063 3 50.99529567  
CW 31 99 19 205 11.4 28 258 11.4 0.0063 3 54.40382487  
CW 32 105 28 258 11.4 30 315 11.4 0.0063 3 57.71949785  
CW 33 119 -298 -34 10.8 -235 -22 10.8 0.0063 3 64.90226708  
CW 34 125 -235 -22 10.8 -168 -12 10.8 0.0063 3 68.55506412  
CW 35 135 -168 -12 10.8 -96 -4 10.8 0.0063 3 73.31239808  
CW 36 111 -96 -4 10.8 -36 0 10.8 0.0063 3 60.85478374  
CW 37 33 -36 0 10.8 -37 17 10.85 0.0063 3 17.23381329  
CW 38 67 -36 0 10.8 0 0 10.8 0.0063 3 36.432  
CW 39 67 0 0 10.8 0 -36 10.8 0.0063 3 36.432  
CW 40 107 0 -36 10.8 -2 -94 10.8 0.0063 3 58.73088618  
CW 41 81 -2 -94 10.8 -44 -83 10.8 0.0063 3 43.93758573  
CW 42 109 -44 -83 10.8 -89 -120 10.8 0.0063 3 58.95714321  
CW 43 37 -2 -94 10.8 18 -96 10.8 0.0063 3 20.34094826  
CW 44 91 0 0 10.8 2 49 10.8 0.0063 3 49.62928893  
CW 45 107 2 49 10.8 -14 104 10.8 0.0063 3 57.96737413  
CW 46 105 -14 104 10.8 1.9517 157.69 11.7 0.0063 3 56.68901019  
CW 47 93 1.9517 157.69 11.7 19 205 10.8 0.0063 3 50.89958235  
CW 48 99 19 205 10.8 28 258 10.8 0.0063 3 54.40382487  
CW 49 105 28 258 10.8 30 315 10.8 0.0063 3 57.71949785  
CW 50 119 -298 -34 9.6 -235 -22 9.6 0.0063 3 64.90226708  
CW 51 125 -235 -22 9.6 -168 -12 9.6 0.0063 3 68.55506412



Powerline30.nec

CW 52 135 -168 -12 9.6 -96 -4 9.6 0.0063 3 73.31239808  
 CW 53 111 -96 -4 9.6 -36 0 9.6 0.0063 3 60.85478374  
 CW 54 33 -36 0 9.6 -37 17 7.5 0.0063 3 17.36428044  
 CW 55 67 -36 0 9.6 0 0 9.6 0.0063 3 36.432  
 CW 56 67 0 0 9.6 0 -36 9.6 0.0063 3 36.432  
 CW 57 107 0 -36 9.6 -2 -94 9.6 0.0063 3 58.73088618  
 CW 58 81 -2 -94 9.6 -44 -83 9.6 0.0063 3 43.93758573  
 CW 59 109 -44 -83 9.6 -89 -120 9.6 0.0063 3 58.95714321  
 CW 60 37 -2 -94 9.6 18 -96 9.6 0.0063 3 20.34094826  
 CW 61 91 0 0 9.6 2 49 9.6 0.0063 3 49.62928893  
 CW 62 107 2 49 9.6 -14 104 9.6 0.0063 3 57.96737413  
 CW 63 105 -14 104 9.6 1 158 9.6 0.0063 3 56.71716058  
 CW 64 93 1 158 9.6 19 205 9.6 0.0063 3 50.93286515  
 CW 65 99 19 205 9.6 28 258 9.6 0.0063 3 54.40382487  
 CW 66 105 28 258 9.6 30 315 9.6 0.0063 3 57.71949785  
 GW 67 19 -235 -22 9.6 -235 -22 0 0.0063  
 GW 68 19 -168 -12 9.6 -168 -12 0 0.0063  
 GW 69 19 -96 -4 9.6 -96 -4 0 0.0063  
 GW 70 15 -37 17 7.5 -37 17 0 0.0063  
 GW 71 19 2 49 9.6 2 49 0 0.0063  
 GW 72 19 28 258 9.6 28 258 0 0.0063  
 GW 73 19 -89 -120 9.6 -89 -120 0 0.0063  
 GW 74 7 -235 -22 0 -235 -22 -3 0.0063  
 GW 75 7 -168 -12 0 -168 -12 -3 0.0063  
 GW 76 7 -96 -4 0 -96 -4 -3 0.0063  
 GW 77 7 -37 17 0 -37 17 -3 0.0063  
 GW 78 7 2 49 0 2 49 -3 0.0063  
 GW 79 7 28 258 0 28 258 -3 0.0063  
 GW 80 7 -89 -120 0 -89 -120 -3 0.0063  
 GW 81 7 1.02 158.04 0 1.02 158.04 3 0.0063  
 GW 82 7 0.97 158.04 0 0.97 158.04 3 0.0063  
 GW 83 7 0.945 158 0 0.945 158 3 0.0063  
 GW 84 7 0.97 157.95 0 0.97 157.95 3 0.0063  
 GW 85 7 1.02 157.95 0 1.02 157.95 3 0.0063  
 GW 86 7 1.045 158 0 1.045 158 3 0.0063  
 GW 87 7 1.02 158.04 3 1.02 158.04 6 0.0063  
 GW 88 7 0.97 158.04 3 0.97 158.04 6 0.0063  
 GW 89 7 0.945 158 3 0.945 158 6 0.0063  
 GW 90 7 0.97 157.95 3 0.97 157.95 6 0.0063  
 GW 91 7 1.02 157.95 3 1.02 157.95 6 0.0063  
 GW 92 7 1.045 158 3 1.045 158 6 0.0063  
 GW 93 7 1.02 158.04 6 1.02 158.04 9 0.0063  
 GW 94 7 0.97 158.04 6 0.97 158.04 9 0.0063  
 GW 95 7 0.945 158 6 0.945 158 9 0.0063  
 GW 96 7 0.97 157.95 6 0.97 157.95 9 0.0063  
 GW 97 7 1.02 157.95 6 1.02 157.95 9 0.0063  
 GW 98 7 1.045 158 6 1.045 158 9 0.0063  
 GW 99 7 1.02 158.04 0 1.02 158.04 -3 0.0063  
 GW 100 7 0.97 158.04 0 0.97 158.04 -3 0.0063  
 GW 101 7 0.945 158 0 0.945 158 -3 0.0063  
 GW 102 7 0.97 157.95 0 0.97 157.95 -3 0.0063  
 GW 103 7 1.02 157.95 0 1.02 157.95 -3 0.0063  
 GW 104 7 1.045 158 0 1.045 158 -3 0.0063  
 GW 105 7 0.02 -35.96 0 0.02 -35.96 3 0.0063  
 GW 106 7 -0.03 -35.96 0 -0.03 -35.96 3 0.0063  
 GW 107 7 -0.055 -36 0 -0.055 -36 3 0.0063  
 GW 108 7 -0.03 -36.05 0 -0.03 -36.05 3 0.0063  
 GW 109 7 0.02 -36.05 0 0.02 -36.05 3 0.0063  
 GW 110 7 0.045 -36 0 0.045 -36 3 0.0063  
 GW 111 7 0.02 -35.96 3 0.02 -35.96 6 0.0063  
 GW 112 7 -0.03 -35.96 3 -0.03 -35.96 6 0.0063  
 GW 113 7 -0.055 -36 3 -0.055 -36 6 0.0063  
 GW 114 7 -0.03 -36.05 3 -0.03 -36.05 6 0.0063

Powerline30.nec

GW 115 7 0.02 -36.05 3 0.02 -36.05 6 0.0063  
GW 116 7 0.045 -36 3 0.045 -36 6 0.0063  
GW 117 7 0.02 -35.96 6 0.02 -35.96 9 0.0063  
GW 118 7 -0.03 -35.96 6 -0.03 -35.96 9 0.0063  
GW 119 7 -0.03 -36.05 6 -0.03 -36.05 9 0.0063  
GW 120 7 0.02 -36.05 6 0.02 -36.05 9 0.0063  
GW 121 7 0.045 -36 6 0.045 -36 9 0.0063  
GW 122 7 0.02 -35.96 0 0.02 -35.96 -3 0.0063  
GW 123 7 -0.03 -35.96 0 -0.03 -35.96 -3 0.0063  
GW 124 7 -0.055 -36 0 -0.055 -36 -3 0.0063  
GW 125 7 -0.03 -36.05 0 -0.03 -36.05 -3 0.0063  
GW 126 7 0.02 -36.05 0 0.02 -36.05 -3 0.0063  
GW 127 7 0.045 -36 0 0.045 -36 -3 0.0063  
GW 128 7 18.2 -95.96 6 18.2 -95.96 9 0.0063  
GW 129 7 18.15 -95.96 6 18.15 -95.96 9 0.0063  
GW 130 7 18.125 -96 6 18.125 -96 9 0.0063  
GW 131 7 18.15 -96.05 6 18.15 -96.05 9 0.0063  
GW 132 7 18.2 -96.05 6 18.2 -96.05 9 0.0063  
GW 133 7 18.225 -96 6 18.225 -96 9 0.0063  
GW 134 7 18.2 -95.96 3 18.2 -95.96 6 0.0063  
GW 135 7 18.15 -95.96 3 18.15 -95.96 6 0.0063  
GW 136 7 18.125 -96 3 18.125 -96 6 0.0063  
GW 137 7 18.15 -96.05 3 18.15 -96.05 6 0.0063  
GW 138 7 18.2 -96.05 3 18.2 -96.05 6 0.0063  
GW 139 7 18.225 -96 3 18.225 -96 6 0.0063  
GW 140 7 18.2 -95.96 0 18.2 -95.96 3 0.0063  
GW 141 7 18.15 -95.96 0 18.15 -95.96 3 0.0063  
GW 142 7 18.125 -96 0 18.125 -96 3 0.0063  
GW 143 7 18.15 -96.05 0 18.15 -96.05 3 0.0063  
GW 144 7 18.2 -96.05 0 18.2 -96.05 3 0.0063  
GW 145 7 18.225 -96 0 18.225 -96 3 0.0063  
GW 146 7 18.15 -95.96 0 18.15 -95.96 -3 0.0063  
GW 147 7 18.125 -96 0 18.125 -96 -3 0.0063  
GW 148 7 18.15 -96.05 0 18.15 -96.05 -3 0.0063  
GW 149 7 18.2 -96.05 0 18.2 -96.05 -3 0.0063  
GW 150 7 18.225 -96 0 18.225 -96 -3 0.0063  
GW 151 7 18.2 -95.96 0 18.2 -95.96 -3 0.0063  
GW 152 7 18.175 -96 0 18.175 -96 -3 0.0063  
GW 153 7 0 -36 0 0 -36 3 0.0063  
GW 154 7 0 -36 3 0 -36 6 0.0063  
GW 155 7 0 -36 6 0 -36.005 9 0.0063  
GW 156 7 0 -36 0 0 -36 -3 0.0063  
GW 157 7 0.9983 158 0 0.9983 158 3 0.0063  
GW 158 7 0.9983 158 3 0.9983 158 6 0.0063  
GW 159 7 0.9983 158 6 0.9983 158 9 0.0063  
GW 160 7 0.9983 158 0 0.9983 158 -3 0.0063  
GW 161 7 18.175 -96 6 18.175 -96 9 0.0063  
GW 162 7 18.175 -96 3 18.175 -96 6 0.0063  
GW 163 7 18.175 -96 0 18.175 -96 3 0.0063  
GW 164 7 -298.125 -33.975 6 -298.125 -33.975 9 0.0063  
GW 165 7 -298.175 -33.975 6 -298.175 -33.975 9 0.0063  
GW 166 7 -298.2 -34.015 6 -298.2 -34.015 9 0.0063  
GW 167 7 -298.175 -34.065 6 -298.175 -34.065 9 0.0063  
GW 168 7 -298.125 -34.065 6 -298.125 -34.065 9 0.0063  
GW 169 7 -298.1 -34.015 6 -298.1 -34.015 9 0.0063  
GW 170 7 -298.125 -33.975 3 -298.125 -33.975 6 0.0063  
GW 171 7 -298.175 -33.975 3 -298.175 -33.975 6 0.0063  
GW 172 7 -298.2 -34.015 3 -298.2 -34.015 6 0.0063  
GW 173 7 -298.175 -34.065 3 -298.175 -34.065 6 0.0063  
GW 174 7 -298.125 -34.065 3 -298.125 -34.065 6 0.0063  
GW 175 7 -298.1 -34.015 3 -298.1 -34.015 6 0.0063  
GW 176 7 -298.125 -33.975 0 -298.125 -33.975 3 0.0063  
GW 177 7 -298.175 -33.975 0 -298.175 -33.975 3 0.0063

Powerline30.nec

GW 178 7 -298.2 -34.015 0 -298.2 -34.015 3 0.0063  
GW 179 7 -298.175 -34.065 0 -298.175 -34.065 3 0.0063  
GW 180 7 -298.125 -34.065 0 -298.125 -34.065 3 0.0063  
GW 181 7 -298.1 -34.015 0 -298.1 -34.015 3 0.0063  
GW 182 7 -298.175 -33.975 0 -298.175 -33.975 -3 0.0063  
GW 183 7 -298.2 -34.015 0 -298.2 -34.015 -3 0.0063  
GW 184 7 -298.175 -34.065 0 -298.175 -34.065 -3 0.0063  
GW 185 7 -298.125 -34.065 0 -298.125 -34.065 -3 0.0063  
GW 186 7 -298.1 -34.015 0 -298.1 -34.015 -3 0.0063  
GW 187 7 -298.125 -33.975 0 -298.125 -33.975 -3 0.0063  
GW 188 7 -298.15 -34.015 0 -298.15 -34.015 -3 0.0063  
GW 189 7 -298.15 -34.015 6 -298.15 -34.015 9 0.0063  
GW 190 7 -298.15 -34.015 3 -298.15 -34.015 6 0.0063  
GW 191 7 -298.15 -34.015 0 -298.15 -34.015 3 0.0063  
GW 192 7 -37 17 7.5 -37 17 10.85 0.0063  
GW 193 3 -96 -4 9.6 -96 -4.55 10.8 0.0063  
GW 194 3 -96 -4 11.4 -96 -4.55 10.8 0.0063  
GW 195 3 -168 -12 9.6 -168 -12.5 10.75 0.0063  
GW 196 3 -168 -12 12 -168 -12.5 10.75 0.0063  
GW 197 3 -235 -22 9.6 -235 -22 10.8 0.0063  
GW 198 3 -89 -120 11.4 -89.25 -120.25 10.5 0.0063  
GW 199 3 -89 -120 9.6 -89.25 -120.25 10.5 0.0063  
GW 200 3 2 49 10.8 2 49 9.6 0.0063  
GW 201 3 28 258 9.6 28.5 258 10.75 0.0063  
GW 202 3 28 258 12 28.5 258 10.75 0.0063  
GW 203 7 -0.055 -36 6 -0.055 -36 9 0.0063  
GW 204 3 1.75 157.75 10.8 1.9517 157.69 11.7 0.0063  
GW 205 7 0.5102 157.65 10.8 0.04829 158.31 11.7 0.0063  
GW 206 13 1 158 12 0.95 158.25 9.6 0.0063  
GW 207 3 0.95 158.25 9.6 0.9983 158 9 0.0063  
GW 208 11 0.5102 157.65 10.8 0.9983 158 9 0.0063  
GW 209 11 1.75 157.75 10.8 0.9983 158 9 0.0063  
GW 210 3 0 -36 10.8 0.32 -35.7 10.3 0.0063  
GW 211 7 0 -36 12 0.35 -36.3 10.35 0.0063  
GW 212 5 0 -36 11.4 -0.35 -36 10.35 0.0063  
GW 213 7 0.32 -35.7 10.3 0 -36.005 9 0.0063  
GW 214 7 0.35 -36.3 10.35 0 -36.005 9 0.0063  
GW 215 7 -0.35 -36 10.35 0 -36.005 9 0.0063  
GW 216 3 18.125 -96 9 18 -96 9.6 0.0063  
GW 217 7 18 -96 10.8 18.1 -95.75 9.6 0.0063  
GW 218 9 18 -96 11.4 18.35 -96 9.6 0.0063  
GW 219 3 18.35 -96 9.6 18.175 -96 9 0.0063  
GW 220 13 18 -96 12 18.125 -96.25 9.6 0.0063  
GW 221 3 18.125 -96.25 9.6 18.175 -96 9 0.0063  
GW 222 3 -298.1 -34.015 9 -298 -34 9.6 0.0063  
GW 223 7 -298 -34 10.8 -298.075 -34.15 9.6 0.0063  
GW 224 9 -298 -34 11.4 -298.25 -34 9.6 0.0063  
GW 225 13 -298 -34 12 -298.075 -33.875 9.6 0.0063  
GW 226 3 -298.075 -34.15 9.6 -298.15 -34.015 9 0.0063  
GW 227 3 -298.25 -34 9.6 -298.15 -34.015 9 0.0063  
GW 228 3 -298.075 -33.875 9.6 -298.15 -34.015 9 0.0063  
GW 229 3 18.175 -96 9 18.1 -95.75 9.6 0.0063  
GE -1  
LD 0 192 1 1 3 0.005  
LD 0 193 1 1 3 0.005  
LD 0 195 1 1 3 0.005  
LD 0 197 1 1 3 0.005  
LD 0 199 1 1 3 0.005  
LD 0 200 1 1 3 0.005  
LD 0 201 1 1 3 0.005  
LD 0 213 6 6 30 0  
LD 0 214 6 6 30 0  
LD 0 215 6 6 30 0

Powerline30.nec

```
LD 0 207 2 2 30 0
LD 0 208 10 10 30 0
LD 0 209 10 10 30 0
LD 0 219 2 2 30 0
LD 0 221 2 2 30 0
LD 0 226 2 2 30 0
LD 0 227 2 2 30 0
LD 0 228 2 2 30 0
LD 0 229 2 2 30 0
LD 5 0 0 0 58000000
GN 2 0 0 0 15 0.005
FR 0 1 0 0 30.000 0
EX 0 3 1 0 1 0
EN
CM Complex Power Line Model
CM Excitation Point 3
CM Excitation point for ionospheric study
CM 30 MHz
CM NTIA 2004
CE
CW 1 119 -298 -34 12 -235 -22 12 0.0063 3 64.90226708
CW 2 125 -235 -22 12 -168 -12 12 0.0063 3 68.55506412
CW 3 135 -168 -12 12 -96 -4 12 0.0063 3 73.31239808
CW 4 111 -96 -4 12 -36 0 12 0.0063 3 60.85478374
CW 5 67 -36 0 12 0 0 12 0.0063 3 36.432
CW 6 67 0 0 12 0 -36 12 0.0063 3 36.432
CW 7 107 0 -36 12 -2 -94 12 0.0063 3 58.73088618
CW 8 81 -2 -94 12 -44 -83 12 0.0063 3 43.93758573
CW 9 109 -44 -83 12 -89 -120 12 0.0063 3 58.95714321
CW 10 37 -2 -94 12 18 -96 12 0.0063 3 20.34094826
CW 11 91 0 0 12 2 49 12 0.0063 3 49.62928893
CW 12 107 2 49 12 -14 104 12 0.0063 3 57.96737413
CW 13 105 -14 104 12 1 158 12 0.0063 3 56.71716058
CW 14 93 1 158 12 19 205 12 0.0063 3 50.93286515
CW 15 99 19 205 12 28 258 12 0.0063 3 54.40382487
CW 16 105 28 258 12 30 315 12 0.0063 3 57.71949785
CW 17 119 -298 -34 11.4 -235 -22 11.4 0.0063 3 64.90226708
CW 18 125 -235 -22 11.4 -168 -12 11.4 0.0063 3 68.55506412
CW 19 135 -168 -12 11.4 -96 -4 11.4 0.0063 3 73.31239808
CW 20 111 -96 -4 11.4 -36 0 11.4 0.0063 3 60.85478374
CW 21 67 -36 0 11.4 0 0 11.4 0.0063 3 36.432
CW 22 67 0 0 11.4 0 -36 11.4 0.0063 3 36.432
CW 23 107 0 -36 11.4 -2 -94 11.4 0.0063 3 58.73088618
CW 24 81 -2 -94 11.4 -44 -83 11.4 0.0063 3 43.93758573
CW 25 109 -44 -83 11.4 -89 -120 11.4 0.0063 3 58.95714321
CW 26 37 -2 -94 11.4 18 -96 11.4 0.0063 3 20.34094826
CW 27 91 0 0 11.4 2 49 11.4 0.0063 3 49.62928893
CW 28 107 2 49 11.4 -14 104 11.4 0.0063 3 57.96737413
CW 29 105 -14 104 11.4 0.04829 158.31 11.7 0.0063 3 56.77149123
CW 30 93 0.04829 158.31 11.7 19 205 11.4 0.0063 3 50.99529567
CW 31 99 19 205 11.4 28 258 11.4 0.0063 3 54.40382487
CW 32 105 28 258 11.4 30 315 11.4 0.0063 3 57.71949785
CW 33 119 -298 -34 10.8 -235 -22 10.8 0.0063 3 64.90226708
CW 34 125 -235 -22 10.8 -168 -12 10.8 0.0063 3 68.55506412
CW 35 135 -168 -12 10.8 -96 -4 10.8 0.0063 3 73.31239808
CW 36 111 -96 -4 10.8 -36 0 10.8 0.0063 3 60.85478374
CW 37 33 -36 0 10.8 -37 17 10.85 0.0063 3 17.23381329
CW 38 67 -36 0 10.8 0 0 10.8 0.0063 3 36.432
CW 39 67 0 0 10.8 0 -36 10.8 0.0063 3 36.432
CW 40 107 0 -36 10.8 -2 -94 10.8 0.0063 3 58.73088618
CW 41 81 -2 -94 10.8 -44 -83 10.8 0.0063 3 43.93758573
CW 42 109 -44 -83 10.8 -89 -120 10.8 0.0063 3 58.95714321
CW 43 37 -2 -94 10.8 18 -96 10.8 0.0063 3 20.34094826
```

Powerline30.nec

CW 44 91 0 0 10.8 2 49 10.8 0.0063 3 49.62928893  
 CW 45 107 2 49 10.8 -14 104 10.8 0.0063 3 57.96737413  
 CW 46 105 -14 104 10.8 1.9517 157.69 11.7 0.0063 3 56.68901019  
 CW 47 93 1.9517 157.69 11.7 19 205 10.8 0.0063 3 50.89958235  
 CW 48 99 19 205 10.8 28 258 10.8 0.0063 3 54.40382487  
 CW 49 105 28 258 10.8 30 315 10.8 0.0063 3 57.71949785  
 CW 50 119 -298 -34 9.6 -235 -22 9.6 0.0063 3 64.90226708  
 CW 51 125 -235 -22 9.6 -168 -12 9.6 0.0063 3 68.55506412  
 CW 52 135 -168 -12 9.6 -96 -4 9.6 0.0063 3 73.31239808  
 CW 53 111 -96 -4 9.6 -36 0 9.6 0.0063 3 60.85478374  
 CW 54 33 -36 0 9.6 -37 17 7.5 0.0063 3 17.36428044  
 CW 55 67 -36 0 9.6 0 0 9.6 0.0063 3 36.432  
 CW 56 67 0 0 9.6 0 -36 9.6 0.0063 3 36.432  
 CW 57 107 0 -36 9.6 -2 -94 9.6 0.0063 3 58.73088618  
 CW 58 81 -2 -94 9.6 -44 -83 9.6 0.0063 3 43.93758573  
 CW 59 109 -44 -83 9.6 -89 -120 9.6 0.0063 3 58.95714321  
 CW 60 37 -2 -94 9.6 18 -96 9.6 0.0063 3 20.34094826  
 CW 61 91 0 0 9.6 2 49 9.6 0.0063 3 49.62928893  
 CW 62 107 2 49 9.6 -14 104 9.6 0.0063 3 57.96737413  
 CW 63 105 -14 104 9.6 1 158 9.6 0.0063 3 56.71716058  
 CW 64 93 1 158 9.6 19 205 9.6 0.0063 3 50.93286515  
 CW 65 99 19 205 9.6 28 258 9.6 0.0063 3 54.40382487  
 CW 66 105 28 258 9.6 30 315 9.6 0.0063 3 57.71949785  
 GW 67 19 -235 -22 9.6 -235 -22 0 0.0063  
 GW 68 19 -168 -12 9.6 -168 -12 0 0.0063  
 GW 69 19 -96 -4 9.6 -96 -4 0 0.0063  
 GW 70 15 -37 17 7.5 -37 17 0 0.0063  
 GW 71 19 2 49 9.6 2 49 0 0.0063  
 GW 72 19 28 258 9.6 28 258 0 0.0063  
 GW 73 19 -89 -120 9.6 -89 -120 0 0.0063  
 GW 74 7 -235 -22 0 -235 -22 -3 0.0063  
 GW 75 7 -168 -12 0 -168 -12 -3 0.0063  
 GW 76 7 -96 -4 0 -96 -4 -3 0.0063  
 GW 77 7 -37 17 0 -37 17 -3 0.0063  
 GW 78 7 2 49 0 2 49 -3 0.0063  
 GW 79 7 28 258 0 28 258 -3 0.0063  
 GW 80 7 -89 -120 0 -89 -120 -3 0.0063  
 GW 81 7 1.02 158.04 0 1.02 158.04 3 0.0063  
 GW 82 7 0.97 158.04 0 0.97 158.04 3 0.0063  
 GW 83 7 0.945 158 0 0.945 158 3 0.0063  
 GW 84 7 0.97 157.95 0 0.97 157.95 3 0.0063  
 GW 85 7 1.02 157.95 0 1.02 157.95 3 0.0063  
 GW 86 7 1.045 158 0 1.045 158 3 0.0063  
 GW 87 7 1.02 158.04 3 1.02 158.04 6 0.0063  
 GW 88 7 0.97 158.04 3 0.97 158.04 6 0.0063  
 GW 89 7 0.945 158 3 0.945 158 6 0.0063  
 GW 90 7 0.97 157.95 3 0.97 157.95 6 0.0063  
 GW 91 7 1.02 157.95 3 1.02 157.95 6 0.0063  
 GW 92 7 1.045 158 3 1.045 158 6 0.0063  
 GW 93 7 1.02 158.04 6 1.02 158.04 9 0.0063  
 GW 94 7 0.97 158.04 6 0.97 158.04 9 0.0063  
 GW 95 7 0.945 158 6 0.945 158 9 0.0063  
 GW 96 7 0.97 157.95 6 0.97 157.95 9 0.0063  
 GW 97 7 1.02 157.95 6 1.02 157.95 9 0.0063  
 GW 98 7 1.045 158 6 1.045 158 9 0.0063  
 GW 99 7 1.02 158.04 0 1.02 158.04 -3 0.0063  
 GW 100 7 0.97 158.04 0 0.97 158.04 -3 0.0063  
 GW 101 7 0.945 158 0 0.945 158 -3 0.0063  
 GW 102 7 0.97 157.95 0 0.97 157.95 -3 0.0063  
 GW 103 7 1.02 157.95 0 1.02 157.95 -3 0.0063  
 GW 104 7 1.045 158 0 1.045 158 -3 0.0063  
 GW 105 7 0.02 -35.96 0 0.02 -35.96 3 0.0063  
 GW 106 7 -0.03 -35.96 0 -0.03 -35.96 3 0.0063

Powerline30.nec

GW 107 7 -0.055 -36 0 -0.055 -36 3 0.0063  
 GW 108 7 -0.03 -36.05 0 -0.03 -36.05 3 0.0063  
 GW 109 7 0.02 -36.05 0 0.02 -36.05 3 0.0063  
 GW 110 7 0.045 -36 0 0.045 -36 3 0.0063  
 GW 111 7 0.02 -35.96 3 0.02 -35.96 6 0.0063  
 GW 112 7 -0.03 -35.96 3 -0.03 -35.96 6 0.0063  
 GW 113 7 -0.055 -36 3 -0.055 -36 6 0.0063  
 GW 114 7 -0.03 -36.05 3 -0.03 -36.05 6 0.0063  
 GW 115 7 0.02 -36.05 3 0.02 -36.05 6 0.0063  
 GW 116 7 0.045 -36 3 0.045 -36 6 0.0063  
 GW 117 7 0.02 -35.96 6 0.02 -35.96 9 0.0063  
 GW 118 7 -0.03 -35.96 6 -0.03 -35.96 9 0.0063  
 GW 119 7 -0.03 -36.05 6 -0.03 -36.05 9 0.0063  
 GW 120 7 0.02 -36.05 6 0.02 -36.05 9 0.0063  
 GW 121 7 0.045 -36 6 0.045 -36 9 0.0063  
 GW 122 7 0.02 -35.96 0 0.02 -35.96 -3 0.0063  
 GW 123 7 -0.03 -35.96 0 -0.03 -35.96 -3 0.0063  
 GW 124 7 -0.055 -36 0 -0.055 -36 -3 0.0063  
 GW 125 7 -0.03 -36.05 0 -0.03 -36.05 -3 0.0063  
 GW 126 7 0.02 -36.05 0 0.02 -36.05 -3 0.0063  
 GW 127 7 0.045 -36 0 0.045 -36 -3 0.0063  
 GW 128 7 18.2 -95.96 6 18.2 -95.96 9 0.0063  
 GW 129 7 18.15 -95.96 6 18.15 -95.96 9 0.0063  
 GW 130 7 18.125 -96 6 18.125 -96 9 0.0063  
 GW 131 7 18.15 -96.05 6 18.15 -96.05 9 0.0063  
 GW 132 7 18.2 -96.05 6 18.2 -96.05 9 0.0063  
 GW 133 7 18.225 -96 6 18.225 -96 9 0.0063  
 GW 134 7 18.2 -95.96 3 18.2 -95.96 6 0.0063  
 GW 135 7 18.15 -95.96 3 18.15 -95.96 6 0.0063  
 GW 136 7 18.125 -96 3 18.125 -96 6 0.0063  
 GW 137 7 18.15 -96.05 3 18.15 -96.05 6 0.0063  
 GW 138 7 18.2 -96.05 3 18.2 -96.05 6 0.0063  
 GW 139 7 18.225 -96 3 18.225 -96 6 0.0063  
 GW 140 7 18.2 -95.96 0 18.2 -95.96 3 0.0063  
 GW 141 7 18.15 -95.96 0 18.15 -95.96 3 0.0063  
 GW 142 7 18.125 -96 0 18.125 -96 3 0.0063  
 GW 143 7 18.15 -96.05 0 18.15 -96.05 3 0.0063  
 GW 144 7 18.2 -96.05 0 18.2 -96.05 3 0.0063  
 GW 145 7 18.225 -96 0 18.225 -96 3 0.0063  
 GW 146 7 18.15 -95.96 0 18.15 -95.96 -3 0.0063  
 GW 147 7 18.125 -96 0 18.125 -96 -3 0.0063  
 GW 148 7 18.15 -96.05 0 18.15 -96.05 -3 0.0063  
 GW 149 7 18.2 -96.05 0 18.2 -96.05 -3 0.0063  
 GW 150 7 18.225 -96 0 18.225 -96 -3 0.0063  
 GW 151 7 18.2 -95.96 0 18.2 -95.96 -3 0.0063  
 GW 152 7 18.175 -96 0 18.175 -96 -3 0.0063  
 GW 153 7 0 -36 0 0 -36 3 0.0063  
 GW 154 7 0 -36 3 0 -36 6 0.0063  
 GW 155 7 0 -36 6 0 -36.005 9 0.0063  
 GW 156 7 0 -36 0 0 -36 -3 0.0063  
 GW 157 7 0.9983 158 0 0.9983 158 3 0.0063  
 GW 158 7 0.9983 158 3 0.9983 158 6 0.0063  
 GW 159 7 0.9983 158 6 0.9983 158 9 0.0063  
 GW 160 7 0.9983 158 0 0.9983 158 -3 0.0063  
 GW 161 7 18.175 -96 6 18.175 -96 9 0.0063  
 GW 162 7 18.175 -96 3 18.175 -96 6 0.0063  
 GW 163 7 18.175 -96 0 18.175 -96 3 0.0063  
 GW 164 7 -298.125 -33.975 6 -298.125 -33.975 9 0.0063  
 GW 165 7 -298.175 -33.975 6 -298.175 -33.975 9 0.0063  
 GW 166 7 -298.2 -34.015 6 -298.2 -34.015 9 0.0063  
 GW 167 7 -298.175 -34.065 6 -298.175 -34.065 9 0.0063  
 GW 168 7 -298.125 -34.065 6 -298.125 -34.065 9 0.0063  
 GW 169 7 -298.1 -34.015 6 -298.1 -34.015 9 0.0063

Powerline30.nec

GW 170 7 -298.125 -33.975 3 -298.125 -33.975 6 0.0063  
 GW 171 7 -298.175 -33.975 3 -298.175 -33.975 6 0.0063  
 GW 172 7 -298.2 -34.015 3 -298.2 -34.015 6 0.0063  
 GW 173 7 -298.175 -34.065 3 -298.175 -34.065 6 0.0063  
 GW 174 7 -298.125 -34.065 3 -298.125 -34.065 6 0.0063  
 GW 175 7 -298.1 -34.015 3 -298.1 -34.015 6 0.0063  
 GW 176 7 -298.125 -33.975 0 -298.125 -33.975 3 0.0063  
 GW 177 7 -298.175 -33.975 0 -298.175 -33.975 3 0.0063  
 GW 178 7 -298.2 -34.015 0 -298.2 -34.015 3 0.0063  
 GW 179 7 -298.175 -34.065 0 -298.175 -34.065 3 0.0063  
 GW 180 7 -298.125 -34.065 0 -298.125 -34.065 3 0.0063  
 GW 181 7 -298.1 -34.015 0 -298.1 -34.015 3 0.0063  
 GW 182 7 -298.175 -33.975 0 -298.175 -33.975 -3 0.0063  
 GW 183 7 -298.2 -34.015 0 -298.2 -34.015 -3 0.0063  
 GW 184 7 -298.175 -34.065 0 -298.175 -34.065 -3 0.0063  
 GW 185 7 -298.125 -34.065 0 -298.125 -34.065 -3 0.0063  
 GW 186 7 -298.1 -34.015 0 -298.1 -34.015 -3 0.0063  
 GW 187 7 -298.125 -33.975 0 -298.125 -33.975 -3 0.0063  
 GW 188 7 -298.15 -34.015 0 -298.15 -34.015 -3 0.0063  
 GW 189 7 -298.15 -34.015 6 -298.15 -34.015 9 0.0063  
 GW 190 7 -298.15 -34.015 3 -298.15 -34.015 6 0.0063  
 GW 191 7 -298.15 -34.015 0 -298.15 -34.015 3 0.0063  
 GW 192 7 -37 17 7.5 -37 17 10.85 0.0063  
 GW 193 3 -96 -4 9.6 -96 -4.55 10.8 0.0063  
 GW 194 3 -96 -4 11.4 -96 -4.55 10.8 0.0063  
 GW 195 3 -168 -12 9.6 -168 -12.5 10.75 0.0063  
 GW 196 3 -168 -12 12 -168 -12.5 10.75 0.0063  
 GW 197 3 -235 -22 9.6 -235 -22 10.8 0.0063  
 GW 198 3 -89 -120 11.4 -89.25 -120.25 10.5 0.0063  
 GW 199 3 -89 -120 9.6 -89.25 -120.25 10.5 0.0063  
 GW 200 3 2 49 10.8 2 49 9.6 0.0063  
 GW 201 3 28 258 9.6 28.5 258 10.75 0.0063  
 GW 202 3 28 258 12 28.5 258 10.75 0.0063  
 GW 203 7 -0.055 -36 6 -0.055 -36 9 0.0063  
 GW 204 3 1.75 157.75 10.8 1.9517 157.69 11.7 0.0063  
 GW 205 7 0.5102 157.65 10.8 0.04829 158.31 11.7 0.0063  
 GW 206 13 1 158 12 0.95 158.25 9.6 0.0063  
 GW 207 3 0.95 158.25 9.6 0.9983 158 9 0.0063  
 GW 208 11 0.5102 157.65 10.8 0.9983 158 9 0.0063  
 GW 209 11 1.75 157.75 10.8 0.9983 158 9 0.0063  
 GW 210 3 0 -36 10.8 0.32 -35.7 10.3 0.0063  
 GW 211 7 0 -36 12 0.35 -36.3 10.35 0.0063  
 GW 212 5 0 -36 11.4 -0.35 -36 10.35 0.0063  
 GW 213 7 0.32 -35.7 10.3 0 -36.005 9 0.0063  
 GW 214 7 0.35 -36.3 10.35 0 -36.005 9 0.0063  
 GW 215 7 -0.35 -36 10.35 0 -36.005 9 0.0063  
 GW 216 3 18.125 -96 9 18 -96 9.6 0.0063  
 GW 217 7 18 -96 10.8 18.1 -95.75 9.6 0.0063  
 GW 218 9 18 -96 11.4 18.35 -96 9.6 0.0063  
 GW 219 3 18.35 -96 9.6 18.175 -96 9 0.0063  
 GW 220 13 18 -96 12 18.125 -96.25 9.6 0.0063  
 GW 221 3 18.125 -96.25 9.6 18.175 -96 9 0.0063  
 GW 222 3 -298.1 -34.015 9 -298 -34 9.6 0.0063  
 GW 223 7 -298 -34 10.8 -298.075 -34.15 9.6 0.0063  
 GW 224 9 -298 -34 11.4 -298.25 -34 9.6 0.0063  
 GW 225 13 -298 -34 12 -298.075 -33.875 9.6 0.0063  
 GW 226 3 -298.075 -34.15 9.6 -298.15 -34.015 9 0.0063  
 GW 227 3 -298.25 -34 9.6 -298.15 -34.015 9 0.0063  
 GW 228 3 -298.075 -33.875 9.6 -298.15 -34.015 9 0.0063  
 GW 229 3 18.175 -96 9 18.1 -95.75 9.6 0.0063  
 GE -1  
 LD 0 192 1 1 3 0.005  
 LD 0 193 1 1 3 0.005

Powerline30.nec

```
LD 0 195 1 1 3 0.005
LD 0 197 1 1 3 0.005
LD 0 199 1 1 3 0.005
LD 0 200 1 1 3 0.005
LD 0 201 1 1 3 0.005
LD 0 213 6 6 30 0
LD 0 214 6 6 30 0
LD 0 215 6 6 30 0
LD 0 207 2 2 30 0
LD 0 208 10 10 30 0
LD 0 209 10 10 30 0
LD 0 219 2 2 30 0
LD 0 221 2 2 30 0
LD 0 226 2 2 30 0
LD 0 227 2 2 30 0
LD 0 228 2 2 30 0
LD 0 229 2 2 30 0
LD 5 0 0 0 58000000
GN 2 0 0 0 15 0.005
FR 0 1 0 0 30.000 0
EX 0 11 1 0 1 0
EN
```



tri310n.nec

```

CM Catenary three-wire BPL model
CM Center-fed, triangular-horizontal configuration
CM Multi-grounded neutral, three transformers
CM 1.0 meter wire spacing
CM 50 MHz
CE NTIA 2004
CW 1 143 0.0 0.0 12.0 42.5 0.0 12.0 0.0063 3 43.0
CW 2 143 42.5 0.0 12.0 85.0 0.0 12.0 0.0063 3 43.0
CW 3 143 85.0 0.0 12.0 127.5 0.0 12.0 0.0063 3 43.0
CW 4 143 127.5 0.0 12.0 170.0 0.0 12.0 0.0063 3 43.0
CW 5 143 -170.0 0.0 12.0 -127.5 0.0 12.0 0.0063 3 43.0
CW 6 143 -127.5 0.0 12.0 -85.0 0.0 12.0 0.0063 3 43.0
CW 7 143 -85.0 0.0 12.0 -42.5 0.0 12.0 0.0063 3 43.0
CW 8 143 -42.5 0.0 12.0 0.0 0.0 12.0 0.0063 3 43.0
CW 9 143 0.0 1.0 12.25 42.5 1.0 12.25 0.0063 3 43.0
CW 10 143 42.5 1.0 12.25 85.0 1.0 12.25 0.0063 3 43.0
CW 11 143 85.0 1.0 12.25 127.5 1.0 12.25 0.0063 3 43.0
CW 12 143 127.5 1.0 12.25 170.0 1.0 12.25 0.0063 3 43.0
CW 13 143 -170.0 1.0 12.25 -127.5 1.0 12.25 0.0063 3 43.0
CW 14 143 -127.5 1.0 12.25 -85.0 1.0 12.25 0.0063 3 43.0
CW 15 143 -85.0 1.0 12.25 -42.5 1.0 12.25 0.0063 3 43.0
CW 16 143 -42.5 1.0 12.25 0.0 1.0 12.25 0.0063 3 43.0
CW 17 143 0.0 2.0 12.0 42.5 2.0 12.0 0.0063 3 43.0
CW 18 143 42.5 2.0 12.0 85.0 2.0 12.0 0.0063 3 43.0
CW 19 143 85.0 2.0 12.0 127.5 2.0 12.0 0.0063 3 43.0
CW 20 143 127.5 2.0 12.0 170.0 2.0 12.0 0.0063 3 43.0
CW 21 143 -170.0 2.0 12.0 -127.5 2.0 12.0 0.0063 3 43.0
CW 22 143 -127.5 2.0 12.0 -85.0 2.0 12.0 0.0063 3 43.0
CW 23 143 -85.0 2.0 12.0 -42.5 2.0 12.0 0.0063 3 43.0
CW 24 143 -42.5 2.0 12.0 0.0 2.0 12.0 0.0063 3 43.0
CW 25 143 0.0 1.0 9.0 42.5 1.0 9.0 0.0063 3 43.0
CW 26 143 42.5 1.0 9.0 85.0 1.0 9.0 0.0063 3 43.0
CW 27 143 85.0 1.0 9.0 127.5 1.0 9.0 0.0063 3 43.0
CW 28 143 127.5 1.0 9.0 170.0 1.0 9.0 0.0063 3 43.0
CW 29 143 -170.0 1.0 9.0 -127.5 1.0 9.0 0.0063 3 43.0
CW 30 143 -127.5 1.0 9.0 -85.0 1.0 9.0 0.0063 3 43.0
CW 31 143 -85.0 1.0 9.0 -42.5 1.0 9.0 0.0063 3 43.0
CW 32 143 -42.5 1.0 9.0 0.0 1.0 9.0 0.0063 3 43.0
GW 33 31 0.0 1.0 9.0 0.0 1.0 0.0 0.0063
GW 34 31 170.0 1.0 9.0 170.0 1.0 0.0 0.0063
GW 35 31 -170.0 1.0 9.0 -170.0 1.0 0.0 0.0063
GW 36 33 0.0 1.0 0.0 0.0 1.0 -2.5 0.0063
GW 37 33 170.0 1.0 0.0 170.0 1.0 -2.5 0.0063
GW 38 33 -170.0 1.0 0.0 -170.0 1.0 -2.5 0.0063
GW 39 7 0.0 1.0 9.0 0.0 0.0 12.0 0.0063
GW 40 7 -170.0 1.0 9.0 -170.0 1.0 12.25 0.0063
GW 41 7 170.0 1.0 9.0 170.0 2.0 12.0 0.0063
GE -1
LD 5 0 0 0 58000000.0 0.0
LD 2 31 1 1 7.7 0.0
LD 0 32 1 1 7.7 0.0
LD 0 33 1 1 7.7 0.0
EX 0 1 1 0 1.0 0.0
GN 2 0 0 0 15.0 .005
FR 0 1 0 0 50 0.0
EN

```

tri310.nec

```
CM Catenary three-wire BPL model
CM Center-fed, triangular-horizontal configuration
CM No multi-grounded neutral, no transformers
CM 1.0 meter wire spacing
CM 50 MHz
CE NTIA 2004
CW 1 143 0.0 0.0 12.0 42.5 0.0 12.0 0.0063 3 43.0
CW 2 143 42.5 0.0 12.0 85.0 0.0 12.0 0.0063 3 43.0
CW 3 143 85.0 0.0 12.0 127.5 0.0 12.0 0.0063 3 43.0
CW 4 143 127.5 0.0 12.0 170.0 0.0 12.0 0.0063 3 43.0
CW 5 143 -170.0 0.0 12.0 -127.5 0.0 12.0 0.0063 3 43.0
CW 6 143 -127.5 0.0 12.0 -85.0 0.0 12.0 0.0063 3 43.0
CW 7 143 -85.0 0.0 12.0 -42.5 0.0 12.0 0.0063 3 43.0
CW 8 143 -42.5 0.0 12.0 0.0 0.0 12.0 0.0063 3 43.0
CW 9 143 0.0 1.0 12.25 42.5 1.0 12.25 0.0063 3 43.0
CW 10 143 42.5 1.0 12.25 85.0 1.0 12.25 0.0063 3 43.0
CW 11 143 85.0 1.0 12.25 127.5 1.0 12.25 0.0063 3 43.0
CW 12 143 127.5 1.0 12.25 170.0 1.0 12.25 0.0063 3 43.0
CW 13 143 -170.0 1.0 12.25 -127.5 1.0 12.25 0.0063 3 43.0
CW 14 143 -127.5 1.0 12.25 -85.0 1.0 12.25 0.0063 3 43.0
CW 15 143 -85.0 1.0 12.25 -42.5 1.0 12.25 0.0063 3 43.0
CW 16 143 -42.5 1.0 12.25 0.0 1.0 12.25 0.0063 3 43.0
CW 17 143 0.0 2.0 12.0 42.5 2.0 12.0 0.0063 3 43.0
CW 18 143 42.5 2.0 12.0 85.0 2.0 12.0 0.0063 3 43.0
CW 19 143 85.0 2.0 12.0 127.5 2.0 12.0 0.0063 3 43.0
CW 20 143 127.5 2.0 12.0 170.0 2.0 12.0 0.0063 3 43.0
CW 21 143 -170.0 2.0 12.0 -127.5 2.0 12.0 0.0063 3 43.0
CW 22 143 -127.5 2.0 12.0 -85.0 2.0 12.0 0.0063 3 43.0
CW 23 143 -85.0 2.0 12.0 -42.5 2.0 12.0 0.0063 3 43.0
CW 24 143 -42.5 2.0 12.0 0.0 2.0 12.0 0.0063 3 43.0
GE -1
LD 5 0 0 0 58000000.0 0.0
EX 0 1 1 0 1.0 0.0
GN 2 0 0 0 15.0 .005
FR 0 1 0 0 50 0.0
EN
```

tri210n.nec

CM Catenary two-wire BPL model  
 CM Center-fed, triangular-horizontal configuration  
 CM Multi-grounded neutral, three transformers  
 CM 1.0 meter wire spacing  
 CM 50 MHz  
 CE NTIA 2004  
 CW 1 143 0.0 0.0 12.0 42.5 0.0 12.0 0.0063 3 43  
 CW 2 143 42.5 0.0 12.0 85.0 0.0 12.0 0.0063 3 43  
 CW 3 143 85.0 0.0 12.0 127.5 0.0 12.0 0.0063 3 43  
 CW 4 143 127.5 0.0 12.0 170.0 0.0 12.0 0.0063 3 43  
 CW 5 143 -170.0 0.0 12.0 -127.5 0.0 12.0 0.0063 3 43  
 CW 6 143 -127.5 0.0 12.0 -85.0 0.0 12.0 0.0063 3 43  
 CW 7 143 -85.0 0.0 12.0 -42.5 0.0 12.0 0.0063 3 43  
 CW 8 143 -42.5 0.0 12.0 0.0 0.0 12.0 0.0063 3 43  
 CW 9 143 0.0 1.0 12.0 42.5 1.0 12.0 0.0063 3 43  
 CW 10 143 42.5 1.0 12.0 85.0 1.0 12.0 0.0063 3 43  
 CW 11 143 85.0 1.0 12.0 127.5 1.0 12.0 0.0063 3 43  
 CW 12 143 127.5 1.0 12.0 170.0 1.0 12.0 0.0063 3 43  
 CW 13 143 -170.0 1.0 12.0 -127.5 1.0 12.0 0.0063 3 43  
 CW 14 143 -127.5 1.0 12.0 -85.0 1.0 12.0 0.0063 3 43  
 CW 15 143 -85.0 1.0 12.0 -42.5 1.0 12.0 0.0063 3 43  
 CW 16 143 -42.5 1.0 12.0 0.0 1.0 12.0 0.0063 3 43  
 CW 17 143 0.0 0.5 9.0 42.5 0.5 9.0 0.0063 3 43  
 CW 18 143 42.5 0.5 9.0 85.0 0.5 9.0 0.0063 3 43  
 CW 19 143 85.0 0.5 9.0 127.5 0.5 9.0 0.0063 3 43  
 CW 20 143 127.5 0.5 9.0 170.0 0.5 9.0 0.0063 3 43  
 CW 21 143 -170.0 0.5 9.0 -127.5 0.5 9.0 0.0063 3 43  
 CW 22 143 -127.5 0.5 9.0 -85.0 0.5 9.0 0.0063 3 43  
 CW 23 143 -85.0 0.5 9.0 -42.5 0.5 9.0 0.0063 3 43  
 CW 24 143 -42.5 0.5 9.0 0.0 0.5 9.0 0.0063 3 43  
 GW 25 31 0.0 0.5 9.0 0.0 0.5 0.0 0.0063  
 GW 26 31 170.0 0.5 9.0 170.0 0.5 0.0 0.0063  
 GW 27 31 -170.0 0.5 9.0 -170.0 0.5 0.0 0.0063  
 GW 28 33 0.0 0.5 0.0 0.0 0.5 -2.5 0.0063  
 GW 29 33 170.0 0.5 0.0 170.0 0.5 -2.5 0.0063  
 GW 30 33 -170.0 0.5 0.0 -170.0 0.5 -2.5 0.0063  
 GW 31 7 0.0 0.5 9.0 0.0 0.0 12.0 0.0063  
 GW 32 7 170.0 0.5 9.0 170.0 1.0 12.0 0.0063  
 GW 33 7 -170.0 0.5 9.0 -170.0 1.0 12.0 0.0063  
 GE -1  
 LD 5 0 0 0 58000000.0 0.0  
 LD 2 31 1 1 7.7 0.0  
 LD 0 32 1 1 7.7 0.0  
 LD 0 33 1 1 7.7 0.0  
 EX 0 1 1 0 1.0 0.0  
 GN 2 0 0 0 15.0 .005  
 FR 0 1 0 0 50 0.0  
 EN

tri210.nec

```
CM Catenary two-wire BPL model
CM Center-fed, triangular-horizontal configuration
CM No multi-grounded neutral, no transformers
CM 1.0 meter wire spacing
CM 50 MHz
CE NTIA 2004
CW 1 143 0.0 0.0 12.0 42.5 0.0 12.0 0.0063 3 43
CW 2 143 42.5 0.0 12.0 85.0 0.0 12.0 0.0063 3 43
CW 3 143 85.0 0.0 12.0 127.5 0.0 12.0 0.0063 3 43
CW 4 143 127.5 0.0 12.0 170.0 0.0 12.0 0.0063 3 43
CW 5 143 -170.0 0.0 12.0 -127.5 0.0 12.0 0.0063 3 43
CW 6 143 -127.5 0.0 12.0 -85.0 0.0 12.0 0.0063 3 43
CW 7 143 -85.0 0.0 12.0 -42.5 0.0 12.0 0.0063 3 43
CW 8 143 -42.5 0.0 12.0 0.0 0.0 12.0 0.0063 3 43
CW 9 143 0.0 1.0 12.0 42.5 1.0 12.0 0.0063 3 43
CW 10 143 42.5 1.0 12.0 85.0 1.0 12.0 0.0063 3 43
CW 11 143 85.0 1.0 12.0 127.5 1.0 12.0 0.0063 3 43
CW 12 143 127.5 1.0 12.0 170.0 1.0 12.0 0.0063 3 43
CW 13 143 -170.0 1.0 12.0 -127.5 1.0 12.0 0.0063 3 43
CW 14 143 -127.5 1.0 12.0 -85.0 1.0 12.0 0.0063 3 43
CW 15 143 -85.0 1.0 12.0 -42.5 1.0 12.0 0.0063 3 43
CW 16 143 -42.5 1.0 12.0 0.0 1.0 12.0 0.0063 3 43
GE -1
LD 5 0 0 0 58000000.0 0.0
EX 0 1 1 0 1.0 0.0
GN 2 0 0 0 15.0 .005
FR 0 1 0 0 50 0.0
EN
```

tri36n.nec

```

CM Catenary three-wire BPL model
CM Center-fed, triangular-horizontal configuration
CM Multi-grounded neutral, three transformers
CM 0.6 meter wire spacing
CM 50 MHz
CE NTIA 2004
CW 1 143 0.0 0.0 12.0 42.5 0.0 12.0 0.0063 3 43.0
CW 2 143 42.5 0.0 12.0 85.0 0.0 12.0 0.0063 3 43.0
CW 3 143 85.0 0.0 12.0 127.5 0.0 12.0 0.0063 3 43.0
CW 4 143 127.5 0.0 12.0 170.0 0.0 12.0 0.0063 3 43.0
CW 5 143 -170.0 0.0 12.0 -127.5 0.0 12.0 0.0063 3 43.0
CW 6 143 -127.5 0.0 12.0 -85.0 0.0 12.0 0.0063 3 43.0
CW 7 143 -85.0 0.0 12.0 -42.5 0.0 12.0 0.0063 3 43.0
CW 8 143 -42.5 0.0 12.0 0.0 0.0 12.0 0.0063 3 43.0
CW 9 143 0.0 .6 12.25 42.5 .6 12.25 0.0063 3 43.0
CW 10 143 42.5 .6 12.25 85.0 .6 12.25 0.0063 3 43.0
CW 11 143 85.0 .6 12.25 127.5 .6 12.25 0.0063 3 43.0
CW 12 143 127.5 .6 12.25 170.0 .6 12.25 0.0063 3 43.0
CW 13 143 -170.0 .6 12.25 -127.5 .6 12.25 0.0063 3 43.0
CW 14 143 -127.5 .6 12.25 -85.0 .6 12.25 0.0063 3 43.0
CW 15 143 -85.0 .6 12.25 -42.5 .6 12.25 0.0063 3 43.0
CW 16 143 -42.5 .6 12.25 0.0 .6 12.25 0.0063 3 43.0
CW 17 143 0.0 1.2 12.0 42.5 1.2 12.0 0.0063 3 43.0
CW 18 143 42.5 1.2 12.0 85.0 1.2 12.0 0.0063 3 43.0
CW 19 143 85.0 1.2 12.0 127.5 1.2 12.0 0.0063 3 43.0
CW 20 143 127.5 1.2 12.0 170.0 1.2 12.0 0.0063 3 43.0
CW 21 143 -170.0 1.2 12.0 -127.5 1.2 12.0 0.0063 3 43.0
CW 22 143 -127.5 1.2 12.0 -85.0 1.2 12.0 0.0063 3 43.0
CW 23 143 -85.0 1.2 12.0 -42.5 1.2 12.0 0.0063 3 43.0
CW 24 143 -42.5 1.2 12.0 0.0 1.2 12.0 0.0063 3 43.0
CW 25 143 0.0 .6 9.0 42.5 .6 9.0 0.0063 3 43.0
CW 26 143 42.5 .6 9.0 85.0 .6 9.0 0.0063 3 43.0
CW 27 143 85.0 .6 9.0 127.5 .6 9.0 0.0063 3 43.0
CW 28 143 127.5 .6 9.0 170.0 .6 9.0 0.0063 3 43.0
CW 29 143 -170.0 .6 9.0 -127.5 .6 9.0 0.0063 3 43.0
CW 30 143 -127.5 .6 9.0 -85.0 .6 9.0 0.0063 3 43.0
CW 31 143 -85.0 .6 9.0 -42.5 .6 9.0 0.0063 3 43.0
CW 32 143 -42.5 .6 9.0 0.0 .6 9.0 0.0063 3 43.0
GW 33 31 0.0 .6 9.0 0.0 .6 0.0 0.0063
GW 34 31 170.0 .6 9.0 170.0 .6 0.0 0.0063
GW 35 31 -170.0 .6 9.0 -170.0 .6 0.0 0.0063
GW 36 33 0.0 .6 0.0 0.0 .6 -2.5 0.0063
GW 37 33 170.0 .6 0.0 170.0 .6 -2.5 0.0063
GW 38 33 -170.0 .6 0.0 -170.0 .6 -2.5 0.0063
GW 39 7 0.0 .6 9.0 0.0 0.0 12.0 0.0063
GW 40 7 -170.0 .6 9.0 -170.0 .6 12.25 0.0063
GW 41 7 170.0 .6 9.0 170.0 1.2 12.0 0.0063
GE -1
LD 5 0 0 0 58000000.0 0.0
LD 2 31 1 1 7.7 0.0
LD 0 32 1 1 7.7 0.0
LD 0 33 1 1 7.7 0.0
EX 0 1 1 0 1.0 0.0
GN 2 0 0 0 15.0 .005
FR 0 1 0 0 50 0.0
EN

```

tri36.nec

```
CM Catenary three-wire BPL model
CM Center-fed, triangular-horizontal configuration
CM No multi-grounded neutral, no transformers
CM 0.6 meter wire spacing
CM 50 MHz
CE NTIA 2004
CW 1 143 0.0 0.0 12.0 42.5 0.0 12.0 0.0063 3 43.0
CW 2 143 42.5 0.0 12.0 85.0 0.0 12.0 0.0063 3 43.0
CW 3 143 85.0 0.0 12.0 127.5 0.0 12.0 0.0063 3 43.0
CW 4 143 127.5 0.0 12.0 170.0 0.0 12.0 0.0063 3 43.0
CW 5 143 -170.0 0.0 12.0 -127.5 0.0 12.0 0.0063 3 43.0
CW 6 143 -127.5 0.0 12.0 -85.0 0.0 12.0 0.0063 3 43.0
CW 7 143 -85.0 0.0 12.0 -42.5 0.0 12.0 0.0063 3 43.0
CW 8 143 -42.5 0.0 12.0 0.0 0.0 12.0 0.0063 3 43.0
CW 9 143 0.0 0.6 12.25 42.5 0.6 12.25 0.0063 3 43.0
CW 10 143 42.5 0.6 12.25 85.0 0.6 12.25 0.0063 3 43.0
CW 11 143 85.0 0.6 12.25 127.5 0.6 12.25 0.0063 3 43.0
CW 12 143 127.5 0.6 12.25 170.0 0.6 12.25 0.0063 3 43.0
CW 13 143 -170.0 0.6 12.25 -127.5 0.6 12.25 0.0063 3 43.0
CW 14 143 -127.5 0.6 12.25 -85.0 0.6 12.25 0.0063 3 43.0
CW 15 143 -85.0 0.6 12.25 -42.5 0.6 12.25 0.0063 3 43.0
CW 16 143 -42.5 0.6 12.25 0.0 0.6 12.25 0.0063 3 43.0
CW 17 143 0.0 1.2 12.0 42.5 1.2 12.0 0.0063 3 43.0
CW 18 143 42.5 1.2 12.0 85.0 1.2 12.0 0.0063 3 43.0
CW 19 143 85.0 1.2 12.0 127.5 1.2 12.0 0.0063 3 43.0
CW 20 143 127.5 1.2 12.0 170.0 1.2 12.0 0.0063 3 43.0
CW 21 143 -170.0 1.2 12.0 -127.5 1.2 12.0 0.0063 3 43.0
CW 22 143 -127.5 1.2 12.0 -85.0 1.2 12.0 0.0063 3 43.0
CW 23 143 -85.0 1.2 12.0 -42.5 1.2 12.0 0.0063 3 43.0
CW 24 143 -42.5 1.2 12.0 0.0 1.2 12.0 0.0063 3 43.0
GE -1
LD 5 0 0 0 58000000.0 0.0
EX 0 1 1 0 1.0 0.0
GN 2 0 0 0 15.0 .005
FR 0 1 0 0 50 0.0
EN
```

tri26n.nec

```

CM Catenary two-wire BPL model
CM Center-fed, triangular-horizontal configuration
CM Multi-grounded neutral, three transformers
CM 0.6 meter wire spacing
CM 50 MHz
CE NTIA 2004
CW 1 143 0.0 0.0 12.0 42.5 0.0 12.0 0.0063 3 43
CW 2 143 42.5 0.0 12.0 85.0 0.0 12.0 0.0063 3 43
CW 3 143 85.0 0.0 12.0 127.5 0.0 12.0 0.0063 3 43
CW 4 143 127.5 0.0 12.0 170.0 0.0 12.0 0.0063 3 43
CW 5 143 -170.0 0.0 12.0 -127.5 0.0 12.0 0.0063 3 43
CW 6 143 -127.5 0.0 12.0 -85.0 0.0 12.0 0.0063 3 43
CW 7 143 -85.0 0.0 12.0 -42.5 0.0 12.0 0.0063 3 43
CW 8 143 -42.5 0.0 12.0 0.0 0.0 12.0 0.0063 3 43
CW 9 143 0.0 0.6 12.0 42.5 0.6 12.0 0.0063 3 43
CW 10 143 42.5 0.6 12.0 85.0 0.6 12.0 0.0063 3 43
CW 11 143 85.0 0.6 12.0 127.5 0.6 12.0 0.0063 3 43
CW 12 143 127.5 0.6 12.0 170.0 0.6 12.0 0.0063 3 43
CW 13 143 -170.0 0.6 12.0 -127.5 0.6 12.0 0.0063 3 43
CW 14 143 -127.5 0.6 12.0 -85.0 0.6 12.0 0.0063 3 43
CW 15 143 -85.0 0.6 12.0 -42.5 0.6 12.0 0.0063 3 43
CW 16 143 -42.5 0.6 12.0 0.0 0.6 12.0 0.0063 3 43
CW 17 143 0.0 0.3 9.0 42.5 0.3 9.0 0.0063 3 43
CW 18 143 42.5 0.3 9.0 85.0 0.3 9.0 0.0063 3 43
CW 19 143 85.0 0.3 9.0 127.5 0.3 9.0 0.0063 3 43
CW 20 143 127.5 0.3 9.0 170.0 0.3 9.0 0.0063 3 43
CW 21 143 -170.0 0.3 9.0 -127.5 0.3 9.0 0.0063 3 43
CW 22 143 -127.5 0.3 9.0 -85.0 0.3 9.0 0.0063 3 43
CW 23 143 -85.0 0.3 9.0 -42.5 0.3 9.0 0.0063 3 43
CW 24 143 -42.5 0.3 9.0 0.0 0.3 9.0 0.0063 3 43
GW 25 31 0.0 0.3 9.0 0.0 0.3 0.0 0.0063
GW 26 31 170.0 0.3 9.0 170.0 0.3 0.0 0.0063
GW 27 31 -170.0 0.3 9.0 -170.0 0.3 0.0 0.0063
GW 28 33 0.0 0.3 0.0 0.0 0.3 -2.5 0.0063
GW 29 33 170.0 0.3 0.0 170.0 0.3 -2.5 0.0063
GW 30 33 -170.0 0.3 0.0 -170.0 0.3 -2.5 0.0063
GW 31 7 0.0 0.3 9.0 0.0 0.0 12.0 0.0063
GW 32 7 170.0 0.3 9.0 170.0 0.6 12.0 0.0063
GW 33 7 -170.0 0.3 9.0 -170.0 0.6 12.0 0.0063
GE -1
LD 5 0 0 0 58000000.0 0.0
LD 2 31 1 1 7.7 0.0
LD 0 32 1 1 7.7 0.0
LD 0 33 1 1 7.7 0.0
EX 0 1 1 0 1.0 0.0
GN 2 0 0 0 15.0 .005
FR 0 1 0 0 50 0.0
EN

```

tri26.nec

```
CM Catenary two-wire BPL model
CM Center-fed, triangular-horizontal configuration
CM No multi-grounded neutral, no transformers
CM 0.6 meter wire spacing
CM 50 MHz (maximum number of segments)
CE NTIA 2004
CW 1 143 0.0 0.0 12.0 42.5 0.0 12.0 0.0063 3 43
CW 2 143 42.5 0.0 12.0 85.0 0.0 12.0 0.0063 3 43
CW 3 143 85.0 0.0 12.0 127.5 0.0 12.0 0.0063 3 43
CW 4 143 127.5 0.0 12.0 170.0 0.0 12.0 0.0063 3 43
CW 5 143 -170.0 0.0 12.0 -127.5 0.0 12.0 0.0063 3 43
CW 6 143 -127.5 0.0 12.0 -85.0 0.0 12.0 0.0063 3 43
CW 7 143 -85.0 0.0 12.0 -42.5 0.0 12.0 0.0063 3 43
CW 8 143 -42.5 0.0 12.0 0.0 0.0 12.0 0.0063 3 43
CW 9 143 0.0 0.6 12.0 42.5 0.6 12.0 0.0063 3 43
CW 10 143 42.5 0.6 12.0 85.0 0.6 12.0 0.0063 3 43
CW 11 143 85.0 0.6 12.0 127.5 0.6 12.0 0.0063 3 43
CW 12 143 127.5 0.6 12.0 170.0 0.6 12.0 0.0063 3 43
CW 13 143 -170.0 0.6 12.0 -127.5 0.6 12.0 0.0063 3 43
CW 14 143 -127.5 0.6 12.0 -85.0 0.6 12.0 0.0063 3 43
CW 15 143 -85.0 0.6 12.0 -42.5 0.6 12.0 0.0063 3 43
CW 16 143 -42.5 0.6 12.0 0.0 0.6 12.0 0.0063 3 43
GE -1
LD 5 0 0 0 58000000.0 0.0
EX 0 1 1 0 1.0 0.0
GN 2 0 0 0 15.0 .005
FR 0 1 0 0 50 0.0
EN
```



ver1n.nec

```
CM Catenary one-wire BPL model
CM Center-fed, vertical configuration
CM Multi-grounded neutral, three transformers
CM n/a meter wire spacing
CM 50 MHz
CE NTIA 2004
CW 1 143 0.0 0.0 12.0 42.5 0.0 12.0 0.0063 3 43
CW 2 143 42.5 0.0 12.0 85.0 0.0 12.0 0.0063 3 43
CW 3 143 85.0 0.0 12.0 127.5 0.0 12.0 0.0063 3 43
CW 4 143 127.5 0.0 12.0 170.0 0.0 12.0 0.0063 3 43
CW 5 143 -170.0 0.0 12.0 -127.5 0.0 12.0 0.0063 3 43
CW 6 143 -127.5 0.0 12.0 -85.0 0.0 12.0 0.0063 3 43
CW 7 143 -85.0 0.0 12.0 -42.5 0.0 12.0 0.0063 3 43
CW 8 143 -42.5 0.0 12.0 0.0 0.0 12.0 0.0063 3 43
CW 9 143 0.0 0.0 9.0 42.5 0.0 9.0 0.0063 3 43
CW 10 143 42.5 0.0 9.0 85.0 0.0 9.0 0.0063 3 43
CW 11 143 85.0 0.0 9.0 127.5 0.0 9.0 0.0063 3 43
CW 12 143 127.5 0.0 9.0 170.0 0.0 9.0 0.0063 3 43
CW 13 143 -170.0 0.0 9.0 -127.5 0.0 9.0 0.0063 3 43
CW 14 143 -127.5 0.0 9.0 -85.0 0.0 9.0 0.0063 3 43
CW 15 143 -85.0 0.0 9.0 -42.5 0.0 9.0 0.0063 3 43
CW 16 143 -42.5 0.0 9.0 0.0 0.0 9.0 0.0063 3 43
GW 17 31 0.0 0.0 9.0 0.0 0.0 0.0 0.0063
GW 18 31 170.0 0.0 9.0 170.0 0.0 0.0 0.0063
GW 19 31 -170.0 0.0 9.0 -170.0 0.0 0.0 0.0063
GW 20 33 0.0 0.0 0.0 0.0 0.0 -2.5 0.0063
GW 21 33 170.0 0.0 0.0 170.0 0.0 -2.5 0.0063
GW 22 33 -170.0 0.0 0.0 -170.0 0.0 -2.5 0.0063
GW 23 7 0.0 0.0 12.0 0.0 -1.32105 10.50161 0.0063
GW 24 7 170.0 0.0 12.0 171.6 0.0 10.2 0.0063
GW 25 7 -170.0 0.0 12.0 -171.6 0.0 10.2 0.0063
GW 26 7 0.0 0.0 9.0 0.0 -1.32105 10.50161 0.0063
GW 27 7 -170.0 0.0 9.0 -171.6 0.0 10.2 0.0063
GW 28 7 170.0 0.0 9.0 171.6 0.0 10.2 0.0063
GE -1
LD 5 0 0 0 58000000.0 0.0
LD 2 26 1 1 7.7 0.0
LD 0 27 1 1 7.7 0.0
LD 0 28 1 1 7.7 0.0
EX 0 1 1 0 1.0 0.0
GN 2 0 0 0 15.0 .005
FR 0 1 0 0 50 0.0
EN
```

ver36.nec

```
CM Catenary three-wire BPL model
CM Center-fed, vertical configuration
CM No multi-grounded neutral, no transformers
CM 0.6 meter wire spacing
CM 50 MHz
CE NTIA 2004
CW 1 143 0.0 0.0 12.0 42.5 0.0 12.0 0.0063 3 43
CW 2 143 42.5 0.0 12.0 85.0 0.0 12.0 0.0063 3 43
CW 3 143 85.0 0.0 12.0 127.5 0.0 12.0 0.0063 3 43
CW 4 143 127.5 0.0 12.0 170.0 0.0 12.0 0.0063 3 43
CW 5 143 -170.0 0.0 12.0 -127.5 0.0 12.0 0.0063 3 43
CW 6 143 -127.5 0.0 12.0 -85.0 0.0 12.0 0.0063 3 43
CW 7 143 -85.0 0.0 12.0 -42.5 0.0 12.0 0.0063 3 43
CW 8 143 -42.5 0.0 12.0 0.0 0.0 12.0 0.0063 3 43
CW 9 143 0.0 0.0 11.4 42.5 0.0 11.4 0.0063 3 43
CW 10 143 42.5 0.0 11.4 85.0 0.0 11.4 0.0063 3 43
CW 11 143 85.0 0.0 11.4 127.5 0.0 11.4 0.0063 3 43
CW 12 143 127.5 0.0 11.4 170.0 0.0 11.4 0.0063 3 43
CW 13 143 -170.0 0.0 11.4 -127.5 0.0 11.4 0.0063 3 43
CW 14 143 -127.5 0.0 11.4 -85.0 0.0 11.4 0.0063 3 43
CW 15 143 -85.0 0.0 11.4 -42.5 0.0 11.4 0.0063 3 43
CW 16 143 -42.5 0.0 11.4 0.0 0.0 11.4 0.0063 3 43
CW 17 143 0.0 0.0 10.8 42.5 0.0 10.8 0.0063 3 43
CW 18 143 42.5 0.0 10.8 85.0 0.0 10.8 0.0063 3 43
CW 19 143 85.0 0.0 10.8 127.5 0.0 10.8 0.0063 3 43
CW 20 143 127.5 0.0 10.8 170.0 0.0 10.8 0.0063 3 43
CW 21 143 -170.0 0.0 10.8 -127.5 0.0 10.8 0.0063 3 43
CW 22 143 -127.5 0.0 10.8 -85.0 0.0 10.8 0.0063 3 43
CW 23 143 -85.0 0.0 10.8 -42.5 0.0 10.8 0.0063 3 43
CW 24 143 -42.5 0.0 10.8 0.0 0.0 10.8 0.0063 3 43
GE -1
LD 5 0 0 0 58000000.0 0.0
EX 0 1 1 0 1.0 0.0
GN 2 0 0 0 15.0 .005
FR 0 1 0 0 50 0.0
EN
```

ver1.nec

```
CM Catenary one-wire BPL model
CM Center-fed, vertical configuration
CM No multi-grounded neutral, no transformers
CM n/a meter wire spacing
CM 50 MHz
CE NTIA 2004
CW 1 143 0.0 0.0 12.0 42.5 0.0 12.0 0.0063 3 43
CW 2 143 42.5 0.0 12.0 85.0 0.0 12.0 0.0063 3 43
CW 3 143 85.0 0.0 12.0 127.5 0.0 12.0 0.0063 3 43
CW 4 143 127.5 0.0 12.0 170.0 0.0 12.0 0.0063 3 43
CW 5 143 -170.0 0.0 12.0 -127.5 0.0 12.0 0.0063 3 43
CW 6 143 -127.5 0.0 12.0 -85.0 0.0 12.0 0.0063 3 43
CW 7 143 -85.0 0.0 12.0 -42.5 0.0 12.0 0.0063 3 43
CW 8 143 -42.5 0.0 12.0 0.0 0.0 12.0 0.0063 3 43
GE -1
LD 5 0 0 0 58000000.0 0.0
EX 0 1 1 0 1.0 0.0
GN 2 0 0 0 15.0 .005
FR 0 1 0 0 50 0.0
EN
```

```

CM Catenary two-wire BPL model
CM Center-fed, vertical configuration
CM Multi-grounded neutral, three transformers
CM 0.6 meter wire spacing
CM 50 MHZ
CE NTIA 2004
CW 1 143 0.0 0.0 12.0 42.5 0.0 12.0 0.0063 3 43
CW 2 143 42.5 0.0 12.0 85.0 0.0 12.0 0.0063 3 43
CW 3 143 85.0 0.0 12.0 127.5 0.0 12.0 0.0063 3 43
CW 4 143 127.5 0.0 12.0 170.0 0.0 12.0 0.0063 3 43
CW 5 143 -170.0 0.0 12.0 -127.5 0.0 12.0 0.0063 3 43
CW 6 143 -127.5 0.0 12.0 -85.0 0.0 12.0 0.0063 3 43
CW 7 143 -85.0 0.0 12.0 -42.5 0.0 12.0 0.0063 3 43
CW 8 143 -42.5 0.0 12.0 0.0 0.0 12.0 0.0063 3 43
CW 9 143 0.0 0.0 11.4 42.5 0.0 11.4 0.0063 3 43
CW 10 143 42.5 0.0 11.4 85.0 0.0 11.4 0.0063 3 43
CW 11 143 85.0 0.0 11.4 127.5 0.0 11.4 0.0063 3 43
CW 12 143 127.5 0.0 11.4 170.0 0.0 11.4 0.0063 3 43
CW 13 143 -170.0 0.0 11.4 -127.5 0.0 11.4 0.0063 3 43
CW 14 143 -127.5 0.0 11.4 -85.0 0.0 11.4 0.0063 3 43
CW 15 143 -85.0 0.0 11.4 -42.5 0.0 11.4 0.0063 3 43
CW 16 143 -42.5 0.0 11.4 0.0 0.0 11.4 0.0063 3 43
CW 17 143 0.0 0.0 9.0 42.5 0.0 9.0 0.0063 3 43
CW 18 143 42.5 0.0 9.0 85.0 0.0 9.0 0.0063 3 43
CW 19 143 85.0 0.0 9.0 127.5 0.0 9.0 0.0063 3 43
CW 20 143 127.5 0.0 9.0 170.0 0.0 9.0 0.0063 3 43
CW 21 143 -170.0 0.0 9.0 -127.5 0.0 9.0 0.0063 3 43
CW 22 143 -127.5 0.0 9.0 -85.0 0.0 9.0 0.0063 3 43
CW 23 143 -85.0 0.0 9.0 -42.5 0.0 9.0 0.0063 3 43
CW 24 143 -42.5 0.0 9.0 0.0 0.0 9.0 0.0063 3 43
GW 25 31 0.0 0.0 9.0 0.0 0.0 0.0 0.0063
GW 26 31 170.0 0.0 9.0 170.0 0.0 0.0 0.0063
GW 27 31 -170.0 0.0 9.0 -170.0 0.0 0.0 0.0063
GW 28 33 0.0 0.0 0.0 0.0 0.0 -2.5 0.0063
GW 29 33 170.0 0.0 0.0 170.0 0.0 -2.5 0.0063
GW 30 33 -170.0 0.0 0.0 -170.0 0.0 -2.5 0.0063
GW 31 7 0.0 0.0 12.0 0.0 -1.32105 10.50161 0.0063
GW 32 7 170.0 0.0 11.4 171.6 0.0 10.2 0.0063
GW 33 7 -170.0 0.0 11.4 -171.6 0.0 10.2 0.0063
GW 34 7 0.0 0.0 9.0 0.0 -1.32105 10.50161 0.0063
GW 35 7 -170.0 0.0 9.0 -171.6 0.0 10.2 0.0063
GW 36 7 170.0 0.0 9.0 171.6 0.0 10.2 0.0063
GE -1
LD 5 0 0 0 58000000.0 0.0
LD 2 34 1 1 7.7 0.0
LD 0 35 1 1 7.7 0.0
LD 0 36 1 1 7.7 0.0
EX 0 1 1 0 1.0 0.0
GN 2 0 0 0 15.0 .005
FR 0 1 0 0 50 0.0
EN

```

ver26.nec

```
CM Catenary two-wire BPL model
CM Center-fed, vertical configuration
CM No multi-grounded neutral, no transformers
CM 0.6 meter wire spacing
CM 50 MHz
CE NTIA 2004
CW 1 143 0.0 0.0 12.0 42.5 0.0 12.0 0.0063 3 43
CW 2 143 42.5 0.0 12.0 85.0 0.0 12.0 0.0063 3 43
CW 3 143 85.0 0.0 12.0 127.5 0.0 12.0 0.0063 3 43
CW 4 143 127.5 0.0 12.0 170.0 0.0 12.0 0.0063 3 43
CW 5 143 -170.0 0.0 12.0 -127.5 0.0 12.0 0.0063 3 43
CW 6 143 -127.5 0.0 12.0 -85.0 0.0 12.0 0.0063 3 43
CW 7 143 -85.0 0.0 12.0 -42.5 0.0 12.0 0.0063 3 43
CW 8 143 -42.5 0.0 12.0 0.0 0.0 12.0 0.0063 3 43
CW 9 143 0.0 0.0 11.4 42.5 0.0 11.4 0.0063 3 43
CW 10 143 42.5 0.0 11.4 85.0 0.0 11.4 0.0063 3 43
CW 11 143 85.0 0.0 11.4 127.5 0.0 11.4 0.0063 3 43
CW 12 143 127.5 0.0 11.4 170.0 0.0 11.4 0.0063 3 43
CW 13 143 -170.0 0.0 11.4 -127.5 0.0 11.4 0.0063 3 43
CW 14 143 -127.5 0.0 11.4 -85.0 0.0 11.4 0.0063 3 43
CW 15 143 -85.0 0.0 11.4 -42.5 0.0 11.4 0.0063 3 43
CW 16 143 -42.5 0.0 11.4 0.0 0.0 11.4 0.0063 3 43
GE -1
LD 5 0 0 0 58000000.0 0.0
EX 0 1 1 0 1.0 0.0
GN 2 0 0 0 15.0 .005
FR 0 1 0 0 50 0.0
EN
```

```

CM Catenary three-wire BPL model
CM Center-fed, vertical configuration
CM Multi-grounded neutral, three transformers
CM 1.0 meter wire spacing
CM 50 MHZ
CE NTIA 2004
CW 1 143 0.0 0.0 12.0 42.5 0.0 12.0 0.0063 3 43
CW 2 143 42.5 0.0 12.0 85.0 0.0 12.0 0.0063 3 43
CW 3 143 85.0 0.0 12.0 127.5 0.0 12.0 0.0063 3 43
CW 4 143 127.5 0.0 12.0 170.0 0.0 12.0 0.0063 3 43
CW 5 143 -170.0 0.0 12.0 -127.5 0.0 12.0 0.0063 3 43
CW 6 143 -127.5 0.0 12.0 -85.0 0.0 12.0 0.0063 3 43
CW 7 143 -85.0 0.0 12.0 -42.5 0.0 12.0 0.0063 3 43
CW 8 143 -42.5 0.0 12.0 0.0 0.0 12.0 0.0063 3 43
CW 9 143 0.0 0.0 11.0 42.5 0.0 11.0 0.0063 3 43
CW 10 143 42.5 0.0 11.0 85.0 0.0 11.0 0.0063 3 43
CW 11 143 85.0 0.0 11.0 127.5 0.0 11.0 0.0063 3 43
CW 12 143 127.5 0.0 11.0 170.0 0.0 11.0 0.0063 3 43
CW 13 143 -170.0 0.0 11.0 -127.5 0.0 11.0 0.0063 3 43
CW 14 143 -127.5 0.0 11.0 -85.0 0.0 11.0 0.0063 3 43
CW 15 143 -85.0 0.0 11.0 -42.5 0.0 11.0 0.0063 3 43
CW 16 143 -42.5 0.0 11.0 0.0 0.0 11.0 0.0063 3 43
CW 17 143 0.0 0.0 10.0 42.5 0.0 10.0 0.0063 3 43
CW 18 143 42.5 0.0 10.0 85.0 0.0 10.0 0.0063 3 43
CW 19 143 85.0 0.0 10.0 127.5 0.0 10.0 0.0063 3 43
CW 20 143 127.5 0.0 10.0 170.0 0.0 10.0 0.0063 3 43
CW 21 143 -170.0 0.0 10.0 -127.5 0.0 10.0 0.0063 3 43
CW 22 143 -127.5 0.0 10.0 -85.0 0.0 10.0 0.0063 3 43
CW 23 143 -85.0 0.0 10.0 -42.5 0.0 10.0 0.0063 3 43
CW 24 143 -42.5 0.0 10.0 0.0 0.0 10.0 0.0063 3 43
CW 25 143 0.0 0.0 9.0 42.5 0.0 9.0 0.0063 3 43
CW 26 143 42.5 0.0 9.0 85.0 0.0 9.0 0.0063 3 43
CW 27 143 85.0 0.0 9.0 127.5 0.0 9.0 0.0063 3 43
CW 28 143 127.5 0.0 9.0 170.0 0.0 9.0 0.0063 3 43
CW 29 143 -170.0 0.0 9.0 -127.5 0.0 9.0 0.0063 3 43
CW 30 143 -127.5 0.0 9.0 -85.0 0.0 9.0 0.0063 3 43
CW 31 143 -85.0 0.0 9.0 -42.5 0.0 9.0 0.0063 3 43
CW 32 143 -42.5 0.0 9.0 0.0 0.0 9.0 0.0063 3 43
GW 33 31 0.0 0.0 9.0 0.0 0.0 0.0 0.0063
GW 34 31 170.0 0.0 9.0 170.0 0.0 0.0 0.0063
GW 35 31 -170.0 0.0 9.0 -170.0 0.0 0.0 0.0063
GW 36 33 0.0 0.0 0.0 0.0 0.0 -2.5 0.0063
GW 37 33 170.0 0.0 0.0 170.0 0.0 -2.5 0.0063
GW 38 33 -170.0 0.0 0.0 -170.0 0.0 -2.5 0.0063
GW 39 7 0.0 0.0 12.0 0.0 -1.0 10.75 0.0063
GW 40 7 0.0 0.0 9.0 0.0 -1.0 10.75 0.0063
GW 41 7 -170.0 0.0 9.0 -170.0 0.0 10.0 0.0063
GW 42 7 170.0 0.0 11.0 171.5 0.0 10.3 0.0063
GW 43 7 170.0 0.0 9.0 171.5 0.0 10.3 0.0063
GE -1
LD 5 0 0 0 58000000.0 0.0
LD 2 40 1 1 7.7 0.0
LD 0 41 1 1 7.7 0.0
LD 0 43 1 1 7.7 0.0
EX 0 1 1 0 1.0 0.0
GN 2 0 0 0 15.0 .005
FR 0 1 0 0 50 0.0
EN

```

```

CM Catenary three-wire BPL model
CM Center-fed, vertical configuration
CM No multi-grounded neutral, no transformers
CM 1.0 meter wire spacing
CM 50 MHz
CE NTIA 2004
CW 1 143 0.0 0.0 12.0 42.5 0.0 12.0 0.0063 3 43
CW 2 143 42.5 0.0 12.0 85.0 0.0 12.0 0.0063 3 43
CW 3 143 85.0 0.0 12.0 127.5 0.0 12.0 0.0063 3 43
CW 4 143 127.5 0.0 12.0 170.0 0.0 12.0 0.0063 3 43
CW 5 143 -170.0 0.0 12.0 -127.5 0.0 12.0 0.0063 3 43
CW 6 143 -127.5 0.0 12.0 -85.0 0.0 12.0 0.0063 3 43
CW 7 143 -85.0 0.0 12.0 -42.5 0.0 12.0 0.0063 3 43
CW 8 143 -42.5 0.0 12.0 0.0 0.0 12.0 0.0063 3 43
CW 9 143 0.0 0.0 11.0 42.5 0.0 11.0 0.0063 3 43
CW 10 143 42.5 0.0 11.0 85.0 0.0 11.0 0.0063 3 43
CW 11 143 85.0 0.0 11.0 127.5 0.0 11.0 0.0063 3 43
CW 12 143 127.5 0.0 11.0 170.0 0.0 11.0 0.0063 3 43
CW 13 143 -170.0 0.0 11.0 -127.5 0.0 11.0 0.0063 3 43
CW 14 143 -127.5 0.0 11.0 -85.0 0.0 11.0 0.0063 3 43
CW 15 143 -85.0 0.0 11.0 -42.5 0.0 11.0 0.0063 3 43
CW 16 143 -42.5 0.0 11.0 0.0 0.0 11.0 0.0063 3 43
CW 17 143 0.0 0.0 10.0 42.5 0.0 10.0 0.0063 3 43
CW 18 143 42.5 0.0 10.0 85.0 0.0 10.0 0.0063 3 43
CW 19 143 85.0 0.0 10.0 127.5 0.0 10.0 0.0063 3 43
CW 20 143 127.5 0.0 10.0 170.0 0.0 10.0 0.0063 3 43
CW 21 143 -170.0 0.0 10.0 -127.5 0.0 10.0 0.0063 3 43
CW 22 143 -127.5 0.0 10.0 -85.0 0.0 10.0 0.0063 3 43
CW 23 143 -85.0 0.0 10.0 -42.5 0.0 10.0 0.0063 3 43
CW 24 143 -42.5 0.0 10.0 0.0 0.0 10.0 0.0063 3 43
GE -1
LD 5 0 0 0 58000000.0 0.0
EX 0 1 1 0 1.0 0.0
GN 2 0 0 0 15.0 .005
FR 0 1 0 0 50 0.0
EN

```

```
CM Catenary two-wire BPL model
CM Center-fed, vertical configuration
CM Multi-grounded neutral, three transformers
CM 1.0 meter wire spacing
CM 50 MHZ
CE NTIA 2004
CW 1 143 0.0 0.0 12.0 42.5 0.0 12.0 0.0063 3 43
CW 2 143 42.5 0.0 12.0 85.0 0.0 12.0 0.0063 3 43
CW 3 143 85.0 0.0 12.0 127.5 0.0 12.0 0.0063 3 43
CW 4 143 127.5 0.0 12.0 170.0 0.0 12.0 0.0063 3 43
CW 5 143 -170.0 0.0 12.0 -127.5 0.0 12.0 0.0063 3 43
CW 6 143 -127.5 0.0 12.0 -85.0 0.0 12.0 0.0063 3 43
CW 7 143 -85.0 0.0 12.0 -42.5 0.0 12.0 0.0063 3 43
CW 8 143 -42.5 0.0 12.0 0.0 0.0 12.0 0.0063 3 43
CW 9 143 0.0 0.0 11.0 42.5 0.0 11.0 0.0063 3 43
CW 10 143 42.5 0.0 11.0 85.0 0.0 11.0 0.0063 3 43
CW 11 143 85.0 0.0 11.0 127.5 0.0 11.0 0.0063 3 43
CW 12 143 127.5 0.0 11.0 170.0 0.0 11.0 0.0063 3 43
CW 13 143 -170.0 0.0 11.0 -127.5 0.0 11.0 0.0063 3 43
CW 14 143 -127.5 0.0 11.0 -85.0 0.0 11.0 0.0063 3 43
CW 15 143 -85.0 0.0 11.0 -42.5 0.0 11.0 0.0063 3 43
CW 16 143 -42.5 0.0 11.0 0.0 0.0 11.0 0.0063 3 43
CW 17 143 0.0 0.0 9.0 42.5 0.0 9.0 0.0063 3 43
CW 18 143 42.5 0.0 9.0 85.0 0.0 9.0 0.0063 3 43
CW 19 143 85.0 0.0 9.0 127.5 0.0 9.0 0.0063 3 43
CW 20 143 127.5 0.0 9.0 170.0 0.0 9.0 0.0063 3 43
CW 21 143 -170.0 0.0 9.0 -127.5 0.0 9.0 0.0063 3 43
CW 22 143 -127.5 0.0 9.0 -85.0 0.0 9.0 0.0063 3 43
CW 23 143 -85.0 0.0 9.0 -42.5 0.0 9.0 0.0063 3 43
CW 24 143 -42.5 0.0 9.0 0.0 0.0 9.0 0.0063 3 43
GW 25 31 0.0 0.0 9.0 0.0 0.0 0.0 0.0063
GW 26 31 170.0 0.0 9.0 170.0 0.0 0.0 0.0063
GW 27 31 -170.0 0.0 9.0 -170.0 0.0 0.0 0.0063
GW 28 33 0.0 0.0 0.0 0.0 0.0 -2.5 0.0063
GW 29 33 170.0 0.0 0.0 170.0 0.0 -2.5 0.0063
GW 30 33 -170.0 0.0 0.0 -170.0 0.0 -2.5 0.0063
GW 31 7 0.0 0.0 12.0 0.0 -1.32105 10.50161 0.0063
GW 32 7 170.0 0.0 11.0 171.6 0.0 10.2 0.0063
GW 33 7 -170.0 0.0 11.0 -171.6 0.0 10.2 0.0063
GW 34 7 0.0 0.0 9.0 0.0 -1.32105 10.50161 0.0063
GW 35 7 -170.0 0.0 9.0 -171.6 0.0 10.2 0.0063
GW 36 7 170.0 0.0 9.0 171.6 0.0 10.2 0.0063
GE -1
LD 5 0 0 0 58000000.0 0.0
LD 2 34 1 1 7.7 0.0
LD 0 35 1 1 7.7 0.0
LD 0 36 1 1 7.7 0.0
EX 0 1 1 0 1.0 0.0
GN 2 0 0 0 15.0 .005
FR 0 1 0 0 50 0.0
EN
```



ver210.nec

```
CM Catenary two-wire BPL model
CM Center-fed, vertical configuration
CM No multi-grounded neutral, no transformers
CM 1.0 meter wire spacing
CM 50 MHz
CE NTIA 2004
CW 1 143 0.0 0.0 12.0 42.5 0.0 12.0 0.0063 3 43
CW 2 143 42.5 0.0 12.0 85.0 0.0 12.0 0.0063 3 43
CW 3 143 85.0 0.0 12.0 127.5 0.0 12.0 0.0063 3 43
CW 4 143 127.5 0.0 12.0 170.0 0.0 12.0 0.0063 3 43
CW 5 143 -170.0 0.0 12.0 -127.5 0.0 12.0 0.0063 3 43
CW 6 143 -127.5 0.0 12.0 -85.0 0.0 12.0 0.0063 3 43
CW 7 143 -85.0 0.0 12.0 -42.5 0.0 12.0 0.0063 3 43
CW 8 143 -42.5 0.0 12.0 0.0 0.0 12.0 0.0063 3 43
CW 9 143 0.0 0.0 11.0 42.5 0.0 11.0 0.0063 3 43
CW 10 143 42.5 0.0 11.0 85.0 0.0 11.0 0.0063 3 43
CW 11 143 85.0 0.0 11.0 127.5 0.0 11.0 0.0063 3 43
CW 12 143 127.5 0.0 11.0 170.0 0.0 11.0 0.0063 3 43
CW 13 143 -170.0 0.0 11.0 -127.5 0.0 11.0 0.0063 3 43
CW 14 143 -127.5 0.0 11.0 -85.0 0.0 11.0 0.0063 3 43
CW 15 143 -85.0 0.0 11.0 -42.5 0.0 11.0 0.0063 3 43
CW 16 143 -42.5 0.0 11.0 0.0 0.0 11.0 0.0063 3 43
GE -1
LD 5 0 0 0 58000000.0 0.0
EX 0 1 1 0 1.0 0.0
GN 2 0 0 0 15.0 .005
FR 0 1 0 0 50 0.0
EN
```

```

CM Catenary three-wire BPL model
CM Center-fed, vertical configuration
CM Multi-grounded neutral, three transformers
CM 0.6 meter wire spacing
CM 50 MHz
CE NTIA 2004
CW 1 143 0.0 0.0 12.0 42.5 0.0 12.0 0.0063 3 43
CW 2 143 42.5 0.0 12.0 85.0 0.0 12.0 0.0063 3 43
CW 3 143 85.0 0.0 12.0 127.5 0.0 12.0 0.0063 3 43
CW 4 143 127.5 0.0 12.0 170.0 0.0 12.0 0.0063 3 43
CW 5 143 -170.0 0.0 12.0 -127.5 0.0 12.0 0.0063 3 43
CW 6 143 -127.5 0.0 12.0 -85.0 0.0 12.0 0.0063 3 43
CW 7 143 -85.0 0.0 12.0 -42.5 0.0 12.0 0.0063 3 43
CW 8 143 -42.5 0.0 12.0 0.0 0.0 12.0 0.0063 3 43
CW 9 143 0.0 0.0 11.4 42.5 0.0 11.4 0.0063 3 43
CW 10 143 42.5 0.0 11.4 85.0 0.0 11.4 0.0063 3 43
CW 11 143 85.0 0.0 11.4 127.5 0.0 11.4 0.0063 3 43
CW 12 143 127.5 0.0 11.4 170.0 0.0 11.4 0.0063 3 43
CW 13 143 -170.0 0.0 11.4 -127.5 0.0 11.4 0.0063 3 43
CW 14 143 -127.5 0.0 11.4 -85.0 0.0 11.4 0.0063 3 43
CW 15 143 -85.0 0.0 11.4 -42.5 0.0 11.4 0.0063 3 43
CW 16 143 -42.5 0.0 11.4 0.0 0.0 11.4 0.0063 3 43
CW 17 143 0.0 0.0 10.8 42.5 0.0 10.8 0.0063 3 43
CW 18 143 42.5 0.0 10.8 85.0 0.0 10.8 0.0063 3 43
CW 19 143 85.0 0.0 10.8 127.5 0.0 10.8 0.0063 3 43
CW 20 143 127.5 0.0 10.8 170.0 0.0 10.8 0.0063 3 43
CW 21 143 -170.0 0.0 10.8 -127.5 0.0 10.8 0.0063 3 43
CW 22 143 -127.5 0.0 10.8 -85.0 0.0 10.8 0.0063 3 43
CW 23 143 -85.0 0.0 10.8 -42.5 0.0 10.8 0.0063 3 43
CW 24 143 -42.5 0.0 10.8 0.0 0.0 10.8 0.0063 3 43
CW 25 143 0.0 0.0 9.0 42.5 0.0 9.0 0.0063 3 43
CW 26 143 42.5 0.0 9.0 85.0 0.0 9.0 0.0063 3 43
CW 27 143 85.0 0.0 9.0 127.5 0.0 9.0 0.0063 3 43
CW 28 143 127.5 0.0 9.0 170.0 0.0 9.0 0.0063 3 43
CW 29 143 -170.0 0.0 9.0 -127.5 0.0 9.0 0.0063 3 43
CW 30 143 -127.5 0.0 9.0 -85.0 0.0 9.0 0.0063 3 43
CW 31 143 -85.0 0.0 9.0 -42.5 0.0 9.0 0.0063 3 43
CW 32 143 -42.5 0.0 9.0 0.0 0.0 9.0 0.0063 3 43
GW 33 31 0.0 0.0 9.0 0.0 0.0 0.0 0.0063
GW 34 31 170.0 0.0 9.0 170.0 0.0 0.0 0.0063
GW 35 31 -170.0 0.0 9.0 -170.0 0.0 0.0 0.0063
GW 36 33 0.0 0.0 0.0 0.0 0.0 -2.5 0.0063
GW 37 33 170.0 0.0 0.0 170.0 0.0 -2.5 0.0063
GW 38 33 -170.0 0.0 0.0 -170.0 0.0 -2.5 0.0063
GW 39 7 0.0 0.0 12.0 0.0 -1.0 10.75 0.0063
GW 40 7 0.0 0.0 9.0 0.0 -1.0 10.75 0.0063
GW 41 7 -170.0 0.0 9.0 -170.0 0.0 10.8 0.0063
GW 42 7 170.0 0.0 11.4 171.5 0.0 10.3 0.0063
GW 43 7 170.0 0.0 9.0 171.5 0.0 10.3 0.0063
GE -1
LD 5 0 0 0 58000000.0 0.0
LD 2 40 1 1 7.7 0.0
LD 0 41 1 1 7.7 0.0
LD 0 43 1 1 7.7 0.0
EX 0 1 1 0 1.0 0.0
GN 2 0 0 0 15.0 .005
FR 0 1 0 0 50 0.0
EN

```

Underground.nec

CM Underground Model  
CM 340-meter URD, center fed, primary distribution-type  
CM Center live with three surrounding grounded neutral wires  
CM Single phase  
CM Driven by excitation in wire-mesh pad-mounted  
CM Transformer structure (above ground)  
CM Note: No meaningful result from AGT at 22 MHz.  
CM Experimental slight lengthening and shortening  
CM of long wires (+/- 0.5 m) resulted in good  
CM AGT values with minimal (+/- .01 dB) change in  
CM radiated power, field and gain values calculated at  
CM 22 MHz with standard (170 m) model wire lengths.  
CM NTIA 2004

CE  
GW 1 3 -0.5 0.5 0.5 -0.25 0.5 0.5 0.002  
GW 2 3 -0.25 0.5 0.5 0.0 0.5 0.5 0.002  
GW 3 3 0.0 0.5 0.5 0.25 0.5 0.5 0.002  
GW 4 3 0.25 0.5 0.5 0.5 0.5 0.5 0.002  
GW 5 3 -0.5 0.5 0.375 -0.25 0.5 0.375 0.002  
GW 6 3 -0.25 0.5 0.375 0.0 0.5 0.375 0.002  
GW 7 3 0.0 0.5 0.375 0.25 0.5 0.375 0.002  
GW 8 3 0.25 0.5 0.375 0.5 0.5 0.375 0.002  
GW 9 3 -0.5 0.5 0.25 -0.25 0.5 0.25 0.002  
GW 10 3 -0.25 0.5 0.25 0.0 0.5 0.25 0.002  
GW 11 3 0.0 0.5 0.25 0.25 0.5 0.25 0.002  
GW 12 3 0.25 0.5 0.25 0.5 0.5 0.25 0.002  
GW 13 3 -0.5 0.5 0.125 -0.25 0.5 0.125 0.002  
GW 14 3 -0.25 0.5 0.125 0.0 0.5 0.125 0.002  
GW 15 3 0.0 0.5 0.125 0.25 0.5 0.125 0.002  
GW 16 3 0.25 0.5 0.125 0.5 0.5 0.125 0.002  
GW 17 1 -0.25 0.5 0.5 -0.25 0.5 0.375 0.002  
GW 18 1 -0.25 0.5 0.375 -0.25 0.5 0.25 0.002  
GW 19 1 -0.25 0.5 0.25 -0.25 0.5 0.125 0.002  
GW 20 1 -0.25 0.5 0.125 -0.25 0.5 0.0 0.002  
GW 21 1 0.0 0.5 0.5 0.0 0.5 0.375 0.002  
GW 22 1 0.0 0.5 0.375 0.0 0.5 0.25 0.002  
GW 23 1 0.0 0.5 0.25 0.0 0.5 0.125 0.002  
GW 24 1 0.0 0.5 0.125 0.0 0.5 0.0 0.002  
GW 25 1 0.25 0.5 0.5 0.25 0.5 0.375 0.002  
GW 26 1 0.25 0.5 0.375 0.25 0.5 0.25 0.002  
GW 27 1 0.25 0.5 0.25 0.25 0.5 0.125 0.002  
GW 28 1 0.25 0.5 0.125 0.25 0.5 0.0 0.002  
GW 29 3 -0.5 -0.5 0.5 -0.25 -0.5 0.5 0.002  
GW 30 3 -0.25 -0.5 0.5 0.0 -0.5 0.5 0.002  
GW 31 3 0.0 -0.5 0.5 0.25 -0.5 0.5 0.002  
GW 32 3 0.25 -0.5 0.5 0.5 -0.5 0.5 0.002  
GW 33 3 -0.5 -0.5 0.375 -0.25 -0.5 0.375 0.002  
GW 34 3 -0.25 -0.5 0.375 0.0 -0.5 0.375 0.002  
GW 35 3 0.0 -0.5 0.375 0.25 -0.5 0.375 0.002  
GW 36 3 0.25 -0.5 0.375 0.5 -0.5 0.375 0.002  
GW 37 3 -0.5 -0.5 0.25 -0.25 -0.5 0.25 0.002  
GW 38 3 -0.25 -0.5 0.25 0.0 -0.5 0.25 0.002  
GW 39 3 0.0 -0.5 0.25 0.25 -0.5 0.25 0.002  
GW 40 3 0.25 -0.5 0.25 0.5 -0.5 0.25 0.002  
GW 41 3 -0.5 -0.5 0.125 -0.25 -0.5 0.125 0.002  
GW 42 3 -0.25 -0.5 0.125 0.0 -0.5 0.125 0.002  
GW 43 3 0.0 -0.5 0.125 0.25 -0.5 0.125 0.002  
GW 44 3 0.25 -0.5 0.125 0.5 -0.5 0.125 0.002  
GW 45 1 -0.25 -0.5 0.5 -0.25 -0.5 0.375 0.002  
GW 46 1 -0.25 -0.5 0.375 -0.25 -0.5 0.25 0.002  
GW 47 1 -0.25 -0.5 0.25 -0.25 -0.5 0.125 0.002  
GW 48 1 -0.25 -0.5 0.125 -0.25 -0.5 0.0 0.002  
GW 49 1 0.0 -0.5 0.5 0.0 -0.5 0.375 0.002

Underground.nec

CM Underground Model  
CM 340-meter URD, center fed, primary distribution-type  
CM Center live with three surrounding grounded neutral wires  
CM Single phase  
CM Driven by excitation in wire-mesh pad-mounted  
CM Transformer structure (above ground)  
CM Note: No meaningful result from AGT at 22 MHz.  
CM Experimental slight lengthening and shortening  
CM of long wires (+/- 0.5 m) resulted in good  
CM AGT values with minimal (+/- .01 dB) change in  
CM radiated power, field and gain values calculated at  
CM 22 MHz with standard (170 m) model wire lengths.  
CM NTIA 2004

CE  
GW 1 3 -0.5 0.5 0.5 -0.25 0.5 0.5 0.002  
GW 2 3 -0.25 0.5 0.5 0.0 0.5 0.5 0.002  
GW 3 3 0.0 0.5 0.5 0.25 0.5 0.5 0.002  
GW 4 3 0.25 0.5 0.5 0.5 0.5 0.5 0.002  
GW 5 3 -0.5 0.5 0.375 -0.25 0.5 0.375 0.002  
GW 6 3 -0.25 0.5 0.375 0.0 0.5 0.375 0.002  
GW 7 3 0.0 0.5 0.375 0.25 0.5 0.375 0.002  
GW 8 3 0.25 0.5 0.375 0.5 0.5 0.375 0.002  
GW 9 3 -0.5 0.5 0.25 -0.25 0.5 0.25 0.002  
GW 10 3 -0.25 0.5 0.25 0.0 0.5 0.25 0.002  
GW 11 3 0.0 0.5 0.25 0.25 0.5 0.25 0.002  
GW 12 3 0.25 0.5 0.25 0.5 0.5 0.25 0.002  
GW 13 3 -0.5 0.5 0.125 -0.25 0.5 0.125 0.002  
GW 14 3 -0.25 0.5 0.125 0.0 0.5 0.125 0.002  
GW 15 3 0.0 0.5 0.125 0.25 0.5 0.125 0.002  
GW 16 3 0.25 0.5 0.125 0.5 0.5 0.125 0.002  
GW 17 1 -0.25 0.5 0.5 -0.25 0.5 0.375 0.002  
GW 18 1 -0.25 0.5 0.375 -0.25 0.5 0.25 0.002  
GW 19 1 -0.25 0.5 0.25 -0.25 0.5 0.125 0.002  
GW 20 1 -0.25 0.5 0.125 -0.25 0.5 0.0 0.002  
GW 21 1 0.0 0.5 0.5 0.0 0.5 0.375 0.002  
GW 22 1 0.0 0.5 0.375 0.0 0.5 0.25 0.002  
GW 23 1 0.0 0.5 0.25 0.0 0.5 0.125 0.002  
GW 24 1 0.0 0.5 0.125 0.0 0.5 0.0 0.002  
GW 25 1 0.25 0.5 0.5 0.25 0.5 0.375 0.002  
GW 26 1 0.25 0.5 0.375 0.25 0.5 0.25 0.002  
GW 27 1 0.25 0.5 0.25 0.25 0.5 0.125 0.002  
GW 28 1 0.25 0.5 0.125 0.25 0.5 0.0 0.002  
GW 29 3 -0.5 -0.5 0.5 -0.25 -0.5 0.5 0.002  
GW 30 3 -0.25 -0.5 0.5 0.0 -0.5 0.5 0.002  
GW 31 3 0.0 -0.5 0.5 0.25 -0.5 0.5 0.002  
GW 32 3 0.25 -0.5 0.5 0.5 -0.5 0.5 0.002  
GW 33 3 -0.5 -0.5 0.375 -0.25 -0.5 0.375 0.002  
GW 34 3 -0.25 -0.5 0.375 0.0 -0.5 0.375 0.002  
GW 35 3 0.0 -0.5 0.375 0.25 -0.5 0.375 0.002  
GW 36 3 0.25 -0.5 0.375 0.5 -0.5 0.375 0.002  
GW 37 3 -0.5 -0.5 0.25 -0.25 -0.5 0.25 0.002  
GW 38 3 -0.25 -0.5 0.25 0.0 -0.5 0.25 0.002  
GW 39 3 0.0 -0.5 0.25 0.25 -0.5 0.25 0.002  
GW 40 3 0.25 -0.5 0.25 0.5 -0.5 0.25 0.002  
GW 41 3 -0.5 -0.5 0.125 -0.25 -0.5 0.125 0.002  
GW 42 3 -0.25 -0.5 0.125 0.0 -0.5 0.125 0.002  
GW 43 3 0.0 -0.5 0.125 0.25 -0.5 0.125 0.002  
GW 44 3 0.25 -0.5 0.125 0.5 -0.5 0.125 0.002  
GW 45 1 -0.25 -0.5 0.5 -0.25 -0.5 0.375 0.002  
GW 46 1 -0.25 -0.5 0.375 -0.25 -0.5 0.25 0.002  
GW 47 1 -0.25 -0.5 0.25 -0.25 -0.5 0.125 0.002  
GW 48 1 -0.25 -0.5 0.125 -0.25 -0.5 0.0 0.002  
GW 49 1 0.0 -0.5 0.5 0.0 -0.5 0.375 0.002

Underground.nec

GW 50 1 0.0 -0.5 0.375 0.0 -0.5 0.25 0.002  
GW 51 1 0.0 -0.5 0.25 0.0 -0.5 0.125 0.002  
GW 52 1 0.0 -0.5 0.125 0.0 -0.5 0.0 0.002  
GW 53 1 0.25 -0.5 0.5 0.25 -0.5 0.375 0.002  
GW 54 1 0.25 -0.5 0.375 0.25 -0.5 0.25 0.002  
GW 55 1 0.25 -0.5 0.25 0.25 -0.5 0.125 0.002  
GW 56 1 0.25 -0.5 0.125 0.25 -0.5 0.0 0.002  
GW 57 3 -0.5 -0.5 0.5 -0.5 -0.25 0.5 0.002  
GW 58 3 -0.5 -0.25 0.5 -0.5 0.0 0.5 0.002  
GW 59 3 -0.5 0.0 0.5 -0.5 0.25 0.5 0.002  
GW 60 3 -0.5 0.25 0.5 -0.5 0.5 0.5 0.002  
GW 61 3 -0.5 -0.5 0.375 -0.5 -0.25 0.375 0.002  
GW 62 3 -0.5 -0.25 0.375 -0.5 0.0 0.375 0.002  
GW 63 3 -0.5 0.0 0.375 -0.5 0.25 0.375 0.002  
GW 64 3 -0.5 0.25 0.375 -0.5 0.5 0.375 0.002  
GW 65 3 -0.5 -0.5 0.25 -0.5 -0.25 0.25 0.002  
GW 66 3 -0.5 -0.25 0.25 -0.5 0.0 0.25 0.002  
GW 67 3 -0.5 0.0 0.25 -0.5 0.25 0.25 0.002  
GW 68 3 -0.5 0.25 0.25 -0.5 0.5 0.25 0.002  
GW 69 3 -0.5 -0.5 0.125 -0.5 -0.25 0.125 0.002  
GW 70 3 -0.5 -0.25 0.125 -0.5 0.0 0.125 0.002  
GW 71 3 -0.5 0.0 0.125 -0.5 0.25 0.125 0.002  
GW 72 3 -0.5 0.25 0.125 -0.5 0.5 0.125 0.002  
GW 73 1 -0.5 -0.5 0.5 -0.5 -0.5 0.375 0.002  
GW 74 1 -0.5 -0.5 0.375 -0.5 -0.5 0.25 0.002  
GW 75 1 -0.5 -0.5 0.25 -0.5 -0.5 0.125 0.002  
GW 76 1 -0.5 -0.5 0.125 -0.5 -0.5 0.0 0.002  
GW 77 1 -0.5 -0.25 0.5 -0.5 -0.25 0.375 0.002  
GW 78 1 -0.5 -0.25 0.375 -0.5 -0.25 0.25 0.002  
GW 79 1 -0.5 -0.25 0.25 -0.5 -0.25 0.125 0.002  
GW 80 1 -0.5 -0.25 0.125 -0.5 -0.25 0.0 0.002  
GW 81 1 -0.5 0.0 0.5 -0.5 0.0 0.375 0.002  
GW 82 1 -0.5 0.0 0.375 -0.5 0.0 0.25 0.002  
GW 83 1 -0.5 0.0 0.25 -0.5 0.0 0.125 0.002  
GW 84 1 -0.5 0.0 0.125 -0.5 0.0 0.0 0.002  
GW 85 1 -0.5 0.25 0.5 -0.5 0.25 0.375 0.002  
GW 86 1 -0.5 0.25 0.375 -0.5 0.25 0.25 0.002  
GW 87 1 -0.5 0.25 0.25 -0.5 0.25 0.125 0.002  
GW 88 1 -0.5 0.25 0.125 -0.5 0.25 0.0 0.002  
GW 89 1 -0.5 0.5 0.5 -0.5 0.5 0.375 0.002  
GW 90 1 -0.5 0.5 0.375 -0.5 0.5 0.25 0.002  
GW 91 1 -0.5 0.5 0.25 -0.5 0.5 0.125 0.002  
GW 92 1 -0.5 0.5 0.125 -0.5 0.5 0.0 0.002  
GW 93 3 0.5 -0.5 0.5 0.5 -0.25 0.5 0.002  
GW 94 3 0.5 -0.25 0.5 0.5 0.0 0.5 0.002  
GW 95 3 0.5 0.0 0.5 0.5 0.25 0.5 0.002  
GW 96 3 0.5 0.25 0.5 0.5 0.5 0.5 0.002  
GW 97 3 0.5 -0.5 0.375 0.5 -0.25 0.375 0.002  
GW 98 3 0.5 -0.25 0.375 0.5 0.0 0.375 0.002  
GW 99 3 0.5 0.0 0.375 0.5 0.25 0.375 0.002  
GW 100 3 0.5 0.25 0.375 0.5 0.5 0.375 0.002  
GW 101 3 0.5 -0.5 0.25 0.5 -0.25 0.25 0.002  
GW 102 3 0.5 -0.25 0.25 0.5 0.0 0.25 0.002  
GW 103 3 0.5 0.0 0.25 0.5 0.25 0.25 0.002  
GW 104 3 0.5 0.25 0.25 0.5 0.5 0.25 0.002  
GW 105 3 0.5 -0.5 0.125 0.5 -0.25 0.125 0.002  
GW 106 3 0.5 -0.25 0.125 0.5 0.0 0.125 0.002  
GW 107 3 0.5 0.0 0.125 0.5 0.25 0.125 0.002  
GW 108 3 0.5 0.25 0.125 0.5 0.5 0.125 0.002  
GW 109 1 0.5 -0.5 0.5 0.5 -0.5 0.375 0.002  
GW 110 1 0.5 -0.5 0.375 0.5 -0.5 0.25 0.002  
GW 111 1 0.5 -0.5 0.25 0.5 -0.5 0.125 0.002  
GW 112 1 0.5 -0.5 0.125 0.5 -0.5 0.0 0.002

Underground.nec

GW 113	1	0.5	-0.25	0.5	0.5	-0.25	0.375	0.002
GW 114	1	0.5	-0.25	0.375	0.5	-0.25	0.25	0.002
GW 115	1	0.5	-0.25	0.25	0.5	-0.25	0.125	0.002
GW 116	1	0.5	-0.25	0.125	0.5	-0.25	0.0	0.002
GW 117	1	0.5	0.0	0.5	0.5	0.0	0.375	0.002
GW 118	1	0.5	0.0	0.375	0.5	0.0	0.25	0.002
GW 119	1	0.5	0.0	0.25	0.5	0.0	0.125	0.002
GW 120	1	0.5	0.0	0.125	0.5	0.0	0.0	0.002
GW 121	1	0.5	0.25	0.5	0.5	0.25	0.375	0.002
GW 122	1	0.5	0.25	0.375	0.5	0.25	0.25	0.002
GW 123	1	0.5	0.25	0.25	0.5	0.25	0.125	0.002
GW 124	1	0.5	0.25	0.125	0.5	0.25	0.0	0.002
GW 125	1	0.5	0.5	0.5	0.5	0.5	0.375	0.002
GW 126	1	0.5	0.5	0.375	0.5	0.5	0.25	0.002
GW 127	1	0.5	0.5	0.25	0.5	0.5	0.125	0.002
GW 128	1	0.5	0.5	0.125	0.5	0.5	0.0	0.002
GW 129	3	-0.5	-0.25	0.5	-0.25	-0.25	0.5	0.002
GW 130	3	-0.25	-0.25	0.5	0.0	-0.25	0.5	0.002
GW 131	3	0.0	-0.25	0.5	0.25	-0.25	0.5	0.002
GW 132	3	0.25	-0.25	0.5	0.5	-0.25	0.5	0.002
GW 133	3	-0.5	0.0	0.5	-0.25	0.0	0.5	0.002
GW 134	3	-0.25	0.0	0.5	0.0	0.0	0.5	0.002
GW 135	3	0.0	0.0	0.5	0.25	0.0	0.5	0.002
GW 136	3	0.25	0.0	0.5	0.5	0.0	0.5	0.002
GW 137	3	-0.5	0.25	0.5	-0.25	0.25	0.5	0.002
GW 138	3	-0.25	0.25	0.5	0.0	0.25	0.5	0.002
GW 139	3	0.0	0.25	0.5	0.25	0.25	0.5	0.002
GW 140	3	0.25	0.25	0.5	0.5	0.25	0.5	0.002
GW 141	3	-0.25	-0.5	0.5	-0.25	-0.25	0.5	0.002
GW 142	3	-0.25	-0.25	0.5	-0.25	0.0	0.5	0.002
GW 143	3	-0.25	0.0	0.5	-0.25	0.25	0.5	0.002
GW 144	3	-0.25	0.25	0.5	-0.25	0.5	0.5	0.002
GW 145	3	0.0	-0.5	0.5	0.0	-0.25	0.5	0.002
GW 146	3	0.0	-0.25	0.5	0.0	0.0	0.5	0.002
GW 147	3	0.0	0.0	0.5	0.0	0.25	0.5	0.002
GW 148	3	0.0	0.25	0.5	0.0	0.5	0.5	0.002
GW 149	3	0.25	-0.5	0.5	0.25	-0.25	0.5	0.002
GW 150	3	0.25	-0.25	0.5	0.25	0.0	0.5	0.002
GW 151	3	0.25	0.0	0.5	0.25	0.25	0.5	0.002
GW 152	3	0.25	0.25	0.5	0.25	0.5	0.5	0.002
GW 153	1	-0.25	0.5	0.0	-0.25	0.5	-0.125	0.002
GW 154	1	0.0	0.5	0.0	0.0	0.5	-0.125	0.002
GW 155	1	-0.25	-0.5	0.0	-0.25	-0.5	-0.125	0.002
GW 156	1	0.0	-0.5	0.0	0.0	-0.5	-0.125	0.002
GW 157	1	0.25	-0.5	0.0	0.25	-0.5	-0.125	0.002
GW 158	1	-0.5	-0.5	0.0	-0.5	-0.5	-0.125	0.002
GW 159	1	-0.5	-0.25	0.0	-0.5	-0.25	-0.125	0.002
GW 160	1	-0.5	0.0	0.0	-0.5	0.0	-0.125	0.002
GW 161	1	-0.5	0.25	0.0	-0.5	0.25	-0.125	0.002
GW 162	1	-0.5	0.5	0.0	-0.5	0.5	-0.125	0.002
GW 163	1	0.5	-0.5	0.0	0.5	-0.5	-0.125	0.002
GW 164	1	0.5	-0.25	0.0	0.5	-0.25	-0.125	0.002
GW 165	1	0.5	0.0	0.0	0.5	0.0	-0.125	0.002
GW 166	1	0.5	0.25	0.0	0.5	0.25	-0.125	0.002
GW 167	1	0.5	0.5	0.0	0.5	0.5	-0.125	0.002
GW 168	1	0.25	0.5	0.0	0.25	0.5	-0.125	0.002
GW 169	830	-2.0	-0.01	-0.994	-170.0	-0.01	-0.994	0.001
GW 170	830	-2.0	0.0	-1.012	-170.0	0.0	-1.012	0.001
GW 171	830	170.0	0.01	-0.994	2.0	0.01	-0.994	0.001
GW 172	830	170.0	-0.01	-0.994	2.0	-0.01	-0.994	0.001
GW 173	830	170.0	0.0	-1.012	2.0	0.0	-1.012	0.001
GW 174	830	-2.0	0.0	-1.0	-170.0	0.0	-1.0	0.005
GW 175	830	-170.0	0.01	-0.994	-2.0	0.01	-0.994	0.001

Underground.nec

GW 176 830 170.0 0.0 -1.0 2.0 0.0 -1.0 0.005  
GW 177 5 -0.225 0.0 0.0 -0.225 0.0 0.2 0.005  
GW 178 11 -0.225 0.0 0.2 0.225 0.0 0.2 0.005  
GW 179 5 0.225 0.0 0.2 0.225 0.0 0.0 0.005  
GW 180 24 2.0 0.0 -1.0 1.04 0.0 -1.0 0  
GC 2 0 0 .005 .005 .2 .04  
GW 181 24 2.0 0.0 -1.012 1.04 0.0 -1.012 0  
GC 2 0 0 .001 .001 .2 .04  
GW 182 24 2.0 0.01 -0.994 1.04 0.01 -0.994 0  
GC 2 0 0 .001 .001 .2 .04  
GW 183 24 2.0 -0.01 -0.994 1.04 -0.01 -0.994 0  
GC 2 0 0 .001 .001 .2 .04  
GW 184 1 1.04 0.0 -1.012 0.9943 0.0 -1.012 0.001  
GW 185 1 1.04 0.01 -0.994 1.003 0.01 -0.994 0.001  
GW 186 1 1.04 -0.01 -0.994 1.003 -0.01 -0.994 0.001  
GW 187 24 -2.0 0.0 -1.0 -1.04 0.0 -1.0 0  
GC 2 0 0 .005 .005 .2 .04  
GW 188 24 -2.0 0.0 -1.012 -1.04 0.0 -1.012 0  
GC 2 0 0 .001 .001 .2 .04  
GW 189 24 -2.0 -0.01 -0.994 -1.04 -0.01 -0.994 0  
GC 2 0 0 .001 .001 .2 .04  
GW 190 24 -2.0 0.01 -0.994 -1.04 0.01 -0.994 0  
GC 2 0 0 .001 .001 .2 .04  
GW 191 31 -1.0 0.0 -1.0 -0.249 0.0 -0.032 0.005  
GW 192 31 -0.994 0.0 -1.012 -0.243 0.0 -0.044 0.001  
GW 193 1 -1.04 0.0 -1.012 -0.994 0.0 -1.012 0.001  
GW 194 1 -1.04 -0.01 -0.994 -1.003 -0.01 -0.994 0.001  
GW 195 1 -1.04 0.01 -0.994 -1.003 0.01 -0.994 0.001  
GW 196 1 1.04 0.0 -1.0 1.0 0.0 -1.0 0.005  
GW 197 1 -1.04 0.0 -1.0 -1.0 0.0 -1.0 0.005  
GW 198 1 -0.249 0.0 -0.032 -0.225 0.0 0.0 0.005  
GW 199 1 -0.252 -0.01 -0.026 -0.232 -0.01 0.0 0.001  
GW 200 1 -0.243 0.0 -0.044 -0.209 0.0 0.0 0.001  
GW 201 1 -0.252 0.01 -0.026 -0.232 0.01 0.0 0.001  
GW 202 31 1.0 0.0 -1.0 0.2494 0.0 -0.032 0.005  
GW 203 31 0.9943 0.0 -1.012 0.2433 0.0 -0.044 0.001  
GW 204 31 1.003 0.01 -0.994 0.2521 0.01 -0.026 0.001  
GW 205 31 1.003 -0.01 -0.994 0.2521 -0.01 -0.026 0.001  
GW 206 1 0.2494 0.0 -0.032 0.225 0.0 0.0 0.005  
GW 207 1 0.2521 0.01 -0.026 0.232 0.01 0.0 0.001  
GW 208 1 0.2433 0.0 -0.044 0.2092 0.0 0.0 0.001  
GW 209 1 0.2521 -0.01 -0.026 0.232 -0.01 0.0 0.001  
GW 210 31 -1.003 -0.01 -0.994 -0.252 -0.01 -0.026 0.001  
GW 211 31 -1.003 0.01 -0.994 -0.252 0.01 -0.026 0.001  
GE -1  
GN 2 0 0 0 13 .005  
LD 5 0 0 0 58000000 0  
LD 5 1 0 0 1390000 0  
LD 5 2 0 0 1390000 0  
LD 5 3 0 0 1390000 0  
LD 5 4 0 0 1390000 0  
LD 5 5 0 0 1390000 0  
LD 5 6 0 0 1390000 0  
LD 5 7 0 0 1390000 0  
LD 5 8 0 0 1390000 0  
LD 5 9 0 0 1390000 0  
LD 5 10 0 0 1390000 0  
LD 5 11 0 0 1390000 0  
LD 5 12 0 0 1390000 0  
LD 5 13 0 0 1390000 0  
LD 5 14 0 0 1390000 0  
LD 5 15 0 0 1390000 0  
LD 5 16 0 0 1390000 0

Underground.nec

LD 5 17 0 0 1390000 0  
LD 5 18 0 0 1390000 0  
LD 5 19 0 0 1390000 0  
LD 5 20 0 0 1390000 0  
LD 5 21 0 0 1390000 0  
LD 5 22 0 0 1390000 0  
LD 5 23 0 0 1390000 0  
LD 5 24 0 0 1390000 0  
LD 5 25 0 0 1390000 0  
LD 5 26 0 0 1390000 0  
LD 5 27 0 0 1390000 0  
LD 5 28 0 0 1390000 0  
LD 5 29 0 0 1390000 0  
LD 5 30 0 0 1390000 0  
LD 5 31 0 0 1390000 0  
LD 5 32 0 0 1390000 0  
LD 5 33 0 0 1390000 0  
LD 5 34 0 0 1390000 0  
LD 5 35 0 0 1390000 0  
LD 5 36 0 0 1390000 0  
LD 5 37 0 0 1390000 0  
LD 5 38 0 0 1390000 0  
LD 5 39 0 0 1390000 0  
LD 5 40 0 0 1390000 0  
LD 5 41 0 0 1390000 0  
LD 5 42 0 0 1390000 0  
LD 5 43 0 0 1390000 0  
LD 5 44 0 0 1390000 0  
LD 5 45 0 0 1390000 0  
LD 5 46 0 0 1390000 0  
LD 5 47 0 0 1390000 0  
LD 5 48 0 0 1390000 0  
LD 5 49 0 0 1390000 0  
LD 5 50 0 0 1390000 0  
LD 5 51 0 0 1390000 0  
LD 5 52 0 0 1390000 0  
LD 5 53 0 0 1390000 0  
LD 5 54 0 0 1390000 0  
LD 5 55 0 0 1390000 0  
LD 5 56 0 0 1390000 0  
LD 5 57 0 0 1390000 0  
LD 5 58 0 0 1390000 0  
LD 5 59 0 0 1390000 0  
LD 5 60 0 0 1390000 0  
LD 5 61 0 0 1390000 0  
LD 5 62 0 0 1390000 0  
LD 5 63 0 0 1390000 0  
LD 5 64 0 0 1390000 0  
LD 5 65 0 0 1390000 0  
LD 5 66 0 0 1390000 0  
LD 5 67 0 0 1390000 0  
LD 5 68 0 0 1390000 0  
LD 5 69 0 0 1390000 0  
LD 5 70 0 0 1390000 0  
LD 5 71 0 0 1390000 0  
LD 5 72 0 0 1390000 0  
LD 5 73 0 0 1390000 0  
LD 5 74 0 0 1390000 0  
LD 5 75 0 0 1390000 0  
LD 5 76 0 0 1390000 0  
LD 5 77 0 0 1390000 0  
LD 5 78 0 0 1390000 0  
LD 5 79 0 0 1390000 0



Underground.nec

LD 5 80 0 0 1390000 0  
LD 5 81 0 0 1390000 0  
LD 5 82 0 0 1390000 0  
LD 5 83 0 0 1390000 0  
LD 5 84 0 0 1390000 0  
LD 5 85 0 0 1390000 0  
LD 5 86 0 0 1390000 0  
LD 5 87 0 0 1390000 0  
LD 5 88 0 0 1390000 0  
LD 5 89 0 0 1390000 0  
LD 5 90 0 0 1390000 0  
LD 5 91 0 0 1390000 0  
LD 5 92 0 0 1390000 0  
LD 5 93 0 0 1390000 0  
LD 5 94 0 0 1390000 0  
LD 5 95 0 0 1390000 0  
LD 5 96 0 0 1390000 0  
LD 5 97 0 0 1390000 0  
LD 5 98 0 0 1390000 0  
LD 5 99 0 0 1390000 0  
LD 5 100 0 0 1390000 0  
LD 5 101 0 0 1390000 0  
LD 5 102 0 0 1390000 0  
LD 5 103 0 0 1390000 0  
LD 5 104 0 0 1390000 0  
LD 5 105 0 0 1390000 0  
LD 5 106 0 0 1390000 0  
LD 5 107 0 0 1390000 0  
LD 5 108 0 0 1390000 0  
LD 5 109 0 0 1390000 0  
LD 5 110 0 0 1390000 0  
LD 5 111 0 0 1390000 0  
LD 5 112 0 0 1390000 0  
LD 5 113 0 0 1390000 0  
LD 5 114 0 0 1390000 0  
LD 5 115 0 0 1390000 0  
LD 5 116 0 0 1390000 0  
LD 5 117 0 0 1390000 0  
LD 5 118 0 0 1390000 0  
LD 5 119 0 0 1390000 0  
LD 5 120 0 0 1390000 0  
LD 5 121 0 0 1390000 0  
LD 5 122 0 0 1390000 0  
LD 5 123 0 0 1390000 0  
LD 5 124 0 0 1390000 0  
LD 5 125 0 0 1390000 0  
LD 5 126 0 0 1390000 0  
LD 5 127 0 0 1390000 0  
LD 5 128 0 0 1390000 0  
LD 5 129 0 0 1390000 0  
LD 5 130 0 0 1390000 0  
LD 5 131 0 0 1390000 0  
LD 5 132 0 0 1390000 0  
LD 5 133 0 0 1390000 0  
LD 5 134 0 0 1390000 0  
LD 5 135 0 0 1390000 0  
LD 5 136 0 0 1390000 0  
LD 5 137 0 0 1390000 0  
LD 5 138 0 0 1390000 0  
LD 5 139 0 0 1390000 0  
LD 5 140 0 0 1390000 0  
LD 5 141 0 0 1390000 0  
LD 5 142 0 0 1390000 0

Underground.nec

```
LD 5 143 0 0 1390000 0
LD 5 144 0 0 1390000 0
LD 5 145 0 0 1390000 0
LD 5 146 0 0 1390000 0
LD 5 147 0 0 1390000 0
LD 5 148 0 0 1390000 0
LD 5 149 0 0 1390000 0
LD 5 150 0 0 1390000 0
LD 5 151 0 0 1390000 0
LD 5 152 0 0 1390000 0
LD 5 153 0 0 1390000 0
LD 5 154 0 0 1390000 0
LD 5 155 0 0 1390000 0
LD 5 156 0 0 1390000 0
LD 5 157 0 0 1390000 0
LD 5 158 0 0 1390000 0
LD 5 159 0 0 1390000 0
LD 5 160 0 0 1390000 0
LD 5 161 0 0 1390000 0
LD 5 162 0 0 1390000 0
LD 5 163 0 0 1390000 0
LD 5 164 0 0 1390000 0
LD 5 165 0 0 1390000 0
LD 5 166 0 0 1390000 0
LD 5 167 0 0 1390000 0
LD 5 168 0 0 1390000 0
IS 0 174 0 0 2.2 .0625 .011
IS 0 176 0 0 2.2 .0625 .011
IS 0 191 0 0 2.2 .0625 .011
IS 0 196 0 0 2.2 .0625 .011
IS 0 197 0 0 2.2 .0625 .011
IS 0 198 0 0 2.2 .0625 .011
IS 0 202 0 0 2.2 .0625 .011
IS 0 206 0 0 2.2 .0625 .011
FR 0 1 0 0 30 0
EX 0 178 6 0 1 0
EN
```